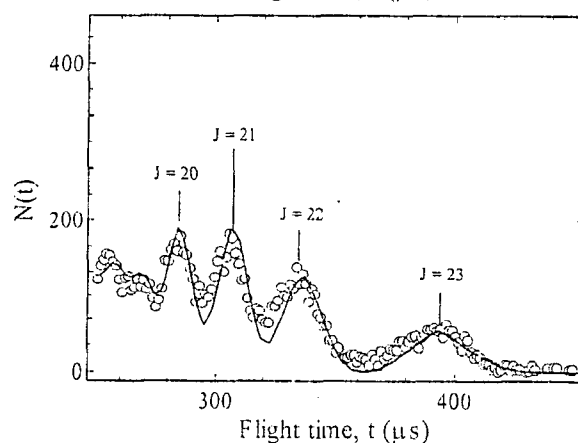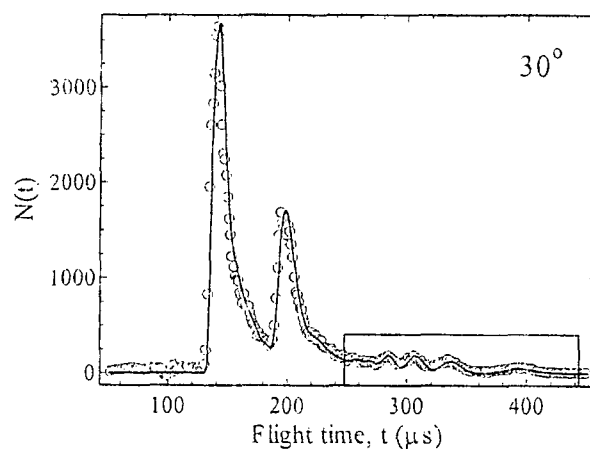# 24th Annual Combustion Research Conference

U.S. Department of Energy
Office of Basic Energy Sciences

Granlibakken Conference Center
Tahoe City, California
May 27 – May 30, 2003

Cover Figure: Top panel: TOF spectrum for O ($^3P_2$) from NO_2 photodissociation at 355 nm, at 30° (open circles) along with fit (solid line). Bottom panel: Expanded region showing rotationally resolved levels of recoiling NO (v=1) counterfragment (*Bimolecular Dynamics of Combustion Reactions*, H. Floyd Davis, p 67)

FOREWORD

The achievement of National goals for energy conservation and environmental protection will rely on technology more advanced than we have at our disposal today. Combustion at present accounts for 85% of the energy generated and used in the U.S. and is likely to remain a dominant source of energy for the coming decades. Achieving energy conservation while minimizing unwanted emissions from combustion processes could be greatly accelerated if accurate and reliable means were at hand for quantitatively predicting process performance.

The reports appearing in this volume present work in progress in basic research contributing to the development of a predictive capability for combustion processes. The work reported herein is supported by the Department of Energy's Office of Basic Energy Sciences (BES) and in large measure by the chemical physics program. The long-term objective of this effort is the provision of theories, data, and procedures to enable the development of reliable computational models of combustion processes, systems, and devices.

The development of reliable models for combustion requires the accurate knowledge of chemistry, turbulent flow, and the interaction between the two at temperatures and pressures characteristic of the combustion environment. In providing this knowledge, the research supported by BES addresses a wide range of continuing scientific issues of long standing.

➢ For even the simplest fuels, the chemistry of combustion consists of hundreds of reactions. Key reaction mechanisms, the means for developing and testing these mechanisms and the means for determining which of the constituent reaction rates are critical for accurate characterization are all required.

➢ For reactions known to be important, accurate rates over wide ranges of temperature, pressure and composition are required. To assess the accuracy of measured reaction rates or predict rates that would be too difficult to measure, theories of reaction rates and means for calculating their values are needed. Of particular importance are reactions involving open shell systems such as radicals and excited electronic states.

➢ To assess the accuracy of methods for predicting chemical reaction rates, the detailed, state-specific dynamics of prototypical reactions must be characterized.

➢ Methods for observing key reaction species in combustion environments, for interpreting these observations in terms of species concentrations, and for determining which species are key are all required

➢ Energy flow and accounting must be accurately characterized and predicted.

➢ Methods for reducing the mathematical complexity inherent in hundreds of reactions, without sacrificing accuracy and reliability are required. Methods for reducing the computational complexity of computer models that attempt to address turbulence, chemistry, and their interdependence and also needed.

Although the emphasis in this list is on the development of mathematical models for simulating the gas phase reactions characteristic of combustion, *such models, from the chemical dynamics of a single molecule to the performance of a combustion device,*

have value only when confirmed by experiment. Hence, the DOE program represented by reports in this volume supports the development and application of new experimental tools in chemical dynamics, kinetics, and spectroscopy.

The success of this research effort will be measured by the quality of the research performed, the profundity of the knowledge gained, as well as the degree to which it contributes to goals of resource conservation and environmental stewardship. In fact, without research of the highest quality, the application of the knowledge gained to practical problems will not be possible.

The emphasis on modeling and simulation as a basis for defining the objectives of this basic research program has a secondary but important benefit. Computational models of physical processes provide the most efficient means for ensuring the usefulness and use of basic theories and data. The importance of modeling and simulation remains well recognized in the Department of Energy and is receiving support through the Scientific Discovery through Advanced Computing (SciDAC) initiative; several work-in-progress reports funded through SciDAC are included in this volume.

During the past year, the Chemical Physics program has continued to benefit from the involvement of Dr. William Kirchhoff, program manager for the Chemical Physics program, Dr. Eric Rohlfing, program manager for the Atomic, Molecular and Optical Physics program and, recently, team leader for the Fundamental Interactions programs, and Dr. Allan Laufer, team leader for the Fundamental Interactions programs, now retired. Allan's many contributions to the scientific programs described herein are well known and greatly appreciated. The efforts of Andreene Witt, Karen Jones, Rachel Smith, and Deborah Garland of the Oak Ridge Institute for Science Education and Karen Talamini of the Division of Chemical Sciences, Geosciences, and Biosciences, Office of Basic Energy Sciences in the arrangements for the meeting are also much appreciated.

Frank P. Tully, SC-141
Division of Chemical Sciences, Geosciences, and Biosciences
Office of Basic Energy Sciences

May 27, 2003

24th Annual Combustion Research Conference
U. S. Department of Energy
Office of Basic Energy Sciences

Agenda

Tuesday, May 27, 2003

3:00 pm   *Registration*

6:30 pm   *Dinner and Reception*

Wednesday, May 28, 2003
Morning Session

David R. Yarkony, Chair

8:15 am   *Welcome and Introduction*, Frank P. Tully

8:30 am   *"Multiscale Modeling of Chemically Reacting Flow Systems - - From
Atoms to Reactors to Chemical Plants,"* Gregory J. McRae

9:45 am   *"Theoretical Studies of the Dynamics of Chemical Reactions,"* Albert F.
Wagner..317

10:15 am   *Break*

10:30 am   *"Theoretical Chemical Kinetics,"* Stephen J. Klippenstein...............168

11:00 am   *"Theoretical Studies of Molecular Systems,"* William A. Lester,
Jr...178

11:30 am   *"Dynamical Analysis of Highly Excited Molecular Spectra,"* Michael E.
Kellman...156

12:15 pm   *Lunch*

5:00 pm   *Dinner*

Wednesday, May 28, 2003
Evening Session

Robert F. Curl, Chair

Thursday, May 29, 2003
Morning Session

William H. Green, Jr., Chair

12:15 pm *Lunch*

Thursday, May 29, 2003
Afternoon and Evening Session

Gregory E. Hall, Chair

5:30 pm *Break*

7:30 pm *Cash Bar*

8:00 pm *Dinner*

Friday, May 30, 2003
Morning Session

David S. Perry, Chair

Table of Contents

Photoelectron Photoion Coincidence Studies: Heats of Formation of Ions, Molecules, and Free Radicals

Tomas Baer (baer@unc.edu)
Department of Chemistry
University of North Carolina
Chapel Hill, NC 27599-3290
DOE Grant DE-FG02-97ER14776

Program Scope

The photoelectron photoion coincidence (PEPICO) technique is utilized to investigate the dissociation dynamics and thermochemistry of energy selected medium to large organic molecular ions. Extensive modeling of the dissociation rate constant using the RRKM theory or variational transition state theory (VTST) is used in order to determine the dissociation limits of energy selected ions. These studies are carried out with the aid of molecular orbital calculations of both ions and the transition states connecting the ion structure to their products. The results of these investigations yield accurate heats of formation of ions and free radicals. In addition, they provide information about the potential energy surface that governs the dissociation process. Isomerization reactions prior to dissociation are readily inferred from the PEPICO data.

The PEPICO Experiment

Although the PEPICO experiment is now about 30 years old, a major improvement has been the incorporation of velocity focusing optics for detecting electrons, and the collection of both threshold PEPICO as well as "hot" electron PEPICO signal. But subtracting the two, a true PEPICO spectrum is obtained with out contamination by "hot" electrons. The photoelectron photoion coincidence (PEPICO) experiment in Chapel Hill is carried out with a laboratory H_2 discharge light source. The threshold electrons provide the start signal for measuring the ion time of flight distribution. When ions dissociate in the microsecond time scale, their TOF distributions are asymmetric. The dissociation rate constant can be extracted by modeling the asymmetric TOF distribution. A high-resolution version of this experiment is being constrctued at the Chemical Dynamics Beamline of the ALS, in which a resolution of 1 meV is expected. When combined with coincidence ion detection, the results permit the measurement of ion dissociation limits to within 1 meV or 0.1 kJ/mol.

Recent Results

TPEPICO experiments with velocity focusing of threshold electrons

A major step forward in threshold photoelectron photoion coincidence (TPEPICO) has been the incorporation of velocity focusing for the detection of low energy electrons. Velocity focusing optics, discovered by Chandler and Parker, permits ions or electrons to be focused to concentric rings whose diameter is related to the electron/ion velocity in a direction perpendicular to the extraction field. The resolution is particularly high for low energy electrons/ions. Two features of velocity focusing make this an ideal match for coincidence experiments. The relatively high extraction field permits ions to be extracted with good efficiency and narrow time of flight peaks. Secondly, a large ionization region (10 mm) can be readily focused to a 1 mm hole. The use of such a small hole reduces the hot electron background signal that routinely compromises the traditional TPEPICO experiments. The

introduction of velocity focusing resulted in a 10-fold increase in threshold electron collection efficiency and the simultaneous improvement in the resolution from 25 to 12 meV.

The most recent innovation has achieved the complete suppression of hot electrons. The electron detector has been replaced by a multi-channel plate that collects the threshold electrons through a 1 mm diameter hole as well as a ring of electrons that strike the collector between diameters of 5 and 7 mm. Because the outer ring collects only hot electrons, while the central electrode collects a combination of true zero energy electrons and a few hot electrons, it is now possible to subtract the hot electrons from the central electrode signal thereby yielding the true zero electron signal. A new chamber has been constructed with a reflectron TOF mass analysis.

Consecutive and parallel dissociation of energy selected $Co(CO)_3NO^+$ ions

Photoelectron photoion coincidence (PEPICO) spectroscopy has been used to investigate the dissociation dynamics of the cobalt tricarbonyl nitrosyl ion, $Co(CO)_3NO^+$. The ionization energy of $Co(CO)_3NO$ was measured from the threshold photoelectron spectrum to be 8.33 ± 0.03 eV. The dissociation of the molecular ion proceeds by two sequential carbonyl-loss steps and then a parallel carbonyl- or nitrosyl-loss step. The first two reactions were observed to be slow (lifetimes in the microsecond range). By simulating the resulting asymmetric time-of-flight peak shapes and the relative ion abundances (breakdown curves), 0 K onsets for the following fragment ions were determined: $Co(CO)_2NO^+$: 9.28 ± 0.02 eV, $CoCONO^+$: 10.43 ± 0.02 eV, $CoNO^+$: 12.00 ± 0.02 eV, $CoCO^+$: 12.07 ± 0.02 eV. Combining these onsets with the experimental adiabatic ionization energy of $Co(CO)_3NO^+$, the three cobalt–carbonyl bond energies in $Co(CO)_xNO^+$ (x = 1 – 3) were determined along with the cobalt-nitrosyl bond energy in $CoCONO^+$. Using a literature value for the $[Co–CO]^+$ bond energy, the 0K heats of formation of the above mentioned molecular and fragment ions and of the neutral compound, $Co(CO)_3NO$, were determined. Using these thermochemical data, the cobalt–nitrosyl bond energies were also derived for $Co(CO)_3NO^+$ and $CoNO^+$. The latter is in good agreement with a theoretical literature value, while the first one explains why there is no observable NO-loss from the molecular ion, $Co(CO)_3NO^+$. Room temperature values of the heats of formation are also given using the calculated harmonic frequencies.

Dissociation dynamics of ethylene glycol ions studied by photoelectron photoion coincidence

Density functional theory (DFT) and threshold photoelectron-photoion coincidence spectroscopy (TPEPICO) have been used to investigate the dissociation dynamics of the ethylene glycol ion. Thirteen isomers of the ethylene glycol ion ($C_2H_6O_2^+$) and the transition states connecting them were obtained at the B3LYP/6-31G(d) level. The TPEPICO experimental results show that the $CH_3OH_2^+$ and CH_2OH^+ ions are the two dominant products. The H_2O loss channel, the lowest dissociation energy channel according to the DFT calculations, requires an isomerization reaction that needs to overcome a high-energy barrier; thus, only weak $C_2H_4O^+$ ion signal was observed in the experiments. For the $CH_3OH_2^+$ ion, the product of a double hydrogen transfer reaction, its time-of-flight distributions exhibit characteristics of a two-component reaction rate. A two-well-two-channel model is proposed to describe the isomerization and dissociation process. The simulations combined with RRKM theory suggest that the production of the $CH_3OH_2^+$ ion involves a hydrogen-bridged reaction intermediate and the slow component of reaction rate is dominantly caused by tunneling through the isomerization barrier connecting the ethylene glycol ion (1^+) and the hydrogen-bridged structure, $CH_3OH(H)OCH^+$ (4^+). The 0 K appearance energies of the $CH_3OH_2^+$ and CH_2OH^+ ions are determined to be 10.52 ± 0.02 and

11.09 ± 0.04 eV, respectively. The 298 K heat of formation of the ethylene glycol molecule is determined to -404.7 ± 6.0 kJ/mol.

Future Plans

Velocity focusing TPEPICO experiments at the ALS: The logical next step in the use of velocity focusing in TPEPICO experiments is the use of an imaging detector for the electrons. In this experiment, to be performed at the chemical dynamics beamline of the ALS, all electrons between 0 and 1 eV will be collected on an imaging plate and the ions will be collected in coincidence with each of these electrons. SIMION calculations suggest that a resolution of 1 meV for threshold electrons should be readily possible. This improved resolution results from a combination of the higher photon resolution available at the beamline and the much smaller ion source region associated with the tightly focused ALS beam. The TPEPICO approach should thus rival the recently developed PFI-PEPICO experiments in terms of resolution. However, the big advantage of TPEPICO is that increased signal can be obtained by degrading electron resolution, a flexibility not possible with pulsed field ionization experiments. In addition, the velocity focusing TPEPICO approach does not require a dark gap in the synchrotron operation. Considerable pressure is being exerted to reduce the dark gap to 20 ns, which would make PFI experiments impossible. The final advantage of using an imaging plate detector for low energy electrons is the ability to collect a complete photoelectron spectrum from 0-1 eV with excellent resolution at low energies. This will make possible the collection of vibrationally resolved PES for tenuous targets such as free radicals.

Heats of formation for R° RCO⁺ and RCO° radicals. The new imaging PEPICO experiment with complete suppression of hot electrons will be used to study the dissociation dynamics of a series of mono and di-ketones, such as 2,3 butane-dione, 2 butanone, 2,3 pentane-dione, etc. From this series, all free radical and ion heats of formation can be determined. In addition, the heats of formation of several starting compounds, such as 2,3-butane-dione can also be determined. A second project will involve the accurate determination of the I atom loss from $C_3H_7I^+$. This dissociative ionization onset has been investigated by four different methods, which all result in different onsets that are well beyond the claimed accuracy of each method. The most striking disagreement is between the two most accurate methods, namely PFI-PEPICO (done at the ALS) and a more recent laser based MATI study. There is no obvious explanation except that the ion dissociation is slow and that the two methods are not only sensitive to this, but are not capable of detecting slow dissociations. Because our TPEPICO apparatus is ideal for rate measurements, it should be possible to resolve this discrepancy.

Rate measurements from 10^3 to 10^8 sec^{-1}: Velocity focusing optics permits the use of high electric fields to extract the ions and electrons. Coupled with a molecular beam sample introduction (at the ALS), it should be possible to measure dissociation rate constants for ions such as iodobenzene up to 10^8 sec^{-1}. (The large mass difference between the parent and daughter ions will result in very asymmetric daughter ion peaks.) At the same time, the use of a reflectron TOF mass analyzer in our Chapel Hill apparatus will permit us to measure rates down to 10^3 sec^{-1}. Such a broad range of rates has never been measured for any reaction and should provide a benchmark for statistical theories. This work is being done in collaboration with J. Troe. In particular, it will be possible to compare variational transition state theory for such a loose reaction with the statistical adiabatic channel (SAC) model of Troe

Research Publications Resulting from DOE grant 2001 – 2003

Y.Li, B. Sztaray, and T. Baer, The dissociation kinetics of energy selected $CpMn(CO)_3^+$ ions studied by threshold photoelectron photoion coincidence spectroscopy, *J.Am.Chem.Soc.* **123** 9388-9396 (2001)

K.-M. Weitzel, G. Jarvis, M. Malow, Y. T. Baer, Song, and C. Y. Ng, Observation of Accurate Ion Dissociation Thresholds in Pulsed Field Ionization Photoelectron Studies, *Phys. Rev. Lett.*, **86** 3526-3529 (2001)

Y.Li and T. Baer, Threshold photoelectron-photoion coincidence spectroscopy: Dissociation of the 1-chloroadamantane ion and the heat of formation of the 1-adamantyl cation, *J.Phys.Chem. A*, **106** 272-278 (2002)

F. Qi, L. Sheng, M. Ahmed, D.S. Peterka, and T. Baer, Exclusive production of excited state sulfur (^{1}D) from 193 nm photolysis of thietane, *Chem.Phys. Lett.* **357** 204-208 (2002)

Y.Li, J.E. McGrady, and T. Baer, Metal-benzene and metal-CO bond energies in neutral and ionic $C_6H_6Cr(CO)_3$ studied by threshold photoelectron photoion coincidence spectroscopy and DFT theory, *J. Am. Chem. Soc.*, **124** 4487-4494 (2002)

T. Baer, Photoelectron spectroscopy, threshold photoelectron spectroscopy, and pulsed field ionization, Chapt. 4 of Volume 1, Encyclopedia of Mass Spectrometry, Elsevier in press (2002)

T. Baer, Measuring fragment ion appearance energies by photoionization methods, Chapt. 5 volume 1, Encyclopedia of Mass Spectrometry, Elsevier, in press (2002)

Y. Li and T. Baer, Neutral and ionic bond energies in $(C_6H_6)_2Cr$ studied by threshold photoelectron photoion coincidence spectroscopy, *J. Phys. Chem. A*. **106** 9820-9826 (2002)

T. Baer and Y. Li, Threshold photoelectron spectroscopy with velocity focusing: An ideal match for coincidence studies, *Int. J. Mass Spectrom.* **219** 381-389 (2002)

Y. Li, B. Sztaray, and T. Baer, The dissociation kinetics of energy selected Cp_2Mn^+ ions studied by threshold photoelectron photoion coincidence spectroscopy, *J.Am.Chem.Soc.* **124** 5843-5849 (2002)

B. Sztáray, L. Szepes, and T. Baer, Neutral Cobalt–Carbonyl Bond Energy By Combining Threshold Photoelectron Photoion Coincidence Spectroscopy with He(I) Photoelectron Spectroscopy, *J.Am.Chem.Soc.* (2002) submitted

Y. Li and T. Baer, Theoretical studies on the isomerization and dissociation of the acrolein ions, *Int. J. Mass Spectrom* **218** 19-37 (2002).

Y. Li and T. Baer, The Dissociation Dynamics and Thermochemistry of the Acrolein Ion Studied by Threshold Photoelectron-Photoion Coincidence Spectroscopy, *Int. J. Mass Spectrom.* **218** 37-48 (2002)

Y. Li and T. Baer, Dissociation dynamics of ethylene glycol ions studied by photoelectron photoion coincidence, *J.Phys.Chem.A* **106** 8656-8666 (2002)

B. Sztaray and T. Baer, Consecutive and parallel dissociation of energy selected $Co(CO)_3NO^+$ ions, *J. Phys. Chem.A* **106** 8046-8053 (2002)

Turbulence-Chemistry Interactions in Reacting Flows

Robert S. Barlow
Combustion Research Facility
Sandia National Laboratories, MS 9051
Livermore, California 94551
barlow@ca.sandia.gov

Program Scope

This experimental program is directed toward achieving a more complete understanding of turbulence-chemistry interactions in flames and providing a quantitative basis for the evaluation and further development of advanced models for turbulent combustion. Spontaneous Raman scattering, Rayleigh scattering, and laser-induced fluorescence are applied simultaneously in hydrocarbon flames to obtain spatially and temporally resolved measurements of temperature, the concentrations of all major species, and selected minor species. Several additional scalar quantities are derived from these measurements, including mixture fraction or local equivalence ratio, reaction progress, and differential diffusion parameters. Our experimental approach has expanded from its previous focus on single-point measurements to include measurements of scalar gradients and scalar dissipation. Detailed results on the instantaneous spatial structure of reaction zones in turbulent flames, as well as the thermochemical states within those reaction zones, provide new fundamental insights on the coupling of turbulent fluid dynamics and chemical kinetics. Experiments are conducted in the Turbulent Combustion Laboratory, which is a relatively new user laboratory at the CRF.

In addition to our experimental work, this program has the leading role in organizing the International Workshop on Measurement and Computation of Turbulent Nonpremixed Flames (TNF). The TNF Workshop facilitates collaboration among experimental and computational researchers, who are working on fundamental issues of turbulence-chemistry interaction. A central theme of the workshop series, which began in 1996, is to contribute to the development and validation of advanced, science-based, predictive models for turbulent combustion. Most of our visiting experiments and external collaborations are carried out in the context of the TNF Workshop, and this arrangement gains significant leverage for the BES Combustion Program.

Recent Progress

The focus of recent and current work is on measurements of scalar dissipation, which is a central concept in the theory and modeling of turbulent flames. Scalar dissipation is defined as $\chi = 2D_\xi (\nabla \xi \bullet \nabla \xi)$, where ξ is the mixture fraction and D_ξ is its diffusivity. Submodels for scalar dissipation in turbulent flames are central to many modeling approaches, yet they are largely unproven because accurate measurements of scalar dissipation are difficult to achieve, particularly in hydrocarbon flames. Last year, we reported measurements of the radial component of scalar dissipation in piloted CH_4/air jet flames, based on line measurements of temperature and all the major species. Since then we have added capability to determine the instantaneous orientation of the reaction zone as it intersects the measured line. This allows determination of the flame-normal direction at each point along the measured line, such that the

measured one-dimensional gradient in mixture fraction can be corrected to yield estimates of the full three-dimensional gradient, $\nabla \xi$, and the full scalar dissipation.

The optical configuration for these three-dimensional measurements of flame structure is shown in Fig. 1. Three cameras are used for line imaging of spontaneous Raman scattering, Rayleigh scattering, and CO-LIF. Two additional cameras are used for planar laser-induced fluorescence (PLIF) imaging of OH in two planes that intersect the measured line. The Raman imaging system uses a Sandia-developed rotating mechanical shutter (9 μs gate) in combination with an imaging spectrograph and an unintensified, back-illuminated, cryogenically cooled CCD array detector. The high collection efficiency, wide dynamic range, and low noise achieved with this system are critical for the measurement of scalar dissipation, χ, which is determined from the square of the spatial derivative of the mixture fraction, ξ.
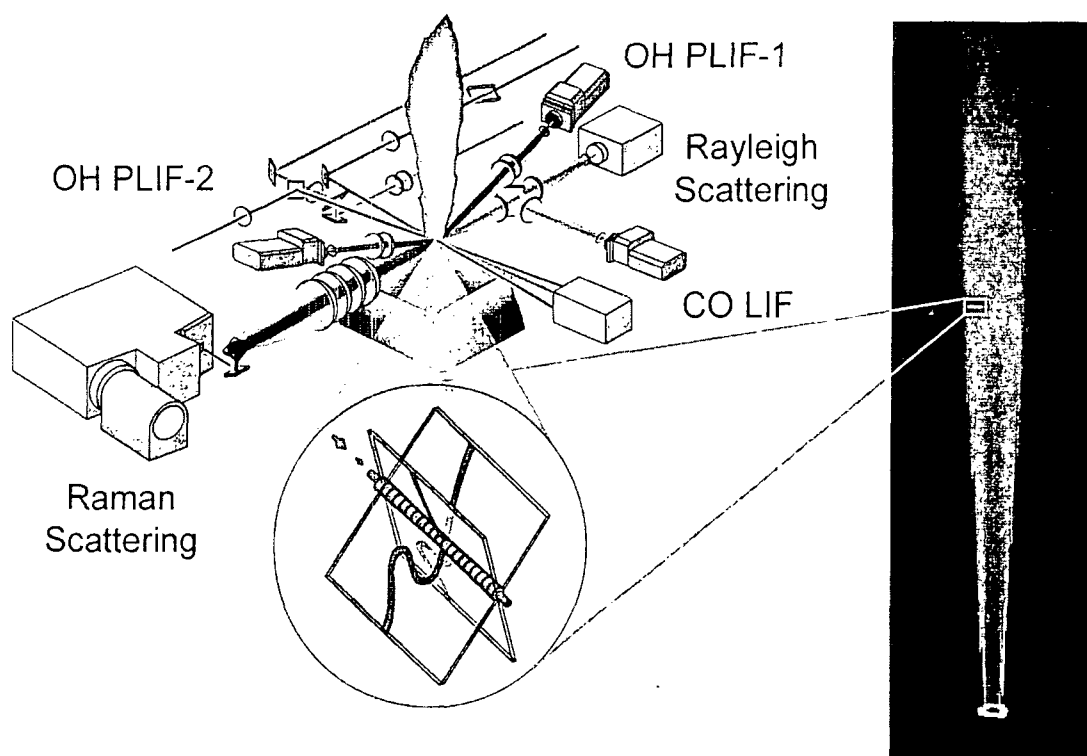
Fig. 1. Experimental system for scalar dissipation measurements in turbulent flames. The photo shows a piloted CH4/air flame (Sandia flame D). The inset in the flame photo shows the location corresponding to measurements in Fig. 2.

Figure 2 shows an example of single-shot results obtained at x/d=30 in a piloted CH4/air jet flame. The OH fluorescence images (smoothed to reduce noise in the calculated flame normal direction) are shown on the left, with the location of the intersection line marked by contrasting color in each image. The measured profile of mixture fraction on a 7-mm segment of this line is shown in the graph, along with the corresponding profiles of the measured 1D scalar dissipation and the derived 3D scalar dissipation.

A complex structure is revealed at this location in the turbulent flame. Regions of high scalar dissipation are localized in peaks that are 1 mm or less in width. Analysis of measured results has shown that the correlation length for fluctuations in scalar dissipation is well under a 1 mm in the in these flames. The flame normal direction also changes significantly over the length of the measured segment, as indicated by large variation in the ratio of χ_{3D} to χ_{1D}. Experiments are in progress in the partially premixed, piloted, CH$_4$/air jet flame (Sandia flames C, D, E, and F), which are already established as benchmarks for testing turbulent combustion models. Joint statistics of scalar dissipation and mixture fraction for both 1D and 3D measurements are key results to be compared with current scalar dissipation models.
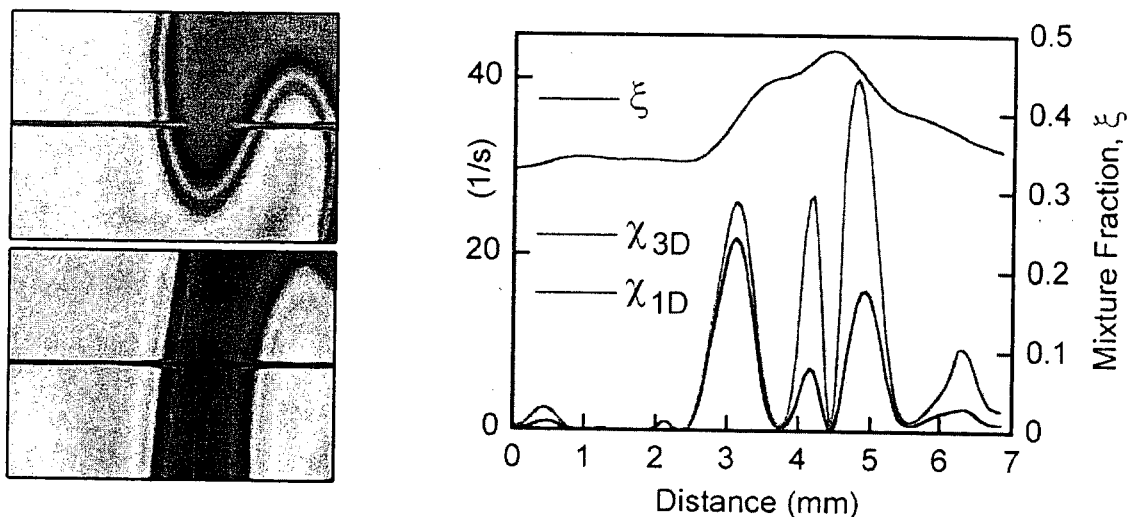
Fig. 2.   Example of single-shot results for OH fluorescence in the two intersecting planes (left) and corresponding profiles of mixture fraction and scalar dissipation (right).

Future Plans

In addition to experiments on the established benchmark flames mentioned above, which have a fuel-side equivalence ratio of $\phi=3.17$, partially premixed flames with higher and lower equivalence ratios will be measured. Experiments on partially premixed flames with CH$_4$/H$_2$ (1:1 by volume) plus air are also planned. Such flames are more robust than CH$_4$/air flames, allowing measurements in fully turbulent flames over a range of jet Reynolds number without significant levels of localized extinction. This will allow a more complete evaluation of scalar dissipation models. The measurement capability described here may also yield unique insights on the structure of reaction zones in the stabilization region of lifted flames, so lifted flame experiments are also planned. Detached or lifted flames are common in practical combustion systems, so it is important to develop predictive capabilities for this class of flames. Accordingly, lifted flames will be added as targets for the TNF Workshop.

More generally, a focus of this program will be to couple more closely with computational research based on direct numerical simulation (DNS) and high-fidelity large-eddy simulation (LES). This coupled experimental/computational approach is intended to accelerate the development of accurate, science-based LES sub-grid models for reacting flows.

BES Supported Publications (2001 - present)

R. S. Barlow, A. N. Karpetis, J. H. Frank, and J.-Y. Chen, "Scalar Profiles and NO Formation in Laminar Opposed-Flow Partially-Premixed Methane/Air Flames," *Combust. Flame* **127**:2102 (2001).

R. S. Barlow, C. D. Carter, R. W. Pitz, "Multiscalar Diagnostics in Turbulent Flames," in *Applied Combustion Diagnostics*, J. B. Jeffries and K. Kohse-Hoeinghaus, eds., Taylor & Francis, 2002.

R. Cabra, T. Myhrvold, J.-Y. Chen, R. W. Dibble, A. N. Karpetis, and R. S. Barlow, "Simultaneous Laser Raman-Rayleigh-LIF Measurements and Numerical Modeling Results of a Lifted Turbulent H2/N2 Jet Flame in a Vitiated Coflow," *Proc. Comb. Inst.* in press, 2002.

B. B. Dally, A. R. Masri, R. S. Barlow, and G. J. Fiechtner, "Two-Photon Laser-Induced Fluorescence Measurements of CO in Turbulent Nonpremixed Bluff Body Flames," *Combust. Flame* 132:272-274 (2002).

B. B. Dally, A. N. Karpetis, and R. S. Barlow, "Structure of Turbulent Nonpremixed Jet Flames in a Dilute Hot Coflow," *Proc. Comb. Inst.* in press, 2002.

P. A. M. Kalt, Y. M. Al-Abdeli, A. R. Masri, and R. S. Barlow, "Swirling Turbulent Nonpremixed Flames of Methane: Flowfield and Compositional Structure," *Proc. Comb. Inst.* in press, 2002.

Y. Zheng, R. S. Barlow, and J. P. Gore, "Measurements and Calculations of Mean Spectral Radiation Intensities for Turbulent Non-Premixed and Partially Premixed Flames," *J. Heat Trans.* (accepted).

X. L. Zhu, J. P. Gore, A. N. Karpetis, and R. S. Barlow, "The Effects of Self-Absorption of Radiation on an Opposed Flow Partially Premixed Flame," *Combust. Flame* 129:342-345 (2002).

Web-Based Information
http://www.ca.sandia.gov/CRF/staff/barlow.html   Research Page
http://www.ca.sandia.gov/TNF   TNF Workshop

Energy Partitioning in Elementary Chemical Reactions

Richard Bersohn
Department of Chemistry
Columbia University
New York, NY 10027
E-mail rb18@columbia.edu

The goals of this research are 1) to measure the yields of all the important channels of the reactions of $O(^3P)$ with unsaturated hydrocarbons and radicals and 2) by measurement of state distributions to understand the detailed mechanism. i.e. the trajectories of the atoms during the reactive collision.

I. A better method for generating HCCO

HCCO has ben commonly made by photodissociation of ketene at 193 nm. There are two difficulties with this method. On is that CH_2 and CO are produced in even larger yield. The second is that the absorption of ketene at 193 nm is very weak.[1] Rohlfing shifted the 193 nm light using a high pressure hydrogen cell to xxx nm.[2] He was then able to obtain stronger LIF excitation spectra of the radical and found that the fluorescence quantum yield is only of the order of a few %. The vinoxy radical is efficiently made by dissociating ethyl or methyl vinyl ether at 193 nm. It occurred to us that ethyl ethynyl ether might be photodissociated at the same wavelength to produce HCCO and C_2H_5

The two photodissociation processes share the property that the vinoxy and the ketenyl radicals can not be observed by LIF immediately after their formation. One has to wait for times of the order of tens of μs i.e. for perhaps 10-20 collisions. In the case of vinoxy, the delay is required to rotationally relax the nascent radicals. We obtained a beautiful set of hot bands which enable measurement of vibrational relaxation times as a function of internal energy. The figures on the following page show that this was not possible with HCCO.

II. H atom abstraction from hydrocarbons by $Cs(9^2P_{3/2})$

We had earlier studied the reaction $Cs (9^2 P) + H_2 \longrightarrow CsH + H$ and determined the rovibrational state distribution of the CsH by LIF. The majority of the exoergicity is released as translational energy which means that the reactants are close when the electron transfer occurs. The reaction of excited Cs atoms with hydrocarbon molecules had nit been previously studied. The C-H bond strengths of alkanes are less than that of H_2 by 6-9 kcal/mol so it was confidently expected that there would be abundant CsH product. None was detected. The major collision product is $Cs(6^2P)$. This result was obtained for methane, ethane, propane, cyclohexane and cyclopropane. The most striking aspects are the absence of chemical reaction and the apparent scalar interaction evidenced by the P--> P transition.. The latter can be justified because the 9p electron is so remote from the Cs^+ ion core. The shape of the molecule does not matter..
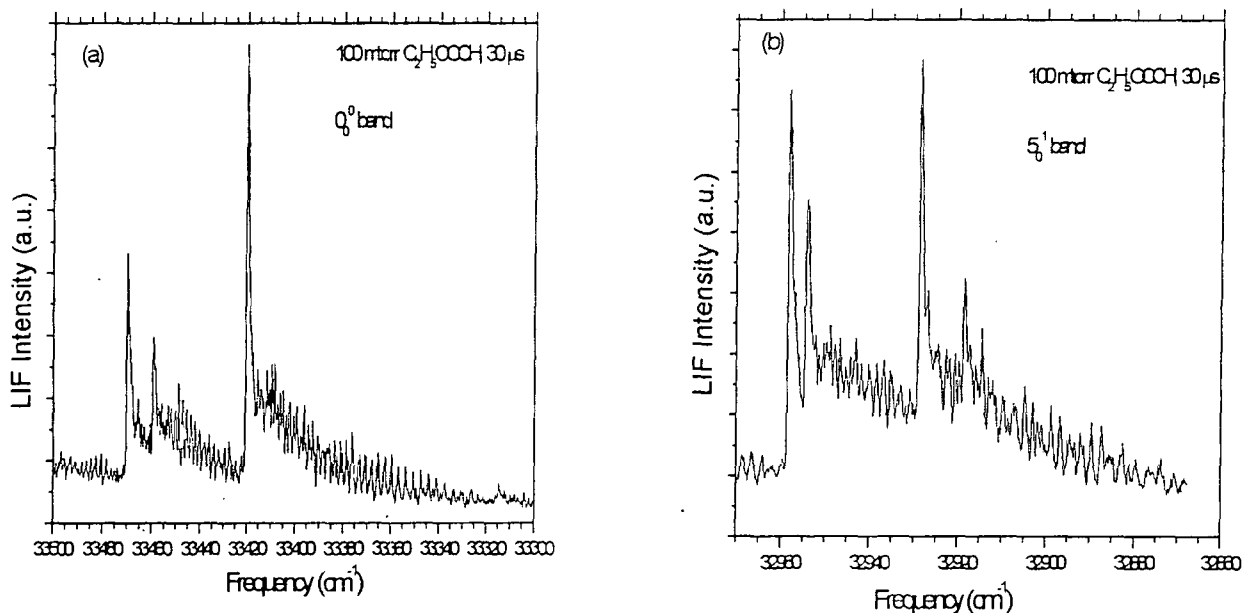
Figure 1. The LIF excitation spectra of HCCO taken at 30 μs after the photodissociation of 100 mtorr of C_2H_5OCCH: (a) 0_0^0 band and (b) 5_1^0 band.
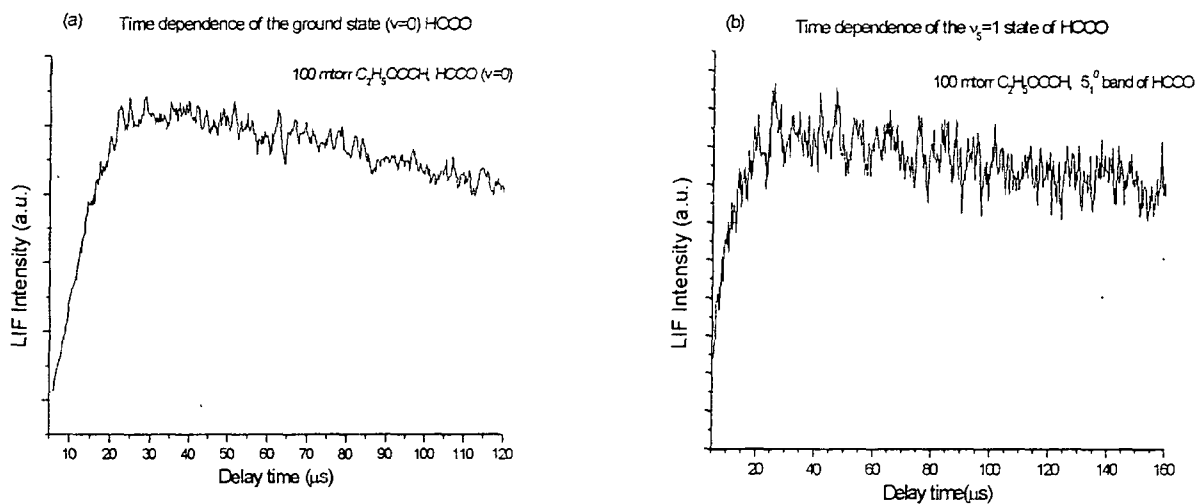
Figure 2. LIF excitation intensity as a function of time delay between the 193nm laser pulse and the probe laser pulse: (a) 0_0^0 band and (b) 5_1^0 band.

Propene whose allylic C-H bond strength is only 86 kcal/mol does indeed react with Cs(9^2P) to give a cold CsH implying again that most of the energy release is into translation.

Future experiments

A molecular beam machine has been constructed in which a mixture of SO_2 and an unsaturated hydrocarbon is expanded through a pulsed valve, then irradiated with 193 nm to form O(^{3}P). The radical reaction products are ionized by a beam of 118.3 nm light. An appropriately timed high voltage pulse prevents the unwanted ions generated by the 193 nm laser alone from reaching the detector. The next year will be devoted solely to this work.

References

1 .L.R.Brock,B.Mischler,E.A.Rohlfing,R.T.Bise,D.Neumark,
   J.Chem.Phys. 107,665(1997)
2. L.R.Brock,B.Mischler,E.A.Rohlfing, J.Chem.Phys. 110,6773((1999)

Publications in years 2001, 2002 and 2003

1. Vibrational state distribution and relaxation of vinoxy radicals,
   Honmei Su and Richard Bersohn J.Chem.Phys. .115,217(2001)
2. Mechanisms of Formation of Vinoxxy Radicals in the Reaction of O(^{3}P)
   with Terminal Alkenes, Honmei Sdu and Richard Bersohn,
   J.Phys.Chem.A 105,9178(2001)
3. Radicals Containing Hydrogen, Carbon and Oxygen Atoms,
   Richard Bersohn, Journal of the Chinese Chemical Society, 49,291(2002)
4. Inelastic and reactive collisions of Cs($9^2P_{3/2}$) with hydrocarbons,
   Hongmei Su and Richard Bersohn, J.Chem.Phys.117,8412(2002)
5. Photodissociation dynamics of ethyl ethynyl ether: A new ketenyl precursor
   M.J.Krisch,J.L.Miller,L.J.Butler,H.Su,R.Bersohn,J.Shu,
   J.Chem.Phys. (2003) submitted

Theoretical Studies of Combustion Dynamics

Joel M. Bowman
Cherry L. Emerson Center for Scientific Computation and
Department of Chemistry, Emory University
Atlanta, GA 30322,
bowman@euch4e.chem.emory.edu

Program Scope

The focus of the research funded by the Department of Energy is the theoretical and computational effort to develop and apply rigorous quantum dynamical methods to chemical processes of importance in gas-phase combustion. These include quantum calculations of bimolecular and unimolecular reactions and the *ab initio*-based potentials that govern these processes. Recent work has focused on acetylene/vinylidene isomerization and the $O(^3P)+HCl$ reaction. We have made major progress in both projects.

Recent Progress

Acetylene/vinylidene isomerization

The existence and charactrer of the vinylidene isomer has been of intense interest to both experimentalists and theorists for nearly twenty years.[1-8] Last year we reported reduced dimensionality quantum calculation, in four degrees of freedom, that clearly showed the existence of vinylidene molecular eigenstates.[9] In the past year we have been able to do calculations in full dimensionality. This required a new code, some new strategies to perform the calculations, and finally access to a large memory computer where it was possible to diagonalize Hamiltonian matrices of order 40,000. The first set of calculations, reported as a Communication,[10] used a potential energy surface which, although correct in the energetics and stationary point configurations, does not describe the CC-stretch in vinylidene correctly. We decided to develop a new global potential for this isomerization and did so using high quality *ab initio* calculations.[11] This potential was used in extensive calculations for both C_2H_2 and C_2D_2, including a calculation of the photodetachment spectra. This work has been accepted for publication and is in press.[12]

The coordinates used in the Hamiltonian that change very significantly for the acetylene and vinyidene minima are R, the distance between the centers of mass of the H_2 and C_2 fragments and r_{HH}. Thus, expectation values of these distances were calculated for each molecular eigenstate. For low energy acetylene states <R> is roughly 0.5 bohr and $< r_{HH}>$ is roughly 6.3 bohr. A plot of these expectation values in the high energy region is shown below. As clearly seen, there is a set of states with very different values of these expectation values in the midst of a "sea" of acetylenic states . These other states correspond to vinylidene-like states. Note at the vinylidene minimum R = 2.3 bohr and r_{HH} = 3.5 bohr, and these values correspond well to some of the expectation values in this plot.

The photodetachment spectrum was also calculated (in the usual Franck-Condon approximation and using a new *ab initio* force field for the anion) and is compared with the experimental one[1] below. As seen, there is very good agreement with the experiment in both the position and intensities of the peaks. (The broadening in the experimental spectrum is due to various inhomogeneous effects and is not indicative of a lifetime.)
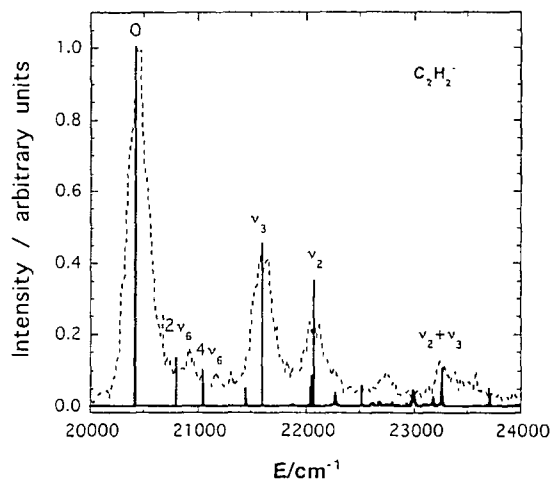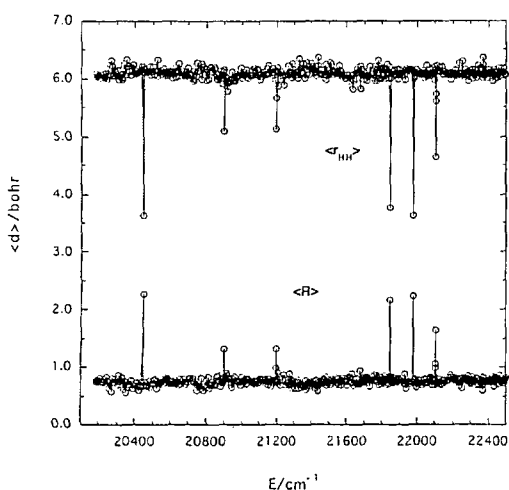
O(^{3}P)+HCl

We have nearly completed quantum reactive scattering studies of this reaction on both the ^{3}A" and ^{3}A' potential energy surfaces. These are very new potentials obtained by Ramuchandran and Peterson.[13] Rate constants on both potentials have been calculated and (finally) good agreement with experiment is found, except at temperatures above 2000 K, where there is disagreement with new experiments of Lee and co-workers.[14] The ^{3}A" surface contains significant van der Waals wells, which influence the rate constant at low temperatures and which appear to be the major source of disagreement with the ICVT/μOMT rate constant obtained using 'POLYRATE'[15] at temperatures below 500 K.

Future Plans

We plan to investigate the unimolecular dissociation dynamics of H_2CO including the cis and trans isomers. This will proceed by first obtaining a global *ab initio* potential energy surface. We hope to investigate the quantum dynamics using the methods and code that we have written for acetylene/vinylidene. We also plan to continue work on the O(^{3}P)+HCl reaction on the two potentials beyond the rate constant to compare directly with the detailed state-to-state experiments of Zare and co-workers.[16]

References

1. K. M. Ervin, J. Ho, and W. C. Lineberger, J. Chem. Phys. **91**, 5974 (1989).
2. (a) M. P. Jacobson, J. P. O'Brian, R. J. Silbey, and R. W. Field, J. Chem. Phys. **109**, 121 (1998); (b) M. P. Jacobson and R.W. Field, J. Phys. Chem A, **104**, 3073 (2000), and references therein.
3. J. Levin, H. Feldman, A. Baer, D. Ben-Hamu, O. Heber, D. Zajfman, and Z. Vager, Phys. Rev. Lett. **81**, 3347 (1998).
4. T. Carrington Jr., L. M. Hubbard, H. F. Schaefer, III, and W. H. Miller, J. Chem. Phys. **80**, 4347 (1984).
5. J. F. Stanton and J. Gauss, J. Chem. Phys. **110**, 6079 (1999) and private communication.
6. T. Germann and W. H. Miller, J. Chem. Phys. J. Chem. Phys. **109**, 94 (1998).
7. (a) R. Schork and H. Köppel, J. Chem. Phys. **115**, 7907 (2001); (b) R. Schork and H. Köppel, Phys. Chem. Chem. Phys. **3**, 891 (2001).

8. R. L. Hayes, E. Fattal, N. Govind, and E. A. Carter, J. Amer. Chem. Soc. **123**, 641 (2001).

9. S. Zou and J. M. Bowman, J. Chem. Phys. **116**, 6667 (2002).

10. S. Zou and J. M. Bowman, J. Chem. Phys. **117**, 5507 (2002).

11. S. Zou and J. M. Bowman, Chem. Phys. Lett. **368**, 421 (2003).

12. S. Zou and J. M. Bowman, and A. Brown, J. Chem. Phys., in press.

13. B. Ramachandran and K. A. Peterson, to be published.

14. C. C. Hsiao, Y. P. Lee, N. S. Wang, J. H. Wang, and M. C. Lin, J. Phys. Chem. **A106**, 10231 (2002).

15. Y.-Y. Chuang, J. C. Corchado, P. Fast, L. Villà, W.-P. Hu, Y.-P. Liu, G. C. Lynch, C. F. Jackels, K. A. Nguyen, M. Z. Gu, M. Z.; I. Rossi, E. L. Coitiño, C. Clayton, V. S. Melissas, B. J. Lynch, R. Steckler, B. C. Garrett, A. D. Isaacson, and D. G. Truhlar, POLYRATE-version 8.4.1, University of Minnesota, MN, 1998.

16. R. Zhang, W. J. van der Sande, M. Bronikowksi, and R. N. Zare, J. Chem. Phys **94**, 2704 (1991).

PUBLICATIONS SUPPORTED BY THE DOE (2001-present)

Thermal and state-selected rate coefficients for the $O(^3P)$ + HCl reaction and new calculations of the barrier height and width, S. Skokov, S. Zou, J. M. Bowman, T. C. Allison, D. G. Truhlar, Y. Lin, B. Ramachandran, B. C. Garrett, and B. J. Lynch, J. Phys. Chem. **105** 2298 (2001).

State-to state reactive scattering via real L^2 wave packet propagation for reduced dimensionality AB + CD reactions, S. Skokov and J. M. Bowman, J. Phys. Chem. A **105**, 2502 (2001).

Ab initio calculation of resonance energies and widths of $HOCl(7v_{OH})$ and $(8v_{OH})$ and comparison with experiment, S. L. Zou, S. Skokov, and J. M. Bowman, Chem. Phys. Lett. **339**, 290 (2001

A reduced dimensionality, six-degree-of-freedom, quantum calculation of the $H+CH_4 \rightarrow H_2+CH_3$, D. Wang and J. M. Bowman, J. Chem. Phys. **115**, 2055 (2001).

The importance of an accurate CH_4 vibrational partition function in full dimensionality calculations of the $H + CH_4 \rightarrow H_2 + CH_3$ reaction, J. M. Bowman, D. Wang, X. Huang, F. Huarte-Larrañaga and U. Manthe, J. Chem. Phys. **114**, 9683 (2001).

The unimolecular dissociation of the OH stretching states of HOCl: Comparison with experimental data, J. Weiss, J. Hauschildt, R. Schinke, O. Haan, S. Skokov, J. M. Bowman, V. A. Mandelshtam, and K. A. Peterson, J. Chem. Phys. **115**, 8880 (2001).

The challenge of high resolution dynamics: Rotationally mediated unimolecular dissociation of HOCl, J. M. Bowman, in <u>Accurate Description of Low-Lying Electronic States</u>, edited by M. Hoffman (ACS, Washington, DC, 2002).

A quasiclassical trajectory study of $O(^1D)$+HCl reactive scattering on an improved *ab initio* surface, K. M. Christoffel and J. M. Bowman, J. Chem. Phys. **116**, 4842 (2002).

Reduced dimensionality quantum calculations of acetylene $\leftrightarrow$ vinylidene isomerization, S.-L.

Zou and J. M. Bowman, J. Chem. Phys. **116**, 6667 (2002).

Resonances in the O(^{3}P)+HCl reaction due to Van der Waals minima, T. Xie, D. Wang, J. M. Bowman, and D. E. Manolopoulos, J. Chem. Phys. **116**, 7461 (2002).

Overview of reduced dimensionality quantum approaches to reactive scattering, J. M. Bowman, Theor. Chem. Acc. **108**, 125 (2002).

Full dimensionalty quantum calculations of acetylene ↔ vinylidene isomerization, S. Zou and J. M. Bowman, J. Chem. Phys. **117**, 5507 (2002).

A new *ab initio* potential energy surface describing acetylene/vinylidene isomerization, S. Zou and J. M. Bowman, Chem. Phys. Lett. **368**, 421 (2003).

Full dimensionalty quantum calculations of acetylene ↔ vinylidene isomerization, S. Zou and J. M. Bowman, and A. Brown, J. Chem. Phys., in press.

Very High Pressure Single Pulse Shock Tube Studies of Aromatic Species

Kenneth Brezinsky
Department of Mechanical Engineering (M/C 251)
University of Illinois at Chicago
842 W. Taylor St.
Chicago, IL 60661
Kenbrez@uic.edu

Program Scope

This program is focused on understanding the oxidation and pyrolysis chemistry of aromatic molecules and radicals with the aim of developing a comprehensive model at conditions that are relevant to practical combustion devices. The experimental approach uses a very high pressure single pulse shock tube, HPST, equipped with GC and GC/MS analyses, to obtain experimental data over the pressure range 5-1000 atm at pre-flame temperatures and a broad spectrum of equivalence ratios. Subsequent simulations of the experimental data using kinetic models are used to improve and develop a comprehensive model.

Toluene Oxidation

Experimental

The majority of the work in this reporting period has focused on the oxidation of toluene which forms the initial point in our program of aromatic oxidation studies and draws on our prior work [1]. Experiments have been performed in the HPST using two reaction mixtures with different equivalence ratios, $\Phi=1$ and $\Phi=5$. The initial toluene concentration range in the reagent mixtures was 8-14 ppm which is very low. However, during these experiments the shock tube and GC sample rig were not heated and it was necessary to use low initial concentrations of toluene to prevent loss of this species by wall condensation. The experiments were performed behind the reflected shock wave at a nominal pressure of 613 atm over the temperature range 1250-1450 K. Samples of the pre-shock and post-shock gases were collected for each experiment and the stable species identities and concentrations were determined by GC and GC/MS. Experimental temperatures were obtained from prior temperature calibrations using chemical thermometers [2].

The temperature dependent profiles for the major species are shown in Figs. 1 and 2 for the $\Phi=1$ and $\Phi=5$ experiments respectively. For the $\Phi=1$ experiments the major products are benzene, CO and CO_2, whereas for the $\Phi=5$ experiments CO_2 was not observed but C_2H_2 was formed as well as benzene and CO. For both sets of experiments the carbon balances are good indicating that no heavy products are condensing in the shock tube or the sample system.

Modeling

We have selected the toluene oxidation mechanism by Klotz et al. [1], KBG model, as the starting point for developing a comprehensive aromatics oxidation model. The KBG model was rigorously tested by the original authors against atmospheric pressure flow reactor data for equivalence ratios around $\Phi=1$ at temperatures up to 1200 K, just below the low end of our experimental data, and it simulates these data very well.

The original KBG model also simulates the lowest temperature data from the HPST quite accurately i.e. where there is only a small extent of reaction. However as the reaction time is increased the KBG model under predicts the consumption of toluene for both the $\Phi=1$ and $\Phi=5$ mixtures, Figs. 3 and 4. It follows that if the model does not predict the experimentally observed toluene concentration accurately then the predictions for the other species will also not match the experimental data. However, it is encouraging that a model developed at 1 atm is able to predict the onset of reaction accurately at 613atm.

Sensitivity and reaction path analyses have been used to identify the key reactions affecting the toluene concentration and the more significant of these are shown in Table 1 along with some additional reactions that were absent in the KBG model but are likely to be important at high pressures and for very rich, $\Phi=5$, experiments. The final model is capable of simulating the new high pressure shock tube data for both $\Phi=1$ and $\Phi=5$ rather well, Figs. 3 and 4, and the modified model still simulates the toluene profile from the original flow tube data well.

From the modifications that have been made to the original KBG model the most striking improvements occurred from adjusting the rates for the reactions of benzyl and phenyl radicals with O_2 as well as the initial rate for toluene + O_2 which is important in the $\Phi=1$ experiments. This tends to highlight the need for further studies on these systems particularly at elevated pressures where no experimental data currently exist.

Future Work

We have recently built a heated sample rig to allow us to work with higher initial toluene concentrations and if necessary we will also heat the driven section of the shock tube. These modifications will allow us to obtain much more accurate measurements of concentrations for products such as benzene and a number of minor species such as butadiene which have been observed in the current experiments at the 1 ppm or less level. Using this additional information we will be able to tackle the simulation of minor as well as major stable species which in turn will help highlight further reactions which require more study.

The experimental range is being extended to cover a number of nominal reaction pressures from 5 atm to 1000 atm to provide a comprehensive data set that overlaps the existing lower pressure experimental data and extends beyond the pressures obtained in real combustion devices. This work should be complete in the next six months.

We also plan to initiate the study of the oxidation of the phenyl radical at very high pressures and focus on obtaining a branching ratio for the reaction with oxygen by monitoring the formation of stable species unique to each channel.

Publications based on the DOE supported work:

Tranter R.S., Fulle D. and Brezinsky K., "Design of a High Pressure Single Pulse Shock Tube for Chemical Kinetic Investigations", Rev. Sci. Inst., 72, 3046 (2001).

Tranter R.S., Sivaramakrishnan R., Srinivasan N. and Brezinsky K., "Calibration of Reaction Temperatures in a Very High Pressure Shock Tube Using Chemical Thermometers", Int. J. Chem. Kinet., 33, 722 (2001).

Tranter R.S., Sivaramakrishnan R., Brezinsky K. and Allendorf M.D., High Pressure, High Temperature Shock Tube Studies of Ethane Pyrolysis and Oxidation", Phys. Chem., Chem. Phys. 4, 2001-2010, 2002.

Tranter R.S., Ramamoorthy H., Raman A., Brezinsky K., Allendorf M.D., "High Pressure Single Pulse Shock Tube Investigation of Rich and Stoichiometric Ethane Oxidation", In Press, 29th International Symposium on Combustion, 2002.

Presentations:

Tranter R.S., Ramamoorthy H., Raman A., Sivaramakrishnan, R. and Brezinsky K., "Shock Tube Investigations of Hydrocarbon Oxidation and Pyrolysis Over Very Wide Pressure

Ranges", Proceedings of the 2002 Technical Meeting of the Central States Section of the Combustion Institute.

Tranter R.S., Sivaramakrishnan R. and Brezinsky K., "High Pressure Shock Tube Studies of Aromatics", AIChE Annual Meeting, November, 2002, Indianapolis, Indiana.

Brezinsky K., Tranter R.S., Sivaramakrishnan R., Durgam S. and Vasudevan H., "High Temperature, High Pressure Oxidation of Toluene", Third Joint Meeting of the U.S. Sections of The Combustion Institute, March, 2003.

References

1. Klotz S.D.,. Brezinsky K., and Glassman I., Proc. Combust. Inst., **27**(1): 337, (1998)
2. Tranter R.S., Sivaramakrishnan R.,Srinivasan N. and Brezinsky K.,. Int. J. Chem. Kinet.,. **33**(11): 722, (2001)
3. Hippler H., Heckmann E., Troe J., Proc. Combust. Inst., **26**: 543, (1996)
4. Just Th., Frank P., Herzler J., Wahl C., Proc. Combust. Inst., **25**: 833, (1994)
5. Glarborg P., Alzueta M.U., Oliva M., Int. J. Chem. Kinet., **30**(9): 683, (1998)
6. Just Th., Frank P., Herzler J., Wahl C., Proc. Combust. Inst., **25**: 833, (1994)
7. Colket M.B., Seery D.J., Proc. Combust. Inst., **25**: 883, (1994)
8. Baulch D.L., Cobos, .J., Cox R.A., Frank P., Hayman G., Just Th., Kerr J.A., Murrells T., Pilling M.J., Troe J., Walker R.W., Warnatz J., J. Phys. Chem. Ref. Data **23**: 847, (1994)
9. Scherer S., Just Th., Frank P., Proc. Combust. Inst., **28**: 1511, (2000)
10. Colussi A.J., Duran R.P., Amorebieta V.T., J. Phys. Chem., **92**: 636, (1988)
11. Miller J.A., Melius C.F., Combustion and Flame, **91**: 29, (1992)

Rxn #	Reaction	A^a $cm^3\ mol^{-1}\ s^{-1}$	b^a	E^a $cal\ mol^{-1}\ K^{-1}$
498[b]	$C_6H_5CH_2+HO_2=C_6H_5+CH_2O+OH$	**1.17E+14**	**0**	**0**
497[b]	$C_6H_5CH_2+HO_2=C_6H_5CHO+H+OH$	**3.67E+14**	**0**	**0**
492[3]	$C_6H_5+C_6H_5CH_3=C_6H_6+C_6H_5CH_2$	7.94E+13	0	11935
458[4]	$C_6H_5+O_2=C_6H_5O+O$	2.60E+13	0	6120
486[4]	$C_6H_5CH_3+O_2=C_6H_5CH_2+HO_2$	1.81E+12	0	39717
531[6]	$C_6H_5+O_2=p-C_6H_4O_2+H$	3.00E+13	0	8982
532[7]	$C_6H_5CH_2=C_4H_4+C_3H_3$	2.00E+14	0	83600
533[7, adj]	$C_6H_5CH_2=C_2H_2+C_5H_5$	2.00E+14	0	70000
534[8]	$C_6H_6=C_4H_4+C_2H_2$	9.00E+15	0	107430
535[9]	$C_3H_3+C_3H_3=C_6H_6$	7.50E+12	0	0
536[10]	$C_4H_3+C_2H_3=C_6H_6$	2.87E+14	0	817
537[11]	$C_4H_3+C_2H_2=C_6H_5$	2.80E+03	2.9	1400
538[7, adj]	$C_5H_5=C_2H_2+C_3H_3$	3.00E+15	0	71000

[a] $k=AT^b exp^{-(E/RT)}$; [b] estimated, this work. Numerals see references for sources

Table 1: Modifications made to the original KBG toluene oxidation model. Bold font indicates a reaction from the original model. Normal font indicates a reaction that was added to the original KBG model.

Toluene Oxidation Experimental and Modeling results for 613 atm Reaction Pressure.
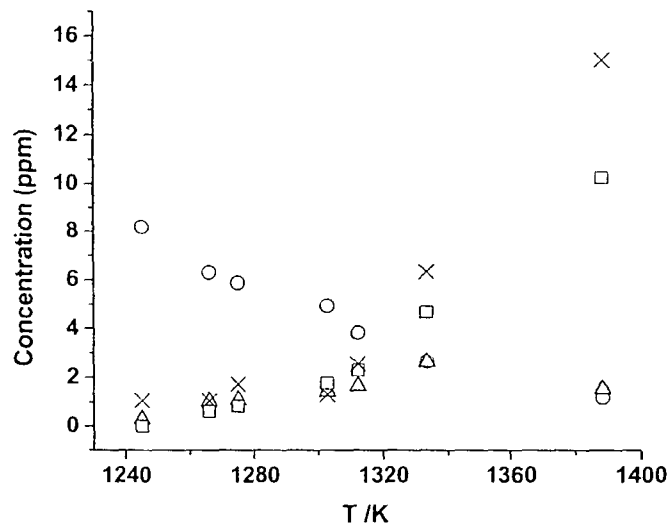
Figure 1: Toluene Oxidation, Φ=1, 8 ppm mix. Open circles-C6H5CH3, Open triangles- C6H6, Open squares- CO, Crosses-CO2.
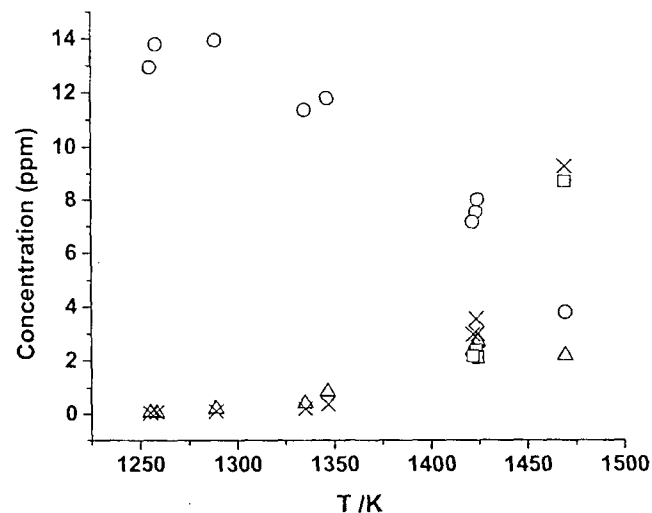
Figure 2: Toluene Oxidation, Φ=5. Open circles- C6H5CH3, Open triangles- C6H6, Open squares- CO, Crosses-C2H2
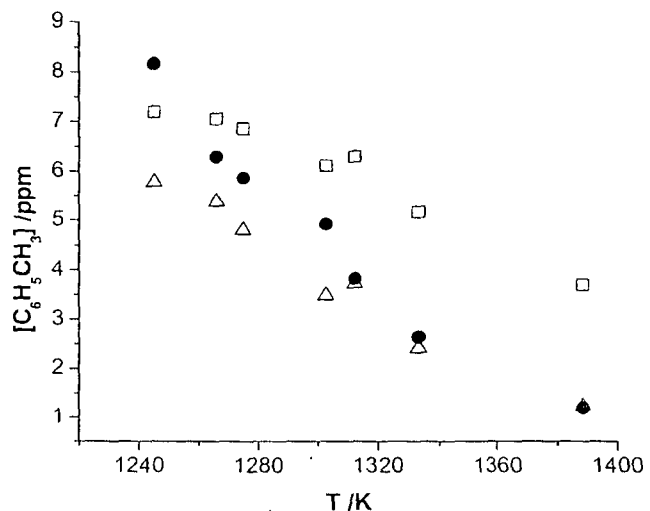
Figure 3: Toluene oxidation, Φ=1, 8 ppm. Closed circles- Experiment. Open squares- KBG model, Open triangles- Modified KBG model.
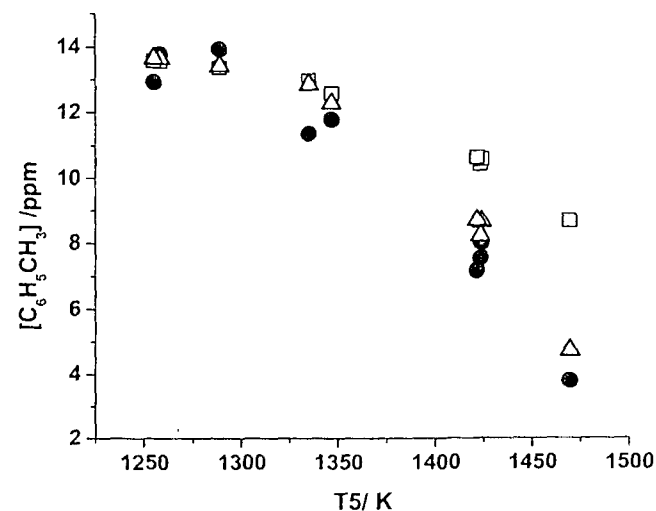
Figure 4: Toluene oxidation, Φ=1, 8 ppm. Closed circles- Experiment. Open squares- KBG model, Open triangles- Modified KBG model.

COMBUSTION CHEMISTRY

Principal Investigator: Nancy J. Brown

Environmental Energy Technologies Division
Lawrence Berkeley National Laboratory
Berkeley, California, 94720
510-486-4241
NJBrown@lbl.gov

PROJECT SCOPE

Combustion processes are governed by chemical kinetics, energy transfer, transport, fluid mechanics, and their complex interactions. Understanding the fundamental chemical processes offers the possibility of optimizing combustion processes. The objective of our research is to address fundamental issues of chemical reactivity and molecular transport in combustion systems. Our long-term research objective is to contribute to the development of reliable combustion models that can be used to understand and characterize the formation and destruction of combustion-generated pollutants. We emphasize studying chemistry at both the microscopic and macroscopic levels. To contribute to the achievement of this goal, our current activities are concerned with three tasks: Task 1) developing models for representing combustion chemistry at varying levels of complexity to use with models for laminar and turbulent flow fields to describe combustion processes; Task 2) developing tools to probe chemistry fluid interactions; and Task 3) modeling and analyzing combustion in multi-dimensional flow fields. A theme of our research is to bring new advances in computing and, in particular, parallel computing to the study of important and computationally intensive combustion problems.

Recent Progress

Task 1: Developing models for representing combustion chemistry at varying levels of complexity to use with models for laminar and turbulent flow fields to describe combustion processes (with Shaheen R. Tonse, Michael Frenklach, and Nigel W. Moriarty): Most practical combustion systems are turbulent, and the dominant computational cost in modeling turbulent combustion phenomena numerically with high fidelity chemical mechanisms is the time required to solve the ordinary differential equations associated with the chemical kinetics. To develop models that describe pollutant formation in practical fuels, the computational burden attributable to chemistry must be reduced. We have pursued an approach that can contribute to this problem, PRISM (Piecewise Reusable Implementation of Solution Mapping). PRISM has been developed as an economical strategy for implementing complex kinetics into high fidelity fluids codes. This approach to mechanism reduction draws upon factorial design, statistics and numerics, caching strategies, data structures, and long term reuse of chemical kinetic calculations. A solution-mapping procedure is applied to parameterize the solution of the initial-value ordinary differential equation system as a set of algebraic polynomial equations. The solution-mapping is done piecewise after dividing the space into N_s+1 dimensional hypercubes with a distinct polynomial parameterization for each. Subsequent calculations in an existing hypercube result in an inexpensive polynomial evaluation rather than an ODE time-integration. The more reuse a hypercube has, the greater the economical gain in CPU time. We have chosen the polynomial order to be quadratic with cross-terms, to give sufficient accuracy. The number of polynomial coefficients scale as $(N_s+2)^2$. The coefficient values are determined by integrating the ODE at various points in the hypercube and then performing a regression calculation, hence the number of ODE calls has to be greater than the number of coefficients. For hydrogen flames, $N_s+2 = 11$, and 151 ODE calls are necessary to determine the coefficients. Consequently, an *a priori* calculation of

the number of expected reuses would help to identify hypercubes with insufficient reuse because we could call the ODE solver rather than construct polynomials for these hypercubes. We determined two strategies for identifying hypercubes that have high reuse before incurring the computational expense of constructing polynomials. One method, named Tvel, utilizes the rate of movement of the chemical trajectory in the hypercube to estimate the number of steps that the trajectory would make though it. The other method, termed DPC, defers polynomial construction until a preset threshold of reuse has been met. Although the latter is an empirical method, it produces a substantial gain and is easy to apply. Both methods have been tested on a 0-D chemical mixture and reactive flows of 1 and 2-D simulations of selected laminar and turbulent H_2 + air flames. The computational performance of PRISM is improved by a factor of two for each method. A paper (Tonse, et al, 2002) describing the methods and their implementation has been submitted for publication.

It is important to clarify the efficiencies we have achieved with PRISM, those associated with polynomial construction and those associated with polynomial evaluation. First we consider the initial simulation using PRISM when the polynomials are being constructed. Polynomial construction is expensive for the reasons given above. The two methods that we have developed to improve PRISM's efficiency reduce the cost of constructing the polynomials. The methods accomplish this by constructing polynomials only for hypercubes that will have a high degree of re-use during the course of the simulation. The two methods each improve PRISM's efficiency by approximately a factor of two. They cannot be used simultaneously to achieve a factor of four because they each identify approximately the same subset of hypercubes where the average usage is quite large. In another part of this abstract, we indicate that replacing orthogonal designs with Gosset designs enables another factor of two and, if applied, would result in a total efficiency gain of a factor of 4 for polynomial construction. A second type of efficiency associated with PRISM can be understood by considering a second or later simulation that occurs after the initial one, that is, a simulation, slightly different from the first. For this simulation, most of the polynomials associated with hypercubes that will be occupied and highly reused have already been constructed during the first simulation. We consider these later simulations to have negligible hypercube construction expenses. In contrast, their only expense is hypercube retrieval and polynomial evaluation. In prior papers, we stated that polynomial retrieval and evaluation was a factor of 10 faster than solving the rate equations; however with recent improvements in programming, we have achieved a factor of 15 improvement in efficiency.

Extension to CH4 flames (with Shaheen Tonse): We have made progress on extending PRISM to CH4/air combustion. We have found that factorial designs produced by the GOSSET program (2003) provide better accuracy than an orthogonal fractional design, and requires approximately half the ODE calls, improving the efficiency of polynomial construction by a factor of two. The high dimensionality remains a problem and to address this we developed a dimensional reduction method. The dynamic dimensional reduction is based on identifying and isolating chemical species that have both fast time-scales and low concentration. The inspiration comes from the steady-state approximation and Intrinsic Low Dimensional Manifold (ILDM) concepts in which concentrations of fast species tend to depend on the concentrations of slow species. This reduces the number of independent variables and makes hypercube construction less costly. The degree of the reduction is dynamic, and it varies from hypercube to hypercube because the properties of chemical composition space vary. For a 32-species GRI-Mech 1.2 reaction set, preliminary results show the number of reduced dimensions for timesteps of 10^{-7}s, 10^{-6}s and 10^{-5}s are approximately 28, 15 and 11, respectively. We are currently studying the accuracy retained from these reductions in flame simulations using the Adaptive Mesh Refinement code of Day and Bell (2000).

Task 2: Developing tools to facilitate building and validating chemical mechanisms (with Kenneth Revzan): We are interested in determining transport parameters that support combustion modeling of simple fuels. Codes have been developed for determining the sensitivity of numerous observables to transport properties and the molecular properties that underlie them. Sensitivity analysis has been used to determine the importance of transport properties in flame modeling and for building chemical mechanisms. This has been accomplished for a number of fuels and mixture ratios. This has revealed that property or observable sensitivities to transport properties are of the same order as the sensitivity to rate parameters. Flame speed is especially sensitive to diffusion coefficients of $H-N_2$, H_2-N_2, and fuel-N_2 for fuel/air flames. For concentration profiles, the transport properties of the species associated with the profile are very important. At the molecular scale, the potential length scaling parameters are especially important and more so than energy scaling parameters. Second-order sensitivities are usually small. Codes have been developed for the Mason and Uribe (1996) and Paul and Warnatz (1998) approaches to transport property evaluation. We verified the code accuracy, and also corrected the Sandia code, Tranlib for an error in the calculation of species thermal conductivities that was identified by Grcar(1998). We have analyzed four approaches for calculating transport properties: the Sandia Tranlib approach with its potential parameters, Tranlib with the new potential parameters listed in the paper of Paul and Warnatz replacing those in the original set, the approach due to Paul and Warnatz, and the approach due to Mason and Uribe. For pure substances, for which there is experimental data, (specifically for rare gases, CO, CO_2, CH_4, N_2, NO, N_2O, O_2, C_2H_4, and C_2H_6) agreement within 15% was found for the various methods; however, the method attributable to Mason and Uribe agrees best with experimental values. The dipole correction due to Paul and Warnatz has a negligible effect on the collision diameter, and for molecules with large dipole moments like OH, H_2O, HO_2, H_2O_2, a substantial effect on the well depth that declines with temperature. We are currently investigating the suitability of the dipole correction and transport parameters for H, H_2 (Midha et al, 2002) and other species important for methane combustion.

Task 3: Modeling combustion in multi-dimensional flow fields (with Shaheen Tonse): We have completed our efforts concerned with finding the dimensionality **d** of chemical composition space. This is important because it allows us to assess PRISM performance and also allows us to begin to characterize the influence of turbulence on the chemistry. We have employed three methods to determine the dimensionality for a 2 D flame that interacts with a velocity field, and we determine how the dimensionality changes with turbulence intensity. The results of the study are described in a paper submitted for publication (Tonse and Brown, 2003).

References

Adifor: http://www.cs.rice.edu/~adifor/AdiforDocs.html

Bzowski, J., Kestin, J., Mason, E.A., and Uribe, F.J., Equilibrium and Transport Properties of Gas Mixtures at Low Density: Eleven Polyatomic Gases and Five Noble Gases. J. Phys. Chem. Ref Data, **19**, 5, 1990.

Day, M.S. and Bell, J.B., Numerical Simulation of Laminar Reacting Flows with Complex Chemistry. Combust. Theory and Modelling, 4(4), pp. 535-556 (2000). Also LBNL Report 44682.

Grcar, J.F., private communication (1998).

Mason, E.A. and Uribe, F.J., The Corresponding-States Principle: Dilute Gases. Millat J, Dymond J.H., and Nieto de Castro CA, eds. **Transport Properties of Fluids.** Cambridge University Press, Cambridge, 1996.

Middha, P., Yang, B., and Wang, H., "A First-Principle Calculation of the Binary Diffusion Coefficients Pertinent to Kinetic Modeling of Hydrogen-Oxygen-Helium Flames." Proceedings of the Combustion Institute 29, (2002).

Paul, P. and Warnatz, J.A., Re-evaluation of the Means Used to Calculate Transport Properties of Reacting Flows. Twenty-seventh Symposium (International) on Combustion. The Combustion Institute, 1998, 495-504.

Sloane, N.J. GOSSET: A General Purpose Program for Designing Experiments.
http://www.research.att.com/~njas/gosset/

Publications

Bell, J.B., Brown, N.J., Day, M.S., Frenklach, M., Grcar, J.F., Propp, R.M., and Tonse, S.R., "Scaling and Efficiency of PRISM in Adaptive Simulations of Turbulent Premixed Flames," (2000) Proceedings of the Combustion Institute 28, 107-113. Also Lawrence Berkeley National Laboratory Report No. LBNL-44732

Bell, J.B., Brown, N.J., Day, M.S., Frenklach, M., Grcar, J.F., and Tonse, S.R., "Effect of Stoichiometry on Vortex-Flame Interactions," (2000) Proceedings of the Combustion Institute 28, 1933-1939. Also Lawrence Berkeley National Laboratory Report No. LBNL-44730

Tonse, Shaheen R. and Brown, N.J., "Emulation of Chemical ODE System by Response Surfaces in CH_4 Combustion," Division of Fluid Dynamics, American Physical Society, Washington DC, November 2000.

Tonse, Shaheen R., Bell, J.B., Brown, N.J., and Day, M.S.,"The Dimensionality of a Chemical Manifold through a Progressing Reaction, 2nd Joint Symposium of the Combustion Institute at Oakland, CA, March 2001.

Tonse, Shaheen R. and Brown, N.J., "Improving the Efficiency of PRISM through Deferred Polynomial Construction." Fall Meeting of Western States Section of The Combustion Institute, Salt Lake City, UT. Oct 2001.

Tonse, S.R., Moriarty, N.W., Frenklach, M., and Brown, N.J., "Computational Economy Improvements in PRISM." Submitted to Intl. J. Chem. Kin. (2002). Also Lawrence Berkeley National Laboratory Report No. LBNL-48858.

Tonse, S.R. and Brown, N.J., "Dimensionality Estimate of the Manifold in Chemical Composition Space for a Turbulent Premixed H2+air flame," Submitted to Intl. J. Chem. Kin. (2003). Also Lawrence Berkeley National Laboratory Report No. LBNL-52058.

Tonse, S.R. and Brown, N.J., "Computational Economy Improvements in PRISM." Proceedings The 3rd Joint Symposium of the U.S. Sections of the Combustion Inst. (2003), Paper-B36 (2003). Also Lawrence Berkeley National Laboratory Report No. LBNL-48858.

Molecular Beam Studies of Radical Combustion Intermediates

Laurie J. Butler
The University of Chicago, The James Franck Institute
5640 South Ellis Avenue, Chicago, IL 60637
L-Butler@uchicago.edu

I. Program Scope

Polyatomic radical intermediates play a key role in a wide range of combustion processes. The DOE-supported experiments[1-5] in my lab pursue three avenues of research on the reaction dynamics of radicals. The first two extend our previous work by 1) investigating competing product channels in photodissociation processes used to generate radical intermediates important in combustion and 2) generalizing a method for determining absolute branching ratios for competing radical and molecular product channels in ground state bimolecular reactions in mass spectrometric experiments. The third avenue of research is new, the methodology growing from work we initiated two years ago on the competing dissociation channels of high-energy hydrocarbon radical isomers. The work seeks to probe dynamics on key portions of the potential energy surface for O + hydrocarbon radical reactions by generating a highly internally excited radical intermediate, such as CH_3O, and investigating the branching between the ensuing product channels of the energized radical under collisionless conditions. Our technique disperses the radical intermediates by velocity and thus by internal energy, and then measures the velocity of the reaction products, allowing us to identify the product branching as a function of internal energy in the radical intermediate for energies that span the lowest energy product channels. Our experimental studies use a combination of techniques including analysis of product velocity and angular distributions in a crossed laser-molecular beam apparatus, emission spectroscopy of dissociating molecules, and high-n Rydberg H atom time-of-flight spectroscopy (HRTOF). Much of the work also serves to test and develop our fundamental understanding of chemical reaction dynamics. We focus on testing the range of applicability of two fundamental assumptions used in calculating reaction cross sections and the branching between energetically-allowed product channels: the assumption of complete intramolecular vibrational energy redistribution often used in transition state theories and the assumption of electronic adiabaticity invoked in many quantum scattering calculations and assumed in most statistical transition state estimates of reaction rates. The influence of angular momentum on product branching is also of increasing interest.

II. Recent Progress

Our work in the last year included: 1) completing[5] our crossed-laser molecular beam experiments on the photodissociation of ethyl ethynyl ether, a new photolytic precursor of the HCCO radical; 2) initiating experiments on d-2 allyl iodide to investigate the marked stability of the CH_2CDCH_2 radical as compared to the CH_2CHCH_2 radical due to centrifugal effects in the dissociation to H (or D) + allene and the isomerization to 2-propenyl radical; 3) pursuing experiments to probe the unimolecular dissociation channels of the CH_2CHCO radical and the CH_3CH_2CO radical produced from the photodissociation of acryloyl chloride and propionyl chloride respectively; and 4) assessing the viability of using the CH_3OCl precursor to investigate the unimolecular dissociation of CH_3O to the two competing product channels H + H_2CO and H_2 + HCO as a function of internal energy in the radical.

A. Photodissociation dynamics of ethyl ethynyl ether: A new ketenyl radical precursor

We completed and submitted for publication[5] our molecular beam photofragmentation experiments to investigate the generation of the HCCO radical from the 193 nm

photodissociation of ethyl ethynyl ether. (The work was motivated by R. Bersohn. The paper includes his LIF studies of the HCCO product as well as data we took in collaboration with J. Shu.) The reaction of HCCO with NO has been shown to be the major NO removal pathway in the reburning of hydrocarbon fuels at low temperature, yet there was no clean photolytic source of the HCCO radical for kinetic studies trying to measure the product branching.

The experiments investigated the dynamics of the photodissociation of ethyl ethynyl ether at 193.3 nm with photofragment translational spectroscopy and laser-induced fluorescence. The data from two crossed laser-molecular beam apparatuses, one with VUV photoionization detection and one with electron bombardment detection, showed only cleavage of the C-O bond to form a C_2HO radical and a C_2H_5 (ethyl) radical occurs. We observed neither cleavage of the other C-O bond nor molecular elimination to form C_2H_4 + CH_2CO (ketene). The C_2HO radical is formed in two distinct product channels, with 37% of the radicals formed from a channel with recoil kinetic energies extending from 6 to 71 kcal/mole and the other 63% formed from a channel with lower average recoil energies ranging from 0 to 40 kcal/mole. The measurements using photoionization detection reveal that the C_2HO radical formed in the higher recoil kinetic energy channel has a larger ionization cross section for photon energies between 10.3 and 11.3 eV than the radical formed in the lower recoil kinetic energy channel, and that the transition to the ion is more vertical. The radicals formed in the higher recoil kinetic energy channel could be either $\tilde{X}(^2A'')$ or $\tilde{A}(^2A')$ state ketenyl (HCCO) product and the shape of the recoil kinetic energy distribution fitting this data does not vary with ionization energy between 10.3 eV and 11.3 eV. The C_2HO formed in the channel with the lower kinetic energy release is tentatively assigned to the spin forbidden $\tilde{a}(^4A'')$ state of the ketenyl radical, reached through intersystem crossing. Bersohn's signal from laser-induced fluorescence of the HCCO photofragment was detected at the electronic origin and the 5^0_1 band. The fluorescence signal peaks after a 20 µs delay, indicating that HCCO is formed with a significant amount of internal energy and then subsequently relaxes to the lowest vibrational level of the ground electronic state. The data show that the photodissociation of ethyl ethynyl ether produces C_2HO with unit quantum yield, establishing it as the first clean photolytic precursor of the ketenyl radical. See D. Osborn's abstract for its utilization in kinetics expts.

B. Centrifugal Effects in the Unimolecular Dissociation of the Allyl Radical: Comparing the CH_2CDCH_2 radical with the CH_2CHCH_2 radical

Radical intermediates typically have many energetically accessible isomeric forms; unraveling the competing isomerization and dissociation reactions of these radicals is important in many combustion mechanisms. Our molecular beam scattering method allows us to resolve the branching between the competing C-H and C-C bond fission channels isomerically selected hydrocarbon radicals as a function of internal energy in the selected radical at energies that span the lowest dissociation and isomerization barriers. The data on product branching is sensitive to the relative barrier heights of the competing dissociation channels to within less than a couple kcal/mol. Our prior work reported in Pub. 4 used photofragment translational spectroscopy and H atom Rydberg time-of-flight (HRTOF) spectroscopy to study the photolytic generation at 193 nm of the allyl radical from allyl iodide and the ensuing dissociation of the nascent allyl radicals as a function of their internal energy. Our data showed that a substantial fraction of the allyl radicals from the I $(^2P_{1/2})$ channel formed with internal energies as high as 15 kcal/mol above the 60 kcal/mol barrier were stable to H atom loss. We attributed the stability to centrifugal effects caused by significant rotational energy imparted to the allyl radical during the precursor

photolysis and the small impact parameter and reduced mass characterizing the loss of an H atom from an allyl radical to form allene + H. A photoionization efficiency (PIE) curve identified the major C_3H_4 secondary dissociation products as allene. Comparison of the mass 40 signal in the TOF spectra at two photoionization energies showed that branching to H + propyne doesn't occur at near threshold internal energies, indicating the experimentally determined allyl $\rightarrow$ 2-propenyl radical isomerization barrier, which is lower than recent ab initio calculations of the barrier by ~15 kcal/mol, is far too low.

In the new experiments this year we sought to probe the relative stability of the CH_2CDCH_2 radical as compared to the CH_2CHCH_2 radical. This required synthesizing d-2 allyl iodide using a modified version of the synthesis used by P. Chen. Our data at the ALS dispersed the CH_2CDCH_2 radicals from the I ($^2P_{1/2}$) + CH_2CDCH_2 channel to determine which of the radicals were formed stable to direct dissociation to allene + D (and to isomerization to 2-propenyl and subsequent dissociation.) As in our prior work on CH_2CHCH_2 radicals, a large fraction of the radical with higher internal energy than the barrier to C-D bond fission were stable to C-D bond fission due to centrifugal effects. The data we took evidences the differences in the survival probability of highly rotationally excited CH_2CDCH_2 radicals as compared to CH_2CHCH_2 radicals. The competing effects evidence the profound effect that conservation of total angular momentum ($|\mathbf{L}_{allyl}| = |\mathbf{L}_{allene}| + \mu v_{rel}b$) can have on the dissociation of allyl radicals. The centrifugal barrier and the resulting stability of highly internally excited d-2 allyl versus undeuterated allyl radicals depends on 1) the reduced mass μ for C-D fission in CH_2CDCH_2 is almost 2 times higher than for C-H fission in CH_2CHCH_2 radicals; 2) the amplitude of the C-D bending and wagging motion is more restricted in the zero point level at the transition state than the amplitude of C-H bending and wagging, so the range of impact parameters accessed by the deuterated radical is smaller; and 3) the zero-point correction to the barrier results in the barrier to C-D fission in CH_2CDCH_2 being slightly higher than the barrier to C-H fission in CH_2CHCH_2. The latter two effects suggest the d-2 allyl radicals with high internal energies will show even a larger probability of surviving secondary dissociation; this is what our data evidences.

C. <u>Unimolecular dissociation channels of the CH_2CHCO radical and the CH_3CH_2CO radical</u>

Armed with this novel method to investigate the competing dissociation channels of radicals dispersed as a function of their internal energy, we have pursued studies of the unimolecular dissociation of the CH_2CHCO radical and the CH_3CH_2CO radical this year. Fei Qi had already taken extensive data on acryloyl chloride photodissociation at 193 nm on Endstation 1 at the ALS and asked us to analyze the data for him. Our analysis shows that acryloyl chloride photodissociation at 193 nm evidences competing C-Cl fission and HCl elimination channels. The former produces CH_2CHCO radicals dispersed by the velocity imparted to them in the C-Cl bond fission, so thus dispersed by internal energy. The data clearly show that all the CH_2CHCO radicals produced undergo secondary dissociation via C-C bond fission to vinyl radical + CO (C-H fission in the radical to form propadienal + H does not compete significantly with C-C fission in the radical). Propanedienal is only produced in the HCl elimination from $CH_2CHCOCl$ itself. We plan to continue with experiments at 248 nm to determine the barrier energy to C-C fission in this radical when Endstation 1 at the ALS is again available.

Our experiments this year on the unimolecular dissociation of the CH_3CH_2CO radical produced from photodissociation of propionyl chloride show that the dominant unimolecular decomposition channel of the radical is C-C fission to form ethyl + CO; the C-H fission channel to form methyl ketene ($CH_3HC=C=O$) + H does not compete with C-C fission in the radical. We are currently analyzing data from both the 193 nm and the 248 nm photodissociation of the precursor; the latter may determine the C-C fission barrier energy in the radical.

D. Assessing the viability of using the CH$_2$OCl precursor to investigate the unimolecular dissociation of rotationally excited CH$_3$O radicals

We did considerable work this year on experiments designed to investigate the product branching from a radical intermediate of the O(^{3}P) + CH$_3$ bimolecular reaction. We desired to measure the unimolecular dissociation of CH$_3$O to the two competing product channels H + H$_2$CO and H$_2$ + HCO (the HCO unimolecularly dissociates to H + CO in the bimolecular reaction) as a function of internal energy in the radical. Since significant branching to the H$_2$ + HCO is only predicted for high J in the bimolecular reaction, our experimental approach was to generate rotationally hot unstable CH$_3$O radicals in a scattering apparatus dispersed by internal energy. Such collision-free data on the dissociation of rotationally hot CH$_3$O radicals as a function of internal energy in the radical would provide a critical test of the most important regions of the *ab initio* potential energy surface (Harding et al.) used to obtain predictive ability for the O + CH$_3$ bimolecular reaction. Working with Prof. F. Blase at Haverford we developed a synthesis for CH$_3$OCl and reproduced the synthesis in our lab. We used this precursor to investigate the production of rotationally excited CH$_3$O radicals both in our lab at Chicago and out at the ALS where the subsequent experiments on the unimolecular dissociation of CH$_3$O radicals would need to be done. However, the 248 nm photodissociation of this precursor produces radicals with a distribution of internal energies that leaves them stable to secondary dissociation and the 193 nm data is plagued by the photodissociation of a contaminant in the molecular beam source, so we have not been successful in this study. L. Harding has also done further calculations which suggest that the branching to the interesting H$_2$ + HCO channel only occurs at much higher internal energies of the radical intermediate.

III. Future Plans

We are engaged in writing up the work on the deuterated allyl radical dissociation dynamics and analyzing data on the acryloyl chloride and propionyl chloride systems. We plan to apply our new method to determine the branching between unimolecular dissociation channels of isomerically-selected radicals to a number of oxygen containing radicals.

IV. Publications Acknowledging DE-FG02-92ER14305 (2001 or later)

1. Photodissociating Methyl Vinyl Ether to Calibrate O + Ethylene Product Branching and to Test Propensity Rules for Product Channel Electronic Accessibility, M. L. Morton, D. E. Szpunar, and L. J. Butler, J. Chem. Phys. 115, 204-16 (2001).

2. C-Cl Bond Fission, HCl Elimination, and Secondary Radical Decomposition in the 193 nm Photodissociation of Allyl Chloride, M. L. Morton, L. J. Butler, T. A. Stephenson, and F. Qi,, J. Chem. Phys. 116, 2763-75 (2002).

3. Theoretical Investigation of the Transition States Leading to HCl Elimination in 2-Chloropropene, B. F. Parsons, L. J. Butler, and B. Ruscic, Molecular Physics 100, 865-74 (2002).

4. Primary and Secondary Dissociation of Allyl Iodide Excited at 193 nm: Centrifugal Effects in the Unimolecular Dissociation of the Allyl Radical, D. E. Szpunar, M. L. Morton, L. J. Butler, and P. M. Regan, J. Phys. Chem. B 106, 8086-8095 (2002).

5. Photodissociation Dynamics of Ethyl Ethynyl Ether: A new ketenyl radical precursor, M. J. Krisch, J. L. Miller, L. J. Butler, H. Su, R. Bersohn, and J. Shu, J. Chem. Phys., in press (2003).

Independent Generation and Study of Key Radicals in Hydrocarbon Combustion (DE-FG02-98ER14857)

PI: Barry K. Carpenter
Department of Chemistry and Chemical Biology
Cornell University
Ithaca, NY 14853-1301
E-mail: bkc1@cornell.edu

New Pathways in the Reactions of Vinyl Radicals with O_2

The reaction of the parent vinyl radical, C_2H_3, with O_2 is an important part of the combustion of alkanes, and for that reason has been the subject of extensive experimental and computational investigation. In collaboration with Stephen Klippenstein, Jim Miller, and Phil Westmoreland, we have re-examined the vinyl + O_2 reaction using the best available multireference *ab initio* electronic structure theory. Three issues have driven this study:

1. Until recently, the C_2H_3 + O_2 reaction was thought to follow two principal paths.
   The low-temperature channel, **A**, is:
   $$C_2H_3 + O_2 \rightarrow CH_2O + CHO \qquad \textbf{A}$$
   The high-temperature channel, **B**, is:
   $$C_2H_3 + O_2 \rightarrow CH_2CHO + O \qquad \textbf{B}$$
   Since reaction **B** is chain-branching whereas **A** is not, the overall modeling of alkane combustion is sensitive to the temperature at which channel **B** becomes dominant.

2. Recent experimental evidence suggests that there may be a third significant channel:
   $$C_2H_3 + O_2 \rightarrow CH_3 + CO_2(v_3\ v=4) \qquad \textbf{C}$$
   but no computational study to date has given a plausible explanation for this reaction.
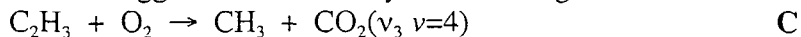
3. Substituted vinyl radicals are believed to play important roles in some mechanisms of soot formation. Their interception by O_2 can lead to reactions similar to those for C_2H_3 + O_2, as well as additional reactions involving the substituent. Correct assessment of the temperature-dependent ratio of these reactions is important in determining the competition between the oxidative degradation of the intermediates and their progress on to PAHs and soot.

1. High-Level Calculations on Reactions A and B

Previously we had carried out CASPT2(23,15)//CASSCF(23,15)/cc-pVTZ calculations on reaction **A**. These calculations have now been extended by using the so-called g3 correction to the Fock operator in the CASPT2 calculations, and by using Klippenstein's formula for extrapolating cc-pVDZ and cc-pVTZ data to an estimate of the result for a complete basis set. In addition, the calculations have been carried out on reaction **B**. The CASPT2 calculations show a larger $\Delta H_0^{\ddagger}$ difference, in favor of channel **A**, than found in earlier calculations using single-reference methods. This implies prediction of a significantly higher crossover temperature from the CASPT2 results.

2. New Reactions from Dioxiranylmethyl: a Plausible Route to $CH_3 + CO_2$

The low-temperature reaction, **A**, is now believed to occur by way of the dioxiranylmethyl radical. Two reactions have been considered so far for this intermediate. One is its rearrangement to oxiranyloxy, and thence, *via* formyloxymethyl,

Dioxiranylmethyl   Oxiranyloxy   Formyloxymethyl
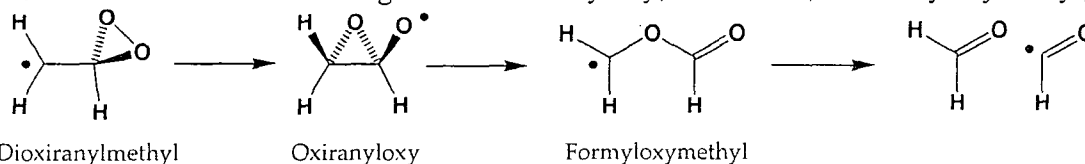
on to $CHO + CH_2O$. The other is a hydrogen migration, leading to methyldioxiranyl radical, and thence to $CH_3 + CO_2$. The latter reaction does not seem a plausible source of the CO_2 recently observed in time-resolved IR emission experiments on vinyl + O_2, since the hydrogen migration is calculated to have a barrier some 40–50 kcal/mol above that

Dioxiranylmethyl   Methyldioxiranyl   Acetoxy
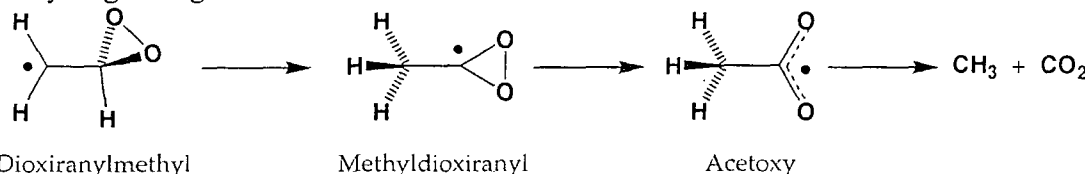
for the rearrangement to oxiranyloxy. The only other route to $CH_3 + CO_2$ considered to date has been a 1,3 hydrogen migration in formyloxymethyl. It is calculated to have a barrier between 6 and 11 kcal/mol higher than the simple fragmentation of formyloxymethyl to $CHO + CH_2O$.

Formyloxymethyl
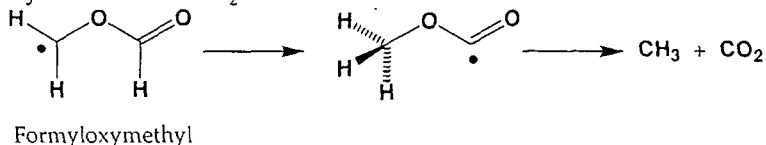
The hydrogen migration also has a less favorable A factor, and so there is no temperature at which it should be able to compete with the fragmentation.

We have now found three previously unrecognized reactions of dioxiranylmethyl, one of which does provide a plausible route to $CH_3 + CO_2$. Simple internal rotation about the C–C bond of dioxiranylmethyl is calculated, at the CASSCF(23,15)/cc-pVTZ level, to lead to spontaneous scission of the O–O bond and the formation of a doublet-state triradical, which is calculated to sit on a plateau-like region of the potential energy surface, as is commonly found for singlet-state biradicals. This triradical has a small barrier for the very exothermic hydrogen migration leading to the acetoxy radical, which

Dioxiranylmethyl   Triradical   Acetoxy
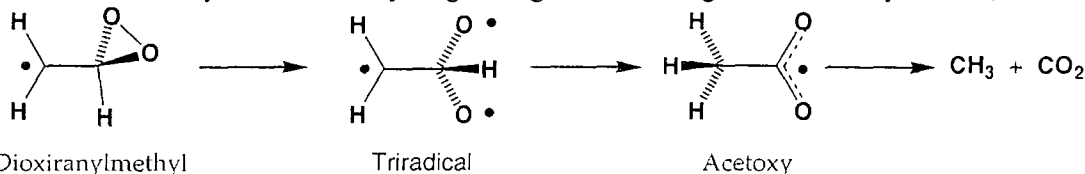
is known to give $CH_3 + CO_2$ very readily. At the CASPT(g3) level, the rate-determining step in this sequence is calculated to have a barrier that is 4 kcal/mol above that for oxiranyloxy formation. Significantly, though, the A factor for the channel leading to CH_3

+ CO$_2$ is larger than that for isomerization to oxiranyloxy, and so the hydrogen migration should become increasingly favorable at high temperatures.

The triradical can, in principle, also undergo hydrogen migration to oxygen, giving the carboxymethyl radical. This pathway is still being investigated, but experimental heats of formation show that it is slightly *more* exothermic than the isomerization to the acetoxy radical.

Dioxiranylmethyl   Triradical   Carboxymethyl
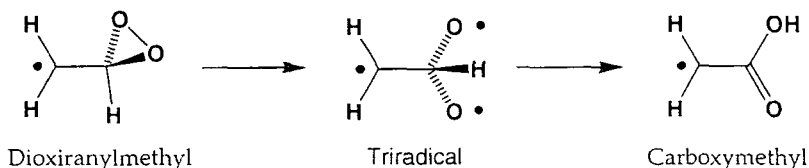
The third new reaction of dioxiranylmethyl is the formation of α-lactone + H:

Dioxiranylmethyl   α-Lactone
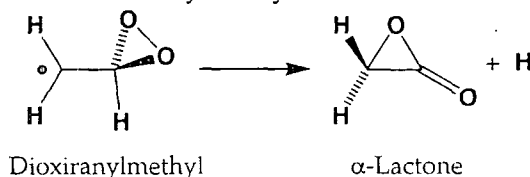
At 298 K, CBS-APNO calculations make this reaction 12 kcal/mol less favorable in overall free energy change than isomerization to oxiranyloxy. However, at 1000K it is found to be 7 kcal/mol more favorable. No new transition state for this reaction has been found. Rather, CASPT2(g3)//CASSCF calculations show that there is a non-steepest-descent path that leads from the TS for formation of oxiranyloxy to α-lactone + H.

3. Oxygen Interception of the β-Styryl Radical

The β-styryl radical plays a pivotal role in the formation of soot by the HACA mechanism. We are interested in the interplay between the increasing-mass aggregation reactions that lead eventually to soot and the decreasing-mass oxidative reactions. The issues are well illustrated by the reaction of the β-styryl radical with O$_2$. Two isomers of the β-styrylperoxy radical are expected to be formed by this reaction. The *E* stereoisomer appears to have little option but to follow reactions similar to those for vinylperoxy, for example giving PhCHO + CHO. The benzaldehyde is, in turn, likely to suffer decarbonylation and simply to return to the beginning of the HACA sequence. In contrast, the *Z* stereoisomer has, in addition to sidechain oxidation, the potential to undergo reactions that would lead eventually to oxidative destruction of the benzene ring.
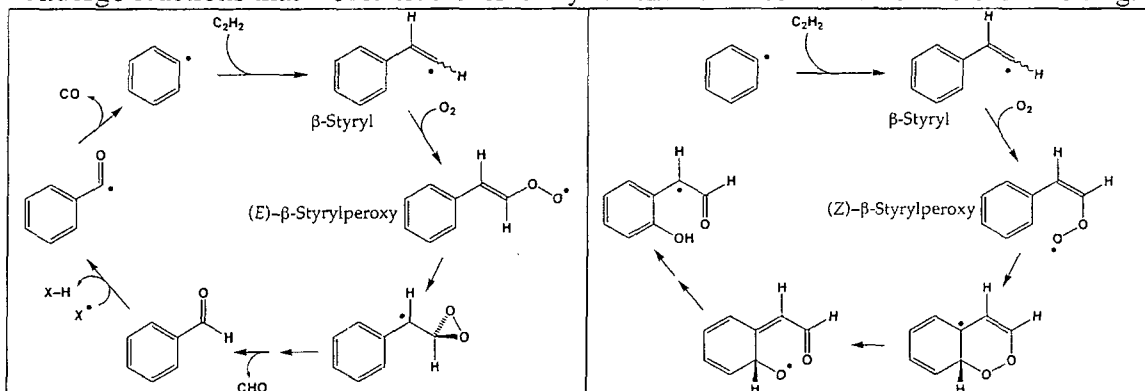
Whether the crucial attack of the peroxyl radical on the benzene ring can compete with the standard vinylperoxy-like reactions of the sidechain is very hard to estimate

-30-

computationally because the large-scale multireference methods used in the vinylperoxy study are not feasible to apply to such large molecules. Simple UB3LYP calculations suggest a very close balance between the two pathways.

We have consequently undertaken an experimental study of the reaction of β-styryl radical with O_2. The β-styryl radical is generated thermally by fragmentation and decarboxylation of cinnamyl peroxide. The products of reaction with O_2 are analyzed by GC-MS. This study is still in progress at the time of writing, but it is already clear that sidechain oxidation occurs to a greater extent than attack on the benzene ring. However, there is also a significant amount of salicaldehyde formed. This is the product expected from O_2 interception of the radical generated in the (Z)-β-styrylperoxy sequence shown above.

Salicaldehyde
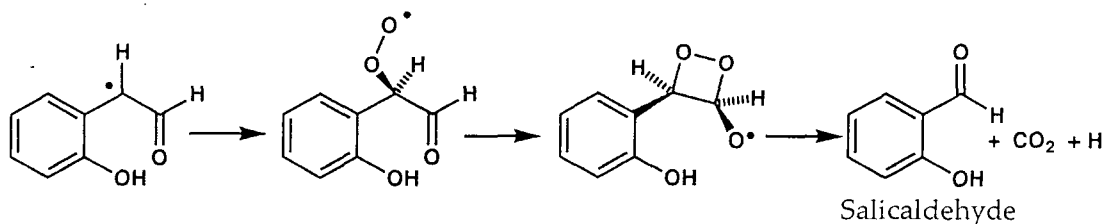
Identification and quantification of all of the products as a function of temperature will provide experimental data concerning the relative heights of the barriers for the sidechain oxidation and ring oxidation.

Publications from 2001 on citing DOE support

(1) "Evidence of a Double Surface Crossing Between Open- and Closed-Shell Surfaces in the Photodissociation of Cyclopropyl Iodide," Arnold, P.A.; Cosofret, B.R.; Dylewski, S.M.; Houston, P.L.; Carpenter, B.K. *J. Phys. Chem. A* **2001**, *105*, 1693.

(2) "The Ring Opening of Dioxiranylmethyl Radical: A Caution on the Use of G2-Type Ab Initio MO Models for Mechanistic Analysis," Carpenter, B.K. *J. Phys Chem. A* **2001**, *105*, 4585.

(3) "Polarized Infrared Absorption Spectrum of Matrix-Isolated Allyl Radicals," Nandi, S.; Arnold, P.A.; Carpenter, B.K.; Nimlos, M.R.;Dayton, D.R.; Ellison, G.B. *J. Phys Chem. A* **2001**, *105*, 7514.

(4) "Nonexponential Decay of Reactive Intermediates. New Challenges for Spectroscopic Observation, Mechanistic Interpretation, and Kinetic Modeling," Carpenter, B.K. *J. Phys. Org. Chem* **2003**, in press.

Ion Imaging Studies of Chemical Dynamics

David W. Chandler
Combustion Research Facility
Sandia National Laboratory
Livermore, CA 94551-0969
Email:chand@sandia.gov

Program Scope

The goal of this program is to study the dynamics of fundamental chemical processes that are of importance to combustion. This includes rotational energy transfer, photodissociation dynamics and reactive scattering. The primary tool we use to study these processes is ion imaging. Ion imaging is a technique for the measurement of the velocity (speed and direction) of a laser-produced ion. As such it extends and enhances the sensitivity of Resonant Enhanced Multi-Photon Ionization (REMPI) detection of molecules and atoms. Ion Imaging was first demonstrated in this laboratory in 1987 in collaboration with Paul Houston (Cornell) in an experiment that showed that a single image was capable of revealing the entire three-dimensional velocity distribution of a photo-fragment.[1] We continue to develop the technique for use in other experiments. Against this background of technique development we are utilizing Ion Imaging in novel ways to better study unimolecular and bimolecular processes of importance to combustion.

Recent Progress

The detailed study of collisional energy transfer has been a focus of this laboratory for several years. From a macroscopic point of view collisional energy transfer is responsible for the maintenance of thermal equilibrium within a reactive system. From a microscopic point of view the study of collisional energy transfer is an important way to gain insight about the potential energy surface of the interaction between atomic and molecular species. At high collision energy the transfer is mainly sensitive to the repulsive wall of the interaction potential, but at lower energies, or in studying collisions that transfer only a small amount of energy, the involvement of the attractive part of the potential energy surface becomes important. In addition, by studying energy transfer involving radical species the interplay of multiple potential energy surfaces can be seen. This is particularly true when studying the rotational or vibrational energy transfer that accompanies the change of electronic state of the molecule. For these reasons we have chosen to study the energy transfer in collisions of the radical NO with atoms (Ar, Ne, He), diatomic molecules (N_2, CO) and polyatomic molecules (CH_4).

Rotational Energy Transfer in Crossed Molecular Beams: NO + Ar

Traditional studies of collisional energy transfer have involved the measurement of energy transfer rates and the determination of the average value of the probability distribution of the energy transfer function. These are not quantities that we attempt to measure. Instead we measure more detailed quantities such as the differential cross section for every rotational quantum state produced in the collision, the alignment of each product molecule as a function of its quantum state and scattering direction, and finally (for the first time) the orientation of the molecule as a function of its final quantum state and scattering direction. This is equivalent to measuring, for the

scattered product, the m_j distribution of each rotational state for every scattering angle. This level of measurement can distinguish between the most sophisticated and detailed potential energy surfaces. This was demonstrated on the NO/Ar system where Millard Alexander[2,3] has generated very high quality potential energy surfaces. Only the latest one is capable of accurately predicting the NO orientation that we observe. This work was done in collaboration with Professor Joe Cline of the University of Nevada at Reno.

Rotational and Electronic Inelastic Collisions: NO + Ar
We find that the differential cross sections are in very good agreement with the predicted differential cross sections for both the NO ground ($^2\Pi_{3/2}$) and NO electronically excited ($^2\Pi_{1/2}$) products. This result is in contrast to earlier measurements of the differential cross sections for the electronically excited NO ($^2\Pi_{1/2}$) that was measured in the laboratory of Suzuki.[4] The differential cross sections for the NO/Ar system are believed to be well predicted and the agreement of theory and experiment can in some sense be seen as a validation of our apparatus and our ability to extract quantitative differential cross sections from the ion images. In fact, our results indicate that holding the bond length constant in the calculations is a valid approximation.

Dissociation of Charge Transfer Dimers: Cyclohexane + O_2 and Cyclohexane + Cl_2.
The dissociation of charge transfer clusters is an excellent opportunity to study non-adiabatic chemistry in a controlled manner.[5] We have compared the dissociative chemistry of two similar clusters: cyclohexane clustered with either Cl_2 or O_2.

We formed van der Waals clusters consisting of cyclohexane bound with either molecular oxygen or molecular chlorine in a pulsed supersonic expansion. These van der Waals clusters exhibit a strong absorption in the ultraviolet not attributable to either molecular subunit but rather to a transition involving transfer of an electron from the organic donor to the diatomic acceptor. The O_2-cyclohexane cluster has a strong absorption to a charge transfer state near 226 nm resulting in dissociation yielding $O(^3P)$. This wavelength is convenient as it also detects the $O(^3P)$ via 2 +1 REMPI transition. A simple model was developed by Mulliken to roughly predict the location of a charge-transfer absorption as has been observed in liquids. The recoil kinetic energy distribution of the atoms from the dissociation of each cluster is analyzed in terms of two possible dissociation mechanisms. The dissociation may be considered to proceed directly on the initially excited charge transfer state where a neutral atom recoils from a atom⁻/cyclohexane⁺ complex. Alternatively, the dissociation may proceed following a non-adiabatic electronic transition to the neutral excited states of the diatomic subunit of the cluster and subsequently dissociate. These two mechanisms lead to different amounts of translational energy available to the exiting atom. For the O_2-cycohexane dissociation the $P(E_t)$ is consistent with dissociation following non-adiabatic electronic transition from the initially accessed electronic state to a dissociative electronic state of the O_2. For the Cl_2-cyclohexane system both mechanisms seem to be present.

NO Dimer Bond Energy:
While performing NO + Ar scattering we observed the formation of both NO/Ar and $(NO)_2$ clusters in the molecular beam. We observed that when exciting these clusters at energies sufficient to dissociate them and form a NO(A) excited electronic state, we

observed ions from absorption of a second photon by the NO(A) product. This fact, along with the ion imaging apparatus that determined the velocity of the NO ions formed, allowed us to determine the bond energy of the NO dimer. We determined it to within 4 cm^{-1}. This is an important species that has been the subject of several calculations and many experimental measurements because it is a radical/radical interaction and therefore fairly strongly bound. We determined the bond strength to be 696 ± 4 cm^{-1}.

Future Plans:

Another area of collisional energy transfer that has been the subject of much attention over the years has been the determination of the shape of the probability distribution for energy transfer from a large, hot polyatomic to a smaller molecule.[6] By colliding a cold molecule (NO) with a large polyatomic (para-difluorobenzene) and measuring the amount of energy that is deposited in the polyatomic, we will be able to measure the shape of the transfer function of vibrational excitation. We will measure this by measuring the velocity distribution of the NO scattered from the polyatomic molecule. Although this is not the same quantity as has been previously measured, the same models that predict the de-excitation results should be capable of predicting our excitation results.

We are also beginning a project to study the reaction of chlorine atoms,[7] both ground and excited state, with small hydrocarbons and H_2. This experiment will require a new arrangement of our molecular beam apparatus as well as the ion imaging detection.

References:
1. David W. Chandler and Paul L. Houston, "Two-dimensional imaging of state-selected photodissociation products detected by multiphoton ionization," J. Chem. Phys. **87**, 1445 (1987).
2. Millard H Alexander, "A new, fully ab initio investigation of the ArNO(X) system. II. Bound states of the Ar-NO complex," J. Chem. Phys., **111**(16), 7435-7439 (1999).
3. Millard H. Alexander, "A new, fully ab initio investigation of the NO(X)Ar system. I. Potential energy surfaces and inelastic scattering," J. Chem. Phys. **111**, 7426-7434 (1999).
4. Hiroshi Kohguchi, Toshinori Suzuki, and Millard H. Alexander, "Fully State-Resolved Differential Cross Sections for the Inelastic Scattering of the Open-Shell NO Molecule by Ar," Science **294**, 832-834 (2001).
5. A. Giardini Guidoni, A. Paladini, M. Veneziani, R. Naaman and T. M. Di Palma, "Laser excited charge transfer processes in oxygen organic molecules mixtures: O(^{3}Pj) formation," Applied Surface Science **154**, 186 (2002).
6. Nancy J. Brown and James A. Miller, "Collisional energy transfer in the low-pressure-limit unimolecular dissociation of HO_2," J. Chem. Phys. **80**, 5568 (1984).
7. Feng Dong, Shih-Huang Lee, and Kopin Liu, "Direct determination of the spin-orbit reactivity in Cl(^{2}P$_{3/2}$,^{2}P$_{1/2}$) +H_2/D_2/HD reactions," J. Chem. Phys. **115**, 1197 (2001).

Publications For 2001 and 2002

1. J. I. Cline, K. T. Lorenz, E. A. Wade, J. W. Barr, and D. W. Chandler, "Ion Imaging Measurement of Collision-induced Rotational Alignment in Ar-NO Scattering," J. Chem. Phys. **115**(14), 6277 (2001).

2. P. L. Houston, D. W. Chandler, B. Cosofret, A. Dixit, S. Dylewski, J. Geiser, J. A. Mueller, R. J. Wilson, P. Pisano, M. S. Westley, and K. T. Lorenz, "Product Imaging Studies of Photodissociation and Bimolecular Reaction Dynamics," J. Chinese Chem. Soc. **48**(#3/SISI), 309-318 (2001).

3. K. T. Lorenz, D. W. Chandler, J. W. Barr, W. Chen, G. L. Barnes, and J. I. Cline, "Direct Measurement of the Preferred Sense of NO Rotation after Collision with Argon," Science 293(5537), 2063-2066 (2001).

4. V. K. Nestorov, R. D. Hinchlitte, R. Uberner, J. I. Cline, K. T. Lorenz, and D. W. Chandler, "Measurement of Bipolar Moments for Photofragment Angular Correlations in Ion Imaging Experiments," J. Chem. Phys. 115(17), 7881-7891 (2001).

5. E.A. Wade, K.T. Lorenz, J.L. Springfield, and D.W. Chandler, "Collisions of HCl with Atoms and Molecules," Chapter 9 in *Imaging in Molecular Dynamics: Technology and Applications (A User's Guide),* B. Whitaker, Ed., Cambridge University Press, May 2003, in press.

6. M. S. Westley, K. T. Lorenz, D. W. Chandler, and P. L. Houston, "Differential Cross Sections for Rotationally Inelastic Scattering of NO_2 from He and D_2," J. Chem. Phys. 114(6), 2669 (2001).

7. D. W. Chandler and J. I. Cline, "Ion Imaging Applied to the Study of Chemical Dynamics," in *Advanced Series in Physical Chemistry: Modern Trends in Chemical Reaction Dynamics,* K. Liu, ed. (unknown, 2002).

8. M. S. Elioff and D. W. Chandler, "State-to-state differential cross sections for spin-multiplet-changing collisions of NO(X (2)Pi(1/2)) with argon," J. Chem. Phys. 117(14), 6455-6462 (2002).

9. K. T. Lorenz, D. W. Chandler, and G. C. McBane, "State-to-State Differential Cross Sections for Rotational Excitation of CO by Ne by Velocity Mapping," J. Phys. Chem. A 106(7), 1144-1151 (2002).

10. E. A. Wade, J. I. Cline, K. T. Lorenz, C. C. Hayden, and D. W. Chandler, "Direct Measurement of the Binding Energy of the NO Dimer," J. Chem. Phys. 116, 4755-4757 (2002).

11. Bradley F. Parsons and David W. Chandler "On the dissociation of van der Waals Clusters of X2-cyclohexane (X=O, Cl) Following Charge Transfer Excitation in the Ultraviolet," J. Phys. Chem. A, accepted (2003).

12. E.A. Wade, K.T. Lorenz, J.L. Springfield, and D.W. Chandler, "Collisions of HCl with Rare Gas and Molecular Colliders," J. Phys. Chem. A, accepted (2003).

13. D.W. Chandler and C. C Hayden "Ion Imaging Techniques for the Measurement of Ion Velocities," for *Volume 5 of the Encyclopaedia of Mass Spectrometry* edited by Peter Armentrout, Elsevier Science, in press (2003).

Direct Numerical Simulation and Modeling of Turbulent Combustion

Jacqueline H. Chen, Evatt Hawkes, Shiling Liu and James Sutherland
Sandia National Laboratories, Mail Stop 9051
Livermore, California 94551-0969
phone: (925) 294-2586
email: jhchen@ca.sandia.gov

Program Scope

Direct numerical simulation (DNS) of turbulence-chemistry interactions has been an invaluable tool in the understanding of complex interactions between combustion chemistry, transport and unsteady flow in gas phase combustion. The scope of the present research is to use massively parallel DNS with detailed chemical mechanisms for hydrocarbon and hydrogen fuels to simulate multi-dimensional unsteady effects relevant to compression ignition, turbulent flame propagation, flame stabilization and flame structure. The physical insights gained from these fundamental studies are being used to guide and validate models of combustion and scalar transport in Reynolds-Averaged Navier-Stokes (RANS) and Large-eddy Simulation (LES) of practical combustion devices.

Recent Progress

In the past year substantial capability has been added to the Sandia S3D DNS code. These capabilities include improved boundary conditions and improved transport property evaluation. Significant improvements have been made to the boundary conditions that allow passage of flames through the computational boundary.[6] This advancement enables the simulation of spatially-developing turbulent jet flames that are statistically stationary and greatly facilitates direct comparisons with experiments.

With the improved code DNS simulations have been used to investigate fundamental combustion problems related to: 1) temperature inhomogeneities on low-temperature autoignition of lean hydrogen/air mixtures, 2) turbulent stretch effects on hydrogen enriched lean premixed methane air flames, 3) product enrichment effect on diluted premixed methane air flames, 4) unsteady scalar dissipation effects on extinction in a turbulent CO/H_2 jet flame, and 5) strain rate effects on high pressure autoignition of n-heptane in counterflow. These simulations were performed on massively parallel computational platforms with up to 256 processors at NERSC and at ORNL using MPI for scaleable parallelism. The results from these simulations are described below.

The Effect of Temperature Inhomogeneity on Low-Temperature Autoignition of Fuel-Lean Premixed Hydrogen/Air Mixtures[1]

The autoignition of lean, compressed hydrogen/air premixtures at elevated pressures in the presence of temperature inhomogeneities was studied using direct numerical simulation with detailed chemistry. The model problem studied by one-dimensional DNS and theoretical analysis corresponds to the autoignition of two hot spots in a closed domain and subsequent ignition front propagation. Initial temperature inhomogeneities lead to ignition first at discrete locations from which emanates an ignited front propagating outward in time. Heat release associated with these fronts promotes the autoignition of the remaining fluid elements through compression heating. Modes of ignition ranging from homogeneous explosion to ignition front propagation and shock-assisted ignition are identified over a range of mixture conditions.

The rate of heat release in the volume is determined by the net effect of the competition between these modes of ignition. A simplified analysis considering single-step chemistry is used to identify the key factors determining the ignition mode. Results are parameterized in terms of the characteristic temperature gradient and the heat release per unit volume of the system. For larger temperature

gradients and less reactive mixtures, laminar deflagration dominates the front propagation. For smaller temperature gradients (or more precisely the gradient of reactants and the exponential of the temperature divided by the effective activation energy) and for greater heat release per unit volume, ignition fronts propagate more rapidly. Depending upon how energetic the mixture is and the initial temperature gradient across the hot spot, combustion heat release-pressure feedback can result in the coalescence of the ignition waves with compression waves as the ignition front propagation approaches sonic velocities, resulting, in some instances, in the formation of developing shock waves from a subsonic ignition propagation. Results from this study may have implications for controlling the rate of heat release for homogeneous charge compression ignition combustion.

Turbulent Stretch Effects on Hydrogen-Enriched Lean Premixed Methane-Air Flames[2]

Lean premixed combustion of natural gas in gas turbines offers the potential to produce power with low NO_x emissions, but suffers from relatively poor combustion stability. The addition of small amounts of H_2 to the fuel could result in enhanced flame stability, and indeed this has been observed experimentally. The goal of this work was to examine the mechanisms that serve to produce a more robust flame when H_2 is added, and the effect of H_2 addition on pollutant formation. Two-dimensional Direct Numerical Simulations (DNS) have been conducted of premixed flames in a random flow field. Two cases were considered: a pure methane case, and a case with 29% H_2 on a molar basis. Both cases have an equivalence ratio of 0.52, which is near the lean limit for the pure methane case. Initial turbulence conditions for the two cases were identical, and the parameters place the combustion within the thin reaction zones regime.

It was found that the enriched fuel flame exhibits a greatly enhanced burning rate (a factor of 2.3 over the pure methane case, compared with 1.4 for the laminar case). The enhanced burning rate is attributed in part to a greater flame area in the enriched flame, due to a greater resistance to extinction and thermal-diffusive effects on the local flame speed, and in part to an effect of the flame structure on the local burning rate per unit area brought about by the focusing of H_2 into elements that protrude into the reactants. The blended case resulted in a lower rate of CO production per unit fuel consumed, but has a higher rate of NO formation per unit fuel consumed, indicating that there may be a trade off between these pollutants. CO levels are lower for the hydrogen flame owing to the greater resistance to strain and extinction. NO levels are higher in the H_2 enriched flame owing to higher local levels of radicals such as H, OH and O that lead to NO formation via a variety of pathways.

Effect of Product Gas Enrichment on the Chemical Response of Premixed Diluted Methane/Air Flames[3]

Turbulent premixed methane-air flames undergoing intense unsteady stretch may encounter tip opening in regions of high curvature due to differential diffusion. In these regions, hot product gases may diffuse through the disruption in the flame front and subsequently be transported back to the reaction front. In a different scenario product gases in recirculation zones may be transported to the flame front, for example, in the corners at the base of a swirl-stabilized lean premixed combustor. To understand the premixed flame response to hot product enrichment, a model problem comprised of a one-dimensional premixed flame perturbed by hot products upstream is studied using direct numerical simulation with detailed methane-air chemistry (GRI-mech 3.0). The product enrichment is characterized by temperature and hydrogen concentration perturbations to the fresh reactants upstream for flames spanning fuel-lean to fuel-rich stoichiometries. Several different perturbation methods were applied to account for different degrees of mixing of product gases with reactants. The perturbation is such that there exists a minimum initial temperature zone, referred to as the preheat zone, which separates the flame and the upstream perturbation.

It is found that the flame response depends on the net rate of temperature and hydrogen concentration change in the preheat zone, which, in turn, depends on three mechanisms: 1) the unperturbed structure and width of the preheat zone; 2) the diffusion of heat and hydrogen from the upstream perturbation and from the flame; and 3) the potential back diffusion of hydrogen from the perturbation to the flame. The competition between the flame response time and the mixing time of the products with the reactants upstream ultimately determines the magnitude of the response. The development of a rigorous flame response and a strong flame acceleration is found to exist in a rich flame when it is perturbed by its own product gases due to the high initial preheat zone temperature and narrower preheat zone width and in a lean flame when it is perturbed by a neighboring rich flame due to a reversal of hydrogen diffusion to the flame. It is found that the chemical response of the perturbed flame, independent of the method of perturbation and the stoichiometry and dilution, is most sensitive to the temperature in the preheat zone, which in turn depends upon its initial unperturbed value and its rate of increase. The only exception to this occurs when the products of a rich flame (namely, hydrogen) are transported to a fuel-lean flame. In this situation, because of its high diffusivity and its crucial chemical role in chain branching, the flame responds more rapidly to the back-diffusion of hydrogen to the flame from upstream.

Direct Numerical Simulation of a Spatially-developing Turbulent CO/H2/N2 Jet Flame[4]
Direct numerical simulation of a spatially-developing $CO-H_2$ turbulent jet flame was performed with detailed kinetics in regimes from fully burning to partial extinction. This configuration is more practically relevant than previous DNS configurations, since many laboratory measurements are available for spatially developing jets. These DNS data was used to perform apriori tests of mixing and reaction models for Large Eddy Simulation (LES). The effect of the LES filter size on model performance was investigated, as well as the number of thermochemical degrees of freedom that must be incorporated into an LES reaction model to accurately capture the thermochemical state of the system. The DNS data shows evidence of flame shortening in regions where the flame is pushed through the shear layer into the slower-moving oxidizer. In these regions, the flame folds back on itself, consuming the remaining oxidizer and extinguishing. Quenching in regions of high scalar dissipation rate between the vortical regions is also observed. Apriori tests of the steady laminar flamelet and equilibrium models coupled with beta-PDF and clipped-Gaussian PDF mixing models show good agreement for major observables, but performed poorly for intermediate species. Overprediction of extinction was observed in several parts of the flow field, suggesting that transient effects may be important in those regions.

Effect of Strain Rate on High-Pressure n-Heptane Autoignition in Counterflow[5]
The effect of steady strain on the transient autoignition of n-heptane at high pressure was studied numerically with detailed chemistry and transport in a counterflow configuration. The global effect of strain on multi-stage ignition is captured in a Damköhler number criteria based on either heat-release rate or the characteristic chain-branching rate. Results show that for low to moderate strain rates, both the low and intermediate temperature chemistry evolve similar to homogeneous systems. At high strain rates diffusive losses may inhibit ignition; for two-stage ignition, it is found that ignition is inhibited during the intermediate-temperature stage. The imposition of an overall temperature gradient further inhibits ignition because reactions zones for key branching reactions with large activation energies are narrowed.

Future Plans
We plan to continue our DNS studies of unsteady multi-dimensional flames with detailed hydrocarbon kinetics on massively parallel distributed memory computational platforms with a focus

towards understanding and modeling inhomogeneous autoignition of hydrocarbon fuels at high pressure, premixed flame stability in the lean limit at high pressure, turbulent flame propagation in autoigniting mixtures, and effects of scalar dissipation rate on quenching mechanisms in turbulent jet flames.

References

[1] J. H. Chen, S. D. Mason, J. C. Hewson, " The Effect of Temperature Inhomogeneity on Low-Temperature Autoignition of Fuel-Lean Premixed Hydrogen/Air Mixtures," 3rd Joint Meeting of the U.S. Sections of the Combustion Institute, Chicago, IL, (2003).

[2] S. Liu and J. H. Chen, "Effect of Product Gas Enrichment on the Chemical Response of Premixed Diluted Methane/Air Flames, " submitted to *Combust. Flame*, (2003).

[3] E. R. Hawkes and J. H. Chen, "Turbulent Stretch Effects on Hydrogen Enriched Lean Premixed Methane/Air Flames," 3rd Joint Meeting of the U.S. Sections of the Combustion Institute, Chicago, IL, (2003).

[4] J. C. Sutherland, P. J. Smith, and J. H. Chen, "DNS of a Nonpremixed CO-H2 Jet Flame using Detailed Chemistry-Toward Improved LES Models," 3rd Joint Meeting of the U.S. Sections of the Combustion Institute, Chicago, IL, (2003).

[5] S. Liu, J. C. Hewson, J. H. Chen, "Effect of Strain Rate on High-Pressure n-Heptane Autoignition in Counterflow," 3rd Joint Meeting of the U.S. Sections of the Combustion Institute, Chicago, IL, (2003).

[6] J. Sutherland and C.A. Kennedy, "Improved Boundary Conditions for Viscous Reacting, Compressible Flows," in review *J. Comp. Phys.*, (2003).

BES Publications (2001-2003)

H. G. Im and J. H. Chen, "Effects of Flow Strain on Triple Flame Propagation," *Combust. Flame* **126**: 1384-1392, (2001).

H. G. Im, J. H. Chen, R. Subramanya and R. Reddy, "Direct Numerical Simulations of Turbulent Premixed Flame Interaction using Parallel Computing, " *I[st] MIT Conference on Applied Mechanics and Fluid Mechanics*, Elsevier Science, June, 2001.

T. Echekki and J. H. Chen, "Direct Numerical Simulation of Autoignition in Non-homogeneous Hydrogen-Air Mixtures," *Combust. Flame*, to appear, (2003).

H. G. Im and J. H. Chen, "Preferential Diffusion Effects on the Burning Rate of Interacting Turbulent Premixed Hydrogen-Air Flames," *Combust. Flame*, 131:246-258 (2002).

S. D. Mason, J. H. Chen, H.G. Im, "Effects of Unsteady Scalar Dissipation Rate on Ignition of Non-premixed Hydrogen/Air Mixtures in Counterflow," *Proceedings of the Combustion Institute, 29*, (2002), 1629-1636.

T. Echekki and J. H. Chen, "High-Temperature Combustion in Autoigniting Non-Homogeneous Hydrogen-Air Mixtures", *Proceedings of the Combustion Institute, 29*, (2002), 2061-2068.

Turbulent Combustion

Robert K. Cheng
Environmental Energy Technologies Div.
Lawrence Berkeley National Laboratory
70 –109, 1 Cyclotron Rd.
Berkeley, CA 94720

E-mail : rkcheng@lbl.gov

Larry Talbot
Dept. of Mechanical Engineering
University of California at Berkeley
6173 Etcheverry Hall
Berkeley, CA 94720-1740

E-mail : Talbot@cmsa.Berkeley

Scope

This research program focuses on lean premixed combustion which is an emerging low emission energy technology being deployed in advanced heat and power generation systems. Our objective is to investigate experimentally the fluid mechanic processes that control combustion intensity, flame stabilization, extinction and pollutant formation. The goal is to provide for energy technologies the scientific underpinnings which can then be captured in models that will become accurate and reliable tools for predicting combustion process performance. This effort is responsive to DOE's mission to "foster a secure and reliable energy system that is environmentally and economically sustainable." Combustion processes of practical interests are turbulent and are not sufficiently characterized or understood to guide the refinement of turbulent combustion models and support the development of robust numerical simulations. Our approach is guided by a theoretical concept to classify premixed flames according to the initial turbulence and chemistry scales. To conduct a systematic exploration of the evolving flame structures at different turbulence intensities and scales, we use laser diagnostics and laboratory burners capable of operating at a wide range of fuel/air ratios and turbulence conditions. The experimental conditions include flames at low velocities (10 m/s <) at standard temperature and high pressures (5 atm <) to flames with high flow velocities (> 30 m/s).

Recent Progress

The capability of our low-swirl burner (LSB) to support very lean flames and very turbulent flames has been exploited in a series of recent studies to test the validity of new concept for classifying premixed turbulent flames. Using 2D imaging diagnostics (planar laser induced fluorescence, PLIF, and planar laser induced Rayleigh scattering) our analysis showed that the wrinkled flame regime may be valid at a turbulence intensity level much higher than previously thought and supports a new 'thin reaction zone' regime for the Kalovitz number range of $1 < Ka < 10$ ($Ka = (u'/s_L)^{3/2} (l_x/d_L)^{1/2}$) proposed by Peters. In this new regime, the smallest turbulent eddy is smaller that the flame front thickness, d_L (about 1 mm) but is still an order of magnitude larger than the reaction zone (about 0.1 mm). The significant change in the flame structures between the wrinkled flame regime and the thin reaction zone regime is the broadening of the preheat zone due to turbulence disturbance. The main implication to modeling is that turbulent transport becomes significant within the pre-heat zone.

To better characterize pre-heat zone broadening, our recent study includes six methane/air flames of equivalence ratio $\phi = 0.7$, $Ka = 1$-17. Within the preheat zone (approximately 400-1000 K) a new approach to analyzing flame front broadening was developed to address issues of flame three dimensionality. Instantaneous progress variable, c, contours extracted from the 2D

Rayleigh images constitute the basic data set. A statistical analysis of three aspects of this data has been developed and performed: a) contour spacing of a conserved scalar c, b) flame front curvature and c) flame surface density Σ. The analyses of c contour spacing have revealed very little change in preheat zone thickness even at the highest Ka numbers. Therefore, the primary effect of increasing turbulence remains to be the wrinkling of flame fronts so to increase the flame surface density. These results indicate that the regime diagrams often used to delimit the various regimes of premixed turbulent combustion and hence guide modeling are based on parameters that need to be carefully investigated to determine their appropriateness. This also argues for the use of the reaction zone thickness as the significant scalar length scale to interpret flame/turbulence interactions.

Our DOE-OIT supported work with combustion equipment manufacturer to scale the LSB to larger sizes has provided valuable insights into premixed turbulent flame behavior under typical operating conditions of practical systems. The fact that our low-swirl burner prototypes with a vane swirler can operate at velocities from 3 to 90 m/s implies a linear relationship between the displacement flame speed and turbulence intensity. This observation contradicts current theoretical consensus on a "bending effect" where the displacement flame speed ceases to increase with increasing turbulence. To better understand the scientific implication of this observation, we built a half-scale low-swirl burner (2.5 cm ID) to access operating conditions approaching 50 m/s. This burner employs an air-jet swirler similar to those used in all our BES studies rather than a vane-swirler.

However, flame stabilization of the small air-jet LSB at lean equivalence ratios was found to be very difficult above a mean velocity of 10 m/s. In those higher ϕ cases where stabilization was possible, the flames were situated close to the burner exit indicating that a much higher swirl number is needed for stabilization than its larger counterparts. Therefore, the smaller burner seems to have breached a lowest size limit for the air-jet LSB design. To continue our pursuit of a platform for the study of premixed turbulent flame behavior at very high flow velocities, we switch to a vane swirler configuration and tested two designs. These vane-swirler burners were found to operate in a wide range of ϕ with approach flow velocities up to 35 m/s and will be used for studying the "bending effect" of displacement flame speed.

We also expanded our diagnostic capabilities to include Particle Image Velocity (PIV). PIV captures instantaneous 2D velocity vectors within a relatively large field of view (typically of 10cm by 10cm) and is ideal for supporting numerical simulation such as large eddies simulations (LES), and adaptive mesh refinement (AMR) methods for direct numerical simulation (DNS). PIV is a relatively mature method and the system we have developed is cost-shared with the NASA Microgravity Combustion Program. It has a dual synchronized YAG laser system interfaced with a PC controlled frame grabber and a 2200 by 2000 pixel digital camera. Data acquisition and analysis software is provided by Mark Wernet of NASA Glenn Research Center.

The PIV system has been applied to v-flames to support our collaboration with the Center for Computational Science and Engineering (CCSE) at LBNL. The CCSE group lead by John Bell is developing methods to resolve the complexities of turbulent combustion using discretization methodology for low Mach number flow using compressible second order Navier-Stokes equations. An especially useful tool, AMR, is one of their major areas of research for use in time dependent 3D simulations of premixed turbulent combustion. The conditions of the PIV experiments are at relatively low turbulence conditions of < 10% RMS to be compatible with the

current capability of the simulation. Data on both non-reacting and reacting flows have been obtained and analyzed to give unconditional mean velocity statistics such as mean, RMS velocities and turbulent shear stresses. The non-reacting data has been used to set the initial conditions for the simulations, and for validation of the results on turbulence intensities and scales. Preliminary results of AMR simulation of our v-flames are very encouraging and a joint publication with the CCSE group is under development.

We also completed the initial commissioning of an experimental facility designed for generating lean premixed turbulent flames at elevated initial pressures and temperatures typical of gas turbine conditions. With the implementation of a preheater in FY05, it will enable us to access a regime of premixed turbulent combustion (1-15 atm and up to 200° C preheat inlet temperature) that has not yet been fully addressed by basic research. The centerpiece of this facility is an optically accessible stainless steel combustion chamber (about 12 cm x 12 cm x 50 cm) that mounts on top of a premixed burner. The burner has a small 2.5 cm diameter exit opening that accommodates different flame stabilizers. With the current system controls it can operate at pressures up to 7 atm. Preliminary experiments thus far include schlieren visualization of turbulent conical flames with mean flow velocity of 1- 3m/s at pressures of 1.5 to 5 atm. The most interesting observation is that the high pressure flames have very fine wrinkle scales and their flame heights do not increase despite the increases in mass flow rates with pressure.

Compared to the experimental efforts, our research on numerical simulation is more modest. From the onset, our focus has been to develop methods that can capture the flame flowfields and simulate evolving flame properties such as flow deflection, turbulence production and dissipation, and flame wrinkling. We focus on the use of 2D vortex dynamics simulation to investigate the dynamics of the turbulent flow and its effects on flame wrinkling of rod-stabilized v-flames. Though other more elaborate numerical approaches have been developed, the discrete vortex method focuses on the fluid mechanical processes and provides a useful and easily interpreted tool to resolve dynamic flame/turbulence interactions that control the development of the turbulent flame brush. The wealth of experimental data we have obtained on v-flames are available for direct comparison with numerical results.

In collaboration with Prof. C. K. Chan of the Hong Kong Polytechnic University our recent achievement include improvement in the simulation of the complex flame fronts by a novel numerical technique called Contour Advection with Surgery. Having been used in geophysical research for more than a decade, CAS is a new numerical scheme for studying flame front propagation. By continuously re-distributing marker nodes at a desired density, CAS is able to avoid the numerical instability caused by the clustering of marker nodes in regions of high curvature. Furthermore, the novel Contour Surgery (CS) accompanying CAS allows topological changes of the flame front while it evolves without causing any difficulty. To test the robustness and accuracy of CAS, we have performed two numerical experiments with carefully selected parameters. The first experiment had a moderate turbulence intensity of 7%; computed velocity statistics as well as flame surface density, when compared to laboratory measurements show good agreement. The second experiment had a higher turbulence intensity of 14%. In this case, contour surgery was found to play an active role in treating the frequent topological changes of the convoluted flame front which results in the formation of small flame islands. In principle, CAS can be extended to other combustion geometries, such as stagnation flame, when the reaction sheet model is employed.

4. Summary of Planned Research

Our work for FY 04 – 06 will be focused on 6 areas.

1. Determine the variation of local flame speed with flame curvature and local strain rate for flames at moderate to intense turbulence.

2. Investigate premixed turbulent flames at high velocities to resolve the "bending effects" of displacement flame speed.

3. Study turbulent flames structures and flowfields at high initial pressures and/or temperatures

4. Develop discrete vortex method for simulation of premixed turbulent v-flames and stagnation flames

5. Collaborate with researcher on computational methods to develop numerical simulations that can capture the flowfield dynamics of premixed turbulent flames

6. Develop an experimental database for premixed turbulent flames to facilitate a closer communication between experimentalists and theoreticians.

Publications

1. Shepherd, I. G. and Cheng, R. K. "Premixed Flame Front Structure in Intense Turbulence" Proceedings of the Combustion Institute, 29, p. 1833-1840 (2002).

2. Lam J. S. L., Chan C. K. Talbot L. and Shepherd I. G. "On the Hign-Resolution Modeling of Turbulent Premixed Open V-flame" submitted to Combustion Theory and Modeling (2002).

ELECTRONIC STRUCTURE STUDIES OF GEOCHEMICAL AND PYROLYTIC FORMATION OF HETEROCYCLIC COMPOUNDS IN FOSSIL FUELS

J.Cioslowski, Department of Chemistry and Biochemistry, Florida State University, Tallahassee, FL 32306
jerzy@csit.fsu.edu, (850) 644-8274

Program scope

This research program has as its objective uncovering of the reaction mechanisms responsible for the formation of various heteroatom-containing combustion emittants. As such, it holds the promise of guiding the practitioners of applied science and engineering in their efforts to significantly reduce the pyrolytic production of carcinogens and other hazardous substances. At the same time, it is slated to test practical limits of the predictive power of modern quantum-chemical methods and shed light on mechanisms of many reactions that are commonly employed in organic syntheses.

Recent progress

The research funded by this grant has thus far yielded 20 papers with the P.I. as the main author or a co-author, of which 18 have already been published (see the enclosed list for the 17 publications that appeared in years 2001-2003). In addition, several papers were published by the co-P.I. (Dr. D. Moncrieff) who has since departed from the research program. In 2002, four research projects were completed.

1. Test G3 calculations on 2,3-didehydronaphthalene confirmed the reliability of the additive correction scheme in the prediction of properties of annelated analogs of 1,2-didehydrobenzene. Such a scheme opens an avenue to facile electronic structure calculations on didehydrogenation reactions of polycondensed heterocyclic compounds with six-membered rings [5].

2. B3LYP/6-311G* electronic structure calculations revealed that the dependence of the complexation energy $E_{cmpl}(z)$ on the longitudinal displacement z of the guest in endohedral complexes of the Na^+ cation with capped [5,5] armchair single-walled carbon nanotubes stems from an interplay between the polarization of the host by the electric field of the guest and the guest-host steric repulsion [9]. Overall, $E_{cmpl}(z)$ is characterized by the presence of a periodic pattern of local minima and maxima that reflect the discrete nature of the tube and of a pair of global minima located at fixed distances from the tube termini. Because of the large barrier height / zero-point energy ratio, the endohedral motion of the Na^+ cation at T = 0 [K] is largely confined to a surface that internally follows the contour of the tube. Vibrations perpendicular to the surface give rise to transitions in the vicinity of 100 [cm^{-1}], whereas the unimpeded motions within the surface result in a plethora of transitions with onsets as low as 0.1 [cm^{-1}].

3. Analysis of the HF/6-31G** and B3LYP/6-311G** relative energies of 25 unbranched catacondensed benzenoid hydrocarbons with six rings revealed a well-pronounced dependence of their thermodynamic stabilities on the presence of simple structural motifs [11]. In particular, the energy contribution due to steric overcrowding is proportional to the number of pairs of adjacent angular annelations of the same helicity, whereas the contribution due to conjugation effects is related to the number and mutual position of linear annelations. Although the arrangement of linear annelations also uniquely determines the number of Kekulé structures, the latter does not correlate directly with the non-steric energy component. This study also demonstrated the uselessness of the simple additive nodal increment model in accurate prediction of thermodynamic stabilities of PAHs.

4. Recognizing the importance of the development of novel electronic structure methods, we decided to investigate the density matrix functional theory (DMFT), which holds the promise of exceeding the currently employed DFT methodology in accuracy. The known asymptotic behavior of the total energy of two weakly interacting systems was found to impose stringent conditions on the exchange-correlation energy as a functional of the one-electron reduced density matrix [13]. Although the first-order conditions that involve Coulomb-type two-electron integrals are relatively trivial to satisfy, the exact functional should also conform to two second-order expressions, and consequently to certain sum rules. The primitive natural spinorbital functionals satisfy the first-order conditions but, lacking terms quadratic in two-electron integrals, are found to be incapable of recovering the dispersion component of the interaction energy. Violating the sum rules, the recently proposed Yasuda functional yields nonvanishing dispersion energy with spurious asymptotic terms that scale like inverse fourth and fifth powers of the intersystem distance. The Legendre transform of an (approximate) expression for the ground-state energy $E_0(\eta, g)$ of an N-electron system was shown to yield the 1-matrix functional $V_{ee}[\Gamma(x', x)]$ for the electron-electron repulsion energy that is given by the function $V_{ee}(n; g)$ of the occupation numbers n pertaining to $\Gamma(x', x)$ and the two-electron repulsion integrals g computed in the basis of the corresponding natural spinorbitals [14]. Extremization of the electronic energy functional, which is a sum of $V_{ee}[\Gamma(x', x)]$ and the contraction of $\Gamma(x', x)$ with the core Hamiltonian, produces the (approximate) ground-state energy even if $E_0(\eta, g)$ itself is not variational. Thanks to this property, any electron correlation formalism can be reformulated in the language of the density matrix functional theory. Ten conditions that have to be satisfied by $V_{ee}(n; g)$ uncover several characteristics of $V_{ee}[\Gamma(x', x)]$. In particular, when applied in conjunction with the homogeneity property, the condition of volume extensivity imposes stringent constraints upon the possible dependence of $V_{ee}(n; g)$ on g.

Future plans

1. The Wellington mechanism of chlorine/hydrogen elimination. The completion of the reactions that lead from elementary sulfur and alkenes, alkynes, or their chloro-derivatives to (chloro) thiophenes requires elimination of hydrogen/chlorine from the 2 and 5 positions of the thiophene ring. Since no evolution of H_2S is observed in such transformations, a free-radical mechanism is unlikely in this case. On the other hand, the concerted elimination that is operational in the well-known unimolecular decompositions of 2,5-dihydroheterocycles to their parent species and H_2 may be involved. In order to either confirm or discard this possibility, electronic structure calculations on the relevant Wellington eliminations are being carried out. In the case of unsubstituted species, the computed activation enthalpies will be compared with the experimental values of 54.8, 44.6, and 48.5 [kcal/mol] for the S, NH, and O heteroatoms, respectively. Stereochemistry of the reaction

will be established and the preferential elimination of H_2 over CH_4 in 2-methyl-2,5-dihydrofuran will be explained.

2. Thermochemistry and kinetics of rearrangements of azynes to aza analogs of cyclopentadienylidenecarbene. The electronic factors affecting the barriers and energetics of these rearrangements are being investigated by analyzing the data produced by G3 and CCSD(T) calculations on didehydroazines and the respective carbene isomers. Stabilities of the latter species with respect to fragmentation are being assessed.

3. The mechanism of thermal decomposition of quinoline and isoquinoline. Pyrolysis of quinoline and isoquinoline produces a large number of products that arise from fragmentation of both the benzene and pyridine moieties. The decomposition pathways of these two species appear to share several intermediates, the most important of which is the 1-indeneimine radical. The following issues concerning these reactions are being addressed:

a) The positional dependence of the energetics of the C-H bond scissions in quinoline and isoquinoline are being studied. Electronic factors affecting stabilities of the resulting radicals are being determined.

b) Kinetic and thermodynamic viabilities of various fragmentation patterns of the quinydyl and isoquinydyl radicals are being evaluated. Possible equilibration among the radicals and/or their fragmentation products is being studied. .

c) The viability of the conjectured equilibria among the intermediates involved in these reactions are being investigated.

The aforedescribed theoretical work will furnish a wealth of data of importance to experimental research. Kinetic models of thermal decompositions of nitrogen-containing heterocyclic compounds will be verified and corrected/augmented if necessary. Mechanistic hypotheses for several reactions will be either proved or rejected, advancing the knowledge of pyrolytic processes.

Publications resulting from the DOE sponsored research (2001-2003)

[1] J.Cioslowski, A.Szarecka, and D.Moncrieff; J.Phys.Chem. A **105** (2001) 501; Conformations and Thermodynamic Properties of Sulfur Homocycles: I. The S_5, S_6, S_7, and S_8 Molecules

[2] J.Cioslowski, A.Szarecka, and D.Moncrieff; Mol.Phys. **100** (2002) 1559; Conformations and Thermodynamic Properties of Sulfur Homocycles: II. The Fluxional S_8^+ Radical Cation

[3] J.Cioslowski, A.Szarecka, and D.Moncrieff; Int.J.Quant.Chem. **90** (2002) 1049; Conformations of the S_5^+ and S_6^+ Homocyclic Radical Cations

[4] J.Cioslowski, A.Szarecka, and D.Moncrieff; Mol.Phys. (in press); Energetics, Electronic Structures, and Geometries of Didehydroazines

[5] J.Cioslowski, A.Szarecka, and D.Moncrieff; Mol.Phys. (in press); Energetics, Electronic Structures, and Geometries of Naphthalene, Quinoline, and Isoquinoline Analogs of 1,2-Didehydrobenzene

[6] Z.Chen, J.Cioslowski, N.Rao, D.Moncrieff, M.Bühl, A.Hirsch, and W.Thiel; Theor.Chem.Acc. **106** (2001) 364; Endohedral Chem.Shifts in Higher Fullerenes with 72-86 Carbon Atoms

[7]   J.Cioslowski, N.Rao, A.Szarecka, and K.Pernal; Mol.Phys. **99** (2001) 1229 Theoretical Thermochemistry.of the $C_{60}F_{18}$, $C_{60}F_{36}$, and $C_{60}F_{48}$ Fluorofullerenes

[8]   J.Cioslowski, N.Rao, and D.Moncrieff; J.Amer.Chem.Soc. **124** (2002) 8485; Electronic Structures and Energetics of [5,5] and [9,0] Single-Walled Carbon Nanotubes

[9]   J.Cioslowski, N.Rao, K.Pernal, and D.Moncrieff; J.Chem.Phys. **118** (2003) 4456; Endohedral Motions Inside Capped Single-Walled Nanotubes

[10]   J.Cioslowski and A.Szarecka; J.Comp.Chem. **22** (2001) 1279; First-Principles Conformational Analysis of the $C_{36}H_{36}$ Spheriphane, a Prototype Hydrocarbon Host Cage

[11]   J.Cioslowski and J.C.Dobrowolski; Chem.Phys. Letters **371** (2003) 317; Structural Dependence of Thermodynamic Stability of Unbranched Catacondensed Benzenoid Hydrocarbons

[12]   J.Cioslowski and K.Pernal; J.Chem.Phys. **115** (2001) 5784; Response Properties and Stability Conditions in Density Matrix Functional Theory

[13]   J.Cioslowski and K.Pernal; J.Chem.Phys. **116** (2002) 4802; Density Matrix Theory of Weak Intermolecular Interactions

[14]   J.Cioslowski, K.Pernal, and P.Ziesche; J.Chem.Phys. **117** (2002) 9560; Systematic Construction of Approximate 1-Matrix Functionals for the Electron-Electron Repulsion Energy

[15]   J.Cioslowski, P.Ziesche, and K.Pernal; J.Chem.Phys. **115** (2001) 8725; Description of a High-Density Homogeneous Electron Gas with the Yasuda Density Matrix Functional

[16]   J.Cioslowski and K.Pernal; J.Chem.Phys. **117** (2002) 67; Variational Density Matrix Functional Theory Calculations with the Lowest-Order Yasuda Functional

[17]   M.Taut, K.Pernal, J.Cioslowski, and V.Staemmler; J.Chem.Phys.**118** (2003) 4861; Three Electrons in a Harmonic Oscillator Potential: Pairs vs. Single Particles

Dynamics and Energetics of Elementary Combustion Reactions and Transient Species
Grant DE-FG03-98ER14879

Robert E. Continetti
Department of Chemistry and Biochemistry
University of California San Diego
9500 Gilman Drive
La Jolla, CA 92093-0340
rcontinetti@ucsd.edu
April 11, 2003

Program Scope and Direction

This research program focuses on the transition-state dynamics of OH radical reactions and the energetics and dynamics of radical species. The dynamics of hydroxyl radical reactions have been studied using negative-ion photodetachment techniques to prepare energy-selected neutral complexes in configurations near the transition-state for the corresponding bimolecular reactions. The products and dissociation dynamics of the nascent neutral complexes are then measured using translational spectroscopy. Previously this technique was applied to the OH + H_2O and OH + OH reactions and in the last year a study of the OH + CO $\rightarrow$ HOCO $\rightarrow$ H + CO_2 reaction was published. The central goal is to study the reaction dynamics of these species, providing experimental benchmarks for the evaluation of potential energy surfaces and dynamics calculations on these important systems. These studies will be continued in the coming year by examining the OH + F, Cl reactions and the simplest 4-atom system, OH + H_2, by photodetachment of the corresponding precursor anions. The relative simplicity of these systems, from both an electronic structure and dynamics perspective should facilitate a direct comparison with detailed dynamics calculations on accurate potential energy surfaces.

We have also been studying the unimolecular dissociation dynamics and energetics of a number of reactive free radicals. Previously, the predissociation of the formyloxyl radical, HCO_2, was studied by photodetachment of the formate anion, yielding H + CO_2 products. These studies have now been extended to the acetate anion, producing the acetoxyl radical, CH_3CO_2. This species predissociates to CH_3 + CO_2 products in addition to the production of a small fraction of stable CH_3CO_2 radicals. Studies of a number of 3, 4 and 5-carbon alkynoxide species have also been completed, and it has recently been shown that these experiments also yield information on the substituted acetylides. Studies of free radicals will be extended in the coming year by carrying out VUV photodetachment experiments on small hydrocarbon anions. An apparatus has been assembled to allow tripling of 100 ps 355 nm radiation and 1.8 ps 386 nm radiation in Kr. Initial experiments will be carried out on iodo-substituted species that are expected to have very large photodetachment cross-sections, and then move on to characterize the excited states and dissociation dynamics of radicals including vinylidene, allyl and cyclopentadienyl.

Recent Progress

1. Probing the HOCO potential energy surface by photodetachment of HOCO⁻

The most exciting recent development in our studies of the half-collision dynamics of elementary combustion reactions has been our success at production of the HOCO⁻ anion and our study of the dissociative photodetachment (DPD) of this species. Formed in a pulsed-discharge ion source containing N_2O, CH_4 and CO, this anion has a photoelectron spectrum vastly different from the previously studied formate anion, HCO_2^-. The most interesting aspect of this anion, however, is the observation that upon photodetachment this species yields stable HOCO radical and both combustion-relevant product channels, $H + CO_2 + e^-$ and $OH + CO + e^-$, showing that this photodetachment process probes the relevant region of the important combustion reaction $OH + CO \rightarrow H + CO_2$.

Calculations of the equilibrium geometry of both cis- and trans-HOCO⁻ and HOCO were carried out by Prof. J. Francisco of Purdue University to support these experiments. The equilibrium geometry of the anion showed that photodetachment is expected to lead to production of excited HOCO radicals. Some of these radicals will have insufficient energy to dissociate, yielding stable radicals, while a fraction will undergo unimolecular decomposition. Unimolecular decomposition to OH + CO products occurs over little or no barrier, yielding a product translational energy distribution peaking near a translational energy $E_T = 0$, while unimolecular decomposition to $H + CO_2$ products is accompanied by a barrier releasing up to 1.3 eV between $H + CO_2$. This is expected to lead to a product translational energy distribution peaking away from $E_T = 0$. These expectations are consistent with our observations: approximately 80% stable HOCO radicals are produced, with 14% OH + CO products and 6 % $H + CO_2$ products. The OH + CO dissociation channel peaks near $E_T = 0$, while the $H + CO_2$ channel peaks at $E_T = 0.6$ eV. In addition, a small high energy OH + CO dissociation channel is observed, peaking at $E_T = 1.6$ eV. This is believed to occur by direct dissociative photodetachment to a repulsive excited electronic state of HOCO, marking the first observation of excited electronic states of the neutral HOCO species.

This work was published in the Journal of Chemical Physics last fall, marking the first characterization of the HOCO⁻ molecular anion, and more importantly the insights mentioned above into the dynamics on both ground and electronically excited state HOCO surfaces. Given the attention focused on the neutral potential energy surface for this system, future dynamics calculations for comparison with these results should be possible and will be of great interest. We are also interested in carrying out experiments on DOCO as well, but owing to the cost of the perdeuterated methane precursor we are currently putting this measurement off until there has been a theoretical assessment of our results on the HOCO system. Other synthetic approaches to the HOCO⁻ anion and the related CH_3OCO^- anion are also under consideration, but have yet to yield results.

2. Energetics of Free Radicals: Photoelectron Spectroscopy and Photodetachment Imaging of Alkynoxides and Substituted Acetylides

In our studies of combustion intermediates, we turned our attention in the last year to the radicals generated from alkynol species. Propargyl alcohol, $HOCH_2CCH$, is the simplest alkynol and is an energetic species owing to the presence of the acetylenic triple bond. In these studies, we have characterized the electron affinities of the corresponding alkynoxy radicals produced by

abstraction of the alcoholic proton by O^-. In addition, we have recently shown that O^- can abstract the acetylenic proton, yielding the corresponding acetylides for alkynols that are only carbon substituted on one end of the carbon-carbon triple bond. This was demonstrated by synthesizing the alkyne-nitrite species and preparing the anions by simple electron impact on the nitrite in the absence of a significant source of the strong gas-phase base O^-. In this manner the spectra were simplified considerably, and a feature that previously appeared to be an excited state of the alkynoxy radicals was shown to disappear, while the ground state of the alkynoxy radicals was unaffected. A number of 3, 4 and 5 membered species have now been studied, including 2-butyn-1-ol, 3-butyn-1-ol, 4-pentyn-1-ol and 2,2-dimethyl-2-butyn-1-ol. The alkynoxy radicals are characterized by electron affinities of ca 2 eV, while the radicals produced from the acetylides have electron affinities on the order of 3.2 eV. These studies have benefitted from our recent implementation of threshold photodetachment techniques for carrying out high-resolution photodetachment studies.

3. Dissociative Photodetachment of the Acetate Anion

Expanding on our previous study of the formate anion, HCO_2^-, and the subsequent predissociation of the formyloxyl radical, HCO_2, we have carried out studies of the acetate anion at 258, 340 and 355 nm. In these experiments we have found that nearly all of the radicals dissociate to $CH_3 + CO_2$ products with a large kinetic energy release, peaking at $E_T = 0.65$ eV for 355 nm excitation, although a small fraction of stable radical is clearly observed as well. A tunable light source in the laboratory has made near-threshold photodetachment studies of this system possible. The photoelectron spectra at 340 and 355 nm are structured, showing that this is a system that undergoes sequential dissociative photodetachment. A number of low-lying electronic states have been predicted for this system and may play a role in the branching between stable and dissociative radicals. Further studies involving deuterated acetic acid are currently underway to help clarify the observed dynamics.

4. VUV Photodetachment

We have assembled a test chamber and have undertaken preliminary studies for the production of VUV radiation by tripling 100 ps 355 nm radiation and 1.8 ps 386 nm radiation in Kr and Xe. A design for installation of the VUV cell on the photoelectron spectrometer will soon be submitted to the machine shop, so we should be able to attempt the first studies of VUV photodetachment within the next few months. The goal here is to study the energetics and dissociative states of a number of small hydrocarbon radicals by photodetachment of the corresponding anions. Initial efforts will focus on large cross-section iodo compounds, and will then move to species including vinylidene, allyl and cyclopentadienyl radicals.

Publications: 2001 – Present

1. H.-J. Deyerl, L.S. Alconcel and R.E. Continetti, "Photodetachment Imaging Studies of the Electron Affinity of CF_3.", J. Phys. Chem. A **105**, 552-557 (2001).
2. A. Rohrbacher and R.E. Continetti, "A Multiple-Ion-Beam Time-of-Flight Mass Spectrometer.", Rev. Sci. Instrum. **72**, 3386-3389 (2001).
3. R.E. Continetti, "Coincidence Spectroscopy.", Annual Reviews of Physical Chemistry, Vol. 52, (2001), pp. 165-192.

4. T.G. Clements and R.E. Continetti, "Predissociation Dynamics of HCO_2/DCO_2 studied by the Dissociative Photodetachment of HCO_2^-/DCO_2^- + hv → H/D + CO_2 + e$^-$.", J. Chem. Phys. **115**, 5345-5348 (2001).

5. H.-J. Deyerl, T.G. Clements, A.K. Luong and R.E. Continetti, "Transition state dynamics of the OH + OH → O + H_2O reaction studied by dissociative photodetachment of $H_2O_2^-$.", J. Chem. Phys. **115**, 6931-6939 (2001).

6. T.G. Clements, R.E. Continetti and J.S. Francisco, "Exploring the OH + CO → H + CO_2 potential surface via dissociative photodetachment of $(HOCO)^-$," J. Chem. Phys. **117**, 6478-6488 (2002).

Flame Sampling Photoionization Mass Spectrometry

Terrill A. Cool
School of Applied and Engineering Physics
Cornell University, Ithaca, New York 14853
tac13@cornell.edu

Project Scope

Progress in minimizing environmental pollution associated with hydrocarbon combustion requires the continuing development of kinetic models for the combustion of ethylene, ethane, propene, propane, propyne, and higher hydrocarbons including 1,3-butadiene and benzene. Improved modeling is also needed for oxygenated hydrocarbon fuels (*e.g.*, dimethyl ether, methanol, ethanol, propanol) with clean-burning characteristics (low NO_x, low soot). Kinetic model development in all of these reaction systems requires direct measurements of the absolute concentrations of combustion intermediates in laboratory flames under carefully controlled and documented flame conditions.

Vacuum ultraviolet (VUV) photoionization mass spectrometry (PIMS), applied to the selective detection of flame species, is a powerful new approach for studies of flame chemistry [1-3], which provides a valuable supplement to the traditional use of electron impact mass spectrometry for such studies. A flame-sampling time-of-flight mass spectrometer (TOFMS), recently designed and constructed for use with a synchrotron radiation light source [4] (LBNL Advanced Light Source) provides significant improvements over previous facilities that have employed tunable VUV laser sources [1-3]. These include superior signal-to-noise, soft ionization, and photon energies readily tunable over the 8 to 15 eV range required for comprehensive flame species concentration measurements.

The new facility is routinely used for measurements of concentration profiles and photoionization efficiency (PIE) curves for species sampled from well-characterized low-pressure laminar flames. Both stable and radical intermediates are detectable at mole fractions as low as 10^{-6}. Individual isomeric species may often be selectively detected and identified; this is one of the most important advantages of VUV PIMS.

Recent Progress

Direct measurements of the absolute concentrations of flame species are possible with VUV PIMS when species photoionization cross sections are known [2]. In our work we measure photoionization cross sections for "target" species by comparing ion signals recorded from a binary mixture of the target with a "standard" species of known photoionization cross section. Photoionization cross sections for allene, propyne, ethylene and acetaldehyde, measured for photon energies from 9.7 to 11.7 eV, using propene as a standard, enable us to

determine the absolute concentrations of the allene and propyne isomers of C_3H_4 (m/e 40) in premixed laminar flames of ethylene/oxygen and benzene/oxygen. The separate contributions of ethenol and acetaldehyde isomers of C_2H_4O (m/e 44) are also distinguishable in fuel-rich ethylene/oxygen flames. This is the first observation of ethenol (vinyl alcohol) in a hydrocarbon flame and may confirm a previous suggestion [5] that vinyl alcohol may be a stable product of the reaction of O_2 with the $HO \bullet C_2H_4$ adduct formed by the addition of OH to ethylene at the C=C double bond [6]:

$$OH + C_2H_4 \rightarrow OH \bullet C_2H_4 \qquad (1)$$
$$OH \bullet C_2H_4 + O_2 \rightarrow CH_2CHOH + HO_2 \qquad (2)$$
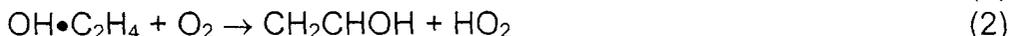
Allene/propyne isomeric composition in ethylene/oxygen and benzene/oxygen flames. Fig. 1 displays the ion signal (dark circles) for the C_3H_4 species at m/e=40 for a fuel-rich (Φ=1.9) 30 Torr ethylene/oxygen flame recorded for photon energies from 9.7 to 10.6 eV. The ion signals have been normalized point-by-point by the photon flux to remove the influence of flux variations with photon energy. These data were recorded with molecular beam sampling from a flame position where the concentration of C_3H_4 species approaches its maximum value. The onset of photoionization of propyne near 10.35 eV is seen superimposed on the allene contribution that rises from its threshold near 9.7 eV. Because we have measured the photoionization cross sections for both allene and propyne over this energy range, the photoionization cross section for an arbitrary mixture of the two isomers may be calculated. Assumed values for the allene and propyne mixture fractions of the C_3H_4 isomers were varied by trial and error to closely match the observed flux-normalized ion signals with the calculated photoionization cross sections for the assumed mixture composition. The arbitrary scale of the ion signals was adjusted as
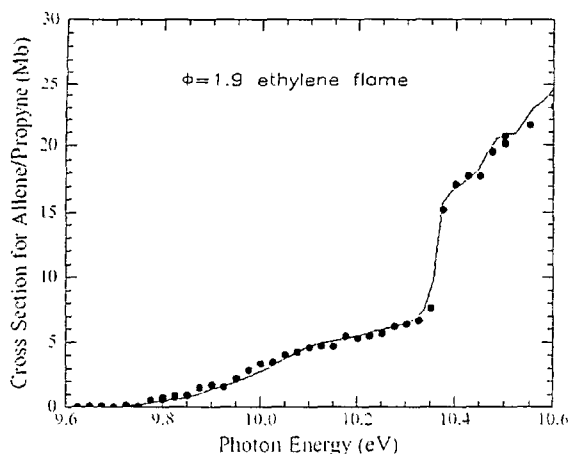
Fig. 1. A comparison of the m/e=40 ion signal (dark circles), recorded for a fuel-rich $C_2H_4/O_2/Ar$ flame, with the computed photoionization cross section (solid curve) for an assumed isomeric composition of 42% allene and 58% propyne.
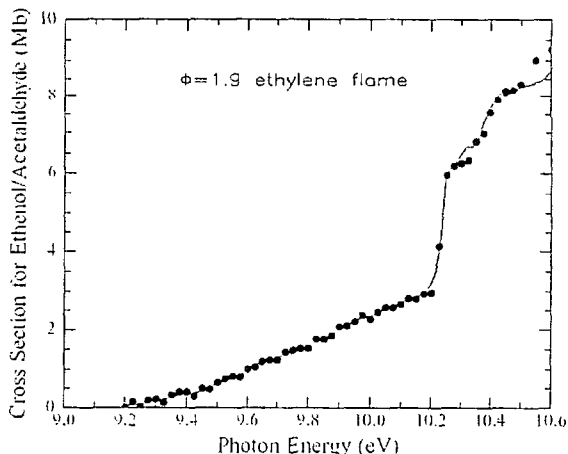
Fig. 2. A comparison of the m/e=44 ion signal (dark circles), recorded for the flame of Fig. 1, with the photoionization cross section (solid line) computed for an assumed isomeric composition of 37% ethenol and 63% acetaldehyde.

needed to assist in the curve fitting. A good match between the calculated cross section (solid curve) and the ion signals is obtained for an assumed isomeric composition of 42±4% allene and 58±4% propyne. This procedure was also used to determine the C_3H_4 isomeric compositions of fuel-rich (Φ=1.4) and fuel-lean (Φ=0.7) benzene/oxygen flames.

Ethenol/acetaldehyde isomeric composition in ethylene/oxygen flames.

An interesting result of this study is the observation of ethenol, a species apparently never before observed in a hydrocarbon flame, although Ruscic and Berkowitz have observed ethenol and acetaldehyde as products of reactions between atomic fluorine and ethanol [7].

The ion signals for m/e=44 displayed in Fig. 2 exhibit a dependence on photon energy qualitatively similar to that shown for the allene/propyne data of Fig. 1. The onset of ionization of acetaldehyde near 10.2 eV is clearly visible, superimposed on the ion signal for a second species with apparent ionization energy near 9.3 eV. The only plausible assignment for this species is ethenol with an IE of 9.33 eV [7]. The solid curve shown with the data of Fig. 2 is based on our measured cross sections for acetaldehyde and estimated cross sections for ethenol. A reasonable fit of the solid curve to the m/e=44 ion signals, displayed in Fig 2, is obtained for an acetaldehyde/ethenol concentration ratio $[CH_3CHO]/[CH_2CHOH]$ = 1.7±0.4.

If we estimate the difference in Gibbs free energy between ethenol and acetaldehyde at 1650 K to be 8.5 kcal/mol, then the ethenol/acetaldehyde ratio $[CH_2CHOH]/[CH_3CHO]$ for thermal equilibrium at 1620 K is only 0.07. Despite the thermodynamic stability of acetaldehyde relative to ethenol, a very high barrier ($\approx$ 56 kcal/mol) for the unimolecular tautomerization of ethenol to acetaldehyde exists [8]. This suggests that once ethenol is formed it is quite stable; the decompositions of the two isomers are uncoupled, and may therefore occur at different rates and by different flame reaction mechanisms.

Additional Completed Studies

1. Species concentration profiles were measured for reaction intermediates in ethylene/oxygen, benzene/oxygen, and 1,3-butadiene/hydrogen/oxygen flames.

2. PIE curves have been recorded for 24 flame species including CH_3, C_2H_2, H_2CO, C_3H_3, C_3H_4 (allene), C_3H_4 (propyne), C_3H_6 (propene), CH_2CO (ketene), CH_3CHO (acetaldehyde), C_2H_6O (dimethyl ether), $HCOOH$ (formic acid), C_4H_2 (diacetylene), C_4H_4 (vinyl acetylene), C_4H_6 (1,3-butadiene), $(CHO)_2$ (glyoxal), $C_4H_{10}O$ (diethyl ether), and C_6H_6 (benzene). These measurements demonstrate that the apparent ionization thresholds for species directly sampled from flames may be reliably used for species identifications.

3. Absolute photoionization cross sections for photon energies ranging from the ionization threshold to typically 1.5 to 2 eV above threshold have been determined for numerous stable flame species including acetylene, diacetylene, vinyl acetylene, ethylene, dimethyl ether, diethyl ether, acetaldehyde, 1,3-butadiene, allene, propyne, formic acid, and benzene.

Future Plans

During the past year we have refined and optimized our measurement capabilities to provide the confidence needed to routinely pursue studies of the chemistry of new flame systems. We have demonstrated that absolute photoionization cross sections for stable intermediates are measurable over the range from 9.7 to 11.75 eV with a probable accuracy of ±25%. We will now extend our cross section measurements to include additional key species in several reaction systems to assist in kinetic model development. We will perform comprehensive measurements of species concentration profiles for each of these systems under both fuel-rich and fuel-lean stoichiometries. The systems to be studied during the coming year are the benzene/oxygen, dimethyl ether/oxygen, propene/oxygen, ethanol/oxygen, and propanol/oxygen flames. In parallel with these experimental measurements, which will be performed at the LBNL ALS, a collaborative kinetic modeling effort will be initiated.

References

1. J. H. Werner and T. A. Cool, "The Combustion of Trichloroethylene Studied with VUV Photoionization Mass Spectrometry", *Twenty-Seventh Symposium (International) on Combustion, The Combustion Institute* (1998), 413-423.
2. J. H. Werner and T. A. Cool, "A Kinetic Model for the Decomposition of DMMP in a Hydrogen/Oxygen Flame", *Combustion and Flame*, **117**, 78 (1999); "The Kinetics of the Combustion of Trichloroethylene for Low Cl/H Ratios", *Combustion and Flame* **120**, 125 (2000).
3. A. McIlroy, T. D. Hain, H. A. Michelsen, and T. A. Cool, "A Laser and Molecular Beam Mass Spectrometer Study of Low-Pressure Dimethyl Ether Flames", *Twenty-Eighth Symposium (International) on Combustion, The Combustion Institute* (2000), 1647-1653.
4. T. A. Cool, A. McIlroy, F. Qi, P. R. Westmoreland, L. Poisson, D. S. Peterka and M. Ahmed, "A photoionization mass spectrometer for studies of flame chemistry with a synchrotron light source", unpublished.
5. C. J. Howard, *J. Chem. Phys.* **65**, 4771 (1976).
6. F. P. Tully, *Chem. Phys. Letters* **143**, 510 (1988); **96**, 148 (1983).
7. B. Ruscic and J. Berkowitz, *J. Chem. Phys.* **101**, 10936 (1994).
8. E. Lewars and I. Bonnycastle, *J. Mol. Structure THEOCHEM,* **418** 17 (1997).

STATE CONTROLLED PHOTODISSOCIATION OF VIBRATIONALLY EXCITED

MOLECULES AND HYDROGEN BONDED DIMERS

F.F. Crim
Department of Chemistry
University of Wisconsin–Madison
Madison, Wisconsin 53706
fcrim@chem.wisc.edu

Our research investigates the chemistry of vibrationally excited molecules. The properties and reactivity of vibrationally energized molecules are central to processes occurring in environments as diverse as combustion, atmospheric reactions, and plasmas and are at the heart of many chemical reactions. The goal of our work is to unravel the behavior of vibrationally excited molecules and to exploit the resulting understanding to determine molecular properties and to control chemical processes. A unifying theme is the preparation of a molecule in a specific vibrational state using one of several excitation techniques and the subsequent photodissociation of that prepared molecule. Because the initial vibrational excitation often alters the photodissociation process, we refer to our double resonance photodissociation scheme as *vibrationally mediated photodissociation*. In the first step, fundamental or overtone excitation prepares a vibrationally excited molecule and a second photon, the photolysis photon, excites the molecule to an electronically excited state. Vibrationally mediated photodissociation provides new vibrational spectroscopy, measures bond strengths with high accuracy, alters dissociation dynamics, and reveals the properties of and couplings among electronically excited states.

Several recent measurements illustrate the scope of the approach and point to new directions. We have completed an extensive study the spectroscopy and non-adiabatic dissociation dynamics of ammonia (NH_3) and have new results on the vibrationally mediated photodissociation of methanol (CH_3OH). In each case, the goals are understanding and exploiting vibrations in the ground electronic state, studying the vibrational structure of the electronically excited molecule, and probing and controlling the dissociation dynamics of the excited state.

Ammonia (NH_3)

Ammonia is a famously well-studied molecule that holds interesting opportunities for vibrationally mediated photodissociation experiments because it has both an adiabatic dissociation to yield ground state $NH_2 + H$ and a nonadiabatic dissociation to form excited state $NH_2^* + H$. We have used vibrationally mediated photodissociation spectroscopy to observe the symmetric N-H stretching vibration (v_1), the antisymmetric N-H stretching vibration (v_3), and the first overtone of the bending vibration ($2v_4$), obtaining simplified spectra originating in the lowest few rotational states. In addition, we have observed combination bands with the umbrella vibration (v_2) for each of these states, ($v_1 + v_2$), ($v_2 + v_3$), and ($v_2 + 2v_4$). The action spectra come from observing the production of the excited state NH_2^* from photolysis well above the threshold energy for its formation. We observe the first hint of the effect of vibrational excitation on the dissociation dynamics in these experiments, finding that the relative yield of excited products is *lower* for photodissociation of molecules containing a quantum of the symmetric stretching vibration in the ground state compared to those with antisymmetric

stretching or bending excitation. This differential dissociation disappears completely upon addition of a quantum of the umbrella vibration in the ground state.

The electronic spectroscopy available through vibrationally mediated photodissociation is particularly informative. Because the initial vibrational excitation of NH_3 molecules cooled in a supersonic expansion selects single rotational states of vibrationally excited molecules, both the Franck-Condon factors and positions of the transitions change from the one-photon spectra. By using this extra dimension, we are able for the first time to identify unambiguously the progression in the excited state bending vibration (v_4), the combination bands between the bending and excited state umbrella vibration (v_2+v_4), and the origin of the excited state symmetric stretch vibration (v_1). The resulting new harmonic frequencies and anharmonicities are $\omega_2^0 = 881\pm12$ cm^{-1}, $x_{22} = 6\pm2$ cm^{-1}, $\omega_4^0 = 910\pm23$ cm^{-1}, $x_{44} = 9\pm6$ cm^{-1}, $g_{44} = 16\pm7$ cm^{-1}, and $x_{24} = 56\pm13$ cm^{-1}. The values for the umbrella vibration (v_2) agree well with those previously determined by Vaida, and the large off-diagonal anharmonicity between the umbrella and bending vibrations is consistent with their near degeneracy, which prevented the direct observation of v_4 in the past. Our necessarily less precise estimate of the origin of the broad excited state symmetric stretch vibration (v_1) is $\omega_1^0 \approx 2360$ cm^{-1}

Information about the excited state structure makes it possible to investigate the dynamics of the dissociation of the different excited states using resonant enhanced multiphoton ionization to perform Doppler spectroscopy on the H atom fragment. In agreement with previous measurements, we observe both slow and fast components in the distribution of recoil velocities upon excitation of different excited state umbrella vibrations. The excited state bending vibrations behave similarly with a slightly larger fraction of fast hydrogen atoms. The dramatic different is in the stretching vibrations, which we can excite unambiguously for the first time. Dissociation from the state containing one quantum of symmetric stretch (v_1) produces a distribution with both fast and slow components that are similar to that for the origin. Dissociation from the antisymmetric N-H stretch state (v_3), however, produces dramatically different results. It forms *only* slow hydrogen atoms, perhaps reflecting preferential decomposition to make solely the excited state product. A major experimental advance is the implementation of Rydberg tagging as a means of detecting the hydrogen atoms from photolysis, a scheme that potentially determines the internal energy of the accompanying NH_2 fragment. We used this approach to study the vibrationally mediated photodissociation of NH_3 molecules with excited bending or umbrella vibrations, but the signal was too small to detect the photolysis of molecules with excited stretching vibrations.

Methanol (CH₃OH)

Our first explorations of the vibrationally mediated photodissociation of methanol allowed us to obtain vibrational overtone spectra of the second and third overtone of the O-H stretching vibration in the cooled molecules that agreed well with other measurements. We have also obtained similar spectra in the fundamental region and made the first measurements of the vibrationally mediated photodissociation dynamics detecting the H-atom product in order to obtain the ultraviolet spectra of the vibrationally excited molecules.

FUTURE DIRECTIONS

The two near term goals of the project are to study of the dissociation of vibrationally excited methanol and its dimers. Both studies are likely to involve Rydberg atom time-of-flight techniques along with our existing capabilities for laser induced fluorescence and resonant multiphoton ionization detection. The next step is to investigate the dimers of other well characterized systems to determine how simple complexation influences these well-understood dissociation dynamics.

PUBLICATIONS SINCE 2001 ACKNOWLEDGING DOE SUPPORT

Relative Product Yields in the One-Photon and Vibrationally Mediated Photolysis of Isocyanic Acid (HNCO). H. Laine Berghout, Shizuka Hsieh, and F. Fleming Crim, J. Chem. Phys. **114**, 10832 (2001).

Vibrational Spectroscopy and Photodissociation of Jet-Cooled Ammonia. Andreas Bach, J. Matthew Hutchison, Robert J. Holiday, and F. Fleming Crim, J. Chem. Phys. **116**, 4955 (2002).

Vibronic Structure and Photodissociation Dynamics of the A State of Jet–cooled Ammonia. Andreas Bach, J. Matthew Hutchison, Robert J. Holiday, and F. Fleming Crim, J. Chem. Phys. **116**, 9315 (2002).

Competition between Adiabatic and Nonadiabatic Pathways in the Photodissociation of Vibrationally Excited Ammonia. Andreas Bach, J. Matthew Hutchison, Robert J. Holiday, and F. Fleming Crim, J. Phys. Chem. A, (2003) *(in press)*.

Photodissociation of Vibrationally Excited Ammonia: Rotational Excitation in the NH₂ Product. Andreas Bach, J. Matthew Hutchison, Robert J. Holiday, and F. Fleming Crim, J. Chem. Phys., (2003) *(in press)*.

INFRARED ABSORPTION SPECTROSCOPY AND CHEMICAL KINETICS OF FREE RADICALS

Robert F. Curl and Graham P. Glass
Department of Chemistry and Rice Quantum Institute
Rice University, Houston, TX 77251
(713)348-4816 (713)348-3285
rfcurl@rice.edu gglass@rice.edu

PROGRAM SCOPE

This research is directed at the detection, monitoring, and study of the chemical kinetic behavior by infrared absorption spectroscopy of small free radical species thought to be important intermediates in combustion. In the last year, work on the reaction of OH with acetaldehyde has been completed and work on the reaction of $O(^1D)$ with acetaldehyde is very near to completion. In addition, the ratio of the H atom production to CH_3 production in the reaction between CH_4 and $O(^1D)$ has been measured.

PRODUCT YIELDS IN THE REACTION OF OH WITH ACETALDEHYDE

There has been a minor controversy about the relative importance of addition and abstraction in the reaction of OH with CH_3CHO. The majority view.[1, 2, 3] is that abstraction of the aldehydic H atom to produce CH_3CO is the dominant channel. However, Taylor et al[4] on the basis of a small negative enthalpy of activation and ab initio calculations proposed that addition was a major process at low temperatures. Including both abstraction and addition, the four channels of possible interest are

$$OH + CH_3CHO \rightarrow H_2O + CH_3CO \quad \Delta H=-139.6 \text{ kJ/mol} \quad (1a)$$
$$\rightarrow H_2O + CH_2CHO \quad \Delta H=-102.6 \text{ kJ/mol} \quad (1b)$$
$$\rightarrow CH_3 + HCOOH \quad \Delta H=-106.2 \text{ kJ/mol} \quad (1c)$$
$$\rightarrow H + CH_3COOH \quad \Delta H=-87.4 \text{ kJ/mol} \quad (1d)$$
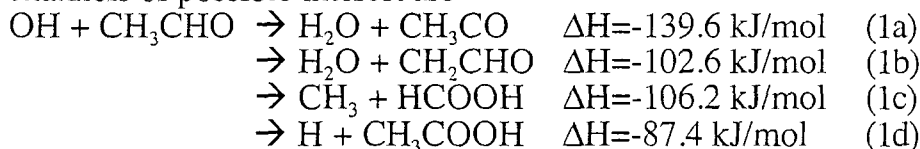
The evidence for the existence and even dominance of channel (1a) is strong. However, this does not preclude more minor contributions by other channels most particularly channels (1c) and (1d), which clearly require addition of OH to the carbonyl end followed by dissociation of the complex.

We have measured the yield of the water producing channels, which we believe is dominated by (1a) and the yield of (1c) and of (1d) at room temperature. The method employed was to produce OH by the reaction of $O(^1D)$ with H_2O in a system flooded with a large excess of water.

$$O(^1D) + H_2O \rightarrow 2OH \qquad (2)$$

This reaction is known to be extremely fast ($k_2 = 2.4 \times 10^{-10} \text{ cm}^3 \text{ s}^{-1}$) and produces at least 1.9 molecules of OH for every molecule of $O(^1D)$ consumed. $O(^1D)$ was produced by the flash photolysis of N_2O at 193 nm. The yield of H_2O (actually HDO) was measured by reacting OH with CD_3CDO and measuring the ratio of the infrared absorption signal of HDO to that of OH. Since the infrared absorption cross-sections of both HDO and OH are known, the HDO yield can be calculated. The yield of HDO thus obtained was 84±8%.

Although CH_3 could be detected in the acetaldehyde, water, $O(^1D)$ production systems under various circumstances, the detected signal typically rose too rapidly to be caused by reaction (1c) except when O_3 was used as the source of $O(^1D)$, CO_2. Then additional CH_3 was observed, suggesting that the reaction

$$CH_3CO + O_3 \rightarrow CH_3 + CO_2 + O_2 \qquad (3)$$

was occurring. Because the reaction of $O(^1D)$ with acetaldehyde produces CH_3 in about 50% yield, care had to be taken to keep the acetaldehyde concentration much smaller than that of water and to vary the acetaldehyde concentration. The detection limit was quantified to the CH_3 signal obtained when the acetaldehyde and water were replaced by a large excess of CH_4 keeping the $O(^1D)$ precursor concentration and laser power constant. The reaction of $O(^1D)$ with CH_4 produces CH_3 in 75% yield.[5] The yield of CH_3 from reaction (1) is less than 10%.

The yield of H was obtained using NO_2 instead of N_2O as the source of $O(^1D)$ again photolysing at 193 nm, where it is known[6] that the yield of $O(^1D)$ is 55%, in the water-flooded system. When CD_3CDO is used, the D atoms produced by channel (1d) then react with NO_2

$$D + NO_2 \rightarrow OD + NO \qquad (4)$$

and the OD thus produced reacts with CD_3CDO producing mostly D_2O. By comparing the D_2O signal thus produced with that produced in a system flooded with D_2 rather than H_2O using the reactions

$$O(^1D) + D_2 \rightarrow OD + D \qquad (5)$$
$$D + NO_2 \rightarrow OD + NO \qquad (6)$$

The yield of D atoms can be calculated after making several small corrections. These include the competition between CD_3CDO and NO_2 for $O(^3P)$ in addition to the corrections from $O(^1D)$ reacting with CD_3CDO. The resulting D yield appears to be about 10%. However, we suspect it is smaller. Indeed, because of some uncertainties about the other possible sources of a transient D_2O signal, which we are trying to reduce, it is not possible to say with certainty that H is produced in reaction (1)

Thus the reaction between OH and acetaldehyde is primarily an H atom abstraction. Any contribution at room temperature from addition channels is small.

PRODUCT YIELDS IN THE REACTION OF $O(^1D)$ WITH ACETALDEHYDE

$O(^1D)$ inserts into CH bonds and into double bonds creating rapidly dissociating, very energetic addition complexes that have a number of exit channels energetically available. In the case, the reaction of $O(^1D)$ with acetaldehyde, the following reaction channels seem plausible.

$$
\begin{array}{lll}
O(^1D) + CH_3CHO \rightarrow CH_3 + CO_2 + H & \Delta H = -262.6 \text{ kJ/mol} & (7a) \\
\rightarrow CH_3 + HCO_2 & \Delta H = -281.2 \text{ kJ/mol} & (7b) \\
\rightarrow CH_3 + HOCO & \Delta H = -350.1 \text{ kJ/mol} & (7c) \\
\rightarrow CH_2OH + HCO & \Delta H = -261.8 \text{ kJ/mol} & (7d) \\
\rightarrow CH_3O + HCO & \Delta H = -213.7 \text{ kJ/mol} & (7e) \\
\rightarrow OH + CH_3CO & \Delta H = -258.4 \text{ kJ/mol} & (7f) \\
\rightarrow CH_4 + CO_2 & \Delta H = -741.4 \text{ kJ/mol} & (7g)
\end{array}
$$

$$\rightarrow H + CH_2OHCO \quad \Delta H= ? \quad (7h)$$

We have observed infrared absorption lines of CH_3, HCO, OH, CH_4 and CO_2 from this reaction, but were unable to observe any transient absorption signals at the known frequencies of the strongest lines of the HOCO OH stretch fundamental. We have observed H indirectly through the NO_2 precursor method described above. The yield of CH_3 is about 50%. We are still in the process of quantifying the other channels. There are issues of the importance of secondary reactions that will require modeling of the reaction system to obtain quantitative branching ratios. Our qualitative observations are that H is a major product and HCO, OH, CH_4 and CO_2 are relatively minor products.

RATIO OF H YIELD TO CH_3 YIELD IN $O(^1D)$ REACTION WITH CH_4

The reaction between $O(^1D)$ and CH_4 has several open channels.[7]

$$O(^1D) + CH_4 \rightarrow CH_3 + OH \quad (8a)$$
$$\rightarrow (CH_2OH \text{ or } CH_3O) + H \quad (8b)$$
$$\rightarrow CH_2O + H_2 \quad (8c)$$
$$\rightarrow O(^3P) + CH_4 \quad (8d)$$
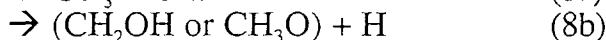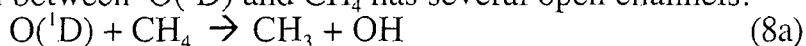
The H atom channel (8b) was measured by Satyaphal et al[8] in a molecular beam as 25±8% and later in a low pressure gas mixture as 14±3% by Matsumi et al.[9] We can conveniently measure an OH signal corresponding to the sum of channels (8a) and (8b) by using NO_2 as the source of $O(^1D)$ as it is known[6] that photolysis of NO_2 at 193 nm produces $O(^1D)$ in about 50% yield and H is converted into OH by reaction (16) with D replaced by H. The photolysis of N_2O produces OH only by channel (8a). Thus by comparing the ratio of the OH signal to the CH_3 signal with NO_2 as the $O(^1D)$ source to the same ratio with N_2O as the $O(^1D)$ source, the ratio of channel (8b) to channel (8a) can be calculated. Let $R(NO_2)$ be the ratio of the OH signal to the CH_3 signal when NO_2 is the $O(^1D)$ source and $R(N_2O)$ be the same ratio with N_2O as the $O(^1D)$ source. Then

$$\frac{(8b)}{(8a)} = \frac{R(NO_2) - R(N_2O)}{R(N_2O)} \quad (9)$$

The ratio (8b)/(8a) obtained by such measurements is 0.44±0.10. A fairly recent evaluation[7] gives 0.27 for this ratio with large uncertainties.

FUTURE PLANS

Electronically excited $O(^1D)$ is an extremely reactive reagent that typically reacts by inserting into CH or double bonds. The addition complex thus produced is highly energetic decomposing very rapidly into a variety of products many of which are free radicals. Under our typical conditions, $O(^1D)$ disappears from the system either by reaction or by quenching to $O(^3P)$ within a few microseconds. Thus $O(^1D)$ should be a powerful, flexible reagent for the production of a number of small free radicals. As an example, it is quite possible its reaction with NH_3 may produce $NH_2O + H$ in addition to NH_2 and OH, and its reaction with ethylene may produce CH_2CHO (vinoxy) and H in addition to OH $+ C_2H_3$ (vinyl). In the case of this last example, we are interested in attempting to determine product branching ratios. We also plan to examine and measure product branching ratios for the reactions of $O(^1D)$ with acetylene.

References

[1]   J. V. Michael, D. G. Keil, and R. B. Klemm, Journal of Chemical Physics **83**, 1630 (1985).

[2]   J. R. Alvarez-Idaboy, N. Mora-Diez, R. J. Boyd, and A. Vivier-Bunge, Journal of the American Chemical Society **123**, 2018 (2001).

[3]   G. S. Tyndall, J. J. Orlando, T. J. Wallington, M. D. Hurley, M. Goto, and M. Kawasaki, Physical Chemistry Chemical Physics **4**, 2189 (2002).

[4]   P. H. Taylor, M. S. Rahman, M. Arif, B. Dellinger, and P. Marshall, Symposium (International) on Combustion, [Proceedings] **26th**, 497 (1996).

[5]   W. B. DeMore, S. P. Sander, D. M. Golden, R. F. Hampson, M. J. Kurylo, C. J. Howard, A. R. Ravishankara, C. E. Kolb, and M. J. Molina, Report No. 97-4, 1997.

[6]   F. Sun, G. P. Glass, and R. F. Curl, Chem. Phys. Lett. **337**, 72 (2001).

[7]   W. B. DeMore, S. P. Sanders, D. M. Golden, R. F. Hampson, M. J. Kurylo, C. J. Howard, A. R. Ravishankara, C. E. Kolb, and M. J. Molina, Report No. 94-26, 1994.

[8]   S. Satyapal, J. Park, R. Bersohn, and B. Katz, J. Chem. Phys **91**, 6873 (1989).

[9]   Y. Matsumi, K. Tonokura, Y. Inagaki, and M. Kawasaki, J. Phys. Chem. **97**, 6816 (1993).

Publications

1.   "The Photolysis of NO$_2$ at 193 nm," F. Sun, G. P. Glass, and R. F. Curl, *Chem. Phys. Lett.* **337**, 72-78 (2001).

2.   "The reaction of NH$_2$ with NO$_2$: the reaction of OH with NH$_2$O," F. Sun, J. D. DeSain, Graham Scott, P.Y. Hung, R. I. Thompson, G. P. Glass, and R. F. Curl, *J. Phys. Chem. A* **105**, 6121-6128 (2001).

3.   "High-resolution infrared spectra of jet-cooled allyl radical (CH$_2$-CH-CH$_2$): v_2, v_3, and v_{14} C-H stretch vibrations," J-X. Han, Yu. Utkin, H-B. Chen, N. T. Hunt, and R. F. Curl, *J. Chem. Phys.* **116**, 6505-6512 (2002).

Vibrational Spectroscopy and Reactions of Transient Radicals

Hai-Lung Dai
Department of Chemistry, University of Pennsylvania
Philadelphia, PA 19104-6323; dai@sas.upenn.edu

I. Introduction

Aiming at characterizing the spectroscopy and structure of unknown transient radicals that are important to energy production and consumption processes, we have developed an approach based on the nanosecond time resolved Fourier Transform IR Emission Spectroscopy (TR-FTIRES) technique. In this approach the transient radical species of interest is produced with high vibrational excitation through UV photolysis of a precursor molecule. The IR emission from the highly excited species through its IR active vibrational modes is detected with fast time resolution using the TR-FTIR technique. The gas sample usually contains low concentration of precursor molecules imbedded in inert gases that can collisionally quench the excited radicals to the lowest excited vibrational level and allow the fundamental vibrational transition of the unknown transient species to be identified.

This approach also allows the reactions of the excited radical and the photolysis reaction of the precursor molecules to be characterized as the time-resolved emission spectra contain all the information related to the concentrations of all the relevant species in the gaseous sample as a function of time. Photodissociation of Acrylonitrile has been examined this way. Acrylonitrile, also known as vinyl cyanide, is an important molecule whose photodissocaition reaction following UV irradiation has been intensively studied using molecular beam techniques by several laboratories. The TR-FTIRES technique in our laboratory can be used to monitor the identity of the dissociation products as well as their internal energy content. The IR emission results complement the Mass spectrometry detection in molecular beam studies as the latter can discern the atomic make up of the molecules while the IR emission can reveal their structures. This advantage has proven valuable in the study of this dissociation reaction. Based on the detection of the HCN species through Mass spectrometry, molecular beam studies have concluded that the primary dissociation channel at 193 nm irradiation is through a 3-centered transition state. Out time-resolved IR emission study on the other hand shows that HNC may actually be the primary product. This finding suggests that other reaction channels such as the 4-centered transition state ought to be considered.

So far using this approach we have detected all the nine vibrational modes of the vinyl radical. In the past grant year we have reported the structure and vibrational modes of the cyanovinyl radical: the CN stretch at 2563 cm^{-1} and the CH$_2$ out of plane bend at 965 cm^{-1} have been determined and its structure is deduced to be bent at the CCC angle. In addition, the vibrational modes of the OCCN radical that have never been characterized previously, have been detected.

Usually in the detection of the IR emission from the desirable transient radical, which is produced from photolysis of a precursor, many other emission bands from other molecules, including the precursor molecule itself and the other product molecules from often several available photolysis channels, are also recorded. It is a challenge to decipher among all the observed bands which ones are from the target radical species. In order to assist in the identification of the radical bands, we have used the strategy in that different precursor molecules that may result in the same target radical are used. In order to improve the signal to noise in the analysis of the emission spectra we have developed a cross-spectral correlation technique that is based on the 2-dimensional correlation analysis. In this analytical scheme, since all the emission bands from the same target radical share the same time-dependence, which can be used as the perturbation parameter, the cross correlation between two different spectra will allow the same set of emission bands to be revealed.

II. The OCCN Radical

The vibrational spectroscopy of the OCCN radical, a species important to combustion environment where nitrogen is abundant and to atmospheric chemistry, is experimentally characterized for the first time. Its CN stretch is identified at 2093 cm^{-1}. The method of detection was by nanosecond Fourier-transform infrared emission spectroscopy. The radical was produced through UV photodissociation (λ=193 nm) of carbonyl cyanide, $CO(CN)_2$ and pivaloyl cyanide, $CO(CN)(CH_3)_3$ which leaves the radical with sufficient internal excitation. Infrared and near-infrared emission from all vibrationally excited species was detected. Pressure dependence, rotational band contour analysis and *ab initio* calculations all aided in assignment.

III. Two Dimensional Cross-Spectra Correlation Analysis of Time Resolved Fourier Transform Emission Spectra: Determination of Unknown Vibrational Bands of a Transient Radical

The 2-D correlation analysis has been applied to the assignment of time resolved infrared emission spectra. Each individual spectrum contains emission bands from the radical species of interest, which is generated from photolysis of a particular precursor molecule. When different precursor molecules are used for generating the same radical, all the corresponding emission spectra obtained should contain the same set of emission bands from this radical. This allows a 2-D correlation analysis across the different sets of spectra. Previously, the 2-D correlation analysis has been applied only to the same spectrum in which an external perturbation has been applied to provide additional phase information to the individual spectral peaks. We have developed the theoretical basis for analyzing spectral peaks from correlations among different spectra. Here the similar time-dependence and frequency shift of the same emission peak from the species of interest in all the emission spectra provide the phase information needed for the correlation analysis. The effectiveness of this cross-spectra correlation analysis is demonstrated on the OCCN radical, which can be generated from using three different precursors mentioned above.

The figure below shows first the longer time emission spectra (10 μs after the photolysis pulse in a sample with about 0.1 Torr precursor in 4 Torr Ar) from experiments using three different kinds of precursors (listed on the spectra). Emission peaks in the longer time spectra mimic more of the fundamental transitions of the vibrational modes. The figure at the bottom shows the spectra after correlation treatment among all three spectra. The CN stretch at 2093 cm^{-1} appears apparently.
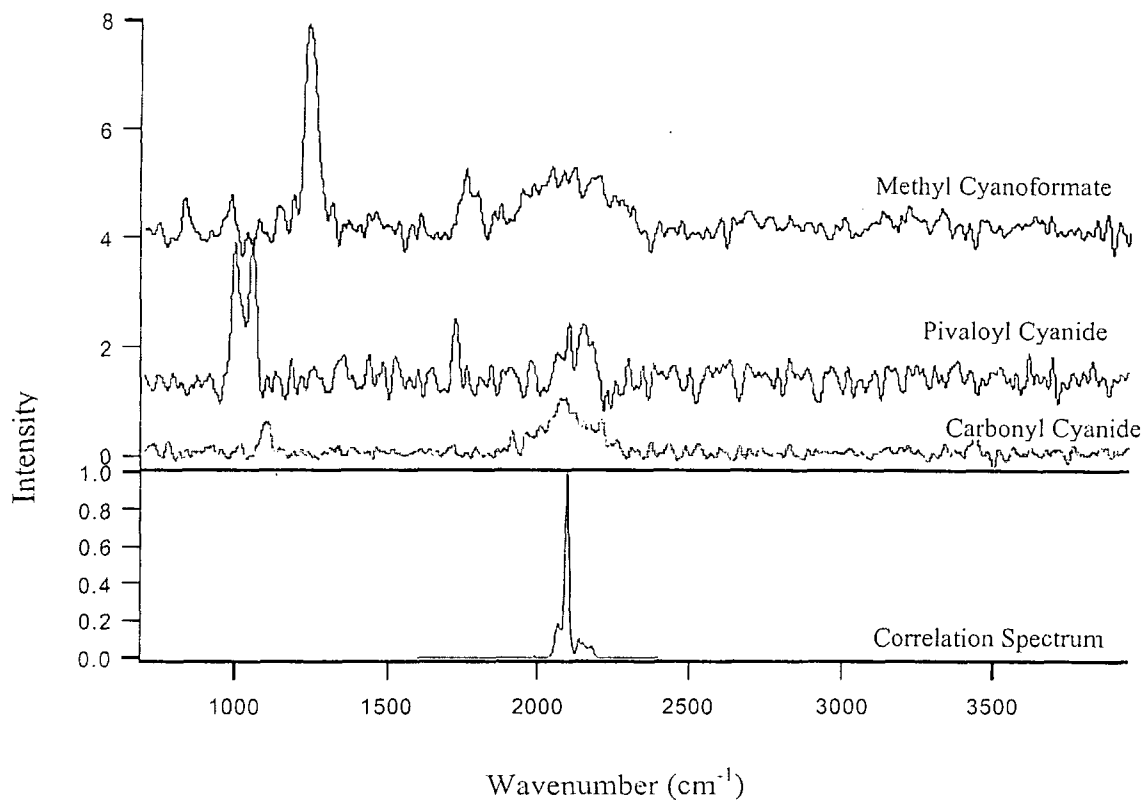
Publications since 2000 acknowledging support from this grant

Vibrational Spectroscopy of a Transient Species through Time-Resolved Fourier Transform Emission Spectroscopy: The Vinyl Radical
  J. Chem. Phys., [communication], 112, 9209-12 (2000)
  Laura Letendre, Dean-Kuo Liu, Charles D. Pibel, Joshua B. Halpern and Hai-Lung Dai

V-V Energy Transfer from Highly Vibrationally Excited Molecules through Transition Dipole Coupling: A QuantitativeTest on Energy Transfer from SO_2 to $SF_6(3_1)$

        J. Phys. Chem. A, 104, 10460-3 (2000) [C.B. Moore issue]

        Dong Qin, Gregory V. Hartland and Hai-Lung Dai

Collisional Deactivation of Highly Vibrationally Excited SO_2: A Time Resolved Fourier Transform Emission Spectroscopy Study

        Z. Phys. Chem., 214, 1501-19 (2000) [J. Troe issue]

        D. Qin, G.V. Hartland, C.L. Chen and H.L. Dai

193 nm Photolysis of Vinyl Bromide: Nascent Product Distribution of the $C_2H_3Br \rightarrow C_2H_2$(vinylidene) + HBr Channel

        J. Chem. Phys. 115, 1734-41 (2001)

        Dean-Kuo Liu, Laura T. Letendre and Hai-Lung Dai

Structure and Vibrational Modes of the Cyanovinyl Radical: A Study by Time-Resolved FTIR Emission Spectroscopy

        J. Phys. Chem. A, 106, 12035-40 (2002)

        Laura Letendre and Hai-Lung Dai

Bimolecular Dynamics of Combustion Reactions

H. Floyd Davis
Department of Chemistry and Chemical Biology
Baker Laboratory, Cornell University, Ithaca NY 14853-1301
hfd1@cornell.edu

1. Program Scope:

This aim of this project is to better understand the mechanisms and product energy disposal in bimolecular reactions fundamental to combustion chemistry. Using the crossed molecular beams method, a molecular beam containing highly reactive free radicals is crossed at right angles with a second molecular beam. The angular and velocity distributions of the products from single reactive collisions are measured.

II. Recent Progress:

a. Oxygen atom Rydberg Time-of-Flight Spectroscopy.

We have extended the hydrogen atom Rydberg time-of-flight (HRTOF) method, used previously in our laboratory and elsewhere, to the detection of ground state oxygen atoms, O (^3P_J). A particular spin-orbit state of oxygen is "tagged" by a double-resonance two-photon excitation to high-n Rydberg states. By selecting appropriate VUV wavelengths near 130 nm, each of the three O $(^3P_{0,1,2})$ spin orbit levels may be excited to a common O$(^3S_1)$ state. A second photon near 304 nm then pumps the excited atoms to a selected Rydberg level. The Rydberg O atoms fly to a detector where they are field ionized and collected.

Figure 1 shows the Rydberg excitation spectrum recorded by scanning the Rydberg tagging dye laser while holding the photolysis and VUV lasers at fixed wavelengths. The progression of peaks corresponds to excitation to Rydberg levels ranging from $n = 14$ to $n = 48$. The signal intensity of each peak depends on several factors, such as the oscillator strength for the excitation process, the fraction of Rydberg atoms surviving to the detector, and the fraction of Rydberg atoms field ionized at the detector. It was found that excitation to $n = 21$ produced the largest signal level.

We have characterized this method by studying the photodissociation dynamics of NO_2 in the near ultraviolet. We have demonstrated that the lifetimes of oxygen Rydberg atoms are long compared to their flight time to the detector (100 μs). Our measurements of the photodissociation dynamics of NO_2 at 355 nm are in good agreement with those obtained previously using other experimental means. For the channel leading to
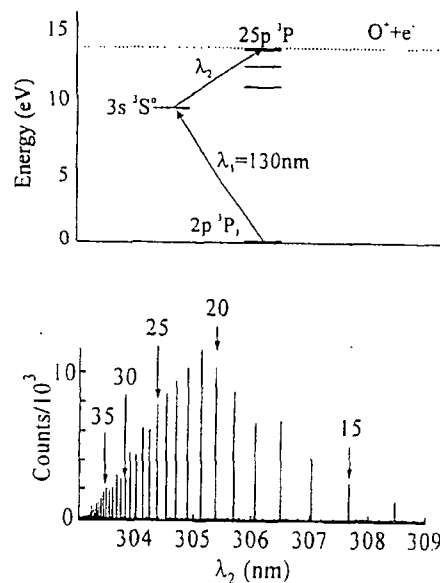
Fig. 1- Top: Oxygen atom Rydberg pumping scheme. Bottom: Rydberg Excitation spectrum obtained by scanning λ_1

production of NO (v = 1) in high-J levels, rotational resolution was achieved (Fig. 2). These studies indicate that ORTOF is suitable as a general method for probing the O (^3P_J) products from photodissociation or bimolecular reactions in crossed molecular beams.

The ORTOF method seems well-suited for studies of the reaction H + O_2 → OH ($^2\Pi$) + O (^3P_J), in which the OH fragment is preferentially formed in high-N levels at collision energies above the reaction endoergicity (Fig. 3). We have recently set up our crossed beams apparatus to study the bimolecular reaction H + O_2 → OH + O (^3P_J). This reaction is very important in combustion processes, and is known to produce OH primarily in v = 0 in high rotational levels. By measuring the O (^3P_J) velocity distributions using Rydberg tagging, we expect to learn about the internal distribution of the OH counterfragment as a function of scattering angle. As indicated in Fig. 3, the spacings between different levels of the OH product are sufficiently large that it may be possible to observe structure corresponding to different OH rotational states.
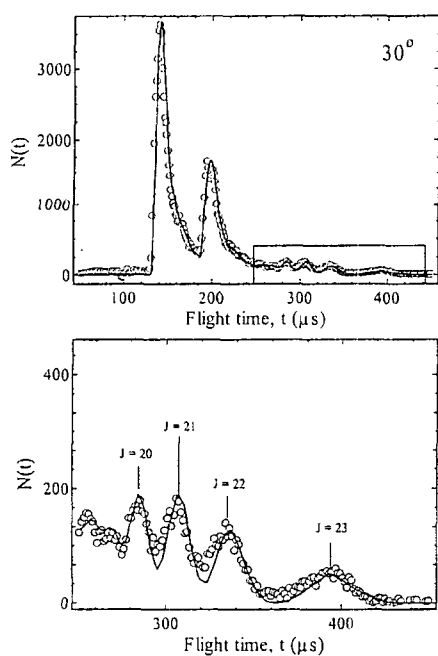
Fig 2- Top panel: TOF spectrum for O ($^3P_2$) from NO_2 photodissociation at 355 nm, at 30° (open circles) along with fit (solid line). Bottom panel: Expanded region showing rotationally resolved levels of recoiling NO (v=1) counterfragment.
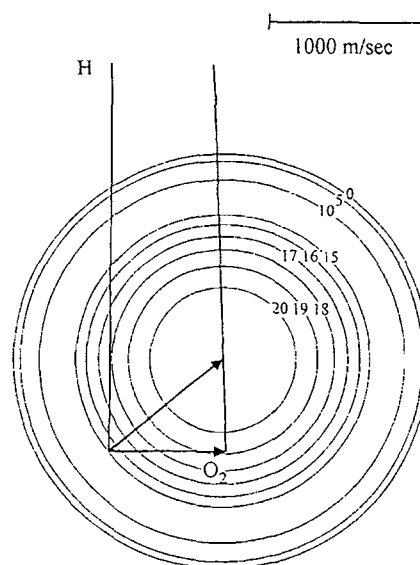
Fig. 3- Newton diagram in velocity space for H + O_2 → OH + O ($^3P_2$) reaction at E_{coll} = 1.8 eV. Circles denote O ($^3P_2$) velocities for indicated rotational levels of OH (v=0)

b.   Progress Towards Studies of OH + D_2 (v=1) → HOD + D

During the first year of the funding period, we were able to demonstrate mode specific energy disposal in the OH + D_2 → HOD + D reaction. In that case, translational energy was employed to surmount the potential energy barrier for reaction. Recently, a number of groups have done calculations on the reaction OH + D_2 (v = 1) → HOD + D. An experimental study in which the HOD product vibrational distribution is measured as a function of scattering angle would provide an important test of the PES.

We have configured our apparatus to study the title reaction. The D_2 is pumped to $v = 1$ by stimulated Raman pumping using two laser beams (532 nm and 633 nm, produced by Raman shifting in D_2). Although this method has been demonstrated by several groups to be very efficient, we have found that we are unable to pump a sufficient fraction of the D_2 molecules using our existing Nd:YAG laser, due to its broad linewidth ($1\ cm^{-1}$). We have therefore set this project aside for the moment until we acquire an injection-seeded Nd:YAG laser in order to complete these experiments.

We also plan to study the reactive quenching process OH ($A^2\Sigma^+$) + $D_2 \rightarrow$ HOD + D. Although this reaction has been studied by Lester's group, and two chemical channels were identified, the angular distributions of the products have not been measured. This should provide important new insight into the mechanism of this reaction.

III. Publications since 2001:

1. Vibrationally Inelastic Scattering of High-n Rydberg H atoms from N_2 and O_2. B. Strazisar, C. Lin and H.F. Davis, *Physical Review Letters* **86**, 3997 (2001).

2. Oxygen Atom Rydberg Time-of-Flight spectroscopy- ORTOF, C. Lin, M.F. Witinski, and H. Floyd Davis, to appear July 1 2003 in *J. Chem. Phys*.

Multiple–time–scale kinetics

Michael J. Davis

Chemistry Division
Argonne National Laboratory
Argonne, IL 60439
Email: davis@tcg.anl.gov

Research in this program focuses on three interconnected areas. The first involves the study of intramolecular dynamics, particularly of highly excited systems. The second area involves the use of nonlinear dynamics as a tool for the study of molecular dynamics and complex kinetics. Recently, this work has been extended to spatially distributed systems (reaction-diffusion equations). The third area is the study of the classical/quantum correspondence for highly excited systems, particularly systems exhibiting classical chaos.

Recent Progress

Two projects have been initiated and a number of results have been generated. The first project is a collaboration with Skodje (Colorado) and involves the study of the Boltzmann equation from a dynamical-systems approach, with an emphasis on the geometrical structure of the phase space. In particular, we wish to understand the asymptotic behavior of the phase space by investigating the approach to equilibrium along low–dimensional manifolds. The long-term goal of this work is to better understand nonequilibrium effects and the nature of transport coefficients derived from the Boltzmann equation. It is natural to try an approach based on low-dimensional manifolds, because they can be used to convert microscopic information to macroscopic information.

We have studied the dynamics of a model Boltzmann equation, which has been studied a number of times before, starting with Refs. 1 and 2. It is a one-dimensional, spatially homogeneous case with the collision integral approximated with a discrete quadrature and a simple form for the collision cross section. The figure shows some
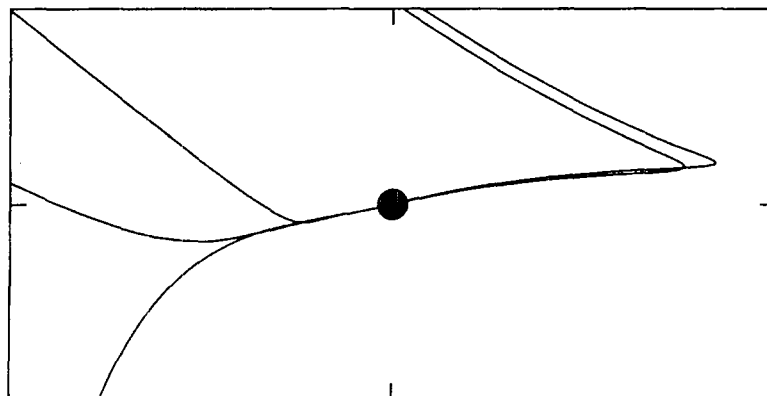
numerical results. Five initial non-equilibrium velocity distributions were propagated with the model Boltzmann equation. The axes of the plot show the population in two of the velocity bins. The solid lines show the relaxation of the five distributions to equilibrium (solid dot). Three of the distributions approach equilibrium from the cold end on the left and two from the hot end on the right. Note that the dynamics first approach a one–dimensional manifold in the high dimensional space of the discretized velocity space.

By mapping out the approach to equilibrium along the manifold, we were able to show that there are two distinct asymptotic solutions. Researchers[1,2] had concentrated on one of these because it can be derived analytically and were surprised when they found the other one and have presumed that it negated earlier conclusions concerning the first, Our investigations demonstrate that distributions approach equilibrium along one-dimensional manifolds from either side, although the cold end does not have a self-similar form observed earlier in Refs. 1 and 2 for the hot end.

The second project is an analysis of low-dimensional manifolds in reaction–diffusion equations and is a collaboration with Kaper (Boston) and Kaper (MCS/ANL). We have studied a number of simple reaction-diffusion equations and results for one of them, originally studied in Ref. 3, are presented here. This system consists of a chain branching mechanism with diffusion, for three species. The system is a simple model of an isothermal, imperfectly stirred reactor in one dimension. A methods-of-lines calculation was performed and the resulting system of ordinary differential equations was studied. This generates a 3N-dimensional dynamical system (the spatial grid from the original PDE consisted of N points). The equilibrium point of the set of ODEs describes the three equilibrium distributions of the species in the PDE. Stability analysis of the equilibrium point of the ODEs elucidates a set of linear manifolds, which describe the approach to equilibrium, in the near vicinity of the equilibrium point as demonstrated in the figure.

The plot on the left demonstrates a result familiar from the low-dimensional manifold literature of ODEs. The chemical kinetics approaches a one-dimensional manifold in the species space for all points along the six distributions included in the plot.

species 3 (x = 0.90)   species 3 (x = 0.90)
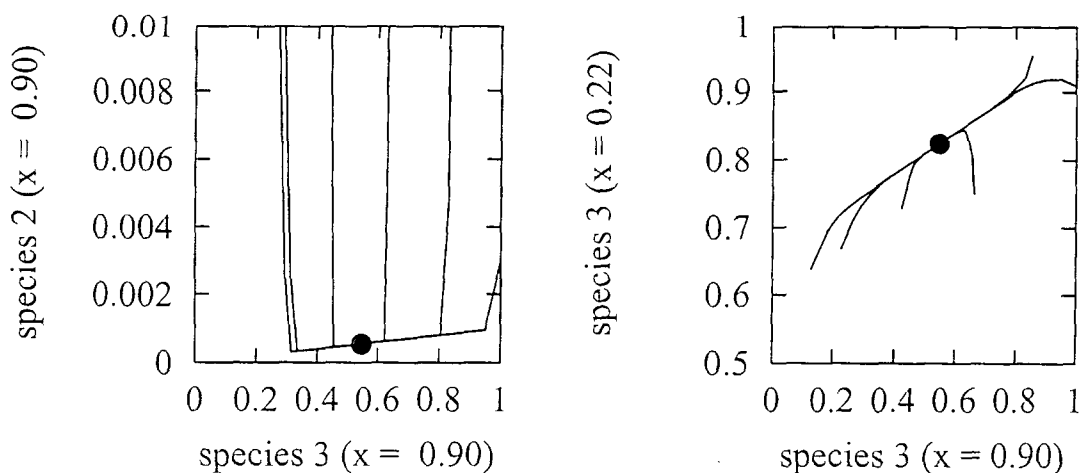
This indicates a reduction of the number of PDEs from three to one. However there is a much deeper reduction as implied by the plot on the right, where different points along the distribution for one of the species are shown. This plot indicates that at times longer than the reduction seen in the left plot, the system is reduced from the infinite dimensions of a single PDE to a one-dimensional system embedded in the infinite-dimensional phase space. In the sense of a spectral picture, the system is reduced to a single mode. Analysis of this mode in terms of a proper orthogonal decomposition[4] is under way.

Future Plans

The project on the Boltzmann equation will be extended in several ways. The main extension will be inclusion of the advection term, via a discrete velocity model. This will also extend the calculation to more than one spatial dimension. An attempt will be made to derive transport coefficients along low-dimensional manifolds. The work on reaction–diffusion equations will also be extended to higher dimensional systems and the analysis of these systems in terms of both low-dimensional manifolds and a proper orthogonal decomposition will be attempted, with a focus on a comparison between the two. Finally, a project on low-dimensional manifolds in open systems will be initiated with Tomlin (Leeds).

References

1. J. Tjon and T.T. Wu, Phys. Rev A **19**, 883 (1979).
2. J. Tjon, Phys. Lett. A **70**, 369 (1979).
3. M. Hadjinicolaou and D. A. Goussis, SIAM J. Sci. Comput. **20**, 781 (1999).
4. G. Berkooz, P. Holmes, and J. L. Lumley, Ann. Rev. Fluid Mech. **25**, 537 (1993).

Publications

M. J. Davis and R. T. Skodje, "Geometric approach to multiple-time-scale kinetics: A nonlinear master equation describing vibration-to-vibration relaxation", Z. Phys. Chem. **215**, 233 (2001).

R. T. Skodje and M. J. Davis, "Geometrical simplification of complex kinetic systems", J. Phys. Chem. A. **105**, 10356 (2001).

M. J. Davis and J. H. Kiefer, "Modeling of nonlinear vibrational relaxation of large molecules in shock waves with a nonlinear, temperature-varying master equation", J. Chem. Phys. **116**, 7814 (2002).

M. J. Davis, "Dynamics of a nonlinear master equation: Low-dimensional manifolds and the nature of vibrational relaxation", J. Chem. Phys. **116**, 7828 (2002).

M. J. Davis and S. J. Klippenstein, "Geometric investigation of association/dissociation kinetics with an application to the master equation for $CH_3 + CH_3 \leftrightarrow C_2H_6$", J. Phys. Chem. A **106**, 5860 (2002).

COMPREHENSIVE MECHANISMS FOR COMBUSTION CHEMISTRY: EXPERIMENT, MODELING, AND SENSITIVITY ANALYSIS

Frederick L. Dryer

Department of Mechanical and Aerospace Engineering
Princeton University, Princeton, New Jersey 08544-5263
fldryer@princeton.edu
Grant No. DE-FG02-86ER-13503

Program Scope

Experiments conducted in a large diameter Variable Pressure Flow Reactor (VPFR) at pressures from 0.3 to 20 atm, temperatures from 500 K to 1200 K, and with observed reaction times from 0.5×10^{-2} to 2 seconds are combined with numerical studies to develop and validate chemical kinetic reaction mechanisms and to determine important elementary rates. Continuing efforts are: (1) utilizing the perturbations of the H_2/O_2 and $CO/H_2O/Oxidant$ reaction systems by the addition of small amounts of other species to further clarify elementary reaction properties; (2) further elucidating the reaction mechanisms for the pyrolysis and oxidation of small hydrocarbons (alkanes, olefins) and oxygenates (aldehydes, alcohols, and ethers).

Recent Progress

Experimental and computational studies on propene oxidation kinetics were described briefly in last year's abstract, and continuing efforts have recently been summarized in Zheng et al. ("Experimental Study of Propene Oxidation at Low and Intermediate Temperatures", *Third Joint Meeting of the U.S. Sections of The Combustion Institute, University of Illinois, Chicago, March 16-19, 2003*). An important result of this work is that at low and intermediate temperatures, no negative temperature coefficient (NTC) behavior is observed in high-pressure oxidation experiments in the VPFR. Prior static-reactor experiments (Wilk et al. *Combust. Sci. Technol.* 52:39-58, 1987) and modeling of these experiments Wilk, et al. *(Combust. Flame* 77:145-170, 1989) show this behavior, as does recent modeling of the same experiments by Heyberger et al. *(Combust. Flame* 126:1780-1802, 2001). However, no negative temperature coefficient (NTC) region is predicted by Heyberger et al. or Qin et al. *(Proc. Combust. Inst.* 28:1663-1669, 2000) at the higher pressures and shorter reaction times of the VPFR experiments. The results suggest that the oxidation kinetics of propene that result in NTC-type behavior are not relevant under conditions in practical combustion systems. An improved oxidation mechanism is under development, based upon the earlier work of Qin et al., the mechanisms presented in our recently published work, [1,2][+], and additional consideration of the reactions involving allyl radicals, hydroxyl radicals, and their reaction products.

Progress in two additional areas, among others that are presently underway, is described in more detail below.

1. Rate Constants for Ethanol Thermal Decomposition Reactions

The decomposition of ethanol into ethylene and water is a major source of ethylene production in the oxidation of ethanol at VPFR conditions [3]. Accurate representation of this channel is critical to assessing the relative importance of radical abstraction reactions and their branching ratios to the overall destruction rate of ethanol. Additional ethanol decomposition channels produce radical species that lead to secondary reactions involving H abstraction from ethanol, but these effects can be removed by terminating the important radicals. Mechanisms exist that can be used to estimate the interactions of toluene as a terminating species. On the other hand, tri-methylbenzene has been successfully used in similar work in shock tubes (Herzler et al., *J. Phys. Chem.*, 101:5500-5508, 1997). Both species are mutually soluble with ethanol, simplifying the experimental aspects of the present work. We used a combined mechanism based upon the works of Marinov *(Int. J. Chem. Kinet.* 31:183-220, 1999) and Emdee et al. *(J. Phys. Chem.* 96:2151-2161, 1992) to estimate the terminating characteristics of toluene in our experiments (Fig. 1). Calculations show that for initial mole fraction ratios of toluene/ethanol greater than one, more than 92% of the observed C_2H_4 yield is produced by $C_2H_5OH \rightarrow C_2H_4 + H_2O$, (R1). By measuring the concentrations of C_2H_5OH and C_2H_4 formation rate in pyrolysis experiments seeded with a radical trapper, the rate constant of the reaction (R1), k_1, can be determined experimentally. We performed such experiments in the Variable Pressure Flow Reactor (VPFR) at 1.7-3.0 atm pressure and at 1045-1080 K with 0.12% ethanol and 0.12% toluene or 0.12% tri-methylbenzene. The determined rate constants have experimental uncertainties of less than ±15%, with less than ±0.4% uncertainty in the measured temperature. Figure 2 shows that the data that are determined using either terminating species are in excellent agreement with each other.

The multi-channel unimolecular decomposition reactions of ethanol were also investigated theoretically based upon the RRKM/master equation approach (Gilbert and Smith, *Theory of Unimolecular and Recombination Reactions*, Blackwell Scientific Publications, Oxford, U.K., 1990). Consistent with the *ab initio* results of Park et al. *(J. Chem. Phys.* 117:3224, 2002), we only considered the two dominant decomposition channels (R1) and (R2), $C_2H_5OH \rightarrow CH_3 + CH_2OH$, in the analysis. Equilibrium geometries and vibrational frequencies of the reactants, transition states and products were optimized by second-order Moller-Plesset perturbation theory (MP2) with the 6-

---

[+] Bracketed references in the text refer to our recent publications listed at the end of this abstract.

311G(d,p) basis set. Electronic energies of the species were evaluated at G2 level of theory. We also investigated the geometries by the hybrid density functional B3LYP method with the 6-31G(d) basis set and energies at G3B3 level of theory. The results of G2//MP2(FC)/6-311G(d,p) calculations agree very well with those using G3B3//B3LYP/6-31G(d). We used the Gaussian 98 package (*Gaussian 98, Revision A.1*, Gaussian, Inc., Pittsburgh, PA, 1998) for all the molecular orbital calculations.

The rate constants were computed by using the recently updated version of ChemRate (*ChemRate, Version 1.19*, NIST, Gaithersburg, MD, 2002). The molecular parameters were based on MP2(FC)/6-311G(d,p) calculations. The two lowest vibrational frequencies of the tight transition state C_2H_4-H_2O were adjusted to match the present experimental data (Fig.2). The energies for stable compounds were adjusted to match the thermochemical and kinetic data available experimentally. As implemented in ChemRate, the Marcus-Miller quantum approach with a one-dimensional unsymmetrical potential was employed to account for the hydrogen tunneling effect in reaction (R1). At 1 atm pressure, the calculated rate constants k_1 and k_2 indicate that the H_2O elimination reaction dominates over the entire temperature range. Our experimental data and theoretical results for k_1 (Fig. 4) are in excellent agreement with the shock tube data of Herzler et al. and the theoretical work of Tsang (*2nd Joint Meeting of the US Sections of the Combustion Institute*, Paper 92, Oakland, CA, March 2001). At 1 atm pressure and 1100 K, the present theoretical results are about 35% higher than those of Marinov and about 3 times higher than that of Park et al.

2. Comparison of Numerical Computations and Experimental Kinetic Data from Flow Reactors

Flow reactor experiments conducted by various laboratories are frequently compared with zero-dimensional (zero-D) numerical kinetic calculations, thus implying that the experiments involve an initially homogeneous mixture and negligible radial and axial diffusive transport effects. However, finite rate heating and/or mixing phenomena are present in *all* such experiments. These "inlet effects" cause uncertainties in drawing equivalence of a flow reactor residence time computed on a plug-flow basis to an absolute chemical reaction time. However, experimental and computed relative reaction times can be accurately compared. Reactions occurring during the mixing region are concentration- and temperature-dependent, and hence species concentrations downstream where the above assumptions apply may differ from those defined by the initial reactant flow rates to the mixing region.

In some works, e.g. those of Bendtsen et al. (*Combust. Sci. Tech.* 151:1, 2000) and Hunter et al. (*Combust. Flame* 97:201,1994), these issues are implicitly ignored, and the calculated reaction times are referenced to the experimental point of mixing. However, several other approaches can be applied to remove or explicitly include these effects in the comparison of computations and experiments. In cases where the mixing issue only affects the time for radical pool development in both computation and experiment, chemical reactions proceed in the fully mixed, plug flow region downstream, with little perturbation. A time-shifting method with initial composition determined by reactant inlet-flows (Yetter and Dryer, *Combust. Sci. Tech.* 79:129, 1991) can be applied to match the computation and experiment. Uncertainties in the matching parameters can be included in the comparison of experiment and computation, e.g. see Scire [1] and Scire et al. [4], to extract kinetic information. Reactions may also proceed in the mixing region sufficiently to considerably modify the mixture composition entering the downstream plug flow region. We have recently shown that a quasi-steady-state approach can be used to compare the experiment and calculation in the plug flow region. [3]. Finally, entrainment mixing/reactive flow models can be applied when mixing effects potentially occur over the majority of the observed reaction time scale (e.g., Schmidt and Bowman, *Combust. Flame* 127:1958, 2001).

The concepts of matching experiments and computations for flow reactors are frequently questioned by elementary kineticists and modelers. As a result, we have recently presented another fundamental demonstration of the issues by performing some simple calculations using a perfectly-stirred reactor (PSR) model to simulate mixing upstream of the plug flow reacting (PFR) region (Gokulakrishnan et al., *Third Joint Meeting of the U.S. Sections of The Combustion Institute*, University of Illinois, Chicago, March 16-19, 2003). The idealized model represents the two limiting cases for real systems: where instantaneous mixing applies, and where a finite rate mixing occurs upstream of a plug flow reaction zone. In the calculations shown below, the overall reaction time, τ_{res}, is the sum of a characteristic residence time in the perfectly stirred reactor, τ_{psr}, and a plug flow reactor time, τ_{pfr}. The mixing time, τ_{psr}, is varied relative to overall reaction time.

An application of the time-shifting method is shown in Fig. 5 for the moist CO oxidation (Mueller, M. A., et al. *Int. J. Chem. Kinet.* 31:705, 1999), where a PFR calculation (*i.e.*, $\tau_{psr} = 0$) is time-shifted by 101 ms to match the 50% consumption CO in the experiment and computation. A PSR-PFR model ($\tau_{psr} = 180$ ms) calculation is also observed to agree well with the experimental data and time-shifted, PFR computation. A similar comparison using n-heptane VPFR experiments and an appropriate mechanism (Held, T. J. et al., *Combust. Sci. Tech.*, 123:107, 1997) is shown in Fig 6, again demonstrating similar agreement of the PSR-PFR result ($\tau_{psr} = 125$ ms) with the time-shifted (140 ms) PFR computation and the experimental data.

A final example demonstrates issues that can become important where the experiments themselves inseparably involve the mixing perturbations within the measurement method. In isothermal flow reactor experiments on pure methane oxidation (Bendtsen et al.), the experimental PFR reaction time was changed by varying the flow rate

through the reactor. Experiments were compared directly with PFR computations in which τ_{pfr} was defined as the axial distance from the mixing-to-sampling location divided by volume flow rate for each experiment. Figure 7 compares the experimental data and computed results for CH_4 and CO volume fractions (in ppm), with initial reaction temperatures from 1125 to 1225 K. Figure 8 depicts the CO time-history profile (at the initial temperature of 1165 K) calculated using a PSR-PFR simulation with $0 < \tau_{psr} < 50$ ms. For an experimental observation time of $\tau_{psr} + \tau_{pfr} = 214$ ms, the results show that the predicted CO at the reactor exit depends strongly on mixing times over nearly all values that are experimentally realistic. Yet, the actual computed species time-histories for the predicted CO measurement essentially overlap if time-shifting is applied for cases where τ_{psr} reasonably small in comparison to τ_{pfr}. Unfortunately, the experimental data cannot identify separately the mixing and plug flow region, and time shifting cannot be applied. Appropriate model comparisons must couple mixing *and* reaction.

In summary, comparisons of zero-D, homogeneous kinetics computations with flow reactor experiments using time-shifting methods require careful testing with each chemical system *and* proposed kinetic mechanism. We have shown elsewhere (Li et al.) that when time-shifting cannot be applied, quasi-steady approximations may be used for experimental/computational comparisons. In essence, these approaches permit "reaction gradient" comparisons of flow reactor species time-history experiments and zero-D computations. Partially stirred reactor models coupled with a plug flow reactor may also be an approach of interest and will be investigated in future work. Gradient comparison rather than absolute time scale methods are also beneficial in shock tube studies to remove perturbations of observations by the shock condition or impurities affecting overall reaction time observations.

Plans

Reaction systems of present interest over the coming year, in addition to those discussed above, include continued efforts on the pyrolyses and oxidations of acetaldehyde, methyl formate, and toluene, all over a range of pressures and temperatures similar to our previous work.

Publications, 2001 – Present

1. J.J. Scire, "Determination of Elementary Rate Constants by Fitting Complex Reaction Mechanisms: Application to Intermediate-Temperature Hydrocarbon Kinetics", PhD Thesis, Princeton University, Princeton, NJ, 2002, MAE 3101-T.
2. T. Carriere, P.R. Westmoreland, A. Kazakov, A., Y.S. Stein, and F.L. Dryer, "Modeling Ethylene Combustion From Low To High Pressure", 29th International Symposium on Combustion (2002). In press.
3. J. Li, A. Kazakov, and F.L. Dryer, "Ethanol Pyrolysis Experiments in a Variable Pressure Flow Reactor", *Int. J. Chem. Kin.* 33:859-867 (2001).
4. J.J. Scire, R.A. Yetter, and F.L. Dryer, "Comparison of Global and Local Sensitivity Techniques for Rate Constants Determined Using Complex Reaction Mechanisms", *Int. J. Chem. Kin.* 33:780-852 (2001).
5. J.J. Scire, Jr., S. D. Klotz, and F.L. Dryer, "Initial Observations of Ketene in Flow Reactor Kinetic Studies", *Zeitscheift fur Physikalishche Chemie* 215:1011-1023 (2001).
6. J.C. Lee, R.A. Yetter, F.L. Dryer, A.G. Tomboulides, and S.A. Orszag, "Simulation and Analysis of Laminar Flow Reactors", *Combust. Sci and Tech.* 159:199-212 (2001).
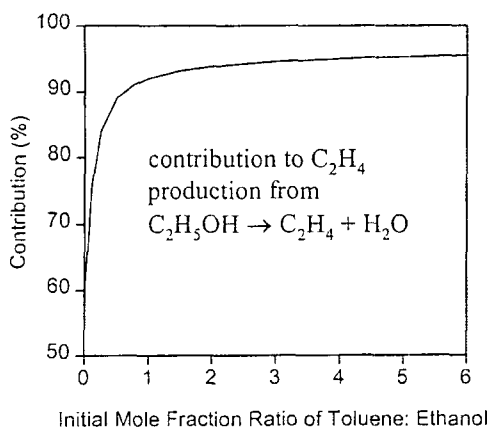
Figure 1 - Integrated contributions of the reaction $C_2H_5OH \rightarrow C_2H_4 + H_2O$ to C_2H_4 yield in a pyrolysis as a function of the toluene/ethanol mole fraction in the initial mixture. Model: ethanol (Marinov, 1999) and toluene (Emdee et al., 1992). Initial conditions: T = 1050 K, P = 3 atm, C_2H_5OH = 0.15% with corresponding toluene and balanced N_2.
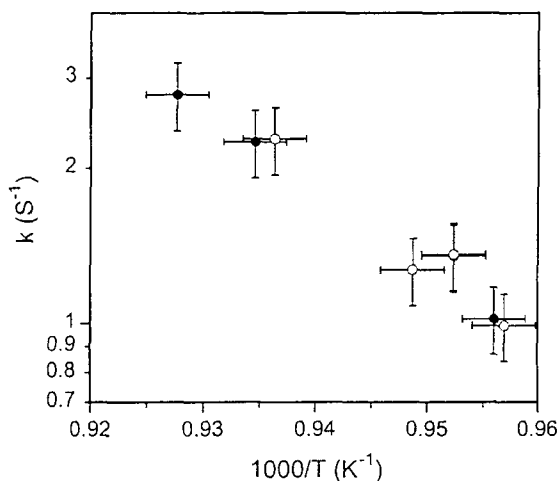
Figure 2 - Rate constant for the reaction $C_2H_5OH \rightarrow C_2H_4 + H_2O$ determined in the present flow reactor experiments. Open symbols represent results by using toluene as a radical trapper, closed symbols by using 1,3,5-trimethylbenzene as a radical trapper.
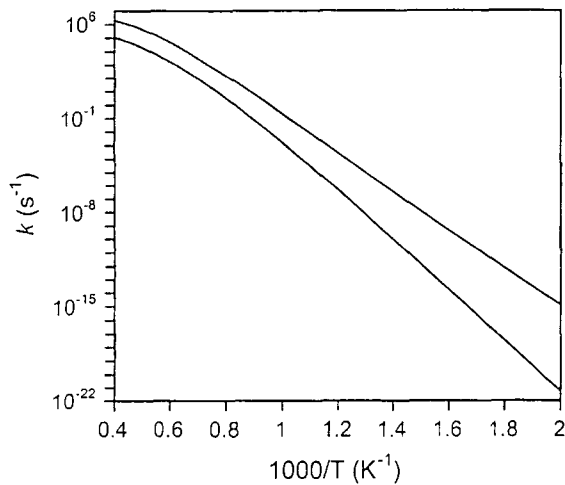
Figure 3 - Rate constants of the ethanol decomposition reactions at 1 atm.

Figure 4 - Rate constant for the reaction $C_2H_5OH \rightarrow C_2H_4 + H_2O$. Symbols represent experimental data; lines are theoretical calculation results at 1 atm, except that of Setser et al. (*J. Phys. Chem.* 98:10779, 1994) which represents the high-pressure limit rate constant.

Figure 5 - CO oxidation at 3.5 atm and 1038 K in the VPFR. Symbols show the experimental data from Mueller *et al.* The solid-line indicates the plug-flow modeling with a time-shift of 101 ms. The dashed lines show the PSR-PFR modeling results for $\tau_{psr} = 0$ and 180 ms.
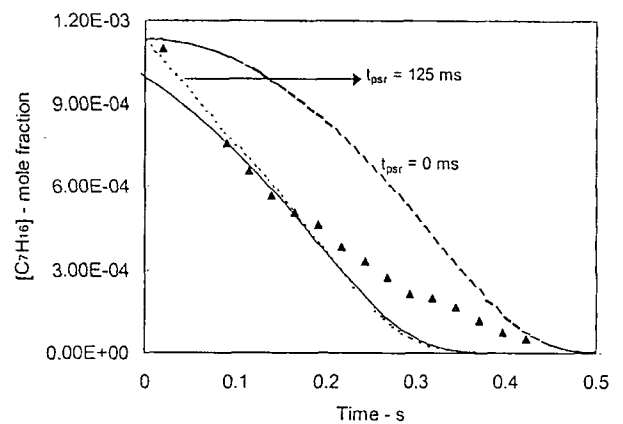
Figure 6 - n-C_7H_{16} oxidation at 3 atm and 940 K in the VPFR. Symbols show the experimental data from Held *et al.* The solid-line indicates the plug-flow modeling with a time-shift of 140 ms. The dashed lines show the PSR-PFR modeling results for $\tau_{psr} = 0$ and 125 ms.

Figure 7 - Concentrations of CO and CH_4 measured at the exhaust of an isothermal, tubular flow reactor during the oxidation of CH_4 from Bendtsen et al. The inlet gas composition to the reactor was 2276 ppm CH_4, 3.69mole% O_2 and 4 mole% H_2O in N_2. The symbols denote the experimental measurements (circle – CH_4 & triangle – CO), and the lines represent the plug-flow modeling results. The residence time = 249.6/T.

Figure 8- Time-history profile of CO calculated for different τ_{psr} values at 1165 K for the experimental conditions specified in Fig. 7. The experimental overall residence time of interest ($\tau_{psr} + \tau_{pfr}$) consistent with the experimental correlation presented in Fig. 7 is 0.214 s.

LASER PHOTOELECTRON SPECTROSCOPY OF IONS

G. Barney Ellison
Department of Chemistry & Biochemistry
University of Colorado
Boulder, CO 80309-0215
Email: **barney@JILA.colorado.edu**

1. <u>Organic Radicals as Revealed by Photoelectron and Matrix Spectroscopy</u>

We have used negative ion photoelectron spectroscopy to study the peroxide ions: (HOO^-, CH_3OO^-, $CH_3CH_2OO^-$) and the cyanocarbenes: ($HCCN^-$, and $HCNC^-$). We find the electron affinities of all the peroxyl radicals to be about 1 eV and the term values of the lowest lying near-IR state to be roughly 0.9 eV. Thus $EA(HOO) = 1.078 \pm 0.006$ eV and $T_0(\tilde{X}\,^2A'' - \tilde{A}\,^2A') = 0.872 \pm 0.007$ eV; $EA(CH_3OO) = 1.161 \pm 0.005$ eV and $T_0(\tilde{X}\,^2A'' - \tilde{A}\,^2A')[CH_3OO] = 0.914 \pm 0.005$ eV; $EA(CH_3CH_2OO) = 1.186 \pm 0.004$ eV and $T_0(\tilde{X}\,^2A'' - \tilde{A}\,^2A')\,[CH_3CH_2OO] = 0.938 \pm 0.004$ eV. The electron affinities of cyanocarbene have been measured to be $EA(HCCN\ \tilde{X}\,^3\Sigma^-) = 2.003 \pm 0.014$ eV and $EA(DCCN\ \tilde{X}\,^3\Sigma^-) = 2.009 \pm 0.020$ eV. Photodetachment of $HCCN^-$ shows a 0.4 eV long vibrational progression in v_5, the H-CCN bending mode; the $HCCN^-$ photoelectron spectra reveal excitations up to 10 quanta in v_5. The term energies for the excited singlet state are found to be $T_0(HCCN\ \tilde{a}\,^1A') = 0.515 \pm 0.016$ eV and $T_0(DCCN\ \tilde{a}\,^1A') = 0.518 \pm 0.027$ eV. For the isocyanocarbene, the two lowest states switch and HCNC has a singlet ground state and an excited triplet state. The electron affinities are $EA(HCNC\ \tilde{X}\,^1A') = 1.883 \pm 0.013$ eV and $EA(\tilde{X}\,^1A'\ DCNC) = 1.877 \pm 0.010$ eV. The term energy for the excited triplet state is $T_0(HCNC\ \tilde{a}\,^3A'') = 0.050 \pm 0.028$ eV and $T_0(DCNC\ \tilde{a}\,^3A'') = 0.063 \pm 0.030$ eV.

We have begun to use a hyperthermal nozzle to generate organic radicals for matrix isolation spectroscopy. Our nozzle is patterned after the pioneering work of Peter Chen's device and a description of our matrix experiment is presented in Rev. Sci. Instruments. Fig. 1 is a sketch of our pulsed hyperthermal nozzle. The hyperthermal nozzle is mounted on a cryostat and fires at a rate of 30 — 100 Hz and is open for roughly 150 μsec. The nozzle generates about 10^{13} radicals pulse^{-1} and a nozzle residence time of approximately 30 μsec.

Hyperthermal Nozzle Production of Organic Radicals: $RX + \Delta \rightarrow R + X$

$$[R] \cong 10^{13} \text{ pulse}^{-1}$$
$$\tau(\text{nozzle}) \cong 30 \text{ } \mu\text{sec}$$

1 mm ID SiC tube
@ 300–1800 K

← R$^+$ photoions:
TOF detection

1 Torr RX in $\cong$ 1.5 atm Ar
behind a pulsed valve

Supersonic Jet of
Radicals/Ar into 10^{-5} Torr

118.2 nm VUV
Photoionization Laser

$h\nu + R \rightarrow R^+ + e^-$

20 K CsI window for
Matrix IR spectroscopy
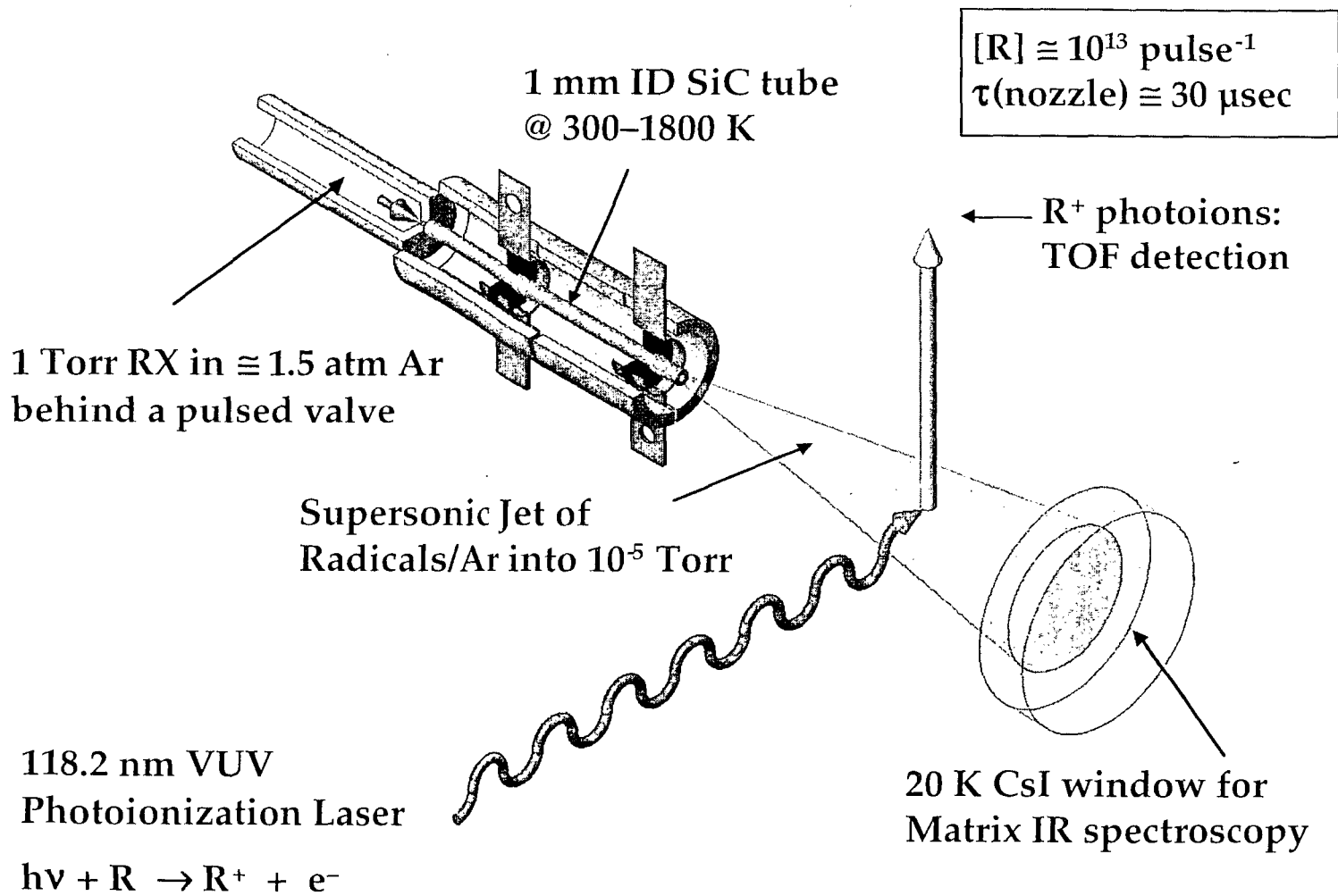
Recently we have used the hyperthermal nozzle to generate samples of the phenyl radical (C_6H_5), the allyl radical (CH_2CHCH_2), the methyl radical (CH_3), and the methylperoxyl radical (CH_3OO). Because we have a "rational synthesis" for these radicals, it is possible to measure a vibrational force field for each of these species.

2. Thermochemistry of Organic Radicals and Ions

In collaboration with Prof. H. F. Schaefer XIII, we have published a review of all atomic and molecular electron affinities. This paper lists that experimental electron affinities of 1100 atoms and molecules. For many years we have used the negative ion/acidity thermochemical cycle that connects the gas phase acidity of a hydrocarbon, $\Delta_{acid}H_{298}(RH)$, with the bond dissociation enthalpy, $DH_{298}(R\text{-}H)$, and the electron affinity of the radical, $EA(R)$: $\Delta_{acid}H_{298}(RH) = DH_{298}(R\text{-}H) + IE(R) - EA(R)$. This cycle permits us to measure the bond energies of many polyatomic molecules. We have completed a small review of bond energies (aimed at experimental chemists) that lists roughly 110 bond enthalpies.

3. Reaction Dynamics of Organic Peroxyl Radials and NO

The conversion of peroxyl radicals to organic nitrates *via* reaction with NO is of importance in combustion and atmospheric chemistry: $ROO + NO \rightarrow RONO_2$. The mechanism for nitrate formation is obscure; no previous theoretical results have been even vaguely consistent with the experimental evidence. We propose a simple valence bond argument to rationalize how an initially formed pernitrite, $ROO\text{-}N=O$, can decompose to an alkoxy radical and NO_2 or rearrange to $RONO_2$. This qualitative mechanism, which involves the coupling of two valence bond states, is supported by coupled-cluster electronic structure calculations that predict a pernitrite/nitrate isomerization barrier of *ca.* 20–30 kcal mol^{-1}. The exothermicity of the radical/radical addition provides the chemical activation for reaction. In addition to its importance for atmospheric chemistry, it is likely that this mechanism is also responsible for the thermal decomposition of nitramines and organic nitro compounds (explosives and solid propellants), $RNO_2 + heat \rightarrow products$.

DOE Publications

- A.V. Friderichsen, J. G. Radziszewski, M. R. Nimlos, P. R. Winter, D. C. Dayton, D. E. David and G. B. Ellison, "The Infrared Spectrum of the Matrix-Isolated Phenyl Radical", J. Am. Chem. Soc., **123**, 1977-1988 (2001).
- S. J. Blanksby, T. M. Ramond, G. E. Davico, M. R. Nimlos, S. Kato, V. M. Bierbaum, W. C. Lineberger, G. B. Ellison and M. Okumura, "Negative Ion Photoelectron Spectroscopy, Gas Phase Acidity, and Thermochemistry of the Peroxyl Radicals CH_3OO and CH_3CH_2OO", J. Am. Chem. Soc.,**123**, 9585-9596 (2001).
- Syomin, J. Kim, B. E. Koel and G. B. Ellison, "Identification of Adsorbed Phenyl (C_6H_5) Groups on Metal Surfaces: Electron-induced Dissociation of Benzene on Au(111)", J. Phys. Chem. B, **105**, 8387-8394 (2001).
- S. Nandi, P. A. Arnold, B. K. Carpenter, M. R. Nimlos, D. C. Dayton and G. B. Ellison, "Polarized Infrared Absorption Spectrum of Matrix-Isolated Allyl Radicals", J. Phys. Chem. A, **105**, 7514-7524 (2001).
- Jon C. Rienstra-Kiracofe, G. S. Tschumper, Henry F. Schaefer III, Sreela Nandi and G. Barney Ellison, "Atomic and Molecular Electron Affinities: Photoelectron Experiments and Theoretical Computations," *Chem. Revs.*, **102**, 231-282 (2002).
- S. Nandi, S. R. Blanksby, X. Zhang, M. R. Nimlos, D. R. Dayton and G. B. Ellison, "Polarized Infrared Absorption Spectra of Matrix-Isolated Methylperoxyl Radicals, CH_3OO $\tilde{X}$ $^2A''''$", J. Phys. Chem. A, **106**, 7547-7556 (2002).
- M. R. Nimlos, G. E. Davico, C. M. Geise, P. G. Wenthold, W. C. Lineberger, S. J. Blanksby, C. M. Hadad, G. A. Petersson, G. B. Ellison, "Photoelectron spectroscopy of $HCCN^-$ and $HCNC^-$ reveals the quasilinear triplet carbenes, HCCN and HCNC," J. Chem. Phys., **117**, 4323-4339 (2002).
- S. J. Blanksby, S. Kato, V. M. Bierbaum, G. B. Ellison, "Ion Induced Fragmentation of Alkylhydroperoxides," *J. Am. Chem. Soc.* 2002, *124*, 3196-3197 (2002).
- T. M. Ramond, S. J. Blanksby, S. Kato, V. M. Bierbaum, G. E. Davico, R. L. Schwartz, W. C. Lineberger and G. B. Ellison, "The Heat of Formation of the Hydroperoxyl Radical HOO *via* Negative Ions", J. Phys. Chem. A, **106**, 9641-9647 (2002).
- Stephen J. Blanksby and G. Barney Ellison, "Bond Dissociation Energies of Organic Molecules," Acct. Chem. Res. **(in press, 2003).**
- X. Zhang, A. V. Friderichsen, J. T. McKinnon, T. G. Lindeman, D. E. David, D. C. Dayton, S. Nandi, G. B. Ellison, and M. R. Nimlos, "An Intense, Hyperthermal Source of Organic Radicals for Matrix-Isolation Spectroscopy" Rev. Sci. Instrum. **(in press, Feb. 2003).**
- Stephen J. Blanksby, Veronica M. Bierbaum, G. Barney Ellison, and Shuji Kato, "Fragmentations of Deprotonated Alkyl Hydroperoxides (ROO^-) Upon Collisional Activation: A Combined Experimental and Computational Study, Australian J. Chemistry **(submitted, Jan. 2003).**
- G. Barney Ellison, Stephen J. Blanksby, and Evan Jochnowitz, and John F. Stanton, "The Role of a Novel Diradical Pathway in Reactions between Alkylperoxyl Radicals and NO", Science **(submitted, March 2003).**

Thermochemistry of Hydrocarbon Radicals:
Guided Ion Beam Studies

Kent M. Ervin
Department of Chemistry/216
University of Nevada, Reno
Reno, Nevada 89557
Telephone: 775-784-6676
E-mail: ervin@chem.unr.edu

Project Scope

Gas phase negative ion chemistry methods are employed to determine enthalpies of formation of hydrocarbon radicals that are important in combustion processes and to investigate the dynamics of ion–molecule reactions. Using guided ion beam tandem mass spectrometry, we measure collisional threshold energies of endoergic proton transfer and hydrogen atom transfer reactions of hydrocarbon molecules with negative reagent ions. The measured reaction threshold energies for proton transfer yield the relative gas phase acidities. In an alternative methodology, competitive collision-induced dissociation of proton-bound ion–molecule complexes provides accurate gas phase acidities relative to a reference acid. Combined with the electron affinity of the R· radical, the gas phase acidity yields the RH bond dissociation energy of the corresponding neutral molecule, or equivalently the enthalpy of formation of the R· organic radical. The threshold energy for hydrogen abstraction from a hydrocarbon molecule yields its hydrogen atom affinity relative to the reagent anion, providing the RH bond dissociation energy directly. Electronic structure calculations are used to evaluate the possibility of potential energy barriers or dynamical constrictions along the reaction path, and as input for RRKM and phase space theory calculations. In new experiments, we are measuring the product velocity distributions to obtain additional information on the energetics and dynamics of the reactions.

Recent Progress

Product Velocity Distribution Measurements

We are taking two approaches toward measuring velocity distributions of the products of ion molecule reactions. These will provide information on the energy partitioning in the reactions. First, we have modified our guided ion beam tandem mass spectrometer to do time-of-flight measurements on product ions. Our first results are described below. Second, in a longer-term project, we are constructing a new instrument for ion product velocity imaging from pulsed crossed beam reactions.

To perform product velocity measurements, the octopole beam guide has been split into two sections, with a reaction cell in the first section and a time-of-flight region in the second

longer section. The ion beam is pulsed by a set a deflectors following the first mass spectrometer. The times-of-flight of reactant and product ions are measured and converted into relative product velocities in the center-of-mass frame. Our first publication using the guided beam product velocity distribution techinque[1] is a study of the $Cl^- + CH_3Br \rightarrow ClCH_3 + Br^-$ reaction, chosen because its kinetic energy release had been investigated before using other techniques. We observed new features in both the total cross sections and the product velocity distributions, with three main regimes: (1) a statistical product energy distributions at near-thermal collision energies, (2) forward-scattered $ClCH_3$ (relative to Cl^-) at 0.2–0.5 eV collision energy, and (3) back-scattering at higher collision energies of 1–4 eV.

We are now conducting a series of experiments measuring the product velocity distributions for hydrogen atom transfer reactions of S^- with H_2, CH_4, and C_2H_6. We have investigated the collision energy dependence of the total reaction cross sections for these reactions with the hope of using the threshold energies to obtain the radical product enthalpies of formation. Although this worked well for the hydrogen reaction,[2] for the hydrocarbons we observed large reverse activation energy barriers. Ab initio potential energy surfaces show either no (H_2) or low (CH_4, C_2H_6) energy barriers along the reaction path, but these latter barriers are not high enough to explain the elevated threshold energies.
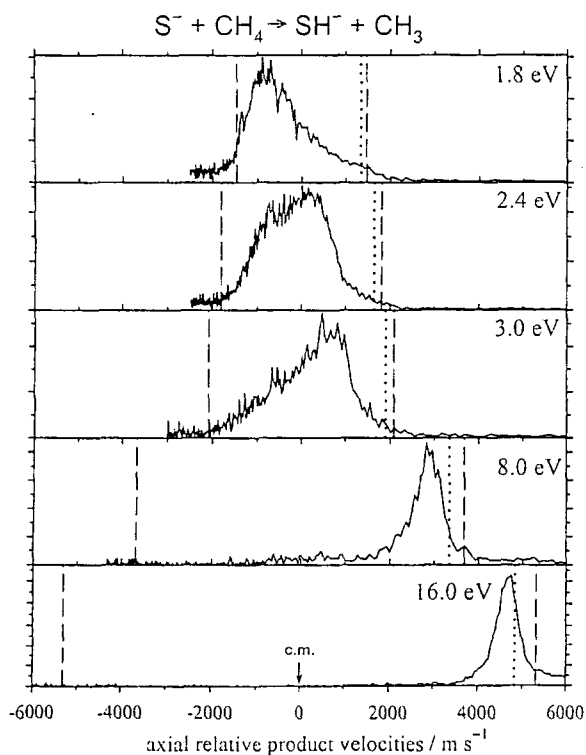
Examining the product velocities provides a handle on the dynamics of the reactions. The figure shows product velocities for $S^- + CH_4$ for several collision energies from just above threshold and higher. Near threshold, the SH^- product is back-scattered, consistent with direct collisions with low impact parameters needed to drive the endoergic reaction. At higher energies, a forward scattered feature becomes dominant.

$$S^- + CH_4 \rightarrow SH^- + CH_3$$

axial relative product velocities / m s^{-1}

The dashed vertical lines are energy limits (neglecting experimental broadening), and the dotted vertical line is the spectator stripping velocity, approached at the highest collision energy. We are exploring modeling the velocity distributions to obtain reaction energetics information.

Proton Transfer

Proton transfer reactions have been our favored method for using ion thermochemistry to derive neutral radical thermochemistry. We measure gas phase acidities via proton transfer

reactions, and then use literature electron affinities of the radicals from negative ion photoelectron spectroscopy to derive the CH bond energies. With former student Vincent DeTuri (Department of Chemistry, Ithaca University), we carried out a computational and thermochemical reexamination of the gas phase acidity scale,[3] which is required for calibrating our relative acidity measurements. New experimental results from our group and others were utilized to construct an accurate gas phase acidity scale at 0 K. The gas phase acidities were also calculated by several different levels of theory, comparing their accuracy. It was found that G3, CBS, and DFT methods are insufficiently accurate for benchmark acidities, but CCSD(T)/aug-cc-pVTZ or a higher level of theory is usually adequate (but impractical for large systems).

A series of endoergic proton transfer reactions have been studied to determine the limits of accuracy of the threshold method. In most cases, the observed threshold is at the thermochemical endothermicity. Detailed modeling of the threshold behavior shows that translational and vibrational energy are fully available for promoting these reactions, but that the internal rotational energy of the reactants may not be fully available. However, for a few systems there are large excess energy thresholds, even though the potential energy surface has no barrier above the reaction endothermicity. We are currently completing a detailed theoretical study of the potential energy surfaces for the "well behaved" and "poorly behaved" proton transfer systems. None of the surfaces have a double well associated with proton transfer, but a key feature for the systems with high threshold energies appears to be a plateau in the product channel related to transfer of the proton from reactant to product.

Polyyne Thermochemistry

Experimental work on proton transfer and hydrogen atom transfer reactions of C_n^- and C_nH^- ions (n = 2,4, 6, and 8) has been completed, extending preliminary work published on diacetylene.[4] We reported preliminary results for the C–H bond dissociation energies of $C_{2n}H_2$ (n = 2, 3, 4) at 2002 DOE Combustion Research Meeting. Finalizing the analyses with proper rigor requires additional ab initio calculations on transitions states and a major revision of our RRKM modeling code to hand multi-well potentials. The RRKM coding has been mostly completed, but there has been a computational bottleneck for completing the ab initio calculations and finding all of the transition states. The UNR Chemistry Department recently acquired a Beowulf cluster that will speed progress on this project.

Future Directions

Our new experimental capability to distinguish reaction mechanisms via product energy distributions will enhance our understanding of proton transfer and hydrogen atom transfer reactions related to combustion chemistry. We further plan to use the energy release distributions for thermochemical measurements, as an adjunct to reaction threshold energy measurements. By fixing the reactant collision energy and measuring the product energies, we can use energy balance to determine reaction enthalpies (either directly from the maximum kinetic energy release or via models of the dynamics). This method should be useful for systems where we have previously found collision energy barriers in excess of the reaction endothermicity.

References

(1) Angel, L. A.; Ervin, K. M. *J. Am. Chem. Soc.* **2003**, *125*, 1014-1027.

(2) Rempala, K.; Ervin, K. M. *J. Chem. Phys.* **2000**, *112*, 4579-4590.

(3) Ervin, K. M.; DeTuri, V. F. *J. Phys. Chem. A* **2002**, *106*, 9947-9956.

(4) Shi, Y.; Ervin, K. M. *Chem. Phys. Lett.* **2000**, *318*, 149-154.

Publications, 2001–present

"Experimental techniques in gas phase ion thermochemistry", K. M. Ervin, *Chem. Rev.* **101**, 391-444 (2001). Erratum, *ibid.* **102**, 855 (2002).

"Dynamics of the gas-phase reactions of fluoride ions with chloromethane", L. A. Angel and K. M. Ervin, *J. Phys. Chem. A*, **105**, 4042-4051 (2001).

"Naphthyl radical: Negative ion photoelectron spectroscopy, Franck-Condon simulation, and thermochemistry", K. M. Ervin, T. M. Ramond, G. E. Davico, R. L. Schwartz, S. M. Casey, W. C. Lineberger, *J. Phys. Chem. A*, 105, 10822-10831 (2001).

"Dynamics of the gas-phase reactions of chloride ions with fluoromethane", L. A. Angel, S. P. Garcia, and K. M. Ervin, *J. Am. Chem. Soc.* **124**, 336-345 (2002).

"Microcanonical analysis of the kinetic method. The meaning of the 'apparent entropy'", K. M. Ervin, *J. Am. Soc. Mass Spectrom.* **13**, 435-452 (2002).

"Anchoring the gas-phase acidity scale", K. M. Ervin and V. F. DeTuri, *J. Phys. Chem. A*, **106**, *9947-9956* (2002).

"Gas-phase S_N2 and bromine abstraction reactions of chloride ion with bromomethane: Reaction cross sections and energy disposal into products", L. A. Angel and K. M. Ervin, *J. Am. Chem. Soc.* **125**, 1014-1027 (2003).

Experimental Kinetics and Mechanistic Investigations of Hydrocarbon Radicals Relevant to Combustion Modeling

Askar Fahr
Physical & Chemical Properties Division
National Institute of Standards and Technology
Gaithersburg, MD 20899-8382
askar.fahr@nist.gov

SCOPE OF THE PROGRAM

This project is concerned with the kinetics, dynamics, and mechanistic studies of key hydrocarbon radical reactions of importance to the formation of aromatic and polyaromatic hydrocarbons and relevant to the inception of soot. The investigation is currently focused on determining rate parameters, branching ratios and products of radical-radical and radical-molecule reactions involving vinyl (C_2H_3) and propargyl ($HCCCH_2$) radicals. Reactions of these radicals are often included in models for hydrocarbon polymerization and soot formation, however, the proposed mechanisms are somewhat speculative since detailed and concrete relevant laboratory data for confirmation and/or calibration of computational predictions are very limited or are unavailable.

Methods employed for our studies include, excimer-laser photolysis for generating the radicals, time-resolved UV-absorption spectroscopy for direct kinetic studies, GC/MS methods for identification and quantification of final reaction products as well as for comparative rate determinations. Detailed kinetic modeling is used for data analysis and interpretations. For a detailed understanding of the reaction mechanisms emphasis is given to determination of the isomeric nature of the products and on examining the effects of pressure and temperature on product channels and on the nature and yields of the reaction products.

RECENT PROGRESS

a. C_3H_3 + C_3H_3: The combination reaction of propargyl radicals, C_3H_3 + C_3H_3 -->C_6H_6, is believed to be a key cyclization step in hydrocarbon combustion reactions which can initiate subsequent formation of larger polyaromatic hydrocarbons and soot. Despite the importance of this reaction only limited experimental product studies, in very narrow ranges of pressure and/or temperature conditions, have been reported.[1,2] Miller and Klippenstein[3] have recently reported a comprehensive computational study of the C_3H_3+C_3H_3 reaction predicting thermal rate coefficients, potential energy surfaces for various isomerization paths, and product distributions. Detailed knowledge of the isomeric distribution of C_6H_6 products and effects of temperature and pressure on yields and nature of the products are of significance. In continuation of our efforts to understand properties of propargyl radicals, we have carried out detailed product studies of the propargyl combination reaction over wider ranges of pressure (20 to 700 Torr) and temperature (295 to 525 °K) than earlier studies. Propargyl radicals were

generated, in most experiments, by the 248 nm excimer laser photolysis of propargyl bromide. In addition, the 193 nm photolysis of propargyl chloride or allene were also used as propargyl radical sources. The final reaction products were separated, identified and quantified using an on-line gas chromatograph/mass spectrometer system. A number of available C_6H_6 isomeric calibration samples were used for isomeric identification of the products. Calibration samples of fulvene and dimethylenecyclobutene were synthesized in our laboratory specifically for this study. Six C_6H_6 isomeric final products were separated and detected and four could be identified. The identified products are, 1,5-hexadiyne, dimethylenecyclobutene, fulvene and benzene. One of the unidentified C_6H_6 products has retention time close to that of 1,5-hexadiyne, but its identity could not be established with certainty due to unavailability of a calibration sample. However, this product is likely to be 1,2-hexadiene-5-yne which is expected to be formed from the "head-to-tail" addition of propargyl radicals and has been detected in two previous product studies (one from our laboratory) of the propargyl combination reaction.[1,2] The formation of this isomer has also been predicted computationally.[3] No evidence of phenyl radical formation, under the experimental conditions of this study, was detected.

The following table lists the relative yields of various C_6H_6 products at two sets of pressure and temperature conditions.

Relative yields (%) of C_6H_6 isomeric products formed from the propargyl combination reaction.

C$_6$H$_6$ Product	P=700 Torr		P=20 Torr	
	T=295 K	T=525 K	T=295 K	T=525 K
1,5-Hexadiyne	55	39.	42	23
1,2-Hexadiene-5-yne*	28.5	31.5	25	18.5
Dimethylenecyclobutene	2	12	4.5	24
Fulvene	0.5	~0.1	1	0.5
Benzene	6	3.5	21	22
Unidentified	8	14	6.5	12

* Predicted isomer

The relative yields of the major reaction products show significant pressure and temperature dependencies. Under pressure and temperature conditions of this study 1,5-hexadiyne is the most abundant product and its relative yield decreases with reducing the pressure or increasing the temperature. The relative yield of dimethylenecyclobutene, another major product, is larger at lower pressures and higher temperatures. Fulvene appears to be a minor product at all conditions of the study. The relative yields of dimethylenecyclobutene and fulvene, determined experimentally, are significantly lower than the predicted yields. Interestingly, appreciable amounts of benzene is formed, particularly at lower pressures, with relative yields considerably higher than those predicted computationally (<1% at T=500K, P=20 Torr).

A manuscript describing our results is near completion.

b. $C_2H_3+C_2H_4$, $C_2H_3+HCCCH_3$ and $C_2H_3+H_2CCCH_2$: We have initiated investigations of the pressure and temperature dependent kinetics and product studies of vinyl radical reactions with ethylene, propyne and allene. The direct kinetic studies are

(and will be) performed both at NIST and at CRF, in collaboration with Dr. Craig Taatjes. Product studies are performed at NIST. Vinyl radicals in these studies are generated either by 248 nm photolysis (NIST) or 266 nm photolysis (CRF) of vinyl iodide. Time profiles of vinyl radicals are probed directly at 230 nm region (NIST) or 420 nm, using a multipass Herriott-type cell (CRF).

Preliminary kinetic results for the $C_2H_3+C_2H_4$ reaction, determined at 720 K, suggest a rate constant of $\sim2 \times 10^{-13}$ cm^3 molecule^{-1} s^{-1}. Product studies identified 1-butene and 1,3-butadiene as the major final products. The yield of these products show significant pressure and temperature dependencies.

Preliminary results for the $C_2H_3+HCCCH_3$ reaction indicate a room temperature rate constant of $(0.5$ to $1)\times10^{-15}$ cm^3 molecule^{-1} s^{-1}. Product studies, performed at ambient temperature, indicate formation of ethane, acetylene, butadiene and allene as major products. Allene is formed from isomerization of photoexcited propyne. The C_2H_4/C_2H_2 ratio indicated minor formation of ethylene from channel(s) other than vinyl combination, most likely from the H-abstraction from propyne. The follow-up studies will be performed at elevated temperatures.

For the reaction $C_2H_3+H_2CCCH_2$, a rate constant of $\sim2\times10^{-15}$ cm^3 molecule^{-1} s^{-1} at room temperature has been determined. Product analysis studies at room temperature indicated the formation of propyne (from isomerization of allene) as one of the major products. In addition, ethane, ethylene, propene, butadiene and trace amounts of a number of C_5 and C_6 hydrocarbons were detected. At elevated temperatures (up to about 420 K) very congested GC/MS traces of reaction mixtures indicated formation of a large number of products, with significantly higher yields than those at room temperature or formation of products which were not detected at low temperatures. These additional products included several isomeric forms of C_4H_6, C_4H_8, C_5H_6, C_6H_6 (5 isomers) and C_6H_8. These are very interesting and potentially important findings. To help in identifying the reaction(s) leading to these products, a number of test experiments were performed. The preliminary results indicated a significant photodissociation (248 nm) of allene at higher temperatures resulting to a number of products also formed in photolyzed vinyliodide/allene/Ar samples. The photodissociation of allene at 248 nm (as in the case of the 193 nm photolysis) most likely leads to the formation of radical species, particularly propargyl radicals and H-atoms. The subsequent radical-radical and radical-molecule reactions can have significant contributions to the formation of larger hydrocarbons as evidenced from the product analysis results. Therefore, kinetics and products studies of the vinyl+allene at high temperatures should follow a detailed investigation of the photolysis of allene at elevated temperatures.

FUTURE PLANS

Our immediate future work will focus on continuing and completing the kinetics and product studies of the vinyl radical reactions, $C_2H_3+C_2H_4$, $C_2H_3+HCCCH_3$ and $C_2H_3+H_2CCCH_2$. Particular attention will be given to see if any of the addition products will undergo isomerization and/or cyclization. Based on our preliminary results, these reactions are relatively slow. Thus most kinetics and product studies will be performed at elevated temperatures.

In addition, the following radical-radical and radical-molecule reactions involving vinyl and propargyl radicals will be investigated.

Radical-Radical Reactions. We will expand our investigations of the radical-radical reactions and examine effects of pressure and temperature on the combination reactions, **vinyl+vinyl**, and **vinyl+propargyl**. Once again, the emphasis of the studies will be on the nature and yields of the combination products as a function of temperature and pressure

Propargyl + Acetylene. This important process can yield cyclopentadienyl. An interesting issue is the pressure dependence of the process. The product analysis should be particularly intriguing. Will a C_8 adduct or C_{10} adduct be formed? The nature of the latter is particularly interesting. It is possible that cyclopentadienyl combination produces naphthalene.

Propargyl + Allene has been cited by Westmoreland et al[4] as an important source of benzene. The rate constant determinations and product analysis studies should yield valuable information on the importance of this reaction.

Vinyl + 1,3-Butadiene can yield 1,3,5-hexatriene or 1,3-butadienyl-1. The latter can react further with 1,3-butadiene to form 1,3,5,7-octatetraene. Both are candidate precursors for cyclization via a molecular channel.

References:
1. Fahr A.; Nayak. A. K. Intl. J. Chem. Kinetics **2000**, *32*, 118.
2. Alkemade U. and K. H. Homann, Zeitsch. Phys. Chem., **1999**, *161*, 19.
3. Miller, J. A. and Klippenstein, S. J.; *J.Phys.Chem.A* **2001**, *105*, 7254 .
4. Westmoreland, P.R., Dean, A.M. Howard, J.B. and Longwell J.P., *J. Phys Chem.* **1989**, *93*, 8171

Low Energy Ion-Molecule Reactions

James M. Farrar
Department of Chemistry
University of Rochester
Rochester, NY 14627
E-mail: farrar@chem.rochester.edu

Program Scope

This research effort probes elementary collision dynamics in ionic systems, both in the gas phase and at liquid interfaces, at chemically relevant energies. The objective of this study is to use crossed beam techniques at low collision energy to provide fundamental dynamical information that validates, tests, and extends theories and models for elementary reaction rates. The concepts, methods, and results can be transferred to the complex environment of hydrocarbon combustion. The long-standing goal of the dynamical studies conducted at Rochester is to probe the potential energy surfaces for elementary gas phase ionic reactions. Questions of preferred reactant orientation, potential surface constraints that are both energetic and entropic in nature, and product energy disposal at the quantum state-resolved level have been studied in the context of ionic systems, but the general concepts and models are applicable to all elementary reactive processes important in combustion. In recent years, a significant portion of our gas phase work has been on benchmark systems such as $O^- + D_2$ and HF and $OH^- + D_2$, as well as more complex systems such as $O^- + H_2O$, NH_3, and CH_4. A long-standing goal of our gas phase research effort has been to extend the simple concepts that correlate potential surface topology in model $A + BC$ systems to reactions of greater complexity. Much of the insight that our studies have provided has come from recognition that only a few key coordinates must be considered in detail in elucidating the dynamics of complex systems.

Recent Progress

Our recent work has focused on hydrogen atom abstraction and charge transfer in the reaction of O^+, OH^+ and H_2O^+ ions with hydrocarbons. Tabulated thermochemical data show that the abstraction reactions of hydrogen atoms from alkanes, alkenes, and alkynes by O^+ are exothermic by 0.25 to 0.7 eV, with the exothermicity increasing with increasing saturation. The OH^+ ion also undergoes abstraction reactions with these substrates, with the exothermicities approximately 0.3 to 0.6 eV larger than for the corresponding O^+ reaction. Consequently, good model systems in the gas phase are reactions of these ions with small hydrocarbons. We have begun such studies on the reactions of OH^+ with C_2H_4. We have performed measurements of differential cross sections for reactive channels in this system, listed here:

$$OH^+ + C_2H_4 \rightarrow OH + C_2H_4^+ \qquad \Delta H = -2.7 \text{ eV} \qquad \text{(charge transfer)}$$
$$OH^+ + C_2H_4 \rightarrow O + C_2H_5^+ \qquad \Delta H = -2.3 \text{ eV} \qquad \text{(proton transfer)}$$
$$OH^+ + C_2H_4 \rightarrow H_2O + C_2H_3^+ \qquad \Delta H = -5.3 \text{ eV} \qquad \text{(hydride transfer)}$$
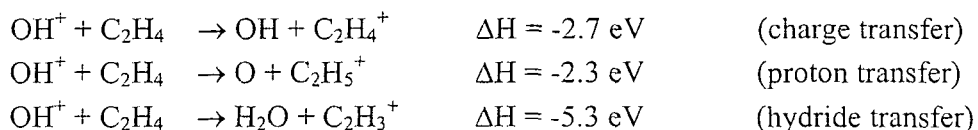
These measurements have been made at collision energies of 0.33, 0.67, and 1.0 eV. In of these reactions, the charge remains on the hydrocarbon fragment. We have not observed the reaction of hydrogen atom transfer to form $C_2H_3 + H_2O^+$, even though the process is exothermic. We expect to carry out *ab initio* calculations to understand key features of the potential energy surfaces that control these branching ratios. The three processes indicated above are all facile in the energy range we have examined, all proceeding as direct reactions. Both proton transfer and hydride transfer mimic the charge transfer process to the extent that these reactions appear to proceed as large impact parameter processes.

Publications, 2000-2003

Susan Troutman Lee, Elizabeth Richards O'Grady, Michael A. Carpenter, and James M. Farrar, "Dynamics of the Reaction of O⁻ with D_2 at Low Collision Energies: Reagent Rotational Energy Effects", *Phys. Chem. Chem. Phys.*, **2**, 679 (2000).

Susan Troutman Lee and James M. Farrar, "Dynamics of the OH⁻ + D_2 Isotope Exchange Reaction: Reactive and Nonreactive Decay of the Collision Complex", *J. Chem. Phys.* **112**, 581 (2000).

James M. Farrar, "Ion Kinetics and Energetics", in *Encyclopedia of Physical Science and Technology*, Third edition, Volume 8 (Academic, New York, 2001), pp. 65-82.

James M. Farrar, "Steric and Solvent Effects in Ionic Reactions", *Science* **295**, 2222 (2002).

James M. Farrar, "Crossed Beam Methods for Ion Collisions", in *Encyclopedia of Mass Spectrometry*, Volume 1, edited by Peter B. Armentrout (Elsevier, Amsterdam, 2003), in press.

Nonlinear Raman spectroscopy of jet-cooled organic radicals and radical complexes

Peter M. Felker

Box 951569, Department of Chemistry, University of California
Los Angeles, CA 90095-1569

Program Scope:

The DoE-sponsored project in this laboratory involves (a) the development of non-linear spectroscopic methods for use in characterizing the geometries, level structures and dynamics of species in sparse, gaseous samples and (b) the application of such techniques to the study of species, including organic free radicals, radical complexes, and molecular clusters in cold, molecular beams.

Recent Progress:

In the past year we have advanced in the following areas: (1) We have made significant strides in relating the information available from the vibrational and rotational spectroscopic methods employed in our laboratory to the intermolecular forces and dynamics that pertain to weakly bound molecular complexes and clusters. (2) We have made progress in the application of mass-selective, ionization-detected stimulated Raman spectroscopy (IDSRS) to the study of organic free radicals.

1. Studies of intermolecular forces and intermolecular dynamics

We have used mass-selective IDSRS and rotational coherence spectroscopy (RCS) to obtain a considerable body of data pertaining to the intermolecular level structures and geometries of weakly bound clusters, including clusters composed of molecules directly relevant to combustion processes. Such results can be very informative as to intermolecular potential-energy surfaces (IPS's) and intermolecular dynamics. However, for this to be achieved there must be close coupling between experiment and theory, given the highly-coupled, large-amplitude nature of the intermolecular motions within a cluster. In collaboration with Dr. Berta Fernández of the University of Sanitago Compostela and co-workers and with Prof. Samuel Leutwyler's group at the University of Bern we have gained access to the expertise required for high-quality *ab initio* computations of IPS parameters. For our part (in collaboration with Prof. Daniel Neuhauser at UCLA) we have developed methods for the quantitative solution of the Schrödinger equations relevant to the inter-molecular rotational-vibrational-tunneling states of various types of cluster species.[1,2] We are now able to make direct comparison between experimental and computational results related to intermolecular states. By so doing, we can converge on IPS functions that accurately reflect true IPSs.

Benzene-N_2 complex is one species to which we have applied this approach.[3] An IPS

function derived from fitting to *ab initio* results from Dr. Fernandez's group was used in dynamically-exact (within the rigid-monomer approximation) calculations of $J = 0$ intermolecular states for several benzene-N$_2$ isotopomers. Rotational constants and Raman-scattering coefficients for the intermolecular states were also computed. The computational results are in excellent agreement with all extant experimental results, including intermolecular Raman spectra measured by our group. The upshot is that we have obtained considerable understanding of the nature of, and dynamics on, the low-energy portion of the 5-D benzene-N$_2$ IPS. Further, we have contributed to the assessment of the quality of *ab initio* calculations required to yield IPS results suitable for quantitative interpretation of spectroscopic results on weakly bound species.

Benzene-ammonia is of interest, in part, because it is a model system for the investigation of N-H—π hydrogen bonding. It is a second species for which we have (a) measured intermolecular Raman spectra, (b) obtained *ab initio* results (from Dr. Fernandez' group) pertaining to the IPS, and (c) performed dynamically exact (6-D) intermolecular level structure calculations based on an IPS function derived from the *ab initio* results. The comparison of experiment and theory has been very valuable in the assignment of the previously unassignable Raman spectra. This has allowed the characterization of the van der Waals bending and stretching vibrations in the species and has shed light on its internal-rotation level structure and equilibrium geometry. This work will be submitted for publication shortly. Additionally, further *ab initio* calculations on the species are underway with the aim of a more complete characterization of the IPS.

A third species for which we have obtained intermolecular Raman results, *ab initio* results pertaining to its IPS, and computational results relating to its intermolecular level structure is benzene-He. The species is an important model system for the information that its study can reveal about molecule-helium interactions, interactions whose characterization has become increasingly important given the marked increase in interest in doped helium clusters. Our aim in this ongoing project is to obtain accurate IPS parameters by comparison of experimental and computational results.

As part of our effort to help facilitate the calculation of intermolecular states and intermolecular spectra of molecular clusters, we have, during the current project period, obtained results pertaining to the kinetic-energy operators ($\hat{T}_v$) of solute-(solvent)$_n$ clusters of the form B-A$_n$, where the A are atoms. In particular, we have shown[4] that $\hat{T}_v$ takes a particularly simple and computationally useful form when the intermolecular coordinates are taken to be components of the vectors from the center of mass of B to the A nuclei, as measured with respect to a body-fixed axis system that coincides with the principal axes of B. We have applied the results in dynamically exact calculations of intermolecular states in anthracene-(He)$_2$ clusters, species for which experimental spectroscopic results have been obtained by other researchers.[5] One of the main results of this project is the demonstration of how the intermolecular states of double-sided aromatic-A$_n$ clusters (m A moieties on one side of the aromatic ring plane and $n-m$ on the other) can be quantitatively described in terms of the intermolecular eigenstates of B-A$_m$ and B-A$_{n-m}$ clusters. The result is

useful in both a conceptual sense and because it points the way to an extensive reduction in the cost of intermolecular level structure calculations on such species.

We have also extended the foregoing approach toward formulating the intermolecular Hamiltonians of B-A_n species to the case where A is a molecule. And, we have measured intermolecular Raman spectra on several such species (e.g., benzene-$(N_2)_2$, benzene-$(NH_3)_2$). We are currently involved in computational studies of the intermolecular level structures of these species. We are confident that the combined experimental and computational approach will yield significant progress in elucidating the intermolecular forces and dynamics that characterize the clusters.

2. Nonlinear Raman spectroscopy of organic free radicals

A primary focus of the present DoE project is to extend IDSRS measurements of vibrational transitions in isolated species to organic radicals and complexes thereof. In this regard we have made some progress, though much remains to be done. Specifically, we have measured intramolecular Raman spectra at 0.03 cm^{-1} resolution of the benzyl radical in a seeded supersonic molecular beam.[6] The radical was generated by discharge-induced electrolysis of benzyl chloride. Mass-selective IDSRS was implemented with a photoionization probe involving two-color, resonantly-enhanced two-photon ionization (R2PI). Measurements have pertained to the ν_{12} fundamental (a CC stretch) of the species, which has been observed as a narrow, polarization-sensitive band near 988 cm^{-1}. The observation of other Raman bands has also been made. This study has given us a very good idea of the stringent requirements that must be met if one wishes to make routine measurements of nonlinear Raman spectra for jet-cooled radicals. In conjunction with these studies, we have purchased and set up an ArF excimer-based photolysis source of radicals. We have made some progress in obtaining mass-selective REMPI spectra of cold radicals produced by this source. We shall now focus our efforts on extending IDSRS methods to these species.

Future Work:

We plan to continue to apply the combined experimental (IDSRS)/computational approach that was described above for several species toward the characterization of intermolecular forces and dynamics in molecular complexes and clusters. In this area, there are numerous candidate species involving three, five, and six intermolecular degrees of freedom. We also plan to focus attention on the measurement and interpretation of intermolecular Raman spectra and rotational spectroscopic results on trimers and larger clusters.

We also plan to persist in efforts to render viable the nonlinear Raman spectroscopy of cold free radicals and radical-containing complexes by IDSRS. These studies will involve photolysis generation, as well as pulsed-discharge generation of radicals in supersonic expansions. The interest will be to characterize the vibrational level structures of these species in spectral regions difficult to access by other means.

References

1. W. Kim, D. Neuhauser, M. R. Wall, and P. M. Felker, J. Chem. Phys. **110**, 8461 (1999).
2. For example, P. M. Felker, D. Neuhauser, and W. Kim, J. Chem. Phys. **114**, 1233 (2001). P. M. Felker, J. Chem. Phys. **114**, 1233 (2001).
3. S. Lee, J. Romascan, P. M. Felker, T. B. Pedersen, B. Fernandez, and H. Koch, J. Chem. Phys. **118**, 1230-1241 (2003)
4. P. M. Felker, D. Neuhauser, et al. – to be submitted.
5. I. Al-Hroub, U. Even, and J. Jortner, J. Chem. Phys. **115**, 2069 (2001).
6. S. Lee, P. M. Felker, et al. – to be submitted.

Publications 2001-2003

1. P. M. Felker, D. Neuhauser, and W. Kim:
   "Efficient calculation of molecular constants and transition intensities in weakly bound species from $J = 0$ eigenstates: Benzene-Ar as test case,"
   J. Chem. Phys. **114**, 1233-1241 (2001).

2. P. M. Felker:
   "Calculation of rovibrational states of weakly bound complexes by transformation from an Eckart frame: Benzene-N_2,"
   J. Chem. Phys. **114**, 7901-7910 (2001).

3. S. Lee, J. Romascan, P. M. Felker, T. B. Pedersen, B. Fernandez, and H. Koch:
   "Study of the benzene-N_2 intermolecular potential-energy surface,"
   J. Chem. Phys. **118**, 1230-1241 (2003).

4. C. Tanner, D. Henseler, S. Leutwyler, L. L. Connell, and P. M. Felker:
   "Structural study of the hydrogen-bonded 1-naphthol-$(NH_3)_2$ cluster,"
   J. Chem. Phys. **118**, xxx (2003).

Spectroscopic and Dynamical Studies of Highly Energized Small Polyatomic Molecules

Robert W. Field and Robert J. Silbey
Massachusetts Institute of Technology
Cambridge, MA 02139
rwfield@mit.edu

Program Definition: Our research program is centered on the development and application of experimental and theoretical methods for studying the dynamics (Intramolecular Vibrational Redistribution and Isomerization) and kinetics of combustion species. The primary focus is the dynamics of acetylene at internal energies above the acetylene↔vinylidene isomerization barrier in the S_0 $\tilde{X}$ state and the cis ↔ trans barrier in the S_1 $\tilde{A}$ state.

Recent Progress

It is rare that a molecule permits direct spectroscopic characterization of a potential energy surface isomerization barrier region. Our effort to illuminate spectroscopically the acetylene ↔ vinylidene isomerization barrier on the S_0 $\tilde{X}^1\Sigma_g^+$ potential energy surface has taken a dramatic detour. In order to gain systematic access to the isomerization barrier region on one potential surface, it is necessary to characterize and exploit the barrier region on another potential surface. Spectroscopic perturbations (anharmonic, Coriolis, spin-orbit) can provide spectroscopic access to classes of states to which access is nominally prohibited by the usual spectroscopic selection and propensity (Franck-Condon) rules. Our immediate goal is to more completely characterize the anharmonic and Coriolis perturbations on the S_1 $\tilde{A}^1 A_u$ surface, particularly those involving the three bending modes (ν'_3 trans-bend, ν'_4 torsion, and ν'_6 asymmetric in-plane bend).

Previous studies of the $S_1 - S_0$ Dispersed Fluorescence (DF) spectrum have established that, from the acetylene side, the minimum energy isomerization path involves almost exclusively a local-bender motion of one CCH and that this local-bender motion becomes increasingly decoupled from other vibrational modes as one approaches the transition state. Thus, in order to illuminate spectroscopically the transition state, one needs a "local-bender pluck". Such a pluck cannot be achieved based on the Franck-Condon active normal modes. However, by exploiting spectroscopic perturbations between Franck-Condon bright and dark normal modes, nominally forbidden $S_1 \leftarrow S_0$ excitation transitions borrow sufficient intensity to provide an experimental basis for the necessary and elusive local-bender pluck.

Accurate Franck-Condon (FC) calculations are of great importance as a means of gaining insight into the $\tilde{A}$ state using what is known regarding the $\tilde{X}$ state and vice versa. For example, with FC results in hand, one can use experimentally determined intensities of related transitions to reveal the coordinate dependence of electronic band oscillator strengths. Of particular interest is the oscillator-strength dependence along the trans bend coordinate in the $\tilde{A}$ state. Knowledge of FC factors is also relevant to determining the sources of brightness of ν'_4 and ν'_6 – two normal modes comprising the important $4\nu'_{bend}$ polyad in the $\tilde{A}$ state. Nominally, the FC bright modes in the $\tilde{A}$ state are the CC stretch ν'_2, which is near resonance with ν'_4 and ν'_6, and ν'_3, which is off-resonance.

Another important way in which we exploit FC calculations is to help determine the identity of intermediate ($\tilde{A}$-state) levels in DF spectroscopy. More specifically, DF spectra from members of the $4\nu'_{bend}$ polyad levels display interference effects among transitions terminating in multiple $\tilde{X}$-state levels with common ℓ''_{total}, but different values of ℓ''_4 and ℓ''_5. Encoded in this interference is the identity of the particular $4\nu'_{bend}$ level, and accurate FC calculations will serve as a tool to identify a spectroscopically accessible intermediate level with a large component of ν'_6, which previous work has established is the key local bender pluck required for acetylene-vinylidene transition-state spectroscopy.

Our study of the DF spectrum of HCCH has demonstrated the importance (and difficulty) of achieving a local-bender pluck to gain Franck-Condon access to the acetylene → vinylidene barrier region. The asymmetric HCCD isotopomer is inherently a local-mode molecule. Large amplitude plucks of either local HCC or DCC bending vibrations are offered on a silver platter. DF spectra of HCCD have been recorded and partially analyzed. Long progressions in the DCC bend are prominent in the spectra, but the HCC bend appears unexpectedly to be largely silent in these spectra. One possible reason for this is that the HCC

bend undergoes much more rapid Intramolecular Vibrational Redistribution (IVR) than the DCC bend owing to a uniquely strong (unidentified) anharmonic resonance. Franck-Condon calculations will demonstrate whether intensity is in fact "missing" from HCC bending transitions and also permit quantitative extraction of the fractionated patterns illuminated by the intensity borrowed from the HCC progressions.

Several new FC calculation results have recently been obtained. These calculations have in common a novel local-mode, RKR-inversion-based approach. One significant result was the calculation of FC factors for transitions between the trans-bending mode (ν_4'') in the $\tilde{X}$ state and totally-symmetric $\tilde{A}$-state levels including the $\tilde{A}$-state zero-point level, $2\nu_3'$, $\nu_2' + \nu_3'$, and $\nu_2' + 2\nu_3'$. A comparison of experimental and calculated FC profiles reveal that FC "nodes" and FC maxima agree within two quanta of transbend. Multidimensional FC calculations were also performed, this time considering the same set of $\tilde{A}$-state levels but both the ν_4'' and CC stretch (ν_2'') modes in the ground state. Our results represent a marked improvement over existing multidimensional calculations, which predict experimentally FC-dark states to be FC-bright.

A number of collaborations exist, most of which are aimed at learning more about the S_1 state. We have benefitted from IR-UV double-resonance spectra recorded by Professor F. Fleming Crim and Dr. Sarah Henton (University of Wisconsin). An S_1-state potential energy surface has been computed by John Stanton (University of Texas). Professor Anthony Merer (University of British Columbia) has been an invaluable source for spectroscopic insight and savvy. A two-day workshop held in March, 2002, and attended by several of our collaborators was enormously helpful in increasing our understanding of the S_1 state.

Recently at MIT the Differential-Temperature Laser-Induced Fluorescence (DT-LIF) technique was developed to aid in our search for and interpretation of subtle yet important spectroscopic features in the S_1-state LIF spectra that are obscured by nearby stronger structure. In this technique, two LIF spectra at different temperatures (270 K and 350 K) are recorded in parallel, and hot- and cold-band features can be separated by exploiting their differing intensity dependence on temperature. Initially, hot- and cold-band features were disentangled using the eXtended Cross Correlation (XCC) algorithm, which was developed several years ago by us to facilitate interpretation of DF spectroscopy. More recently, the DT-LIF method-
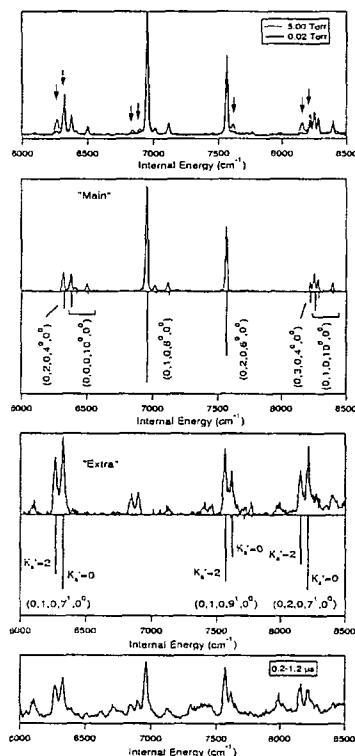
Figure 1: Unexpected sharp features (identified by vertical arrows in the top spectrum) in the Dispersed Fluorescence (DF) spectrum of acetylene (upper state is $2\nu_3'$, $J = K = 1$) due to K-changing collisions. Since we claim that our polyad model accounts for every feature in the DF spectrum, an explanation for all sharp "extra" features is essential. The pressure- and gate-dependence of the spectra suggest that the extra features are due to collisions. The extra features become more prominent relative to the expected features as pressure is increased (light trace in the top spectrum) or as fluorescence is collected within a later-opening gate (the bottom spectrum shows the effect of an early gate). The clincher is provided by the DF spectrum from $K' = 1$, excited via a cold band (second spectrum), compared to a DF spectrum from $K' = 0$ or 2, excited via a hot band (third spectrum). Fluorescence from odd-K' upper state rotational levels terminates in even-ℓ'', even-v_4'' lower state vibrational levels (except for weak axis-switching bands) and that from even-K' levels of the same upper state vibrational level terminates in odd-ℓ'', odd-v_4'' lower state vibrational levels. Thus K'-changing transitions have a very prominent effect on the DF spectrum, as illustrated by the complementarity of the second and third spectra.

ology has been improved by the development and implementation of the Structure-Based Cross Correlation (SBCC) to separate hot- and cold-band features. SBCC represents a significant improvement by taking into account the temperature dependence of relative intensity of rotational features *within a single rovibronic band*. Figure 2 shows hot- and cold-band features separated cleanly using DT-LIF accompanied by the SBCC analysis.
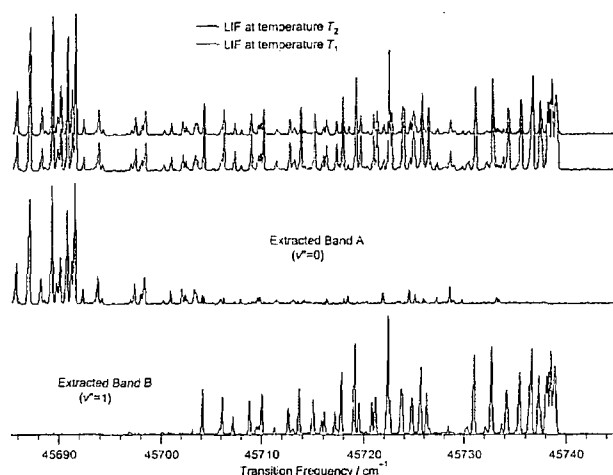
Figure 2: Structure-Based Cross-Correlation (SBCC) used to separate hot bands from cold bands in a Differential Temperature Laser Induced Fluorescence Spectrum (DT-LIF) of acetylene. Two LIF spectra are recorded simultaneously at ~ 270 and ~ 350 K in a pair of interconnected static gas cells. The intensity of the hot-band $(v_4'' = 1)$ is much more sensitive to temperature than the cold band $(v_4'' = 0)$. Since the hot-cell:cold-cell intensity ratio is dependent on lower state rotational as well as vibrational quantum number, the SBCC method was devised to take account explicitly of all rotational intensity information in a vibrational band in order to obtain an optimized separation of hot from cold bands.

An *ab initio* study of the origins of the isomerization barriers for vinylidene, fluorovinylidene, and difluorovinylidene has been carried out. The goal of these calculations was to explain the relative kinetic stabilities of species that can undergo 1,2-atom shift isomerizations across an unsaturated bond. The high barrier for difluorovinylidene is a consequence of the large energetic penalty of the C–F bond cleavage yielding a covalently unbound fluorine atom in the transition state. In contrast, for vinylidene a strong covalent bond between the migrating hydrogen atom and the C=C moiety exists at the transition state.

Future Directions

We plan to record LIF, DF, and SEP spectra of $^{13}C_2H_2$ using the ν_6' local-bender pluck. The permutation doublets observable in the DF and SEP spectra will provide a unique class of spectroscopic information about the location of the small number of vibrational levels localized on the vinylidene side of the S_0 state isomerization barrier and the strength of the coupling of those levels with the very sparse manifold of acetylene-localized pure local-bender eigenstates that are uniquely capable of sampling the isomerization barrier at its lowest and thinnest region.

A collaboration has been established with Hua Guo of the University of New Mexico. Using a full-dimensional, exact Hamiltonian, Guo and coworkers have calculated vibrational energy levels with $J = 0$ up to $13\,000$ cm^{-1} in energy on the S_0 electronic energy surface of C_2H_2. Calculations carried out using the Lanczos algorithm and a mixed-basis/grid representation produced four simulated DF spectra, using the origin, ν_2, $2\nu_3$, and $\nu_2 + 2\nu_3$ levels in the S_1 state as intermediates. These spectra, with "infinite resolution" (corresponding to long-time dynamics), contrast our experimental DF spectra, whose resolution corresponds to dynamics on the picosecond timescale. Treating these calculated spectra as "unknown" spectra, we have begun to apply the XCC algorithm, which will provide insight into the extent of the breakdown of the polyad (effective Hamiltonian) model – and corresponding approximate constants of motion – on very long timescales.

The HCN $\leftrightarrow$ HNC isomerization is the simplest example of bond-breaking isomerization. Calculations suggest that vibrational eigenstates delocalized onto both sides of the S_0 state isomerization barrier will have greater Franck-Condon accessibility from the HNC than HCN side of the S_1 state barrier. The HNC $S_1 \leftarrow S_0$ electronic transition has never been observed, suggesting that fluorescence from the S_1 state competes poorly with predissociation into H + CN. We propose to produce HNC (free of CN) in a pyrolysis jet and to record

Stimulated Emission Pumping spectra of HNC by monitoring dips in the production of CN as the frequency of the DUMP laser is scanned. Collaborations have been established with the research groups of Joel Bowman (predissociation rates in the S_1 state, calculation of Franck-Condon factors for transitions into "isomerization states") and Peter Chen (pyrolysis jet).

Recent DOE-Supported Publications (Since 2001)

1. M.L. Silva, M.P. Jacobson, Z. Duan, and R.W. Field, "Anomalous Simplicity of the Dispersed Fluorescence Spectrum of $^{13}C_2H_2$," J. Mol. Struc. 565, 87-91 (2001).

2. M.L. Silva, R. Jongma, R.W. Field, and A.M. Wodtke, "The Dynamics of 'Stretched Molecules': Experimental Studies of Highly Vibrationally Excited Molecules with Stimulated Emission Pumping," Annu. Rev. Phys. Chem. 52, 811-852 (2001).

3. K. Hoshina, A. Iwasaki, K. Yamanouchi, M.P. Jacobson, and R.W. Field, "The Infrared-Ultraviolet Dispersed Fluorescence Spectrum of Acetylene: New Classes of Bright States," J. Phys. Chem. A 114, 7424 (2001).

4. M.L. Silva, M.P. Jacobson, Z. Duan, and R.W. Field, "Unexpected Simplicity in the $S_1 - S_0$ Dispersed Fluorescence Spectra of $^{13}C_2H_2$," J. Chem. Phys. 116, 93 (2002).

5. Z.-H. Loh and R.W. Field, "Contrasting origins of the isomerization barriers for vinylidene, fluorovinylidene, and difluorovinylidene," J. Chem. Phys. 118, 4037 (2003).

6. A.J. Merer, N. Yamakita, S. Tsuchiya, J.F. Stanton, Z. Duan, and R.W. Field, "New vibrational assignments in the $\widetilde{A}\,^1A_u - \widetilde{X}\,^1\Sigma_g^+$ electronic transition of acetylene, C_2H_2: the ν_1' frequency," Mol. Phys. 101, 663 (2003).

Laser Studies of Chemical Reaction and Collision Processes

George Flynn, Department of Chemistry, Columbia University
Mail Stop 3109, 3000 Broadway, New York, New York 10027
flynn@chem.columbia.edu

Introduction and Overview

Our Department of Energy sponsored work has for many years involved the study of vibrational energy transfer in the gas phase using laser pump and probe techniques. Most recently this work has been focused on the quenching of molecules with chemically significant amounts of vibrational energy, an aspect of combustion chemistry in which vibrational energy transfer plays a critical role.

Over the past ten years substantial progress has been made in the application of laser devices to experimental studies of chemical reactions and relaxation phenomena in the electronic, vibrational, and rotational degrees of freedom of various molecular systems.[1-7] These studies are of considerable importance to chemical physicists, theoretical chemists, and biochemists interested in energy transfer mechanisms and chemical reactivity of relatively complex species. Until recently an improved understanding of the exchange of energy between translational, rotational, vibrational, and electronic degrees of freedom in molecules was largely of fundamental interest to energy transfer specialists. However, increasing efforts are now being focused on attempts to relate energy transfer information to the detailed nature of both bimolecular and unimolecular combustion reactions, as well as to understand the competition between reaction and energy transfer. Indeed a complete knowledge of the potential energy surface for a dynamical process would describe both reactive and energy transfer events. It is this intimate coupling between chemical reaction dynamics and energy transfer processes that makes studies of molecular relaxation phenomena so interesting and important.

The major focus of our gas phase collision dynamics work has been on the relaxation of molecules having "chemically significant" amounts of vibrational energy (enough energy to rupture a chemical bond). The quenching of such high energy molecules is one of the three major steps in the Lindemann unimolecular reaction mechanism.[8,9] One of our experiments can be illustrated by the following equations:

$$C_4N_2H_4 + h\nu \ (248 \ nm) \rightarrow C_4N_2H_4^{(E)} \ [Excitation]$$
$$C_4N_2H_4^{(E)} + CO \ (v=0; \ J',V') \rightarrow C_4N_2H_4^{(E-\Delta E)} + CO \ (v=0; \ J,V) \ [Quench].$$
$$CO \ (v=0; \ J,V) \ h\nu(4.8\mu m) \rightarrow CO(v=1,J\pm1,V) \ [Diode \ Laser \ Probing]$$
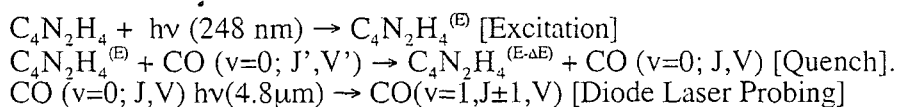
Here pyrazine ($C_4N_2H_4$) is excited by a pulse from an excimer laser. Left in this excited state with 5 eV of internal energy, the pyrazine would fragment into acetylene and HCN. However, fragmentation or unimolecular decomposition can be prevented by quenching collisions with molecules like CO as illustrated here. In principle internal energy in the pyrazine can be removed as center of mass translational energy of the pyrazine/CO pair, which is reflected in the velocity of the CO measured through the Doppler shift of the infrared absorption of CO. In addition the quenching can involve the excitation of rotational motion in the CO, which is sensed by the value of the rotational angular momentum, J, or the production of vibrational excitation, which is sensed by a change in the CO vibrational quantum number, v. The resolution of the infrared diode laser probe at 4.8 μm used in our experiments is sufficient to determine how much of the internal energy of the pyrazine goes into CO translational, rotational, and vibrational motions.

Studies of these high energy relaxation processes are of considerable importance in combustion chemistry since many of the key processes in this field turn out to involve unimolecular events. Our approach to this problem has been very direct and simple. The studies that we have performed are designed to accomplish two major goals: (1) to illuminate the core microscopic mechanism which controls energy loss for these chemically reactive species; (2) to obtain the energy transfer distribution function P(E,E'),[10-14] which gives the probability that a molecule $C_4N_2H_4^{(E)}$, initially at an energy E, will undergo a collision induced transition to an energy E', with a corresponding change in vibrational energy $\Delta E=E'-E$. We made a breakthrough over the last five years that allows us to obtain P(E,E') from a direct inversion of our data. A knowledge of this function is important both in testing detailed theoretical energy transfer calculations and in modeling unimolecular chemical reactions using master equation methods that require P(E,E'). There are remarkably few methods for obtaining P(E,E') directly from experiment, despite its importance, and most studies of unimolecular reactions make use of an assumed form for this important distribution function.

Results:

We have used this experimental method to probe collisions between cool bath molecules and vibrationally hot molecules with chemically significant amounts of energy in an effort to determine the quenching mechanism for unimolecular chemical reactions.[15-23] Several main conclusions can be drawn from these studies:

1) A "soft" collision process is responsible for the transfer of vibrational energy from a donor with "chemically significant amounts of energy" to the vibrations of a bath molecule. These vibration-vibration (V-V) energy transfer processes are accompanied by almost no rotational or translational excitation of the bath and are responsible for the loss of very little energy from the donor (typically much less than 10%).

2) Hard (impulsive) collisions that transfer the internal vibrational energy of the donor to the translational and rotational degrees of freedom of the bath constitute the dominant relaxation process taking place at chemically significant energies. These collision events can be described by a probability distribution function P(E,E') that can be obtained from the experimental data and, so far, has been successfully modeled by a double exponential fit. The high energy tail of the P(E,E') distribution constitutes what are generally referred to in the literature as "super collisions".[10-14]

3) Angular momentum constraints exist for both soft and impulsive energy transfer collisions that significantly restrict the amount of **rotational** excitation occurring in the bath due to a collision with a high energy donor. For soft collisions this constraint is extremely severe with the dominant change in angular momentum being $\Delta J=\pm1$. The angular momentum constraints for impulsive collisions are far less severe and appear to be describable by a simple classical model in which the shape (mostly the length) of the bath molecule is a critical factor. The maximum rotational energy of the bath molecules resulting from such impulsive collisions is well below that set by energy conservation in the collision process.

4) Impulsive encounters that lead to "super collisions" represent events in which the maximum rotational excitation of the bath molecules is accompanied by truly impressive translational recoil.

Present and Future Experimental Program

We plan to finish the present energy transfer theme of our experiments by investigating one final system that should illustrate the importance of the above angular momentum constraints in these kinds of collisions. Acetylene provides an excellent probe molecule for

this effort. The center of mass is in the middle of the C≡C triple bond making the maximum impact length, **b**, roughly the length of a C-H bond plus half a C≡C triple bond [a total length of 1.66 Å]. Experiments to test for angular momentum constraints in this system can be described by the following equations

$$C_4N_2H_4 + h\nu \text{ (248 nm)} \rightarrow C_4N_2H_4^{(E)} \text{ [Excitation]}$$

$$C_4N_2H_4^{(E)} + C_2H_2 (0000^00^0,J') \rightarrow C_4N_2H_4^{(E-\Delta E)} + C_2H_2(0000^00^0,J,V) \text{ [Quench]}$$

$$C_2H_2(0000^00^0,J,V) + h\nu(13.7\mu m) \rightarrow C_2H_2(0000^0 1^\Gamma,J,V) \text{ [Diode Laser Probing]}$$
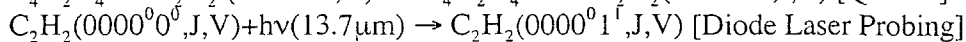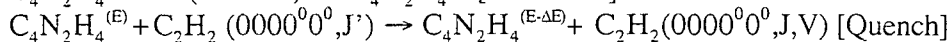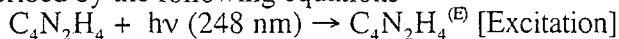
For acetylene the mean J at room temperature is roughly 13 and we expect the mean ΔJ for this molecule to be approximately (1.66/1.23)60=80 [for CO_2 the maximum **b** is 1.23 Å and the observed maximum ΔJ is roughly 60]. Thus, we predict a maximum J for these experiments to be around 80+13=93, noticeably higher than that for CO_2 (J~80) and much larger than that found for CO (J~40). We have purchased an infrared diode that operates in the spectral region of the transition

$$C_2H_2(0000^00^0,J,V) + h\nu(13.7\mu m) \rightarrow C_2H_2(0000^0 1^1,J,V)$$
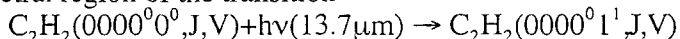
The oscillator strength for this vibration in acetylene rivals that of the $00^00 \rightarrow 00^01$ transition in CO_2, which we have used to study energy transfer processes of this kind for some time. We expect the study of energy transfer from pyrazine to acetylene to be finished by the end of the present grant period. The results of these experiments, especially when compared to similar data for CO_2 and CO, should provide clear evidence for the validity of the simple angular momentum constraint picture described above.

There are, of course, features of the donor/acceptor interaction potential that will influence the maximum angular momentum transferred in the collision. In particular when treating the potential surface of each of the bath molecules as a rigid ellipsoid, the curvature of the ellipsoidal surface is known to have an effect on the angular momentum transfer to the acceptor molecule.[24,25] Variations in the potential are unlikely to be great for the three molecules, C_2H_2, CO_2 and CO, but in any case it should be possible to model these effects by an extension of the rigid ellipsoid scattering model, which we have used before for hot atom/molecule collsions.[24] The reduced mass of the donor/acceptor collision pair will also have some effect on the angular momentum transfer, making comparisons between CO and C_2H_2 the most appropriate.

References

1. Ralph E. Weston, Jr. and George W. Flynn, Annu. Rev. Phys. Chem. 43, 559-589 (1992)
2. P. L. Houston, Accts. Chem. Res., 28, 453-460 (1995)
3. F. F. Crim, Accts. Chem. Res., 32 877-884 (1999)
4. L. J. Butler, Ann. Rev. Phys. Chem. 49 125-171 (1998)
5. S. A. Reid and H. Reisler, Ann. Rev. Phys. Chem. 47 495-525 (1996)
6. J. M. Bowman and G.C. Schatz, Annu. Rev. Phys. Chem., 46, 169-195 (1995)
7. R. E. Continetti, "Coincidence Spectroscopy", Annual Reviews of Physical Chemistry 52, 165-192 (2001)
8. F. A. Lindemann, Trans. Faraday Soc., 17, 598-606 (1922);
9. D. C. Tardy and B. S. Rabinovitch, Chem. Rev. 77, 369-408 (1977)
10. N. J. Brown and J. A. Miller, J. Chem. Phys. 80 5568-5580 (1984)
11. Jurgen Troe, J. Chem. Phys. 97, 288-292 (1992)
12. Victor Bernshtein and Izhack Oref, J. Phys. Chem. 97, 12811-12818 (1993)
13. Hassoon, I. Oref, and C. Steel, J. Chem. Phys., 89, 1743-1744 (1988)
14. G. A. Fisk and F. F. Crim, Accts. Chem. Res. 10, 73-79 (1977)
15. Amy S. Mullin, Chris A. Michaels, and George W. Flynn, J. Chem. Phys., 102,

6032-6045 (1995)

16. Chris A. Michaels, Amy S. Mullin, and George W. Flynn, J. Chem. Phys., 102, 6682-6695(1995)
17. Chris A. Michaels and George W. Flynn, J. Chem. Phys. 106, 3558-3566 (1997)
18. Chris A. Michaels, Amy S. Mullin, Jeunghee Park, James Z. Chou, and George W. Flynn, J. Chem. Phys., 108, 2744-2755 (1998)
19. E.T. Sevy, C. A. Michaels, H. C. Tapalian, and G.W. Flynn, J. Chem. Phys., 112, 5844-51 (2000)
20. E. T. Sevy, S. M. Rubin, Z. Lin, and G. W. Flynn, J. Chem. Phys., 113, 4912-4932 (2000)
21. Cortney Higgins, Quan Ju, Natalie Seiser, George Flynn and Sally Chapman, J. Phys. Chem. A, 105, 2858-2866, (2001)
22. Natalie Seiser, Kavita Kannappan, and George Flynn, "Long Range Collisional Energy Transfer from Highly Vibrationally Excited Pyrazine to CO Bath Molecules: Excitation of the v=1 CO Vibrational Level", J. Phys. Chem., accepted.
23. Natalie Seiser, Kavita Kannappan, Quan Ju and George Flynn, "Collisional Energy Transfer from Highly Vibrationally Excited Pyrazine to CO Bath Molecules: Excitation of the v=0 CO(J) Vibrational Levels", in preparation.
24. Thomas G. Kreutz and George W. Flynn, J. Chem. Phys., 93, 452-465(1990).
25. D. Beck, U. Ross and W. Schepper, Z. Physik A, 293, 107-117 (1979); D. Beck, U. Ross and W. Schepper, Z. Physik A, 299, 97-104 (1981);

DOE Publications: (2001-2003)

1. Cortney Higgins, Quan Ju, Natalie Seiser, George Flynn and Sally Chapman, "Classical Trajectory Study of Energy Transfer in Pyrazine-CO Collisions", J. Phys. Chem. A, 105, 2858-2866, (2001)
2. George W. Flynn, Encyclopedia of Chemical Physics and Physical Chemistry, Volume III: Applications, Part C3 Chemical Kinetics and Dynamics, "Energy Transfer in Gases", John Moore and Nicholas Spencer, Eds., Institute of Physics Publishing, Bristol and Philadelphia, pp 2681-2700, (2002)
3. Natalie Seiser, Quan Ju, Eric Sevy, and George Flynn, "Quenching of Pyrazine by CO: Angular Momentum Constraints for Impulsive Encounters", in preparation
4. Natalie Seiser, Kavita Kannappan, and George Flynn, "Long Range Collisional Energy Transfer from Highly Vibrationally Excited Pyrazine to CO Bath Molecules: Excitation of the v=1 CO Vibrational Level", J. Phys. Chem., accepted.

Quantitative Imaging Diagnostics for Reacting Flows

Jonathan H. Frank
Combustion Research Facility
Sandia National Laboratories, MS 9051
Livermore, CA 94551
jhfrank@ca.sandia.gov

Program Scope

The primary objective of this project is the development and application of laser-based imaging diagnostics for studying reacting flows. Imaging diagnostics provide temporally and spatially resolved measurements of species, temperature, and velocity distributions over a wide range of length scales. Multi-dimensional measurements are necessary to determine spatial correlations, scalar and velocity gradients, flame orientation, curvature, and connectivity. Our current efforts focus on planar laser-induced fluorescence (PLIF) and Rayleigh scattering techniques for probing the detailed structure of both isolated flow-flame interactions and turbulent flames. The investigation of flow-flame interactions is of fundamental importance in understanding the coupling between turbulence and chemistry in turbulent flames. These studies require the development of a new suite of imaging diagnostics to measure key species in the hydrocarbon-chemistry mechanism as well as to image rates of reaction and scalar dissipation.

Recent Progress

Recent research has continued to emphasize the development of diagnostics for probing the detailed structure of reaction zones during flow-flame interactions. The coupling of measurements with simulations also remains an essential element of this program. Research activities have included the following: i) Reaction-rate imaging with CO and OH PLIF in turbulent jet flames, ii) Simultaneous 2-D measurements of mixture fraction, temperature, and reaction-rate in turbulent jet flames, iii) A study of a new imaging diagnostic for vinyl (C_2H_3) and acetylene (C_2H_2) to provide insight into the C2 branch of reaction pathways in rich premixed flames, iv) Investigation of premixed vortex-flame interactions, v) A study of nanosecond vs. picosecond excitation for atomic oxygen LIF imaging, vi) An investigation of effects of flow transients on ignition kernels.

Reaction-rate Imaging Joint CO/OH PLIF imaging was used to perform 2-D measurements of the forward reaction rate of the reaction $CO+OH \Rightarrow CO_2 + H$ in turbulent jet flames. The diagnostic technique uses simultaneous CO and OH PLIF to derive an image of the forward rate of the reaction $CO + OH \Rightarrow CO_2 + H$. This reaction represents the primary pathway for the formation of CO_2 in a methane-air flame. The basic concept of the diagnostic involves using the product of simultaneous OH and CO PLIF measurements to obtain a signal that is proportional to the reaction rate. We performed instantaneous CO/OH reaction-rate imaging in turbulent partially premixed CH_4/air jet flames with varying levels of local extinction and are using these measurements to analyze the instantaneous structure of the reaction-rate field.

Mixture Fraction and Temperature Imaging We recently developed a three-scalar technique for 2-D measurements of mixture fraction (ξ) and temperature in partially premixed jet flames using a combination of polarized and depolarized Rayleigh scattering and CO LIF. Multidimensional measurements of mixture fraction are needed to determine scalar dissipation ($\chi = 2D|\nabla\xi|^2$), which is a metric for the rate of molecular mixing and is a critical parameter in nonpremixed and partially premixed flames. Mixture fraction can be determined by measuring all major species. However, it is

impractical to do this in two dimensions. Mixture fraction imaging thus requires the identification of a subset of measurements that can provide an accurate measure of mixture fraction with enough signal for 2-D measurements. We have coupled fuel concentration and temperature measurements with CO LIF to provide single-shot 2-D measurements of mixture fraction. Fuel concentration and temperature are measured by combined depolarized and polarized Rayleigh scattering. This technique was implemented in collaboration with M. Long (Yale Univ.). Recently, we compared results in turbulent jet flames with line measurements of R. Barlow (Sandia) to appreciate the effects of spatial resolution on measured scalar dissipation rates. We also compared imaging measurements of conditional scalar dissipation rates with predictions from the one-dimensional turbulence model of A. Kerstein (Sandia) and T Echekki (NC State). The agreement between experiments and model is encouraging.

Development of C2-Species Imaging Diagnostic We have initiated the second stage of an investigation into a new imaging diagnostic for probing C2 chemical reaction pathways in premixed flames. With this technique it may be possible to obtain single-pulse images of vinyl (C_2H_3) or acetylene (C_2H_2) that would offer unique information about the flux of carbon through C2 pathways. In the first stage of the study, we performed measurements in a low-pressure cell and identified multi-photon laser-induced fragmentation fluorescence (LIFF) from vinyl and acetylene as the two possible sources of laser-generated $C_2(d{\to}a)$ emission. Results showed that photodissociation of C_2H_3 (at $\lambda=230$ nm) is between 200 and 1300 times more efficient at generating $C_2(d{\to}a)$ emission than is photodissociation of C_2H_2. The relative efficiency depends on the initial internal excitation of the vinyl radical. At high internal energy, a two-photon dissociation of C_2H_3 is possible, while at lower internal energy three photons are required. Acetylene LIFF occurs via a three-photon process. Vinyl photodissociation is considerably more efficient than acetylene because the initial H-atom dissociation requires a single photon for vinyl and two photons for acetylene. In the second stage of this investigation, we are examining the temperature dependence of the LIFF process in flames. We combine laser diagnostics and molecular beam mass spectrometry (MBMS) to measure LIFF and species profiles in low-pressure premixed flames. Details of the flame chamber and MBMS system are available in Ref. 1. We performed simultaneous LIFF and MBMS measurements in premixed Ar-diluted methane, ethylene, and acetylene flames. Measurements in lean ($\phi=0.5$) acetylene flames were used to investigate the temperature dependence of LIFF from acetylene. In these flames, acetylene is the only source of C_2 LIFF since the formation of vinyl is improbable at an equivalence ratio of 0.5. A comparison of LIFF and acetylene spatial profiles indicates a significant enhancement of LIFF from acetylene at elevated temperatures. This enhancement is consistent with improved Frank-Condon factors in vibrationally excited acetylene. Further flame experiments are underway to quantify the temperature dependence of LIFF from acetylene and vinyl. This project is conducted in collaboration with D. Osborn (Sandia).

Study of Premixed Flame-Vortex Interactions We have made significant progress in resolving differences between experimental and computational studies of flame-vortex interactions. Previously unresolved differences in rich premixed N_2-diluted CH_4 flames included the experimental observation of a sudden increase in OH as a line-vortex pair impinged on a V-flame.[2] This OH 'burst' was not predicted by computations, and the discrepancy was previously attributed to missing steps in C1-C2 chemical mechanisms.[3] However, our recent measurements of the OH response in rich ($\phi=1.2$ and 1.4) premixed H_2 flames also showed an OH burst. Furthermore, measurements of a toroidal vortex interacting with a rich premixed CH_4 counterflow flame did not show an OH 'burst'.[4] These experimental results prompted a more detailed analysis of the V-flame apparatus. An analysis of the vortex formation process revealed that the vortex could be hotter than the surrounding premixed flow. Both 1-D and 2-D calculations showed that an elevated vortex temperature could contribute to increased OH levels.[5] Further investigation of the V-flame burner revealed that excess air was mixed into the vortex generator resulting in a vortex with a leaner equivalence ratio than the main fuel/air mixture. Our

recent experiments demonstrate that this difference in composition is the primary cause of the OH 'burst'. The elimination of the excess air results in the disappearance of the OH 'burst'. Numerical studies using 1-D laminar flame calculations indicate that these highly diluted premixed CH_4 flames are significantly more sensitive to perturbations of stoichiometry and temperature than undiluted flames. The 1-D calculations exhibit excellent agreement with the centerline OH profiles from the full 2-D calculations. The use of 1-D calculations facilitates rapid parametric studies of flame response.

Atomic Oxygen Imaging We are investigating the use of picosecond lasers to reduce photolytic interference in two-photon O-atom LIF imaging.[6] Quantitative measurements of atomic oxygen concentrations in flames are needed to better understand the detailed chemistry of combustion and in particular, nitric oxide formation. Two-photon LIF can provide sensitive detection of atomic oxygen in flames. However, previous studies using nanosecond pulsed lasers have shown that photolytically produced O-atoms cause a significant interference to measurements of the naturally occurring oxygen. Until recently, the photochemically generated O-atom was primarily attributed to the photodissociation of vibrationally excited O_2. We conducted a comparison of O-atom LIF line imaging with ps- and ns-laser excitation at 226 nm $(3p^3P \leftarrow \leftarrow 2p^3P)$ and detection at 845 nm $(3p^3P \rightarrow 2s^3S)$ in lean premixed methane and hydrogen flames. Methane flames showed significantly more photolytic interference than hydrogen flames suggesting that vibrationally excited CO_2 is a significantly more effective photolytic precursor than O_2. The ps laser pulses offer an advantage because at 226 nm the O-atom excitation is a two-photon process, and the photolysis is a single-photon process. The use of ps lasers is a promising alternative for O-atom LIF with dramatically reduced interference from photolysis. We attained comparable O-atom LIF signals from the ps and ns lasers with a ps-laser energy that was less than 1/50th of the ns-laser energy. The lower ps-laser energy gave a significant reduction in photolytic interference. The line imaging results also demonstrated Using ps excitation, we demonstrated 2-D O-atom LIF imaging in a steady premixed CH_4-air flame. This project is conducted in collaboration with T. Settersten (Sandia).

Interaction of Flow Transients and Ignition Kernels We have initiated a collaboration with K. Seshadri (UCSD) to explore the effects of flow transients on ignition processes in an opposed flow burner. We have measured the effects of a pulsed flow on the temporal evolution of the OH field during ignition of nonpremixed hydrogen flames. Results are being coupled with computations by J. Chen (Sandia).

Future Plans
In the near term, we will continue to expand our suite of novel laser-based imaging diagnostics and apply these techniques to the study of flow-flame interactions in highly reproducible, building-block flames. Diagnostic techniques will be extended to single-shot measurements in turbulent flames whenever possible. Ultimately, these efforts are aimed at achieving our long-term goal of using imaging diagnostics to apply our understanding of building-block flames to turbulent flow-flame interactions. In all of these endeavors, we will strive to couple experimental measurements with simulation and modeling efforts.

Reaction-rate Imaging We plan to continue the development and application of diagnostics that provide imaging measurements of reaction-rates. In the near future, our primary emphasis will be further developing the simultaneous CO/OH measurement technique to obtain the spatial distribution of the forward reaction rate of the CO + OH $\Rightarrow CO_2$ + H reaction in both reproducible flow-flame interactions and turbulent flames.

Mixture Fraction We will expand our initial demonstration of simultaneous 2-D mixture-fraction and temperature measurements by implementing the technique in a wider range of turbulent jet flames and

repeatable flow-flame interactions. The diagnostic technique will be further evaluated using comparisons with results from multiscalar point and line measurements performed in collaboration with R. Barlow. Further developments are needed to determine the uncertainty of the scalar dissipation rates and to extend the technique to flames having localized extinction.

C_2-Species Diagnostic We will expand our understanding of laser-induced fragmentation fluorescence (LIFF) of vinyl (C_2H_3) and acetylene (C_2H_2) in flames. Measurements of temperature profiles in low-pressure flames will be combined with LIFF and MBMS to quantify the temperature dependence of the LIFF process. This research will be performed in collaboration with A. McIlroy and D. Osborn.

Flame-Vortex Interactions Future studies on flame-vortex interactions will focus on a counterflow flame interacting with a toroidal vortex. This burner geometry has boundary conditions that are better defined than those of the V-flame configuration. This will greatly facilitate comparisons of computations and experiments. We will experimentally compare the effects of flow transients in highly diluted and undiluted premixed flames using a suite of imaging diagnostics. Experiments will be coupled with new 2-D computations by H. Najm. Investigations of nonpremixed flames will be conducted in collaboration with A. Gomez and M. Smooke (Yale Univ.).

Atomic Oxygen Imaging We will continue to develop the use of ps lasers for O-atom LIF imaging and apply this diagnostic to the study of repeatable flow-flame interactions. Additional amplification stages will be added to the ps dye laser to increase the PLIF signal to noise ratio.

Interaction of Flow Transients and Ignition Kernels We compare experiments and computations of the effects of flow perturbations on ignition processes in H_2 and hydrocarbon fuels. These experiments will be conducted in collaboration with J. Chen (Sandia) and K. Seshadri (UCSD).

Cited References

1. A. McIlroy, T. D. Hain, H. A. Michelsen, and T. A. Cool, *Proc. Combust. Inst.* 28:1647 (2002).
2. V. Nguyen, and P. H. Paul, *Proc. Combust. Inst.* 26:357-364 (1996).
3. H. N., Najm, P. H. Paul, O. M. Knio, and A. McIlroy, *Combust. Flame* 125:879 (2001).
4. See Ref. 3 below.
5. C. M. Vagelopoulos, J. H. Frank, and H. N., Najm, The Joint Meeting of the US Sections of the Combustion Institute, Chicago, IL, March 17-19, 2003.
6. J. H. Frank, T. B. Settersten, B. Patterson, and X. Chen, The Joint Meeting of the US Sections of the Combustion Institute, Chicago, IL, March 17-19, 2003.

Recent DOE Supported Publications

1. J. H. Frank, S. A. Kaiser, and M. B. Long, "Reaction-rate, Mixture Fraction, and Temperature Imaging in Turbulent Methane/Air Jet Flames," *Proc. Combust. Inst.* Vol. 29, in press (2002).
2. J. Fielding, J. H. Frank, S. A. Kaiser, M. D. Smooke, and M. B. Long, "Polarized/Depolarized Rayleigh Scattering for Determining Fuel Concentrations in Flames," *Proc. Combust. Inst.* Vol. 29, in press (2002).
3. C. M. Vagelopoulos and J. H. Frank, "Effects of Flow and Chemistry on OH Levels in Premixed Flame-Vortex Interactions," *Proc. Combust. Inst.* Vol. 29, in press (2002).
4. D. L. Osborn and J. H. Frank, "Laser-induced Fragmentation Fluorescence Detection of the Vinyl Radical and Acetylene", *Chem. Phys. Lett.* 349:43 (2001).
5. R. S. Barlow, A. N. Karpetis, J. H. Frank, and J.-Y. Chen, "Scalar Profiles and NO Formation in Laminar Opposed-Flow Partially-Premixed Methane/Air Flames," *Combust. Flame* 127:2102 (2001).

MECHANISM AND DETAILED MODELING OF SOOT FORMATION

Principal Investigator: Michael Frenklach
Department of Mechanical Engineering
The University of California
Berkeley, CA 94720-1740
Phone: (510) 643-1676; E-mail: myf@me.berkeley.edu

Project Scope: Soot formation is one of the key environmental problems associated with operation of practical combustion devices. Mechanistic understanding of the phenomenon has advanced significantly in recent years, shifting the focus of discussion from conceptual possibilities to specifics of reaction kinetics. However, along with the success of initial models comes the realization of their shortcomings. This project focuses on fundamental aspects of physical and chemical phenomena critical to the development of predictive models of soot formation in the combustion of hydrocarbon fuels, as well as on computational techniques for the development of predictive reaction models and their economical application to CFD simulations. The work includes theoretical and numerical studies of gas-phase chemistry of gaseous soot particle precursors, soot particle surface processes, particle aggregation into fractal objects, and development of economical numerical approaches to reaction kinetics.

Recent Progress:

Particle Aggregation with Simultaneous Surface Growth—Transition from Coalescent to Fractal Growth (with P. Mitchell and M. Balthasar)

Transformation of gas into particulate matter is at the core of a variety of natural phenomena and industrial processes; examples may include formation of atmospheric fog, combustion soot, interstellar dust, carbon black, and commodity ceramics like fumed silica and pigmentary titania. Conventional description of the particulate inception begins with homogeneous nucleation of precursors in the gas phase, leading to the appearance of the first recognizable particles. These *primary* particles are assumed to be spherical and collisions among them coalescent, i.e., forming larger spherical particles. In the case of solid particulates, the collected samples often exhibit characteristics of fractal-like aggregates. It is understood therefore that the initial period of coalescent growth must transition to particle aggregation. Surface deposition also contributes to particle growth. Gas phase species attach themselves to the surface of the particles during both the coalescent and aggregation stages of formation. This adds a layer of mass on the particle surface.

While the formation of particle aggregates is well documented and their fractal-like appearance is well characterized, the transition between the formation of primary particles and chain-like aggregates is not well understood. In the past few years, we investigated this transition using dynamic Monte-Carlo simulations. The simulations construct soot particles via ensemble-averaged collisions between small geometrically perfect spheres. Simultaneously with the collisions, the particle sphere surfaces grow at a prescribed rate. The result is a union of overlapping spheres. A point sampling algorithm was implemented to compute particle center of mass, volume, surface area, fractal dimension, and radius of gyration. Using the results of these detailed Monte Carlo simulations, we developed a working definition of the transition between

coalescent coagulation and fractal aggregation. The developed theory is based on shape descriptors, δ and Δ, introduced to quantify the geometric differences between particles. Descriptor δ quantifies a particle's geometric proximity to either a perfectly round ball or a chain-like aggregate. For a given shape, Δ identifies a particle's direction of geometric change.

During the past year, we developed a formulation that captures the essential physics of the detailed Monte Carlo model but in a numerical form that allowed us to incorporate the aggregation phenomena into the method of moments. The latter was coupled with our detailed chemical kinetic mechanism of soot formation. The combined model was applied to ensemble-average simulations of a number of burner stabilized premixed laminar flames and the results were validated against experimental observations of soot yields and particle sizes.

This represents reaching another milestone in soot modeling: *a practical model that predicts the evolution of particle shape from first principles.*

Equipped with the developed code, we investigated the predicted trends for the transition from coalescent to aggregate growth in a numerically simulated series of freely propagating laminar premixed flames. The location of transition and the degree of aggregation were analyzed against variations in fuel type, fuel/air equivalence ratio, and pressure. The simulations showed that the degree of aggregation and the location at which transition from coalescent to aggregate growth occurs are governed by a complex interaction of nucleation, coagulation, and surface growth. The strength of particle nucleation appears to be the dominant factor controlling the particle shape and the time of transition, since it determines the number of small particles available for coagulation. The abundance of small particles leads to the formation of aggregates that are more readily covered by surface growth and hence, depending on the rate of surface growth, exhibit a more spherical shape. Not only the peak of nucleation but also the rate of nucleation in the post flame zone appears to play a significant role: secondary nucleation can defer transition from coalescent to aggregate growth and thereby enhance the sphericity of the formed aggregates.

The results imply a shift in the paradigm: *particle aggregation is not separated in time from particle nucleation,* as is often presumed.

Application of Solution-Mapping to Geometry Optimization in Quantum Monte Carlo (with S. C. Schuetz, A. C. Kollias, and W. A. Lester, Jr.)

The quantum Monte Carlo (QMC) method is a stochastic many-body approach for solving the Schrödinger equation. While QMC methods yield molecular energies of high accuracy, PES critical points including the equilibrium geometry and the location of reaction energy barriers are traditionally taken from other methods because of the absence of an analytical derivative capability with QMC. It is of interest to develop a method for geometry optimization within the framework of QMC itself that is not dependent on other methods. We are in the process of testing the Solution Mapping methodology for this purpose.

In the Solution Mapping approach an approximation is sought not to the mathematical equations that define the model, but to the *solution* of these equations. The approximation is developed through statistical techniques of response surface design, by performing computer runs with the original model (QMC in the present case) and fitting the numerical results obtained with simple functions such as polynomials. The statistical surrogate thus obtained is then used in subsequent numerical calculations (potential energy minimization in this case), replacing the need for repeated solutions of the original equations or information about gradients.

The statistical surrogates are obtained by means of a relatively small number of computer simulations, referred to as *computer experiments*. The computer experiments are performed at preselected combinations of the optimization variables, and the set of these combinations is called a *factorial design*. These factorial designs originate from rigorous analysis of variance, with the objective of minimizing the number of computer experiments to be performed in order to gain the information required. Hence, this approach is particularly well suited to use with QMC, as a minimum number of calculations are required to develop the potential surface. This is of paramount importance because of the high computational cost of QMC calculations.

Three internal coordinates were chosen to define the potential surface of formaldehyde: the C-O bond length, C-H bond length, and the O-C-H angle. We assumed that the optimal geometry is planar and so an out-of-plane bending coordinate was not included in the design. The design was centered at the experimental values of r(C=O) = 1.21 Å, r(C-H) = 1.12 Å, and <OCH = 121°. The fitted region of the potential surface was ±0.05 Å in bond length and ±3° in OCH angle, or ±5 times the experimental error in the bond length and ±3 times the experimental error in the OCH angle. This choice of the optimization region is a compromise between accuracy of the approximation, which increases as variable spans decrease, and the area of the potential energy surface covered by the surrogate model.

A composite orthogonal design, based on a 2^3 full factorial design, was used in the present study. This design is tailored to producing a quadratic approximation to the functional relationship being sampled. The computer experiments were performed using single point energy calculations from single determinant, pseudopotential VMC and DMC methods. Using the quadratic surrogate, the minimum energy and optimal geometry were found with a nonlinear multivariable optimization; the results are shown in the Table below.

Method	Energy	C-O (Å)	C-H (Å)	C-O-H (°)
VMC				
HF(Soft/Partridge)	–22.7868295	1.197	1.101	121.3
MCSCF (SBK/cc-pVQZ)	–22.7984708	1.204	1.080	120.8
DMC				
HF(Soft/Partridge)	–22.8445736	1.205	1.108	121.4
MCSCF (SBK/cc-pVQZ)	–22.8515749	1.212	1.08	120.2
Experiment	–	1.21(1)	1.12(1)	121(1)

Using the surrogate PES it is also possible to calculate force constants and vibrational frequencies, as well as estimate the uncertainty of the results.

Future Plans

1. *Pre-nucleation Chemistry*: In collaboration with William Lester's group we will continue ab initio quantum-chemical analysis of reactions that are critical to the development of kinetic models of aromatic growth. Our current attention is on QMC analysis of small aliphatic unsaturated C_2-C_5 radicals, and the A and B states of the cyclopentadienyl radical.

   We will explore further the application of Solution Mapping to geometry optimization with QMC. We plan to complete the present testing and follow with its application to other systems.

2. *Soot Particle Aggregation:* We will complete the presently ongoing analysis of freely propagating laminar premixed flames. Our subsequent goal is to perform flame simulations of soot formation, using the new model and with the focus on evolution of soot particle morphology, in more complex reactive flows.

3. *Homogeneous Nucleation of Carbon Nanoparticles.* We will continue molecular dynamics simulations with "on-the-fly" quantum forces, exploring wider ranges of initial conditions. Our current objective is to investigate collisions of different-size aromatics. During the past year, we have carried out MD simulations for collisions of coronene molecules. The initial results indicate that these collisions might be "stickier" than those of pyrene molecules and the underlying mechanism analogous to the one identified for the pyrene case. After we have completed these studies, we plan to study collisions of aromatics smaller than pyrene, like naphthalene and anthracene, and larger than coronene, like circumcoronene Then we intend to study collisions of aromatics of dissimilar sizes, like pyrene-coronene, pyrene-naphthalene, and coronene-naphthalene, as well as radical-molecule collisions.

4. *Graphene Layer Growth.* We will investigate the effect of graphene edge migration reactions, discovered by us a couple years ago under this program, on the formation of surface growth patterns by site-specific time-dependent Monte Carlo simulations. As the first step in this direction, we have been carrying out two-dimensional Monte Carlo simulations on a graphene layer, using an extended set of elementary surface reactions, coupled to the incoming species from the surrounding gas. The very preliminary results show nanopattern formation consistent with our initial proposal and in agreement with recent spectroscopic observation of PAH species in interstellar clouds.

Publications

1. "Solution Mapping Approach to Modeling Combustion," M. Frenklach, in *Computational Fluid and Solid Mechanics*, K. J. Bathe, Ed., Elsevier, New York, 2001, pp. 1177–1179.

2. "The Addition Reaction of Propargyl and Acetylene: Pathways to Cyclic Hydrocarbons," N. W. Moriarty, X. Krokidis, W. A. Lester Jr., and M. Frenklach, 2nd Joint Meeting of the U.S. Sections of the Combustion Institute, Oakland, CA, March 25–28, 2001, paper 102.

3. "A Quantum Monte Carlo Study of Energy Differences in C_4H_3 and C_4H_5 Isomers," X. Krokidis, N. W. Moriarty, W. A. Lester, Jr., and M. Frenklach, *Int. J. Chem. Kinet.* **33**, 808–820 (2001).

4. "Reaction Mechanism of Soot Formation in Flames," *Phys. Chem. Chem.* **4**, 2028–2037 (2002).

5. "Method of Moments with Interpolative Closure," *Chem. Eng. Sci.* 57, 2229–2239 (2002).

6. "On the Formation of the First Aromatic Ring," N. W. Moriarty, X. Krokidis, W. A. Lester Jr., and M. Frenklach, *Preprints of the 224th ACS National Meeting*, Vol. 47, No. 2, 2002, pp. 769–770.

7. "Nucleation of Soot: Molecular Dynamics Simulations of Pyrene Dimerization," C. A. Schuetz and M. Frenklach, *Proc. Combust. Inst.* **29**, in press.

Multiresonant Spectroscopy and the High-Resolution Threshold Photoionization of Combustion Free Radicals

Edward R. Grant
Department of Chemistry
Purdue University
West Lafayette, IN 47907
edgrant@purdue.edu

Program Definition/Scope

In this research we apply methods of multiresonant spectroscopy and rotationally resolved threshold photoionization to characterize the structure, thermochemistry and intramolecular dynamics of excited neutrals and cations derived from combustion free radicals. The objectives of this work are: (1) To measure ionization potentials with wavenumber accuracy for a broad set of polyatomic molecules of relevance to combustion and combustion modeling; (2) To determine vibrational structure for cations as yet uncharacterized by ion absorption and fluorescence spectroscopy, including the study of anharmonic coupling and intramolecular vibrational relaxation at energies approaching thresholds for isomerization; (3) By threshold photoionization scans, referenced in double resonance to specific cation rovibrational states, to obtain information on originating-state level structure useful for the development of neutral-species diagnostics; (4) To measure rotationally detailed state-to-state photoionization cross sections for comparison with theory; and (5) To spectroscopically study near-threshold electron-cation scattering dynamics of relevance, for example, to plasma processes such as dissociative recombination, by acquiring and analyzing rotationally resolved high-Rydberg spectra.

Recent Progress

Ionization-Detected Vibronic Absorption Spectroscopy of the $3p\pi\ ^2\Pi$ state of HCO

The electron plus closed-shell HCO^+ core serves well as a simple prototype for the characterization of resonances formed by quantum-state-detailed electron-cation scattering. These resonances play important roles in such processes as dissociative recombination. Work in our laboratory to isolate associated features spectroscopically has relied on the selectivity of vertical Rydberg-Rydberg transitions from specific levels of the $3p\pi\ ^2\Pi$ intermediate state prepared by an initial step of one-photon absorption.

Results on cation vibrational structure and Rydberg relaxation dynamics have motivated an interest in reaching the higher vibrational states of the core. Work completed in the previous reporting period carried rovibronic analysis up to the level of (030) for HCO and (040) for DCO. These experiments introduced the important technique for HCO in which a low-power UV laser populates levels of the $3p\pi\ ^2\Pi$ state in a step of first-photon absorption followed by detection in a second step of high-power visible laser driven photoionization.

We have now extended measurements to reach levels as high as (080) in HCO by employing first-photon frequencies from 48,000 to 51,000 cm^{-1}, which have been generated by

frequency tripling the output of a Nd:YAG pumped dye laser in successive β-barium borate (BBO) crystals.
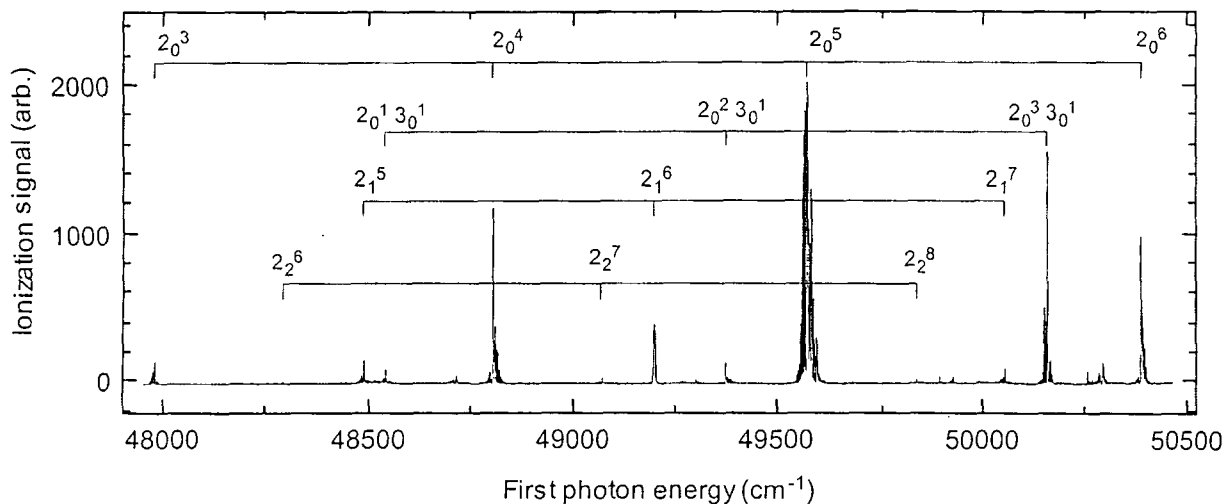
Figure 1 shows an overview of the resulting absorption spectrum. We have assigned all of the features observed. The most prominent features in the spectrum consist of progressions in the bending vibration (v_2). We have yet to observe any level in which the C-H stretching (v_1) mode has been excited. The Renner-Teller effect leads to several sub-bands for each $(0, v_2, v_3)$-$(0, v_2, 0)$ band. For even v_2, we observe principally (K', K") = (1, 0) and (1, 2) sub-bands. For odd v_2, the (K', K") = (0, 1) sub-band dominates. The cold-band progressions include: $(0, v_2, 0)$ - $(0, 0, 0)$, $v_2 = 4, 5, 6$; $(0, v_2, 1)$-$(0, 0, 0)$, $v_2 = 1, 2$, and the transition, $(0, 0, 2)$-$(0, 0, 0)$. We also find the following hot-band progressions: $(0, v_2, 0)$-$(0, 1, 0)$, $v_2 = 5, 6, 7$ and $(0, v_2, 0)$-$(0, 1, 0)$, $v_2 = 6, 7, 8$.

From among these rovibronically resolved states, we select intermediates for double resonance scans of the high Rydberg states of HCO. In such scans, strongly vertical Rydberg-Rydberg transitions isolate autoionizing series converging to specific rotational limits in vibrationally highly excited states of the cation

Dynamics of vibrational auto ionization from highly excited bending levels of HCO

Using the same pulsed molecular beam quadrupole mass spectrometer, we have recorded autoionization spectra originating from a set of $(0, v_2, 0)$ intermediate states with $v_2 = 4, 5, 6$ and 7. The initial rotational state selected in each case is the lowest one allowed by the vibronic angular momentum of the level. Resonant second-photon absorption is marked by the appearance of HCO^+ cations produced following vibrational autoionization.

Linewidths and positions recorded in these spectra reflect the coupling dynamics of a Rydberg electron in a selected orbital with a core excited to successively higher amplitudes of bending. For example, Figure 2 shows the spectrum obtained in a second-photon scan originating from the N' = 0 level selected by first-photon absorption in the (K', K") = (0, 1) sub-

band of the $3p\pi\,^2\Pi$ (0, 5, 0) - X ^{2}A' (0, 0, 0) system. Figure 3 compares scans over the principal quantum number interval from n = 13 to 14 showing transitions originating from N' = 0 in successive levels with odd quanta of bending, v_2 = 3, 5 and 7. Arbitrary second photon scales have been selected to align principal features. Remarkably, the rotational-electronic structure and the Rydberg-vibrational relaxation dynamics appear largely unaltered by significant increases in bending amplitude.
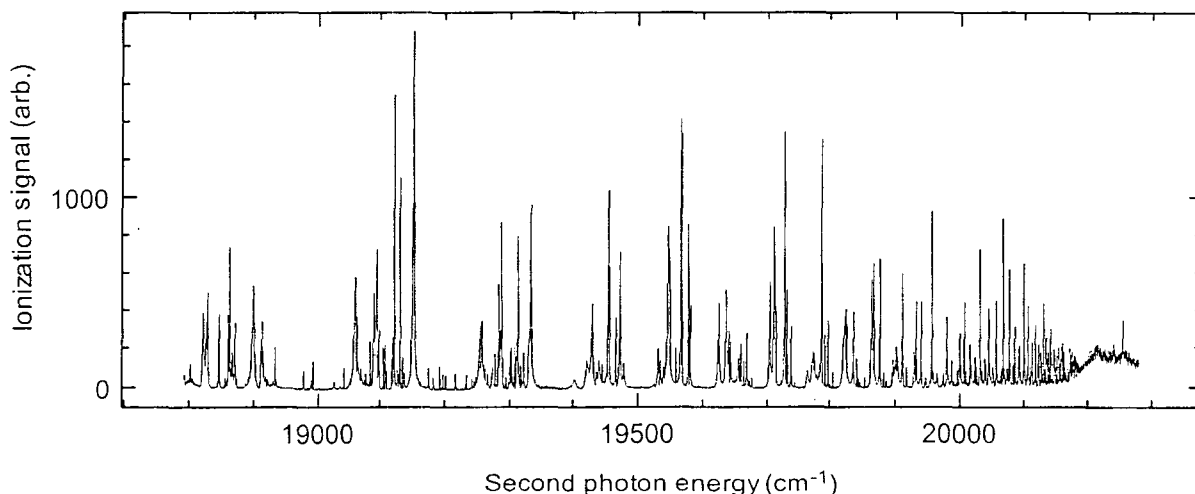
Figure 2 Spectrum of Rydberg series converging to the (050) vibrational state of HCO+ originating from the N' = 0 level of the (0, 5, 0) Σ^- component of the $3p\pi\,^2\Pi$ intermediate state.
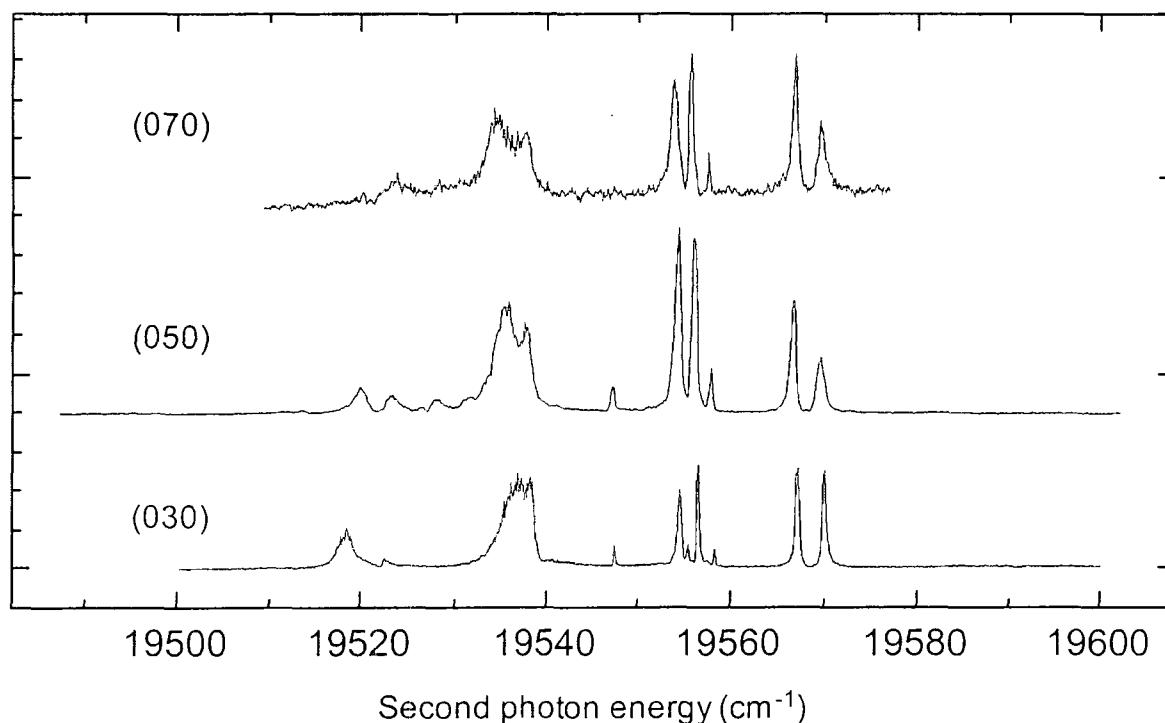
Figure 3 Scans comparing rotational-electronic structure of states with binding energy R/n* for n* in the range from 13, as observed in transitions from N' = 0 for states built on (030), (050) and (070) vibrational levels of the HCO^+ core.

We are currently in the process of analyzing these autoionization spectra to isolate individual series converging to specific rotational levels (typically N^+ = 1 through 3) of HCO^+ vibrational states (0, v_2, 0), with v_2 = 4, 5, 6 and 7. Extrapolation of the series will locate the position of these rovibrational states accurately. This information combined with precise ionization limits for lower vibrational states determined from earlier Rydberg extrapolations and spectroscopic information available from infrared absorption measurements will help to refine force-field parameters for HCO^+ bending.

References to publications of DOE sponsored research (2001-2003)

Double-resonant photoionization efficiency (DR/PIE) spectroscopy: A precise determination of the adiabatic ionization potential of DCO, R. J. Foltynowicz, J. D. Robinson and E. R. Grant, *J. Chem. Phys.* **114**, 5224 (2001).

An experimental measure of anharmonicity in the bending of DCO^+, J. D. Robinson, R. J. Foltynowicz and E. R. Grant, *J. Chem. Phys.* **114**, 878 (2001).

The A $^1\Pi \leftarrow$ X $^1\Sigma^+$ (2,0) Transition in ^{11}BH and ^{10}BH Observed by (1+2)-Photon Resonance-Enhanced Multiphoton Ionization Spectroscopy, J. Clark, M. Konopka, L.-M. Zhang and E. R. Grant, *Chem. Phys. Lett.* **340**, 45 (2001).

Bend-Stretch Fermi Resonance in DCO^+, J. D. Robinson, R. J. Foltynowicz, K. Prentice, P. Bell and E. R. Grant, *J. Chem. Phys.* **116**, 2370 (2002).

Laser-assisted (1+1')-photon ionization-detected absorption spectrum of the 3pπ $^2\Pi$ state of HCO and DCO, R. J. Foltynowicz, J. D. Robinson, K. Prentice, P. Bell and E. R. Grant, *J. Chem. Phys.* . **117**, 8384 (2002).

CHEMICAL DYNAMICS IN THE GAS PHASE: QUANTUM MECHANICS OF CHEMICAL REACTIONS

Stephen K. Gray
Chemistry Division
Argonne National Laboratory
Argonne, IL 60439

E-mail: gray@tcg.anl.gov

PROGRAM SCOPE

This research program focuses on theoretical chemical reaction dynamics, with particular emphasis on the development of rigorous quantum mechanical methods and applications to experimentally relevant and combustion important problems.   A time-dependent or iterative quantum approach is often adopted, which can offer computational advantages and mechanistic insights.   The results of these calculations are also used to gauge the quality of the underlying potential energy surfaces, as well as more approximate chemical dynamics theories.

RECENT PROGRESS

The real wave packet (RWP) approach of Gray and Balint-Kurti [1, 2] was used to carry out two extensive quantum dynamics studies. In the first study, the triatomic $N(^2D) + O_2(X) \rightarrow O(^3P) + NO(X)$ reaction was investigated with Balint-Kurti and co-workers [3].   The two lowest potential energy surfaces were considered, for which potential energy surfaces based on high quality *ab initio* data were available.   A large number of different total angular momenta were considered within the helicity-decoupled approximation, allowing reasonable quality estimates of cross sections and rate constants for this chemical reaction.   Comparison with experiment, quasiclassical trajectory (QCT) and variational transition state theory (VTST) calculations were made.   For example, the quantum rate constant estimates for T $\geq$ 300K agreed reasonably well with the QCT and VTST results and experiment. Discrepancies do exist at lower temperatures which need to be further investigated.

The second wave packet study was for the D_2 + OH $\rightarrow$ HOD + D reaction, carried out in collaboration with Defazio [4]. The recent four-atom implementation of the RWP of Goldfield and Gray [5], which also included a novel finite differencing approach to evaluate the action of the kinetic energy operator [6] was employed. The recent *ab initio* based WSLFH potential energy surface due to Harding, Schatz and their co-workers was employed [7]. As with the triatomic reaction discussed above, extensive helicity-decoupled calculations were carried out leading to quantum estimates of cross sections and rate constants. Consistent with previous results obtained for the H_2 + OH $\rightarrow$ H_2O + H reaction [5], we found that the WSLFH surface consistently underestimates rate constants in comparison with experiment by almost a factor of three. The ratio of rate constants for the H_2 + OH and D_2 + OH reactions was, however, found to be in reasonable accord with available experimental results. It is also interesting to note that VTST calculations incorporating a high level tunneling correction on the same WSLFH surface [8] yield larger rate constants than our quantum ones for both reactions. This may indicate that reaction path curvature effects in the tunneling for this reaction are over-estimated in the

VTST calculations. Inspection of the evolving wave packets, in fact, shows no significant evidence of corner cutting or curvature effects.

Motivated by the exciting experimental results of Lester and co-workers [9], as well as the availability of new high-quality *ab initio* potential energy surfaces [10, 11], a study of the combustion important $OH + CO \rightarrow H + CO_2$ reaction was initiated with Goldfield. Following Lester and co-workers [9], our interest lies in the role of linear reactant-channel complexes of the form $OH\cdots CO$ and $HO\cdots CO$, and their impact on the reaction dynamics. Employing the so-called LTSH potential energy surface of Schatz, Harding and co-workers [11], preliminary wave packet results indicate, for ground state reactants and zero total angular momentum, that the presence of reactant channel wells can indeed have an important effect, particularly at low collision energies, on the reaction probability. Figure 1 below shows the ratio of the reaction probability when the full LTSH surface (with reactant channel wells) is used and the reaction probability for a variation of the LTSH surface with the wells removed. It indicates a significant enhancement of probability occurs when the reactant-channel wells are present. While a variety of different basis set sizes and grid sizes to describe the problem always yields a picture similar to Fig. 1, our results are not yet fully converged. Thus the fine details in Fig. 1 will likely change but the significant enhancement effect at lower energies will probably remain.
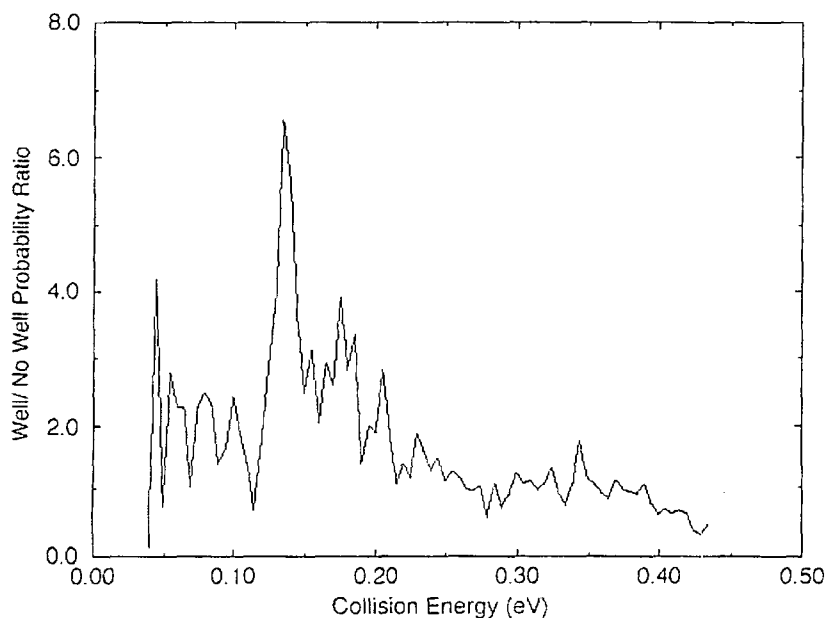
Figure 1. Ratio of reaction probabilities inferred from RWP calculations that include and exclude the presence of reactant-channel complexes for the $OH + CO \rightarrow H + CO_2$ reaction.

FUTURE PLANS

In collaboration with Goldfield and Medvedev, the full-dimensional OH + CO $\rightarrow$ H + CO$_2$ reaction probability calculations will be converged (with the aid of parallel implementations of the RWP code), and estimates of the cumulative reaction probability and rate constants will be made in order to deduce the effect of the reactant-channel complexes. We will also carry out calculations on the unimolecular decay of state-selected unimolecular OH$\cdots$CO complexes in order to compare with more recent work of Lester and co-workers [12]. In particular we will focus on the nature of the resulting OH + CO product distributions that result when these complexes decay.

Finally, in collaboration with Hall and Harding, four-atom wave packet calculations pertaining to NCCN $\rightarrow$ 2CN will be carried out, focusing on the nature of the rotational product distributions which, experimentally [13], are colder than would be expected on the basis of statistical theories. The four-atom implementation of the RWP code [5] and a new and accurate *ab initio* based potential energy surface due to Harding will be employed.

References
[1] S. K. Gray and G. G. Balint-Kurti, J. Chem. Phys. **108**, 950 (1998).
[2] S. K. Gray, J. Theor. Comput. Chem. **2**, 373 (2002).
[3] I. Miquel, M. Gonzalez, R. Sayos, G. G. Balint-Kurti, S. K. Gray, and E. M. Goldfield, J. Chem. Phys. **118**, 3111-3123 (2003).
[4] P. Defazio and S. K. Gray, J. Phys. Chem. A. *in press* (2003).
[5] E. M. Goldfield and S. K. Gray, J. Chem. Phys. **117**, 1604-1612 (2002).
[6] S. K. Gray and E. M. Goldfield, J. Chem. Phys. **115**, 8331-8344 (2001).
[7] G. Wu, G. C. Schatz, G. Lendvay, D.-C. Fang, and L. B. Harding, J. Chem. Phys. **113**, 3150 (2000).
[8] D. Troya, M. L. Lakin, G. C. Schatz, and M. Gonzalez, J. Chem. Phys. **115**, 1828 (2001).
[9] M. I. Lester, B. V. Pond, D. T. Anderson, L. B. Harding, and A. F. Wagner, J. Chem. Phys. **113**, 9889 (2000).
[10] H.-G. Yu, J. T. Muckerman, and T. J. Sears, Chem. Phys. Lett. **349**, 547 (2001).
[11] D. Troya, M. J. Lakin, G. C. Schatz, L. B. Harding, and M. Gonzalez, J. Phys. Chem. B **106**, 8148 (2002).
[12] B. V. Pond and M. I. Lester, J. Chem. Phys. **118**, 2223 (2003).
[13] S. W. North and G. E. Hall, J. Chem. Phys. **106**, 60 (1997).

PUBLICATIONS, S. K. Gray (2001-2003)

1. S. K. Gray, B. G. Sumpter, D. W. Noid, and M. D. Barnes, Quantum mechanical model of localized electrons on the surface of polymer nanospheres, Chem. Phys. Lett. **333**, 308-313 (2001).

2. M. Hankel, G.G. Balint-Kurti, and S. K. Gray , Quantum mechanical calculation of reaction probabilities and branching ratios for the $O(^1D) + HD \rightarrow OH(OD) + D(H)$ reaction on the 1A' and 1A" adiabatic potential energy surfaces, J. Phys. Chem. A. **105,** 2330-2339 (2001).

3. S. K. Gray and E. M. Goldfield, Highly excited bound and low-lying resonance states of H_2O, J. Phys. Chem. A **105,** 2634-2641 (2001).

4. V. Piermarini , G. G. Balint-Kurti, S. K. Gray , F. Gögtas, A. Laganà* and M. L. Hernández, Wave packet calculation of cross sections, product state distributions, and branching ratios for the $O(^1D) + HCl$ reaction, J. Phys. Chem. A **105,** 5743-5750 (2001).

5. K. M. Forsythe, S. K. Gray, S. J. Klippenstein, and G. E. Hall, An *ab initio* molecular dynamics study of S_0 ketene fragmentation, J. Chem. Phys. **115,** 2134-2145 (2001).

6. P. Defazio, C. Petrongolo, S. K. Gray, and C. Oliva, Wave packet dynamics of the $N(^4S) + O_2 \rightarrow NO + O$ reaction on the X^2A' potential energy surface, J. Chem. Phys. **115,** 3208-3214 (2001).

7. S. K. Gray and E. M. Goldfield, Dispersion fitted finite difference method with applications to molecular quantum mechanics, J. Chem. Phys. **115,** 8331-8344 (2001).

8. E. M. Goldfield and S. K. Gray, A quantum dynamics study of $H_2 + OH \rightarrow H_2O + H$ employing the Wu-Schatz-Lendvay-Fang-Harding potential function and a four-atom implementation of the real wave packet method, J. Chem. Phys. **117,** 1604-1612 (2002).

9. S. K. Gray, Chemical reaction dynamics with real wave packets, J. Theor. Comput. Chem. **2,** 373-379 (2002)..

10. I. Miquel, M. Gonzalez, R. Sayos, G. G. Balint-Kurti, S. K. Gray, and E. M. Goldfield, Quantum reactive scattering calculations of cross sections and rate constants for the $N(^2D) + O_2(X) \rightarrow O(^3P) + NO(X)$ reaction, J. Chem. Phys. **118,** 3111-3123 (2003).

11. M. Hankel, G. G. Balint-Kurti, and S. K. Gray, Sinc wavepackets: A new form of wavepacket for time-dependent quantum mechanical reactive scattering calculations, Int. J. Quant. Chem., **92,** 205-211 (2003).

12. P. Defazio and S. K. Gray, Quantum dynamics study of the $D_2 + OH \rightarrow DOH + D$ reaction on the WSLFH potential energy function, P. Defazio and S. K. Gray, J. Phy . Chem. A. *in press* (2003).

Computer-Aided Construction of Chemical Kinetic Models

William H. Green, Jr., MIT Department of Chemical Engineering,
77 Massachusetts Ave., Cambridge, MA 02139. email: whgreen@mit.edu

Project Scope

The combustion chemistry of even simple fuels can be extremely complex, involving hundreds or thousands of kinetically significant species. The most reasonable way to deal with this complexity is to use a computer not only to numerically solve the kinetic model, but also to construct the kinetic model in the first place. We are developing the methods needed to make computer-construction of accurate combustion models practical, as well as tools to make it feasible to handle and solve the resulting large kinetic models.

Most of our work during this grant period has focused on:

1) Development and demonstration of improved rapid reaction rate estimation techniques suitable for systems involving many large molecules

2) Demonstrating methods for automating k(T,P) calculations while building mechanisms with a computer

We have also worked on:

3) Development of a new "Adaptive Chemistry" method for coupling complex chemical kinetics into flame simulations along with other improvements to the numerics

4) "Optimal Model Reduction" for generating the reduced models needed for Adaptive Chemistry simulations

5) "Valid Range Analysis", i.e. methods for identifying the range of reaction conditions over which a kinetic model is valid.

Very recently we have begun developing extensible kinetic-model construction software for wide distribution; this has required development of a new data model for reaction rate and thermochemistry estimation, and compilation of a rate estimation database.

Recent Progress

1. TS Group Additivity for Reaction Rate Estimates

Often the accuracy of combustion simulations is constrained primarily by the accuracy of the high-pressure-limit rate parameters employed. It is unlikely that either experiment or high-quality quantum calculations will be able to provide the very large number of rate constants needed. Instead, we are generalizing from a limited number of quantum calculations and experimental data, using the concept of functional groups. Benson's group additivity scheme very accurately describes thermochemical properties for stable species; we have extended this approach to predict the transition state properties (e.g. the free-energy of activation, needed to compute reaction rates). We have demonstrated for several reaction families that these TS group additivity predictions accurately reproduce individual quantum chemical calculations of rates and thermochemistry. For some reaction families non-nearest-neighbor corrections are important (both for the thermo and the rates), and we have developed effective methods to deal with several examples like this. In general the Complete-Basis-Set (CBS) methods of Petersson et al. are found to achieve the best accuracy at a reasonable computational

cost, though in a handful of cases we have identified technical problems in the CBS extrapolations. We are now preparing to publish a comprehensive database for rate-estimation for the gas phase chemistry of C/H/O compounds, based on the articles reported below [4,5,7,9-11,15] and other manuscripts we have submitted.

2. Automated k(T,P) Calculations

We have developed the first computer algorithms and software for rapidly and accurately computing k(T,P) during computerized model construction. We use an accurate screening technique to compute only the isomerizations and dissociation channels that are numerically significant.[3,12] We have also developed criteria for rapidly determining whether or not a large-molecule reaction will be in the high-pressure limit. We recently completed the integration of these screened k(T,P) calculations into kinetic model generation software, and constructed the first pyrolysis models which account for the pressure-dependence effects on all the reactions. As we complete the rate estimates for reactions of oxygenated radicals we are using this technique to develop combustion/ignition models including k(T,P).

Most of the automated models-with-k(T,P) algorithm development was done by my student David Matheu in collaboration with Jeff Grenda and Tony Dean of ExxonMobil, with initial financial support from a DOE Academic-Industrial partnership award. (Tony Dean is now at Colorado School of Mines; David Matheu recently started an NRC postdoc at NIST.) We are now developing the second generation of these algorithms, in extensible software suitable for wide distribution to the combustion community.

3. Adaptive Chemistry & Numerics for Handling Large Kinetic Models

Reacting flow simulations are most valuable for reactors/combustors with large concentration or temperature gradients, where one expects the chemistry to be dramatically different in different spatial regions. However, currently most reacting flow simulations are performed using the same chemistry model at all mesh positions and at all times. These calculations typically require a very large amount of CPU time and computer memory, limiting most reacting-flow simulations of hydrocarbon combustion to oversimplified chemical kinetic models.

Computational efficiency without sacrificing chemical accuracy is possible by 'adapting' the chemistry model to the local reaction conditions in much the same way that modern simulations use adaptive time-steps and adaptive mesh refinement. The idea in all three cases is to use a lot of detail when it is necessary, but to use a less-detailed description whenever possible without sacrificing accuracy. Our Adaptive Chemistry [14] approach of ignoring chemical reactions and species where they are insignificant is very advantageous, since the best available methods for solving the kinetic equations and for computing the multicomponent diffusion coefficients both scale super-linearly with the number of chemical species considered.

In our quest to reduce the CPU time required to solve large combustion models, we have also developed a numerical method taking advantage of advances in sparse linear algebra and automatic differentiation technology.[6] This approach reduces the CPU time required to solve the LLNL n-heptane/iso-octane model in engine simulations by a factor of 60, making it practical to use this type of very detailed model in rather

complex simulations. We have recently combined these numerics with a new knock criterion we developed to predict the viable operating range of an HCCI engine (SAE 2003-01-1092).

4. Optimal Model Reduction

We have developed a computer program that identifies the smallest valid reduced model for a set of user-specified reaction conditions that it is possible to obtain by eliminating reactions. We have automated this method so that no human intervention is required, and used it to rapidly construct a library of hundreds of reduced kinetic models needed for efficient Adaptive Chemistry reacting-flow simulations of a methane flame. Our work on optimal model reduction has been submitted for publication in *Combustion and Flame*.

5. Valid Range Analysis

In any method that uses or generates multiple kinetic models, one is faced with the problem of identifying which kinetic model is valid for which reaction conditions. We have developed a method that estimates the valid range for an arbitrary kinetic model.[8] However, there is no known way to put a firm bound on the model truncation error in the general case. One can do much better with reduced models, if one assumes that the full model from which they are derived is exact/complete. We are now developing an algorithm for generating valid ranges for reduced models where one can guarantee they will reproduce the full model within user-specified tolerances. This is tricky because there is no guarantee that the region where the reduced model is valid will be convex in the reaction variables (T_o, P, initial concentrations of all the species). We have successfully tackled this problem using interval analysis, in collaboration with Paul Barton and John Tolsma.

Future Plans

We will soon publish a database of high-pressure-limit reaction-family rate estimation rules. For kinetic models with thousands of reactions, it is more reasonable to compare these rules than to try to compare each reaction rate individually. Many of these rate estimates will be derived from the TS group additivity approach described above, which we will apply to a variety free radical reactions of oxygenates. Comparisons will be made with rate estimation rules already in the literature.

We will also develop new thermochemical groups as required using high-level quantum chemistry and advanced models for hindered internal rotation that include the usually neglected couplings between the large-amplitude rotor and the small-amplitude vibrations.

The rate estimation rules and automated k(T,P) calculations will be coupled with computerized model-generation software to construct new combustion chemistry models, with larger valid ranges than existing models. As a first step, we will compute k(T,P) for radical chain-branching from $R+O_2$ and $QOOH + O_2$, where R and Q are the radicals derived from iso-octane using rates derived from high quality quantum calculations for all the isomerization/reaction barriers and wells.

We will also develop the "Adaptive Chemistry" technique into a flexible software library which can be called by a variety of computational fluid dynamics codes, suitable

for wide distribution. This software will include automated model reduction and valid range analysis tools, and software to facilitate control of model-truncation error.

Publications Resulting from DOE Sponsorship (Since 200)

1. H. Richter, O.A. Mazyar, R. Sumathi, W.H. Green, J.B. Howard, & J.W. Bozzelli, "Detailed Kinetic Study of the Growth of Small Polycyclic Aromatic Hydrocarbons. I. 1-Naphthyl + Ethyne", *J. Phys. Chem.* A **105**, 1561-73 (2001).

2. W.H. Green, P.I. Barton, B. Bhattacharjee, D.M. Matheu, D.A. Schwer, J. Song, R. Sumathi, H.H. Carstensen, A.M. Dean, & J.M. Grenda, ' Computer-Construction of Detailed Models for Gas-Phase Reactors", *Ind. Eng. Chem. Res.* **40**, 5362 (2001).

3. D.M. Matheu, T.A. Lada, W.H. Green, A.M. Dean, & J. A. Grenda, "Rate-Based Screening of Pressure-Dependent Reaction Networks", *Comp. Phys. Comm.* **138**, 237-249 (2001).

4. R. Sumathi, H.-H. Carstensen, and W.H. Green, "Reaction Rate Prediction via Group Additivity, Part 1: H Abstraction from Alkanes by H and CH_3", *J. Phys. Chem. A* **105**, 6910-6925 (2001).

5. R. Sumathi, H.-H. Carstensen, and W.H. Green, "Reaction Rate Prediction via Group Additivity, Part 2: H Abstraction from Alkenes, Alkynes, Alcohols and Acids by H atoms", *Journal of Physical Chemistry A* **105** 8969-8984 (2001).

6. D.A. Schwer, J.A. Tolsma, W.H. Green, and P.I. Barton, 'On Upgrading the Numerics in Combustion Chemistry Codes", *Combust. Flame* **128**, 270-291 (2002).

7. R. Sumathi, H.-H. Carstensen, & W.H. Green, "Reaction Rate Prediction via Group Additivity, Part 3: Effect of Substituents with CH_2 as the Mediator", *J. Phys. Chem. A* **106**(22), 5474-5489 (2002).

8. J. Song, G. Stephanopoulos, and W.H. Green, "Valid Parameter Range Analyses for Chemical Reaction Kinetic Models", *Chem. Eng. Sci.* **57**, 4475 (2002).

9. R. Sumathi and W.H. Green, "Thermodynamic Properties of Ketenes: Group Additivity Values from Quantum Chemical Calculations" *J. Phys. Chem. A* **106**(34), 7937-7949 (2002).

10. R. Sumathi and W.H. Green, "*A priori* Rate Constants for Kinetic Modeling", *Theoretical Chemistry Accounts* **108**, 187-213 (2002).

11. R. Sumathi and W.H. Green, "Missing thermochemical groups for large unsaturated hydrocarbons: Contrasting predictions of G2 and CBS-Q" *J. Phys. Chem. A* **106**(46), 11141-11149 (2002).

12. D.M. Matheu, W.H. Green, and J.M. Grenda, "Capturing Pressure-Dependence in Automated Mechanism Generation: Reactions Through Cycloalkyl Intermediates", *Int. J. Chem. Kinet.* **35**, 95-119 (2003).

13. J.M. Grenda, I.P. Androulakis, A.M. Dean, and W.H. Green, "Application of Computational Kinetic Mechanism Generation to Model the Autocatalytic Pyrolysis of Methane", *Ind. Eng. Chem. Res.* **42**, 1000-1010 (2003).

14. D.A. Schwer, P. Lu, and W.H. Green, "An Adaptive Chemistry approach to modeling Complex Kinetics in Reacting Flows", *Combust. Flame* (accepted).

15. C.D. Wijaya, R. Sumathi, and W.H. Green, "Cyclic Ether Formation from Hydroperoxyalkyl Radicals (QOOH)", *Journal of Physical Chemistry A* (accepted).

SPECTROSCOPY AND KINETICS OF COMBUSTION GASES
AT HIGH TEMPERATURES

Ronald K. Hanson and Craig T. Bowman
Department of Mechanical Engineering
Stanford University, Stanford, CA 94305-3032
hanson@me.stanford.edu, bowman@navier.stanford.edu

Program Scope

This program involves two complementary activities: (1) development and application of cw laser absorption methods for the measurement of concentration time-histories and fundamental spectroscopic parameters for species of interest in combustion; and (2) shock tube studies of reaction kinetics and thermochemistry relevant to combustion. Species investigated in the spectroscopic portion of the research include OH and CH_3 using narrow-linewidth ring dye laser absorption, NH_2 using frequency-modulation laser absorption methods, and NO_2 using fixed-frequency absorption. Reactions of interest in the shock tube kinetics portion of the research include: $NH_2 + NO \rightarrow$ Products; $NH_2 + NO_2 \rightarrow$ Products; Benzylamine $\rightarrow$ Products; $CH_3 + O_2 \rightarrow$ Products; and $CH + N_2 \rightarrow$ NCN + H. A new measurement of the enthalpy of formation for OH was made using OH absorption.

Recent Progress: Shock Tube Chemical Kinetics

$NH_2 + NO \rightarrow$ Products: We have completed our study of the overall reaction rate and the branching ratio of the two primary channels of the reaction of NH_2 and NO,

$$NH_2 + NO \rightarrow OH + NNH \tag{1a}$$
$$NH_2 + NO \rightarrow N_2 + H_2O \tag{1b}$$

The branching ratio, $\alpha = k_{1a}/(k_{1a}+k_{1b})$, of these two primary channels is an important parameter in the modeling of NO_X reduction by the Thermal $DeNO_X$ process. Our approach exploited the high sensitivity of NH_2 detection available with frequency-modulation (FM) spectroscopy methods to establish accurate high-temperature values of both the overall rate and the branching ratio. In the temperature range 1340 K - 1670 K, using low (ppm level) concentrations of NH_2 generated by excimer laser photolysis of shock-heated NH_3/NO/Ar mixtures, it was possible to nearly eliminate the dependence of α on the overall rate coefficient. This resulted in a very accurate determination of the branching ratio near $\alpha = 0.5$ that occurs at 1560 K. In the higher temperature region 1826-2159 K, we have measured the branching ratio using thermal decomposition of monomethylamine as a source of NH_2 in mixtures of CH_3NH_2, NO and argon. The final results agree with the theoretical predictions of Miller and Klippenstein (2000).

The overall rate coefficient of the reaction $NH_2 + NO \rightarrow$ products was determined using FM detection of NH_2. NH_2 radicals were produced using the thermal decomposition of two separate source compounds: CH_3NH_2, monomethylamine (MMA), and $C_6H_5CH_2NH_2$, benzylamine (BA). To determine k_{1a+1b}, a perturbation strategy was employed that is based on changes in the NH_2 profiles when NO is added to the MMA or BA/Ar mixtures. Sensitivity analysis shows that NH_2 profiles in these mixtures were sensitive primarily to the overall rate, with significantly lower sensitivity to the branching ratio and other NH_2 reactions. The measured NH_2 profiles were interpreted by detailed kinetic modeling to obtain k_{1a+1b}-values in the temperature range 1700-2500 K using MMA, and were extended to 1300 K using BA. Final results are shown in Fig. 1.

Fig. 1. Summary of k_1: ■ data from $C_6H_5CH_2NH_2$ experiments; □ data from CH_3NH_2 experiments [8]; ○ Lesclaux et al. (1975); △ Silver and Kolb (1982); ▽ Stief et al. (1982); ◇ Atakan et al. (1989); + Wolf et al. (1994); × Park and Lin (1997); ✳ Wolf et al. (1997); — Miller and Klippenstein (2000); - - - Equation (1). The vertical bars represent the combined fitting errors and uncertainties associated with secondary reactions and absorption coefficient.

In figure: $k_1 = 6.83 \times 10^{15}\, T^{-1.203}\, e^{106/T(K)}$; Thermal De-NOx Window
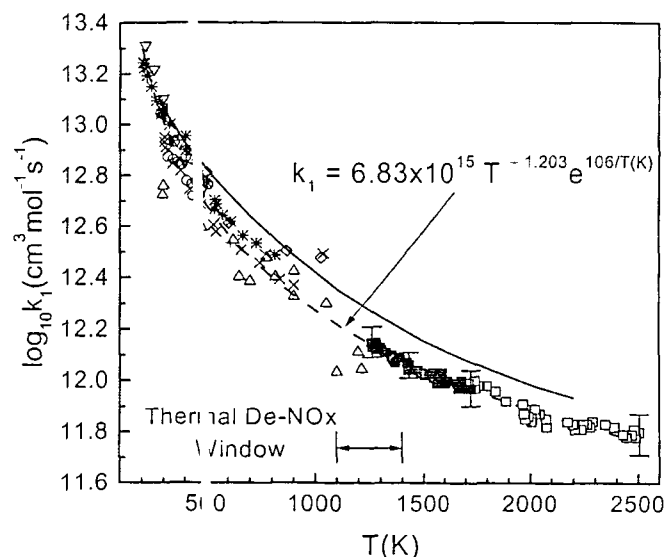
$NH_2 + NO_2 \rightarrow$ Products: We have completed our study of the overall rate coefficient and the branching ratio of the reaction of NH_2 with NO_2. This reaction plays a role during Thermal De-NOx in the recycling of NO_2 back to NO and in N_2O formation. The primary channels are

$$NH_2 + NO_2 \rightarrow N_2O + H_2O \tag{2a}$$
$$NH_2 + NO_2 \rightarrow H_2NO + NO \tag{2b}$$

with the branching ratio defined as $\alpha_2 = k_{2a}/(k_{2a}+k_{2b})$. NH_2 was generated using thermal decomposition of small quantities of benzylamine that was added to NO_2/Ar mixtures. To determine the overall rate coefficient ($k_{2a}+k_{2b}$), we measured NH_2 using FM absorption. Since the sensitivity analysis shows that N_2O traces are sensitive to the branching ratio, we employed IR emission to measure N_2O concentration. NO_2 was also monitored (in absorption) to verify the current reaction mechanism. The reaction rate and branching ratio for these reactions are:

$$k_{2a+2b} = 5.5 \times 10^{12}\ [cm^3/mol/s]\ \{1320\text{-}1530\ K,\ 1.31\text{-}1.49\ atm\}$$
$$\alpha_2 = 0.17 \pm 0.04\ \{1319\text{-}1493\ K\}$$

Decomposition of Benzylamine: In connection with our measurements of the $NH_2 + NO$ and $NH_2 + NO_2$ reactions, we have studied the rate coefficient of the benzylamine (BA) decomposition reaction

$$C_6H_5CH_2NH_2 \rightarrow C_6H_5CH_2 + NH_2 \tag{3}$$
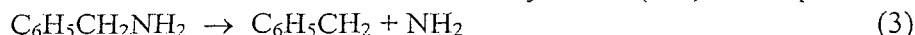
Measuring the initial slope of NH_2 concentration during BA decomposition, we determine the decomposition rate of BA into benzyl and NH_2 radicals. In addition, we performed RRKM calculations that allow inference of the high-pressure-limit values of the decomposition rate of BA and the heat of formation of the benzyl radical, 210 ± 5 kJ/mol, which agrees with the results of Ellison et al. (1996).

$$k_3 = 5.49 \times 10^{14}\ exp(-33110/T)\ [1/s]\ \{1225\text{-}1599\ K,\ 1.19\text{-}1.4\text{?}\ atm\}$$
$$k_\infty = 1.07 \times 10^{16}\ exp(-36470/T)\ [1/s]\ \{1000\text{-}1600\ K\}$$

OH Thermochemistry: We have measured the standard enthalpy of formation of OH using shock tube methods. Recently, workers in multiple laboratories have found evidence of a lower value for the enthalpy of formation of OH. This radical plays an important role in combustion chemistry and has a profound effect on the kinetic modeling of combustion reactions. Our strategy involved sensitive and accurate measurements of OH using narrow-linewidth laser absorption, in shock-heated high temperature H_2-O_2-Ar mixtures where the plateau levels of OH are strongly sensitive to the OH heat of formation and insensitive to kinetic parameters. Over the range of our experimental

conditions (1964-2718 K) we found $\Delta H_{f,298}(OH) = 8.92 +/- 0.16$ kcal/mol, which is ~0.45 kcal/mol below the previously accepted value, and agrees with other recent experimental efforts and theoretical calculations.

Recent Progress: Spectroscopy

OH Spectral Parameters: We have investigated the collision width and shift parameters of key rotational lines in the OH A-X(0,0) band near 307 nm, with the goal of providing missing spectroscopic data and extending the useful pressure range of the OH laser absorption diagnostic. Knowledge of the collision width and shift and their temperature dependences is critical to making accurate, quantitative measurements of species concentration using narrow-linewidth laser diagnostics.

The collision-induced line shift of several rotational lines has been studied at elevated temperatures and pressures behind reflected shock waves in bath gases of Ar and N_2. Experiments at pressures up to 7.5 atm confirmed that the shift is linear with pressure. At 2500 K and 2 atm, the shift was found to increase with lower state rotational quantum number. The collision shift was also found to vary among major rotational branches, and was dependent on the collision partner. Our high temperature measurements for the $P_1(2)$ line can be compared with the room temperature measurements of Shirinzadeh et al. (1985) to ascertain the temperature dependence. Assuming a form of δ_i (T) $\propto T^{-n}$, we find that n = 0.81 for Ar and n = 0.55 for N_2 (see Fig. 2). In the case of the $R_1(5)$ line, the most commonly used absorption line in our laboratory, we found n = 0.76 for Ar.

Fig. 2. Measured OH collision shifts for the $P_1(2)$ transition in N_2 and Ar and the $R_1(5)$ transition in Ar.
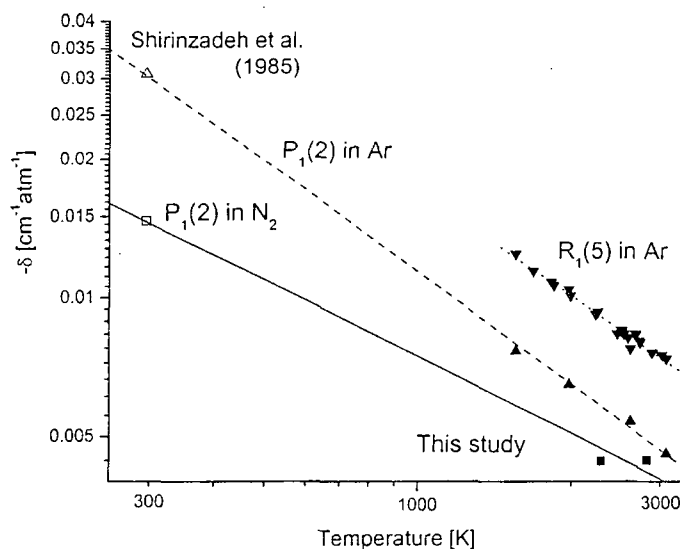
Future Plans

Develop external-cavity frequency-doubling methods for the generation of laser radiation at 216 nm as needed for the improved detection of CH_3. Apply these frequency-doubling methods to other wavelengths of interest including the detection of NCN and HCO at 329 nm and 258 nm respectively.

Develop experimental approaches to measure the overall rate and product branching ratio of the reaction $CH_3+O_2 \rightarrow$ products using OH laser absorption and O-atom ARAS. Develop experimental approaches to measure the reaction rate of $CH+N_2 \rightarrow NCN+H$ using laser absorption.

Recent Publications of DOE Sponsored Research: 2001-2003

1. S. Song, D. M. Golden, R. K. Hanson, C. T. Bowman, J. P. Senosiain, C. B. Musgrave, and G. Friedrichs, "A Shock Tube Study of the Reaction $NH_2+CH_=NH_3+CH_3$ and Comparison with Transition State Theory," accepted for publication, International Journal of Chemical Kinetics.

2. J. T. Herbon, R. K. Hanson, D. M. Golden, and C. T. Bowman, "A Shock Tube Study of the Enthapy of Formation of OH," Proceedings of the Combustion Institute **29**, in press.

3. S. H. Song, R. K. Hanson, C. T. Bowman, and D. M. Golden, "A Shock Tube Study of the NH_2+NO_2 Reaction," Proceedings of the Combustion Institute **29**, in press.

4. S. H. Song, R. K. Hanson, D. M. Golden, and C. T. Bowman, "A Shock Tube Study of the Product Branching Ratio of the NH_2+NO Reaction at High Temperatures," Journal of Physical Chemistry A 106, 9233-9235 (2002).

5. S. Song, D. M. Golden, R. K. Hanson, and C. T. Bowman, "A Shock Tube Study of Benzylamine Decomposition: Overall Rate Coefficient and Heat of Formation of the Benzyl Radical," submitted to Journal of Physical Chemistry A 106, 6094-6098 (2002).

6. R. W. Bates, D. M. Golden, R. K. Hanson, and C. T. Bowman, "Experimental Study and Modeling of the Reaction $H + O_2 + M \rightarrow HO_2 + M$ (M=Ar, N_2, H_2O) at Elevated Pressures and Temperatures between 1050 and 1250 K," Phys. Chem. Chem. Phys. 3, 2337-2342 (2001).

7. D. F. Davidson and R. K. Hanson, "Chapter 5.2: Spectroscopic Diagnostics," *Handbook of Shock Waves: Volume 1*, G. Ben-Dor, O. Igra and T. Elperin, editors, Academic Press, San Diego, pp. 741-785, (2001).

8. J. T. Herbon and R. K. Hanson, "Measurements of Collision-Shift in Absorption Transitions of the OH A-X (0,0) Band Using a Shock Tube," Paper 5734, 23rd International Symposium on Shock Waves, Arlington, Texas (2001).

9. E. L. Petersen and R. K. Hanson, "Non-Ideal Effects Behind Reflected Shock Waves in a High-Pressure Shock Tube," Shock Waves 10, 405-420 (2001).

10. S. Song, R. K. Hanson, C. T. Bowman, and D. M. Golden, "Shock Tube Determination of the Overall Rate of $NH_2+NO \rightarrow$ Products in the Thermal De-Nox Temperature Window," Paper 204 2nd Joint Meeting of the US Section of the Combustion Institute, March (2001).

11. S. Song, R. K. Hanson, C. T. Bowman, and D. M. Golden, "Shock Tube Determination of the Overall Rate of $NH_2+NO \rightarrow$ Products in the Thermal De-NOx Temperature Window," International J. Chemical Kinetics 33, 715-721 (2001).

Theoretical Studies of Potential Energy Surfaces*

Lawrence B. Harding
Chemistry Division
Argonne National Laboratory
Argonne, IL 60439
harding@anl.gov

Program Scope

The goal of this program is to calculate accurate potential energy surfaces for both reactive and non-reactive systems. Our approach is to use state-of-the-art electronic structure methods (MR-CI, CCSD(T), etc.) to characterize multi-dimensional potential energy surfaces. Depending on the nature of the problem, the calculations may focus on local regions of a potential surface (for example, the vicinity of a minimum or transition state), or may cover the surface globally. A second aspect of this program is the development of techniques to fit multi-dimensional potential surfaces to convenient, global, analytic functions that can then be used in dynamics calculations. Finally a third part of this program involves the use of direct dynamics for high dimensional problems to by-pass the need for surface fitting.

Recent Results

H+Vinoxy Radical: Although the vinoxy radical is a resonance stabilized radical, the two resonance structures,

$$H_2C\text{-}CH\text{=}O \longleftrightarrow H_2C\text{=}CH\text{-}O$$
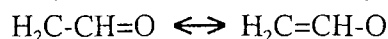
are unequally weighted. The dominant resonance structure has the radical orbital localized on the methylene carbon, while the less important resonance structure has the radical orbital localized on the oxygen. An interesting question in radicals such as this concerns the relative reactivities of the two radical sites. We have completed a 3D analytic potential surface for the interaction of a hydrogen atom with a rigid vinoxy radical. This surface is fit to approximately 9000, CAS+1+2/aug-cc-pvdz energies. The calculations show that there are no barriers for addition to either the methylene carbon or the oxygen atom, however addition to the methylene carbon gives a much more attractive potential. We have also evaluated MEP's for both paths to assess the effect of allowing the vinoxy radical's geometry to relax as the H atom approaches. Geometry relaxation is significantly more important for the oxygen addition pathway but methylene addition remains much more attractive. Basis set corrections using CAS+1+2/aug-cc-pvtz calculations have been evaluated along the MEP's for both paths. These results are now being used by Klippenstein (Sandia) to calculate rates for both paths.

CN+CN: Recent experiments on the photdissociation of NCCN by Hall et al[1,2] (Brookhaven) led to the unexpected result that the product translational energy distributions are consistent with a small (500 cm^{-1}) exit channel barrier. Ab initio, CAS+1+2/aug-cc-pvtz calculations predict no exit channel barrier on the ground state surface and a barrier of ~2500 cm^{-1} on the lowest triplet surface. Neither appear to be consistent with the experiment. This has motivated the development of a four dimensional, analytic, ground state, potential surface for the dissociation of NCCN. In this surface the two CN distances are kept fixed, the remaining four degrees of

freedom are sampled with ~11,000 points at the CAS+1+2/aug-cc-pvtz level. The calculated energies are fit with a combination of a 3D spline and a Fourier expansion. A two dimensional slice of this surface is shown in Figure1. This illustrates that although there is a dipole-dipole
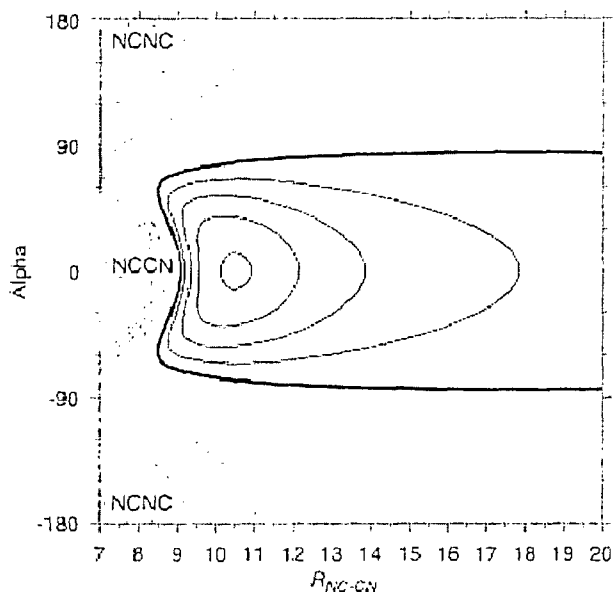
Figure 1. CAS+1+2/aug-cc-pvtz potential surface for the dissociation on NCCN. The thick black contour corresponds to the asymptotic energy of 2CN radicals. Thin black contours denote repulsive energies while gray contours denote attractive energies. The contour increment for repulsive contours is 50 cm^{-1}. The contour increment for attractive contours is 250 cm^{-1}. Alpha is the angle between the line connecting the two CN centers-of-mass and one of the CN bonds. The orientation of the other CN bond is fixed (carbon pointing towards the first CN).

induced barrier for the collinear dissociation of NCCN, barrier-less, non-colinear paths do exist. This surface is now being used by Gray to model the photodissociation experiments.

N+H$_2$: A new analytic global potential surface for $N(^2D)+H_2$ has been fit in collaboration with Ho and Rabitz (Princeton). The new surface is approximately 10 times faster than the previous version and corrects several defects in the older surface. Spurious small scale features have been eliminated and the features of the C_{2v} transition state are in much better agreement with the ab initio calculations. The new surface required roughly a doubling in the number of ab initio calculations. Trajectory calculations on the new surface yield thermal rate constants in significantly better agreement with experiment.

H+HCCH: Recently Knyazev and Slagle[3] reported a combined experimental-theoretical study of reaction (1).

$$C_2H_3 \rightarrow H + C_2H_2 \qquad (1)$$
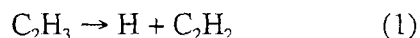
The aim of this study was to resolve existing discrepancies[4] between theory and experiment for reactions (1) and (-1). Two important conclusions from this study were that some of the measured rates for (-1) are not at the high pressure limit (as was previously assumed) and that tunneling significantly influences the shape of the falloff. The theoretical study employed PMP4 calculations which yield a barrier for (-1) of 7.9 kcal/mole. This ab initio barrier had to be scaled to 4.0 kcal/mole inorder to fit the observed rate. This study, together with new high temperature measurements of k_{-1} by Micahel et al, have motivated us to re-examine this reaction.

We have now completed high level, CCSD(T)/aug-cc-pvqz and CAS+1+2/aug-cc-pvqz calculations on this reaction. The calculated CCSD(T) and CAS+1+2+QC barrier heights for (-1) are 3.8 and 4.2 kcal/mole, respectively. To address the question of tunneling we have parameterized a hybrid DFT model (similar in spirit to the MPW1K model proposed by Truhlar[5]) that reproduces the ab initio barrier height, exothermicity, and barrier height location for this specific reaction, (we denote this DFT-SRP). Figure 2 shows a comparison of the
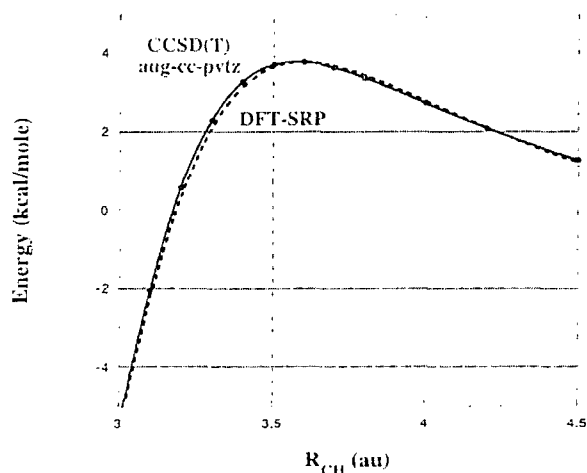
Figure 2. MEP's for the reaction, H+HCCH $\rightarrow$ H$_2$CCH. Solid line and filled symbols are from CCSD(T)/aug-cc-pvtz calculations while the dashed line and open symbols are from the hybrid DFT model (DFT-SRP) described above.

DFT-SRP and CCSD(T) MEP's for this reaction. The DFT-SRP model is then used to calculated IRC's for both H+HCCH and D+HCCH. These IRC's are now being used by Wagner to model both the previous experiments and Michael's new high temperature measurements.

Future Plans

Our direct dynamics/classical trajectory studies on O+CH$_3$ and O+C$_2$H$_5$ have demonstrated that the decomposition of highly energized species can lead to unexpected products. In the coming year we plan to search for more examples of this kind of behavior. One specific system we will study is the dissociation of formaldehyde. At higher energies one might expect to find a new mechanism for the reaction H$_2$CO$\rightarrow$H$_2$+CO in which the molecule starts to dissociate towards H+HCO but before the two fragments completely separate, an abstraction occurs forming the H$_2$+CO products. To address this question we plan to fit an analytic surface at the CAS+1+2 level of theory.

We plan a detailed study of the O atom + vinoxy radical reactions analogous to that described above for H atom +vinoxy. The reverse of the oxygen addition reaction,

$$CH_2=CH-O-O \rightarrow CH_2-CHO + O \qquad (2)$$

may be an important decomposition pathway for the initial adduct formed in the O$_2$+vinyl reaction.

References:

(1) S.W. North, and G. E. Hall, *J. Chem. Phys.* **106**, 60 (1997)
(2) G.E. Hall (private communication)
(3) V. D. Knyazev and I.R. Slagle, *J. Phys. Chem.* **100**,16899 (1996)
(4) L.B. Harding, A.F. Wagner, J.M. Bowman, G.C. Schatz and K. Christoffel,
J. Phys. Chem. **86**, 4312 (1982)
(5) B.J. Lynch, P.L. Fast, M. Harris and D.G. Truhlar, *J. Phys. Chem.* **104**, 4811 (2000)

PUBLICATIONS (2001 - Present):

Evidence for a Lower Enthalpy of Formation of Hydroxyl Radical and a Lower Gas Phase Bond Dissociation Energy of Water, B. Ruscic, D. Feller, D. A. Dixon, K. A. Peterson, L. B. Harding, R. A. Asher, and A. F. Wagner. *J. Phys. Chem. A* **105**, 1-4 (2001)

Construction of reproducing kernel Hilbert space potential energy surfaces for the 1A" and 1A' states of the reaction $N(^2D)+H_2$,
T. Hollebeek, T.-S. Ho, H. Rabitz and L.B. Harding, *J. Chem. Phys.* **114**, 3945-3948 (2001)

Mapping the $OH+CO \rightarrow HOCO$ reaction pathway through infrared spectroscopy of the OH-CO reactant complex, M. I. Lester, B. V. Pond, M.D. Marshall, D. T. Anderson, L. B. Harding, A. F. Wagner, *Faraday Discussions,* **118**, 373-385(2001)

Comment on "On the High Pressure Rate Constants for the H/Mu + O_2 Addition Reactions",
L.B. Harding, J. Troe, and V.G. Ushakov, *Phys. Chem. Chem. Phys.* **3**, 2630-2631 (2001)

A Direct Transition State Theory Based Analysis of the Branching in NH_2+NO, De-Cai Fang, L.B. Harding, S.J. Klippenstein and J.A. Miller, *Faraday Discussions,* **119**, 207-222(2001)

Theoretical and Experimental Investigation of the Dynamics of the Production of CO from the CH_3+O and CD_3+O Reactions, T.P. Marcy, R. R. Diaz, D. Heard, S.R. Leone, L.B. Harding and S.J. Klippenstein, *J. Phys. Chem. A* **105**, 8361-8369 (2001)

On the Enthalpy of Formation of Hydroxyl Radical and Gas Phase Bond Dissociation Energies of Water and Hydroxyl, B. Ruscic, A. F. Wagner, L. B. Harding, R. A. Asher, D. Feller, D. A. Dixon, K. A. Peterson, Y. Song, X. Qian, C.-Y. Ng, J. Liu and W. Chen, *J. Phys. Chem. A* **106**, 2727-2747(2002)

Rate Constants, $1100 \leq T \leq 2000$ K, for $H + NO_2 \rightarrow OH + NO$ Using Two Shock Tube Techniques: Comparison of Theory to Experiment, M.-C. Su, S. S. Kumaran, K. P. Lim, J. V. Michael, A. F. Wagner, L. B. Harding and D. C. Fang, *J. Phys. Chem. A* **106**,8261-8270(2002)

Quasiclassical Trajectory Study of Energy and Angular Distributions for the $H + CO_2 \rightarrow OH + CO$ Reaction, D. Troya, M. J. Lakin, G. C. Schatz, L. B. Harding, and M. Gonzalez, *J. Phys. Chem. B* **106**,8148-8160 (2002)

Resolving the Mystery of Prompt CO_2: The $HCCO+O_2$ Reaction, S.J. Klippenstein, J. A. Miller, and L.B. Harding *28th Symposium (International) on Combustion,* **29**, (in press)

A Theoretical Analysis of the CH_3+H Reaction: Isotope Effects, the High Pressure Limit and Transition State Recrossing, S.J. Klippenstein, Y. Georgievskii, and L.B. Harding
28th Symposium (International) on Combustion, **29**, (in press)

Femtosecond Laser Studies of Ultrafast Intramolecular Processes

Carl Hayden
Combustion Research Facility, MS9055
Sandia National Laboratories
Livermore, CA 94551-0969
CCHAYDE@SANDIA.GOV

Program Scope

The purpose of this research program is to characterize important fundamental chemical processes by probing them directly in time. In this work femtosecond laser pulses are used to initiate chemical processes and follow their progress. The development of new techniques that take advantage of the time resolution provided by femtosecond lasers for studies of chemical processes is an integral part of this research.

Our research focuses on studies of ultrafast energy relaxation and unimolecular reaction processes in highly excited molecules. The goal of these studies is to provide measurements of the time scales for elementary chemical processes that play critical roles in the reaction mechanisms of highly excited reaction intermediates, such as those created in combustion environments by either thermal excitation or exothermic addition reactions. For these studies we have developed the technique of time-resolved photoelectron-photoion coincidence imaging. The apparatus constructed for this work measures fragment recoil velocities and photoelectron velocities in coincidence. This approach provides a wealth of new capabilities for femtosecond time-resolved experiments. Using this technique we have made unique measurements of time-resolved energy correlation spectra for the study of complex dissociation processes[1] and also measured time-resolved, molecular frame photoelectron angular distributions from dissociating molecules.[2]

Recent Progress:

Time-resolved studies of NO dimer photodissociation

We have an ongoing collaboration with Prof. James Shaffer at the University of Oklahoma and Dr. Albert Stolow at the Steacie Institute, NRC, Canada, to study the UV photodissociation of NO dimers. We made preliminary measurements on this system previously and now after some improvements to the apparatus are making more detailed measurements. In these experiments the NO dimer is excited at 211 nm then probed at 258 nm with time-delayed ionization. Coincident ions and electrons are collected on time- and position-sensitive detectors that allow us to calculate the initial velocity vector of each detected fragment ion and its associated electron. The ion detection system also functions as a mass spectrometer, and data on all masses are collected simultaneously. From previous measurements, both in our lab and at the Steacie Institute,[3] we know that the dissociation is relatively slow, occurring on a time scale of ~1 ps. Our current experiments are intended to characterize the excited state of the dimer that undergoes dissociation. The coincidence capabilities of the apparatus are important for these experiments because multiple ionization processes are observed that produce different photoelectron spectra.

At the shortest time delays between the pump and ionization pulses the $(NO)_2$ excited state ionizes to both $(NO)_2^+$ and NO^+. The photoelectron spectrum in coincidence with $(NO)_2^+$

indicates that the neutral state excited at 211 nm has two vibrational quanta in the NO stretching coordinate and that the NO stretching frequency in the dimer excited state is similar to the corresponding frequency in the dimer ion rather than the frequency in the dimer ground state. The ionization of the $(NO)_2$ excited state produces very predominantly NO^+. The photoelectron spectrum coincident with NO^+ shows that it results from ionization of the neutral excited state to the dissociative B state of the dimer ion. This is in marked contrast to the VUV ionization of ground state $(NO)_2$, which ionizes preferentially to $(NO)_2^+$ ground state and only very weakly to the dissociative $(NO)_2^+$ (B) state.

At longer time delays, ionization of the NO(A) state product begins to appear, characterized by photoelectrons with a kinetic energy of 1 eV. The progress of the dissociation is clearly observed in energy correlation spectra for NO^+. An energy correlation spectrum results from correlating the photoelectron energy with the fragment kinetic energy for each individual event detected. The joint probability distribution for electron and fragment kinetic energies can then be plotted. Figure 1 shows a sequence of these spectra. At zero pump-probe delay the dissociative ionization of the dimer excited state is observed. The signal from this process monitors the population of the dimer excited state. At a delay of 300 fs the product NO(A) state is just visible at 1 eV electron energy. Between 300 fs and 800 fs the product grows in rapidly as seen by the development of the peak at 1 eV electron energy, but ionization of the excited dimer persists well past a time delay of one picosecond.

Time-resolved studies of CF₃I dissociative ionization

In another ongoing collaboration, we have performed extensive measurements on the dissociative multiphoton ionization of CF_3I with Anouk Rijs and Dr. Maurice Janssen at Vrije University, Amsterdam, The Netherlands. In these studies the molecule is two-photon excited with a 264 nm pulse in the region of the 7s Rydberg state. The excited molecule is then probed by time-delayed ionization. The experiments reveal a complex process that yields both CF_3^+ and I^+ in conjunction with a substantial contribution from parent ionization.[4] The maximum production of fragment ions occurs when the ionization pulse is delayed by about 100 fs and the fragment ion yield decays with a time constant of approximately 250 fs. Very rapid changes in the vibrational energy distribution in the neutral molecule are observed, resulting in rapid changes in the ionization and fragmentation of the molecule.

There are many ionization processes that occur in this experiment. With sufficiently large coincident data sets we can examine individual process in detail. A particularly interesting ionization mechanism is observed to produce CF_3^+. CF_3^+ is detected with recoil energies up to about 0.5 eV associated with two discrete photoelectron energies separated by 0.2 eV. This separation is the C-F stretching vibrational energy in CF_3^+. The lack of correlation between the photoelectron energy and the ion recoil energy suggests these ions result from a dissociative autoionization process. We can also extract the distribution of photoelectron recoil angles with respect to the dissociation axis to generate a molecular frame photoelectron angular distribution (PAD) referenced to the dissociation axis. For the autoionization process that yields CF_3^+ the electrons are found to have a strong propensity to recoil in the direction of the departing CF_3^+. This forward-backward asymmetry along the dissociation axis is evidence that the dissociation and ionization are strongly coupled because the two fragments must be in close proximity when the electron is ejected to break the symmetry along the dissociation axis.

Future Plans

We will continue our collaboration with Prof. James Shaffer and Dr. Albert Stolow to study the UV photodissociation of NO dimers. Our current results imply that the NO dimer state excited at 211 nm is vibrationally excited with two quanta in an NO stretch. By reducing the excitation frequency by an amount corresponding to one NO stretch quantum we will test this result at a lower excitation level. Another important goal of these new experiments will be to take the large data sets necessary to generate accurate PADs. Since the PADs are sensitive to angular momentum alignment, measurement of PADs for the NO just after dissociation should make it possible to determine if there is torsional motion in the excited state or if the dissociating complex remains planar.

We will also collaborate with Prof. James Shaffer to study dissociation dynamics dimethylformamide and dimethylnitramine. Previous studies of the photodissociation of dimethylformamide indicate that upon excitation to its S_2 state the molecule undergoes charge transfer that results in dissociation on the S_1 surface.[5] Two of the products are HCO and $N(CH_3)_2$. Dimethylnitramine can undergo a seemingly similar dissociation to NO_2 and $N(CH_3)_2$,[6] but in this case charge transfer is not thought to be involved. The dissociation dynamics of these molecules can be compared using time-resolved photoionization as described above to measure photoelectron spectra and photoelectron angular distributions.

References

1. J.A. Davies, J.E. LeClaire, R.E. Continetti and C.C. Hayden, J. Chem. Phys. **111**, 1 (1999).
2. J.A. Davies, R.E. Continetti, D.W. Chandler and C.C. Hayden, Phys. Rev. Lett. **84**, 5983 (2000).
3. V. Blanchet, A. Stolow, J. Chem. Phys., **108**, 4371 (1998).
4. W.G. Roeterdink and M.H.M. Janssen, Phys. Chem. Chem. Phys., **4**, 601 (2002).
5. N. R. Forde, L. J. Butler, and S. Abrash, J. Chem. Phys., **110**, 8954(1999).
6. J-C Mialocq and J. C. Stephenson, Chem. Phys., **106**, 281 (1986).

Publications: 2000-Present

1. A.M. Rijs, C.C. Hayden, and M.H.M. Janssen, "Femtosecond Coincidence Imaging Of Dissociative Ionization Dynamics In CF_3I," in *Femtochemistry and Femtobiology: Ultrafast Dynamics in Molecular Science*, A. Douhal and J. Santamaria, World Scientific Publishing Co.Pte.Ltd. (Singapore) (2002), 91.
2. A.M. Rijs, C.C. Hayden, and M.H.M. Janssen, "Time-Resolved Coincidence Imaging of the Dissociative Ionization in CF_3I," in *XIII Ultrafast Phenomena*, Springer-Verlag, in press.
3. J. P. Shaffer, T. Schultz, J. G. Underwood, C. C. Hayden and A. Stolow, "Time-Resolved Photoelectron Spectroscopy: Charge & Energy Flow in Molecules," in *XIII Ultrafast Phenomena*, Springer-Verlag, in press.
4. E. A. Wade, J. I. Cline, K. T. Lorenz, C. C. Hayden, and D. W. Chandler, "Direct measurement of the binding energy of the NO dimer," J. Chem. Phys. **116**, 4755 (2002).
5. D. W. Chandler and C. C. Hayden, "Ion Imaging Techniques for the Measurement of Ion Velocities," for *Vol. 5 of the Encyclopedia of Mass Spectrometry*, ed. Peter Armentrout, Elsevier Science, in press.
6. R. E. Continetti and C. C. Hayden, "Coincidence Imaging Techniques," in Advanced Series in Physical Chemistry: Modern Trends in Chemical Reaction Dynamics, ed. K. Liu and X. Yang, World Scientific, Singapore, in press.

0 fs delay

300 fs delay

800 fs delay
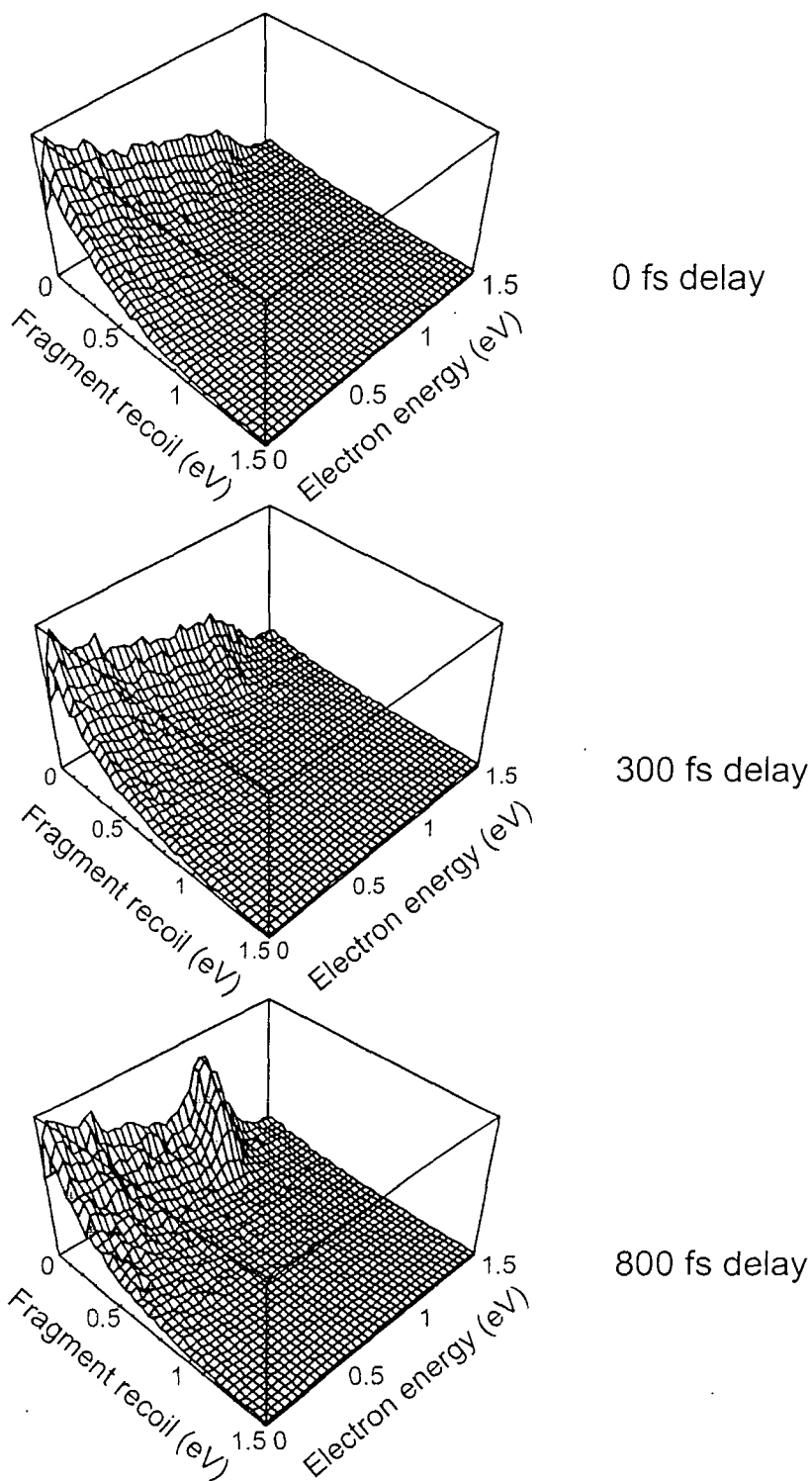
Figure 1. A sequence of energy correlation spectra for NO^+ from NO dimer at increasing time delays between excitation and ionization. Ionization of the NO(A) state product yielding a 1 eV electron can be clearly seen at the longest delay.

CHEMICAL ACCURACY FROM
AB INITIO MOLECULAR ORBITAL CALCULATIONS

Martin Head-Gordon
Department of Chemistry, University of California, Berkeley, and,
Chemical Sciences Division, Lawrence Berkeley National Laboratory,
Berkeley, CA 94720.
mhg@cchem.berkeley.edu

1.   Scope of Project.

Short-lived reactive radicals and intermediate reaction complexes are believed to play central roles in combustion, interstellar and atmospheric chemistry. Due to their transient nature, such molecules are challenging to study experimentally, and our knowledge of their structure, properties and reactivity is consequently quite limited. To expand this knowledge, we develop new theoretical methods for reliable computer-based prediction of the properties of such species. We apply our methods, as well as existing theoretical approaches, to study prototype radical reactions, often in collaboration with experimental efforts. These studies help to deepen understanding of the role of reactive intermediates in diverse areas of chemistry. At the same time, these challenging problems sometimes reveal frontiers where new theoretical developments are needed in order to permit better calculations in the future.

2.   Summary of Recent Major Accomplishments.

2.1   Time-dependent density functional theory calculations.

Density functional theory is a simple and effective computational tool for computational studies of the ground and excited states of radicals. For excited states, time-dependent density functional theory (TDDFT) provides an in-principle exact framework for the calculation of excitation energies. Low-lying excited states of radicals can usually be adequately described using TDDFT with existing functionals. This is exciting because such states often involve substantial double excitation character that is tremendously difficult to describe within wavefunction-based approaches. Moving beyond monoradicals, we have recently reported an extension of TDDFT [17] that permits the description of diradicals with good accuracy using TDDFT starting from a triplet ground state and flipping a spin. We are working on exploring chemical applications of TDDFT, as well as probing its present limitations.

The first class of recent chemical applications have been to excited states of polycyclic aromatic hydrocarbon (PAH) cations which are known to be intermediates in sooting flames. They are also of relevance in the interstellar medium, as a likely source of the diffuse interstellar bands (DIB's). A combined experimental and theoretical study of the fluorene cation has also been completed [10], where all key features seen in the experimental spectrum were assigned using electronic structure methods developed under the support of this program. We have probed the excited states of closed shell PAH cations, suggesting that some members of this series will exhibit strong transitions in the

visible [3]. By contrast, our studies of the maximally pericondensed PAH's suggests that the larger members of this class do not necessarily have strong transitions, which has interesting astrophysical implications [18]. In these studies, TDDFT exhibits numerical errors that are typically less than 0.3 eV or so for cations, which makes it ideal for further studies of the excited states of PAH's, while calculations on systems up to about 100 non-hydrogen atoms are feasible on workstations or fast PC's.

A second class of chemical applications of TDDFT involves excited states in biological systems. We have studied excited states of carotenoids involved in the light-harvesting complex of purple bacteria [8], after establishing the performance of TDDFT for related polyene oligomers [1]. Using our recently developed approach to describing intermolecular energy transfer within TDDFT [2], we were then able to describe Coulombic coupling leading to energy transfer from the carotenoid to neighboring bacteriochlorophyll molecules. Recently we have also characterized the excited states of CO bound to a reduced model of myoglobin [15], to probe the origin of the ultrafast photodissociation seen experimentally. We were able to show that a state which is dissociative in the metal-ligand coordinate crosses the lowest allowed excited state for relatively small stretches of the M-L distance.

Third, we have studied the excited states of the phenyl peroxy radical, and related peroxy radicals, using TDDFT methods [9]. Experiments in solution by the Ingold group (NRC), and in the gas phase by Lim (Emory) showed that it has an absorption in the visible. This is in contrast to the vinyl peroxy radical which only absorbs in the UV, based on experiments by Fahr and Laufer. Furthermore, based on examination of the calculations, we are able to extract a simple and satisfying qualitative picture of the origin of the substituent effects [9].

2.2 New methods for high accuracy electronic structure calculations.

While density functional calculations are extremely valuable, the highest levels of accuracy currently possible come from wavefunction-based electronic structure calculations, such as CCSD(T) (which are also dramatically more expensive). We have performed systematic benchmarks of the performance of existing electronic structure methods for structure and vibrational frequency prediction for radicals [7]. We found that advanced coupled cluster methods performed significantly less well for radicals than for closed shell molecules, with the widely used CCSD(T) method offering no net improvement over CCSD.

To try to overcome the deficiencies of (T) corrections for radicals and for the related problem of bond-dissociation to radical fragments, we have developed a new correction to singles and doubles coupled cluster methods [4,12]. This new method is a true second order correction to a coupled cluster reference, and therefore we denote the correction as (2). The physics of this correction, when applied to a singles and doubles coupled cluster reference, is that it accounts for the leading 3 and 4-electron correlations between electrons. The reference itself only accounts for pair correlations.

In addition to the general formulation, we have developed specific versions to correct the coupled cluster singles and doubles method, as CCSD(2) [4], and the quadratic coupled cluster doubles method [14], as QCCD(2) [11]. It will of course be some time before the strengths and weaknesses of our new (2) corrections relative to

CCSD(T) are completely clear. The most striking result we have obtained to date is a 4 to 5-fold reduction in error for QCCD(2) versus CCSD(T) for predicting the structure and harmonic frequency of N_2 (errors are relative to exact calculations). The level of accuracy obtained by QCCD(2) for this problem actually approaches CCSDTQ! This provides strong incentive for further testing and development of the (2) corrections.

2.3 How compact can the exact many-body wavefunction be?

An exciting result was obtained [6] on the ability to write the exact wave function in a very compact form, as a generalized coupled cluster doubles wave function, depending on a number of variables only equal to the degrees of freedom in the two-particle density matrix. The usual linear expansion of the exact wavefunction involves a factorial number of degrees of freedom! This compact form may offer a way around the problems of n-representability that have plagued attempts to develop electronic structure theory based on the 2-particle density matrix. While (as far as we can tell!) not directly useful for practical calculations, this may be a basis for novel approximations in the future.

3. Summary of Research Plans.

3.1 Density functional theory for excited states of radicals.

We are planning further development and application of the time-dependent density functional (TDDFT) approach to excited states of large molecules, particularly radicals. We are completing a combined theoretical and experimental study of the perylene, terrylene ($C_{30}H_{16}$) and quaterrylene ($C_{40}H_{20}$) series, examining neutral, radical cation and radical anion of each species. We hope to assign the main peak seen experimentally and explain trends in oscillator strength. Calculations probing the role of charge-transfer excited states between carotenoids and chlorophyll are underway. We are also working on extensions of TDDFT to explore excited potential energy surfaces via gradient and possibly hessian evaluation. This should later permit prediction of lineshapes, and possibly also non-radiatiive lifetimes.

3.2 Accurate electronic structure methods.

Motivated by the very exciting preliminary results we have obtained so far, we are in the process of systematically testing our new (2) approach to see whether the weaknesses of CCSD(T) seen for radicals can be corrected using methods such as CCSD(2). We are starting to explore the usefulness of our theoretical methods for characterizing diradicals. We are also thinking about how best to characterize radical and diradical character in reactive molecules to obtain chemical insight.

4. Publications from DOE Sponsored Work, 2001-present.

[1] "Excitation Energies from Time-Dependent Density Functional Theory for Linear Polyene Oligomers: Butadiene to Decapentaene", C.-P.Hsu, S.Hirata and M.Head-Gordon, J. Phys. Chem. A 105, 451-458 (2001).

[2] "Excitation Energy Transfer in Condensed Media", C.-P. Hsu, G.R. Fleming, M. Head-Gordon, and T. Head-Gordon, J. Chem. Phys. 114, 3065-3072 (2001).

[3] "Electronic Spectra and Ionization Potentials of a Stable Class of Closed Shell Polycyclic Aromatic Hydrocarbon Cations", J. L. Weisman, T. J. Lee, and M. Head-Gordon, Spectrochim. Acta A, 57, 931-945 (2001).

[4] "A second order correction to the coupled cluster singles and doubles method: CCSD(2)", S. R. Gwaltney and M. Head-Gordon, J. Chem. Phys. 115, 2014-2021 (2001).

[5] "Two body coupled cluster expansions", T. Van Voorhis and M. Head-Gordon, J. Chem. Phys. 115, 5033-5040 (2001).

[6] "Calculating the Equilibrium Structure of the BNB Molecule: Real Versus Artifactual Symmetry Breaking", S.R. Gwaltney and M. Head-Gordon, Phys. Chem. Chem. Phys. 3, 4495-4500 (2001).

[7] "The theoretical prediction of molecular radical species: a systematic study of equilibrium geometries and harmonic vibrational frequencies", E.F.C. Byrd, C.D. Sherrill, and M. Head-Gordon, J. Phys. Chem. A 105, 9736-9747 (2001).

[8] "The role of the S1 state of carotenoids in photosynthetic energy transfer: the light harvesting complex II of purple bacteria", C.-P. Hsu, P.J. Walla, M. Head-Gordon, and G.R. Fleming, J. Phys. Chem. B 155, 11016-11025 (2001).

[9] "On the Origin of Substituent Effects in the Absorption Spectra of Substituted Peroxy Radicals: Time-Dependent Density Functional Theory Calculations", J.L. Weisman and M. Head-Gordon, J. Am. Chem. Soc. 123, 11686-11694 (2001).

[10] "Vibrational and Electronic Spectroscopy of the Fluorene Cation", J. Szczepanski, J. Banisaukas, M. Vala, S. Hirata, R.J. Bartlett, and M. Head-Gordon, J. Phys. Chem. A 106, 63-73 (2002).

[11] "A Perturbative Correction to the Quadratic Coupled Cluster Doubles Method for Higher Excitations", S. R. Gwaltney, E. F. C. Byrd, T. Van Voorhis, and M. Head-Gordon, Chem. Phys. Lett. 353, 359-367 (2002).

[12] "Coupled cluster methods for bond-breaking", M. Head-Gordon, T. Van Voorhis, S.R. Gwaltney and E.F.C. Byrd, in, "Low-Lying Potential Energy Surfaces", edited by M.R. Hoffman, and K.G. Dyall (ACS Symposium Series, volume 828, 2002), pp. 93-108.

[13] "Can coupled cluster singles and doubles be approximated by a valence active space model?", G.J.O. Beran, S.R. Gwaltney, and M. Head-Gordon, J. Chem. Phys. 117, 3040-3048 (2002).

[14] "Quadratic coupled-cluster doubles: implementation and assessment of perfect-pairing optimized geometries", E.F.C. Byrd, T. Van Voorhis, and M. Head-Gordon, J. Phys. Chem. B 106, 8070-8077 (2002).

[15] "Characterization of the relevant excited states in the photodissociation of CO ligated hemoglobin and myoglobin", A. Dreuw, B.D. Dunietz, and M. Head-Gordon, J. Am. Chem. Soc. 124, 12070-12071 (2002).

[16] "Implementation of generalized valence-bond inspired coupled cluster theories", T. Van Voorhis and M. Head-Gordon, J. Chem. Phys. 117, 9190-9201 (2002).

[17] "The spin-flip approach within time-dependent density functional theory: theory and application to diradicals", Y. Shao, M. Head-Gordon, and A.I. Krylov, J. Chem. Phys. 118, 4807-4818 (2003).

[18] "Time Dependent Density Functional Theory Calculations of Large Compact PAH Cations: Implications for the Diffuse Interstellar Bands" J.L. Weisman, T.J. Lee, F. Salama, and M. Head-Gordon, Astrophys. J. 587, 256-261 (2003).

Laser Studies of the
Combustion Chemistry of Nitrogen

John F. Hershberger

Department of Chemistry
North Dakota State University
Fargo, ND 58105
john.hershberger@ndsu.nodak.edu

Time-resolved infrared diode laser spectroscopy is used in our laboratory to study the kinetics and product channel dynamics of chemical reactions of importance in the gas-phase combustion chemistry of nitrogen-containing radicals. This program is aimed at improving the kinetic database of reactions crucial to the modeling of NO_x control strategies such as Thermal de-NO_x, RAPRENO$_x$, and NO-reburning. The data obtained is also useful in the modeling of propellant chemistry. The emphasis in our study is the quantitative measurement of both total rate constants and product branching ratios.

A. CCO + NO_x Kinetics

We have recently completed data collection for our study of the kinetics of the CCO radical. Previously, only a room temperature CCO+NO rate constant has been known,[1] with no published information available on the branching ratios. No reports of the CCO+NO_2 reaction have been previously published. Originally, we had planned to use LIF to detect CCO but we found that the infrared transitions of CCO near 1970 cm^{-1} (the v_1 band)[2] are sufficiently strong to permit kinetic measurements, at least at near ambient temperatures.

We produce CCO by laser photolysis of carbon suboxide. When using 193 nm photolysis radiation, the transients have rather long risetimes of ~50 μsec, possibly because CCO is initially formed in an exited singlet electronic state. Upon 248 or 266 nm photolysis, somewhat faster risetimes are observed, which is consistent with other reports that mostly ground electronic state CCO is produced at this wavelength.[3] As a result, most of our kinetic data have been collected using 248 or 266 nm:

$$C_3O_2 + h\nu \ (266 \ nm) \rightarrow CCO + CO$$

Possible exothermic product channels include:

$$
\begin{array}{lll}
CCO + NO & \rightarrow NCO + CO & \Delta H_r^0 = -328 \ kJ/mole \\
 & \rightarrow CN + CO_2 & \Delta H_r^0 = -335 \ kJ/mole \\
 & & \\
CCO + NO_2 & \rightarrow CN + CO + O_2 & \\
 & \rightarrow NCO \ (or \ CNO) + CO_2 &
\end{array}
$$

$$\rightarrow NO + 2\ CO$$
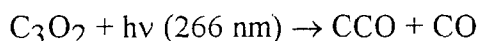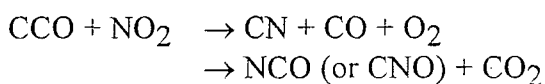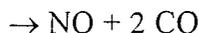
Using infrared detection of CCO under pseudofirst order conditions, we have measured the total rate constant over the range 298-605 K. The rate constants are nearly temperature independent, and can be represented by:

$$k_{CCO\ +\ NO} = (1.37 \pm 0.44) \times 10^{-10}\ exp[(-316 \pm 11)/T] \qquad (cm^3\ molecule^{-1}\ s^{-1})$$

$$k_{CCO\ +\ NO_2} = (5.60 \pm 0.42) \times 10^{-11}\ exp[(-32.6 \pm 22.6)/T].$$

Our initial approach to determine product yields of CCO+NO was to detect CO, CO_2, and N_2O as a function of NO pressure. N_2O (as well as additional CO and CO_2) is produced from the secondary reaction:

$$NCO + NO \quad \rightarrow N_2O + CO$$
$$\rightarrow N_2 + CO_2$$
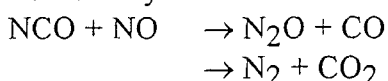
Unfortunately, a large amount of background CO is produced from the C_3O_2; CO yields were found to be roughly the same with and without NO reagent. Quantification of [CO] therefore did not yield useful information towards obtaining the branching ratio. Furthermore, CO_2 detection was made difficult by the presence of CO_2 impurities in the carbon suboxide samples which proved difficult to purify. We also tried to directly detect the CN radical product, but were unsuccessful.

The approach we used to overcome these problems was to use isotopically labeled reagents:

$$CCO + N^{18}O \qquad \rightarrow NC^{18}O + CO$$
$$\rightarrow CN + {}^{16}O^{12}C^{18}O$$
$$NC^{18}O + N^{18}O \qquad \rightarrow N_2{}^{18}O + C^{18}O$$
$$\rightarrow N_2 + {}^{18}O^{12}C^{18}O$$
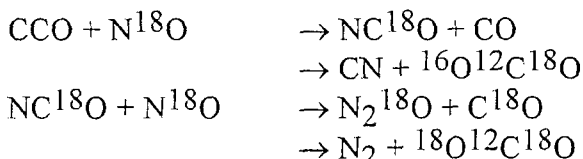
By detecting both the singly and doubly-labeled CO_2 isotopes, we separated the CO_2 that originated from the primary and secondary reactions, and also were able to discriminate from the background due to CO_2 impurities. Since we know the CO_2 yield from the NCO+NO reaction, we were able to unambiguously obtain the branching ratios of CCO+NO. Using this approach, we obtain $\phi(NCO+CO) = 0.87 \pm 0.05$, and $\phi(CN+CO_2) = 0.13 \pm 0.05$ at 298 K.

This approach makes one crucial assumption, that the labelled oxygen-18 in the NO reactant ends up on the NCO and not the CO product. We have conducted QCISD(T)/6-311G(2df,2pd) *ab initio* calculations of portions of the potential energy surface in order to examine this assumption. We find a low-energy path to NCO+CO products involving an ONCCO intermediate, that rearranges via a three membered ring (ONC)-CO structure, eventually yielding NCO+CO, and satisfying our assumption regarding the isotopic labeling. A path that would put the oxygen-18 on the CO product involved an NOCCO intermediate rearranging through a four-membered ring. Although this rearrangement may be feasible, our calculations indicate that formation of the NOCCO is endoergic and proceeds over a

substantial barrier. We are therefore quite confident that our assumption is valid, and that the quoted branching ratios are reliable.

Another issue is whether we are produced NCO or CNO radicals in this experiment. We have no way of detecting CNO, but we have compared the N_2O yields with the $^{18}O^{12}C^{18}O$ yields. Since both of these molecules are postulated to originate from the NCO+NO reaction, they should be present in ratios comparable to the known branching ratios of NCO+NO. They are, suggesting that either we are making NCO and not CNO, or that CNO+NO has similar branching ratios as NCO+NO.

CCN Kinetics

We have begun work on kinetic measurements of the CCN radical. At present, the best precursor we have for this species is HBr_2CCN. This precursor is known to produce HCCN upon 193 nm photolysis.[4] We have found that by weakly focusing the excimer beam, we produce significant amounts of CCN via multiphoton dissociation. CCN is then detected by laser-induced fluorescence at ~403 nm. Although use of focused photolysis light introduces some additional problems, this approach is adequate for total rate constant measurements using LIF, and we have a preliminary estimate of the CCN+NO rate constant of $(2.98\pm0.8)\times10^{-12}$ cm^3 molecule^{-1} s^{-1} at 300 K. We are currently investigating the temperature dependence of the CCN+NO and CCN+O_2 reactions.

Several product channels are possible:

$$
\begin{aligned}
CCN + NO \quad &\rightarrow CN + NCO & \Delta H_r^0 &= -208.6 \text{ kJ/mol} \\
&\rightarrow CCO + N_2 & \Delta H_r^0 &= -393.4 \text{ kJ/mol} \\
&\rightarrow C_2 + N_2O & \Delta H_r^0 &= +118.6 \text{ kJ/mol} \\
&\rightarrow CO + CNN & \Delta H_r^0 &= -313.4 \text{ kJ/mol} \\
&\rightarrow CO + NCN & \Delta H_r^0 &= -434.0 \text{ kJ/mol}
\end{aligned}
$$
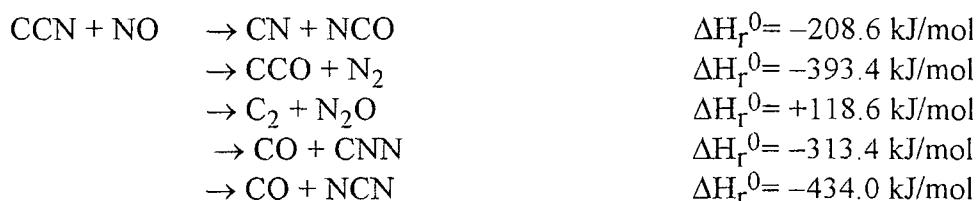
Unfortunately, our photolytic precursor is not particularly suitable for product yield measurements, because of the HCCN that is also produced. We do see some differences between product yields when comparing experiments with focused and unfocused beams. For example, CO is produced in much higher yield relative to N_2O and CO_2 when using focused photolysis light. This CO could have come from channels (d) or (e), or from secondary chemistry of NCO or CCO from (a) or (b). We do not believe it is practical to obtain more than qualitative information from the data using this precursor.

We have tried to use NCCNO, variously called cyanofulminate or cyanogen N-oxide, as an alternative precursor. The synthesis of this semi-stable species has been reported recently,[7] but the photodissociation channels have not been previously investigated. We have found that this molecule absorbs fairly strongly at 193 nm (but not at 248 nm). Unfortunately, we have been unable to observe LIF signals attributable to CCN radicals upon 193-nm photolysis of NCCNO. We have detected CN radicals (using infrared absorption), and we estimate a photolysis quantum yield for CN+(CNO) production of 0.38 ± 0.16.

HCCO+NO Reaction

We have renewed our investigation of the HCCO+NO reaction, which is an important step in NO-reburning mechanisms. Two channels are active:

$$HCCO+NO \rightarrow HCN + CO_2$$
$$\rightarrow CO + HCNO$$

Previous experimental measurements of the branching ratio have varied from $\phi(CO_2)$=0.12-0.28.[4-6] All previous studies have suffered from significant secondary chemistry. Following a suggestion of Richard Bersohn and some mass spectrometric experiments of Laurie Butler, we are using ethyl ethynyl ether, C_2H_5OCCH, as our HCCO precursor. This appears to be a cleaner HCCO source than previous methods, but still produces a CO background (i.e., CO is produced upon 193-nm photolysis of a C_2H_5OCCH/buffer gas mixture). This CO is probably produced by reactions of HCCO which are suppressed in the presence of an excess of NO, but because of this problem, we have chosen to measure the branching ratio by quantifying the HCNO product rather than CO. We have detected both CO_2 and HCNO, and are in process of quantifying the yields. Preliminary data, based on CO_2 and HCNO yields, appears to confirm our previous low value of $\phi(CO_2)\sim0.12$ at 296 K.

References

1. Donnelly, V. M.; Pitts, W. M.; McDonald, J. R. *Chem. Phys.* **1980**, *49*, 289.
2. Yamada, C.; Kanamori, H.; Horiguchi, H.; Tsuchiya, S.; Hirota, E. *J. Chem. Phys.* **1986**, *84*, 2573.
3. Anderson, D. J.; Rosenfeld, R. N. *J. Chem. Phys.* **1991**, *94*, 7857.
4. Nguyen, M. T.; Boullart, W.; Peeters, J. *J. Phys. Chem.* **1994**, *98*, 8030.
5. Eickhoff, U.; Temps, F. *Phys. Chem. Chem. Phys.* **1999**, *1*, 243.
6. Rim, K. T.; Hershberger, J. F. *J. Phys. Chem. A* **2000**, *104*, 293.
7. Pasinszki, T.; Westwood, N. P. C. *J. Phys. Chem.* **1996**, *100*, 16857.

Publications acknowledging DOE support (2001-present)

"Recent Progress in Infrared Absorption techniques for Elementary Gas Phase Reaction Kinetics", C. Taatjes and J.F. Hershberger, Ann. Rev. Phys. Chem. **52**, 41 (2001).

"Kinetics of HCCl + NO_x Reactions", R.E. Baren, M. Erickson, and J.F. Hershberger, Int. J. Chem. Kinet. **34**, 12 (2002).

"Kinetics of the NCN Radical", R.E. Baren and J.F. Hershberger, J. Phys. Chem. A, **106**, 11093 (2002).

"Kinetics of the SiH_3+O_2 and $SiH_3+H_2O_2$ Reactions", J. Meyer and J.F. Hershberger, submitted to J. Phys. Chem. A.

"Kinetics of the CCO+NO and CCO+NO_2 Reactions, W.D. Thweatt, M.A. Erickson, and J.F. Hershberger, manuscript in preparation.

PRODUCT IMAGING OF COMBUSTION DYNAMICS

P. L. Houston

Department of Chemistry
Cornell University
Ithaca, NY 14853-1301
plh2@cornell.edu

Program Scope

The technique of product imaging is being used to investigate several processes important to a fundamental understanding of combustion. The imaging technique produces a "snapshot" of the three-dimensional velocity distribution of a state-selected reaction product.

Research in three main areas is planned. First, the imaging technique will be used to measure rotationally inelastic energy transfer on collision of closed-shell species with several important combustion radicals. Such measurements improve our knowledge of intramolecular potentials and provide important tests of *ab initio* calculations. Second, product imaging will be used to investigate the reactive scattering of radicals or atoms with species important in combustion. These experiments, while more difficult than studies of inelastic scattering, are now becoming feasible. They provide both product distributions of important processes as well as angular information important to the interpretation of reaction mechanisms. Finally, experiments using product imaging at the Advanced Light Source will explore the vacuum ultraviolet photodissociation of CO_2 and other important species. Little is known about the highly excited electronic states of these molecules and, in particular, how they dissociate. These studies will provide product vibrational energy distributions as well as angular information that can aid in understanding the symmetry and crossings among the excited electronic states.

Recent Progress

Two-photon Photodissociation of NO through Rydberg Levels in the 265-278 nm region

The spectroscopy and dynamics of the NO photodissociation through Rydberg levels near 74,000 cm^{-1} have been investigated following two-photon excitation. The $6d\pi^-(v=1)$ and $5s\sigma(v=3)$ levels overlap near 74,070 cm^{-1}. Assignment of the rotational transitions for these levels has been aided by the use of the photo-product angular distributions measured using product imaging techniques. Product imaging was also used to investigate the $8d\pi^-(v=1)$ and $5s\sigma(v=2)$ regions assigned by previous investigators. In all cases, the major products were $N(^2D) + O(^3P)$. As shown in Fig. 1, the angular distributions vary strongly with rotational transition and with the assumed intermediate in the two-photon excitation
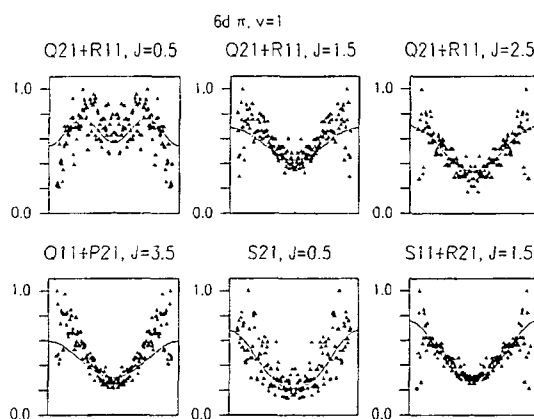
Figure 1 Comparison between measured and predicted angular distributions. The x axis in all cases is from 0 to π radians.

scheme. They can be predicted by calculation and demonstrate that the major contribution to the two-photon line strength is via a Π intermediate, likely the C $^2\Pi$ state, with less than a 30% amplitude contribution from either a Σ or Δ intermediate.

Photodissociation of O_2

One experiment that arose as a by-product of our use of 130 nm as a detection wavelength for O atoms in the CN + O_2 reaction is a study of the photodissociation of O_2 itself. O atoms are resonantly ionized by the same wavelength used to dissociate the O_2. The cross section for O_2 absorption at this wavelength is only about 10 atm^{-1} cm^{-1}, or about 4 x 10^{-19} cm^2. Nonetheless, we can still observe the O image from photodissociation of O_2, as shown in Fig. 2. The signal, though weak, is still detectable even though the cross section is so small. In the diagram, the polarization vector of the dissociating light is roughly 45° to the vertical and runs between the upper left and lower right in the plane of the image.
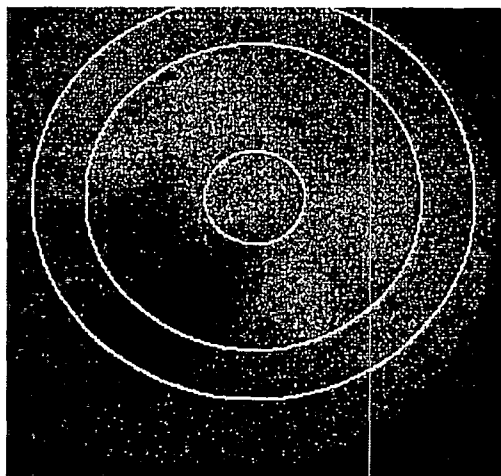
Figure 2 O(^{3}P) image following photodissociation of O_2 at 130 nm.

Thus, the image indicates that the transition is a parallel one. The energetics indicate that the predominant sibling atom to O(^{3}P) is O(^{1}D) -- the energetic limit for this channel is given by the middle circle. Both this identification of the main dissociation channel and the determination of the symmetry of the final state are in agreement with previous measurements.[1-4] We do not see evidence for O(^{1}S) + O(^{3}P) above the (unsubtracted) background within the innermost circle. However, there is a faint signal just inside the outer circle due to the O(^{3}P) + O(^{3}P) channel, not previously observed. More careful study of these will produce quantitative branching ratios.

Photodissociation of N_2O

Encouraged by the example above, we decided to investigate a 130-nm photodissociation that had a more reasonable cross section; N_2O has $\sigma \approx 4$ x 10^{-17} cm^2. Somewhat to our surprise, the 130/212 combination ionized several products. While the dominant signal when the VUV was tuned to the O resonance was O$^+$, as expected, we also observed N_2^+ and NO$^+$, whether or not the 130 nm was tuned to the O resonance. Figures 3 and 4 show the images of O and NO obtained from this preliminary study. Figure 3 indicates that the O(^{3}P) is produced in coincidence with electronically excited N_2. The outer circle gives the velocity limit for O(^{3}P) + $N_2(A, v=0)$ while the inner circle gives the velocity limit for O(^{3}P) + $N_2(B, v=0)$. Figure 4 indicates that the majority of N_2^+ comes from a channel producing O(^{1}S) and $N_2(X)$. The outer ring is for this channel with the N_2 in $v=2$, while the inner ring is for N_2 in $v=10$. Observation of O(^{1}S) and $N_2(A)$ are in agreement with some previous observations,[5] but O(^{1}D) should also
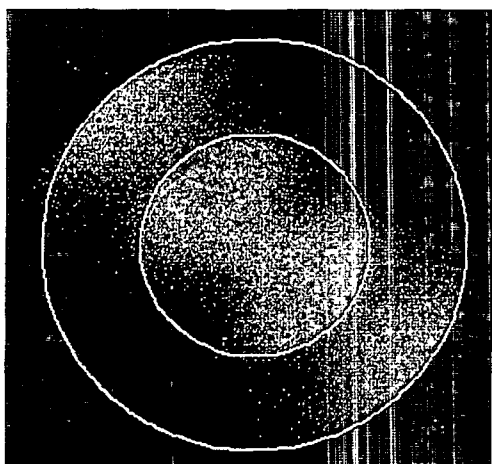
Figure 3 O from photodissociation of N_2O at 130 nm. The outer ring is $O + N_2(A, v=0)$, while the inner ring is $O + N_2(B, v=0)$.
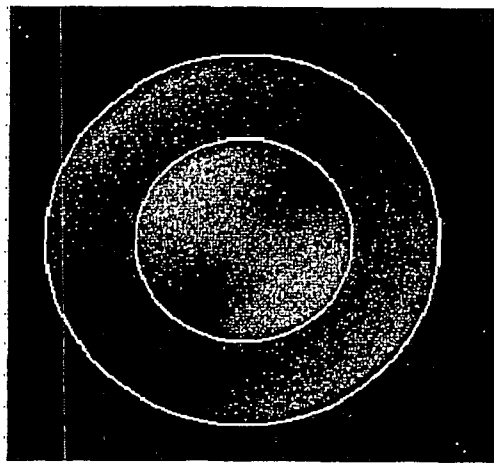
Figure 4 N_2 from photodissociation of N_2O at 130 nm. The outer ring is $O(^1S) + N_2(X, v=2)$, while the inner ring is $O(^1S) + N_2(X, v=10)$.

be present. It is clear that a more thorough investigation of these and other images will be necessary to sort out the dissociation channels.

Future Directions

Research in three main areas is planned. First, product imaging will be used to investigate the reactive scattering of radicals or atoms with species important in combustion. These experiments, while more difficult than studies of inelastic scattering or photodissociation, are now becoming feasible. They provide both product distributions of important processes as well as angular information important to the interpretation of reaction mechanisms. Preliminary work on the CN $+O_2$ reaction has begun. Second, the imaging technique will be used to measure rotationally inelastic energy transfer on collision of closed-shell species with important combustion radicals. Such measurements improve our knowledge of intramolecular potentials and provide important tests of ab $initio$ calculations. Work on Ar + SO is underway. Finally, experiments using product imaging will explore the vacuum ultraviolet photodissociation of O_2, N_2O, SO_2, and other important species. Little is known about the highly excited electronic states of these molecules and, in particular, how they dissociate. These studies will provide product vibrational energy distributions as well as angular information that can aid in understanding the symmetry and crossings among the excited electronic states.

References

1.   E. J. Stone, G. M. Lawrence, and C. E. Fairchild, *J. Chem. Phys.* **65**, 5083-92 (1976).
2.   G. A. Germany, G. J. Salamo, and R. J. Anderson, *Journal of Applied Physics* **54**, 4573-7 (1983).
3.   J. B. Nee and P. C. Lee, *Journal of the Korean Physical Society* **32**, 338-341 (1998).
4.   J. J. Lin, D. W. Hwang, Y. T. Lee, and X. Yang, *Journal of Chemical Physics* **109**, 1758-1762 (1998).
5.   G. Black, R. L. Sharpless, T. G. Slanger, and D. C. Lorents, *J. Chem. Phys.* **62**, 4266-73 (1975); D. G. Hopper, *J. Chem. Phys.* **80**, 4290-316 (1984); E. Patsilinakou, R. T. Wiedmann, C. Fotakis, and E. R. Grant, *J. Chem. Phys.* **91**, 3916-25 (1989); W. F.

Chan, G. Cooper, and C. E. Brion, *Chem. Phys.* **180**, 77-88 (1994); J. B. Nee, J. C. Yang, P. C. Lee, X. Y. Wang, and C. T. Kuo, *Journal of Physics B: Atomic, Molecular and Optical Physics* **31**, 5175-5181 (1998); H. Umemoto, M. Kashiwazaki, and T. Yahata, *Journal of the Chemical Society, Faraday Transactions* **94**, 1793-1795 (1998); W. C. Trogler, *Coordination Chemistry Reviews* **187**, 303-327 (1999); P. C. Lee and J. B. Nee, *Journal of Chemical Physics* **112**, 1763-1768 (2000); J. B. Nee and P. C. Lee, *APPC 2000, Proceedings of the Asia-Pacific Physics Conference, 8th, Taipei, Taiwan, Aug. 7-10, 2000* , 250-252 (2001).

Publications Prepared with DOE Support 2001-present

M. S. Westley, K. T. Lorenz, D. W. Chandler, and P. L. Houston, "Differential Cross Sections for Rotationally Inelastic Scattering of $NO(X^2\Pi_{1/2}, v=0, J=0.5, 1.5)$ from He or D_2 to $NO(X^2\Pi_{1/2}, J=2.5-12.5)$," *J. Chem. Phys.* **114**, 2669-2680 (2001).

P. A. Arnold, B. R. Cosofret, S. M. Dylewski, P. L. Houston, and B. K. Carpenter, "Evidence of a Double Surface Crossing Between Open and Closed Shell Surfaces in the Photodissociation of Cyclopropyl Iodide," *J. Phys. Chem. A*, **105**, 1693-1701 (2001).

P. L. Houston, B. R. Cosofret, A. Dixit, S. M. Dylewski, J. D. Geiser, J. A. Mueller, R. J. Wilson, P. J. Pisano, M. S. Westley, K. T. Lorenz, and D. W. Chandler, "Product Imaging Studies of Photodissociation and Bimolecular Reaction Dynamics," *J. Chinese Chem. Soc.*, **48**, 309-318 (2001).

A. A. Dixit, P. J. Pisano, and P. L. Houston, "Differential cross section for rotationally inelastic scattering of vibrationally excited $NO(v=5)$ scattered from Ar," J. Phys. Chem. **105**, 11165-11170 (2001).

P. L. Houston, "Charged Particle Imaging in Chemical Dynamics: An Historical Perspective," in *Imaging in Molecular Dynamics: Technology and Applications*, B. Whitaker, ed. (Cambridge University Press, in press).

Bogdan R. Cosofret, H. Mark Lambert, and Paul L. Houston, "$N(^2D)$ Product Velocity Mapped Imaging in the VUV Photolysis of Nitrous Oxide at 118.2 nm," Bull. Korean Chem. Soc. **23**, 179-183 (2002). (K.-H. Jung commemorative issue).

Bogdan R. Cosofret, H. Mark Lambert, and Paul L. Houston, "Two-photon Photodissociation of NO through Rydberg Levels in the 265-278 nm region: Spectra and Photofragment Angular Distributions," J. Chem. Phys. **117**, 8787-8799 (2002)

These publications may be accessed at http://www.ccmr.cornell.edu/~plh2/group/publicat.html

AROMATICS OXIDATION AND SOOT FORMATION IN FLAMES

J. B. Howard and H. Richter
MIT Department of Chemical Engineering
77 Massachusetts Avenue
Cambridge, MA 02139-4307
e-mail: jbhoward@mit.edu

Scope

This project is concerned with the kinetics and mechanisms of aromatics oxidation and the growth process to polycyclic aromatic hydrocarbons (PAH) of increasing size, soot and fullerenes formation in flames. The overall objective of the experimental aromatics oxidation work is to extend the set of available data by measuring concentration profiles for decomposition intermediates such as phenyl, cyclopentadienyl, phenoxy or indenyl radicals which could not be measured with molecular-beam mass spectrometry to permit further refinement and testing of benzene oxidation mechanisms. The focus includes PAH radicals which are thought to play a major role in the soot formation process while their concentrations are in many cases too low to permit measurement with conventional mass spectrometry. The radical species measurements are used in critical testing and improvement of a kinetic model describing benzene oxidation and PAH growth. Thermodynamic property data of selected species are determined computationally, for instance using density functional theory (DFT). Potential energy surfaces are explored in order to identify additional reaction pathways. The ultimate goal is to understand the conversion of high molecular weight compounds to nascent soot particles, to assess the roles of planar and curved PAH and relationships between soot and fullerenes formation. The specific aims are to characterize both the high molecular weight compounds involved in the nucleation of soot particles and the structure of soot including internal nanoscale features indicative of contributions of planar and/or curved PAH to particle inception.

Recent Progress

The development of a kinetic model describing the oxidation of hydrocarbons including the formation of PAH under fuel-rich conditions has been continued. Thermodynamic and kinetic property data have been continuously updated. Thermodynamic property data were taken from the literature or were determined by means of density functional theory (DFT). Isodesmic reactions allowed for the determination of heats of formation of unknown compounds including most radical species. Entropies and heat capacities were obtained using vibrational analysis including treatment of pertinent rotors as free rotors. Chemically activated reactions were analyzed by means of Quantum Rice-Ramsperger-Kassel (QRRK) [1] analysis and rate constants for low-pressure and atmospheric pressure conditions were determined. Model computations were conducted for rich premixed low-pressure benzene flames [2-4] using experimental temperature profiles and for ethylene combustion in well-stirred/plug-flow reactors at atmospheric pressure covering temperatures from 1530 to 1720 K [5]. All model computations were conducted with the *Chemkin* software package. The built-in postprocessor was used for subsequent reaction pathway analysis. The comparison of model predictions with experimental data showed good to excellent agreements for nearly all detected species pertinent to the oxidation of the initial fuel, i.e., benzene or ethylene, including radicals at low-pressure and atmospheric pressure conditions. This observation is consistent with recently published results from this project [6] in which the predictive capability of a previous version of the present model was tested for the combustion of acetylene, ethylene and benzene in premixed low-pressure flames.

However, comparison of model predictions with experimental data [3] showed significant underpredictions for major PAH such as pyrene and these discrepancies were found to increase with the size of the molecules. A careful analysis of potential sources of error led to the conclusion that additional PAH formation pathways not currently included in the model might exist. Two potential additional PAH

growth routes were explored: a) direct addition of acetylene to vinyl-PAH adducts (PAH-CHCH) with subsequent ring closure followed by hydrogen loss and b) the contribution of C_3 species.

a) Direct addition of acetylene to vinyl adducts (see (1))

A recent investigation of the potential energy surface of phenanthrene formation from biphenyl and naphthalene using density functional theory (DFT) and *ab initio* computations provided high-pressure rate constants for all known pertinent elemental reactions steps [7]. Many of the reported reactions pathways are chemically activated and, in the present study, QRRK computations [1] were conducted in order to determine kinetic data describing processes relevant for PAH growth under different pressure and temperature conditions. Particularly, direct addition of acetylene to vinyl-adducts (1), initially suggested by Bittner and Howard [2], was investigated and the relative contribution of this pathway assessed.
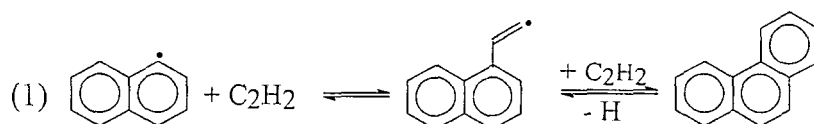
The contribution of direct addition of acetylene to vinyl adducts to phenanthrene formation at low (20 torr), atmospheric and high pressure (20 atm) was investigated. At low pressure, direct addition of acetylene to 1-vinylnaphthalene was found to play a minor role in comparison to acetylene addition to biphenyl radicals, ring-ring condensation or fusion of five-membered ring structures. However, an increasing contribution of the acetylene + 1-vinylnaphthalene was observed at higher pressures, particularly at moderate temperatures. In addition, increasing size of vinyl adducts is expected to favor their formation in comparison to the corresponding PAH-C_2H + H product channel. In conclusion, under high-pressure/moderate temperature conditions, direct addition of acetylene to vinyl-PAH adducts is likely to play a significant role in the formation of large PAH and possibly of soot. Reactions describing formation of PAH of increasing size will be added to the model after determination of the corresponding rate constants by means of QRRK computations.

b) Contribution of C_3 species

Interest in the contribution of C_3 species to PAH growth was triggered by the identification of a large number of PAH with an odd number of carbon atoms by Homann and co-workers [8]. Concentrations of the corresponding radicals, i.e., PAH with odd numbers of carbon and hydrogen atoms (o,o-PAH) were found to be surprisingly high, in the case of larger species even higher than those of the parent molecules (o,e-PAH).

In the present work, formation of phenalene from 1-naphthyl + C_3H_3 was investigated in some detail. The potential energy surface was explored using B3LYP density functional theory with a cc-pvdz basis set. All computations were conducted with the *Gaussian 98* sofware. Finally, two pathways were identified to be overall exothermic and to play a potential role in the formation of o,e-PAH:
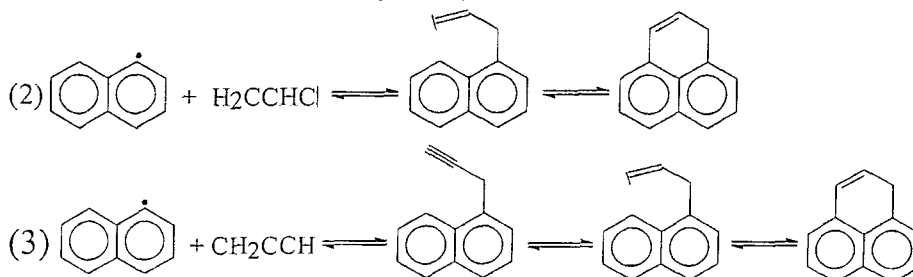
Major features of both pathways are hydrogen-shift and carbon-insertion reactions. In the case of (2), isomerization via hydrogen migration from 2-propynyl (propargyl, CH_2CCH) to 2-propene-1-yl-3-ylidene (H_2CCC) takes place prior to the initial growth reaction while in pathway (3) such isomerization occurs

subsequently. After completion of the potential energy surfaces including transition states, rate constants of the individual reaction steps will be determined. Pathway (3) is expected to be chemically activated; therefore, QRRK computations will be conducted.

The geometry of the phenalene radical was optimized on a B3LYP cc-pvdz level and the heat of formation was determined by means of the following isodesmic reaction:

$$(4) \quad \text{[chemical structures]} + \text{[chemical structure]} \longrightarrow \text{[chemical structures]} + \text{[chemical structure]}$$
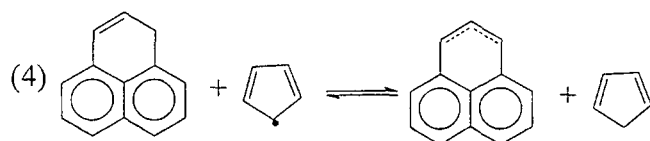
$\Delta H_f^0 = 55.8$ kcal mole^{-1} was found for the phenalene radical and the difference of only ≈ 8 kcal mole^{-1} (phenalene: $\Delta H_f^0 = 47.5$ kcal mole^{-1}) relative to the parent molecule reveals significant resonance stabilization. In addition, geometries of the adducts of 5-acenapthyl + CH_2CCH and of 1-phenanthryl + CH_2CCH, as well as of the corresponding o,e-PAH and o,o-PAH radicals were optimized. Consistent with the results for 1-napththyl + CH_2CCH, ring structures were found to be significantly more stable than the substituted isomers (i.e., propyne derivatives) and similar stabilities relative to the corresponding parent molecules were found for all o,o-PAH radicals. QRRK computations will allow for the assessment of the effect of molecule size on the relative abundances of o,e-PAH and the corresponding propyne derivatives. The possibility of further PAH growth via reaction of C_3 species (C_3H_3 or C_3H_2) with o,o-radicals was explored but no viable reaction pathway could be identified at this stage.

The formation of young soot particles has been modeled in two benzene/oxygen/argon low-pressure flames with equivalence ratios $\phi = 1.8$ and 2.0 [2,3] and compared with model predictions for an even more sooting benzene flame of $\phi = 2.4$ [4]. This approach permits assessment of changes in the flame chemistry close to the sooting limit and therefore offers the potential for gaining improved understanding of soot inception. The kinetic model describing the formation of young soot particles with particle diameters of up to 7 nm by means of a sectional technique has been developed in parallel research at MIT [9]. Its ability to describe PAH and soot formation has been demonstrated for the above-mentioned rich benzene/oxygen/argon flame at $\phi = 2.4$ [10]. Soot inception was found to depend strongly on the equivalence ratio and to occur at the investigated conditions at an equivalence ratio between $\phi = 2.0$ and 2.4. The comparison of maximum PAH concentrations showed a general increase with equivalence ratio, ranging from $\approx 40\%$ in the case of acenaphthylene to ≈ 4-fold for pyrene (between $\phi = 1.8$ and 2.4). Particularly for larger PAH, the increase between $\phi = 2.0$ and 2.4 is more pronounced than that between $\phi = 1.8$ and 2.0. Maximum concentrations of particles with diameters of up to ≈ 2 nm are similar in all three investigated flames while significant amounts of larger particles were predicted only in the flame with $\phi = 2.4$. For instance, the predicted concentrations of particles with a diameter of ≈ 7 nm are more than three orders of magnitude higher than in the flames with $\phi = 1.8$ and 2.0. This observation is consistent with a lack of depletion of smaller particles in the latter flames.

In studying the relationship between fullerenes formation and soot formation, it has been found that the formation of fullerenic nanotubes in low-pressure premixed flames can be competitive with soot formation if a catalyst such as iron is present in the gas phase. The results reveal the presence of a window of residence times and fuel equivalence ratios in which single-walled nanotubes form before significant soot formation occurs.

Future Plans
The work will include finishing the analysis of, and reporting, PAH radical concentration measurements in two benzene/oxygen flames, and extension of flame modeling calculations and critical

comparison of the results against the experimental measurements. PAH growth via direct addition of acetylene to vinyl adducts will be extended to larger PAH. Vibrational frequencies, necessary as input for the QRRK analysis, will be determined after geometry optimization by means of density functional theory computations. PAH radicals with odd numbers of carbon and hydrogen atoms as well as their parent molecules will be included in the model and the resulting impact on PAH growth will be investigated. For this purpose, rate constants of chemically activated reactions between PAH radicals and C_3H_3 species (H_2CCCH and $CHCHCH$) will be determined using QRRK analysis and the effect of pressure and molecular size on the formation of PAH derivatives with odd numbers of carbon atoms will be assessed.

References

1. Chang, A. Y., Bozzelli, J. W. and Dean, A. M. Kinetic Analysis of Complex Chemical Activation and Unimolecular Dissociation Reactions Using QRRK Theory and the Modified Strong Collision Approximation. Z. Phys. Chem. **214**, 1533-1568 (2000).
2. Bittner, J. D. and Howard, J. B. Composition Profiles and Reaction Mechanisms in a Near-Sooting Premixed Benzene/Oxygen/Argon flame. Proc. Combust. Inst. **18**, 1105-1116 (1981).
3. Benish, T. G., PAH Radical Scavenging in Fuel-Rich Premixed Benzene Flames. Ph.D. thesis, Massachusetts Institute of Technology, Cambridge, MA 1999.
4. Grieco, W. J., Lafleur, A. L., Swallow, K. C., Richter, H., Taghizadeh, K. and Howard, J. B. Fullerenes and PAH in Low-Pressure Premixed Benzene/Oxygen Flames. Proc. Combust. Inst. **27**, 1669-1675 (1998).
5. Marr, J. A., PAH Chemistry in a Jet-Stirred/Plug-Flow Reactor System. Ph.D. thesis, Massachusetts Institute of Technology, Cambridge, MA 1993.
6. Richter, H. and Howard, J. B. Formation and Consumption of Single-Ring Aromatic Hydrocarbons and Their Precursors in Premixed Acetylene, Ethylene and Benzene Flames. Phys. Chem. Chem. Phys. **4**, 2038-2055 (2002).
7. Kislov, V. V., Mebel, A. M. and Lin, S. H. Ab Initio and DFT Study of the Formation Mechanisms of Polycyclic Aromatic Hydrocarbons: The Phenanthrene Synthesis from Biphenyl and Naphthalene. J. Phys. Chem. A **106**, 6171-6182 (2002).
8. Homann, K.-H., Fullerenes and Soot Formation – New Pathways to Large Particles in Flames. Angew. Chem. Int. Ed. **37**, 2434-2451 (1998).
9. National Science Foundation, Formation of Polycyclic Aromatic Hydrocarbon Structures and their Role in Soot Formation. Award 0123345, 2002.
10. Richter, H., Granata, S., Howard, J. B. and Kronholm, D. F., Modeling of PAH and Soot Formation in a Laminar Premixed Benzene/Oxygen/Argon Low-Pressure Flame. Presented at the Third Joint Meeting of the U.S. Sections of the Combustion Institute, Chicago, March 2003.

Publications of DOE Sponsored Research, 2001-2003

1. Richter, H., Mazyar, O.A., Sumathi, R., Green, W. H., Howard, J. B. and Bozzelli, J. W. Detailed Kinetic Study of the Growth of Small Polycyclic Aromatic Hydrocarbons. 1. 1-Naphthyl + Ethyne. J. Phys. Chem. A **105**, 1561-1573 (2001).
2. Goel, A., Hebgen, P., Vander Sande, J. B. and Howard, J. B. Combustion Synthesis of Fullerenes and Fullerenic Nanostructures. Carbon **40** 177-182 (2002).
3. Richter, H. and Howard, J. B. Formation and Consumption of Single-Ring Aromatic Hydrocarbons and Their Precursors in Premixed Acetylene, Ethylene and Benzene Flames. Phys. Chem. Chem. Phys. **4**, 2038-2055 (2002).
4. Goel, A. and Howard, J.B. Rate Constant for C60 Fullerene Oxidation by Molecular Oxygen, Carbon (to be published).

IONIZATION PROBES OF MOLECULAR STRUCTURE AND CHEMISTRY

Philip M. Johnson
Department of Chemistry
State University of New York, Stony Brook, NY 11794
Philip.Johnson@sunysb.edu

PROGRAM SCOPE

Photoionization processes provide very sensitive probes for the detection and understanding of molecules and chemical pathways relevant to combustion processes. Laser based ionization processes can be species-selective by using resonances in the excitation of the neutral molecule under study or by exploiting the fact that different molecules have different sets of ionization potentials. Therefore the structure and dynamics of individual molecules can be studied, or species monitored, even in a mixed sample. We are continuing to develop methods for the selective spectroscopic detection of molecules by ionization, to use these spectra for the greater understanding of molecular structure, and to use these methods for the study of some molecules of interest to combustion science.

RECENT PROGRESS

The exploitation of Rydberg molecules has enabled orders-of-magnitude increases in the resolution available for recording the spectra of molecular ions. These spectra provide information equivalent to photoelectron spectra, but contain much more information by virtue of that resolution and the versatility of laser preparation of the states involved.

We primarily use techniques developed in our laboratory called mass analyzed threshold ionization spectroscopy (MATI) and photoinduced Rydberg ionization spectroscopy (PIRI) to provide high resolution spectra of the various electronic states of ions. The resonant nature of MATI and PIRI are usually multilaser techniques, and the multiresonant nature of the overall process is of great use in sorting out the vibrational structure of some ionic states.

I. A new way of studying metastable states of molecules

Various metastable states of molecules, such as long-lived triplet states, are difficult to study because they have little oscillator strength in transitions from the stable ground state. In many molecules even such fundamental quantities as gas-phase triplet energies are not known accurately. Traditionally emission spectroscopy in condensed phase has been used to gain some information, but the structure in those spectra is mostly due to the lower state. Absorption spectra in condensed phase have also been used, but these also do not contain as much information as a gas phase spectrum. MATI spectroscopy of triplet states provides a gas phase method for getting information about the metastable state via hot band structure, and additionally provides additional information about cation properties. A problem in using MATI spectroscopy is providing a high enough density of triplet states.

For our experiments we used an electric discharge in a pulsed supersonic nozzle to generate the triplet state of benzene. The mass resolution of MATI enabled the triplet parent molecules to be distinguished from the various fragments created in the discharge. This technique created substantial amounts of vibrationally excited triplets, enabling the

measurements of the gas phase energies of several triplet vibrations and a new MATI spectrum of the cation ground state.

Thus the first MATI spectra from molecular excited triplet states were collected for benzene and perdeuterobenzene from the $^3B_{1u}$, lowest triplet state. From these spectra the C_6H_6 $^3B_{1u}$ state energy is found to be 29627 ± 12 cm^{-1} and the C_6D_6 $^3B_{1u}$ state energy is found to be 29828 ± 12 cm^{-1}. The MATI spectrum for each species was collect from 1000 cm^{-1} below the ionization threshold to ~2000 cm^{-1} above the threshold. Hot band structure allowed for the first higher-resolution gas phase vibrational measurement of the v_1, v_8, and v_6 frequencies in the $^3B_{1u}$ state. They were found at 927, 229, and 575 cm^{-1} in the protonated molecule, and 832, 200, and 528 cm^{-1} for the deuterated molecule. New vibrational structure has also been observed in the cation ground state of both molecules.

II. The Jahn-Teller effect in benzene cation

Almost all previous spectroscopic work on the Jahn-Teller effect in benzene has focused on the ground state of the cation. While the ground state of benzene cation provides a fertile ground for the testing of Jahn-Teller methods, as one moves to the first excited electronic state of this cation, one finds a doubly degenerate state that represents a much more complicated situation. This $^2E_{2g}$ state provides a greater challenge to spectroscopic analysis and a more demanding test of Jahn-Teller models.

The presence of a nearby $^2A_{2u}$ state subjects the state to pseudo-JT coupling, in addition to its having the normal linear and quadratic Jahn-Teller (JT) effects. However, the amount of intrastate coupling was not determined, due to the complexity of the vibrational structure. Using information from the electronic structure calculations, we have been able to make a more complete vibrational analysis of the B-X transitions of both $C_6H_6^+$ and $C_6D_6^+$, and determine the linear and quadratic intrastate coupling parameters for the major low frequency JT modes using multimode JT calculations based on the classical model of Longuet-Higgins.

In our previous work, determination of the linear JT coupling was made difficult because of a lack of any knowledge of expected coupling parameters to use as starting points for the fitting of the spectral lines to the JT model. While some previous theoretical work indicated very large couplings in several modes, the classical model as used in the calculation of the vibrational patterns contains an angular momentum (Λ) selection rule for the Hamiltonian matrix elements that would indicate the coupling could be very small.

The states of the benzene cation provide an opportunity to examine the effects of Λ upon the Jahn-Teller coupling strength. First, the molecule approaches circular symmetry. Second, while the ground state has one electronic node containing the C_6 axis, the first excited $^2E_{2g}$ state (termed the state for historical reasons concerning the splitting of the ground state degeneracy in substituted benzenes) has two nodes. Third, the spectra of benzene cation are well enough resolved that individual vibronic state assignments are possible. In both states the linear Jahn-Teller effect activates the e_{2g} vibrations v_6, v_7, v_8, and v_9. In addition, in both states there is considerable activity in the e_{1u} modes v_{16} and v_{17}, with splittings caused by both the quadratic and pseudo-Jahn-Teller effects (these cannot be distinguished experimentally).

The linear coupling parameters for the e_{2g} vibrations of the state were derived from electronic structure calculations. With this information, a few initial assignments could be made and much of the remaining vibronic structure assigned by reference to classical multimode Jahn-Teller calculations. Most of the structure can be ascribed to various combinations of modes 6 and 16, with minor contributions from 4, 17, and 18 (using Wilson's numbering convention). In

qualitative agreement with parameters derived from electronic structure calculations, the linear coupling parameter for mode 6 is very large (D=1.39 in $C_6H_6^+$ and 1.28 in $C_6D_6^+$). This raises questions about certain angular momentum selection rules in the classical Jahn-Teller model.

In work on the cation ground state, we have also been able to reproduce the vibrational state energies appearing in various MATI spectra from different neutral (S_0, S_1, and T_1) states using multimode Jahn-Teller calculations. By itself, however, that process does not bring a particular insight into the vibrational motions of the molecule because the vibrational eigenvectors are complicated combinations of the fundamental normal modes. By using derivatives of the state energies with respect to the Jahn-Teller parameters, and by animated pictures of the vibrational wave functions in both normal coordinate space and molecular space, we have been able to make some qualitative observations about the motional character of the states and provide some guidance as to the vibrational character at least some of the states in the classical terms of molecular spectroscopy.

III. Nanoclusters

In collaboration with Trevor Sears and Michael White at Brookhaven National Laboratory, we have been looking into methods for the production of more intense sources of metal containing nanoparticles. The eventual goal is to examine the spectroscopy and chemistry of these particles in a coordinated way that provides insight in their uses in catalysis.

Using the laser ionization mass spectrometers in this laboratory, we have been able to generate and measure useful quantities of TiO and clusters of Molybdenum carbides, nitrides and sulfides up to 3000 amu.

Molybdenum carbide, nitride and sulfide clusters were created via laser ablation in the presence of dilute and neat reactive carrier gases. Distributions of the neutral products were characterized by time-of-flight mass-spectrometry after photoionization with 193 nm radiation. The carbide clusters show an increase in ion intensity up to Mo_8C_{12} at which point there is a sharp drop in intensity. The latter suggests that the Mo_8C_{12} neutral and/or ion is particularly stable, which we attribute to a Met-Car-like structure analogous to that observed for other early transition metal carbides. Carbide clusters containing 10-23 Mo atoms exhibit a Mo_xC_{x+3} stoichiometry, while those containing >23 Mo atoms are closer to Mo_xC_{x+2}, indicative of near cubic nanocrystallite structures. At low mass (Mo_x, $x \leq 6$), cluster ions produced in expansions of ammonia gas were found to contain up to three nitrogen atoms, however, heavier species (Mo_x, $x \leq 40$) appear to be pure molybdenum metal clusters. The mass distributions for the sulfide clusters indicate a "magic number" structure at $Mo_6S_4^+$ which is attributed to a stable structure previously observed for the $[Cu_6S_4]^-$ anion. Also, the dependence of cluster distributions on the fluence of the ionizing laser was investigated to gain insight on the observed cluster ion distributions using a simple, qualitative kinetic model.

Theoretical work on these clusters indicate that they have their lowest transitions in the infrared region (often about 2 microns), and at present we are searching for resonances in their multiphoton ionization transitions.

FUTURE PLANS

We are in the process of setting up a pulsed amplified CW dye laser system in order to obtain higher resolution electronic spectra of molecular cations using the multiphoton dissociation, and PIRI techniques. This system will enable rotational resolution to be obtained for medium sized molecules and molecular clusters. The pulse nature of this high resolution

source will couple well with our established spectroscopic techniques and with the pulsed coherent vuv generation used to prepare Rydberg states. It will also enable the generation of infrared wavelengths for the measurement of low-lying electronic states and for vibrational spectroscopy. The goal is to develop a general method for cation spectroscopy with orders of magnitude higher optical resolution than current techniques.

DOE PUBLICATIONS

Andrew Burrill and Philip Johnson, "Torsional analyses of trans-2-butene and propene cations: A comparative investigation of two prototypical ions with different degrees of symmetry", Journal of Chemical Physics, **115**, 133 (2001).

Andrew Burrill and Philip Johnson, "The ionization potential and ground state cation vibrational structure of 1,4-dioxane", Chemical Physics Letters, **350**, 473 (2001).

Philip Johnson, "The Jahn-Teller effect in the lower electronic states of benzene cation: Part I. Calculation of linear parameters for the e_{2g} modes." J. Chem. Phys., 117, 9991-10000 (2002).

Philip Johnson, "The Jahn-Teller effect in the lower electronic states of benzene cation: Part II. Vibrational analysis and coupling constants of the B $^2E_{2g}$ state." J. Chem. Phys. 117, 10001-10007 (2002).

Andrew Burrill, Jia Zhou and Philip Johnson, "The Mass Analyzed Threshold Ionization Spectra of $C_6H_6^+$ and $C_6D_6^+$ obtained via the $^3B_{1u}$ Triplet State," J. Phys. Chem. In press.

DYNAMICAL ANALYSIS OF HIGHLY EXCITED MOLECULAR SPECTRA

Michael E. Kellman
Department of Chemistry, University of Oregon, Eugene, OR 97403
kellman@oregon.uoregon.edu

PROGRAM SCOPE:

Spectra of highly excited molecules are essential to understanding intramolecular processes of fundamental importance for combustion, including intramolecular energy transfer and isomerization reactions. The goal of our program is new theoretical tools to unlock information about intramolecular dynamics encoded in highly excited experimental spectra. Due to anharmonicity, ordinary normal modes behavior is transcended in highly excited states, with the birth in bifurcations of new anharmonic modes, and the onset of widespread chaotic classical dynamics. In a bifurcation, a normal mode changes character, with an abrupt change in the natural motions of the molecule. This results in severe disturbance of the ordinary spectral patterns associated with normal modes. New spectral effects are expected on the pathway to isomerization and beyond in systems such as acetylene.

The current goal is to relate bifurcation dynamics to time-dependent processes including spectra of isomerizing systems up to and above the isomerization barrier. For this, development of our previous methods using spectroscopic fitting Hamiltonians is needed, for example, for systems with multiple barriers.

RECENT PROGRESS: DYNAMICS FROM SPECTRA OF HIGHLY EXCITED SYSTEMS APPROACHING ISOMERIZATION.

Bifurcation analysis: Branchings of the normal modes into new anharmonic modes. Our approach to highly excited vibrational spectra uses bifurcation analysis of the classical version of the effective Hamiltonian used to fit spectra. We have applied this to a bifurcation analysis of the bend degrees of freedom of acetylene. The pure bending system is a stepping-stone to inclusion of the stretch degrees of freedom and an attack on the above-barrier isomerization problem for vinylidene-acetylene isomerization, both described below. We are extending our investigation of the pure bends system with development of a simplified approximate independent resonance analysis. The reason to do this is the need to simplify the bifurcation analysis as much as possible for larger systems, for example with addition of the stretch modes of acetylene. The prospects for this are described in more detail in our Future Plans, below.

Visualization of complex molecular dynamics. One of the most important goals of our research is to convert the fairly abstract dynamical knowledge of the bifurcation analysis into a directly visualizable representation. For this, we are using computer animation techniques to make movies of the anharmonic modes born in bifurcations. Examples of our animations can be found on a web-site at http://darkwing.uoregon.edu/$\sim$meklab/, which the interested reader is invited to access.

Spectral patterns of isomerizing systems. Our earlier work has demonstrated spectral patterns associated with bifurcations and the new modes which they produce. These patterns are robust as the barrier to isomerization is approached in a system such as acetylene [3,4]. Of great interest then is to extend the bifurcation and spectral analysis to isomerizing systems. We have begun this with an investigation [8] of a model of an isomerizing system of coupled stretch and bend, intended to have some of the features of a realistic model of the acetylene-vinylidene isomerization. Below the barrier there are patterns expected from previous work; and there are wholly new patterns associated with multiple barriers and above-barrier motion. These patterns are interpreted in terms of nonlinear resonance-type couplings, similar to anharmonic Fermi resonances, between the stretch and bend. There is conventional Fermi resonance below the barrier, and a new type of "cross-barrier" resonance.

Semiclassical quantization of systems of spectral models. Much of our work seeks to assign novel quantum numbers to highly excited spectra, based on the new modes from our bifurcation analysis, when the ordinary normal modes quantum numbers no longer suffice. A fundamental question is whether these quantum numbers can be given a precise meaning. In a series of investigations [3-6] on semiclassical quantization of wavefunctions, we are finding that this can be answered this in the affirmative, even for chaotic systems [6].

FUTURE PLANS: TIME-DEPENDENT AND REACTIVE DYNAMICS.

Our current goal is to extend or methods to larger systems and systems undergoing intramolecular reactions, i.e. isomerization reactions involving a potential barrier. We are interested in the particular chemical problem of the acetylene-vinylidene isomerization.

The key challenges are: (1) Making current methods practical for more complex systems, with more degrees of freedom. In acetylene, this means inclusion of the stretches in addition to the pure bends previously analyzed; (2) The problem of extending the spectroscopic Hamiltonian to handle qualitatively new physical situations, in particular, motion in multiple potential wells, and very large-amplitude motion above two or more wells.

Adding complexity. The acetylene/vinylidene isomerization involves the stretches as well as the bends. As the dimensionality of the problem becomes larger, one of the

challenges is whether our analysis can be performed in a way that is still understandable and useful.

One key to making larger systems tractable is use of the polyad quantum number. Even for many degrees of freedom with multiple resonances couplings and chaos, the bifurcation problem is thereby reduced from numerical searching to the much simpler task of finding the solutions of analytical (polynomial) equations. Still, the results are formidably complex to interpret. To address this, building on our investigation of the bifurcation behavior of the pure bends spectral fitting Hamiltonian, we are developing an approximate independent resonance analysis. This is much easier to understand than the exact bifurcation analysis, but our simplified Hamiltonian can be *exactly* carried over to the full, exact spectroscopic Hamiltonian, so there is a smooth continuation from approximate to exact analysis. Furthermore, the method appears to be scalable to larger systems.

Time dependent dynamics. Our prior work has focused on extracting information from spectra, i.e. time-independent phenomena. A major reason is to understand dynamics. Part of this means understanding the new modes that take over from the normal modes after bifurcations. However, dynamics must also certainly include time-dependent phenomena, for example intramolecular relaxation, and isomerization reactions. We are currently applying our spectroscopic Hamiltonians to time-dependent vibrational relaxation dynamics. One goal is to understand Coulomb explosion and related studies of the vinylidene/acetylene system. The system is believed to "cycle" between the vinylidene and acetylene forms in a very highly excited condition. This goes on for an extremely long time, up to a microsecond. The reason for this extraordinary lifetime is presently a mystery. The question is why the system doesn't relax out of the reaction coordinate into the dense "bath" modes when it is on the acetylene side of the reaction barrier. We are currently modeling this with the spectroscopic Hamiltonian, and attempting to understand it in terms of the knowledge of the molecular phase space. This means understanding the role of the approximate conserved polyad number, breaking of the polyad number, and formation of phase space "zones of stability" described by our bifurcation analysis. .

Spectroscopic Hamiltonians for multiple wells and above barrier spectroscopy. The remaining and least-explored challenge in dealing with isomerization problems in our approach is to include above barrier spectroscopy, and multiple wells, in the spectroscopic Hamiltonian; and to develop techniques such as bifurcation analysis to obtain dynamical information. We have begun this, using model systems until such time as experimental data become available. We are using some of the ideas developed in our paper [8] on spectral patterns of isomerizing systems.

Recent publications (in print or in press since 2001) related to DOE supported research:

1. M.E. Kellman, J.P. Rose, and Vivian Tyng, "Spectral Patterns and Dynamics of Planar Acetylene", European Physical Journal D 14, 225 (2001).

2. M.E. Kellman, "Internal Molecular Motion", Encyclopedia of Chemical Physics and Physical Chemistry, J.H. Moore, Ed. (Institute of Physics, London, 2001).

3. S. Yang and M.E. Kellman, "Addendum: Direct Trajectory Method for Semiclassical Wavefunctions", Phys. Rev. A. 65, 034103 (2002).

4. S. Yang and M.E. Kellman, "Semiclassical Wave Function Near a Strong Resonance", Phys. Rev. A 65, 064101 (2002).

5. S. Yang and M.E. Kellman, "Perspective on Semiclassical Quantization: How Periodic Orbits Converge to Quantizing Tori", Phys. Rev. A. 66, 052113 (2002).

6.. S. Yang and M.E. Kellman, "Semiclassical wave function from a quantizing cantorus", submitted to Phys. Rev. A.

7. C.Zhou, D. Xie, R.Chen, G.Yan, H.Guo, V. Tyng, and M.E. Kellman, "Highly Excited Vibrational Energy Levels of $CS_2(\tilde{X})$ on a New Empirical Potential Energy Surface and Semiclassical Analysis of the 1:2 Fermi Resonance", Spetrcochimica Acta A 58, 727-746 (2002).

8. S. Yang, V. Tyng, and M.E. Kellman, "Spectral Patterns of Isomerizing Systems", in press, J. Phys. Chem. A.

9. M.E. Kellman, M.W. Dow, and Vivian Tyng, "Dressed Basis for Highly Excited Vibrational Spectra", in press, J. Chem. Phys.

High Energy Processes

Alan R. Kerstein
Combustion Research Facility
Sandia National Laboratories
Livermore, CA 94551-0969
Email: arkerst@sandia.gov

PROJECT SCOPE

The goals of this project are to develop and demonstrate new capabilities for numerical simulation of turbulent flow couplings to multiple chemical and physical processes, such as the couplings that govern turbulent combustion, and to use the new capabilities to explore fundamental science issues. Current and planned model development efforts focus on flows involving turbulence-chemistry interactions, compressibility effects, momentum and thermal couplings between the fluid phase and dispersed suspensions (particles or droplets), gravitational coupling to mixing-induced density changes, and surface-tension effects at fluid-fluid interfaces. Capabilities developed during this project are applied to turbulent non-premixed, premixed, and partially premixed combustion.

Improved model representation of these phenomena is sought by fully resolving, in space and time, the operative physical processes and their couplings. It is common practice to employ coarse-grained descriptions in which processes and couplings that are not spatially and temporally resolved are parameterized. Increasing recognition that parameterization is inadequate for complex flows involving multiple, strongly non-linear couplings has motivated the development of synthetic-field modeling approaches designed to resolve these couplings within a simplified framework.

To accomplish this without incurring the overwhelming computational cost of fully resolving these couplings in three spatial dimensions, synthetic fields of reduced dimensionality have been formulated. This approach has been pursued during this project, resulting in the development of a novel 1D synthetic-field approach denoted One-Dimensional Turbulence (ODT).

1D synthetic-field models typically involve random sequences of additive or multiplicative operations that emulate the wide range of spatial scales of turbulent flow fluctuations. This approach represents fluctuation effects in detail, and in fact is designed specifically for the study of these fluctuations. However, it contains no representation of the physical processes that drive these fluctuations, so it is useful primarily for studying the generic (universal) properties of turbulent fluctuations rather than flow-specific effects. In particular, it does not capture multi-physics couplings or structural inhomogeneities induced by initial or boundary conditions or body forces.

To broaden its capabilities, ODT combines this approach with the conventional 1D boundary-layer formulation of the fluid-dynamical equations. For application to turbulence, this formulation has previously been used to represent ensemble-averaged behavior, with the role of turbulence represented by enhancement of viscous momentum transport. Thus, a diffusive process, which damps fluctuations, is used to represent an advective process that generates flow fluctuations. At best, such an approach captures the overall transfer of momentum, mass, and heat without resolving local fluctuations that strongly influence subprocess interactions.

In ODT, turbulence effects within the 1D boundary-layer framework are not represented by enhanced diffusion. Rather, the 1D boundary-layer equations are treated as instantaneous equations. Turbulence effects are incorporated by performing a random sequence of operations somewhat analogous to the stochastic approach. Each operation is the model analog of an individual turbulent eddy. The resulting formulation captures both turbulent cascade properties, as in previous stochastic models, and the coupling of cascade dynamics to the initial and boundary conditions and forcings corresponding to various inhomogeneous turbulent flows of practical interest. Numerous demonstrations of the novel predictive capabilities of this approach have been performed, including several recent demonstrations that are described below.

RECENT PROGRESS

At low Mach number (the ratio of the typical flow speed to the speed of sound), fluid pressure is constant to a good approximation. As Mach number of order unity is approached, pressure fluctuations become significant and flow kinematics and thermodynamics become intimately coupled. Despite this coupling, published direct-numerical-simulation (DNS) studies indicate that turbulent flow kinematics may be explained largely as a sonic-eddy effect. Namely, turbulent eddy motions whose speed is comparable to or larger than the sound speed do not occur because they would imply supersonic communication across the eddy, so forcing mechanisms that might create such an eddy will instead create a shocklet or a collection of subsonic eddies.

Although the sonic-eddy effect may explain observed Mach-number dependencies, it has not hitherto been a basis for prediction of these dependencies. One of the salient characteristics of ODT is the use of an explicit representation of an individual turbulent eddy as the basic building block of turbulent flow simulation. Within this framework, it is straightforward to incorporate a suppression mechanism based on an eddy-Mach-number criterion. Proceeding in this manner, a model formulation has been developed that reproduces the key Mach-number dependencies of flow kinematics (fluctuation statistics as well as mean behavior) that were noted in the DNS studies. This result indicates that the kinematics of compressible flow can be modeled successfully without addressing flow thermodynamics. It also provides a useful foundation for future incorporation of compressible-flow thermodynamics into ODT by establishing a distinction between thermodynamic effects *per se* and their coupling to flow kinematics (see the next section).

The combined influence of turbulent mixing and gravitational effects can induce buoyancy reversal, an important dynamical effect in a variety of geophysical and astrophysical flows. A common manifestation of this effect results from the nonmonotonic temperature dependence of the density of water. Lakes often have a warm layer above a denser cold layer, such that turbulent mixing of the layers can produce water denser than the cold layer, inducing gravitational instability. The instability accelerates the mixing process, causing a runaway that ceases only when the intense turbulence has mixed out the instability (e.g., by depleting one of the layers). ODT has been used to simulate buoyancy reversal in a flow configuration studied experimentally. This application is the first demonstration of a capability to predict this phenomenon quantitatively. In addition, the dependence of flow evolution on Prandtl number (the ratio of thermal diffusivity to fluid viscosity) has been examined using ODT. This study indicated the relationship between flow evolution observed experimentally at high Prandtl number and the anticipated flow evolution in atmospheric buoyancy-reversing configurations at near-unity Prandtl number. (Atmospheric buoyancy reversal is a multiphase process driven by evaporative cooling in clouds.)

Though ODT by itself can be used to address a wide variety of turbulent flow phenomena, the

fullest realization of its potential contribution to high-fidelity modeling requires coupling of ODT to a multi-dimensional flow solver. The first step toward this goal has been taken. An ODT subprocess has been incorporated into each wall-adjacent cell of a 3D large-eddy simulation (LES) of channel flow [11]. Turbulent mixing in a channel blends out velocity gradients in the central region of the flow, expelling the gradients toward the walls. The high near-wall shear induces intense small-scale turbulence that strongly effects the overall dynamics, but cannot be resolved affordably by the LES mesh. The ODT near-wall subprocesses provide the wall-normal spatial refinement needed to capture the near-wall flow behavior. Comparison of computed results to DNS of channel flow demonstrates that ODT is advantageous in this regard [11]. Based on experience gained during this initial effort, a strategy for complete LES subgrid closure using ODT has been developed [8] and implementation has begun (see next section).

FUTURE PLANS

Several of the planned extensions of ODT will broaden its applicability to turbulent combustion processes. Planned incorporation of compressible thermodynamics will address important engine combustion phenomena, including density and temperature fluctuations that influence reaction rates and pressure fluctuations that can cause engine knock. An ongoing effort to incorporate a dispersed phase (particles and/or droplets) will address issues relevant to spray combustion and pulverized coal combustion as well as soot formation and evolution in flames. Planned incorporation of fluid interfaces subject to surface tension will enable the study of liquid-jet breakup during fuel injection in diesel engines. Further extensions of ODT subgrid modeling within LES will combine the detailed fine-scale representation within ODT with the capability of LES to capture the effects of complex geometry. These are the key requirements for comprehensive high-fidelity computational modeling of turbulent combustion processes.

The basic strategy for incorporating compressible thermodynamics into ODT is to couple ODT eddy processes to conventional 1D gas-dynamic evolution. Preliminary development of this approach has identified some issues that need to be addressed as the effort proceeds. The main concern is that acoustic radiation associated with gas-dynamic evolution tends to damp pressure fluctuations rapidly. In 3D flow, the pressure-fluctuation level is sustained by a quasi-steady (on acoustic time scales) balance between pressure gradients and solenoidal fluid motions. This mechanism is not inherent within ODT, so a method to incorporate its effects has been formulated and will be tested.

Two aspects of multiphase flow will be addressed in future work. One is the exchange of momentum, mass, and heat between advected particles and the surrounding fluid. Momentum coupling will be based on a conventional drag law. The simplest approach is to use fluid velocity profiles evolved by ODT to represent the flow seen by the particles. This has the disadvantage that it is inaccurate in the marker-particle limit (no slip between the particles and the surrounding fluid) because particles are not displaced when the fluid elements containing them are displaced by ODT eddies. Therefore a more elaborate procedure, involving an interaction between particles and eddies that emulates particle response to 3D eddy turnover, will be tested.

The other planned multiphase flow extension addresses liquid-jet breakup. For this application, the ODT domain represents a line normal to the axis of the liquid column. A potential energy per unit area arising from surface tension is associated with each liquid-gas interface along the 1D domain. Each eddy operation within the simulation triples the number of interfaces contained within the eddy. The energy stored in the newly formed interfaces is subtracted from the energy available to drive the eddy, and accordingly, reduces the likelihood of eddy occurrence. This formulation emulates the inhibition of jet breakup by surface tension.

The extension of ODT closure of LES from the near-wall region to the entire flow introduces a key complication that must be addressed. Near-wall closure requires spatial refinement only in the wall-normal direction, but in a more general closure, spatial refinement in all three coordinate directions is needed. The ODT substructure is then a 3D latticework of 1D subprocesses. Consistent coupling of these subprocesses to each other and to the large-scale multi-dimensional flow evolution captured by LES time advancement poses several challenges. An overall strategy for addressing these challenges has been developed [8]. As a first step beyond near-wall closure, a full closure suitable for constant-property flow will be implemented.

In addition to the proposed model extensions, a variety of applications of capabilities developed to date will be pursued. ODT will be used to support simultaneous line-Raman measurements of multiple species concentrations in turbulent diffusion flames, performed in the Turbulent Combustion Laboratory at the Sandia Combustion Research Facility. ODT simulations of turbulent diffusion flames will address the fundamental question of whether flame structure becomes independent of turbulence intensity at very high intensities. Turbulent autoignition processes will be simulated in coordination with ongoing investigation of this topic at the Combustion Research Facility using DNS. Turbulent premixed combustion in an astrophysical context will be investigated; specifically, the coupling of nuclear reactions and buoyancy-driven mixing that initiates supernova explosions will be simulated. In a geophysical context, buoyant density-stratified turbulent boundary layers will be simulated in order to demonstrate that ODT provides a useful representation of atmospheric mixing for purposes of future air-quality studies that incorporate pollutant chemistry.

PUBLICATIONS SINCE 2001

1. S. Wunsch and A. R. Kerstein, "A Model for Layer Formation in Stably Stratified Turbulence," Phys. Fluids **13**, 702 (2001).
2. T. Echekki, A. R. Kerstein, J.-Y. Chen, and T. D. Dreeben, "One-Dimensional Turbulence Simulation of Turbulent Jet Diffusion Flames: Model Formulation and Illustrative Applications," Combust. Flame **125**, 1083 (2001).
3. A. R. Kerstein, Wm. T. Ashurst, S. Wunsch, and V. Nilsen, "One-Dimensional Turbulence: Vector Formulation and Application to Free Shear Flows," J. Fluid Mech. **447**, 85 (2001).
4. A. R. Kerstein, "Kinematics of Small Scale Anisotropy in Turbulence," Phys. Rev. E **64**, 036306 (2001).
5. A. R. Kerstein, "Prandtl-Number Dependence of Turbulent Flame Propagation," Phys. Rev. E **64**, 066306 (2001).
6. J. C. Hewson and A. R. Kerstein, "Stochastic Simulation of Transport and Chemical Kinetics in Turbulent CO/H2/N2 Flames," Combust. Theor. Model. **5**, 669 (2001).
7. J. C. Hewson and A. R. Kerstein, "Local Extinction and Reignition in Nonpremixed Turbulent CO/H2/N2 Jet Flames," Combust. Sci. Tech. **174**, 35 (2002).
8. A. R. Kerstein, "One-Dimensional Turbulence: A New Approach to High-Fidelity Subgrid Closure of Turbulent Flow Simulations," Computer Phys. Commun. **148**, 1 (2002).
9. Wm. T. Ashurst, A. R. Kerstein, L. M. Pickett, and J. B. Ghandhi, "Passive Scalar Mixing in a Spatially Developing Shear Layer: Comparison of ODT Simulations with Experimental Results," Phys. Fluids **15**, 579 (2003).
10. A. R. Kerstein, "Turbulence in Combustion Processes: Modeling Challenges," Proc. Combust. Inst., in press (2003).
11. R. C. Schmidt, A. R. Kerstein, S. Wunsch, and V. Nilsen, "Near-Wall LES Closure Based on One-Dimensional-Turbulence Modeling," J. Comput. Phys., in press (2003).

KINETICS OF COMBUSTION-RELATED PROCESSES
AT HIGH TEMPERATURES

J. H. Kiefer and R.S. Tranter
Department of Chemical Engineering
University of Illinois at Chicago
Chicago, IL 60607
(kiefer@uic.edu; rtranter@uic.edu)

Program Scope

This program involves the use of the shock tube with laser-schlieren, laser-flash absorption, and dump-tank GC/MS analysis diagnostics to explore reactions and energy transfer processes over an extremely wide range of temperatures and pressures. We are interested primarily in the kinetics of unimolecular reactions at combustion temperatures, and, in particular, the effects of unimolecular falloff. Over the past year we have considerably extended our efforts to include some new results on relaxation and incubation. We have also begun the construction of a shock-tube, time-of-flight mass spectrometer, briefly described herein.

Falloff, relaxation, and incubation in unimolecular reactions.

Our most recent efforts include the study of decomposition in neopentane and isobutene. This work was initiated in the belief that the combination of reliable dissociation rates at very high T and existing reliable data at lower temperatures would permit the extraction of a more precise dissociation barrier, and thus a better estimate of the $\Delta_f H^o{}_{298}$ for the *tert*-butyl radical. It was quickly realized that reliable data for reactions of the major isobutene product were unavailable, so a parallel study of this decomposition was begun. Both projects are now completed; the neopentane work has appeared (publication #1) and the isobutene is in press (publication #2). The rate data from neopentane are reproduced in the attached Fig. 1, where a RRKM fit of the strong falloff and the derived k_∞ are also shown. A $\Delta_f H^o{}_{298} = 12.8 \pm 2$ kcal/mol was finally obtained.

Vibrational relaxation in methyl hydrocarbons

To our surprise, we found we were able to observe vibrational relaxation in both neopentane and isobutene, at least at high T and very low P. An example laser-schlieren (LS) raw signal and semilog gradient plot are given in Fig. 2. The relaxation is extremely fast here, $P\tau \sim 40$ ns-atm, but this is still much slower than the room-T time of 4 ns-atm [1]. We have now been able to resolve relaxation in a number of methyl hydrocarbons, and a large selection of our results is summarized in the Landau-Teller plot of Fig. 3. In all cases the relaxation times show an 'inverted' T-dependence, slowing with increasing T. This appears to be a consequence of energy transfer that is already so fast at room T (4 ns-atm is ~ 5 collisions), that it cannot much increase, and the process just appears slowed by the much greater amount of energy that has to be transferred at higher T. This is quite consistent with preliminary analyses, either using the rather crude "series" model [2] for P_{10}, or calculating a $<\Delta E>_{down}$ from the relaxation equation.

Values for $<\Delta E>_{down}$ can be obtained rather simply from experiments with accurate exponential energy relaxation by considering the relaxation equation at $t = 0$. Here $(dE_{vib}/dt) = E_{vib}^{eq}/\tau$, and we introduce $\tau = P\tau/P$, $P = (M)RT$, and divide through by the collision frequency, $Z_c(M)$. On the left is then $<\Delta E>_{up}$, the average collisional energy transferred on excitation from the ground state

$$< \Delta E >_{up} = \frac{RTE_{vib}^{eq}}{P\tau Z_c}$$

These excitation energies are then easily converted to the desired $<\Delta E>_{down}$ using the gap law and molecular frequencies as

$$< \Delta E >_{up} = \frac{\sum_{n=0} E_n g_n e^{-\alpha E_n}}{\sum_{n=0} g_n e^{-\alpha E_n}}$$

where $\alpha = \dfrac{1}{< \Delta E >_{down}} + \dfrac{1}{kT}$. The E_n and g_n are taken from Beyer-Swinehart calculations, and the $<\Delta E>_{down}$ found by iteration.

In both simple analyses the results are surprisingly reasonable; the P_{10} are all < 1, and increase weakly with T, and in neopentane the $<\Delta E>_{down}$ also increase with T, from $60 - 80$ cm^{-1} over $600 - 1500$ K. In toluene they are nearer 150 cm^{-1}. This work on relaxation has been submitted to Chem. Phys.

Incubation in unimolecular dissociation

In many of the above experiments conducted at the highest temperatures and lowest pressures, both relaxation and dissociation are seen. An example of such an experiment is shown in Fig. 4. Here there is an initial, very fast relaxation followed by an extended non-exponential tail from dissociation. From experiments like these it is possible to estimate incubation times and these are given in pubs. #1 and #2. In general they are similar to those found in previous work [3,4], a few times larger than corresponding relaxation times.

Development of a Time-of-Flight Mass Spectrometer (TOF)

Since the last report, we have completed the design and begun construction of a state-of-the-art TOF to be attached to the low-pressure shock tube. In this effort we have received financial help from DOE, and the loan of equipment form Sandia and Argonne Nat'l Labs.

Currently the vacuum chamber and interface between tube and TOF have been built, and the ion optics of the Jordan TOF is being modified by the manufacturer for E. I. ionization. When the TOF is finally coupled to the tube it will first be used in the usual fashion, on the reflected shock, but as we gain experience we hope to bring it to bear on the incident shock with the eventual aim of performing coincident LS and TOF measurements.

Dissociation and relaxation in 1,1,1-trifluoroethane

We continue to investigate the odd behavior of this simple dissociation, which defies application of standard RRKM theory. The reaction is solely $CF_3CH_3 \rightarrow CF_2CH_2 + HF$, and is a popular chemical thermometer. We have now been able to resolve relaxation in this molecule with very interesting results. More on this will be reported at the meeting.

Future plans

Of course we hope to put the TOF into operation before the year is out. To begin with this we will return to some earlier TOF work for testing and confirmation. For one thing we plan to return, once again, to ethane decomposition, and perhaps look at azomethane and the combination of methyl. We also hope to extend the isomerization (and relaxation?) in methylisocyanide to much higher T.

References

1. R. Holmes, G. R. Jones, and R Lawrence, Trans. Fara. Soc. **62**, 46 (1965).

2. see T. L. Cottrell and J. C. McCoubrey, *Molecular Energy Transfer in Gases*, Butterworths, London, 1961.

3. D. Fulle, A. Dib, J. H. Kiefer, Q. Zhang, J. Yao, and R.D. Kern, J. Phys. Chem. **102**, 7480 (1998).

4. J. H. Kiefer, S. S. Kumaran, and S. Sundaram, J. Chem. Phys. **99**, 3531 (1993).

Publications

1. "Dissociation, Relaxation, and Incubation in the Pyrolysis of Neopentane: Heat of Formation for *tert*-butyl Radical", N. K. Srinivasan, J. H. Kiefer, and R.S. Tranter, J. Phys. Chem. **107**, 1532 (2003).

2. "A Shock-Tube, Laser-Schlieren Study of the Pyrolysis of Isobutene: Relaxation, Incubation, and Dissociation Rates", S. Santhanam, J. H. Kiefer, R.S. Tranter and N. K. Srinivasan, Int. J. Chem. Kinet. in press.

3. "The Application of Densitometric Methods to the Measurement of Rate Processes in Shock Waves", J. H. Kiefer, in "Handbook of Shock Waves" Chapter 16.2, Academic Press, New York; p. 29 - 76 (2001).

4. "Thermodynamic Functions for the Cyclopentadienyl Radical: The Effect of Jahn-Teller Distortion, J. H. Kiefer, R. S. Tranter, H. Wang and A. F. Wagner, Int. J. Chem. Kinet. **33**, 834 (2001).

5. "Modeling of Nonlinear Vibrational Relaxation of Large Molecules in Shock Waves with a Nonlinear, Temperature-Varying Master Equation, M. J. Davis and J. H. Kiefer, J. Chem. Phys. **116**, 7814 (2002).

Fig. 1: Dissociation Rates neopentane/Kr

T (K)
1900 1800 1700 1600 1500 1400 1300

□ – 2 %, 400 Torr
▲ – 2 %, 100 Torr
○ – 5 %, 25 Torr
Solid lines – RRKM 400– 25 Torr

k_∞

k_1 (s^{-1})

1000/T
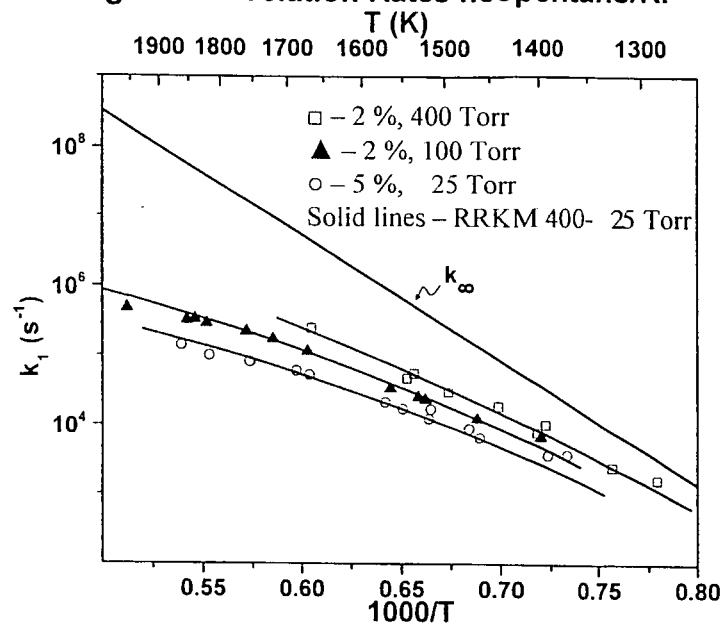
Fig. 2: 5% isobutene/Kr, Vibrational Relaxation

1092 K
12 torr

$d\rho/dx$
gm/cm^4

t(μs)

LS
Raw signal

t (μs)

Fig. 3: Relaxation times

T (K)
2000   1000   300

P_τ (ns-atm)

$T^{-1/3}$
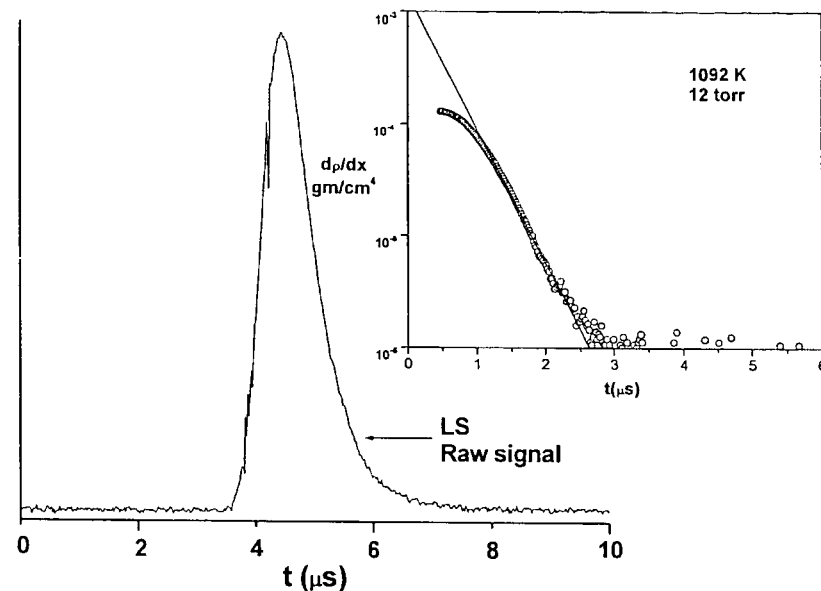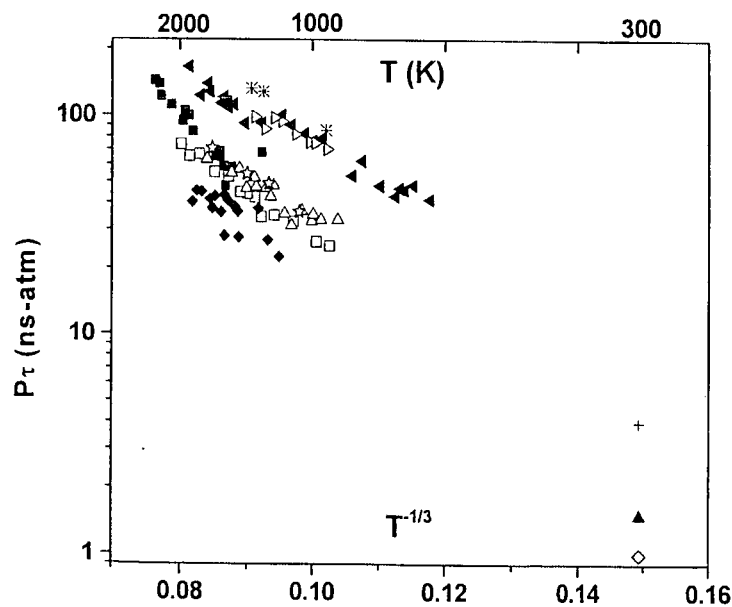
* 20 % C$_5$H$_{12}$/Kr   ◀ 5 % C$_5$H$_{12}$/Kr   ☆ 10 % C$_5$H$_{12}$/Kr   + 300 K C$_5$H$_{12}$
◆ 5 % i- C$_4$H$_8$/Kr   ■ 10% i- C$_4$H$_8$/Kr   ▷ 5 % C$_7$H$_8$/Kr   △ 5 % i- C$_4$H$_{10}$/Kr
□ 5 % C$_3$H$_8$/Kr   ▲ 300 K i- C$_4$H$_{10}$ ◇ 300 K C$_3$H$_8$

Fig. 4: 10% isobutene/Kr
Relaxation, Dissociation, & Incubation
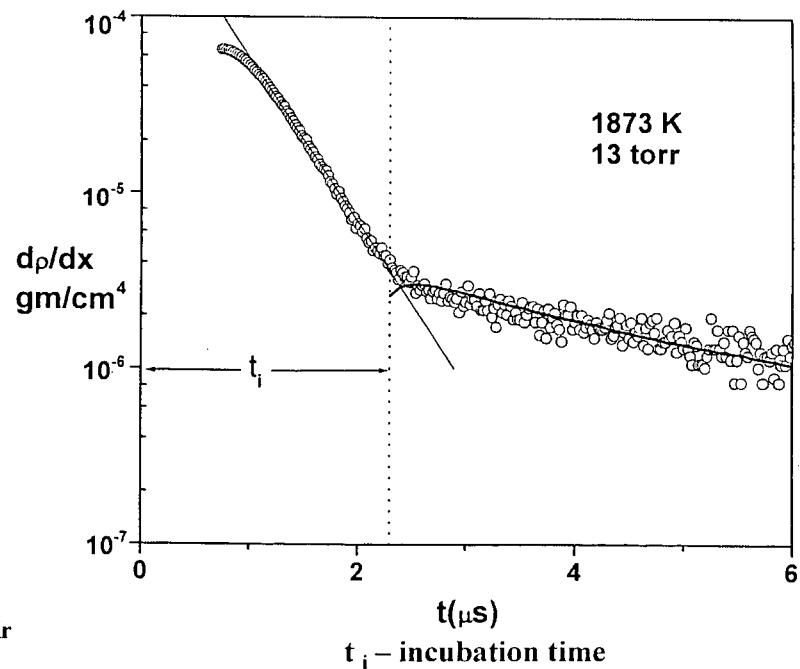
1873 K
13 torr

$d\rho/dx$
gm/cm^4

t_i

t(μs)

t $_i$ – incubation time

THEORETICAL CHEMICAL KINETICS

Stephen J. Klippenstein
Combustion Research Facility
Sandia National Laboratories
Livermore, CA, 94551-0969
E-mail: sjklipp@sandia.gov

Program Scope

The focus of this program is the theoretical estimation of the kinetics of elementary reaction steps of importance in combustion chemistry. The research involves a combination of *ab initio* quantum chemistry, variational transition state theory, direct dynamics, and master equation simulations. The emphasis of our current applications is on (i) reactions of importance in soot formation, (ii) radical oxidation reactions, and (iii) NO_x chemistry. We are also interested in a detailed understanding of the limits of validity of and, where feasible, improvements in the accuracy of specific implementations of transition state theory. Detailed comparisons with experiments, and with other theoretical methods, are used to explore and improve the predictive properties of the transition state theory models. Direct dynamics simulations are being performed as a means for testing the statistical assumptions, for exploring reaction mechanisms, and for generating theoretical estimates where statistical predictions are clearly inadequate. Master equation simulations are used to study the pressure dependence of the kinetics and to produce phenomenological rate coefficients for use in kinetic modeling.

Recent Progress

Propargyl Radical Kinetics (in collaboration with Jim Miller)

Using a combination of electronic-structure methods, we have explored in some detail the regions of the C_6H_6 potential that are important for describing the recombination of propargyl (C_3H_3) radicals. Using this information in an RRKM-based master equation, we have been able to predict rate coefficients for a variety of elementary reactions, including the $C_3H_3+C_3H_3$ recombination itself. Generally, the agreement between the theory and the limited amount of experimental information available is very good, although some discrepancies remain. The most important new feature of the present analysis (over our previous one) is the inclusion of a path on the potential that connects 1,2,4,5-hexatetraene to 1, 3-hexadiene-5-yne and then goes on to benzene and phenyl + H without passing through fulvene. The inclusion of this path in the analysis allows a number of experimental observations to be accounted for by the theory. From the results of the master-equation calculations, we propose a simple, contracted model for describing the rate coefficient and product distribution of the $C_3H_3 + C_3H_3$ recombination reaction (and subsequent isomerizations) for use in flame modeling. Modified Arrhenius expressions are provided for the rate coefficients of the reactions appearing in the simplified model.

Radical Oxidation

In collaboration with John DeSain and Craig Taatjes, we have completed a joint experimental and theoretical study of the chlorine atom initiated oxidation of neopentane. The production of HO_2 in the neopentane oxidation is attributed to secondary reactions of the RO_2 or QOOH radicals, since the neopentylperoxy radical cannot form a conjugate alkene and formation of 1,1-dimethylcyclopropane + HO_2 is energetically inaccessible. As a result, this oxidation system provides a valuable test of our understanding of RO_2 to QOOH isomerization. A simple kinetic model was constructed based on comparison with previous time-dependent master equation simulations of analogous processes in the reaction of n-propyl with O_2 and from limited B3LYP density function calculations. The inclusion of formally direct pathways for several chemical activation reactions, especially direct production of OH from R + O_2, were found to be essential to the modeling of the observed time profiles for both OH and HO_2. Furthermore, the isomerization from RO_2 to QOOH occurs significantly more rapidly than previously proposed.

The reaction between vinyl radical (C_2H_3) and molecular oxygen is a pivotal step in the combustion of ethylene and, consequently, in the combustion of higher alkanes under many conditions. The branching between HCO + H_2CO and C_2H_3O + O is of key importance to global combustion models. A prior theoretical study of Lin and coworkers suggests that the crossover temperature, where the branching fractions are equal, is about 900 K. However, a later CASPT2 study of Carpenter suggests that a key barrier height could be in error by 8 kcal/mol. In collaboration with the groups of Carpenter, Harding, Miller, and Westmoreland we are undertaking a complete theoretical reanalysis of this reaction. This analysis is based on a combination of high level ab initio studies of the stationary points (MRCI, CASPT2, and QCISD(T) each extrapolated to the infinite basis set limit), direct VRC-TST estimates, and direct B3LYP/6-31G* trajectory simulations. Preliminary results suggest that the crossing temperature is significantly higher, likely at about 2000 K or higher. We are in the process of considering the effects of such a change in the relative branching on the modeling of ethylene flames. Interestingly, the trajectory simulations indicate that the HCO products are better thought of as H + CO, since they are generally produced with energies exceeding their dissociation threshold. Similarly, H_2CO is expected to be produced very hot, up to just below the dissociation threshold, as has been recently verified in the Taatjes laboratory. The direct statistical analysis for the entrance channel is in good agreement with experimental observations, and suggests that the high pressure addition rate goes through a minimum near 700 K.

NOx Chemistry (in collaboration with Jim Miller and Peter Glarborg)

We have determined that the branching in the HCNO + OH reaction plays a important role in NO_x reburning. Thus, we have undertaken a detailed *ab initio* study of the stationary points in this reaction. This analysis suggests significant branching to NO + CO + H_2, NCO + OH + H, and NCO + H_2O in addition to the previously assumed NO + HCOH products. Kinetic modeling incorporating these additional channels provides considerably improved agreement with experimental observations of the reburning process.

Transition State Theory (in collaboration with Yuri Georgievskii)

We have provided a novel derivation of the canonical, microcanonical, and E/J resolved reactive flux within the variable reaction coordinate transition state theory (VRC-TST) formalism. This derivation, in addition to providing a particularly efficient implementation, also better illustrates the dependence of the kinematic factor on the pivot point location. The

simplicity of the derivation allows for straightforward generalizations to alternative forms for the dividing surface. Specific generalizations to elliptical and planar dividing were presented.

This new methodology was tested through an application to the H + C_2H_3 addition reaction. Comparisons with trajectory simulations of the capture process illustrated the accuracy of the basic VRC-TST formalism. This application also illustrated some of the problems that arise when trying to obtain channel specific estimates which properly satisfy the variational criterion. These problems are related to the difficulties in obtaining channel-specific dividing surfaces which adequately separate the two regions of potential energy surface minima. The incorporation of approximate dividing surfaces, which at least in principle negate the variational principle, yields channel specific results that are in satisfactory agreement with the trajectory results.

More recently we have developed an alternative approach to obtaining transition state theory estimates for multichannel addition reactions. Multiple addition channels are fairly commonplace, arising in resonantly stabilized radicals where the addition can occur to the radical site in each of the resonance structures, in p-orbital radicals where addition can occur from one of two sides, and in ion-molecule reactions where the neutral has multiple electrostatic binding sites. This approach employs a multifaceted dividing surface composed of individual faces for each separate reaction channel. Proper consideration of the contributions through each face again yields a variational result, while maintaining flexibility in the form of the dividing surface for each face. The overall dividing surface is simply specified as

$$min\ (r_{i,j}/s_{i,j}) = 1$$

where $r_{i,j}$ is the distance between i'th pivot point on fragment 1 and the j'th pivot point on fragment 2, and $s_{i,j}$ is the transition state separation for that particular pair of pivot points.

A variety of illustrative applications of this multifaceted dividing surface approach were presented. For the C_3H_3 + H addition, the multifaceted dividing surface results agreed with trajectory results to within 5 to 10%, as do prior approximate VRC-TST results. In contrast, results based on the sums of properly variational single faced results differ more significantly, being 15 to 20% greater. Notably, the optimal multifaceted transition state dividing surfaces are again in qualitative accord with contours of the radical molecular orbital. Applications to the CH_3 + CH_3 and C_2H_3 + O_2 reactions further illustrate the dependence of the results on the use of multiple pivot points, while also illustrating the feasibility and accuracy of employing directly determined density functional interaction energies.

Future Directions

The additions of acetylene to C_4H_3 and/or C_4H_5 have been postulated to be key steps in the formation of aromatic ring compounds. We will investigate each of these reactions, considering both the n and i isomers for each one, since they are effectively separate species with quite different kinetic properties. This study will build on the earlier quantum chemical work of Walch, but will include a more wide-ranging analysis of the reaction pathways. The temperature and pressure dependence of the rate constant will again be estimated via master equation analyses.

Our recent study of the production of OH in radical oxidation reactions suggests that the reaction of ROO radicals with OH to produce RO + HO_2 are important in alkane oxidation. This study also suggested the importance of the reaction of R with HO_2 to form RO + OH, as has often been suggested by Dryer. Our direct transition state theory methodology should provide an ideal procedure for exploring such reactions since each of them are likely barrierless.

DOE Supported Publications, 2001-Present

1. Holger Thiesemann, Eileen P. Clifford, Craig A. Taatjes and Stephen J. Klippenstein, *Temperature Dependence and Deuterium Kinetic Isotope Effects in the CH(CD) + $C_2H_4(C_2D_4)$ Reaction Between 295 and 726 K* , J. Phys. Chem. A, **105**, 5393-5401 (2001).

2. James A. Miller and Stephen J. Klippenstein, *The Recombination of Propargyl Radicals: Solving the Master Equation*, J. Phys. Chem. A, **105**, 7254-7266, (2001).

3. Kelsey M. Forsythe, Stephen K. Gray, Stephen J. Klippenstein, and Gregory E. Hall, *An Ab Initio Molecular Dynamics Study of S_0 Ketene Fragmentation*, J. Chem. Phys., **115**, 2134-2145, (2001).

4. Timothy P. Marcy, Robert R. Diaz, Dwayne Heard, Stephen R. Leone, Lawrence B. Harding, and Stephen J. Klippenstein, *Theoretical and Experimental Investigation of the Dynamics of the Production of CO from the CH_3 + O and CD_3 + O Reactions*, J. Phys. Chem. A, **105**, 8361-8369, (2001).

5. Craig A. Taatjes and Stephen J. Klippenstein, *Kinetic Isotope Effects and Variable Reaction Coordinates in Barrierless Recombination Reactions*, J. Phys. Chem. A, **105**, 8567-8578, (2001).

6. James A. Miller and Stephen J. Klippenstein, *The Reaction Between Ethyl and Molecular Oxygen II: Further Analysis*, Int. J. Chem. Kinet., **33**, 654-668, (2001).

7. David K. Hahn, Stephen J. Klippenstein, and James A. Miller, *A Theoretical Analysis of the Reaction Between Propargyl and Molecular Oxygen*, Faraday Disc., **119**, 79-100, (2001).

8. John D. DeSain, Craig A. Taatjes, James A. Miller, Stephen J. Klippenstein, and David K. Hahn, *Infrared Frequency-Modulation Probing of Product Formation in Alkyl + O_2 Reactions: IV. Reactions of Propyl and Butyl Radicals with O_2*, Faraday Disc., **119**, 101-120, (2001).

9. De-Cai Fang, Lawrence B. Harding, Stephen J. Klippenstein, and James A. Miller, *A Direct Transition State Theory Based Analysis of the Branching in NH_2 + NO*, Faraday Disc., **119**, 207-222, (2001).

10. James A. Miller, Stephen J. Klippenstein, and Christophe Raffy, *Solution Of Some One- And Two-Dimensional Master Equation Models For Thermal Dissociation: The Dissociation Of Methane In The Low-Pressure Limit*, J. Phys. Chem. A, **106**, 4904-4913 (2002).

11. Michael J. Davis and Stephen J. Klippenstein, *Geometric Investigation of Association/Dissociation Kinetics with an Application to the Master Equation for CH_3 + CH_3 $\leftrightarrow$ C_2H_6*, J. Phys. Chem. A, **106**, 5860-5879 (2002).

12. Stephen J. Klippenstein and James A. Miller, *From the Time-Dependent, Multiple-Well Master Equation to Phenomenological Rate Coefficients*, J. Phys. Chem. A, **106**, 9267-9277 (2002).

13. Stephen J. Klippenstein, Yuri Georgievskii, and Lawrence B. Harding, *A Theoretical Analysis of the CH_3 + H Reaction: Isotope Effects, the High Pressure Limit, and Transition State Recrossing*, Proc. Comb. Inst., **29**, *in press* (2002).

14. Stephen J. Klippenstein, James A. Miller, and Lawrence B. Harding, *Theoretical Kinetic Estimates for the Reaction of HCCO with O_2*, Proc. Comb. Inst., **29**, *in press* (2002).

15. John D. DeSain, Stephen J. Klippenstein, Craig A. Taatjes, Michael D. Hurley, and Timothy J. Wallington, *Measurements, Theory, and Modeling of Product Formation in the Cl-Initiated Oxidation of Cyclopropane*, J. Phys. Chem. A, **107**, 1992-2002 (2003).

16. Yuri Georgievskii and Stephen J. Klippenstein, *Variable Reaction Coordinate Transition State Theory: Analytic Results and Application to the C_2H_3 + H $\rightarrow$ C_2H_4 Reaction*, J. Chem. Phys., **118**, 5442-5455 (2003).

17. John D. DeSain, Stephen J. Klippenstein, and Craig A. Taatjes, *Time-Resolved Measurements of OH and HO_2 Product Formation in Pulsed-Photolytic Chlorine-Atom Initiated Oxidation of Neopentane*, Phys. Chem. Chem. Phys. **5**, 1584-1592 (2003).

18. John D. DeSain, Stephen J. Klippenstein, James A. Miller, and Craig A. Taatjes, *Measurements, Theory, and Modeling of OH Formation in the Reactions of Ethyl and Propyl with O_2*, J. Phys. Chem. A, *in press* (2003).

19. James A. Miller and Stephen J. Klippenstein, *From the Multiple-Well Master Equation to Phenomenological Rate Coefficients: Reactions on a C_3H_4 Potential Energy Surface*, J. Phys. Chem. A, *in press*, (2003).

TIME-RESOLVED FTIR EMISSION STUDIES OF LASER PHOTOFRAGMENTATION AND RADICAL REACTIONS

Stephen R. Leone
Departments of Chemistry and Physics
and Lawrence Berkeley National Laboratory
University of California
Berkeley, California 94720
(510) 643-5467 srl@cchem.berkeley.edu

Scope of the Project

Combustion is a complex process involving short-lived radical species, highly excited states, kinetics, transport processes, fluid dynamics, and energy transfer. Detailed measurements of microscopic reaction pathways, rate coefficients, vibrational and rotational product state distributions, and thermochemistry have resulted in considerable new information to aid in the understanding of combustion processes. Infrared emission provides a method of probing the excited states of species that is complementary to many other techniques, such as laser-induced fluorescence, permitting direct detection of vibration-rotation transitions or low-lying electronic states. The time-resolved FTIR method provides a broad overview of all emitting species, which is crucial in identifying novel products and transition state mechanisms, especially 5-member ring transition states, i.e. HOI from O + alkyl iodides, and for products of radical-radical reactions, CO(v) from O + methyl or ethyl reactions. This project explores laser-initiated radical reactions, radical-radical reactions, photofragmentation events, and energy transfer processes related to problems in combustion dynamics. The vibrationally and low-lying electronically excited species generated in such processes are probed by time-resolved Fourier transform infrared (FTIR) emission spectroscopy. Dynamics measurements are obtained by acquiring time-resolved signals from a high repetition rate pulsed excimer laser at each mirror position of the spectrometer. These signals are then assembled into interferograms at a series of time delays, to obtain spectra at each time delay. This is a relatively unique facility, applicable to detect the diatomic and small polyatomic species that are the products of photofragmentation and radical reactions. The current research involves the main thrust to study radical reactions to determine the nascent product species and states formed in a variety of important radical-radical and radical-molecule processes.

The principal investigator recently moved his laboratories to the University of California, Berkeley. After a period of down-time, the time-resolved FTIR instrument is now set up in laboratory space at the Lawrence Berkeley National Laboratory. The principal investigator is also the Director of the Chemical Dynamics Beamline, and through this position he has joined new efforts to study photoionization spectroscopy of radical species, such as CH_3 (with Branko Ruscic), propargyl (postdoctoral fellow at the beamline Christophe Nicolas), and ClCO (with Cheuk Ng). Ongoing work at the Chemical Dynamics Beamline also involves interactions with Terry Cool and Andy McIlroy, in their pursuit of the study of flame chemistry using nozzle sampling and photoionization techniques. A large array of radical species have been detected and used to study the flame chemistry and ionization potentials of the radicals themselves. Molecular beam photofragmentation studies have been completed by a postdoctoral fellow at the beamline, Jinian Shu, on the dissociation of crotonaldehyde (CH3CHCHCHO). Finally, a new laser ablation experiment has been developed at the beamline with Musa Ahmed to study C, C_2, and C_3 species in

photoionization. In that work, a preliminary ionization energy of C_3 is obtained, which is approximately 11.6 eV.

Product State Distributions of Photofragmentation with the FTIR

A large amount of earlier published work involved the development of new tools for spectroscopic pattern recognition and the use of these tools to study complex photodissociation pathways in ammonia and deuterated ammonia molecules. The method of time-resolved FTIR spectroscopy permits the experimentalist to study the progress of many simultaneous reaction pathways, monitoring the infrared-emitting product state distributions and branching ratios of different reaction channels. Detailed analyses of the spectroscopic data obtained, and their variation with reaction conditions, are a necessary prerequisite to the interpretation of other chemical reaction systems under study, as well as to learn about the dynamics on complex polyatomic potential surfaces.

CD_3/CH_3 + O Radical-Radical Reactions

In a joint experimental and theoretical work, together with Larry Harding and Stephen Klippenstein, the relative production of CO in the reactions of CD_3/CH_3 + O was investigated. The yield of CO(v=1) from the deuterated methyl + O reaction was measured to be 69±10% of the yield of CO(v=1) from the hydrogenated methyl + O reaction. Classical trajectory studies confirm the CO producing channel, arising from the sequence $CH_3O \rightarrow HCO + H_2 \rightarrow CO(v) + H + H_2$. The calculations also indicate the experimentally observed lower yield of CO in the deuterated reaction. Finally, the calculations show a key importance of the reaction mechanism. This reaction, which proceeds through methoxy, CH_3O, has no transition state in the potential surface for the production of H_2 from the methoxy intermediate. Instead, the calculations show that the H_2 product is formed by passing over a high energy ridge in the potential, rather than via a minimum energy path. This surprising result explains the theoretical and experimental controversy over the CO producing channel in the methyl + O reaction. The results also mean that such new types of reactive mechanisms must be considered for other highly energized systems, which may not proceed through saddle point transition states.

Ethyl, *n*-Propyl, Isopropyl, and *n*-Butyl Radical Reactions with O atoms

In recent work, a group of symmetric ketones are photodissociated in the presence of SO_2 to study the reactions of larger hydrocarbon radicals with O atoms. The symmetric ketones, acetone, diethyl ketone, di-*n*-propyl ketone, diisopropyl ketone, and di-*n*-butyl ketone, are dissociated with 193 nm light, while the photodissociation of SO_2 produces O atoms simultaneously. The products of the reactions of $O(^3P)$ with methyl, ethyl, *n*-propyl, isopropyl, and *n*-butyl radicals are then observed under low resolution with the FTIR. In earlier work, the reactions of methyl and ethyl were studied in detail, and the CO-producing channel was verified completely. Here the methyl and ethyl reactions are compared with the reactions of the larger hydrocarbons. The reactions of these larger radicals with $O(^3P)$ can yield aldehydes or CO as primary products. Evidence is found that the CO-producing channel occurs for all the alkyl radicals studied, and the form of the kinetics for the *n*-propyl reaction is studied in detail to verify the CO production. In addition, the absorption cross sections for the series of symmetric ketones are quantified at 193 nm and used to set limits on the production of the alkyl radical yields and the relative CO(v) yields from the

reactions. The lower limits on the yields of ethyl, *n*-propyl, *i*-propyl, and *n*-butyl in the photodissociation of the ketones, normalized to 2 for methyl, are 1.3 ± 0.2, 0.8 ± 0.2, 1.8 ± 0.7 and 0.86 ± 0.14, respectively. The relative CO yields from the reactions of the same series of radicals with O atoms were also obtained.

NH_2 + NO, Thermal De-NO_x Reaction with Additional Vibrational Excitation

A study was performed on the reaction of NH_2 with NO, in which the initial NH_2 is formed with electronic and vibrational excitation. Emission is observed from vibrationally excited NO, N_2O, and H_2O. The NO emission occurs by energy transfer from the initially excited NH_2. The N_2O is formed only by the availability of the extra excitation energy, requiring passage over a high barrier. The vibrationally excited H_2O is formed only in a delayed kinetic process that exhibits an induction period. Experimental investigations of this induction period suggest that the water vapor product is only formed after vibrational excitation is removed from the NH_2 radical by collisions. The results provide additional evidence for the interesting temperature dependence of the product branching ratios in the NH_2 + NO reaction and the narrow temperature range over which the water vapor product is formed. With the presence of vibrational excitation in the NH_2, there is a significant probability that the collisions of NO with vibrationally excited NH_2 occur by deactivation and dissociation of the reactive complex, without reaction to form H_2O. This is reasonable, since for the reaction to occur it has to pass through many transition states, breaking all the initial bonds in the reactants and reforming new ones in the products.

Future Plans
New studies of radical reactions and photofragmentation will be pursued, including: C_2H reactions with O atoms, C_2H + NO, CH_3 + N, and kinetic energy enhanced OH reactions with hydrocarbons.

Recent Publications

Timothy P. Marcy, Jonathan P. Reid, Charles X. W. Qian, and Stephen R. Leone, "Addition-insertion-elimination reactions of $O(^3P)$ with halogenated iodoalkanes producing HF(v) and HCl(v)," J. Chem. Phys. 114, 2251 (2001).

Timothy P. Marcy, Robert Richard Díaz, Dwayne Heard, Stephen R. Leone, Lawrence B. Harding, and Stephen J. Klippenstein, "Theoretical and experimental investigation of the dynamics of the production of CO from the CH_3 + O and CD_3 + O reactions," J. Phys, Chem. A 105, 8361 (2001).

Timothy P. Marcy, Dwayne Heard, Stephen R. Leone, "Product studies of inelastic and reactive collisions of NH_2 + NO: Effect of vibrationally and electronically excited NH_2," J. Phys. Chem. A 106, 8249 (2002).

INTERMOLECULAR INTERACTIONS OF HYDROXYL RADICALS ON REACTIVE POTENTIAL ENERGY SURFACES

Marsha I. Lester
Department of Chemistry
University of Pennsylvania
Philadelphia, PA 19104-6323
milester@sas.upenn.edu

PROGRAM SCOPE

The current goal of the DOE-sponsored research in this laboratory is to characterize OH reactant complexes with a series of new partners of combustion relevance, including ethylene and acetylene. For these partners, molecular associations of OH radicals have already been predicted to play a critical role in the reaction mechanism. These systems have strong intermolecular interactions, very low barriers to reaction (often lying below the reactant asymptote), and fast overall rates of reaction. For example, recent high-level *ab initio* calculations by Garrett and coworkers have identified a hydrogen-bonded complex between OH and the π-bond of C_2H_4 as an important precursor in the addition reaction of OH radicals to the double bond of ethylene.[1] An analogous T-shaped complex has been predicted on the reaction path for OH addition to acetylene (C_2H_2).[2]

INFRARED ACTION SPECTROSCOPY OF OH-C_2H_2

We have recently obtained the first spectroscopic evidence of a π-hydrogen-bonded complex between the OH and C_2H_2 reactants in the entrance channel to reaction. The OH-C_2H_2 complexes are generated by photolyzing HNO_3 at 193 nm to produce OH radicals, which are entrained in a premixed 5-10% C_2H_2 / Ar gas mixture at a total pressure of 40-60 psi. We have used infrared action spectroscopy to obtain infrared spectra of the OH-C_2H_2 reactant complex in the regions of the $2\nu_{OH}$ OH stretch overtone of the hydroxyl radical and the ν_3 asymmetric stretch fundamental of acetylene. In addition, we have simultaneously identified the principal OH (v, j_{OH}) product channels that are populated following dissociation of the complex.

The production and/or detection of the OH-C_2H_2 reactant complex by infrared action spectroscopy has been much more challenging than other systems studied to date, namely H_2-OH, CH_4-OH, and OH-CO. The photolytically generated OH radicals can react quickly with C_2H_2 in the carrier gas, $k_{rxn} = 9.0 \times 10^{-13}$ cm^3 molec^{-1} s^{-1} at 298K,[3] which can significantly reduce the number of OH radicals available for complexation with C_2H_2. Additionally, the infrared action technique relies on vibrational predissociation of the OH-C_2H_2 complex and subsequent detection of the inelastically scattered OH fragments. The sensitivity of this technique is reduced when the OH fragments are distributed over many quantum states and, even more importantly, if the complex undergoes significant reactive decay following infrared activation. We do not yet know the branching ratio for reaction upon OH overtone or asymmetric acetylenic stretch excitation of the OH-C_2H_2 complex.

The infrared action spectrum of OH-C_2H_2 in the OH overtone region is centered at 6885.6 cm^{-1}, which is shifted 85.7 cm^{-1} to lower energy of the OH monomer transition. The large spectral shift demonstrates that H-atom of OH is hydrogen-bonded to the acetylene molecule.

The rotational band structure is characteristic of an A-type parallel transition of a near prolate symmetric top. The P- and R-branch line spacings reveal an intermolecular separation distance of 3.34(3) Å. By contrast, the infrared spectrum in the asymmetric stretch region of acetylene is located at approximately 3281 cm^{-1}, indicating a much smaller spectral red shift of 14 cm^{-1}. The relatively small spectral shift confirms that the asymmetric acetylenic stretch is remote from the hydrogen bond. The rotational band structure in this region consists of several peaks arising from multiple Q-branches, as would be expected for a B-type perpendicular transition.

Ab initio calculations predict the structure of the OH-C$_2$H$_2$ reactant complex to be T-shaped, with the H of OH pointing toward the π-bond of acetylene.[2,4] This structure is analogous to that previously determined for closed-shell complexes, such as HCl-C$_2$H$_2$ and HF-C$_2$H$_2$.[5-7] The spectroscopic data is consistent with this minimum energy structure, although the OH-C$_2$H$_2$ spectra are more complicated than seen for HX-C$_2$H$_2$ systems due to the unquenched angular momentum of OH along the intermolecular axis.

The principal OH (v, j_{OH}) product channels that are populated following dissociation of the complex provide information on the stability of the OH-C$_2$H$_2$ complex and the mechanism for inelastic decay. For OH overtone stretch excitation of OH-C$_2$H$_2$, the dominant OH product channels are OH $X^2\Pi_{3/2}$ (v=1, j_{OH}=23/2). By constructing an energy cycle, we can estimate an upper limit for the ground state binding energy of OH-C$_2$H$_2$, $D_0 \leq$ 995 cm^{-1} (2.8 kcal mol^{-1}), assuming minimal translational energy for the recoiling partners and little excess energy deposited as rotational and/or vibrational excitation of the C$_2$H$_2$ fragment. Other significant product channels, OH (v=1, j_{OH}=9/2 and 11/2), likely arise when the correlated C$_2$H$_2$ fragment acquires C≡C stretch excitation (v$_2$) in the dissociation event. Thus, it appears that vibrational predissociation of the OH-C$_2$H$_2$ complex proceeds by transfer of the energy released from OH vibration (v=2→1) to OH rotation or C$_2$H$_2$ (v$_2$) vibration. For asymmetric acetylenic stretch excitation of the OH-C$_2$H$_2$ complex, the OH fragments are observed primarily in OH (v=0, j_{OH}=9/2), although it is difficult to probe lower rotational states due to OH background in the supersonic jet. In this case, it appears that vibrational energy transfer to the v$_2$ C≡C stretch is the dominant decay pathway.

FUTURE PLANS

In the coming year, we will continue our investigation of the OH-C$_2$H$_2$ reactant complex. These studies will include infrared spectroscopy, time and/or frequency domain measurements of the lifetime of the vibrationally activated complex, and probes of the inelastic and/or reactive decay process. We also plan to search for intermolecular bending vibrations that drive the transformation from the reactant complex to the transition state for the addition reaction. Finally, it will be crucial to connect the experimental measurements with *ab initio* calculations of the reaction coordinate. We will also extend our studies to OH-ethylene and OH-cyclopropane systems, the latter of which can be viewed as the prototype pseudo-π unsaturated hydrocarbon.

REFERENCES

[1] S. M. Kathmann, M. Dupuis, and B. C. Garrett, personal communication (2001).

[2] C. Sosa and H. B. Schlegel, *J. Am. Chem. Soc.* **109**, 4193 (1987).

[3] R. Atkinson, *J. Phys. Chem. Ref. Data, Monogr. No. 1* (1989).

[4] M. D. Wheeler, personal communication (2002).

[5] Z. S. Huang and R. E. Miller, *J. Chem. Phys.* **86**, 6059 (1987).

[6] L. Oudejans, D. T. Moore, and R. E. Miller, *J. Chem. Phys.* **110**, 209 (1999).

[7] P. Carcabal, M. Broquier, M. Chevalier, A. Picard-Bersellini, V. Brenner, and P. Millie, *J. Chem. Phys.* **113**, 4876 (2000).

DOE SUPPORTED PUBLICATIONS
2001-2003

1. M. Tsiouris, M. D. Wheeler, and M. I. Lester, "Activation of CH Stretching Vibrations in CH_4-OH Entrance Channel Complexes: Spectroscopy and Dynamics", *J. Chem. Phys.* **114**, 187-197 (2001).

2. M. W. Todd, D. T. Anderson, and M. I. Lester, "Reactive Quenching of OH $A\ ^2\Sigma^+$ in Collisions with Molecular Deuterium via Nonadiabatic Passage through a Conical Intersection", *J. Phys. Chem. A.* **105**, 10031-10036 (2001).

3. M. Tsiouris, I. B. Pollack, and M. I. Lester, "Infrared Action Spectroscopy and Inelastic Recoil Dynamics of the CH_4-OD Reactant Complex", *J. Phys. Chem. A* **106**, 7722-7727 (2002).

Theoretical Studies of Molecular Systems

William A. Lester, Jr.
Chemical Sciences Division,
Ernest Orlando Lawrence Berkeley National Laboratory and
Kenneth S. Pitzer Center for Theoretical Chemistry,
Department of Chemistry, University of California, Berkeley
Berkeley, California 94720-1460
walester@lbl.gov

Program Scope

This research program is directed at extending fundamental knowledge of atoms and molecules. The approach combines the use of ab initio basis set methods and the quantum Monte Carlo (QMC) method to describe the electronic structure, energetics, and reaction pathways of systems of primarily combustion interest.

Recent Progress

Singlet-Triplet Energy Splitting in Ethylene (with O. El Akramine and A. Kollias)
Recent photodissociation experiments at the Advanced Light Source (ALS) by Qi, Suits, and colleagues suggest the formation of triplet ethylene from photodissociation of ethylene sulfide [1,2]. Analysis of the experimental findings raised the question of the accuracy of the adiabatic energy difference between the ground state and the lowest triplet state of ethylene. Using DMC trial functions constructed from Hartree-Fock (HF), complete active space self-consistent field (CASSCF) and multi-configuration HF (MCHF) wave functions, we computed the atomization energy and the heat of formation of both states, and the adiabatic and vertical energy differences between these states using both all-electron and effective core potential (ECP) DMC. The ground state atomization energy and heat of formation are found to agree with experiment to within the error bounds of the computation and experiment. Only theoretical predictions are available of the triplet state atomization energy and heat of formation. We have carried out carried out Moeller-Plesset second-order (MP2) perturbation theory and generalized gradient approximation B3LYP calculations. The DMC adiabatic singlet-triplet energy difference is found to differ by 5 kcal/mol from the value obtained in the recent photodissociation experiment. In a private communication, however, the PI of the ALS experiments, A. G. Suits, has informed us that the experimental error estimate is likely too small and therefore that the apparent discrepancy may not be real [3]

[1] F. Qi, O. Sorkhabi, and A. G. Suits, J.Chem.Phys. 112, 10707 (2000); A. G. Suits and F. Qi, J.Electron Spectrosc.Relat.Phenom. 119, 127 (2001).
[2] F. Qi, O. Sorkhabi, A. G. Suits, S. H. Chien, and W. K. Li, J.Am.Chem.Soc. 123, 148 (2001).
[3] A. G. Suits (private communication).

Hydrogen abstraction from methanol by chlorine (with A. Kollias and O. Couronne)

Abstraction reactions of hydrogen atoms from hydrocarbons are of great importance in combustion, and in atmospheric and interstellar chemistry. The reaction of a chlorine atom with methanol can proceed via two channels:

$$Cl + CH_3OH \rightarrow CH_3O + HCl \qquad \Delta H = 2.4 \text{ kcal/mol} \qquad (1)$$
$$\rightarrow CH_2OH + HCl \qquad \Delta H = -6.8 \text{ kcal/mol} \qquad (2)$$
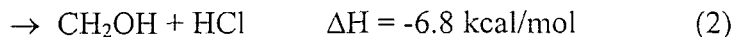
yielding methoxy radical in (1) and hydroxylmethyl radical in (2).

Although the reaction of methanol with Cl has been studied in a number of laboratories, until the recent crossed beam experiment of Ahmed et al. [1], the reaction was thought to proceed with formation of an intermediate complex. The crossed beam experiment ruled out the backward-forward symmetry characteristic of complex formation found in earlier ab initio studies [2]. In the present investigation, the situation was clarified by computation of the reaction path using ab initio intrinsic reaction coordinate procedures. The reactants, transition state, and products were characterized using DMC. The present study identified a collinear pathway for dehydrogenation leading to hydroxymethyl radical. The DMC calculations confirm a modest barrier along the pathway. A manuscript describing this work is in preparation.

[1]M. Ahmed, D. S. Peterka, and A. G. Suits, Chem.Phys.Lett. **317**, 264 (2000); M. Ahmed, D. S. Peterka, and A. G. Suits, PCCP Phys.Chem.Chem.Phys. **2**, 861 (2000).

[2]J. T. Jodkowski, M. T. Rayez, J. C. Rayez, T. Berces, and S. Dobe, J Phys Chem A **102**, 9230 (1998).

Geometry optimization in QMC by the solution mapping (SM) method (with S. C. Schuetz, A. C. Kollias, and M. Frenklach)

Although several QMC studies have examined geometry optimization of molecules, most have treated diatomic systems exclusively. It is of interest to examine the applicability of the QMC method, in the most accurate DMC variant of the approach, to geometry optimization of polyatomic systems.

One aspect of the procedures followed in DMC molecular computations that must be carefully addressed is the specification of geometries at critical points of the potential energy surface. The usual approach is to obtain the equilibrium geometry from non-QMC approaches such as, for example, second-order Moller-Plesset perturbation theory (MP2) or a generalized gradient approximation density functional method such as B3LYP. Although much success has been achieved for the systems studied to date, for the radicals and novel bonding systems that are contemplated for study in this laboratory, it is also important to have a technique that is not dependent on other methods. Work is in progress in collaboration with M. Frenklach to test the SM method for its usefulness for this purpose.

Our test system is formaldehyde. Three internal coordinates were chosen to define the potential surface of formaldehyde: the CO bond length, CH bond length, and the OCH angle. Two trial wave functions were used in the variational Monte Carlo (VMC) and DMC methods. The trial functions were computed using the HF method with soft effective core potentials (ECPs) and the uncontracted Partridge-2 basis set, and the multi-configuration self-consistent field (MCSCF) approach with Stevens-Basch-Krauss (SBK) ECPs and the cc-pVQZ basis set. VMC and DMC energies were calculated for 15 geometries and the results fitted to a second-order polynomial.

Both VMC and DMC optimized structures were found to lie within the error of the experimental formaldehyde bond lengths and angle.

Future Plans

Future work will continue in the direction of establishing fundamental understanding of mechanisms leading to soot formation as well as other molecular species of combustion interest. In addition, there will be an enhanced effort to develop an efficient scheme for the calculation of optimized geometries in the DMC method.

DOE Supported Publications 2001-2003

1. R. N. Barnett, Z. Sun, and W. A. Lester, Jr., "Improved Trial Wave Functions in Quantum Monte Carlo: Application to Acetylene and Its Dissociation Fragments," J. Chem. Phys. 114, 2013 (2001).

2. A. C. Pavão, C. A Taft, T. C. F. Guimarães, M. B. C. Leão, J. R. Mohallem, and W. A. Lester, Jr. "Interdisciplinary Applications of Pauling's Metallic Orbital and Unsynchronized Resonance to Problems of Modern Physical Chemistry: Conductivity, Magnetism, Molecular Stability, Superconductivity, Catalysis, Photoconductivity and Chemical Reaction," (feature article), J. Phys. Chem. 105, 5 (2001).

3. I. Ovcharenko, A. Aspuru-Guzik, and W. A. Lester, Jr., "Soft Pseudopotentials for Efficient Quantum Monte Carlo Calculations: From Be to Ne and Al to Ar," J. Chem. Phys. 114, 7790 (2001).

4. W. A. Lester, Jr., "Research Developments and Progress During the Nineties," J. Mol. Struct. (THEOCHEM) 573, 55 (2001).

5. X. Krokidis, N. W. Moriarty, W. A. Lester, Jr., and M. Frenklach, "A Quantum Monte Carlo Study of Energy Differences in C_4H_3 and C_4H_5 Isomers," Int. J. Chem. Kinetics 33, 808 (2001).

6. N. W. Moriarty, X. Krokidis, W. A. Lester Jr., and M. Frenklach, "The Addition Reaction of Propargyl and Acetylene: Pathways to Cyclic Hydrocarbons," 2nd Joint Meeting of the U.S. Sections of the Combustion Institute, Oakland, CA, March 25–28, 2001, paper 102.

7. N. W. Moriarty, X. Krokidis, W. A. Lester Jr., and M. Frenklach, "On the Formation of the First Aromatic Ring," *Abstracts of the 224th ACS National Meeting*, Vol. 47, No. 2, 2002, pp. 769–770.

8. W. A. Lester, Jr. and J. C. Grossman, "Quantum Monte Carlo for the Electronic Structure of Combustion Systems," in *Recent Advances in Quantum Monte Carlo – Part II*, eds., W. A. Lester, Jr., S. Rothstein, and S. Tanaka, World Scientific Publishing, Singapore, p. 159 (2002).

9. O. El Akramine, W. A. Lester, Jr., X. Krokidis, C. A. Taft, T. C. Guimaraes, A. C. Pavao, and R. Zhu, "Quantum Monte Carlo Study of the CO Interaction with a Model Surface for Cr(110)" Mol. Phys. 101, 277 (2003).

10. J. A. W. Harkless, J. H. Rodriguez, L. Mitas, and W. A. Lester, Jr., "Quantum Monte Carlo and Density Functional Theory Study of Peroxynitrite Anion," J. Chem. Phys. 118, 4987 (2003).

Quantum Dynamics of Fast Chemical Reactions

April 2003

John C. Light

The James Franck Institute and Department of Chemistry

The University of Chicago,Chicago,Illinois 60637

j-light@uchicago.edu

Scope:

The aims of this research and are to develop theoretical infrastructure and computational methods and to apply these methods to determine theoretically reaction rates and other dynamical quantities of interest for chemical reactions.

The past year has been one of rebuilding the research group in this area which was required by a change in personnel and was hampered by delays due to immigration difficulties. During the past year we have focused primarily on two areas: development of better representations for dynamical calculations on larger systems and applications to understand the vibration/rotation structure of molecules of interest in combustion problems. This year we focused on developing efficient direct product angular DVR (DPA-DVR) bases for larger systems, methods for symmetry adaptation of such bases, and the application of this approach to the CO_2 dimer. We have continued work on semiclassical methods mainly on the problems semiclassical methods face in treating reactive systems in which bifurcations occur.

Recent Results:

Angular Basis Representations for molecular motions:

There are three fundamental choices one makes in determining theoretically the quantum states of high energy or floppy molecular systems: the coordinate system to use, the basis to use, and the solution method to use. This latter obviously involves both the basis and the evaluation of the Hamiltonian or its action on the basis.

For four or more atoms the number of internal angular coordinates ranges from $3n-7$ (hyperspherical coordinates) to $2n-5$ (sequential Jacobi for example). Thus for tetra-atomic systems there are 3 to 5 angular coordinates. Coupled angular bases are often used for these degrees of freedom. Since these bases do not take into account the potential, the basis becomes large in order to represent localized motions, and iterative methods do not appear to work. Thus the 3-D angular problem may be limiting for many four atom systems.

We have recently shown that a direct product angular DVR (DPA-DCR) can be used for such systems, yielding several advantages but with a few drawbacks. First, the DPA-DVR primitive basis is larger that the equivalent CAM basis, i.e. the convergence may be slower in the DPA-DVR basis.

However, the advantages are substantial. The angular problem may be solved by sequential diagonalization/truncation, necessary if the basis is very large.Second, the

convergence is *faster* than CAM if the states of interest are localized in angle. Third, the use of angular DVR's make evaluation of the Hamiltonian matrix elements very simple. Fourth we have shown that full symmetrization of the DPA-DVR is relatively simple (for G_{16} for example) thus reducing the basis size.

This was applied to the intermolecular modes of the CO_2 dimer (i.e. rigid monomers) and compared with the CAM calculations of Chen[1] Agreement to .01 cm^{-1} was achieved with a much smaller 4-D basis SDT using the DPA-DVR and thus about a factor of 10 reduction in computation time.

(Sometimes it's not quite a zero-sum game.)

DOE Supported publications, 2002

No papers which cite DOE support appeared in 2002. Research results on the above DPA-DVR are contained in:

H.S. Lee, Hua Chen and J. C. Light, Symmetry Adapted direct product discrete variable representation for the coupled angular momentum operator: Applications to the vibrations of $(CO_2)_2$

J. Chem. Phys. (submitted) [2]

Current research:

Semiclassical methods:

We have been looking at extending the late Gert Billing's "dressed classical dynamics"[3] to treat reactive systems more effectively. Although his approach becomes exact quantum mechanically with sufficient "dressing", the cost in dressing basis becomes exhorbitant for long times and for systems which bifurcate. We have been looking possibilities to treat the bifurcation problem by re-expansion or by combining two different "dressed trajectories". We have not yet had great success but are *continuing to look at this point in time.*

Theoretical spectroscopy of larger systems: H_2CO

The development of the DPA-DVR (above) and the energy selected basis (ESB) iterative method[4] provide the tools for the efficient determination of many energy levels of molecules important for combustion. One of these is formaldehyde, H_2CO. The DPA-DVR permits the determination of zero order potentials for one (or more) angles, the determination of zero order eigenpairs for these degrees of freedom, and the combination of zero order eigenfunctions into product basis functions for the full problem (6-D). This basis is limited by truncation of the basis such that the zero order energies of the basis functions are limited by a cut-off energy. This is a very large reduction.

The zero order bases also permit the definition of PODVR's for all degrees of freedom, including angles. This greatly reduces the size of the direct product grid used for evaluation of the Hamiltonian. Although the ESB is not a direct product basis it is relatively small and iterative solution via transformations to the 6-D truncated grid[5] is possible.

We are in the late stages of this calculation.

Future Directions:

Our newfound ability to generate excellent zero order bases for all degrees of freedom of four atom systems and to combine them into compact energy selected bases which permit iterative solution (we currently use the Arnoldi (IRLM) approach) opens the possibility of accurate reactive scattering solutions for larger systems. Even with

these techniques, however, the scaling problem with number of atoms or dimensionality means that exact solutions for 5 or more atom systems will be few and far between, limited to those systems for which the full density of states at energies of interest for reactions is relatively small. The alternative, much discussed but not often implemented[6], is to isolate the "active" degrees of freedom to treat more or less exactly from the more "spectator" like degrees of freedom. One would like to do this in a fashion in which corrections toward the exact solutions can be obtained.

I believe progress toward this goal can be made by using subsets of the energy selected basis sets which, for example, restrict "spectator" degrees of freedom to the ground state or to a small subset of states. Alternatively, it is likely that only basis functions highly excited in the "active" subspace will contribute to the reaction or CRP. The ability to solve iteratively (e.g. RRGM or spectrally filtered Chebychev propagation) using this basis and a truncated grid should permit quite efficient solution of the CRP via an analogue of the transition state wave packet method[7]. . The basis already does substantial filtering (reducing the spectral range of the representation of the Hamiltonian), so convergence may be rapid.

Overall we will continue the high energy spectroscopic studies of high energy molecules of relevance to combustion as well as reactive studies such as mentioned above.

REFERENCES

[1] Hua Chen. *Theoretical Spectra of Floppy Molecules.* PhD thesis, University of Chicago, Chicago, IL, 60637, 2000.

[2] Hua Chen H. S. Lee and J. C. Light. Symmetry adapted direct product discrete variable representation for the coupled angular momentum operator: Application to the vibrations of $(CO_2)_2$. *J. Chem. Phys.*, (Submitted).

[3] Billing G. D. Quantum-dressed classical mechanics: Theory and application. *PCCP*, 4:2865–2877, 2002.

[4] H. S. Lee and J. C. Light. Molecular vibrations: Iterative solution with energy selected bases. *J. Chem. Phys.*, 118:3458, 2003.

[5] X. G. Wang and T. Carrington, Jr. New ideas for using contracted basis functions with a Lanczos eigensolver for computing vibra- tional spectra of molecules with four or more atoms. *J. Chem. Phys.*, 117:6923, 2002.

[6] M. L. Wang and J. Z. H. Zhang. Generalized semirigid vibrating rotor target model for atom-poly reaction: Inclusion of umbrella mode for H+CH4 reaction. *J. Chem. Phys.*, 117:10426, 2002.

[7] J. C. Light and D. H. Zhang. The quantum transition state wavepacket method. *Faraday Discuss.*, 110:105, 1998.

Kinetics of Elementary Processes Relevant to Incipient Soot Formation

M. C. Lin
Department of Chemistry
Emory University
Atlanta, GA 30322
chemmcl@emory.edu

I. Program Scope

Soot formation and abatement processes are some of the most important and challenging problems in hydrocarbon combustion. The key reactions involved in the formation of polycyclic aromatic hydrocarbons (PAH's), the precursors to soot, remain elusive. Small aromatic species such as C_5H_5, C_6H_6 and their derivatives are believed to play a pivotal role in incipient soot formation.

The goal of this project is to establish a kinetic database for elementary reactions relevant to soot formation in its incipient stages. In the past year, our major focus has been placed on the experimental studies on several reactions of C_6H_5 with n-alkanes, CH_2CO, CH_3CHO and CH_3COCH_3, and computational studies on the reactions with C_2H_2 and C_3H_6, and the thermal decomposition of C_5H_6, $C_5H_5CH_3$, C_2H_5OH and i-C_3H_7OH at the G2M level of theory.[1] These results are briefly summarized below.

II. Recent Progress

A. Experimental studies

We have developed three complementary methods for determination of the kinetics and mechanisms for C_6H_5 reactions with combustion species, including small alkenes and small aromatics. Combination of these methods: cavity ring-down spectrometry (CRDS), pyrolysis/Fourier transform infrared spectrometry (P/FTIRS) and pulsed laser photolysis/mass spectrometry (PLP/MS), allows us to cover a broad temperature range, 300 - 1000 K

1. C_6H_5 + C_3H_8, n-C_4H_{10}, n-C_6H_{14} and n-C_8H_{18} Reactions (ref. # 2)

The kinetics for the C_6H_5 reaction with 4 small alkanes have been investigated to determine the reactivity of the phenyl radical toward the secondary C-H bonds. Using acetophenone as the C_6H_5 source, the total rate constants have been measured by PLP/MS at 3 Torr He pressure in the temperature range 565 < T < 1050 K. The rate constants can be given by the following expressions in units of $cm^3 mol^{-1} s^{-1}$:

$$k(C_3H_8) = 2.95 \times 10^{11} \exp(-1951/T)$$
$$k(C_4H_{10}) = 4.57 \times 10^{11} \exp(-1735/T)$$
$$k(C_6H_{14}) = 4.07 \times 10^{11} \exp(-1541/T)$$
$$k(C_8H_{18}) = 3.65 \times 10^{11} \exp(-1300/T).$$

These rate constants, after the corrections for the primary C-H contributions, give $k_{s\text{-}CH}$:

$$k_{s\text{-}CH} = \left(k_{alkane} - 6 \times k_{p\text{-}CH} \right) / N_{s\text{-}CH}$$

where $N_{s\text{-}CH}$ is the number of s-C-H bonds, 2, 4 and 8 for C_3H_8, n-C_4H_{10} and n-C_6H_{14}, $k_{p\text{-}CH} = 10^{10.40 \pm 0.06}$
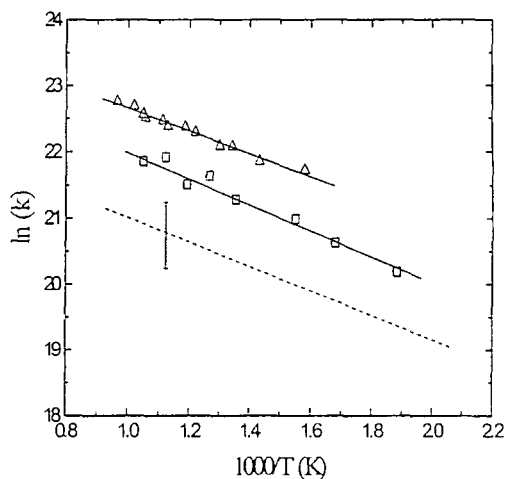
Fig. 1. Arrhenius plot of the rate constant per s-CH bond obtained by the C_6H_5 + C_3H_8 (dashed line with large error), n-C_4H_{10} (□) and n-C_6H_{14} (△) data

exp $[(-1790 \pm 102)/T)]$.[3] The results shown in Fig. 1 reveal a strong dependence of k_{s-CH} on molecular size. The averaged absolute rate constant at 1000 K increases from 1.6×10^9 cm^3 mol^{-1} s^{-1} for C_3H_8 to 3.8×10^9 cm^3 mol^{-1} s^{-1} for n-C_4H_{10} and 7.0×10^9 cm^3 mol^{-1} s^{-1} for n-C_6H_{14}, approximately 2:4:8.

2. C_6H_5 + CH_3CHO → Products (ref. # 4)

Acetaldehyde is an important combustion intermediate. The rate constant for the C_6H_5 with CH_3CHO reaction has been measured by CRDS in the temperature range 299 - 501 K. The total second-order rate constant can be represented by the expression, $k = (2.8 \pm 0.1) \times 10^{11}$ exp$[-(695 \pm 18)/T]$ cm^3 mol^{-1} s^{-1}, which is slightly faster than the analogous C_6H_5 + CH_2O reaction,[5] $k = (4.7 \pm 1.1) \times 10^{11}$ exp$[-(951 \pm 82)/T]$ cm^3 mol^{-1} s^{-1}, determined with the same method in the same temperature range. The experimental data for the CH_3CHO reaction could be reasonably accounted for by TST using the predicted barrier for the aldehydic C-H abstraction 0.5 kcal/mol at the B3LYP/aug-cc-PVTZ//B3LYP/cc-PVDZ level of theory.

3. C_6H_5 + CH_3COCH_3 → Products (ref. # 6)

The absolute rate constants for the C_6H_5 + CH_3COCH_3 and CD_3COCD_3 reactions have been measured by CRDS in the temperature range 299 – 451 K. The rate constants can be represented by the Arrhenius equation, k (C_6H_5 + CH_3COCH_3) = $(4.2 \pm 0.4) \times 10^{11}$ exp$[-(955 \pm 30)/T]$ cm^3 mol^{-1} s^{-1} and k (C_6H_5 + CD_3COCD_3) = $(5.1 \pm 0.6) \times 10^{11}$ exp$[-(1114 \pm 43)/T]$ cm^3 mol^{-1} s^{-1} with a significant kinetic isotope effect. The result of our computational study indicates the reaction is dominated by the abstraction mechanism with negligible contributions from addition to the C=O bond.

4. C_6H_5 + CH_2CO → Products (ref. #7)

Ketene is a potential combustion intermediate which can be formed in O + alkyne reactions. The absolute rate constants for the reactions of C_6H_5 with CH_2CO and CD_2CO reactions have been measured by CRDS at 301 – 474 K and 45 Torr of Ar pressure. The results reveal no detectable kinetic isotope effect with $k = (6.4 \pm 1.1) \times 10^{11}$ exp $[-(1183 \pm 57)/T]$ cm^3 mol^{-1} s^{-1}. The 2.2 kcal/mol activation energy is similar to our measured values for the C_6H_5 + C_2H_4 and C_3H_6 reactions. The mechanism for the C_6H_5 + CH_2CO reaction has also been investigated at the B3LYP/cc-pVDZ level of theory. The result indicates that the reaction is dominated by the addition/decomposition reaction:

$$C_6H_5 + CH_2CO \rightarrow C_6H_5CH_2CO^\dagger \quad \rightarrow C_6H_5CH_2 + CO$$
$$\rightarrow C_6H_5CHCO + H$$
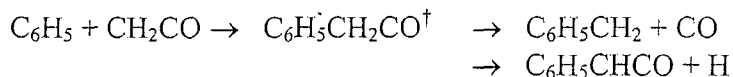
B. Computational Studies
1. Unimolecular Decomposition of C_5H_6 and $C_5H_5CH_3$ (ref. # 8)

We have calculated theoretically the rate constants for the unimolecular decomposition of C_5H_6 (1) and $C_5H_5CH_3$ (2) using canonical variational transition state theory (VTST) and multichannel RRKM-master equation analysis based on the G2M-predicted $\Delta H_0(1)$ = 83.1 kcal/mol and $\Delta H_0(2)$ = 72.5 kcal/mol, which are in good agreement with the reported experimental values : 80.8 ± 1 kcal/mol[9] for (1) and ~75 kcal/mol[10] for (2). The predicted rate constants agree reasonably with earlier experimental results.[9, 11-14]

The rate constants for the dissociation of $C_5H_5CH_3$ to C_5H_5 and CH_3 have been calculated in the same manner. The predicted result compares reasonably with the recent experimental measurements of Ikeda et al.[10] Since the experiment did not distinguish between the three isomers of $C_5H_5CH_3$ (of which only 5-methyl-1,3-cyclopentadiene (5-MCP) has an accessible barrier for dissociation), the reported apparent rate constants are scaled by the factor of 0.1, the calculated equilibrium fraction of 5-MCP.

The following high and low-pressure limiting rate constants evaluated in this work should be useful for kinetic modeling of hydrocarbon combustion:

$$k_1^\infty = 2.07 \times 10^{15} \exp(-41238K/T) \ s^{-1}$$
$$k_1^0 = 5.89 \times 10^{-54} \ T^{-19.6} \exp(-50355/T). \ cm^3 \ s^{-1}$$
$$k_2^\infty = 4.70 \times 10^{15} \exp(-35890K/T) \ s^{-1}$$
$$k_2^0 = 9.71 \times 10^{-60} \ T^{-31.0} \exp(-57527/T) \ cm^3 \ s^{-1}$$

2. Other computational studies (refs. # 15 -17, 19)

Due to space limitation, we briefly cite the systems investigated which are supported in part by this DOE project. The reactions studied include the $C_6H_5 + C_3H_6$ reaction[15] at the UB3LYP/6-311++G(d,p) level, thermal decomposition of C_2H_5OH[16] and i-C_3H_7OH,[17] both are potential alternate fuels or fuel additives. The former, a truly green fuel which can be generated from biomass, is particularly an important fuel of future. The result of our calculation performed at the G2M (RCC2) level of theory[1] indicates that among the 8 product channels identified, the H_2O-elimination process (1) via a four-member-ring transition state is dominant below 10 atm in the temperature range of 700 – 2500 K. At the high – pressure limit and over 1500 K, cleavage of the C-C bond by reaction (2) producing $CH_3 + CH_2OH$ is predicted to be dominant while the $CH_3CH_2 + OH$ channel (8) also becomes competitive. The predicted high-pressure rate constants for the two major product channels can be given by $k_1 = 7.0 \times 10^{13} \exp(-34200/T)$ and $k_2 = 3.7 \times 10^{26} T^{-2.95} \exp(-45600/T)$ s^{-1}, which compare reasonably with earlier data and with our preliminary experimental result obtained in a shock tube and static cell study. At the internal energy corresponding to the $O(^1D)$ + C_2H_6 reaction (140.7 kcal/mol above C_2H_5OH), the predicted branching ratios for the production of CH_3, C_2H_5 and H_2 are in qualitative agreement with the result of a recent cross-molecular beam experiment.[18]

In addition to the decomposition reaction mentioned, we have also calculated the rate constants for H + C_2H_5OH.[19] Among the 4 accessible channels, including OH abstraction, the formation of $H_2 + CH_3CHOH$ products was predicted to be the dominant channel and was found to be in good agreement with available experimental data.[19] The unimolecular decomposition of i-C_3H_7OH was also studied with the G2M method.[17] Among the 6 low-lying product channels identified, the H_2O-elimination process (2) via a four-member-ring transition state is dominant below 760 Torr over the temperature range 500 – 2500 K. At higher pressures and over 1200 K, the cleavage of a C-C bond by reaction (1) producing $CH_3 + CH_3C(H)OH$ is predicted to be dominant. The predicted low- and high-pressure limit rate constants for these two major product channels can be given by $k_1^0 = 6.3 \times 10^{42} T^{-16.21} \exp(-47400/T)$, $k_2^0 = 7.2 \times 10^{44} T^{-14.70} \exp(-35700/T) \ cm^3 \ molecule^{-1} \ s^{-1}$, $k_1^\infty = 8.0 \times 10^{29} T^{-3.75} \exp(-45800/T)$ and $k_2^\infty = 2.0 \times 10^6 T^{2.12} \exp(-30700/T) \ s^{-1}$, respectively. Predicted k_1 values compare reasonably with available experimental data; however, k_2 values are lower than the experimentally determined apparent rate constant for C_3H_6 formation, which may derive in large part from secondary radical reactions. Other minor decomposition products were predicted to have the barriers: $H_2 + CH_3C(O)CH_3$, $E_3^0 = 82.8$

kcal/mol; $H_2O + {}^1CH_3CCH_3$, $E_4{}^0 = 77.9$ kcal/mol; $CH_4 + CH_3C(H)O$, $E_5{}^0 = 84.3$ kcal/mol and $CH_4 + {}^1CH_3COH$, $E_6{}^0 = 81.9$ kcal/mol. The triplet-singlet energy gap for CH_3CCH_3 was predicted to be 5.2 kcal/mol, favoring the singlet state.

III. Future Plans

Currently, we continue the acquisition of kinetic data for C_6H_5 reactions by CRDS and PLP/MS techniques to determine the total rate constants and product branching probabilities in the C_6H_5 reactions with C_3H_4, C_4H_4 and alcohols. Computationally, we will carry out high-level *ab initio* MO calculations to improve our predictive capability for the rate constant and product branching ratios of C_6H_5 reactions with these species and with O_2. We also plan to extend the calculations to include the reaction of C_6H_5 radicals with alkanes to correlate the kinetic data obtained for the abstraction reactions.

IV. References (DOE publications, 2001-present, denoted by *)

1. A. M. Mebel, K. Morokuma and M. C. Lin, J. Chem. Phys., 103, 7414 (1995).
2*. J. Park, L. Wang and M. C. Lin, Int. J. Chem. Kinet., in preparation..
3*. J. Park, S. Gheyas and M. C. Lin, Int. J. Chem. Kinet., 33, 64 (2001).
4*. Y. M. Choi and M. C. Lin, J. Phys. Chem., A, in press.
5. Y. M. Choi, W. S. Xia, J. Park and M. C. Lin, J. Phys. Chem. A, 104, 7030 (2000).
6*. Y. M. Choi and M. C. Lin, J. Phys. Chem., A, submitted.
7*. Y. M. Choi and M. C. Lin, J. Phys. Chem., A, in preparation.
8*. L. V. Moskaleva, I. V. Tokmakov and M. C. Lin, Int. J. Chem. Kinet., in preparation.
9. K. Roy, M. Braun-Unkhoff, P. Frank, and Th. Just, Int. J. Chem. Kinet. 33, 821 (2001).
10. E. Ikeda, R. S. Tranter,, J. H. Kiefer, R. D. Kern, H. J. Singh, Q. Zhang, Proc. of Combust. Inst. 28, 1725 (2000).
11 M. B. Colket, Eastern States Section of Combustion Institute annual meeting, paper no. 1, Orlando, FL, 1990.
12. A. Burcat and M. Dvinyaninov, Int. J. Chem. Kinet. 29:505(1997).
13. K.Roy, Ch. Horn, P. Frank, V. G. Slutsky, and Th. Just, Proc. Combust. Inst. 27, 329 (1998).
14. A. Burcat, M. Dvinianinov, and E. Olchanski, Int. J. Chem. Kinet. 33, 491 (2001).
15*. I. V. Tokmakov, G. J. Nam and M. C. Lin, J. Phys. Chem., A., in preparation.
16*. J. Park, R. S. Zhu and M. C. Lin, J. Chem. Phys., 117, 3224 (2002).
17*. B. H. Bui, R. S. Zhu and M. C. Lin, J. Chem. Phys. 117, 11188 (2002).
18. J. Shu, J. J. Lin, Y. T. Lee and X. Yang, J. Chem. Phys.115, 849 (2001).
19*. J. Park, Z. F. Xu and M. C. Lin, J. Chem. Phys., in press.

Other DOE Publications Not Cited in the Text:

1. I. V. Tokmakov and M. C. Lin, Int. J. Chem. Kinet., 33, 633 (2001).
2. J. Park and M. C. Lin, Int. J. Chem. Kinet., 33, 803 (2001).
3. R. S. Zhu and M. C. Lin, J. Phys. Chem. A., 105, 243 (2001).
4. L. V. Moskaleve and M. C. Lin,. Z. Phys. Chem., 215, 1043-54 (2001).
5. A. M. Mebel, M. C. Lin, D. Chakraborty, J. Park, S. H. Lin and Y. T. Lee, *J. Chem. Phys.* 114, 8421 (2001).
6. R. S. Zhu, C.-C. Hsu and M. C. Lin, J. Chem. Phys. 115, 195 (2001).
7. W. S. Xia, R. S. Zhu, M. C. Lin and A. M. Mebel, Faraday Discuss., 119, 191(2001).
8. L. V. Moskaleva and M. C. Lin, Proc. Combust. Inst. 29, in press.
9. J. Park, Y. M. Choi, I. V. Dyakov and M. C. Lin, J. Phys. Chem., A, 106, 2903 (2002).
10. I. V. Tokmakov, L. V. Moskaleva and M. C. Lin, J. Phys. Chem., A, 107, 1066-76 (2003).

INVESTIGATION OF POLARIZATION SPECTROSCOPY AND DEGENERATE FOUR-WAVE MIXING FOR QUANTITATIVE CONCENTRATION MEASUREMENTS

Principal Investigator: Robert P. Lucht
School of Mechanical Engineering, Purdue University, West Lafayette, IN 47907-2088
(Lucht@purdue.edu)

I. PROGRAM SCOPE

Nonlinear optical techniques such as laser-induced polarization spectroscopy (LIPS) and degenerate four-wave mixing (DFWM) are techniques that show great promise for sensitive measurements of transient gas-phase species, and diagnostic applications of these techniques are being pursued actively at laboratories throughout the world. Over the last year we have also begun to explore the use of three-laser electronic-resonance-enhanced (ERE) coherent anti-Stokes Raman scattering (CARS) as a minor species detection method with enhanced selectivity.

The objective of this research program is to develop and test strategies for quantitative concentration measurements using these nonlinear optical techniques in flames and plasmas. We are investigating the physics of these processes by direct numerical integration (DNI) of the time-dependent density matrix equations for the resonant interaction. Significantly fewer restrictive assumptions are required using this DNI approach compared with the assumptions required to obtain analytical solutions. Inclusion of the Zeeman state structure of degenerate levels has enabled us to investigate the physics of LIPS and of polarization effects in DFWM. We have incorporated the effects of hyperfine structure in our numerical calculations of LIPS signal generation. We have successfully incorporated the multi-axial-mode laser structure that is characteristic of commercial dye lasers into our LIPS calculations, although single-mode diode-laser injection-seeded optical parametric oscillator systems are under development in our laboratory. Experimental measurements are performed in well-characterized flames, gas cells, or nonreacting flows for comparison with our theoretical calculations.

II. RECENT PROGRESS

A. Laser-Induced Polarization Spectroscopy Measurements of the Hydrogen Atom

We have demonstrated a new technique for the measurement of hydrogen atom concentrations in flames over the last year. The two-color LIPS technique is illustrated in Fig. 1. A Nd:YAG pumped dye laser is used to produce 486-nm laser radiation that is frequency-doubled to produce a 243-nm laser beam. The circularly polarized 243-nm pump beam is tuned to the two-photon 1S-2S resonance of the hydrogen atom. The 243-nm pump beam produces an anisotropic Zeeman state distribution in the 2S level; this distribution is probed using a small fraction of the residual 486-nm laser radiation as a probe beam. The 486-nm beam is linearly polarized before entering the flame medium and then directed through a crossed polarization analyzer after passing through the flame medium. The probe intensity that is transmitted through the crossed polarization analyzer is the LIPS signal is directed through bandpass and neutral density filters, focused through an aperture to reduce scattered light, and is then detected using a photomultiplier tube. Resonance line shapes from near-adiabatic hydrogen-air flames stabilized on a Hencken burner are shown in Fig. 2.

We have developed a nonperturbative numerical model of the two-photon, two-color H-atom LIPS process. As depicted in Fig. 1, the hyperfine structure of H-atom is incorporated in the numerical calculations. Because of the selection rule of $\Delta M = \pm 2$ for circularly polarized light for a two-photon transition, the 1S-2S transition is not two-photon-allowed in the absence of the hyperfine effect. The development of the nonperturbative DNI code for the LIPS technique, which involves a two-photon

absorption, is a very significant accomplishment. We have started to study the effects of saturation on the two-photon process, and the effects of Doppler and collisional broadening on the line shapes in both the low laser power limit and under saturation conditions can now be investigated.

B. ERE CARS Measurements of the NO Molecule

Electronic-resonance-enhanced (ERE) coherent anti-Stokes Raman scattering (CARS) measurements of nitric oxide (NO) were performed using a three-color CARS technique. In this dual-pump technique, the second pump beam is an ultraviolet laser beam with a frequency tuned into electronic resonance with specific transitions in the NO molecule. The technique that we have demonstrated is a variant of the dual-pump CARS technique developed for the simultaneous detection of two species [1]. An energy level schematic for the technique is shown in Fig. 3. The first pump and the Stokes beam are visible laser beams with frequencies far from resonance with the $A^2\Sigma^+ - X^2\Pi$ electronic transition. The second pump beam at frequency ω_3 is at or near electronic resonance. This wide separation of the frequencies ω_1 and ω_3 of the two pump beams distinguishes our technique from previous ERE CARS experiments [2], which were performed with the same laser frequency for both pump beams, and with both the pump and Stokes beams at or near electronic resonance.

The Sandia CARS code [3] was modified for the ERE CARS calculations and the NO spectral data was obtained from the spectroscopic database code LIFBASE [4] and from previous high-resolution NO CARS measurements. The square root of the CARS intensity is plotted in Fig. 4 versus the theoretical enhancement factor. The enhancement factor is the square root of the calculated CARS intensity for the ultraviolet pump frequency divided by square root of the calculated CARS intensity for $\lambda_3 = 532$ nm. As can be seen from Fig. 4, there is good agreement between theory and experiment and we observe an enhancement factor of nearly 2500 at the peak of the $Q_1(9.5)$ line. The spectral line assignments in Fig. 4 can be understood by examination of Fig. 3. The main-branch electronic resonances, $Q_1(9.5)$, $R_1(9.5)$, and $P_1(9.5)$ will be predominant in the spectrum when the Raman Q-branch transition between the $J = 9.5 = N+0.5$ levels in the (1,0) band in the $X^2\Pi$ state is probed. The occurrence of the $Q_2(8.5)$, $R_2(8.5)$, and $P_2(8.5)$ lines in the same scan indicates that the Raman Q-branch transition between the $J = 8.5 = N-0.5$ levels in the (1,0) band occurs at nearly the same Raman shift.

We have demonstrated the detection of ERE CARS signals from NO in concentrations as low as 100 ppm. Spectral scans were obtained with fixed Stokes frequency as the ultraviolet pump frequency was varied, and with fixed ultraviolet pump frequency as the Stokes frequency was varied. Good agreement between theory and experiment was obtained for both these cases. The use of the dual-pump ERE CARS technique allows us to separate clearly the process by which the Raman coherence is induced in the medium from the ERE process where the induced coherence is probed with the second pump beam. The separation of these two processes simplifies considerably the modeling of the ERE CARS process, and may enable sensitive, selective detection of small polyatomic molecules in flames and plasmas.

III. FUTURE WORK

Our investigation of the physics of two-photon, two-color LIPS will continue. We have just begun to explore the physics of this process using our direct numerical integration (DNI) code. Using this DNI code, we can explore saturation effects and develop fundamental models of the effects of Doppler broadening and collisions on the two-photon absorption process. We plan to use the two-photon, two-color LIPS technique for measurements of the O-atom and of the C-atom, and to compare the detection limits of the LIPS technique with two-photon LIF techniques. We are also planning to perform H-atom imaging LIPS experiments in collaboration with Tom Settersten at the Combustion Research Facility using his picosecond laser system.

We plan to pursue theoretical and experimental investigations of the ERE CARS process for NO, especially at higher cell pressures where collisional narrowing may result in significant decreases in the detection limits, and for acetylene, which has electronic resonances near 226 nm. The ERE CARS signal is generated only when the frequency difference between the 532-nm pump beam and the Stokes beam is tuned to a Raman vibrational resonance, <u>and</u> when the ultraviolet pump beam is tuned to an electronic resonance. ERE CARS offers sensitivity comparable to DFWM, but with an additional degree of selectivity that may make the selective detection of small hydrocarbon species feasible in flames. The methyl radical is another candidate species for ERE CARS detection. A DNI code will be developed for the ERE CARS method; it will actually be quite similar in structure to the DNI code for the two-photon, two-color LIPS analysis.

We are also developing pulsed, tunable high-resolution laser sources based on diode-laser-seeded ring optical parametric oscillator cavities.

IV. REFERENCES

1. R. P. Lucht, *Optics Letters* **12**, 78-80 (1987).
2. T. Doerk, P. Jauernik, S. Hädrich, B. Pfelzer, and J. Uhlenbusch, *Opt. Comm.* **118**, 637-647 (1995).
3. R. E. Palmer, *The CARSFT Computer Code for Calculating Coherent Anti-Stokes Raman Spectra: User and Programmer Information*, Sandia National Laboratories Report SAND89-8206, Livermore, California, 1989.
4. J. Luque and D. R. Crosley, "LIFBASE: Database and Spectral Simulation Program (Version 1.5), SRI International Report MP 99-009 (1999).

V. BES-SUPPORTED PUBLICATIONS 2001-2003

1. J. Walewski, C. F. Kaminski, S. F. Hanna, and R. P. Lucht, "Dependence of Partially Saturated Polarization Spectroscopy Signals on Pump Intensity and Collision Rate," *Physical Review A* **64 (6)**, 3816-3827 (2001).
2. S. Roy, R. P. Lucht, and T. A. Reichardt, "Polarization Spectroscopy Using Short-Pulse Lasers: Theoretical Analysis," *Journal of Chemical Physics* **116 (2)**, 571-580 (2002).
3. S. Roy, R. P. Lucht, and A. McIlroy, "Mid-Infrared Polarization Spectroscopy of Carbon Dioxide: Experimental and Theoretical Investigation," *Applied Physics B* **75**, 875-882 (2002).
4. R. P. Lucht, S. Roy, and T. A. Reichardt, "Calculation of Radiative Transition Rates for Polarized Laser Radiation," *Progress in Energy and Combustion Science,* accepted for publication (2003).
5. S. F. Hanna, W. D. Kulatilaka, Z. Arp, T. Opatrný, M. O. Scully, J. P. Kuehner, and R. P. Lucht, "Electronic-Resonance-Enhanced (ERE) Coherent Anti-Stokes Raman Scattering (CARS) Spectroscopy of Nitric Oxide," *Applied Physics Letters,* submitted for publication (2003).
6. W. D. Kulatilaka, R. P. Lucht, S. F. Hanna, and V. R. Katta, "Two-Color, Two-Photon Laser-Induced Polarization Spectroscopy Measurements of Atomic Hydrogen in Near-Adiabatic, Atmospheric Pressure Hydrogen/Air Flames," *Combustion and Flame,* submitted for publication.

VI. GRADUATE DISSERTATIONS RESULTING FROM DOE/BES SUPPORT 2001-2003

1. Sukesh Roy, "Laser Diagnostic Investigation of Low-Pressure Diamond-Forming Flames," Ph.D. Thesis, Texas A&M University (2002), supported 50% on BES grant.
2. Sherif F. Hanna, "Investigation of Pump Polarization Effects on Polarization Spectroscopy in Atmospheric Pressure Flames," M.S. Thesis, Texas A&M University (2001).
3. Waruna D. Kulatilaka, "Investigation of Polarization Spectroscopy for Detecting the Hydrogen Atom in Flames," M.S. Thesis, Texas A&M University (2002).
Graduate Students Supported at Present Time: Waruna Kulatilaka (PhD student at Purdue University)
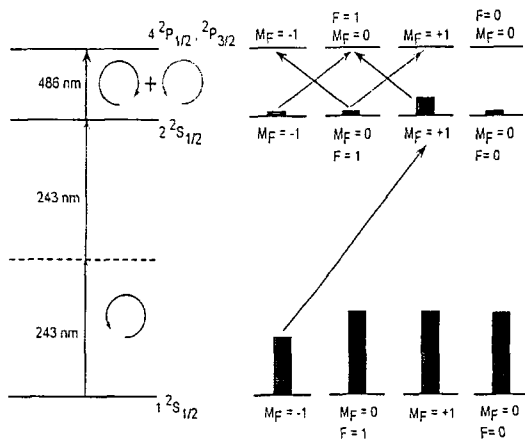
Fig. 1. Energy level schematic diagram for the two-photon, two-color LIPS measurements of the H-atom.

Fig. 3. ERE CARS energy level diagram specialized to the case where the Raman resonance frequency is tuned to the Q-branch resonances between the $J'' = 9.5$ in the $(1,0)$ Raman band.

Fig. 2. Two-photon, two-color LIPS line shapes for the H atom in near-adiabatic hydrogen/air flames.
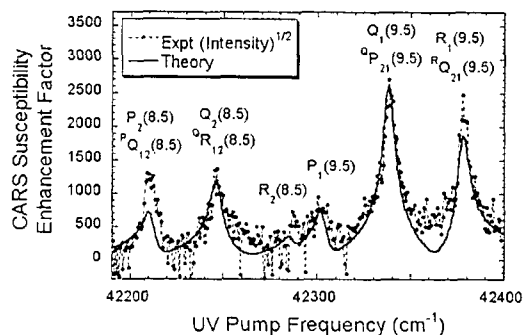
Fig. 4. ERE CARS spectra obtained by scanning the ultraviolet pump beam with the frequency difference between the 532-nm pump beam and the Stokes beam (i.e., the Raman shift) fixed at 1874.35 cm^{-1}. The NO concentration was 1000 ppm and the cell pressure was 13.1 kPa.

Time-Resolved Infrared Absorption Studies of the Dynamics of Radical Reactions

R. G. Macdonald
Chemistry Division
Argonne National Laboratory
Argonne, IL 60439
Email: macdonald@anlchm.chm.anl.gov

Background

There is very little information available about the dynamics of radical-radical reactions. These processes are important in combustion being chain termination steps as well as processes leading to new molecular species. For almost all radical-radical reactions, multiple product channels are possible, and the determination of product channels will be a central focus of this experimental effort. Two approaches will be taken to study radical-radical reactions. In the first, one of the species of interest will be produced in a microwave discharge flow system with a constant known concentration and the second by pulsed-laser photolysis of a suitable photolyte. The rate constant will be determined under pseudo-first order conditions. In the second approach, both transient species will be produced by the same photolysis laser pulse, and both followed simultaneously using two different continuous-wave laser sources. This approach allows for the direct determination of the second-order rate constant under any concentration conditions if the appropriate absorption cross sections have been measured. In both approaches, the time dependence of individual ro-vibrational states of the reactants and/or products will be followed by frequency- and time-resolved absorption spectroscopy. In order to determine branching ratios and second-order rate constants, it is necessary to measure state-specific absorption coefficients and transition moments of radicals and these measurements will play an important role in this experimental study.

Recent Results

The difficulty in studying radical-radical reactions is the necessity to know the time dependence of the absolute concentration of two transient species. In some cases, it may be possible to make measurements in environments where the concentration of one species is in great excess over the other, and its absolute concentration established. These circumstances result in pseudo-first-order conditions, and only the time dependence of the radical with the smaller concentration need be determined, not its absolute concentration. However, such conditions are difficult to generate in practice because of the reactive nature of radicals and self-radical-radical recombination.

In the current work, the above difficulty was eliminated by simultaneously monitoring the time dependence of the absolute concentration of two radical species using state-specific time-resolved absorption spectroscopy. These experiments also illustrate the utility of the time-resolved absorption technique, and the power of infrared spectroscopy to probe a variety of molecular and/or transient species at the individual ro-vibration state level of detail.

(a) $CN(^2\Sigma^+) + OH(^2\Pi)$
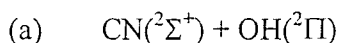
The CN radical plays an important role in the both the generation of NO_X in combustion systems arising from both the reaction of simple hydrocarbon radicals, such as CH and $^1CH_2$ with N_2 (prompt NO_X formation) and the oxidation of HCN (the fuel-fixed nitrogen mechanism for NO_X production). In both cases, the $CN(^2\Sigma^+) + OH(^2\Pi)$ reaction can have an important influence on the radical pool. Furthermore, this reaction exemplifies all of the possible features of radical-radical reactions: multiple potential energy surfaces, multiple spin manifolds and multiple product channels. In C_s geometry, there are only two electronic surfaces that correlate with the reactants in each of the singlet and triplet manifolds, i.e. $^1A'$ and $^1A''$ and $^3A'$ and $^3A''$. Neglecting stabilization products, there are five possible exothermic product channels, in increasing exothermisity:

$$
\begin{aligned}
CN\ (^2\Sigma^+) + OH(^2\Pi) \quad &\rightarrow HNC(X^1\Sigma) + O(^3P) & &1(a) \\
&\rightarrow NH(a^1\Delta) + CO(X^1\Sigma) & &1(b) \\
&\rightarrow HCN(X^1\Sigma) + O(^3P) & &1(c) \\
&\rightarrow NCO(X^2\Pi) + H(^2S) & &1(d) \\
&\rightarrow NH(X^3\Sigma^-) + CO(X^1\Sigma) & &1(e)
\end{aligned}
$$
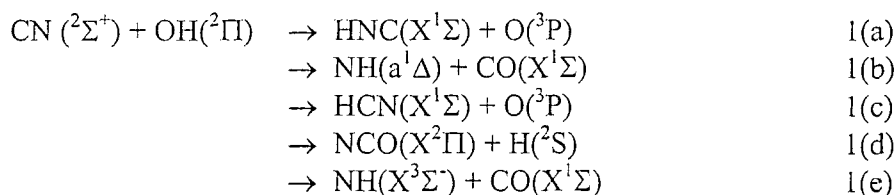
Some of these product channels involve either the singlet (1(b) and 1(d)), triplet (1(a), 1(c), 1(d)and 1(e)) or both 1(d) manifolds. There has been no previous direct measurement of the thermal rate constant or a determination of the product branching ratios.

Time-resolved absorption spectroscopy was used to monitor the reactants, CN and OH, as well as a transient species from each of the possible product channels. The CN radical was monitored in the CN "Red" system using the $CN(A^2\Pi \leftarrow X^2\Sigma)$ (2,0) band at 790 nm, while the other species OH, HNC, NH, HCN, and NCO were monitored in the infrared using a tunable infrared laser. The CN radical was generated by the excimer laser photolysis of $(CN)_2$ at 193 nm and the OH radical from the reaction of O^1D with either H_2 or H_2O. The latter source of the OH radical has several advantages: there is very little generation of HCN from the slow CN + H_2O reaction and there is much less vibrational excitation in the OH reactant. Initial radical concentrations were in the range 3×10^{12} to 2×10^{13} molecules cm.$^{-3}$ The experiments were carried out at a total pressure of 3 - 6 Torr.

Mercifully, this experiment has now been completed. The rate constant was determined by two independent methods. The first, using the integrated-profiles method and the second, based on a detailed chemical model of the system, gave essentially the same rate constant, $1.4 \pm 0.48 \times 10^{-10}$ cm^3 molecule^{-1} s^{-1} at 292 K, where the error includes both systematic and random errors. An estimate of the branching ratios has also been made. The dominant reaction pathway was found to be the NCO + O channel, accounting for $92.9 \pm 3\%$ of the reaction products. No NH($^1\Delta$) product was directly observed so its branching fraction was assumed to be zero. The other product branching ratios were found to be $4.3 \pm 1.6\%$, $2.2 \pm 2.0\%$, and $0.8 \pm 0.2\%$, for channels 1(e), 1(b) and 1(a), respectively, where the uncertainty is one standard deviation from the average. The experiments also provide an indirect measurement of the NH + OH reaction rate constant of 3.0×10^{-11} cm^3 molecules^{-1} s,$^{-1}$ with an uncertainty of about a factor of two. There has been no previous experimental measurement of this reaction rate constant.
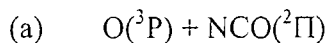
(a) $O(^3P) + NCO(^2\Pi)$

The atom-radical reaction, $O(^3P) + NCO(^2\Pi)$, has three possible reaction channels

$$O(^3P) + NCO(^2\Pi) \rightarrow N(^2D) + CO_2 \qquad\qquad 2(a)$$
$$\rightarrow N(^4S) + CO_2 \qquad\qquad 2(b)$$
$$\rightarrow NO(^2\Pi) + CO \qquad\qquad 2(c)$$
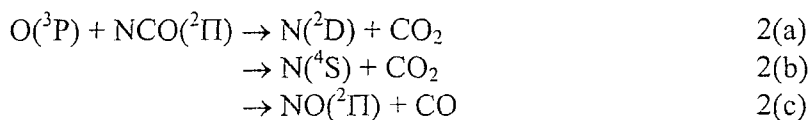
The complexity of the multiple potential energy surface nature of radical-radical interactions becomes much larger for this system as the reactants correlate, in C_s symmetry, to 3A' and 3A" electronic surfaces each in a doublet or quartet spin manifold. The likely product channel, 2(c), only correlates to ^2A' and ^2A" surfaces. Equal concentrations of [O] and [NCO] were created by the photolysis of $(CN)_2$ and the subsequent rapid reaction of $CN + O_2$ to generate O and NCO. The time dependence of the absolute [NCO] was followed using the infrared combination $(10^01) \leftarrow (00^00)$ band. To investigate three body effects, the reaction was studied with Ar and CF_4 as a bath gas over a modest pressure range of 1 – 7 Torr. The rate constant was found to be large 2.1 ± 0.76 x 10^{-10} cm^3 molecule^{-1}s^{-1} in both CF_4 and Ar bath gases, where the error estimate includes both systematic and random error. The rate constant was determined using a model to simulate the [NCO] profiles. A reaction-contribution-factor analysis showed that the O + NCO reaction accounted for over 80% removal of NCO. The measured value was found to be a factor of three larger than a recent room temperature determination. As well, the pressure dependence found in the previous work was not verified in our work.

The large rate constant for this reaction implies that both spin manifolds and almost all the electronic manifolds must participate in the reaction; thus intersystem crossing and internal conversion must play important roles in this reaction.

Future Work

The studies of reactions that are needed to describe the CN-OH model chemistry that have not been well characterized have been a continuing focus of our research effort. The completed study of the NCO + O reaction is an example. In previous work, it appeared that the NCO radical was reacting with N_2O with a rate constant of 5 x 10^{-14} cm^3 molecule^{-1}s.$^{-1}$ However, these experiments were heavily influenced by the NCO + O reaction, and another source of the NCO radical was required to verify this interpretation.

A simple flow system that delivers a small stable ClNCO flow entrained in Ar has been constructed. The unstable ClNCO molecule was produced by thermal dissociation of $(ClNCO)_3$. The photodissociation of ClNCO at 248 nm produces a NCO radical and a Cl atom with unit quantum efficiency.

Initial work has focused on the characterization of this NCO radical source. It was found that the NCO radical was removed by a rapid bimolecular reaction with the Cl atom:

$$NCO(X^2\Pi) + Cl(^2P) \rightarrow NCl(X^3\Sigma) + CO(X^1\Sigma) \qquad\qquad (3)$$
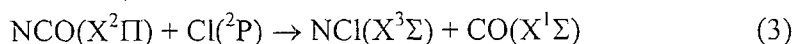
The decay of NCO was monitored by the vibrational $(101) \leftarrow (000)$ band near 3.15 microns. The vibrational transition moment for this transition has been measured in previous experiments in this laboratory. The decay of NCO was found to be purely

second-order and the resulting rate constants were independent of total pressure. Preliminary analysis indicates that the rate constant for reaction 3 is about 8.0×10^{-11} cm^3 molecules^{-1} s^{-1} at 292 K. Work will continue on this system.

The reaction between NCO and N$_2$O was investigated using the photodissociation of ClNCO to generate NCO. The Cl atom does not react with N$_2$O. An upper limit for the NCO + N$_2$O rate constant of 1×10^{-15} cm^3 molecule^{-1} s^{-1} at 292 K has been established.

The rapid reaction between NCO and Cl precludes the use of this NCO radical source for studies of NCO with species that react relatively slowly with NCO, less than 1.0×10^{-13} cm^3 molecule^{-1} s^{-1}; however, the Cl does react rapidly with many hydrocarbon species, RH, to produce HCl and a radical, R. Work has been initiated on the study the radical-radical reaction NCO + CH$_3$. There have been no previous experimental studies of the NCO radical with simple hydrocarbons.

Work will also begin on the investigation of the CH$_3$(^{2}A$_2$") + OH($^2\Pi$), radical – radical reaction. As in the CN + OH work, both species will be interrogated on the same photolysis laser pulse using different laser sources. The product branching ratio into the ^{1}CH$_2$ + H$_2$O channel will be probed using time-resolved absorption spectroscopy of ^{1}CH$_2$ using the vibronic transitions of the ^{1}CH$_2$ (b ^{1}B$_1$) ← (a ^{1}A$_2$) transition in the near infrared. The formation of other product channels will be probed using infrared vibrational spectroscopy.

Publications 2001-2003

Determination of the branching ratios for the reaction of hot H atoms with BrCN and ClCN.
-B. K. Decker, G. He, I. Tokue, and R. G. Macdonald
J. Phys. Chem. 105A, 5759-5767, (2001).

Channeling of products in the hot atom reaction: H + (CN)$_2$ → HCN/HNC + CN, and the reaction of CN with CH$_3$SH.
-B. K. Decker and R. G. Macdonald
J. Phys. Chem. 105A, 6817-6825, (2001).

Determination of the rate constant for the NCO(X$^2\Pi$) + O(^{3}P) reaction at 292 K.
-Y. Gao and R. G. Macdonald
J. Phys. Chem. 107A, (accepted) (2003).

Determination of the rate constant for the radical-radical reaction CN(X$^2\Sigma$) + OH($^2\Pi$) at 292 K.
-B. K. Decker and R. G. Macdonald
J. Phys. Chem. 107A, (submitted) (2003).

Flame Chemistry and Diagnostics

Andrew McIlroy
Combustion Research Facility
Sandia National Laboratories, MS 9051
Livermore, CA 94551-0969
Phone: (925) 294-3054
Email: amcilr@sandia.gov

Program Scope

The goal of this program is to elucidate the chemical mechanisms of combustion through a combination of experiments based on state-of-the-art diagnostics and detailed chemical kinetic modeling. The experimental program concentrates on the development and application of combustion diagnostics for the measurement of key chemical species concentrations. Although much work has been done to develop diagnostics for combustion species, many common radicals such as CH_3 and CH_2 remain challenging to study on a routine basis and many larger radicals remain difficult to detect at all. Comparison of experimental data to models employing detailed chemical kinetics allows us to determine the important chemical kinetic pathways for combustion, to test the accuracy of published models, and to develop new models. For the development and validation of chemical kinetic models, low pressure, one-dimensional laminar flames are studied. Transport issues are minimized in this configuration and well-developed models including detailed chemical kinetics, such as the Sandia PREMIX code, are available. As turbulent combustion models become increasingly sophisticated, accurate chemical kinetic mechanisms will play a larger role in computations of realistic combustion systems. Validated and well-characterized models will be required as inputs to these reactive flow codes. Only after rigorous comparisons of calculated and experimental results for a given chemical kinetic flame model over a wide range of steady conditions can these models be used with any confidence in turbulent codes.

Recent Progress

Progress has been made on the development of new diagnostic methods for probing flame chemistry and on the investigation of the chemistry of important prototype fuels. The areas of investigation will be briefly outlined followed by a more detailed discussion of selected topics. We have investigated several new optical diagnostic methods. In collaboration with David Osborn, we have developed a new expertise in noise-immune, cavity-enhanced, optical heterodyne molecular spectroscopy (NICE-OHMS), a technique that promises greater sensitivity in flames than is achievable with cavity ringdown spectroscopy (CRDS).[1] Working with Ian Kennedy of UC Davis and John Daily of the University of Colorado, Boulder, we have expanded the range of species detectable with CRDS by the first optical detection of CrO in a flame. In collaboration with Bob Lucht of Purdue University, we have demonstrated the application of polarization spectroscopy in the infrared, showing quantitative agreement between a density matrix model and the data. With Terry Cool of Cornel University, Phil Westmoreland of the University of Massachusetts, Amherst, and Musa Ahmed of the Lawrence Berkeley National Laboratory (LBL), we have constructed and made operational a new molecular beam sampling mass spectrometer (MBMS) utilizing photoionization via synchrotron radiation produced at the Chemical Dynamics Beamline of the LBL Advanced Light Source (ALS). The cooling of flame-

sampled species in low-pressure flame MBMS machines was investigated with NO resonance enhanced multiphoton ionization (REMPI) spectroscopy in a joint project with Burak Atakan and Katherina Kohse-Höinghaus of Bielefeld University.

Detailed studies of several flames are underway or have been completed. An extended study of dimethyl ether flame chemistry was complete with Jay Thoman of Williams College using laser diagnostics and photoionization MBMS using the Sandia instrument. Working with Jim Miller, we have carried out a series of experiments using 1,3-butadiene doped $H_2/O_2/Ar$ flames to investigate the role of C4 + C2 reactions in benzene ring formation. We have also begun a detailed study of a series of benzene flames with the goal of enhancing the understanding of benzene oxidation and investigating the formation of larger polyaromatic hydrocarbons (PAHs).

CrO Detection in Flames

The $B^5\Pi$-$X^5\Pi$ electronic transition of CrO was probed by CRDS in a lean ($\phi= 0.38$), low-pressure, flat, laminar $H_2/O_2/Ar$ flame seeded with $Cr(CO)_6$. The previous $B^5\Pi$-$X^5\Pi$ CrO spectrum of Hocking et al. (605.0 nm-606.5 nm) is extended from the band head located at 605.6 nm to 614.4 nm.[2] The temperature profiles of the doped and undoped flames were obtained from measurements of OH laser-induced fluorescence. Seeding the flame with $Cr(CO)_6$ increased the flame temperature by approximately 150 K.

The concentration profile of CrO was measured as a function of height above the burner. CrO absorption signals were converted to concentrations using the measured temperature profile and absorption cross section calculated from lifetimes of Hedgecock et al.[3] This calculation yielded a large cross-section of 2.07×10^{-13} cm^2 compared with the CH and OH A-X cross sections of 8×10^{-15} and 6×10^{-16} cm^2.[4] The calculated CrO cross section is unusually, and perhaps improbably, large. This result assumes the short lifetime measured by Hedgecock et al. is in fact the radiative lifetime of the state. It is possible that intersystem crossing or internal conversion, and not radiation, limits the lifetime of the upper state. In this case, the true radiative lifetime would be longer than the measured lifetime. Thus the τ reported by Hedgecock et al. should be viewed as providing an upper limit on A and σ. Using the calculated cross section, a lower limit peak CrO concentration of 1.6 ppb was found in the flame. Comparisons to calculations using STANJAN indicate that CrO is present in flames at super equilibrium concentrations.

VUV Photoionization Mass Spectrometry

Over the last several years, we have developed single photon ionization MBMS methods for low-pressure flame studies. Recently we have constructed a new MBMS at the ALS in collaboration with Cornell and the University of Massachusetts. The instrument uses Endstation 3 on the Chemical Dynamics Beamline at the ALS. The endstation utilizes a 3-m Eagle monochromator with a resolving power of 1000 and provides a photon flux of 10^{14} photon/s at this resolution. Continuously tunable light is available from 7.8 to 24 eV with the accelerator ring operating in its most common 1.9 GeV mode. Our instrument uses a time-of-flight (TOF) mass spectrometer with pulsed extraction in combination with the essentially continuous ALS beam. We employ high repetition rates (>10,000 scans/s) to maximize the collection duty cycle from our continuous beam source. The burner chamber and sampling probe geometry are identical to those used at Sandia and Cornell to facilitate comparisons between labs. The burner

chamber pressure is servo controlled to 0.1 Torr and calibrated mass flow controllers are used to deliver gas to the burner.

The instrument is configured to collect data in two modes. First the photon energy is fixed, and the burner is scanned to produce mass spectra at each burner height. This data is then reduced to produce species concentration vs. burner height profiles for comparison to models. In the second mode, the burner height is fixed and the photon energy is scanned to produce photoionization efficiency (PIE) curves. With these PIE curves we are able to identify species by photoionization threshold as well as mass. In favorable cases, we are able to identify multiple species at a single mass by observing multiple ionization thresholds at that single mass.

1,3-Butadiene Flame Studies

The formation of benzene is a rate-limiting step in soot production in flames. Recent work has established the recombination of the resonantly stabilized propargyl radical as a primary pathway for benzene formation in flames of small hydrocarbons.[5] The combustion of larger hydrocarbons opens up the possibility for benzene formation from the reaction of acetylene and butadienyl radicals. Jim Miller has initiated an effort to model these processes. In the lab, we are testing these models by examining the prototype system of 1,3-butadiene doped $H_2/O_2/Ar$ flames. The fuel 1,3-butadiene is attractive because abstraction of one hydrogen forms a butadienyl radical, thus maximizing the importance of this channel. Pure 1,3-butadiene flames soot easily and are difficult to work with. By doping into a hydrogen flame, we can form a stable flame that essentially only produces benzene. The next larger PAH, naphthalene, is a factor of ten lower in concentration. Larger species are not observed.

The destruction of 1,3-butadiene, mass 54, is observed, as is the formation of propargyl radicals, mass 39, and ultimately benzene. All of these species are identified from their photoionization thresholds. An unexpectedly large signal is observed at mass 70. This species is unambiguously identified as 2-pentene. The experiments completed to date have been done with the laser-based VUV source at Sandia. Unfortunately, the 212 nm light present from the VUV generation photolyzes the 1,3-butadiene, producing a variety of fragments. A major fragment is at mass 53 and obscures the native butadienyl signal. We are currently undertaking experiments at the ALS where we expect to be able to unambiguously detect this critical intermediate. The 212 nm light does have an advantage though; it easily ionizes naphthalenes through a 1+1 or 1+1' process with cross sections a factor of 10-100 higher than for single photon ionization. The 212 nm light is accidentally on resonance with the strong $^1B_{2u} \leftarrow {}^1A_{1g}$ transition in naphthalene and presumably similar transitions in substituted naphthalenes.[6] A second 212 nm or 425 nm photon can then be absorbed for REMPI generation of these ions.

Future Plans

Our molecular weight growth studies will include further work on 1,3-butadiene doped hydrogen flames and new studies of several benzene flames. We now have a complete initial dataset for two 1,3-butadiene doped flames. Further analysis of this data and comparisons with modeling being done by Jim Miller will almost certainly suggest additional experiments to carry out, either at Sandia or the ALS. Benzene flames are interesting for at least two reasons. Benzene is the simplest aromatic hydrocarbon and is thus the prototype for aromatic combustion. Furthermore, although the rate limiting step in PAH and soot formation is believed to be the formation of benzene, most of the molecular weight growth process happens after benzene formation. Thus, by starting with benzene, we can look at the chemistry leading to higher

molecular weight species. We have collected a limited set of data on low-pressure benzene flames and will need to extend this set before it is useful to compare to models. Measurements of temperature and OH concentration profiles are needed.

We will continue efforts to apply NICE-OHMS to combustion problems. Joakim Bood will construct a cavity compatible with our low-pressure flame chamber and investigate the best method to lock the cavity and laser together. Using a Ti:sapphire laser with <100 kHz of frequency noise, this should produce outstanding sensitivity. With our ~0.75 m cavity, we will use 99.8% reflectivity mirrors to give a cavity mode width of 130 kHz. Initial experiments will probe acetylene, NO, and O_2 using well known transitions within the Ti:Sapphire tuning range. With the success of these experiments, we plan to frequency-double the laser with an external cavity doubler in order to probe CH, C_2, and CH_2O.

We also plan to extend our work in infrared polarization spectroscopy in collaboration with Prof. Lucht of Purdue University. Our initial studies of CO_2 combination bands in both an atmospheric pressure jet and reduced pressure cells showed good agreement with current state-of–the-art models. We obtained sufficient sensitivity to encourage us to extend this work into flames. For our first studies, we will try to detect a stable species such as CO_2 or acetylene in a low-pressure flame. We plan to first look at acetylene in an acetylene low-pressure flame for simplicity and then detect acetylene as an intermediate in methane and ethylene flames.

Recent BES Publications

H. N. Najm, P. H. Paul, O. M. Knio, A. McIlroy, "A numerical and experimental investigation of premixed methane-air flame transient response," *Combustion and Flame* 125, 879 (2001).

A. McIlroy and J. B. Jeffries, "Chapter 4: Cavity ring-down spectroscopy for concentration measurements," in *Applied Combustion Diagnostic*, Eds. K. Kohse-Höinghaus and J. B. Jeffries, Taylor and Francis: London, 2002.

M. Shahu, C.-H. Yang, C. D. Pibel, A. McIlroy, C. A. Taatjes and J. B. Halpern "Vinyl radical visible spectroscopy and excited state dynamics," *Journal of Chemical Physics* 116, 1 (2002).

A. McIlroy, A. H. Steeves and J. W. Thoman, Jr. "Chemical Intermediates in Low-Pressure Dimethyl Ether/Oxygen/Argon Flames," *Combustion and Flame*, accepted.

M. Kamphus, N.-N. Liu, B. Atakan, F. Qi and A. McIlroy "REMPI Temperature measurement in molecular beams sampled from low-pressure flames," *29th International Symposium on Combustion*, in press.

S. Roy, R. P. Lucht and A. McIlroy, "Mid-Infrared Polarization Spectroscopy Of Carbon Dioxide," *Applied Optics*, in press.

Cited Refernces

[1] J. Ye, L.-S. Ma, and J. L. Hall, Journal Of The Optical Society Of America B-Optical Physics 15 (1), 6 (1998).

[2] W. H. Hocking, A. J. Merer, D. J. Milton, W. E. Jones, and G. Krishnamurty, Canadian Journal of Physics 58 (4), 516 (1980).

[3] I. M. Hedgecock, C. Naulin, and M. Costes, Journal of Molecular Spectroscopy 184 (2), 462 (1997).

[4] J. Luque and D. R. Crosley, Report No. MP 99-009, 1999.

[5] C. J. Pope, J. A. Miller, K. H. Homann, and K. Kohse-Hoinghaus, Proceedings of the Combustion Institute 28(pt.2), 1519 (2000).

[6] E. E. Koch, A. Otto, and K. Radler, Chemical Physics Letters 16, 131 (1972); M. Suto, X. Y. Wang, J. Shan, and L. C. Lee, Journal of Quantitative Spectroscopy & Radiative Transfer 48 (1), 79 (1992).

FLASH PHOTOLYSIS-SHOCK TUBE STUDIES

Joe V. Michael

Gas Phase Chemical Dynamics Group, Chemistry Division
Argonne National Laboratory, Argonne, IL 60439
e-mail: michael@anlchm.chm.anl.gov

Using shock tube techniques, the scope of the program is to measure high-temperature thermal rate constants for use in high-temperature combustion. During the past year, rate studies on four bimolecular reactions have been completed. In these studies, the atomic resonance absorption spectroscopic (ARAS) method was used for atom detection in reflected shock wave experiments.

The shock tube technique with D-atom atomic resonance absorption spectrometry (ARAS) detection was previously used to study the thermal decomposition of C_2D_5I showing that two decomposition processes occur yielding $C_2D_5 + I$ and $C_2D_4 + HI$.[1] The first pathway is most important, and the product C_2D_5 radicals instantaneously decompose to give $C_2D_4 + D$. This thermal source of D-atoms was then used to measure bimolecular rate constants for $D + CH_3 \rightarrow CH_2D + H$.[1] These experiments were similar to those already reported from this laboratory for C_2H_5I decomposition[2] and the subsequent study of the $H + NO_2$ reaction.[3] Rate constants can also be determined from measurements of H-atom product profiles. We applied this technique to measure high-temperature rate constants for two bimolecular rate constants and two rate constants involving chemically activated species.

The shock tube technique with both D- and H-atom atomic resonance absorption spectrometric (ARAS) detection has been used to measure rate constants for two isotopic modifications of the most fundamental chemical reaction, $H + H_2 \rightarrow H_2 + H$;

$$D + H_2 \rightarrow HD + H, \tag{1}$$

and,

$$H + D_2 \rightarrow HD + D. \tag{2}$$

Hydrogen atoms were produced from the thermal decomposition of either C_2D_5I or C_2H_5I. Ethyl iodide decomposition above ~1150 K is fast, and the product ethyl-radicals decompose even faster giving ethylene and hydrogen atoms. This clean source of atoms then allows for first-order analyses of both reactant and product hydrogen atoms for determining rate constants. The rate constant results can be described by the Arrhenius expressions:

$$k_1 = 3.17 \times 10^{-10} \exp(-5207 \text{ K/T}) \text{ cm}^3 \text{ molecule}^{-1} \text{s}^{-1}, \tag{3}$$

over the temperature range, 1166-2112 K, and,

$$k_2 = 2.67 \times 10^{-10} \exp(-5945 \text{ K/T}) \text{ cm}^3 \text{ molecule}^{-1} \text{s}^{-1}, \tag{4}$$

over the temperature range, 1132–2082 K.

These new results are compared to earlier results[4,5] and supply additional values for evaluating the rate behavior for both reactions over the very large temperature range, ~200-2200 K.[6-10] These evaluations are then compared to recent quantum mechanical scattering estimations of the thermal rate behavior that are based on a new and quite accurate potential energy surface (i.e., globally

accurate to ~0.01 kcal mole^{-1}).[11] As shown in Fig. 1, there is now complete convergence, within experimental error, between the experimental evaluation and the new theory,[12] bringing to completion a 75-year effort in chemical kinetics and dynamics. This is the first completely solved problem in chemical kinetics.

Similar techniques have been used to measure thermal rate constants for,

$$D + C_2H_2 \rightarrow C_2HD + H. \tag{5}$$

Values were again obtained from both reactant and product hydrogen atom measurements, and these were found to be identical within experimental error. In this case, the reaction proceeds through a vibrationally excited vinyl-radical, and the equivalence of results based on reactant and product measurements suggests that radical stabilization is negligible over the temperature and pressure ranges of the experiments. The results can be described by the linear-least-squares Arrhenius expression:

$$k = (2.77 \pm 0.45) \times 10^{-10} \exp(-3051 \pm 210 \text{ K/T}), \tag{6}$$

in units of cm^3 molecule^{-1} s^{-1}. The one standard deviation of the values from Eq. (6) is $\pm 10.7\%$. Application of RRKM theory with negligible stabilization shows that $k = k_{D\infty}<k_{f\epsilon}/(k_{f\epsilon} + k_{b\epsilon})>$ where the $k_{i\epsilon}$'s refer to RRKM evaluated specific rate constants for forward and backward dissociations, and $k_{D\infty}$ is the high-pressure limiting rate constant for D addition to acetylene. Hence, the present measurements coupled with earlier measurements and modern *ab initio* potential energy determinations allow for specification of the high-pressure limiting rate constants. The same model can then be used for the protonated reaction, $H + C_2H_2$ where a considerable ambiguity has existed for about 30 years.[13-16]

The method for obtaining high-pressure limits for chemically activated systems as shown above for $D + C_2H_2$, prompted us to carry out a similar study on the $D + C_2H_4$ reaction. As is well known, the determination of high-pressure limits for $H + C_2H_4$ has involved RRKM extrapolation of pressure dependent data, particularly at high temperature (i. e., for ethyl-radical decompostition).[17-19] With the same techniques as used for reactions (1), (2), and (5), rate constants were measured for:

$$D + C_2H_4 \rightarrow C_2H_3D + H. \tag{7}$$

Values based on both D-depletion and H-formation were determined and found to be identical within experimental error. The equivalence of these rate constants indicates that pressure stabilization is negligible for the present conditions and that $k = k_{D\infty}<k_{f\epsilon}/(k_{f\epsilon} + k_{b\epsilon})>$. Combining the two sets, the rate constants for reaction (7) can be expressed over the T-range, 1153 to 1616 K, by the Arrhenius expression,

$$k = (2.56 \pm 0.46) \times 10^{-10} \exp(-2797 \pm 239 \text{ K/T}), \tag{8}$$

in units of cm^3 molecule^{-1} s^{-1}. The one standard deviation of the points from the line in the figure is $\pm 10.4\%$. There are no previous high temperature studies of this reaction. However, there are lower temperature studies, and these, combined with the present determinations, are currently being analyzed and will subsequently be compared to theoretical results by L. B. Harding and A. F. Wagner.

Additional atom and radical with molecule reaction studies (e.g., Cl + hydrocarbons, OH + hydrocarbons, $CF_2 + O_2$, etc.) and, also, thermal decomposition investigations (e.g., C_2H_5, C_2H_3, etc.)

are in the planning stage at the present time. These reaction studies are of theoretical interest to chemical kinetics and of practical interest in hydrocarbon combustion or waste incineration.

References

1. M.-C. Su and J. V. Michael, Proc. Combust. Inst. **29**, in press.
2. S. S. Kumaran, M.-C. Su, K. P. Lim, and J. V. Michael, Proc. Combust. Inst. **26**, 605 (1996).
3. M.-C. Su, S. S. Kumaran, K. P. Lim, J. V. Michael, A. F. Wagner, L. B. Harding, and D.-C. Fang, J. Phys. Chem. A **106**, 8261 (2002).
4. J. V. Michael and J. R. Fisher, J. Phys. Chem. **94**, 3318 (1990)
5. J. V. Michael, J. Chem. Phys. **92**, 3394 (1990).
6. B. A. Ridley, W. R. Schulz, and D. J. Le Roy, J. Chem. Phys. **44**, 3344 (1966).
7. A. A. Westenberg and N. de Haas, J. Chem. Phys. **47**, 1393 (1967).
8. D. N. Mitchell and D. J. Le Roy, J. Chem. Phys. **58**, 3449 (1973).
9. W. R. Schulz and D. J. Le Roy, Can. J. Chem. **42**, 2480 (1965).
10. I. S. Jayaweera and P. D. Pacey, J. Phys. Chem. **94**, 3614 (1990).
11. S. L. Mielke, B. C. Garrett, and K. A. Peterson, J. Chem. Phys. **111**, 3806 (1999); **116**, 4142 (2002).
12. S. L. Mielke, K. A. Peterson, D. W. Schwenke, B. C. Garrett, D. G. Truhlar, J. V. Michael, M.-C. Su, and J. W. Sutherland, Phys. Rev. Lett., submitted.
13. W. A. Payne and L. J. Stief, J. Chem. Phys. **64**, 1150 (1976).
14. D. G. Keil, K. P. Lynch, J. A. Cowfer, and J. V. Michael, Int. J. Chem. Kinet. **8**, 825 (1976).
15. L. B. Harding, A. F. Wagner, J. M. Bowman, G. C. Schatz, and K. Christoffel, J. Phys. Chem. **86**, 4312 (1982).
16. V. D. Knyazev and I. R. Slagle, J. Phys. Chem. **100**, 16899 (1996).
17. J. H. Lee, J. V. Michael, W. A. Payne, and L. J. Stief, J. Chem. Phys. **68**, 1817 (1978).
18. M. A. Hanning-Lee, N. J. B. Green, M. J. Pilling, and S. H. Robertson, J. Phys. Chem. **97**, 860 (1993), and references therein.
19. Y. Feng, J. T. Niiranen, A. Bencsura, V. D. Knyazev, D. Gutman, and W. Tsang, J. Phys. Chem. **97**, 871 (1993), and references therein.

PUBLICATIONS FROM DOE SPONSORED WORK FROM 2001-2003

■ *Atomic Resonance Absorption Spectroscopy with Flash or Laser Photolysis in Shock Waves Experiments*, J. V. Michael and Assa Lifshitz, in *Handbook of Shock Waves, Vol. 3* ; G. Ben-Dor, O. Igra, T. Elperin, and A. Lifshitz, Eds., Academic Press, New York, 2001, pp. 77-105.
■ *Rate Constants for H + CH₄, CH₃ + H₂, and CH₄ Dissociation at High Temperature*, J. W. Sutherland, M.-C. Su, and J. V. Michael, Int. J. Chem. Kinet., **33**, 669 (2001).
■ *Rate Constants for H + O₂ + M -> HO₂ + M in Seven Bath Gases*, J. V. Michael, M.-C. Su, J. W. Sutherland, J. J. Carroll, and A. F. Wagner, J. Phys. Chem. A **106**, 5297 (2002).
■ *Rate Constants, 1100≤T≤2000 K, H + NO₂ -> OH + NO, Using Two Shock Tube Techniques: Comparison of Theory to Experiment*, M.-C. Su, S. S. Kumaran, K. P. Lim, J. V. Michael, A. F. Wagner, L. B. Harding, and D.-C. Fang, J. Phys. Chem. A **106**, 8261 (2002).

- *C2D5I Dissociation and D + CH3 -> CH2D + H at High Temperature: Implications to the High Pressure Rate Constant for CH4 Dissociation*, M.-C. Su and J. V. Michael, Proc. Combust. Inst., in press.
- *H + H2 Thermal Reaction: Another Solved Problem of Quantum Mechanics*, S. L. Mielke, K. A. Peterson, D. W. Schwenke, B. C. Garrett, D. G. Truhlar, J. V. Michael, M.-C. Su, and J. W. Sutherland, Phys. Rev. Lett., submitted.
- *New Rate Constants for D + H2 and H + D2 between ~1150 and 2100 K*, J. V. Michael, M.-C. Su, and J. W. Sutherland, J. Phys. Chem. A, submitted.
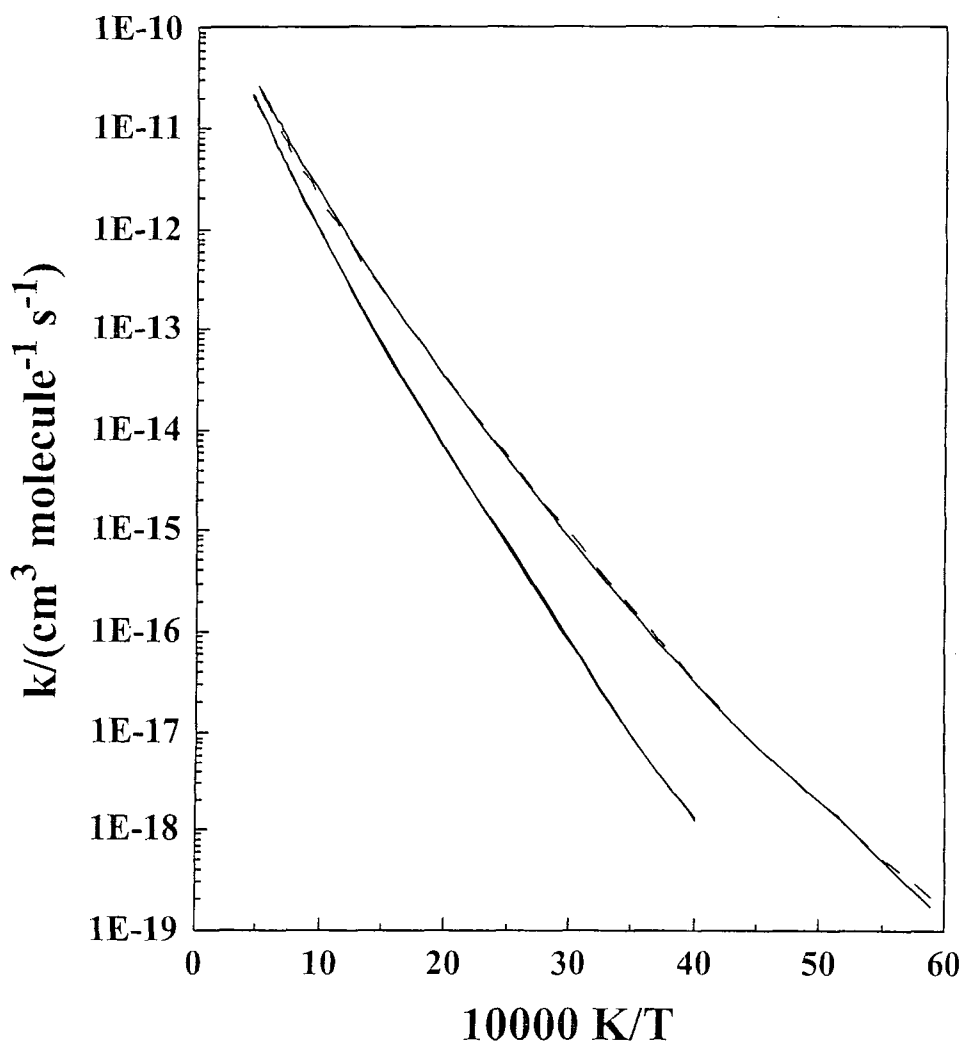
Figure. 1. Arrhenius plots of experimental evaluations, ——————, and theoretical calculations, — — — —, for the D + H2 (Top) and H + D2 (Bottom) reactions.

Particle Diagnostics Development

H. A. Michelsen

Sandia National Labs, MS 9055, P. O. Box 969, Livermore, CA 94551

hamiche@ca.sandia.gov

1. Program Scope

Growing concerns about adverse health, economic, and environmental effects of small particles have prompted intensified research on the formation and impact of combustion-generated particles. Studies of particle formation, however, are hindered by a lack of sensitive, accurate, noninvasive measurements of particle physical characteristics. Our research program focuses on the development of optical diagnostics for particles, primarily soot particles, in combustion environments. The goal of this work is in situ measurements of volume fraction, size, and morphology of such particles with fast time response and high sensitivity. Combustion-generated soot particles consist of small (5-50 nm diameter) carbon spheroids held firmly together at points of contact to form fractal-like, branched-chain aggregates. Small primary particle sizes and non-spherical aggregate shapes complicate optical schemes for measuring sizes and volume fractions of air-borne particles. Over the past year our research has been aimed at assessing the applicability of laser-induced incandescence (LII) for quantitative volume fraction measurements. This work involves experimental measurements of LII from soot produced in flames combined with the development of a comprehensive model of the response of soot particles to laser irradiation over a wide range of laser fluences.

2. Recent Progress

The particle diagnostics research program combines experimental and modeling studies to develop an accurate description of LII. During this past year we have focused on constructing and refining a model that accounts for particle heating by laser absorption, oxidation, and annealing and cooling by sublimation, conduction, and radiation, includes convective and diffusive heat and mass transfer processes, and incorporates mechanisms for phase changes. Recently published experimental data were used to determine the temperature dependence of important parameters included in the model. The most substantial advances in this model over previous models are the inclusion of (1) temperature-dependent thermodynamic parameters for calculating sublimation, conduction, and internal energy storage, (2) wavelength-dependent optical parameters to describe absorption and emission, (3) the introduction of a nonthermal mechanism for evaporative heat and mass loss, (4) the influence of annealing on absorption, emission, and sublimation, and (5) a thermal accommodation coefficient more appropriate for high-temperature conductive cooling. Our goal is to test the model under a wide range of conditions and refine it to the point that it can be used for quantitative analysis of LII signals in a variety of combustion environments.

In our LII experiments the particles are heated with pulses of ~7 ns duration (10 Hz) at 532 nm from an injection-seeded Nd:YAG laser. An aperture is placed in the laser beam and imaged into the flame to provide a homogeneous spatial profile. Since LII is extremely nonlinear with laser fluence, a homogeneous beam profile is critical for interpreting the results. The signal is imaged onto a fast Si photodiode and collected between 570 and 1100 nm. We have collected data to fluences as high as 1 J/cm^2 with a temporal resolution of 0.3 ns. We have varied the fuel, burner dimensions, and flow rates to test the sensitivity of the technique to different conditions.

Comparison of the model with these experimental data has provided valuable insight into the sensitivity of LII signals to measurement conditions and has highlighted uncertainties in the model that result from a lack of understanding of the microphysical mechanisms involved in the LII process. In general the model reproduces the steep rise in LII signal as the particles heat and the decay as the particles cool. At fluences below ~0.2 J/cm^2, temperatures increase rapidly during the laser pulse and slowly decay (on microsecond timescales) following the laser pulse. This slow decay is

predominantly attributable to conductive cooling. At higher fluences particles quickly reach and surpass the sublimation temperature of ~4000 K, becoming superheated, and then cool via sublimation back to the sublimation point. Sublimation also causes particles to decrease in size at these higher fluences, whereas at lower temperatures particles swell slightly with increasing temperature as density decreases.

The microstructure of mature soot is similar to polycrystalline graphite. Soot primary particles have been shown to anneal at temperatures above ~2500 K into multi-shell carbon onions.[1,2] These nested fullerene structures can also form during laser heating.[3] Furthermore, graphite surfaces have been shown to melt at atmospheric pressure when heated rapidly with a laser.[4-7] Changes in the phase of soot primary particles via annealing and melting are likely to influence heating and cooling rates because of differences in physical properties, such as (1) the index of refraction, which controls rates of light absorption and emission, (2) enthalpies and entropies of formation of carbon clusters, which control sublimation rates, and (3) thermal accommodation coefficients, which determine the rate of heat conduction to the ambient atmosphere. Soot annealing rates have not been measured under the conditions encountered during laser heating on nanosecond timescales and are inferred from annealing rates measured on graphite at lower temperatures on longer timescales. At low fluences (temperatures), annealing is associated with di-interstitial migration parallel to the graphite crystallite basal plane and recombination with stationary vacancies.[8] At higher fluences, the shapes and magnitudes of the temporal profiles are strongly influenced by high-temperature annealing processes associated with interstitial and vacancy formation and migration. Model results suggest that rates of these high-temperature processes are consistent with formation of 5- and 7-member ring defects in the flat hexagonal structure of the graphite crystallites, producing curved fullerene precursors. Our results also indicate that the enthalpy of annealing is much less than that measured during annealing of graphite damaged by high-energy neutron or electron radiation.

Understanding absorption and emission rates is crucial to the analysis of LII signals. Furthermore, as particles anneal, their emissivity and absorptivity are estimated to decrease, leading to a decrease in LII signal. There are large uncertainties associated with the wavelength-, temperature-, composition-, and phase-dependence of the optical properties of soot, however, which lead to substantial uncertainties in interpreting LII measurements. Larger uncertainties are associated with the emissivity of the annealed particles. We have successfully generated significant quantities of carbon onions in order to measure the optical properties of the annealed particles. The carbon onions were produced by generating an arc between carbon electrodes submerged in deionized water.[9] The carbon onions were then collected from the surface of the water.

The model descriptions of cooling and mass loss by sublimation and photodissociation are the most important terms for calculating the temporal behavior and magnitude of the LII signal at fluences above 0.1 J/cm^2. This part of the model is also the most complex and, in the case of photodissociation, the most uncertain. Although previous studies have suggested that laser photodesorption of carbon clusters from graphite can proceed by a nonthermal mechanism,[10] the nature of this mechanism, including the number of photons required, is not known. Our model includes such a mechanism with a cross section and enthalpy of reaction approximated by comparing the results with the data. Including the nonthermal photolysis term allows the model to reproduce the fast decay in the temporal profile during the laser pulse at high fluences and the lack of fluence dependence of the peak signal at fluences above 0.1 J/cm^2.

At fluences greater than 0.1 J/cm^2, laser heating of the particles is audible, indicating that the velocity of the sublimed clusters exceeds the speed of sound. Supersonic expansion of desorbed carbon clusters has been observed following laser heating of graphite. The model predicts that supersonic expansion of carbon clusters leaving the surface should occur at 0.12 J/cm^2. This prediction is based on inclusion of the convective transport term. Inclusion of this term, however, has little effect on calculated LII signals.

Future work, described below, will include performing experiments under widely varying conditions to test our understanding of LII. We will also perform experiments to narrow some of the uncertainties associated with our description of the response of particles to laser irradiation.

3. Future plans

1. We are currently using a laser with a pulse duration of ~7 nanoseconds. We will further test our understanding of the high temperature physics and chemistry of soot particles by using a laser with a significantly shorter pulse duration (115 picoseconds) and fast detector (streak camera). This set of experiments will allow us to isolate mechanisms that take place on short timescales (e.g., absorption, nonthermal photolytic desorption) from processes that are predicted to evolve over longer (nanosecond) timescales (e.g., thermal sublimation, annealing).

2. We are currently heating the soot with a visible laser beam (532 nm). Future experiments will use longer wavelengths to heat the particles. Heating the particles with redder light will give us more information about the wavelength response of the nonthermal sublimation component. Our data are consistent with a mechanism that requires at least two photons at 532 nm and is likely to require more photons at longer wavelengths. Switching to longer pump wavelengths will also allow us to avoid interferences from laser-induced fluorescence of polycyclic aromatic hydrocarbons.

3. We have generated carbon onions (30-40 nm) with an arc discharge between carbon electrodes submerged in deionized water. These particles will be used to study the optical properties of the annealed soot. High resolution transmission electron micrographs of the carbon onions generated show some contamination by larger carbon particles (250-750 nm). We will develop a method to purify the carbon onion samples, possible using centrifuge techniques.

4. In the experiments described above we collected broadband LII signal. We are setting up an experiment using a spectrometer with a gatable array detector, which will allow us to record time-resolved emission spectra during and after the laser pulse. Temperatures will be inferred from these spectra using the Planck function with a gray-body assumption and compared with model-predicted temperatures.

5. We have built a soot source that extracts soot from a flame and cools it before it is heated with the laser. A Scanning Mobility Particle Sizer (SMPS) is attached to the source for measuring aggregate size distributions. We will use the new source to investigate the sensitivity of the LII temporal profiles to the initial and ambient temperatures and aggregate size.

6. If LII proves to be applicable over a wide range of combustion conditions, this work will be extended to include investigations of the utility of combining LII with other optical techniques, such as laser-light scattering (LLS) in which light elastically scattered from the sample is measured at one or more angles and multipass extinction.

4. References

1. Bacsa, W. S.; de Heer, W. A.; Ugarte, D.; Châtelain, A. *Chem. Phys. Lett.* **1993**, *211*, 346.
2. de Heer, W. A.; Ugarte, D. *Chem. Phys. Lett.* **1993**, *207*, 480.
3. Vander Wal, R. L.; Ticich, T. M.; Stephens, A. B. *Appl. Phys. B* **1998**, *67*, 115.
4. Venkatesan, T.; Jacobson, D. C.; Gibson, J. M.; Elman, B. S.; Braunstein, G.; Dresselhaus, M. S.; Dresselhaus, G. *Phys. Rev. Lett.* **1984**, *53*, 360.
5. Heremans, J.; Olk, C. H.; Eesley, G. L.; Steinbeck, J.; Dresselhaus, G. *Phys. Rev. Lett.* **1988**, *60*, 452.
6. Malvezzi, A. M.; Bloembergen, N.; Huang, C. Y. *Phys. Rev. Lett.* **1986**, *57*, 146.
7. Reitze, D. H.; Wang, X.; Ahn, H.; Downer, M. C. *Physical Review B* **1989**, *40*, 11.
8. Banhart, F.; Füller, T.; Redlich, P.; Ajayan, P. M. *Chem. Phys. Lett.* **1997**, *269*, 349.
9. Sano, N.; Wang, H; Chhowalla, M.; Alexandrou, I.; Amaratunga, G. A. J. *Nature* **2001**, *414*, 506.
10. Krajnovich, D. J. *J. Chem. Phys.* **1995**, *102*, 726.

5. BES peer-reviewed publications

P. O. Witze, S. Hochgreb, D. Kayes, H. A. Michelsen, and C. R. Shaddix, "Time-resolved laser-induced incandescence and laser elastic scattering measurements in a propane diffusion flame", *Appl. Opt.* **40**, 2443-2452 (2001).

H. A. Michelsen, "The reaction of Cl with CH_4: A connection between kinetics and dynamics", *Acc. Chem. Res.* **34**, 331-337 (2001).

H. A. Michelsen, "Carbon and hydrogen kinetic isotope effects for the reaction of Cl with CH_4: Consolidating chemical kinetics and molecular dynamics measurements", *J. Geophys. Res.* **106**, 12,267-12,274 (2001).

H. A. Michelsen and W. R. Simpson, "Relating state-dependent cross sections to non-Arrhenius behavior for the $Cl+CH_4$ reaction", *J. Phys. Chem. A* **105**, 1476-1488 (2001).

H. A. Michelsen, "Understanding and predicting the temporal response of laser-induced incandescence from carbonaceous particles", *J. Chem. Phys.* **118**, in press (2003).

Chemical Kinetics and Combustion Modeling

James A. Miller

Combustion Research Facility
Sandia National Laboratories
Livermore, CA 94551-0969
Email: jamille@sandia.gov

Program Scope

The goal of this project is to gain qualitative insight into how pollutants are formed in combustion systems and to develop quantitative mathematical models to predict their formation and destruction rates. The approach is an integrated one, combining theory, modeling, and collaboration with experimentalists to gain as clear a picture as possible of the processes in question. My efforts and those of my collaborators are focused on problems involved with the nitrogen chemistry of combustion systems and the formation of soot and PAH in flames, as well as on general problems in hydrocarbon combustion. Current emphasis is on determining phenomenological rate coefficients from the time-dependent, multiple-well master equation for reactions involved in the pre-cyclization and cyclization chemistry of flames burning aliphatic fuels.

Recent Results

From the Multiple-Well Master Equation to Phenomenological Rate Coefficients: Reactions Occurring on a C$_3$H$_4$ Potential Energy Surface (with Stephen Klippenstein).

We have spent most of the last year developing and applying robust, systematic procedures for extracting phenomenological rate coefficients from solutions to the time-dependent, multiple-well master equation. Such an equation can be written in the deceptively simple matrix form

$$\frac{d|w\rangle}{dt} = G|w\rangle, \tag{1}$$

where G is the transition matrix. The solution to Eq. (1) can be written as

$$|w(t)\rangle = \hat{T}|w(0)\rangle, \tag{2}$$

where $\hat{T}$ is the time evolution operator, $\hat{T} = \sum_{j=0}^{N} e^{\lambda_j t} |g_j\rangle\langle g_j|$, and can be constructed from the eigenvalues and eigenvectors of G, $G|g_j\rangle = \lambda_j |g_j\rangle$. Of course, having the solution (2) does not help us very much; what we really want is phenomenological rate coefficients, k(T,p), to use in flame models.

In accomplishing this objective the first point to realize is that, although G will likely have several thousand eigenpairs, only a small number,

$$N_{chem} = S-1,$$ (3)

where S is the number of chemical configurations in the problem (wells plus sets of bimolecular fragments), describe chemical change. The remainder relax much faster than these CSE's (chemically significant eigenpairs) and describe internal energy relaxation. At the same time, there are

$$N_k = \frac{S(S-1)}{2}$$ (4)

"forward" rate coefficients (and all equal number of reverse rate coefficients) embedded in the CSE's.

We have derived 2 different methods of obtaining the rate coefficients from the CSE's. The first (and simplest) is to apply $\hat{T}$ to multiple initial conditions and take the limit as $t \to 0$. In this case, one obtains

$$k_{Ti} = \sum_{j=1}^{N_{chem}} \lambda_j \Delta X_{ij}^{(i)}$$

(5)

and

$$k_{i\ell} = -\sum_{j=1}^{N_{chem}} \lambda_j \Delta X_{\ell j}^{(i)}$$

where k_{Ti} is the total rate coefficient for removal of "species" i, and $k_{i\ell}$ is the $i \to \ell$ rate coefficient. In Eq. 5 ΔX_{ij} is the change in population of the ith configuration (or species) brought about by the jth eigenpair; the superscript i indicates that species i is the initial reactant.

The second method exploits the fact that the time evolution of the chemical system, regardless of the initial condition, is equivalent to the solution of a system of rate equations with the rate coefficients,

$$k_{Ti} = -\sum_{j=0}^{N_{chem}} \lambda_j \, a_{ij} \, b_{ji}$$

(6)

and

$$k_{i\ell} = \sum_{j=0}^{N_{chem}} \lambda_j \, a_{\ell j} \, b_{ji}$$

where $a_{ij} = -\Delta X_{ij} (j \neq 0)$ and $a_{i0} = X_i(\infty)$, the population at $t = \infty$. If the a_{ij} are considered to be the elements of a matrix A, the b_{ij} are the elements of $B = A^{-1}$. The 2 different methods, as expected, give the same results for the rate coefficients.

The power of the methodology is illustrated well by applying it to reactions occurring on the C_3H_4 potential. I will note 2 points specifically:

1. The formalism allows one to distinguish *unambiguously* between the one-step process allene $\rightleftarrows$ propyne and the two-step process allene $\rightleftarrows$ cyclopropene $\rightleftarrows$ propyne even through both processes follow the same reaction path on the potential.

2. It also allows one to distinguish between the dissociations of allene and propyne to propargyl + H, even though the allene $\rightleftarrows$ propyne isomerization equilibrates much faster than either dissociation. In fact, most experiments are sensitive only to the eigenvalue of G that describes the dissociation of the equilibrated isomers (allene, propyne, and cyclopropene).

The Recombination of Propargyl Radicals and Other Reactions on a C_6H_6 Potential
(with Stephen Klippenstein).

Using a combination of electronic-structure methods, we have explored in some detail the regions of the C_6H_6 potential that are important for describing the recombination of propargyl (C_3H_3) radicals. Using this information in an RRKM-based master equation and the methods described above, we have been able to predict rate coefficients for a variety of elementary reactions, including the $C_3H_3 + C_3H_3$ recombination itself. Generally, the agreement between the theory and the limited amount of experimental information available is very good, although some discrepancies remain. The most important new feature of the present analysis (over our previous one) is the inclusion of a path on the potential that connects 1,2,4,5-hexatetraene to 1,3-hexadiene-5-yne and then goes on to benzene and phenyl + H without passing through fulvene. The inclusion of this path in the analysis allows a number of experimental observations to be accounted for by the theory. Most importantly, we are now able to predict the results of Stein's experiments on the pyrolysis of 1,5-hexadiyne (Proc. Combust. Inst. 23, 85-90 (1990)). In these experiments fulvene and benzene are formed *simultaneously* as products between 700K and 800K. Calculations using the older Miller-Melius potential, on which fulvene and benzene are located sequentially along the reaction path, show only fulvene formed in this temperature range, with benzene appearing as a product only for T >1000K. The inclusion of the new path also allows us to predict that 1,3-hexadiene-5-yne is a significant product for T $\approx$ 650K and p = 2-5 Torr, in agreement with the experiments of Alkemade and Homann (Z. Physik. Chemie Neue Folge 161, 19-34 (1989)). This product is energetically inaccessible on the Miller-Melius potential. From the results of the master-equation calculations, we have proposed a simple, contracted model for describing the rate coefficient and product distribution of the $C_3H_3 + C_3H_3$ recombination reaction (and subsequent isomerizations) for use in flame modeling.

Future Directions
Our work in the next year will focus on applying the methods discussed above to a number of reactions implicated in forming the "first ring" in flames of aliphatic fuels. Candidate reactions include n-C_4H_3 + C_2H_2, n-C_4H_5 + C_2H_2, i-C_4H_5 + C_2H_2, i-C_5H_3 + CH_3, and C_3H_3 + CH_3 $\rightarrow$ c-C_5H_5. We shall also collaborate with the CRF flame lab in modeling their experimental results on $H_2/O_2/Ar$ – C_4H_6 flames. Particular issues concerning the nitrogen chemistry of combustion will continue to be of interest, especially those that impact the modeling of NO_x control techniques such as Thermal De-NO_x, RAPRENO$_x$, and reburning.

Publications of James A. Miller
2001 to Present

- J.A. Miller and S.J. Klippenstein, "Propargyl Recombination and Other Reactions on a C_6H_6 Potential", *J. Phys. Chem. A*, submitted (2003).

- J.A. Miller, S.J. Klippenstein, and P. Glarborg, "A Kinetic Issue in Reburning: The Fate of HCNO", *Combustion and Flame*, submitted (2003).

- J.A. Miller and S.J. Klippenstein, "From the Multiple-Well Master Equation to Phenomenological Rate Coefficients: Reactions Occurring on a C_3H_4 Potential Energy Surface," *J. Phys. Chem. A.*, in press (2003).

- S.J. Klippenstein and J.A. Miller, "From the Time-Dependent, Multiple-Well Master Equation to Phenomenological Rate Coefficients" *J. Phys. Chem. A* **106**, 9267-9277 (2002).

- J.D. DeSain, J.A. Miller, S.J. Klippenstein, and C.A. Taatjes, "Measurements and Modeling of OH Formation in Ethyl + O_2 and Propyl + O_2 Reactions", *J. Phys. Chem. A*, submitted (2003).

- S.J. Klippenstein, J.A. Miller, and L.B. Harding, "Resolving the Mystery of Prompt CO_2: The HCCO + O_2 Reaction," *Proceedings of the Combustion Institute* **29**, in press (2002).

- J.A. Miller, S.J. Klippenstein, and C. Raffy "Solution of Some One- and Two-Dimensional Master Equation Models for Thermal Dissociation: The Dissociation of Methane in the Low-Pressure Limit", *J. Phys. Chem. A* **106**, 4904-4913 (2002).

- J.A. Miller "Concluding Remarks", *Faraday Discussions of the Royal Society of Chemistry* **119**, 461-475 (2001).

- J.A. Miller and S.J. Klippenstein, "The Recombination of Propargyl Radicals: Solving the Master Equation," *J. Phys. Chem. A* **105**, 7254-7266 (2001).

- J.A. Miller and S.J. Klippenstein, "The Reaction Between Ethyl and Molecular Oxygen II: Further Analysis," *International Journal of Chemical Kinetics* **33**, 654-668 (2001).

- D.K. Hahn, S.J. Klippenstein, and J.A. Miller, "A Theoretical Analysis of the Reaction Between Propargyl and Molecular Oxygen," *Faraday Discussions of the Royal Society of Chemistry* **119**, 79-100 (2001).

- D.-C. Fang, L.B. Harding, S.J. Klippenstein, and J.A. Miller, "A Direct Transition State Theory Analysis of the Branching in NH_2 + NO," *Faraday Discussions of the Royal Society of Chemistry* **119**, 207-222 (2001).

- J.D. DeSain, C.A. Taatjes, D.K. Hahn, J.A. Miller, and S.J. Klippenstein, "Infrared Frequency-Modulation Probing of Product Formation in Alkyl + O_2 Reactions: IV. Reactions of Propyl and Butyl Radicals with O_2 between 295 and 750K" *Faraday Discussions of the Royal Society of Chemistry* **119**, 101-120 (2001).

Detection and Characterization of Free Radicals Relevant to Combustion Processes

Terry A. Miller
Laser Spectroscopy Facility, Department of Chemistry
The Ohio State University, Columbus OH 43210, email: tamiller+@osu.edu

1 Program Scope

The chemistry of combustion is well-known to be extremely complex. Modern computer codes are now available that employ hundreds of reaction steps and a comparable number of chemical intermediates. Nonetheless the predictions of such models can be no better than the fundamental dynamics and mechanistic data that are their inputs. Spectroscopic identifications and diagnostics for the chemical intermediates in the reaction mechanisms constitute an important experimental verification of the models.

One of our principal aims has been to obtain and analyze the electronic spectra of radicals involved in the oxidation of hydrocarbons, of which some of the most important are the alkoxy, RO·, and the peroxy, RO_2·, radicals. Once the spectra have been identified and analyzed, we can use them to probe the fundamental dynamics of radical intermediates.

Figure 1: Plot of the $\tilde{B} - \tilde{X}$ origin frequency of the various alkoxy radicals, $C_nH_{2n+1}O$, vs number of carbon atoms, n. The different structural isomers, 1, 2, 3, and t, clearly fall on different curves.

2 Recent Progress

Figure 2: Survey LIF spectrum of a) 1-butoxy, and b) 1-pentoxy. Labelled bands have been rotationally analyzed.

During the past year we have spent most of our time studying the alkoxy radicals and so this report will concentrate on those species. A while ago, we observed for the first time the laser induced fluorescence (LIF) of a number of alkoxy radicals, $C_nH_{2n+1}O$ ($n \leq$ 12) in a supersonic free jet expansion. The larger alkoxy radicals exhibit a great deal more structural complexity than the smallest members of this family, methoxy and ethoxy. In the larger family members multiple structural isomers are present. Fig. 1 shows how the origin frequencies of the LIF spectra clearly fall into subsets based upon primary, secondary, or tertiary substitution, and how even different secondary isomers

can be distinguished. In short this plot provides the basis for an isomer specific spectral identification.

Of course these spectra have more structure than just an origin band. Fig. 2 shows this clearly for the spectra of 1-butoxy and 1-pentoxy. Initially it was believed that the higher energy bands corresponded to excited state vibrational structure in the observed $\tilde{B} - \tilde{X}$ electronic transitions. However efforts to assign these bands to vibrational transitions largely failed. Fig. 3 shows why this is the case. The rotational structure of the labelled bands in the butoxy spectrum of Fig. 2 clearly falls into three distinct groups (A), (B, D, F), and (C and E), which are very different.

The detailed rotational analyses of these spectra is beyond the scope of this report. However the results of these analyses and the subsequent comparison of the resulting spectroscopic parameters (rotational and spin-rotation constants) with quantum chemistry calculations establishes unambiguously that these three groups of lines belong to different conformers of 1-butoxy, with similar conclusions having been reached for the LIF spectra of the other observed $C_nH_{2n+1}O$ radicals.

For 1-butoxy, there are 5 possible conformers, G_1T_2, T_1T_2, T_1G_2, G_1G_2, and $G_1'G_2$, where T and G denote *trans* and *gauche* conformations respectively. The subscripts designate the orientation 1) with respect to the O-C_1-C_2 and C_1-C_2-C_3 planes and (2) with respect to the C_1-C_2-C_3 and C_2-C_3-C_4 planes. Unprimed G and primed G correspond to *gauche* clockwise and counterclockwise rotation respectively.
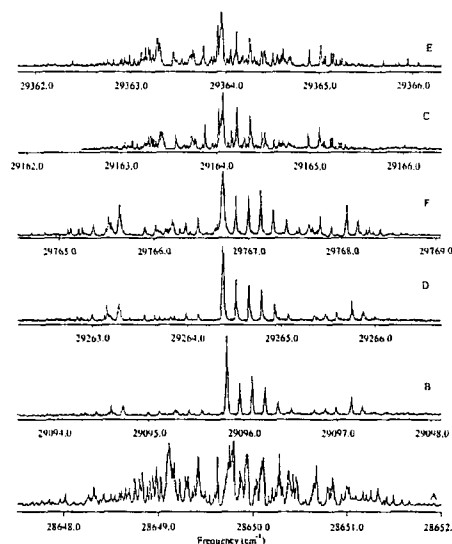
Figure 3: Rotationally resolved spectra of bands A through F in 1-butoxy. Transition (B, D, F) correspond to the T_1T_2 conformer while transition (C, E) are from the T_1G_2 and transition (A) from the G_1T_2 conformers respectively.

Figure 4: Plot of the measured $\tilde{B}$ state lifetimes, $\tau_{v'}$ of the various alkoxy radicals, normalized by the lifetime, τ_0 – taken to be 2.57 μsec, of the vibrationless level of methoxy, vs. excess vibrational energy (above the vibrationless level) in the CO stretch in the species. The v=0 and v=4 CO stretch levels are indicated. Dashed lines indicate that the LIF of the next CO stretch was unobserved implying a $(\tau_{v'}/\tau_0) \lesssim 0.05$.

Of these 5 possible conformers, the spectra of three have been identified with the correlation between the spectral lines and the conformations given in the caption to Fig. 3. It may be interesting to note that the two unidentified conformers, G_1G_2 and $G_1'G_2$, both have cyclic structures, more or less reminiscent of the expected transition state structure for the isomerization of the 1-butoxy to the butyl hydroxy radical.

Once transitions have been identified that are isomer and conformer specific, these lines can be used to follow various dynamical processes in exquisite detail. We have pursued this approach in a couple of different ways. In one case we have measured the lifetime of the excited state and found it to be quite dependent upon several factors: 1) degree of vibrational excitation, 2) isomer, and 3) conformer of a given radical. Fig. 4 is a plot for the smallest alkoxy radicals (CH_3O, C_2H_5O, and C_3H_7O) of the $\tilde{B}$ state lifetime, normalized by its value in the vibrationless level of CH_3O, as a function of excess vibrational energy above the vibrationless level of the $\tilde{B}$ state.

Interestingly Fig. 4 does not show great variation in lifetime for different radical species in the vibrationless level, but it does show some striking dependence on other parameters. The dramatic decrease in lifetime

for v $\approx$ 7 of the CO stretch in methoxy has long been attributed to the onset of a predissociation of the $\tilde{B}$ state by a repulsive level. Because of a lowering of the $\tilde{B}$ state vibrationless level, it is unlikely that the lifetime decreases for any of the other species shown in Fig. 4 can be similarly attributed to predissociation, although we expect that in all cases it does arise from the onset of a non-radiative decay channel.

We note a rather remarkable difference between the decay behavior of the 1-propoxy and 2-propoxy radicals. As Fig. 4 shows for 2-propoxy the CO stretch progression extends through v = 6, which has over 3000 cm^{-1} of excess vibrational energy. However for both T and G conformers of 1-propoxy, there is no longer any LIF signal above v = 1 of the CO stretch indicating the molecule effectively decays by non-radiative processes whenever it possesses greater than $\approx$700 cm^{-1} of excess vibrational energy. Furthermore while the lifetimes of the vibrationaless level of the T and G conformers of 1-propoxy are within $\approx$15%, the lifetimes of their v = 1 stretch levels differ by a factor of $\approx$6. Thus we see that the decay dynamics of the $\tilde{B}$ state of the propoxy radical is strongly isomer and conformer dependent. Similar observations have been made for the structural isomers and conformers of butoxy and pentoxy.

Another experiment that illustrates the different behavior of conformers is illus-

Figure 5: Dispersed fluorescence spectra of three conformers of 1-butoxy, exciting each at its origin. The CO stretch (ν_{24}) progression is indicated.

trated by the dispersed fluorescence spectra, shown in Fig. 5 for the three observed conformers of 1-butoxy. The T_1T_2 conformer with C_s symmetry alone shows a strong line at 290 cm^{-1} above the vibrationless level. We tentatively attribute this to the origin of the $\tilde{A}$ $^2A''$ state. Interestingly for both the T_1T_2 and T_1G_2 conformer, complex mostly unresolved structure is observed approximately 300 cm^{-1} above each member of the CO stretch (ν_{24}) progression. Such structure is either absent or significantly reduced in the G_1G_2 conformer.

3   Future Plans

The assignment of isomer and conformer specific LIF transitions for the larger alkoxy radicals has opened a number of avenues for research. However much more needs to be done to fully characterize the spectroscopy and dynamics of these radicals. For example, while we have spectra for the 2- and t-isomers, no detailed analysis or conformer assignment has yet been performed.

We have recently extended our LIF studies of linear, jet-cooled, alkoxy radicals to cyclohexoxy. It is expected that we will be able to uniquely assign spectral transitions to different conformers; however now the possible conformations likely involve chair and boat forms with an axial or equatorial oxygen.

List of Publications

[1] "Rotationally Resolved Electronic Spectra of the $\tilde{B} - \tilde{X}$ Transition in Multiple Conformers of 1-Butoxy and 1-Pentoxy Radicals," S. Gopalakrishnan, L. Zu, and T. A. Miller, *J. Phys. Chem. A* (submitted).

[2] "Theoretical Prediction of Spectroscopic Constants of 1-Alkoxy Radicals," G. Tarczay, S. Gopalakrishnan, and T. A. Miller, *J. Mol. Spectros.* (submitted).

[3] "Natural Lifetimes of Selected Vibronic Levels of the $\tilde{B}$ State of Alkoxy," S. Gopalakrishnan, L. Zu, and T. A. Miller, *in preparation.*

[4] "Jet-Cooled LIF Spectra of Cyclohexoxy Radical," L. Zu, J. Liu, and T. A. Miller, *in preparation.*

[5] "Dispersed Fluorescence Spectra of 1-Propoxy and 1-Butoxy," J. Jin, A. Bezant, S. Gopalakrishnan, and T. A. Miller, *in preparation.*

Reaction Dynamics in Polyatomic Molecular Systems

William H. Miller

Department of Chemistry, University of California, and
Chemical Sciences Division, Lawrence Berkeley National Laboratory
Berkeley, California 94720-1460
miller@cchem.berkeley.edu

Program Scope or Definition

The goal of this program is the development of theoretical methods and models for describing the dynamics of chemical reactions, with specific interest for application to polyatomic molecular systems of special interest and relevance. There is interest in developing the most rigorous possible theoretical approaches and also in more approximate treatments that are more readily applicable to complex systems.

Recent Progress

Classical molecular dynamics (CMD) simulations ($\equiv$ classical trajectory calculations) are widely used to describe a variety of dynamical processes in complex molecular systems, e.g., chemical reactions rates involving polyatomic molecules. Classical mechanics, of course, cannot describe quantum mechanical effects such as coherence/interference, tunneling, zero-point energy constraints, etc., features that sometimes make significant contributions to the process of interest. The current focus of our research efforts is to develop practical ways for adding quantum effects to CMD by using the initial value representation (IVR) of semiclassical (SC) theory. Paper 3 gives a comprehensive summary of the theoretical development and surveys numerous recent SC-IVR applications.

For complex molecular systems, the dynamical quantity of interest is typically expressed in terms of a time correlation function of the form

$$C_{AB}(t) = tr\left[\hat{A} e^{i\hat{H}t/\hbar}\ \hat{B} e^{-i\hat{H}t/\hbar}\right] , \tag{1}$$

where $\hat{A}$ and $\hat{B}$ are hermitian operators depending on the property of interest, and $\hat{H}$ is the Hamiltonian of the system. E.g., the reaction rate for a chemical reaction is the $t \to \infty$ limit of Eq. (1), where $\hat{A}$ is the Boltzmannized-flux operator and $\hat{B}$ a Heaviside function that is 1 (0) on the product reactant side of a dividing surface in configuration space. If, as is often the case, $\hat{B}$ is a local function of the form $B[s(\mathbf{q})]$, then the 'forward-backward' (FB) version of SC-IVR theory (cf. paper 3) gives the correlation function of Eq. (1) as

$$C_{AB}(t) = (2\pi\hbar)^{-F}\int d\mathbf{p}_0 \int d\mathbf{q}_0 \int dp_s\, \tilde{B}(p_s) < \mathbf{p}_0, \mathbf{q}_0 \mid \hat{A} \mid \mathbf{p}_0', \mathbf{q}_0' > C_0(\mathbf{p}_0, \mathbf{q}_0; p_s)e^{iS_0(\mathbf{p}_0, \mathbf{q}_0; p_s)\hbar} , \tag{2}$$

where $(\mathbf{p}_0, \mathbf{q}_0)$ are the initial conditions for classical trajectories that arrive at phase point $(\mathbf{p}_t, \mathbf{q}_t)$ at time t; at time t there is a momentum 'jump',

$$\mathbf{p}_t \rightarrow \mathbf{p}_t + p_s \frac{s(\mathbf{q}_t)}{\mathbf{q}_t} , \tag{3}$$

and the trajectory is then evolved backward in time to t = 0; $(\mathbf{p}_0', \mathbf{q}_0')$ is the final phase point, S_0 the action integral along this FB trajectory, and C_0 a factor involving the derivatives of final values $(\mathbf{p}_0', \mathbf{q}_0')$ with respect to initial ones $(\mathbf{p}_0, \mathbf{q}_0)$. $\tilde{B}(p_s)$ is the Fourier transform of the function B(s), and $|\mathbf{p}_0, \mathbf{q}_0\rangle$ and $|\mathbf{p}_0', \mathbf{q}_0'\rangle$ are coherent states.

An important example of the above methodology is to the calculation of thermal rate constants for chemical reactions: the rate constant k(T) is given by the long time limit of the flux-side correlation function,[1]

$$k(T) = Q_r(T)^{-1} C_{fs}(t \rightarrow \infty) , \tag{4}$$

where Q_r is the reactant partition function (per unit volume), and $C_{fs}(t)$ is the correlation function of Eq. (1) with

$$\hat{A} = e^{-\frac{\beta \hat{H}}{2}} \hat{F} e^{-\frac{\beta \hat{H}}{2}} , \tag{5a}$$

$$\hat{B} = h(s(\mathbf{q})) \tag{5b}$$

$\hat{F}$ being the flux operator, $\frac{i}{\hbar} [\hat{H}, h(s(\hat{\mathbf{q}}))]$, and $h(s(\mathbf{q}))$ the Heaviside function.

With the time evolution operators (propagator) in Eq. (1), $\exp(\pm i \hat{H} t/\hbar)$, well-described by the SC-IVR approach, there is still the task of evaluating the Boltzmann operator, $\exp(-\beta \hat{H})$, accurately. In some earlier applications it was treated by a local harmonic approximation about the transition state, but this fails at lower temperatures. Paper 14, therefore, undertook to show how one can combine a fully quantum mechanical (QM) treatment of the Boltzmann operator (by Monte Carlo path integration) with the SC-IVR description of the real time propagators. Applications to several test problems shows this combined QM Boltzmann operator + SC-IVR propagator approach to be quantitatively accurate (giving rate constants to a few percent) even when tunneling effects are large ($>10^3$) and also when re-crossing (i.e., transition state theory-violating) dynamics is significant.

Another important step forward is the work described in paper 18, where it is shown how a gas phase reaction can be treated by the SC-IVR approach completely in Cartesian coordinates. I.e., in standard QM treatments of an A + BC → AB + C reaction in 3d, for example, one typically solves the Schrödinger equation separately for each value of total angular momentum J, and then adds up the contribution of each J to the cross section or rate constant. This means that one has to solve a Schrödinger equation involving only 4 degrees of freedom rather than one

with 6 if conservation of J and M_J were not taken into account. For classical trajectory-based approaches, however, the necessary use of curvilinear coordinates that this requires is usually more trouble than it is worth, and this is progressively true for larger molecular systems. In paper 18 the 3d version of the benchmark reaction $D + H_2 \rightarrow HD + H$ is treated using Cartesian Jacobi coordinates (overall center-of-mass translational motion is removed); the Hamiltonian thus retains its simple Cartesian form and the sums over total J are implicitly contained in the average over the phase space of initial conditions (cf. Eq. 2). This version of the methodology is directly applicable to reactions involving essentially any number of atoms.

Future Plans

With the validation of the above SC-IVR methodology for non-trivial model problems, work is underway to apply it to real molecular systems, both gas phase reactions and reactions in complex environments.

References

1. W. H. Miller, J. Chem. Phys. 61, 1823 (1974); W. H. Miller S. D. Schwartz and J. W. Tromp, J. Chem. Phys. 79, 4889 (1983).

2001 - 2003 (to date) DOE Publications

1. H. Wang, M. Thoss, K. Sorge, R. Gelabert, X. Gimenez and W. H. Miller, Semiclassical Description of Quantum Coherence Effects and Their Quenching: A Forward-Backward Initial Value Representation Study, J. Chem. Phys. 114, 2562-2571 (2001); LBNL-46836.

2. R. Gelabert, X. Gimenez, M. Thoss, H. Wang and W. H. Miller, Semiclassical Description of Diffraction and Its Quenching by the Forward-Backward Version of the Initial Value Representation, J. Chem. Phys. 114, 2572-2597 (2001); LBNL-46837.

3. W. H. Miller, The Semiclassical Initial Value Representation: A Potentially Practical Way for Adding Quantum Effects to Classical Molecular Dynamics Simulations, J. Phys. Chem. 105, 2942 2955 (2001); LBNL-46935.

4. M. Thoss, H. Wang and W. H. Miller, "Generalized Forward-Backward Initial Value Representation for the Calculation of Correlation Functions in Complex Systems," J. Chem. Phys. 114, 9220-9235 (2001); LBNL-47268.

5. J. Xing, E. A. Coronado and W. H. Miller, "Some New Classical and Semiclassical Models for Describing Tunneling Processes with Real-Valued Classical Trajectories," J. Phys. Chem. A 105, 6574-6578 (2001); LBNL-47268.

6. H. Wang, M. Thoss and W. H. Miller, "Systematic Convergence in the Dynamical Hybrid Approach for Complex Systems: A Numerically Exact Methodology," J. Chem. Phys. 115, 2979 2990 (2001); LBNL-47557.

7. M. Thoss, H. Wang and W. H. Miller, "Self-Consistent Hybrid Approach for Complex Systems: Application to the Spin-Boson Model with Debye Spectral Density," J. Chem. Phys. 115, 2991 3005 (2001); LBNL-47558.

8. H. Wang, D. E. Manolopoulos and W. H. Miller, "Generalized Filinov Transformation of the Semiclassical Initial Value Representation," J. Chem. Phys. **115**, 6317-6326 (2001); LBNL-48140.

9. W. H. Miller, "Adding Quantum Effects to Classical Molecular Dynamics Simulations via the Semiclassical Initial Value Representation," SIMU Newsletter, Issue 3, 51-62 (2001); LBNL 47984.

10. E. A. Coronado, J. Xing, and W. H. Miller, "Ultrafast Non-Adiabatic Dynamics of Systems with Multiple Surface Crossings: A Test of the Meyer-Miller Hamiltonian with Semiclassical Initial Value Representation Methods," Chem. Phys. Lett. **349**, 521-529, (2001); LBNL-47694.

11. W. H. Miller, "Using the Semiclassical Initial Value Representation to Include Quantum Effects in Molecular Dynamics" in Wide-Amplitude Rovibrational Bound States in Polyatomic Molecules, ed. I. N. Kozin, M. M. Law, and J. N. L. Connor, CCP6, Daresbury, UK (2001); LBNL-49021.

12. W. H. Miller, An Alternate Derivation of the Hermann-Kluk (Coherent State) Semiclassical Initial Value Representation of the Time Evolution Operator, Mol. Phys. **100**, 397-400 (2002); LBNL-47781.

13. V. Guallar, V. S. Batista, W. H. Miller and D. L. Harris, Proton Transfer Dynamics in the Activation of Cytochrome P450eryF, J. Am. Chem. Soc. **124**, 1430-1437 (2002); LBNL-48392.

14. T. Yamamoto, H. Wang, and W. H. Miller, Combining Semiclassical Time Evolution and Quantum Boltzmann Operator to Evaluate Reactive Flux Correlation Function for Thermal Rate Constants of Complex Systems, J. Chem. Phys. **116**, 7335-7349 (2002); LBNL-49465.

15. W. H. Miller, On the Relation between the Semiclassical Initial Value Representation and an Exact Quantum Expansion in Time-Dependent Coherent States, J. Phys. Chem. B **106**, 8132-8135 (2002); LBNL-49606.

16. S. X. Sun and W. H. Miller, Statistical Sampling of Semiclassical Distributions: Calculating Quantum Mechanical Effects Using Metropolis Monte Carlo, J. Chem. Phys. **117**, 5522-5528 (2002); LBNL-51074.

17. Y. Zhao and W. H. Miller, Semiclassical (SC) Initial Value Representation (IVR) for the Boltzmann Operator in Thermal Rate Constants, J. Chem. Phys. **117**, 9605-9610 (2002); LBNL-50669.

18. T. Yamamoto and W. H. Miller, Semiclassical Calculation of Thermal Rate Constants in Full Cartesian Space: The Benchmark Reaction for $D + H_2 \rightarrow DH + H$, J. Chem. Phys. **118**, 2135-2152 (2003); LBNL-51587.

19. W. H. Miller, Y. Zhao, M. Ceotto and S. Yang, Quantum Instanton Approximation for Thermal Rate Constants of Chemical Reactions, J. Chem. Phys. (submitted); LBNL-52311.

Unimolecular Reaction Dynamics of Free Radicals*

C. Bradley Moore,
Principal Investigator
Department of Chemistry
The Ohio State University
Columbus, OH 43210-1106
moore.1@osu.edu

Program Scope

The fundamental goal of this work is a quantitative understanding of the unimolecular reactions of free radicals. These reactions are of crucial importance in combustion and in atmospheric chemistry. Reliable theoretical models for predicting the rates and products of these reactions are required for modeling combustion and atmospheric chemistry systems. In contrast to the benchmark reactions, $CH_2CO \rightarrow {}^{1,3}CH_2 + CO$, the reactions of free radicals occur over barriers sufficiently low that the hypothesis of rapid energy randomization upon which statistical transition state theories depend is in doubt. A study of the rates and dynamics of methoxy and vinyl radicals in their ground electronic states is in progress:

$$CH_2 = CH \rightarrow HC \equiv CH + H, \qquad \Delta H_0 = 11760 \text{ cm}^{-1} \qquad (1)$$
$$CH_3 - O \rightarrow CH_2 = O + H, \qquad \Delta H_0 = 6950 \text{ cm}^{-1} \qquad (2)$$

These should serve as benchmarks for this important class of reactions. The dissociation of CH_3O has a very low barrier, about 8,400 cm^{-1}. As for many other free radicals, this low barrier results from the simultaneous increase in the bond order of C-O as the C-H bond is broken.

The statistical Transition State Theory (TST), i.e. RRKM and its variants, depends on the basic postulate that complete intramolecular vibrational energy redistribution (IVR) is much faster than the chemical reactions of interest. TSTs give reaction rates that are functions of total energy and angular momentum. While TSTs are consistent with much experimental data and have gained practical importance for computational modeling of complex reaction systems, some small and moderate size molecular systems, e.g., HCO and HFCO, are observed to decompose at rates that depend systematically on rovibrational quantum numbers. The dissociation of HCO is quantitatively understood in terms of the coupling of modestly perturbed single quantum states to the H+CO continuum. Lower barriers result in limited IVR due to lower vibrational level densities and smaller matrix elements for mode coupling and level mixing at the lower energies.

Methoxy and vinyl will provide benchmark models for unimolecular dynamics in systems that lie between the statistical and single-quantum-state extremes. Other radicals important in combustion and atmospheric chemistry will also be explored including members of the RO_2 family.

The experiments use a wide range of time and wavelength resolved laser spectroscopies. Radicals are produced by laser flash photolysis of precursors in supersonic jets. Products are observed by laser-induced fluorescence and by state-selective Resonance-Enhanced Multiphoton Ionization (REMPI) with velocity map ion imaging. This allows complete spectroscopic study of the radicals including the intramolecular vibrational couplings revealed in the spectra of highly excited ground electronic state rovibrational energy levels.

Decay time and linewidth measurements then give the dissociation rates of well-characterized rovibronic energy levels. Ion imaging and Doppler-resolved REMPI measurements give vector and scalar correlations of the product energy state distributions.

Recent Progress

Dissociation dynamics and spectroscopy of vinyl radical
Aaron M. Mann, Xiangling Chen, Vladimir A. Lozovsky, C. Bradley Moore

Our previous work[1] revealed the vibrational and rotational structure of the first $\tilde{A}\,^2A''$ excited electronic state of vinyl radical (CH$_2$CH) and it's partially deuterated isotopomer (CD$_2$CH). The vibrationally resolved spectra of the $\tilde{A}\,^2A'' \leftarrow \tilde{X}\,^2A'$ electronic transition of the jet-cooled vinyl radical and CD$_2$CH in the range of 443 – 516 nm have been obtained via action spectroscopy. The resonance of the excitation laser frequency with the frequency of transition to rovibrational levels of the $\tilde{A}\,^2A''$ state is monitored via the appearance of the H or D fragment. The appearance of H or D fragments was detected via 1+1' REMPI through the Lyman-α transition. The action spectra of both CH$_2$CH and CD$_2$CH were assigned with the use of B3LYP/6-311(d)G level of *ab initio* calculations. Excitation to the $\tilde{A}$ state rovibrational levels leads to the dissociation of vinyl radical via internal conversion into highly excited vibrational levels of the $\tilde{X}$ state. The vibrational excitation of the $\tilde{X}$ state is in the range of 6750 – 9940 cm^{-1} above the dissociation barrier.

Based on our previous study, we were able to measure velocity distributions of the H product of reaction (1) as well as the D product of the reaction:

$$CD_2 = CH \rightarrow CD \equiv CH + D \qquad (1')$$

for six vibrational bands of C$_2$H$_3$ and for seven bands of CD$_2$CH of the $\tilde{A}$ state. Two-dimensional (2-D) velocity maps of H and D atoms that are products of CH$_2$=CH and CD$_2$=CH dissociation, respectively, were recorded. A typical H-atom raw 2-D image from vinyl radical excitation to the 6^2, 6^18^1 bands of the $\tilde{A}$ state is shown in Fig. 1(a). In Fig.1(b) the Abel inverse-transformed image is shown. Fig. 2 and Fig. 3 show the H-atom speed distribution and anisotropy parameter extracted from the image data in Fig. 1. These data were obtained for all vibrational bands and gave important dynamical characteristics of unimolecular dissociation of the vinyl radical in its ground $\tilde{X}\,^2A'$ electronic state. The distributions of translational and total internal ($E_{int}=E_{vib} + E_{rot}$) energy of acetylene and di-acetylene products in the excitation energy range 6750 – 9150 cm^{-1} above the dissociation barrier are determined from the H-atom speed distributions by simple conservation of energy and compared with theoretically predicted ones. The possibility of significant H-atom scrambling,

$$CD_2 = CH \rightarrow CHD = CD \qquad (3)$$

followed by dissociation, $CHD = CD \rightarrow CD \equiv CD + H$ (1″), is ruled out by the experimental data shown in Fig. 4.
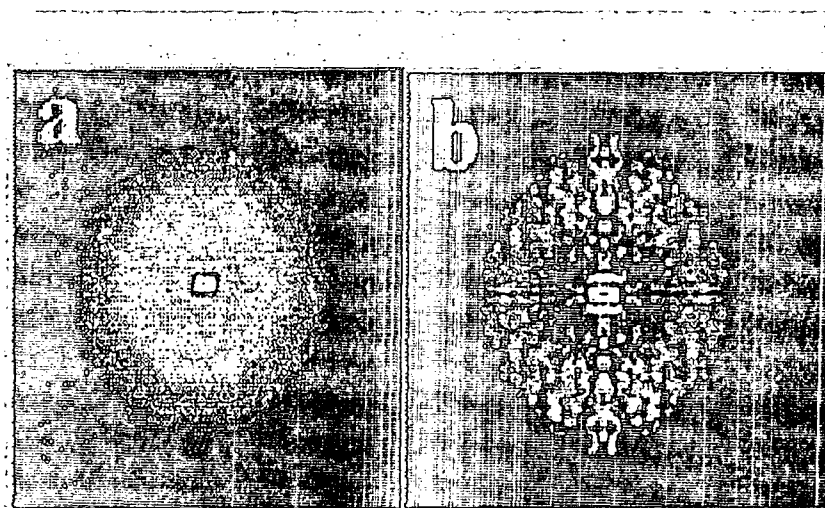
Fig.1. Typical H-atom images from vinyl radical excitation to the 6^2, $6^1 8^1$ bands of C_2H_3 at 22 391 cm^{-1} (a) Raw image and (b) reconstructed image.
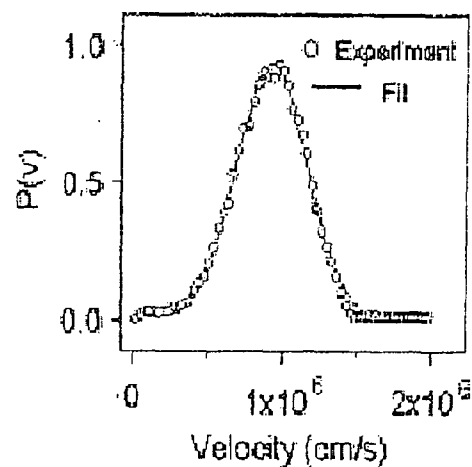
Fig. 2. H atoms speed distribution P(v) is extracted from image data in Fig1.
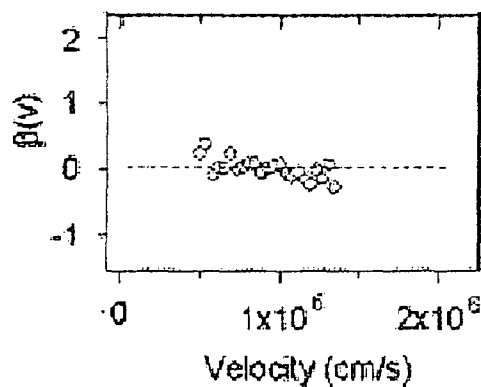
Fig. 3. H atoms anisotropy parameters $\beta(v)$ at selected velocities extracted from image data in Fig. 1.
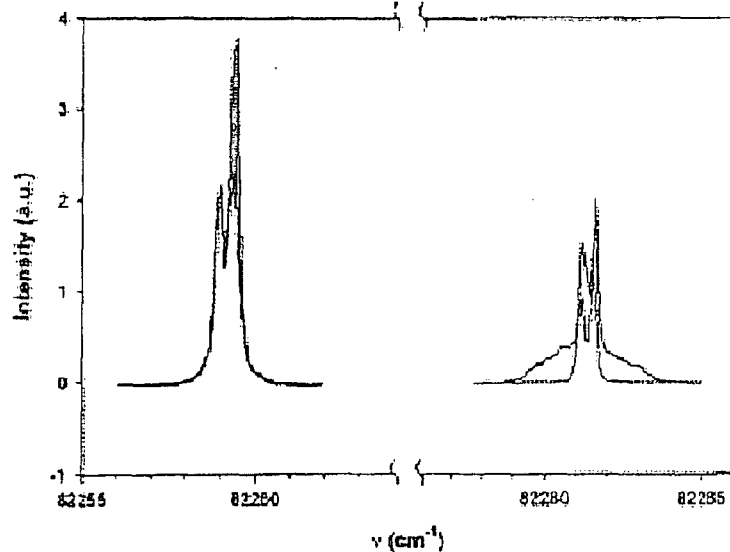
Fig. 4. REMPI spectra of H and D from excitation to the 5^2 band of CD_2CH at 22330 cm^{-1}.

REMPI spectra of both H and D shown in this figure consist of two traces one with and one without the laser that dissociates CD_2CH. The H-atom profiles on the left show little or no difference, reflecting the lack of H-atom products from d_2-vinyl excitation. The D-atom profiles on the right part of Fig. 4 clearly show the "cold" D atoms entrained in the molecular

beam, and the additional translationally "hot" D atoms produced after vinyl excitation. These facts reflected in Fig. 4 allow an upper bound of 1.3×10^{11} s^{-1} to be derived for the rate constant of H-atom scrambling between the α and β carbon atoms.

Future Plans

Work on methoxy radical is currently focused on the spectroscopy of C–H stretching vibrational energy levels. Fluorescence excitation spectra of the $\tilde{A}$ state reveal possible transitions involving C–H stretching. In collaboration with Terry A. Miller's group, dispersed fluorescence spectra unambiguously establish the assignment of levels involving C–H stretching and yield approximate ($\pm$ 10 cm^{-1}) energies of levels with one quantum of C–H stretch for CH$_3$O and CHD$_2$O in the $\tilde{X}$ state. Rotationally resolved spectra are obtained by SEP. Levels with multiple quanta of C–H stretch excited will be studied via IR excitation for both methoxy and vinyl. Dispersed fluorescence spectra of methoxy are recorded at $\tilde{X}$-state energies above the dissociation threshold and give some information on the dynamics of vibrational energy flow and on dissociation. Femtosecond IR multiphoton dissociation studies in collaboration with the Kompa group in Munich have shown that dissociation of diazomethane by excitation of its CNN asymmetric stretch leads to dissociation on a timescale shorter than intramolecular vibrational relaxation.

Publications since 2001

1. M.B. Pushkarsky, A.M. Mann, J.S. Yeston, and C.B. Moore, "Electronic Spectroscopy of Jet-Cooled Vinyl Radical," J. Chem. Phys. 115, 10738-10744 (2001).

2. A.M. Mann, X. Chen and V.A. Lozovsky, C.B. Moore, "Dissociation dynamics of the $\tilde{A}\,^2A''$ state of vinyl radical", J. Chem. Phys. 118, 4452-4455 (2003).

Gas-Phase Molecular Dynamics:
Research in Spectroscopy, Dynamics and Kinetics

James T. Muckerman, Trevor J. Sears, Gregory E. Hall, Jack M. Preses and Christopher Fockenberg
Chemistry Department, Brookhaven National Laboratory, Upton, NY 11973-5000
muckerma@bnl.gov, sears@bnl.gov, gehall@bnl.gov, preses@bnl.gov, fknberg@bnl.gov

The purpose of this program is to explore the energetics, dynamics and kinetics of chemical reactions resulting from molecular collisions in the gas phase. The goal of this work is a fundamental understanding of chemical processes related to combustion. We are interested in the microscopic factors affecting the structure, dynamics and reactivity of short-lived intermediates such as free radicals in gas-phase reactions. Molecular species are studied using both experimental and theoretical tools including high-resolution spectroscopic probes, velocity map imaging, time-of-flight mass spectrometry, *ab initio* electronic structure calculations and both time-dependent and time-independent quantum calculations of nuclear motion. The focus of the program has recently been broadened to include aspects of the chemical physics of catalysis, specifically chemical dynamics and kinetics at surfaces and on metal and metal-containing clusters, and the spectroscopy of metal-containing clusters. The synergy between the experimental and theoretical components of the research is an important element in achieving the goals of the program.

Recent Progress

Axis-switching intensities in floppy molecules

Spectra of several bands in the $\tilde{A} - \tilde{X}$ system of HCCl and HCBr were recorded in order to test axis-switching models for intensity in "forbidden" sub-bands. Transitions terminating in low energy vibrational levels of the $\tilde{A}$ state in these halocarbenes have relative intensities of "allowed" and "forbidden" perpendicular and parallel bands that are well described by the standard small-amplitude theory of Hougen and Watson. In such transitions, which are accompanied by a change in geometry between stiff structures, the "forbidden" intensities provide a quantitative observable in addition to line positions for the determination of structure. High bending levels in the $\tilde{A}$ state, in contrast, exhibit large amplitude excursions from the equilibrium structure, and deviations from the Hougen and Watson theory are expected. Several examples of such axis-switching bands have been recorded. Experimental intensities of axis-switching sub-bands involving highly excited bending states of HCCl and HCBr are substantially stronger than the predictions of the small-amplitude Hougen and Watson model for axis-switching in triatomics. A more general, non-perturbative model has been developed in our group and has been shown to calculate rovibronic energies and wavefunctions efficiently and accurately. The calculated rovibronic transition intensities in this formulation do not rely on a small-amplitude approximation, and should yield good axis-switching intensities even when the perturbative theory fails. Preliminary comparison with the new model provides encouragingly accurate agreement with observed axis-switching intensities for both low- and high-energy upper states.

Collision-induced electronic transitions in methylene

Relaxation from singlet to triplet CH_2 is thought to be induced by collisions in which a sparse set "doorway states" of mixed singlet-triplet parentage play a key role. By observing time-resolved Doppler spectra of selected CH_2 rotational states following pulsed laser photolysis of ketene, the approach to steady-state kinetics has been analyzed during the time characteristic of translational and rotational thermalization in competition with reactive and non-reactive quenching. Preliminary experiments provided evidence for an unusual velocity dependence of collisions producing or destroying mixed states. Further investigations of the unusual kinetics and velocity distribution of a mixed state in the collisional relaxation of singlet methylene have resulted in a satisfactory explanation. A coincidental overlap of spectral lines had led us to an incorrect attribution of signal to a mixed state. The relaxation kinetics can now be interpreted in a more conventional way, and the signature of a special role for mixed-states in the dis-equilibrium evolution of state populations is discernable, though less dramatic than previously thought. A final analysis of the measurements is in progress.

Two-layer Lanczos iteration approach to molecular spectroscopic calculations

A two-layer Lanczos algorithm has been suggested for calculating the rovibrational energy levels of polyatomic molecules in terms of a partitioned Hamiltonian. Such a Hamiltonian is formed in a set of orthogonal polyspherical coordinates. This algorithm solves the full-dimensional eigenvalue problem in a reduced-dimensional (RD) manner. By splitting the coordinates into radial and angular groups, one obtains a small RD Hamiltonian in each coordinate group. The eigenstates of each RD system are computed using either a standard or guided spectral transform (GST) Lanczos method. These two subsystems are exactly coupled *via* a set of diabatic basis functions in the angular degrees of freedom without any dynamical approximation. The two-layer Lanczos algorithm has been illustrated in detail in the context of the variational calculation of the vibrational energies of pentatomic molecules such as CH_4. Numerical results show that the two-layer Lanczos method is substantially more efficient than the conventional Lanczos method.

Accelerated calculation of rovibrational energies of four-atom molecules

The two-layer Lanczos algorithm described above has been extended to study the rovibrational spectrum of four-atom molecules in a mixed grid/finite basis representation basis. This algorithm exploits the partitioned structure of the Hamiltonian in polyspherical coordinates, and calculates the eigenstates in a reduced-dimension (RD) way but exactly. The idea of the approach to rovibrational energies of four-atom molecules is to construct the Hamiltonian with diagonal blocks corresponding to the coupled-states approximation, and with off-diagonal blocks containing the Coriolis coupling. The improved efficiency of the two-layer Lanczos method allows the calculation of the eigenvalues of this rovibrational Hamiltonian as easily as the standard Lanczos method solves for only the vibrational eigenvalues. The initial application of this approach has been to the rovibrational levels of formaldehyde.

An exact variational approach for calculating vibrational energy levels of five-atom molecules

As shown above for the case of tetra-atomic molecules, orthogonal polyspherical coordinates are powerful for describing the internal motion of polyatomic molecules. The resulting quantum Hamiltonian is compact and relatively simple. We are currently extending this approach to study the vibrational energy levels of pentatomic molecules such as CH_4. In order to avoid the huge basis set problem associated with the nine-dimensional coordinate space, a full DVR contracted representation is employed in the variational calculation, together with a one- or two-layer iteration method. As with our four-atom code, we will make this program available to the scientific community free of charge.

Ab initio study of coordinatively unsaturated transition-metal containing species

We have carried out high-level *ab initio* calculations of the geometry and electronic properties of several low-lying electronic states of the met-car precursor molecules TiC_2 and MoC_2. In TiC_2, there are four low-lying, closely-spaced triplet states, one of each irreducible representation in C_{2v} symmetry, that differ only by which two d orbitals on the Ti atom are singly occupied. Somewhat above these are four corresponding singlet states. Our restricted MRCI+Q calculations with full-valence CAS reference functions calculations indicate a $^3B_2$ ground state, in disagreement with the CAS and DFT (B3LYP) results of Sumathi and Hendrickx, with the $^3B_1$ state just 235 cm^{-1} above it. It is noteworthy that the full-valence CAS method, which is usually quite reliable for predicting the correct ordering of low-lying electronic states, in this case produces results that are completely inconsistent with other high-level methods (*e.g.*, CI(SD), RCCSD(T), and MRCI). This anomaly can be explained by the differential correlation energy recovered by active space *vs.* virtual space configuration interaction among the various states.

Yield of allene in the reaction of propargyl radicals with H atoms

During the last year we have been using diode laser absorption spectroscopy to examine two reaction systems. The first involves a radical-radical reaction previously studied using TOFMS: the yield of allene from the reaction of propargyl radicals and hydrogen atoms, utilizing a method similar to that previously applied in our laboratory to determine the CO yield from the reaction of CH_3 radicals and O atoms. A mixture of a few mTorr of propargyl chloride and oxalyl chloride in ~5 T of H_2 was irradiated with pulses of 193 nm radiation. Cl atoms were produced from photolysis of oxalyl chloride. Cl atoms abstracted an H atom from H_2, producing H atoms which then went on to react with propargyl radicals generated from propargyl chloride by the same 193-nm pulse. The concentration of propargyl radicals was determined from the reduction of propargyl chloride absorption near 3-μm and the concentration of allene was determined in early experiments from the magnitude of allene absorption near 5 μm. We have replaced a weak 5 μm diode to take advantage of a better diode for detection of allene C–H bending absorption near 1452 cm^{-1} (6.9 μm), and we are currently acquiring data.

CO vibrational state distribution from 308-nm photodissociation of ketene

There is an extensive literature concerning the study of unimolecular dissociation on barrierless potentials. The CO vibrational-state distribution from the 308-nm photodissociation of ketene may help to diagnose K rotor-adiabatic or K rotor-active dissociation mechanisms. Previous measurements that place the ratio of CO($v=1$) to CO($v=0$) close to 10% favor a K-adiabatic mechanism, while more recent measurements that are significantly lower favor the K-active mechanism. Diode laser absorption provides a direct method to determine this ratio. We have measured the ratio of CO($v=1$) to CO($v=0$) from the 308-nn photodissociation of ketene, and while preliminary data support the lower ratio, consideration of vibrational energy sharing between ketene and CO may raise the value of the ratio.

Variational transition state calculations of methyl-methyl recombination

We complemented last year's experimental study of the methyl-methyl recombination reaction by microcanonical variational transition state calculations using the Variflex® program package by the ANL group. From a new *ab initio* potential surface we derived a new switching function to replace the exponential function used by Wardlaw and Marcus (*J. Phys. Chem.* 1986, **90**, 5383). The change in frequency of the transitional vibrations as well as the symmetry parameter as a function of the reaction coordinate is now expressed by the change in the CH_3 splay angle. The calculations of the pressure and temperature dependence of the recombination reaction for He and Ar as bath gases are in very good agreement with experimental data.

Experimental studies of CH₃ + OH kinetics

Current research is focused on measuring the kinetics and especially the product distribution of the methyl-hydroxyl radical reaction. According to *ab initio* calculations, the energies of almost all transition states lie within a few kcal/mol of the entrance channel making the product distribution very sensitive to pressure and temperature. Initial experiments indicate that no (or very little) methanol is produced at pressures less than 6 Torr. Because small increases of CH_3OH at mass 32 can be obscured by the background signal of O_2, we concentrated our research on the CH_3 + OD reaction. Again, no CH_3OD was found, now on an essentially zero background.

Potential energy surface features for the CH₃ + OH reaction

The stationary point geometries and frequencies on the lowest singlet potential energy surface for the CH_3OH system have been calculated using the CASSCF method with an active space consisting of ten electrons and ten orbitals. The energetics were refined using a restricted internally contracted MRCI (RMRCI) in which configurations with more than two electrons in active space orbitals not populated in the principal configuration are excluded from the CAS reference function. These energies were extrapolated to the complete basis set (CBS) limit using the scheme of Halkier *et al.* with two large basis sets: aug-cc-pVDZ and aug-cc-pVTZ. The implications of our calculated results concerning the $O(^1D)$ + CH_4 and OH + CH_3 reactions are being explored.

Future Work

Search for the HOCO overtone spectrum

The HOCO radical is the intermediate in the OH+CO reaction that is central in combustion of hydrocarbon fuels. Searches for v(OH) overtone transitions in the spectrum of the radical near 10 000 cm⁻¹ are underway. According to calculations performed in our group, the second OH overtone in this radical is above the dissociation energy for both the H+CO_2 and OH+CO asymptotes. Contrary to intuition, the calculations suggest that local excitation in the H-O bond will not lead preferentially to the H+CO_2 channel. Detection of lifetime-broadened absorptions in the radical will lead to new information on the HOCO potential surface in experimentally unexplored regions where two nearly isoenergetic transition states compete.

Spectroscopic studies of coordinatively unsaturated transition metal-containing species

In collaboration with Prof. Philip Johnson (Stony Brook Univ.), new spectroscopic methods for the study of coordinatively unsaturated transition metal-containing species will be developed. This effort has already begun, with the development of pulsed laser sources in the 1.4-3.0 micron region; wavelengths corresponding to energies of 3300-7700 cm⁻¹, where computational work in our group has suggested many of the species have their lowest-lying excited electronic states. The experimental and computational efforts in this area are strongly coupled, with theory suggesting experiments and experimental measurements providing valuable calibration marks for different theoretical approaches. Particular systems of interest are early transition metal (*e.g.*, vanadium, chromium and molybdenum) carbides and alkyls, which are thought to be intermediates in many economically important catalytic processes. A scheme to detect the absorption by 1+1 REMPI spectroscopy is proposed. Here, the first, resonant, photon is in the infrared or near-infrared, while the ionization photon is in the UV.

Improved transient FM spectrometers

The sensitivity of the transient FM spectrometers will be increased by moving the r.f. operating frequency to the GHz regime. This will particularly help in the measurements of spectral lines that are broadened due to photodissociation, or due to extreme translational excitation in photochemically generated radicals. The present sideband spacing is small compared to the line widths in many cases resulting in less than optimum sensitivity. Increasing the sideband spacing by a factor of *ca.* five will result in an immediate sensitivity increase by approximately the same amount.

Determination of rovibrational energies and the anomalous isotope effect of the HXeOH cluster

The rovibrational energy levels of the weakly bound HXeOH cluster and its isotopomers will be calculated using a two-layer Lanczos algorithm in Radau-diatom-Jacobi coordinates, based on a high-level *ab initio* potential energy surface we have calculated. The surface was obtained by fitting 1229 RCCSD(T)/SDB-cc-pVQZ energy points. The equilibrium geometry of HXeOH is determined to have a *trans* configuration with a nearly collinear HXeO bond angle of 177.32°. The well depth of this minimum energy configuration is only 0.6123 eV with respect to the OH + Xe + H dissociation limit. The calculation of vibrational frequencies for this molecule will focus on the anomalous isotopic shift in the H-Xe stretching frequency of HXeOH and HXeOD upon ¹⁸O substitution in contrast to the normal isotopic shift in the D-Xe frequency of DXeOH and DXeOD observed in a Xe solid matrix.

The full-dimensional calculation of the vibrational spectra of six-atom molecules

Two quantum mechanical Hamiltonians have been derived in polyspherical coordinates for the study of the vibrational energies of six-atom molecules. They are expressed in an explicit Hermitian form in the spatial representation. Since one employs a set of orthogonal coordinates, which can be formed by Jacobi and/or Radau vectors, *etc.*, the Hamiltonians are very compact. In particular, the large amplitude motions of a molecule are

naturally described. The matrix representation of the Hamiltonians is described in both mixed grid/basis and full-grid representations. Using a two-layer Lanczos iteration algorithm, we plan to apply this approach to the determination of the vibrational energy levels of the hydrogen trimer $(H_2)_3$.

Experimental kinetics of the CH_3 + OH reaction

In our group, we are bringing to bear several simultaneous experimental and theoretical tools to study the CH_3+OH reaction. The C-H bending vibration of CH_3OH may be within the range of the 1452 cm^{-1} diode and, therefore, may permit us to pursue the answer to a somewhat puzzling TOFMS result: The reaction of CH_3 and OH radicals does not seem to produce any detectable CH_3OH at pressures below 4 Torr. Instead, the signal trace at mass 30 suggests that either CH_2O or HOCH is formed. Since there is greater flexibility for choosing the pressure range in the diode laser experiment we plan to look for methanol using diode laser absorption. If successful, we may be able to determine whether the CH_3OH yield from the CH_3+OH reaction is miniscule or zero, or whether the TOFMS result is an artifact. The experimental method is similar to previous ones: The CH_3 concentration determined from the loss of acetone concentration by monitoring CO appearance will be compared to the concentration of CH_3OH determined from the magnitude of its absorption. In the TOFMS experiment, we will separate signals due to $^{13}C_2H_6$ ($m/e = 32$) from $^{13}CH_2O$ ($m/e = 31$) using ^{13}C-labeled acetone. Together with data from the CH_3+OD study we hope to answer the question of whether CH_2O or HOCH is the primary product of this reaction. The data will be analyzed by simulation calculations, for which will make use of our new computer program based on the Chemkin program package employing genetic and simplex algorithms to find the best fit.

Theoretical direct dynamics of the reactions of $O(^1D)$ with CH_4

We have determined by comparison with features of the accurate potential energy surface for CH_3OH described above that a dual-level direct dynamics method employing a geometry-dependent combination of HF and CCD forces is sufficiently accurate for treating the reaction of $O(^1D)$ with CH_4. We are initiating a direct dynamics study of this reaction with the objective of separating the contributions of "direct" and "complex formation" mechanisms, which may result in very different branching into the various product channels. Direct reactions are deemed to occur in less than 1 ps, when trajectories are stopped and are considered to contribute to a statistical product distribution.

Publications since 2001

"Experimental and theoretical studies of the near IR spectrum of bromomethylene," Hua-Gen Yu, Tomas Gonzalez-Lezana, Andrew J. Marr, James T. Muckerman and T. J. Sears, *J. Chem. Phys.* **115**, 5433-5444 (2001).

"A theoretical study of the potential energy surface for the reaction OH + CO → H +CO_2," H.-G. Yu, J.T. Muckerman and T.J. Sears, *Chem. Phys. Lett.* **349**, 547 (2001).

"An *ab initio* molecular dynamics study of S_0 ketene fragmentation," K. M. Forsythe, S. K. Gray, S. J. Klippenstein and G. E. Hall, *J. Chem. Phys.* **115**, 2134 (2001).

"A direct measurement of the rate constant for the CH_2 (X^3B_1) + CH_3 reaction at 300 K," B. Wang and C. Fockenberg, *J. Phys. Chem. A* **105**, 8449 (2001).

"A general variational algorithm to calculate vibrational energy levels of tetra-atomic molecules," H.-G. Yu and J.T. Muckerman, *J.Molec. Spectrosc.* **214**, 11 (2002).

"Imaging $O(^3P)$ + alkane reactions in crossed molecular beams: vertical *vs.* adiabatic H abstraction dynamics," X. Liu, R.L. Gross, G.E. Hall, J.T. Muckerman and A.G. Suits, *J. Chem. Phys.* **117**, 7947 (2002).

"Radiation chemical effects of x-rays on liquids," R.A. Holroyd and J.M. Preses, in *Chemical Applications of Synchrotron Radiation*, World Scientific, pp. 987-1009 (2002).

"Temperature dependence of the rate constant and product distribution of the reaction of CH_3 radicals with $O(^3P)$ atoms," C. Fockenberg and J.M. Preses, *J. Phys. Chem. A* **106**, 2924 (2002).

"Quantum dynamics of the photoinitiated unimolecular dissociation of HOCO," H.-G. Yu and J.T. Muckerman, *J. Chem. Phys.* **117**, 11193 (2002).

"The $E^3\Pi$ $X^3\Delta$ transition of jet-cooled TiO observed in absorption," K. Kobayashi, G. E. Hall, J. T. Muckerman, T. J. Sears and A. J. Merer, *J. Mol. Spectrosc.* **212**, 133 (2002).

"Axis switching and coriolis coupling in the $A(010)$ $X(000)$ transitions of DCCl and HCCl," A. Lin, K. Kobayashi, H.-G. Yu, G.E. Hall, J.T. Muckerman and T.J. Sears, *J. Molec. Spectrosc.* **214**, 216 (2002).

"Vibrational energy transfer and reactivity in HO + CO collisions," G.D. Billing, J.T. Muckerman and H.-G. Yu, *J. Chem. Phys.* **117**, 4755 (2002).

"A K-dependent adiabatic approximation to the Renner-Teller effect for triatomic molecules," H.-G. Yu, J.T. Muckerman and T.J. Sears, *J. Chem. Phys.* **116**, 1435 (2002).

"An exact variational method to calculate vibrational energies of five atom molecules beyond the normal mode approach," H.-G. Yu, *J. Chem. Phys.*, **117**, 2030 (2002).

"Two-layer Lanczos iteration approach to molecular spectroscopic calculation," H.-G. Yu, J. Chem. Phys., **117**, 8190 (2002).

"Accelerating the calculation of the rovibrational energies of tetraatomic molecules using a two-layer Lanczos algorithm," H.-G.Yu, *Chem. Phys. Lett.* **365**, 189 (2002).

"Vibrational energy levels of methyl cation," H.-G. Yu and T.J. Sears, *J. Chem. Phys.* **117**, 666 (2002).

"The deposition of Mo nanoparticles on Au(111) from a $Mo(CO)_6$ precursor: Effects of CO on Mo-Au intermixing," P. Liu, J.A. Rodriguez, J.T. Muckerman and J. Hrbek, *Surf. Sci. Lett.* (in press).

"The behavior of Mo nanoparticles on Au(111): A theoretical study," P. Liu, J.A. Rodriguez, J.T. Muckerman and J. Hrbek, *Phys. Rev. B* (in press).

"Chemical reactivity of metcar Ti_8C_{12}, nanocrystal $Ti_{14}C_{13}$ and a bulk TiC(001) surface: A density functional study," P. Liu, J.A. Rodriguez, H. Hou and J.T. Muckerman, *J. Chem. Phys.* (in press).

"Hot bands in the A X spectrum of HCBr," B.-C. Chang, J. Guss and T. J. Sears, *J. Molec. Spectrosc.* (in press).

Reacting Flow Modeling with Detailed Chemical Kinetics

Habib N. Najm

Sandia National Laboratories
7011 East Ave, MS 9051, Livermore, CA 94550
hnnajm@ca.sandia.gov

1 Program Scope

The purpose of this research program is to understand the transient behavior of flames in turbulent flow, thereby improving the state of the art in predictive modeling of combustion. The work involves: (1) Using advanced computational tools to investigate the structure and dynamical behaviour of flames in unsteady vortical laboratory-scale flows. (2) Performing detailed validation studies with matched experimental-numerical comparisons to assess the validity of existing flame chemistry and transport models. (3) Developing advanced techniques for the analysis of, and extraction of information from, multidimensional reacting flow computations. (4) Developing improved numerical methods for discretizing large scale reacting flow systems of equations with detailed kinetics and transport. (5) Developing efficient massively parallel programming approaches for computing large scale reacting flow with detailed kinetics.

2 Recent Progress

2.1 Premixed Flame-Vortex Interactions

We conducted a computational study of the transient behavior of premixed H_2-air flames during a 2D flame-vortex interaction. This included comparison to ongoing experimental measurements on the planar V-flame apparatus by J.Frank. As was the case with CH_4-air flames, computational results did not exhibit the OH "burst" observed experimentally at rich flame conditions. However, after a detailed study of the experiment suggested some preheating of the vortex by the flame, we conducted a computational study with a preheated vortex and at rich mixture conditions. At about 150-200 K of preheat the computations exhibited about a 2.5× rise in OH during the interaction with the vortex. This is about the value observed in the experiment, and it is the direct result of the flame burning into preheated reactants once the fuel in front of the vortex is consumed. Some differences persisted, pertaining to the exact amplitude and timing of the OH transient, but the global behavior was consistent. Further analysis of the experiment revealed an additional issue, namely the presence of excess air in the vortex generator, resulting in a vortex that is leaner than the rest of the premixed flow. Given the rich mixture, this effect contributed to the enhanced burning rate of the flame when it met the vortex fluid. Computations with about 10 % excess air in the vortex fluid, in addition to the above preheating, exhibited an even larger rise in centerline-peak-OH (about 5.5× for a $\phi = 1.4$ H_2-air flame) during the interaction. Moreover, the rising OH transient occured earlier in the interaction, consistent with the experiment. This finally removes the *qualitative* disagreement between our computations of transient flame-vortex interaction and observational data.

2.2 Uncertainty Quantification (UQ)

Our UQ work is motivated by a need to quantify limits of predictability in reacting flow models. Without UQ it is difficult to make rational comparisons between predictions and observations. Particularly, it is not possible to conclude whether disagreements are due to model deficiencies or parametric uncertainties. We have pursued two UQ strategies, one "intrusive", requiring reformulation of the model governing equations, and the other "non-intrusive", allowing the utilization of existing codes as black boxes.

2.2.1 Intrusive Spectral Polynomial-Chaos (PC) Reacting Flow UQ

In this approach, uncertain quantities are presumed to depend on random variables, where this dependence is described using spectral polynomial chaos (PC) expansions. By substituting these expansions into the governing equations and applying a Galerkin projection, we arrive at reformulated governing equations. We have implemented this approach for low Mach number reacting flow with detailed kinetics. We have also derived new

approaches for propagation of PC expansions in non-polynomial terms, such as inversion, logarithms, exponentiation. The resulting construction was used for UQ in a 1D premixed H_2-O_2 flame using a 9-species, 19-step mechanism. Tests revealed a need for an alternate, non-gaussian, basis for the spectral expansions. The gaussian measure requires high order in the PC expansion to avoid negative values of strictly-positive physical quantities. This translates into a large computational challenge. No practical high-order was sufficient to maintain stability given the extreme non-linearities of the chemical source terms and associated fast rate of growth of the uncertainty. Remedies for this problem, involving the use of alternate spectral basis functions, are under further investigation, as discussed below.

We investigated one alternative basis, the Haar wavelets. This was done primarily to address situations with fast growth rate of uncertainty. It proved to be efficient in representing system behavior in the vicinity of steep discontinuities, but not sufficiently so in the context of smooth functions. Thus, it may well be a useful piece of the overall machinery in the context of an adaptive construction that uses different bases in different regions of the solution. We used this basis to study Rayleigh-Benard convection, where the degree of unstable temperature/density stratification determines whether pure conduction or convection is dominant. The results showed high fidelity in the description of this bifurcation boundary.

2.2.2 Non-intrusive Spectral PC Reacting Flow UQ

In this construction, spectral PC expansions are also used for model parameters. However, conventional (deterministic) reacting flow codes are used, with parameter values that are sampled from their assigned distributions. In this way, many sample runs of the deterministic model are computed, and the results used to evaluate the PC mode strengths of the model outputs. This is an attractive alternative to the intrusive approach, because it leverages investments in deterministic reacting flow solvers. Moreover, it does not suffer the stability challenges associated with the gaussian measure, non-linear terms, and fast rate of growth of uncertainties. On the other hand, computational costs can become impractical if a large number of samples is required. In this particular area, sampling techniques are key.

We had previously computed a 1D H_2-O_2 flame under super-critical water oxidation conditions. This study used Latin-Hypercube sampling (LHS), which required ~20,000 samples for the statistics to converge. While this is doable with a 1D steady hydrogen flame, it is not practical with more complex reacting flow. We investigated an alternative sampling strategy, based on the conceptual reformulation of the problem as an integration problem. The result was a Gauss-Hermite sampling (GHS) approach which uses the GH quadrature points as samples in 1D, and a corresponding tensor product in multi-D. The advantage here pertained to the need for far fewer samples to evaluate the necessary moments for small numbers of uncertain parameters. Thus, for example, only 81 samples were necessary for convergence with 3 uncertain parameters, versus thousands for LHS. This success dissipated however with higher numbers of uncertain parameters. With ~10 uncertain parameters, GHS was even less efficient than LHS, as both suffer from the curse of dimensionality. More optimal approaches are outlined below.

2.3 Computational Reacting Flow Toolkit

We continued to work on the development of a common-component-architecture (CCA) reacting flow code toolkit for enabling multi-D high-order adaptive mesh refinement (AMR) reacting flow computations. We implemented high-order spatial derivative and interpolation stencils, including filtering operators. We demonstrated computations of the heat equation on a 3-mesh-level adaptive mesh with up to 8th order spatial accuracy. Results suggest advantages for the high-order approach in terms of flattening the mesh hierarchy for equivalent discretization errors. We have also applied operator-split reaction/diffusion time integartion constructions based on a stabilized explicit Runge-Kutta-Chebyshev (RKC) integration for the diffusion operator, and a stiff ODE integrator (CVODE) for the chemical source terms. We have demonstrated high-order reaction-diffusion computations of an H_2-O_2 mixture with detailed kinetics and mixture averaged transport. Work is in progress on the assembly of momentum solution components to arrive at an AMR projection-scheme solver. We have also worked on the development and testing of Half-Explicit Methods (HEMs) for the solution of differential-algebraic eqns. that offer a promise of more robust momentum solvers in low Mach number reacting flow. We have tested HEM methods in the context of simple model problems, and are in the process of implementing them in a more realistic context. We have also implemented two transport libraries (DRFM & EGLIB) as components, and are in the process of testing and comparing their performance and accuracy.

2.4 Computational Singular Perturbation (CSP) Analysis

We have continued to develop CSP analysis tools for multi-D reacting flow analysis. This work has progressed to a point where stable and robust algorithmic structure is being pursued to reduce the sensitivity to computational noise in the data, by improving the condition numbers of matrices being operated on. We have also implemented key elements of the CSP analysis machinery into components under CCA, and have demonstrated component-based CSP analysis of AMR-computed H_2-O_2 ignition data. One clear outcome of this was the clear need for high-order spatial accuracy (higher than second) and/or robust analysis algorithms for handling internal mesh-boundary data, due to small discretization errors resulting from local interpolations. We have demonstrated refinement strategies for reducing errors in CSP analysis, and are in the process of improving the associated algorithms in terms of robustness.

3 Future Plans

3.1 Premixed Flame-Vortex Interactions

Given the resolved qualitative disagreements between experiments and numerics in the flame-vortex interaction, our next goal is the use of automatic chemical mechanism reduction based on computational singular perturbation (CSP) theory, and its application in the context of adaptive chemistry computations in 2D reacting flow. Our work on flame analysis with CSP has clearly showed the spatiotemporal variability of low-dimensional manifolds during the CH_4-air flame-vortex interaction. This points out the need for adaptive chemical mechanism reduction. A single globally simplified/reduced mechanism will by necessity have to satisfy all flame conditions, and therefore would be constrained by the primary flame reaction zone to be effectively very close to the full detailed mechanism. Instead, being able to handle different reduced mechanisms in different regions of the flow allows optimal mechanism reduction. This adaptive chemistry target is feasible in transient flow only with the availability of the CSP analysis tools that we have worked on so far. We will also pursue computational studies of vortex-flame interaction in the context of an opposed jet burner, where the experimental characteristics of the vortex and flame are more controllable. In this context, we should be able to pursue more quantitative comparisons with the experimentally observed transient flame behavior.

3.2 Uncertainty Quantification

3.2.1 Intrusive Spectral Polynomial-Chaos (PC) Reacting Flow UQ

In order to address intrusive PC challenges, it is necessary to use a formulation which preserves the non-negativity of physical quantities even when uncertainties are large, non-linearities are extreme, and relatively low PC order is utilized. While this is possible with the Haar-wavelet approach, this basis is primarily useful in the vicinity of sharp transitions. The Hermite-Gaussian PC implementation does not meet the necessary requirements either. On the other hand, other combinations of orthogonal polynomials and their associated measures are potential alternative options. Thus, for example, the Laguerre polynomials will satisfy the necessary orthogonality relation with respect to the Gamma distribution $G(\alpha, 1)$ on the domain $[0, \infty)$ and with $\alpha > -1$. This and other options for orthogonal polynomial members of the *Askey scheme* will be investigated as alternative basis for the intrusive PC construction. The use of these bases in a mixed-adaptive construction is also of interest as a potentially optimal choice.

3.2.2 Non-intrusive Spectral PC Reacting Flow UQ

The main challenge with the non-intrusive approach is the curse dimensionality. LHS requires too many samples, even with small (~3) numbers of uncertain parameters. GHS requires a number of samples that scales exponentially with the number of dimensions, thus failing at $O(10)$ uncertain parameters. One seemingly viable alternative uses sparse-quadrature, or cubature. Sparse-quadrature sampling (SQS) uses quadrature formulas that are designed for a multi-D, not built based on products of 1D formulae as with GHS. Further, there are well established results on the efficiency of the SQ formulae for multi-D integration. The number of samples does *not* depend exponentially on the number of uncertain dimensions. It has a much milder dependence, which, for about 10 parameters should require on the order of 200 samples only! Thus, there is reason to expect this approach to provide the best means of achieving converged sampling statistics with a realistic number of model runs.

3.3 Computational Reacting Flow Toolkit

We will continue to assemble and test components for reacting flow computations. We are presently testing and debugging a range of high-order interpolants and boundary stencils for both cell-centered and vertex-centered discretizations. We are also working on comparisons of the performance of different transport packages, which have been incorporated under CCA.

3.4 Computational Singular Perturbation Analysis

We will proceed to incorporate more of the CSP machinery under CCA, to arrive at a full suite of analysis codes in the CCA CFRFS reacting flow toolkit. We will also proceed further towards automatic CSP-based chemical reduction, techniques for enabling adaptive chemistry computations based on real-time mechanism choice/reduction, and adaptive tabulation methods for tabulating either the results of CSP analysis or the mechanism choice corresponding to particular state and source-term vectors.

4 DOE-Supported Publications [2001-2003]

[1] Valorani, M., Najm, H.N., and Goussis, D., CSP Analysis of a Transient Flame-Vortex Interaction: Time Scales and Manifolds, *Combustion and Flame* (2003) in press.

[2] Pébay, P.P., Half-Explicit Runge-Kutta Scheme for Low Mach Number Reacting Flows, *Appl. Num. Meth.* (2003) submitted.

[3] Pébay, P.P., Half-Explicit Methods and the Modified Kaps Problem, *Compt. Rendue Acad. Sci. Paris, Serie I Mathematiques* (2003) submitted.

[4] Reagan, M.T., Najm, H.N., Ghanem, R.G., and Knio, O.M., Uncertainty Quantification in Reacting Flow Simulations Through Non-Intrusive Spectral Projection, *Combustion and Flame*, 132 (2003) in press.

[5] Le Maître, O.P., Ghanem, R.G., Knio, O.M., and Najm, H.N., Uncertainty Propagation using Wiener-Haar Expansions, *J. Comp. Phys.* (2003) submitted.

[6] Le Maître, O.P., Reagan, M.T., Debusschere, B.D., Najm, H.N., Ghanem, R.G., and Knio, O.M., Natural Convection in a Closed Cavity under Stochastic, Non-Boussinesq conditions, *SIAM J. Scientific Computing* (2003) submitted.

[7] Debusschere, B.J., Najm, H.N., Matta, A., Knio, O.M., Ghanem, R.G., and Le Maître, O.P., Protein Labeling Reactions in Electrochemical Microchannel Flow: Numerical Simulation and Uncertainty Propagation, *Phys. Fluids* (2003) in press.

[8] Najm, H.N., Knio, O.M., and Paul, P.H., Role of Transport Properties in the Transient Response of Premixed Methane-Air Flames, *Proc. Comb. Inst.*, 29 (2002) in press.

[9] Le Maître, O.P., Reagan, M.T., Najm, H.N., Ghanem, R.G., and Knio, O.M., A Stochastic Projection Method for Fluid Flow II. Random Process, *J. Comp. Phys.*, 181:9–44 (2002).

[10] Najm, H.N., Paul, P.H., McIlroy, A., and Knio, O.M., A Numerical and Experimental Investigation of Premixed Methane-Air Flame Transient Response, *Combustion and Flame*, 125(1-2):879–892 (2001).

[11] Knio, O.M., and Najm, H.N., Numerical Simulation of Unsteady Reacting Flow with Detailed Kinetics, in *Computational Fluid and Solid Mechanics* (K. Bathe, Ed.), volume 2, Elsevier, 2001, , pp. 1261–1264.

[12] Le Maître, O.P., Knio, O.M., Najm, H.N., and Ghanem, R.G., A Stochastic Projection Method for Fluid Flow I. Basic Formulation, *J. Comp. Phys.*, 173:481–511 (2001).

[13] Najm, H.N., Paul, P.H., Knio, O.M., and McIlroy, A., Transient Response of Premixed Methane-Air Flames, in *Computational Fluid and Solid Mechanics* (K. Bathe, Ed.), volume 2, Elsevier, 2001, , pp. 1334–1337.

Free Radical Chemistry and Photochemistry

Daniel M. Neumark
Chemical Sciences Division
Lawrence Berkeley National Laboratory
Berkeley, CA 94720
dan@radon.cchem.berkeley.edu

Program Scope

Although much time and effort has been invested in modeling combustion chemistry, many of the primary processes involved in combustion are poorly understood. In many cases, the primary chemistry of the reactions in combustion models and the thermochemistry of the species involved in these reactions are not known. Examples include the reactions leading to soot formation in flames, and reactions in which NO is produced as a by-product of combustion. Our research program is focused on the photodissociation, photoionization, and bimolecular reaction dynamics of free radicals, with particular emphasis on radicals and radical reactions that play an important role in combustion chemistry. The photodissociation experiments map out the dissociative electronic states of free radicals, the primary photochemical products, and the kinetic energy and angular distribution for each product channel. From this information we can extract bond dissociation energies and heats of formation, and determine whether dissociation occurs on an excited state or by internal conversion to the ground state followed by statistical unimolecular decay. The photoionization experiments yield absolute photoionization cross sections for polyatomic free radicals such as vinyl and propargyl; these cross sections will be exceedingly useful in flame diagnostics experiments based on photoionization. The bimolecular reaction dynamics experiments will focus on identifying and characterizing primary products from the oxidation reactions of the C_2H_3 and CH radicals.

Three instruments are used in these studies: a fast radical beam photofragment translational spectrometer, in which radicals are generated by photodetachment of mass-selected negative ions, and two neutral beam instruments, one which uses electron impact ionization of products and the other (Endstation 1 at the Advanced Light Source) based on ionization of scattered product s by tunable vacuum ultraviolet light.

Recent Progress

The photodissociation dynamics of 1,2- and 1,3- butadiene were investigated at 193 nm using molecular beam photofragment translational spectroscopy. In the 193 nm photodissociation of 1,2-butadiene, two product channels are observed: $CH_3 + C_3H_3$ and $C_4H_5 + H$. Both are bond fission channels; no evidence of products from isomerization to 1,3-butadiene was seen. The C_3H_3 product is identified as the propargyl radical through measurement of its photoionization efficiency curve, whereas the C_4H_5 product cannot be identified definitively. The propargyl channel dominates by approximately 10:1. The translational energy $P(E_T)$ distributions suggest that both channels result from internal conversion to the ground electronic state followed by dissociation. The $P(E_T)$ distribution for the C_4H_5 product was sharply truncated below 7 kcal/mol, indicating spontaneous decomposition of the slowest C_4H_5 product.

The photodissociation dynamics of 1,3-butadiene at 193 nm are considerably more complex. Five product channels are evident from this study: $C_4H_5 + H$, $C_3H_3 + CH_3$, $C_2H_3 + C_2H_3$, $C_4H_4 + H_2$, and $C_2H_4 + C_2H_2$. The translational energy ($P(E_T)$) distributions suggest that these channels result from internal conversion to the ground electronic state followed by statistical unimolecular dissociation; those for the radical production channels peak near zero energy, while those for the molecular elimination channels peak near 20 kcal/mol, characteristic of an exit barrier associated with

a tight transition state. Further studies were carried out using 1,3-butadiene-1,1,4,4-d_4. While the radical channels produced by the dissociation of 1,3-butadiene-1,1,4,4-d_4 could be fit with the $P(E_T)$ distributions obtained from 1,3-butadiene dissociation, the molecular channels required a unique $P(E_T)$ distribution for each product isotopic combination, suggesting the presence of multiple reaction pathways. Branching ratios were determined for the channels listed above using a molecular beam photodissociation instrument with electron impact ionization. These measurements showed C_3H_3 + CH_3 to be the dominant channel. This channel arises from isomerization to 1,2-butadiene on the ground state surface followed by C-C bond fission.

We have recently worked out a scheme by which one can measure absolute photoionization cross sections for free radicals by carrying out photodissociation experiments on Endstation 1. In these experiments, stable molecules are dissociated and both fragments are detected by photoionization with vacuum ultraviolet light. If the absolute photoionization cross section is known for one fragment (a Cl atom, for example), then it can be determined for the other fragment, typically a polyatomic radical. We have used this scheme to obtain absolute photoionization cross sections for the vinyl and propargyl radical from (approximately) 8-11 eV. The determination of these cross sections is central to many of the planned research projects on the Chemical Dynamics Beamline. For example, the determination of branching ratios on both crossed molecular beam and photodissociation experiments on Endstation 1 requires knowledge of the absolute cross sections for the various bimolecular and unimolecular products. A recently implemented flame diagnostics experiment on Endstation 3, in which one measures the photoionization mass spectrum of species in a flame as a function of distance from the burner, can yield quantitative number density data only if absolute photoionization cross sections are known for the species being measured. Finally, planned high resolution radical photoionization measurements on Endstation 2 can also be put on an absolute scale if the cross section is known at a small number of photon energies.

Future Plans

A new detection system based on photofragment coincidence imaging has just been installed on the fast radical beam instrument that will significantly augment the capabilities of this instrument, yielding both improved photofragment collection efficiency and the ability to study dissociation events involving multi-body decay. Its first application has been to examine the three-body decay of $I_2^-\cdot Ar$. It will be next be applied to photodissociation of HCNN, fluorovinoxy, and the larger alkoxy radicals (with three or more carbon atoms).

Radical photodissociation and crossed beam experiments will be carried out on a crossed molecular beams instrument utilizing electron impact ionization of the scattered products. As part of this program, we will develop molecular beam radical sources via laser photolysis of stable precursor molecules. Target systems for radical photodissociation include the vinoxy and ethoxy radicals in order to characterize the H-atom loss channel from both species. Although both of these radicals have been studied previously on our fast beam instrument, the H-atom loss channel is difficult to characterize on that instrument because the large mass disparity between the two photofragments complicates their coincident detection. The bimolecular reaction dynamics experiments will focus on oxidation reactions of the C_2H_3 and CH radicals. The CH + N_2 reaction is also of particular interest because of its role in the mechanism for prompt NO formation in flames; one of the unifying themes of our program is to characterize of the potential energy surface for this reaction by photodissociation of the HNCN and HCNN radicals and by reactive scattering of CH + N_2. While rate constants for many of these reactions have been determined, identification of the primary products and their branching ratios has been challenging, and the proposed dynamics experiments will address this issue directly.

DOE-supported publications (2001-present):

"Photoisomerization and photodissociation pathways of the NCN, CNN, and HNCN radicals", R. T. Bise, A. A. Hoops, H. Choi, and D. M. Neumark, ACS Symposium Series **770**, 296 (2001).

"Photodissociation and photoisomerization pathways of the HNCN free radical" R. T. Bise, A. A. Hoops, and D. M. Neumark, J. Chem. Phys. **114**, 9000 (2001).

"State-resolved translational energy distributions for NCO photodissociation" A. A. Hoops, R. T. Bise, J. R. Gascooke, and D. M. Neumark, J. Chem Phys. **114**, 9020 (2001).

"Photofragment translational spectroscopy of 1,2-butadiene at 193 nm" J. C. Robinson, W. Z. Sun, S. A. Harris, F. Qi, and D. M. Neumark, J. Chem. Phys. **115**, 8359 (2001).

"Photofragment translational spectroscopy of 1,3-butadiene and 1,3-butadiene-1,1,4,4-d4 at 193 nm" J. C. Robinson, S. A. Harris, W. Sun, N. E. Sveum, and D. M. Neumark, J. Am. Chem. Soc. **124**, 10211 (2002).

"An ab initio/RRKM study of product branching ratios in the photodissociation of buta-1,2- and -1,3-dienes and but-2-yne at 193 nm" H. Y. Lee, V. V. Kislov, S. H. Lin, A. M. Mebel, and D. M. Neumark, Chemistry--A European Journal **9**, 726 (2003).

"Fast beam studies of I_2^- and $I_2^-\cdot$Ar photodissociation", A. A. Hoops, J. R. Gascooke, A. E. Faulhaber, K. E. Kautzman, and D. M. Neumark, Chem. Phys. Lett. (in press).

High-Resolution Photoionization and Photoelectron Studies: Determination of Accurate Energetic Database for Combustion Chemistry

C. Y. Ng

Department of Chemistry, University of California at Davis
One Shields Avenue, Davis, California 95616
E-mail Address: cyng@chem.ucdavis.edu

Program scope: The main goal of this project is to obtain accurate thermochemical data, such as ionization energies, dissociative photoionization thresholds, bond dissociation energies, and 0 K heats of formation (ΔH°_{f0}'s) for small and medium sizes molecular species and their ions of relevance to combustion chemistry. Accurate thermochemical data determined by high-resolution photoionization and photoelectron studies for selected polyatomic neutrals and their ions are also useful for the development of the next generation of *ab initio* quantum computational procedures.

Selected recent progress:

1. X.-M. Qian, Y. Song, K.-C. Lau, C. Y. Ng, J. Liu, W. Chen, and G.-Z. He, "A Pulsed Field Ionization Study of the Reaction $D_2O + h\nu \rightarrow OD^+ + D + e^-$", *Chem. Phys. Lett.* <u>353</u>, 19-26 (2002).

    We have examined the dissociative photoionization reaction $D_2O + h\nu \rightarrow OD^+ + D + e^-$ near its threshold using the pulsed field ionization photoelectron-photoion coincidence method. The measured 0 K threshold (18.220±0.002 eV) has made possible the determination more precise values for the 0 K bond dissociation energies for D-DO$^+$ (5.584±0.002 eV) and D-OD (5.191±0.002 eV) and the ΔH°_{f0}'s for OD$^+$ (308.83±0.05 kcal/mol) and OD (8.38±0.05 kcal/mol). We found that the available energetic data for the OD/OD$^+$ and D_2O/D_2O^+ system are in excellent agreement with those obtained recently for the OH/OH$^+$ and H_2O/H_2O^+ system after taking into account the zero-point-vibration-energies of these species.

2. W. Chen, M. Hochlaf, P. Rosmus, G.-Z. He, and C. Y. Ng, "Vacuum Ultraviolet Pulsed Field Ionization Photoelectron Study of OCS in the Energy range of 15.0-19.0 eV", *J. Chem. Phys.* <u>116</u>, 5612-5621 (2002).

    Vacuum ultraviolet pulsed field ionization-photoelectron (PFI-PE) spectra for OCS have been obtained in the energy range 15.0-19.0 eV, covering the vibronic bands of OCS$^+$($A^2\Pi$, $B^2\Sigma^+$, and $C^2\Sigma^+$). The ionization energies for the formation of the ground vibrational levels of OCS$^+$($A^2\Pi_{3/2}$, $A^2\Pi_{1/2}$, $B^2\Sigma^+$, and $C^2\Sigma^+$) from the ground OCS($X^1\Sigma^+$) state have been determined as 15.0759±0.0005 eV, 15.0901±0.0005 eV, 16.0403±0.0005 eV, and 17.9552±0.0005 eV, respectively. We have also generated the theoretical adiabatic three dimensional potential energy functions (PEFs) for OCS$^+$($A^2\Pi$) by employing the complete active space self-consistent field and internally contracted multi-reference configuration interaction methods. Using these PEFs, the spectroscopic constants and low-lying rovibronic energy levels for

$OCS^+(A^2\Pi)$ are calculated variationally. These calculations have made possible the identification of many PFI-PE vibronic bands for $OCS^+(A^2\Pi)$, which are originated from vibronic and Fermi resonance interactions. Owing to the different equilibrium geometries between the $OCS^+(A^2\Pi)$ and $OCS(X^1\Sigma^+)$ states, the PFI-PE spectrum for $OCS^+(A^2\Pi)$ exhibits a long vibronic progression extending well above the $OCS^+(B^2\Sigma^+)$ state. On the contrary, the PFI-PE spectra for $OCS^+(B^2\Sigma^+,$ and $C^2\Sigma^+)$ are overwhelmingly dominated by the ground (0,0,0) bands, exhibiting only weak vibrational progressions.

3.   H. K. Woo, Jiping Zhan, K.-C. Lau, C. Y. Ng, and Y.-S. Cheung, "Vacuum Ultraviolet Laser Pulsed Field Ionization Photoelectron Study of cis-2-Butene", *J. Chem. Phys.* <u>116</u>, 8803-8808 (2002).

The VUV PFI-PE spectra of supersonically cooled *cis*-2-butene (*cis*-CH$_3$CH=CHCH$_3$) have been measured in the photon energy range of 73,560–75,460 cm^{-1}. Using the *ab initio* theoretical rotational constants of *cis*-CH$_3$CH=CHCH$_3$ and its cation (*cis*-CH$_3$CH=CHCH$_3^+$) and a semi-empirical simulation scheme, we have obtained a good fit of the origin vibrational band with partially resolved contours of rotational branches. After taking into account the Stark shift, the ionization energy of *cis*-CH$_3$CH=CHCH$_3$ is determined as 73,595.0±1.5 cm^{-1}. Guided by *ab initio* vibrational frequency calculations, we have also assigned the vibrational bands observed for *cis*-CH$_3$CH=CHCH$_3^+$ in its ground state.

4.   J. Liu, W. Chen, M. Hochlaf, X.-M. Qian, C. Chang, and C. Y. Ng, "Unimolecular Decay Pathways of State-Selected CO_2^+ in the Internal Energy Range of 5.2-6.2 eV: An Experimental and Theoretical Study", *J. Chem. Phys.* <u>118</u>, 149-163 (2003).

The VUV PFI-PE spectrum of CO_2 has been measured in the energy region of 19.0-20.0 eV. The vibrational bands resolved for $CO_2^+(C^2\Sigma_g^+)$ are overwhelmingly dominated by the origin band along with weak vibrational bands corresponding to excitations of the v_1^+ (symmetric stretching), v_2^+ (bending), and v_3^+ (anti-symmetric stretching) modes. The simulation of the rotational contour resolved in the origin PFI-PE band yields a value of 19.3911±0.0005 eV for the ionization energy of CO_2 to form $CO_2^+(C^2\Sigma_g^+)$. A PFI-PE peak is found to coincide with each of the 0 K dissociation thresholds for the formation of $O^+(^4S) + CO(X^1\Sigma^+)$ and $CO^+(X^2\Sigma^+) + O(^3P)$. This observation is tentatively interpreted to result from the lifetime switching effect, arising from the prompt dissociation of excited CO_2 in high-*n* (n≥100) Rydberg states prior to PFI. We have also examined the decay pathways for state-selected CO_2^+ in the internal energy range of 5.2-6.2 eV using the PFI-PE-photoion coincidence scheme. The coincidence TOF data show unambiguously the formation of $O^+(^4S) + CO(X^1\Sigma^+;$ v''= 0, 1) and $CO^+(X^2\Sigma^+;$ v$^+$= 0, 1) + O(^3P). Analysis of the kinetic energy releases of fragment ions suggests that the dissociation of excited CO_2^+ involved is non-statistical and proceeds with an impulsive mechanism. Potential energy functions for the $CO_2^+(C^2\Sigma_g^+)$ state and the lowest quartet states of CO_2^+, together with their spin-orbit interactions, have been calculated using the complete active space self-consistent field and internal contracted multi-reference configuration interaction methods. Based on these PEFs, vibrational levels for $CO_2^+(C^2\Sigma_g^+)$ have been also calculated using a variational approach. With the aid of these theoretical

calculations, vibrational bands resolved in the PFI-PE spectrum for $CO_2^+(C^2\Sigma_g^+)$ have been satisfactorily assigned, yielding a v_3^+ value of 2997 cm^{-1}. The theoretical calculation also provides a rationalization that the predissociation for $CO_2^+(C^2\Sigma_g^+)$ to form $O^+(^4S) + CO(X^1\Sigma^+)$ and $CO^+(X^2\Sigma^+) + O(^3P)$ most likely proceeds via the repulsive $a^4\Sigma_g^-$ and $b^4\Pi_u$ (or $^4B_1$ in a bent geometry) states.

Future Plans:

We are making excellent progress in the photoionization studies of radicals. Using an excimer laser photodissociation radical sources, we have produced and successfully obtained the photoionization efficiency (PIE) spectra for a series of radicals, including methyl radicals (CH_3), vinyl radicals (C_2H_3), propargyl radicals (C_3H_3), and chlorocarbonyl radicals (ClCO), and phenyl radicals (C_6H_5). Reliable ionization energies have been obtained for these radicals. The measured PIE spectra for photofragments also provide valuable information on their internal energy contents acquired in the photodissociation processes. We are currently learning how to perform PFI-PE measurements on these radicals that are of relevance to combustion and atmospheric chemistry.

Publications of DOE sponsored research (2001-present)

1   J. Liu, M. Hochlaf, G. Chambaud, P. Rosmus, and C. Y. Ng, "High Resolution Pulsed Field Ionization-Photoelectron Bands for $CS_2^+(A^2\Pi_u)$: An Experimental and Theoretical Study", *J. Phys. Chem.* **105**, 2183 (2001).

2   K.-M. Weitzel, G. Jarvis, M. Malow, Y. T. Baer, Song, and C. Y. Ng, "Observation of Accurate Ion Dissociation Thresholds in Pulsed Field Ionization Photoelectron Studies", *Phys. Rev. Lett.* **86**, 3526 (2001).

3   Y. Song, C. Y. Ng, G. Jarvis, and R. A. Dressler, "Rotational-Resolved Pulsed Field Ionization-Photoelectron Study of $NO^+(A'^1\Sigma^-, v^+ = 0\text{-}17)$ in the Energy Range of 17.79-20.10 eV", *J. Chem. Phys.* **115**, 2101-2108 (2001).

4   Y. Song, X.-M. Qian, K.-C. Lau, C. Y. Ng, J. Liu and W. Chen, "High Resolution Energy-Selected Study of the Reaction $NH_3^+ \rightarrow NH_2^+ + H$: Accurate Thermochemistry for the NH_2/NH_2^+ and NH_3/NH_3^+ Systems", *J. Chem. Phys.* **115**, 2582-2589 (2001).

5   Y. Song, X.-M. Qian, K.-C. Lau, C. Y. Ng, J. Liu and W. Chen, "High Resolution Energy-Selected Study of the Reactions $CH_3X^+ \rightarrow CH_3^+ + X$: Accurate Thermochemistry for the CH_3X/CH_3X^+ (X= Br and I) System", *J. Chem. Phys.* **115**, 4095 (2001).

6   X.-M. Qian, Y. Song, K.-C. Lau, C. Y. Ng, J. Liu and W. Chen, "A Pulsed Field Ionization Study of the Dissociative Photoionization Reaction $CD_4 + h\nu \rightarrow CD_3^+ + D + e^-$", *Chem. Phys. Lett.* **347**, 51-58 (2001).

7   D. G. Fedorov, M. S. Gordon, Y. Song, and C. Y. Ng, "A Theoretical Study of the Spin-orbit coupling in $O_2^+(A^2\Pi_{3/2,1/2u}, v^+=0\text{-}15; a^4\Pi_{5/2,3/2,1/2,-1/2u}, v^+=0\text{-}18)$", *J. Chem. Phys.* **115**, 7393-7400 (2001).

8 X.-M. Qian, Y. Song, K.-C. Lau, C. Y. Ng, J. Liu, W. Chen, and G.-Z. He, "A Pulsed Field Ionization Study of the Reaction $D_2O + h\nu \rightarrow OD^+ + D + e^{-}$", *Chem. Phys. Lett.* **353**, 19-26 (2002).

9 Branko Ruscic, Albert F. Wagner, Lawrence B. Harding, Robert L. Asher, David Feller, Kirk A. Peterson, Y. Song, X.-M. Qian, C.Y. Ng, J. Liu, and W. Chen, "On the Enthalpy of Formation of Hydroxyl Radical and Gas-Phase Dissociation energies of Water and Hydroxyl", *J. Phys. Chem.* **A106**, 2727-2747 (2002).

10 C. Y. Ng, "Vacuum Ultraviolet Spectroscopy and Chemistry Using Photoionization and Photoelectron Methods", *Ann. Rev. Phys. Chem.* **53**, 101-140 (2002).

11 W. Chen, M. Hochlaf, P. Rosmus, G.-Z. He, and C. Y. Ng, "Vacuum Ultraviolet Pulsed Field Ionization Photoelectron Study of OCS in the Energy range of 15.0-19.0 eV", *J. Chem. Phys.* **116**, 5612 (2002).

12 H. K. Woo, J.-P. Zhan, K.-C. Lau, C. Y. Ng, and Y.-S. Cheung, "Vacuum Ultraviolet Laser Pulsed Field Ionization Photoelectron Study of cis-2-Butene", *J. Chem. Phys.* **116**, 8803 (2002).

13 C. Y. Ng, "State-Selected and State-to-State Ion-Molecule Reaction Dynamics", *J. Phys. Chem. (Invited Feature Article)*, **A106**, 5952-5966 (2002).

14 Y.-J. Chen, P. T. Fenn, K.-C. Lau, C. Y. Ng, C.-K. Law, and W.-K. Li, "A Study of the Dissociation of $CH_3SCH_3^+$ by Collisional Activation: Evidence of Non-Statistical Behavior", *J. Phys. Chem.* **A106**, 9729 (2002).

15 Y.-S. Cheung, C. Y. Ng, S.-W. Chiu, and W.-K. Li, "Application of Three-Center-Four-Electron Bonding for Structural and Stability Predictions of Main Group Hypervalent Molecules: The Fulfillment of Octet Shell Rule", *J. Mol. Struct., Theochem.* **623**, 1-10 (2003).

16 J. Liu, W. Chen, M. Hochlaf, X.-M. Qian, C. Chang, and C. Y. Ng, "Unimolecular Decay Pathways of State-Selected CO_2^+ in the Internal Energy Range of 5.2-6.2 eV: An Experimental and Theoretical Study", *J. Chem. Phys.* **118**, 149 (2003).

17 X. M. Qian, T. Zhang, Y. Chiu, D. J. Levandier, J. S, Miller, R. A. Dressler, and C. Y. Ng,, "Rovibrational State-Selected Study of $H_2^+(X, v^+=0\text{-}17, N^+=1)+Ar$ Using the Pulsed Field Ionization-Photoelectron-Secondary Ion Coincidence Scheme", *J. Chem. Phys. (communication)*, **118**, 2455 (2003).

18 J. Liu, M. Hochlaf, and C. Y. Ng, "Pulsed Field Ionization-Photoelectron Bands for CS_2^+ in the Energy Range of 13.2 −17.6 eV: An Experimental and Theoretical Study", *J. Chem. Phys.* **118**, 4487 (2003).

19 W. Chen, J. Liu, and C. Y. Ng, "Vacuum Ultraviolet Pulsed Field Ionization-Photoelectron Study for N_2O^+ in the Energy Range of 16.3 - 21.0 eV", *J. Phys. Chem.* A, accepted.

20 X.-M. Qian, Andy Kung, T. Zhang, and C. Y. Ng, "Two-Color Photoionization Spectroscopy Using Vacuum Ultraviolet Synchrotron Radiation and Infrared Optical Parametric Oscillator Laser Source, *Rev. Sci. Instrum.*, accepted.

KINETICS AND DYNAMICS OF COMBUSTION CHEMISTRY

David L. Osborn
Combustion Research Facility, Mail Stop 9055
Sandia National Laboratories
Livermore, CA 94551-0969
Telephone: (925) 294-4622
Email: dlosbor@sandia.gov

PROGRAM SCOPE

The goal of this program is to elucidate mechanisms of elementary combustion reactions through the use of broadband and ultrasensitive optical spectroscopy. Two techniques are employed. First, time-resolved Fourier transform spectroscopy (TR-FTS) is used to probe multiple reactants and products with broad spectral coverage (> 1000 cm^{-1}), moderate spectral resolution (0.1 cm^{-1}) and a wide range of temporal resolution (ns – ms). The inherently multiplexed nature of TR-FTS makes it possible to simultaneously measure product branching ratios, internal energy distributions, energy transfer, and spectroscopy of radical intermediates. Together with total rate coefficients, this additional information provides further constraints upon and insights into the potential energy surfaces that control chemical reactivity. Because of its broadband nature, the TR-FTS technique allows a global view of chemical reactions and energy transfer processes that would be difficult to achieve with narrow-band laser-based detection techniques.

Second, cavity-enhanced frequency modulation spectroscopy (a.k.a. NICE-OHMS) is used to provide an ultrasensitive, differential absorption spectroscopic probe. Proof of principle measurements have been made on stable closed- and open-shell species, with the goal of using this technique for measurements of chemical kinetics in flow cells and monitoring of species in flames. This cavity-enhanced FM spectroscopy technique provides very high sensitivity, the generality of absorption spectroscopy, and insensitivity to background absorptions that vary slowly with frequency. These advantages allow the suppression of secondary chemistry by increased dilution of reactive species while still retaining sufficient detection sensitivity.

RECENT PROGRESS

Photodissociation of dicyclopropyl ketone: isomerization produces allyl radicals

Due to some recent experimental improvements, we now have definitive data on this photodissociation that firmly resolves the question of the isomeric nature of the C$_3$H$_5$ product. We have recently completed a set of experiments on the photodissociation dynamics of dicyclopropyl ketone (DCPK), a symmetric ketone analogous to acetone. The original goal of this study was to determine whether DCPK is a suitable photolytic precursor for cyclopropyl radicals. Cyclopropyl (c-C$_3$H$_5$) is a prototype for radical isomerizations, a critically important process in combustion chemistry. The cyclopropyl radical can ring open to the allyl radical (CH$_2$CHCH$_2$) over a (calculated) 20 kcal/mol barrier, with an exothermicity of 32 kcal/mol. A clean source of cyclopropyl radicals is required to study this isomerization experimentally.

We have investigated the 193 nm photodissociation of DCPK using time-resolved FT emission spectroscopy from 800 – 4000 cm^{-1} with improved time-resolution of 100 ns. Following photolysis, prompt emission is seen from free CO, implying that the dissociation products are CO + 2C$_3$H$_5$. Prompt emission is also seen in the C-H stretching region, and in the IR fingerprint region from 800 – 1600 cm^{-1}, both of which are assigned to C$_3$H$_5$. The main question is whether the nascent hydrocarbon emission is due to cyclopropyl, allyl, or a mixture of the two radicals. We can answer this question by examining both the disposal of energy among the fragments and the IR fingerprint spectra of the nascent C$_3$H$_5$ radicals. To characterize energy distribution in this system,

we have examined the internal energy distribution (both vibrational and rotational) of the CO fragment using TR-FTS. In addition, the translational energy distribution of CO is explored using photofragment translational spectroscopy.

By examining time-resolved CO emission with 0.1 cm^{-1} resolution, we obtain nascent vibrational and rotational distributions. The vibrational distribution is fairly well described by a temperature of 2230 ± 170 K, or $<E_{vib}>$ = 1.4 ± 0.1 kcal/mol. Similarly, we can extract a nascent rotational temperature of ~ 2300 K, corresponding to $<E_{rot}>$(CO) ~ 4.6 kcal/mol. The center-of-mass translational energy deposited into CO is not measured in this three-body dissociation. Nevertheless we can gain some insight into the CO translational energy by measuring the lab-frame energy distribution using ion imaging techniques. The translational energy distribution has an average energy of 3.4 kcal/mol, and provides an upper limit for the center-of-mass translational energy. The total energy (T + V + R) in CO is therefore estimated as 8 – 10 kcal/mol.

In DCPK, photodissociation at 193 nm to CO + 2(c-C_3H_5) leaves only 29 kcal/mol of available energy (compared to 53 in acetone). Deposition of 8-10 kcal/mol in CO would leave only 19 – 21 kcal/mol of total internal energy in the two C_3H_5 fragments if they are cyclopropyl radicals. This amount of energy is insufficient for isomerization. However, a two-step, phase-space-theory model for the vibrational distribution of CO shows that dissociation producing cyclopropyl radicals will produce > 99% of the CO molecules in their zero-point level, clearly inconsistent with the data. In contrast, photodissociation to the ring-opened products, CO + 2(allyl), yields 92 kcal/mol of available energy, and the PST predictions for CO are closer to the experimental distributions. Furthermore, an energetically favorable transition state for ring opening in the parent molecule exists on the ground state surface.
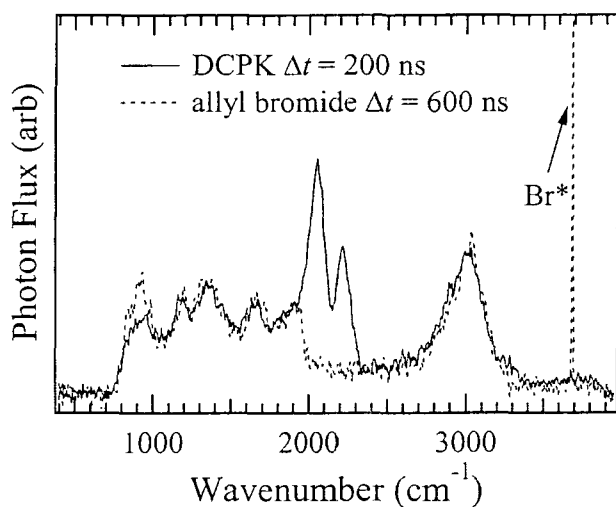
In addition to these energy balance arguments that point to allyl radical production, infrared spectroscopy of the C_3H_5 fragment also provides important isomeric evidence. Dissociation of allyl bromide at 193 nm is known to produce the allyl radical.[1] Fig. 1 shows a comparison of time-resolved FTIR spectra of allyl bromide and DCPK. Although the resolution (8 cm^{-1}) is modest, the good agreement between the spectra throughout the IR fingerprint region argues strongly that dissociation of DCPK at 193 nm produces allyl radicals.

We conclude that the mechanism most consistent with the experimental and theoretical data is internal conversion of the initially excited DCPK to S_0, followed by ring-opening isomerization of the parent molecule and dissociation producing CO + allyl + allyl. The availability of internal isomerization pathways and the influence of electronic delocalization make the dissociation of DCPK qualitatively different from aliphatic ketones.

The reaction of HCCO + O$_2$: experimental evidence of prompt CO$_2$ formation

Acetylene is a ubiquitous species present in the combustion of aliphatic and aromatic hydrocarbons.[2] Acetylene is oxidized in flames exclusively by oxygen atoms:

$$O + C_2H_2 \quad \rightarrow \quad {}^3CH_2 + CO \qquad \Delta H_{rxn} = -47.8 \text{ kcal/mol} \qquad (1a)$$
$$\rightarrow \quad HCCO + H \qquad \Delta H_{rxn} = -19.6 \text{ kcal/mol} \qquad (1b).$$

Shock tube experiments on the ignition of $C_2H_2/O_2/Ar$ mixtures[3] show formation of "prompt" CO_2, meaning that CO_2 is formed with the same time constant as CO. In a recent theoretical paper, Klippenstein, Miller, and Harding[4] proposed a new pathway for prompt CO_2 formation based on the oxidation of the ketenyl radical (HCCO):

$$HCCO + O_2 \rightarrow \quad H + CO + CO_2 \qquad \Delta H_{rxn} = -110.6 \text{ kcal/mol} \qquad (3a)$$
$$\rightarrow \quad OH + CO + CO \qquad \Delta H_{rxn} = -85.7 \text{ kcal/mol} \qquad (3b).$$

Their calculations predict that reaction (3a) represents ~90% of the products of HCCO + O_2.

Four reports of the total rate coefficient of reaction (3) appear in the literature,[5-8] but the identity of the products were not characterized. We applied emission-based TR-FTS to measure the branching ratio and state distributions of reaction (3). HCCO radicals are produced by 193 nm photolysis of ethyl ethynyl ether ($HCCOCH_2CH_3$).[9] Emission from hot HCCO is clearly observed in the $\Delta v_2 = -1$ bands from $1800 - 2040 \text{ cm}^{-1}$, and this emission decays rapidly due to vibrational energy transfer with the precursor. In the presence of O_2, strong emission from hot CO and CO_2 products is obvious. Both products are unambiguously identified at higher resolution from rotationally resolved spectra.

CO and CO_2 have identical rise times, indicating that H + CO + CO_2 is a major product channel, and that OH + CO $\rightarrow$ H + CO_2 is not the source of CO_2. No emission from OH is observed in this system, but two independent calibrations of the spectrometer's sensitivity to OH provide a limit to the branching ratio of $k_{3b} / k_3 \leq 10\%$, in agreement with theoretical predictions. Analysis of the data gives the product state distribution for CO, which can be fairly well fit by a vibrational temperature of 8400 ± 800 K. These results are consistent with the proposed reaction mechanism involving a 4-membered ring intermediate that dissociates to yield H + CO + CO_2. This measurement is the first experimental evidence that prompt CO_2 arises from the HCCO + O_2 reaction.

Ultrasensitive cavity-enhanced frequency modulation spectroscopy

We have built an ultra-sensitive laser absorption spectrometer based on the Noise Immune Cavity Enhanced Optical Heterodyne Molecular Spectroscopy technique (NICE-OHMS) developed by Ye, Hall and coworkers.[10] This technique utilizes frequency modulation (FM) spectroscopy to eliminate sources of technical noise, coupled with a high-finesse sample cavity to provide long absorption pathlengths. An amplitude and frequency-stabilized cw laser (Ti:Sapphire) is locked to a stable high finesse cavity and frequency modulated at 541 MHz, a value equal to the free spectral range (FSR) of the cavity. The carrier and sidebands are detected in transmission, and the heterodyne signal arising from molecular absorption is demodulated at 541 MHz to give the NICE-OHMS signal. While the future goal of this experiment is the detection of transient species in kinetics and flame environments, during this period we have built and tested the spectrometer on weak absorptions of two stable molecules: C_2H_2 and NO.

We have detected transitions in the $(1v_1+3v_3)$ combination band of C_2H_2 at 790.7 nm using mirrors of moderately high reflectivity that give a cavity finesse of 6850. The minimum detectable absorption with this system is $2.5 \times 10^{-10} \text{ cm}^{-1} \text{ Hz}^{-1/2}$, compared to a theoretical shot-noise limited

value of 3×10^{-12} cm^{-1} Hz$^{-1/2}$. Residual frequency noise in our particular Ti:Sapphire laser is the main reason the theoretical limit is not reached.

The spectrometer is nevertheless of sufficient sensitivity that we have recorded the first spectrum of the extremely weak (7 ← 0) vibrational overtone of NO near 796 nm. We have also measured absolute linestrengths and the corresponding vibrational band intensity of $S_v^0 = 2.2 \times 10^{-6}$ cm^{-2}atm^{-1}. The peak absorption cross section of these lines are ~ 7×10^{-26} cm^2/molecule. The measured band intensity is larger than the result obtained from extrapolation of lower overtone band intensities and will lead to a better determination of the electric dipole moment function of NO.

Future Plans

Another area of interest is chemical reactions that may not occur solely on the ground state potential energy surface, but produce radical products in low-lying electronically excited states. For example, in $C_2H_5 + O_2 \rightarrow C_2H_4 + HO_2$, production of HO_2 in its excited $\tilde{A}$ ($^2A'$) state is energetically allowed, and is a possible explanation for inconsistencies in data comparing the forward and reverse reactions. Detection of this species by TR-FTS via the $\tilde{A}$ ($^2A'$) $\rightarrow$ $\tilde{X}$ ($^2A''$) electronic emission would provide clear evidence that multiple electronic surfaces participate in this reaction.

Building upon detection of C_2H_2 and NO using the NICE-OHMS technique, we propose to extend this technique to the observation of transient free radicals. The first candidate radical will be NH_2, which has several attractive qualities for this experiment. First, NH_2 is easily produced from the 193 nm photolysis of NH_3 with no detrimental effects of photochemistry on the cell windows or the high finesse mirrors. Second, NH_2 has only one heavy atom, resulting in high rotational constants and relatively sparse rotational lines. Third, the low-lying $\tilde{A}$($^2A_1$) ← $\tilde{X}$ ($^2B_1$) transition of NH_2 is orders of magnitude stronger than vibrational overtone transitions and yet can be accessed using our current Ti:Sapphire laser in the 790 nm region. Proof of principle kinetics measurements on reactions of NH_2 will follow.

BES sponsored publications

D. L. Osborn and J. H. Frank, "Laser-induced fragmentation fluorescence detection of the vinyl radical and acetylene," *Chem. Phys. Lett.* **349**, 43 (2001).

J. Bood, A. McIlroy, and D. L. Osborn, "Cavity-enhanced Frequency Modulation Absorption Spectroscopy of the Sixth Overtone Band of Nitric Oxide." *Proc. SPIE*, vol. 4962, in press (2003).

D. L. Osborn, "The Reaction of HCCO + O_2: Experimental Evidence of Prompt CO_2 by Time-Resolved Fourier Transform Spectroscopy," *J. Phys. Chem. A*, in press (2003).

References

[1] J. D. DeSain, R. I. Thompson, S. D. Sharma, and R. F. Curl, *J. Chem. Phys.* **109** , 7803 (1998).
[2] H. Gg. Wagner, *Proc. Comb. Inst.* **17**, 3 (1979).
[3] J. B. Homer and G. B. Kistiakowsky, *J. Chem. Phys.* **1967**, 47 5290.
[4] S. J. Klippenstein, J. A. Miller, and L. B. Harding, *Proc. Comb. Inst.* **29** (2002), in press.
[5] J. Peeters, M. Schaekers, and C. Vinckier, *J. Phys. Chem.* **90**, 6552 (1986).
[6] F. Temps, H. Gg. Wagner, and M. Wolf, *Z. Phys. Chem.* **176**, 27 (1992).
[7] K. K. Murray, K. G. Unfried, G. P. Glass, and R. F. Curl, *Chem. Phys. Lett.* **192**, 512 (1992).
[8] S. A. Carl, Q. Sun, and J. Peeters, *J. Chem. Phys.* **114**, 10332 (2001).
[9] M. J. Krisch, J. L . Miller, L. J. Butler, H. Su, R. Bersohn, and J. Shu, *J. Chem. Phys.* in press (2003).
[10] J. Ye, L. S. Ma, and J. L. Hall, *J. Opt. Soc. Am. B* **15**, 6 (1998).

The Effect of Large Amplitude Motion on the Vibrational Level Structure and Dynamics of Internal Rotor Molecules

David S. Perry, Principal Investigator
University of Akron, Akron OH 44325-3601
DPerry@UAkron.edu

Introduction

In the presence of large amplitude motion, a molecular system no longer remains close to a well-defined reference geometry, which challenges the concepts of the traditional theory of molecular vibrations. Among the challenged concepts are normal modes and point group symmetry. The large amplitude coordinate may take on the character of a reaction coordinate along which one must continuously redefine the remaining "normal" coordinates. The consequences are that large amplitude motion can result in novel energy level structures and it can promote coupling between vibrations and hence accelerated IVR.

In this project, we examine the vibrational level structure of molecules with a single internal rotor including methanol, nitromethane, and methylamine. Vibrational fundamental and overtone spectra of the jet-cooled molecules are examined by cavity ringdown, FTIR spectroscopy, and photodissociation spectroscopy (IRLAPS). The ringdown experiments are done in our lab in Akron; the jet-FTIR is done in collaboration with Robert Sams at Pacific Northwest Labs (PNNL); the IRLAPS experiments are done in Thomas Rizzo's lab at the EPFL in Switzerland. To understand the level structures and vibrational mode coupling taking place, we employ high resolution analysis, quantum mechanical modeling, and *ab initio* calculations. Recent progress on several activities under this project is outlined below.

A. Inverted Torsional Tunneling in Methanol and Tests of the Vibrational Born-Oppenheimer Approximation

In previous work under this project,[1] we discovered the inverted torsional tunneling splitting in the asymmetric CH stretch vibrational states ($v_2=1$ and $v_9=1$). These results were successfully explained by our 4-dimensional model calculation that included the three CH stretch coordinates and the torsion.[2] Torsional motion interchanges the identities of the CH bonds *anti* and *gauche* to the OH, and the CH bonds in these positions have different force constants. A single lowest-order coupling term with the required symmetry (A_1 in G_6) was sufficient to reproduce the observed torsional structure. We concluded that the inverted torsional structure was a general phenomenon deriving from molecular symmetry and that the single coupling term results in a myriad of mixed vibrational states throughout the CH stretch-torsion manifold.

Subsequent spectroscopic reports[3] of other asymmetric vibrations, have confirmed the generality of the effect, and a number of theoretical studies[4] have contributed to our understanding. Most recently, Fehrensen, Luckhaus, Quack, Willeke, and Rizzo[5] have

used *ab initio* calculations, a Born-Oppenheimer separation of the torsion from the other vibrations and the concept of geometric phase to account for the torsional structure of excited methanol vibrational states. This successful treatment provides an appealing conceptual unity with electronic spectroscopy, particularly with the Jahn-Teller effect. It is difficult to test the range of applicability and accuracy of the Born Oppenheimer approximation because the relevant full-dimensional calculations needed as a reference are often intractable. In this vibrational case, our 4-dimensional model calculation is the reference calculation needed to evaluate a Born-Oppenheimer separation of the torsion from the three CH stretches. We are engaged in this test of the Born-Oppenheimer approximation to understand its limits of validity, the role of geometric phase, and the extent of nonadiabatic effects.

B. Slit-Jet Cavity-Ringdown Spectra of Methanol

The rotationally resolved overtone spectrum of the OH (v_1) + CH (v_3) stretch combination band of methanol between 6510 and 6550 cm^{-1} has been recorded at sub-Doppler resolution using continuous-wave cavity ringdown spectroscopy (CW-CRDS). The experimental sensitivity has been shown to be close to the theoretical shot noise limit. Of 572 recorded lines, 358 lines have been assigned by ground state combination differences, including the 21 subbands with J' up to 8 and K' up to 3. Perturbations of E $K' = -1$, -2, and -3 levels have been observed and deperturbations carried out. The torsion-rotation constants in the upper state have been obtained by fitting the observed spectrum to the Herbst Hamiltonian and they are found to be in a reasonable agreement with the extrapolated values based on the fundamental bands, v_1 and v_3. This combination band has fewer perturbations than the v_1 fundamental and the coupling matrix elements are smaller, 0.02 to 0.66 cm^{-1} as compared to 0.35 to 1.6 cm^{-1}. Consistent with our previous results on the $2v_1$ and $3v_1$ overtones, we find that these low overtones and combinations of methanol are relatively less perturbed than the relevant fundamentals and much less perturbed than the higher overtones.

C. Higher Symmetry Systems: Nitromethane and Methyl Amine

Nitromethane (CH_3NO_2) and methyl amine (CH_3NH_2) are internal rotor molecules with one more atom than methanol. Each has two equivalent atoms attached to the nitrogen, which increases the molecular symmetry group from G_6 to G_{12}. These molecules serve to test the concepts that are being developed for methanol in section A. above and provide the opportunity to extend them.

In nitromethane, the planarity of the heavy atoms results in a low 6-fold torsional barrier. We have slit-jet FTIR spectra from PNNL of the asymmetric NO stretch. Analogous to the asymmetric methanol vibrations discussed above, we should expect an anomalous ordering of the torsional levels in this nitromethane band. At this point, we have assigned the most intense subbands but much remains to be done. In methyl amine, the amine group is non-planar which results in two large amplitude degrees of freedom, internal rotation with a 3-fold barrier and inversion at the nitrogen. The two degrees of freedom have comparable tunneling frequencies (0.2 to 0.3 cm^{-1}). We have assigned jet spectra of the asymmetric CH stretch and more work on the interpretation is required.

D. A Chemical Reaction Pathway Provides Insight into Vibrational Mode Couplings

IRLAPS spectra of methanol have yielded a wealth of information on intramolecular vibrational interactions including specific information on two kinds of mode coupling: 1) The OH stretch ν_1 is coupled to the ν_2 CH stretch by a 4th order matrix element of 23.5 cm^{-1}. 2) The torsional barrier increases by about 41 cm^{-1} for each quantum of excitation in the OH stretch. Through the application of *ab initio* calculations, we found that these two results could be explained qualitatively by the existence of the potentially reactive channel,

$$CH_3OH \Rightarrow H_2C=O + 2\ H\bullet.$$
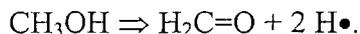
The key feature is that, as hydride bonds are broken at opposite ends of the molecule, a double bond is formed between the carbon and the oxygen. Although this is a relatively high energy unimolecular dissociation channel, it does affect the shape of the potential well down into the bound region and gives rise to vibrational mode couplings.

This appears to be a general concept. Accordingly, we tested it with *ab initio* calculations on the following systems,

$$HOOH \Rightarrow O=O + 2\ H\bullet$$

and

$$CH_3CH_3 \Rightarrow H_2C=CH_2 + 2\ H\bullet,$$
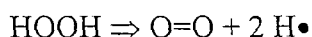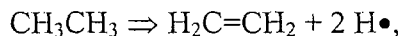
and found qualitatively similar results.

Plans for the Next Year

1. The test of the Born-Oppenheimer approximation described in section A. above will be completed.

2. Additional cavity ringdown spectra will be recorded in the OH + CH combination region of methanol, including particularly the asymmetric CH stretches to further test the concepts outlined in section A. above.

3. Work on the nitromethane analysis (section C. above) will continue.

4. *Ab intitio* calculations on the torsion plus COH bend potential of methanol will be pursued. This 2-dimensional potential has the form of the "Mexican hat" or "Champaign bottle" potential used for water and quasilinear molecules, with the addition of a 3-fold ripple around the bottom. The 3-fold ripple will give rise to torsional tunneling splittings that are a very useful diagnostic of the molecular dynamics. The computed level structures will be used to help us assign the $\nu_1+\nu_6$ and $2\nu_1+\nu_6$ methanol bands, which show anomalous unassigned structure

Cited References

[1] L.-H. Xu, X. Wang, T. J. Cronin, D. S. Perry, G. T. Fraser, and A. S. Pine, J. Mol. Spectrosc. **185**, 158 (1997).

[2] X. Wang and D. S. Perry, J. Chem. Phys. **109**, 10795 (1998).

[3] R. M. Lees and L.-H. Xu, Phys. Rev. Let. **84**, 3815 (2000).

[4] J. T. Hougen, J. Mol. Spectrosc. **181**, 287 (1997); J. T. Hougen, J. Mol. Spectrosc. **207**, 60 (2001); M. A. Temsamani, L.-H. Xu, and D. S. Perry, Can. J. Phys. **79**, 467 (2001).

[5] B. Fehrensen, D. Luckhaus, M. Quack, M. Willike, and T. R. Rizzo, manuscript.

Publications, 2001-2002

1) M.A. Temsamani, L.-H. Xu, and D. S. Perry, Vibrational dependence of the torsional tunneling splitting and the *a* to *b* intensity evolution in the OH overtone spectra of CH_3OH, *Can. J. Phys.* **79**, 467-477 (2001).

2) L. Wang, Y.-B. Duan, I. Mukhopadhyay, D. S. Perry, and K. Takagi, On the physical interpretation of torsion-rotational parameters for CH_3OD isotopomers, *Chem. Phys.* **263**. 263-279 (2001).

3) David Rueda, Oleg V. Boyarkin, Thomas R. Rizzo, Indranath Mukhopadhyay and David S. Perry, Torsion-rotation analysis of OH stretch overtone-torsion combination bands in methanol, *J. Chem. Phys.* **116**, 91-100 (2002).

4) A. Chirokolava, David S. Perry, O.V. Boyarkin, M. Schmid, and T.R. Rizzo, Rotational and torsional analysis of the OH-stretch third overtone in $^{13}CH_3OH$, *J. Mol. Spectrosc.* **211**, 221-227 (2002).

5) Indranath Mukhopadhyay, David S. Perry, Yun-Bo Duan, John C. Pearson, S. Albert, Rebecca A.H. Butler, Eric Herbst, and Frank C. De Lucia, Observation and analysis of high-*J* inter-species transitions in CH_2DOH, *J. Chem. Phys.* **116**, 3710-3717 (2002).

INVESTIGATION OF NON-PREMIXED TURBULENT COMBUSTION

Grant: DE-FG02-90ER14128

Principal Investigator: Stephen B. Pope
Sibley School of Mechanical & Aerospace Engineering
Cornell University
Ithaca, NY 14853
pope@mae.cornell.edu

Introduction

In transportation, process industry and power generation, vast amounts of fossil fuel are consumed, and significant amounts of pollutants are emitted. More advanced combustion technologies are required to address the national goals of energy conservation and environmental protection. The overall goal of this research project is to contribute to the development of predictive capabilities for combustion processes in order to facilitate the development of improved combustion technologies.

In most of the industries that manufacture combustion devices, turbulent combustion models are employed as a primary design tool. These are computer models that predict the combustion performance by solving a set of equations that model the fundamental physical and chemical processes involved. The turbulent combustion models considered in this project are PDF methods, in which a modelled transport equation is solved for the joint probability density function of velocity, turbulence frequency, and the thermochemical composition of the fluid (species mass fractions and enthalpy).

One of the two themes of this research project is to make PDF calculations of non-premixed turbulent flames and to compare the results to detailed measurements obtained at Sandia. Recent work on this topic is described in the next section.

The second theme of the research project is the development of methodologies for the computationally-efficient implementation of combustion chemistry in PDF methods and other modelling approaches. This is an important issue because, as more efficient algorithms are developed, more detailed and accurate descriptions of combustion chemistry can be used at an affordable computational cost. Work on this topic is described in the third section.

PDF Calculations of Bluff Body Stabilized Flames

Over the past three years substantial progress has been made in developing much improved solution algorithms for the PDF equations. This work is described in Jenny et al. (2001a, 2001b), Muradoglu et al. (2001, 2002, 2003) and Cao & Pope (2003). These improvements are now being brought to bear on the calculations of bluff-body stabilized flames.

The flame considered is the bluff-body stabilized flame first studied experimentally by Dally et al. (1998). A jet of methane and hydrogen (1:1 by volume) emerges through the center of a cylindrical bluff body, which is surrounded by a co-flow of air. The calculations are based on the joint PDF of velocity, turbulence frequency and chemical composition. The chemistry is represented by an augmented reduced mechanism (Sung et al. 1998) consisting of 19 species which includes NO chemistry.
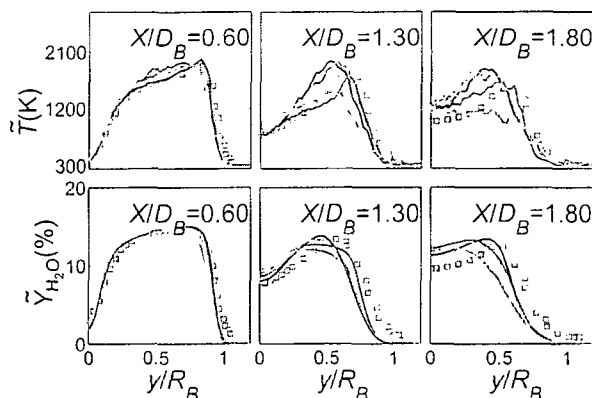
Figure 1: Radial profiles of mean temperature and mean water mass fraction. Symbols: experimental data, JPDF-ARM2 calculations with green solid lines: $C_\phi = 1.5$, magenta dashed lines: $C_\phi = 2.0$, blue dashed-doted lines: $C_\phi = 3.0$, black dotted lines: $C_\phi = 4.0$.

Figure 1 shows the calculated and measured mean profiles of temperature and water mass fraction. As may be seen, there is generally good agreement with the experimental data, and no great sensitivity to the mixing-model constant C_ϕ.

Figure 2 shows scatter plots of temperature vs. mixture fraction from the experiments (left-hand side) and from the calculations (right-hand side). These are at the furthest upstream measurement location $x/D_B = 0.26$, and are divided in radial location to the outer shear layer (top plots) and to the recirculation zone (bottom plots). The solid blue line shows the result of a flamelet calculation. It is interesting to observe that in the shear layer the experiments appear to show non-reactive mixing between the air ($\xi = 0$) and fluid from the recirculation zone ($\xi \approx 0.15$). This finite-rate effect is captured by the calculations. Further downstream the scatter plots (not shown) exhibit near complete combustion (close to the flamelet line).

Computational Implementation of Combustion Chemistry

A major thrust of the current work is the development of methodologies for the computationally-efficient implementation of combustion chemistry. There are two general strategies which can be used in combination. First, a *dimension reduction* is performed to reduce the number of degrees of freedom in the description of the chemistry. Second, a *storage/retrieval* algorithm is used to reduce the number of expensive chemistry calculations that are needed. Dimension-reduction strategies include: skeletal mechanisms (e.g., Smooke 1991); quasi-steady-state assumptions, QSSA (e.g., Peters & Rogg 1993); intrinsic low-dimensional manifolds, ILDM (Maas & Pope 1992); and rate-controlled constrained equilibrium, RCCE (Keck & Gillespie, 1971). Storage/retrieval strategies include: structured tabulation (applicable only in low dimensions); *in situ* adaptive tabulation, ISAT (Pope 1997); artificial neural networks, ANN (e.g., Christo et al. 1996); and PRISM (Tonse et al. 1999).

The approach which we are developing is a combination of ISAT and an extension of RCCE. In application (e.g., Tang, Xu & Pope 2000) ISAT has proved very effective when applied in combination with reduced mechanisms with of order 20 species, and we regard the current algorithm as *quite satisfactory*. Consequently the research effort is focused on the dimension reduction.

Compared to other methodologies, RCCE has clear advantages and disadvantages. Each reduction methodology implies that compositions lie on a low-dimensional manifold in the high-dimensional composition space. The decisive advantage of RCCE is that the implied *constrained*
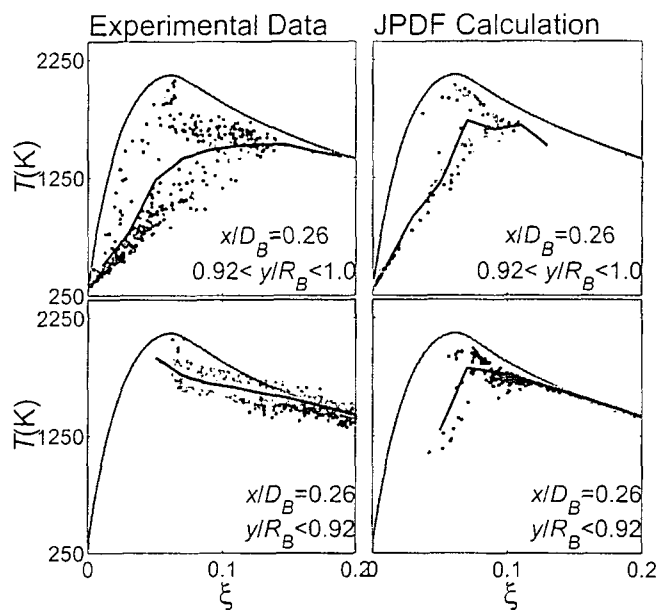
Figure 2: Scatter plot of temperature vs. mixture fraction at $x/D_B = 0.26$. Left-hand side, experimental data; right-hand side, PDF calculations. Lower plots, in the recirculation zone ($r/R_B < 0.92$); upper plots, in the shear layer between the recirculation zone and the co-flow ($0.92 < r/R_B < 1.0$).

equilibrium manifold (CEM) has excellent mathematical properties, namely: existence, uniqueness and smoothness. In contrast intrinsic low-dimensional manifolds can be discontinuous, and may not exist in some regions of the reduced space. The disadvantage is that the CEM is based on thermodynamics rather than on chemical kinetics. We are developing extensions to RCCE, therefore, in which the chemistry enters more directly. Some preliminary work in this direction has been described by Tang & Pope (2003).

References

1. F.C. Christo, A.R. Masri, E.M. Nebot, and S.B. Pope (1996). An integrated PDF/neural network approach for simulating turbulent reacting systems. *Proc. Combut. Inst.* **26**, 43-48.

2. B.B. Dally, D.F. Fletcher, and A.R. Marsi (1998) Flow and mixing fields of turbulent bluff-body jets and flames. *Combust. Theory Modelling* **2**, 193–219.

3. J.C. Keck and D. Gillespie (1971) "Rate-controlled partial equilibrium method for treating reacting gas-mixtures," Combust. Flame **17**, 237–241.

4. K. Liu, S.B. Pope and D.A. Caughey (2003) "Calculations of a turbulent bluff-body stabilized flame," Third Joint Meeting of the U.S. Sections of the Combustion Institute, Chicago.

5. U.A. Maas and S.B. Pope (1992) "Simplifying Chemical Kinetics: Intrinsic Low-Dimensional Manifolds in Composition Space," *Combust. and Flame*, **88**, 239-264.

6. M. Muradoglu, S.B. Pope and D.A. Caughey (2001) "The hybrid method for the PDF equations of turbulent reactive flows: consistency conditions and correction algorithms," *J. Comp. Phys.* **172**, 841–878.

7. M. Muradoglu and S.B. Pope (2002) " Local time-stepping algorithm for solving the probability density function turbulence model equations," AIAA Journal, **40**, 1755-1763.

8. M. Muradoglu, K. Liu and S.B. Pope (2003) "PDF Modeling of a Bluff-Body Stabilized Turbulent Flame," *Combust. Flame* **132**, 115-137.

9. N. Peters and B. Rogg (Eds.) (1993). *Reduced kinetic mechanisms for applications in combustion systems*. Berlin: Springer.

10. S.B. Pope (1997) "Computationally Efficient Implementation of Combustion Chemistry using In Situ Adaptive Tabulation," Combustion Theory and Modelling, **1**, 41–63.

11. M.D. Smooke (Ed.) (1991). *Reduced kinetic mechanisms and asymptotic approximations for methane-air flames*, Volume 384 of *Lecture Notes in Physics*. Berlin: Springer.

12. C. J. Sung, C. K. Law, and J.-Y. Chen (1998). An augmented reduced mechanism for methane oxidation with comprehensive global parametric validation. *Proc. Combust. Inst.* **27**, 295-304.

13. Q. Tang, J. Xu and S.B. Pope (2000) "PDF calculations of local extinction and NO production in piloted-jet turbulent methane/air flames," Proceedings of the Combustion Institute, **28**, 133–139.

14. Q. Tang and S.B. Pope (2003) "A more accurate projection in the rate-controlled constrained equilibrium method for dimension reduction of combustion chemistry." Third Joint Meeting of the U.S. Sections of the Combustion Institute, Chicago.

15. S.R. Tonse, N.W. Moriarty, N.J. Brown, and M. Frenklach (1999). PRISM: Piecewise reusable implementation of solution mapping. An economical strategy for chemical kinetics. *Isreal J. Chem.* **39**, 97-106.

Publications from DOE Research 2001-2003

1. R. Cao and S.B. Pope (2003) "Numerical integration of stochastic differential equations: weak second-order mid-point scheme for applications in the composition PDF method," *J. Comput. Phys.* **185**, 194–212.

2. P. Jenny, S.B. Pope, M. Muradoglu and D.A. Caughey (2001a) "A hybrid algorithm for the joint PDF equation for turbulent reactive flows," *J. Comp. Phys.* **166**, 281–252.

3. P. Jenny, M. Muradoglu, K. Liu, S.B. Pope, D.A. Caughey (2001b) "PDF simulations of a bluff-body stabilized flow," *J. Comp. Phys.* **169**, 1–23.

4. M. Muradoglu, S.B. Pope and D.A. Caughey (2001) "The hybrid method for the PDF equations of turbulent reactive flows: consistency conditions and correction algorithms," *J. Comp. Phys.* **172**, 841–878.

5. M. Muradoglu and S.B. Pope (2002) " Local time-stepping algorithm for solving the probability density function turbulence model equations," AIAA Journal, **40**, 1755-1763.

6. M. Muradoglu, K. Liu and S.B. Pope (2003) "PDF Modeling of a Bluff-Body Stabilized Turbulent Flame," *Combust. Flame* **132**, 115-137.

OPTICAL PROBES OF ATOMIC AND MOLECULAR DECAY PROCESSES

S.T. Pratt
Building 200, D-177
Argonne National Laboratory
9700 South Cass Avenue
Argonne, Illinois 60439

Telephone: (630) 252-4199
E-mail: stpratt@anl.gov

PROJECT SCOPE

Molecular photoionization and photodissociation dynamics can provide considerable insight into how energy and angular momentum flow among the electronic, vibrational, and rotational degrees of freedom in isolated, highly energized molecules. This project involves the study of these dynamics in small polyatomic molecules, with an emphasis on understanding the mechanisms of intramolecular energy flow and determining how these mechanisms influence decay rates and product branching ratios. The experimental approach combines double-resonance laser techniques, which are used to prepare selected highly excited species, with mass spectrometry, ion-imaging, and high-resolution photoelectron spectroscopy, which are used to characterize the decay of the selected species. Additional techniques, including excited-state absorption spectroscopy by fluorescence-dip techniques and zero-kinetic energy-photoelectron spectroscopy are used also as necessary. Photoelectron imaging capabilities are currently being developed to allow the determination of photoelectron angular distributions.

RECENT PROGRESS

In the past year, we have continued to work on the normal-mode dependence of vibrational autoionization in small polyatomic molecules. A study of the relative vibrational autoionization rates for the umbrella and asymmetric bending vibrations of ammonia was published in the Journal of Chemical Physics. [See Publication 3 below.] In addition, a new set of experiments was initiated to study mode-dependent vibrational autoionization in the Rydberg states of NO_2 in collaboration with Ed Grant of Purdue University. Patrice Bell, a graduate student of Ed's, is currently spending the final year of her Ph.D. studies at Argonne to work on these experiments. We are using triple-resonance excitation to prepare autoionizing states of NO_2 and using photoelectron spectroscopy to study how they decay. In particular, we are using the selectivity of the excitation process to prepare states that can vibrationally autoionize via two different vibrational modes, and using photoelectron spectroscopy to determine the relative importance of the two processes. In our first experiments on NO_2, we studied the vibrational autoionization of Rydberg series converging to the (100) and (02^00) vibrational levels of the ground state of NO_2^+. [Here we use the notation (v_1, v_2^l, v_3), where v_1 is the symmetric stretch, v_2 is the bend, and v_3 is the asymmetric stretch. The superscript l refers to the vibrational angular momentum.] The (100) and (02^00) vibrational levels are coupled by Fermi resonance, and the details of this interaction have been characterized previously by Ed's group. As a result of this interaction, the series converging to the (100) and (02^00) ionization thresholds have mixed character, which allows us to compare the relative rates of vibrational autoionization via the symmetric stretching and bending modes. Although Ed's group had previously compared the autoionization rates for these two vibrational modes by measuring the linewidths of the autoionizing

levels, such measurements can give misleading results if other decay mechanisms, such as predissociation or internal conversion, are important. In contrast, the photoelectron measurements provide a direct measurement of the relative importance of autoionization via the two vibrational modes. In this case, the photoelectron measurements confirmed the earlier finding of Ed's group that vibrational autoionization via the symmetric stretch is approximately 30 times faster than via the bending vibration. We have recently completed additional experiments on series converging to the (110) vibrational level of the ion, and the results of these experiments provide another window onto the relative rates of autoionization via the two different modes. We are also working to develop qualitative models based on earlier ideas of Mulliken and Walsh to rationalize these observations.

In the past year, an ion-imaging spectrometer was completed and initial studies using velocity-map imaging were performed to characterize the instrument. This initial work included preliminary studies of the photodissociation of O_2 and CH_3I, which allowed the comparison of our images with those of previous studies. Our first new work was on characterizing the photodissociation dynamics of CF_3I between 275 nm and 305 nm. The two-dimensional ion images provided detailed information on the partition of available energy into kinetic and internal energy of the photofragments. In particular, by velocity-map imaging the I $^2P_{3/2}$ and I* $^2P_{1/2}$ fragments, it was possible to determine the resulting vibrational state distributions of the CF_3 product. As expected, the images showed a series of rings separated by approximately 700 cm^{-1}, which indicated the excitation of the umbrella vibration in the CF_3 fragment. The fragment recoil anisotropies $\beta(I)$ and $\beta(I^*)$ were also determined from the images as a function of the excitation wavelength. The variations in the $\beta(I)$ and $\beta(I^*)$ were interpreted in terms of the crossing between the $^3Q_0$ and $^1Q_1$ dissociative electronic states of CF_3I. The high resolution images allowed the determination of the variation of the anisotropy parameter β as a function of the vibrational level of CF_3 fragment, and provided a complementary method for the determination of the C - I bond energy. The vibrational dependence of the anisotropy values was interpreted in terms of final-state interactions between the CF_3 umbrella motion and the C – I dissociation coordinate, as discussed previously by Hennig et al. [J. Chem. Phys. **84**, 544 (1986)]. The results of this study have been published as Publication 5 listed below.

In our second ion-imaging study, we used resonance enhanced multiphoton ionization via selected vibronic levels of the 6p Rydberg state of CF_3I to prepare vibrationally state-selected CF_3I^+ ions, which were then photodissociated by absorbing an additional photon. This is a very interesting photodissociation process because it produces both $CF_3 + I^+$ and $CF_3^+ + I$. As in an earlier study using time-of-flight mass spectrometry [L. D. Waits et al., J. Chem. Phys. **97**, 7263 (1992)], we observed a bimodal velocity distribution in the $CF_3^+ + I$ channel, indicative of two different dissociation mechanisms. Waits et al. had suggested that the slower velocity component was produced by unimolecular decomposition of hot CF_3I^+ formed by the ionization process, while the faster component was produced by photodissociation of the CF_3I^+. However, by recording high-resolution photoelectron spectra, it was possible to show that the CF_3I^+ ion was formed with very little internal vibrational energy and that $CF_3^+ + I$ can only be produced through photodissociation (i.e., the absorption of an additional photon). Both velocity components in the $CF_3^+ + I$ channel must be produced by excitation to the A $^2A_1$ state or to another dissociative state of the ion, and the ion images are consistent with this conclusion. The bimodal velocity distribution indicates that the dissociation to $CF_3^+ + I$ occurs via two mechanisms. The first corresponds to dissociation to $CF_3^+ + I$ ($^2P_{1/2}$), and results in a large translational energy release consistent with direct dissociation on the excited state surface. The second mechanism results in a small translational energy distribution that has an

appearance similar to that expected for a statistical dissociation process, but statistical models predict a much larger translational energy than observed. Possible explanations for this behavior have been discussed, but none of these is completely satisfactory at this time. In contrast, the dissociation to CF_3 + I^+ appears to be relatively simple. In particular, this process results in the population of the I^+ $^3P_2$ level, and the dissociation process is quite fast. The photoion angular distributions extracted from the ion images were also used to provide a new perspective on earlier studies of the dissociative ionization of CF_3I [P. Downie and I. Powis, Farad. Discuss. **115**, 103 (2000)]. The results of this study have been published as Publication 7 listed below.

The demonstrated ability to do ion-imaging experiments on the photodissociation of state-selected ions has considerable potential for future work. To simplify analysis and to be more generally useful, however, it is necessary to decouple the ionizing laser from the photodissociating laser. In our most recent study, we have extended our work on the photodissociation of CF_3I^+ by preparing the ion with one laser and photodissociating it with a second tunable laser. In this manner, we are able to study the photodissociation of CF_3I^+ near threshold. The ion images provide insight into the vibrational distributions in the CF_3^+ fragment, and by increasing the photon energy it is possible to see how the vibrational distributions change with the opening of new continua, and to see how the angular distributions in a given vibrational channel change with increasing photon energy. We are currently analyzing the results of this initial two-color study, and preparing a manuscript for publication.

FUTURE PLANS
Much of the work in the near future will involve the continuation and extension of projects discussed above. The study of vibrational autoionization via the bending and symmetric stretching vibrations of NO_2 will be extended by comparing the decay of resonances converging to the (110) and (03^{1}0) vibrational levels of the ion, which should show similarities with the comparison of the Rydberg series converging to the (100) and (02^{0}0) ionization thresholds. In addition, the decay of levels involving overtones of the symmetric stretch [e.g., the (200) and (300) levels] may also be studied. Photoelectron spectroscopy will also be used to explore the ability to make vibrationally state selected NO_2^+ by photoionizing selected vibrational levels of the $3p\sigma$ Rydberg state. This latter work is motivated by a request from Ed Grant and Scott Anderson at the University of Utah, who wish will use the schemes we characterize at Argonne to study the vibrational mode dependence of ion-molecule reactions of NO_2^+. Studies of the electronic and vibrational autoionization of H_2O will also continue in collaboration with Wally Glab (Texas Tech).

The two-color study of the photodissociation on state selected CF_3I^+ will be completed in the near future. Additional work will be performed on the ion-imaging of the photodissociation of other ions, as well as of some precursors for the formation of neutral radicals, such as propargyl chloride. Such precursors are often photodissociated in supersonic expansions to produce cold free radicals. However, cooling of vibrational excitation in supersonic expansions is not always very efficient, and thus it is useful to characterize the nascent products of the photodissociation. This work may also provide insight into the spectroscopy of vibrationally and rotationally hot radicals. An important direction for the imaging studies will be to apply the technique to superexcited states of molecules that undergo both autoionization and predissociation. The goal is to characterize both the ionization and dissociation dynamics of such superexcited states for a number of selected molecules. This work

will initially focus on a fairly well-characterized system such as NO, and move to more complex systems like NO_2 and small hydrocarbons.

I am continuing to collaborate with Christian Jungen of the Laboratoire Aime Cotton in Orsay, France on theoretical models of vibrational autoionization in polyatomic molecules. In the coming year, we will attempt to extend our earlier study of simple polyatomic molecules to situations involving degenerate electronic states. In this situation, the Renner-Teller and Jahn-Teller interactions can play an important role. We will also work to develop a better qualitative understanding of the factors that influence the strength of coupling between the vibrational and electronic degrees of freedom in these systems. I have also developed a collaboration with Professor Frederic Merkt of the ETH Zurich to perform very high resolution pulsed field ionization spectroscopy of small molecules. In this work, we will focus on the spectra near the threshold for dissociative ionization, with the goal of developing a better understanding of the steps observed at the dissociative ionization thresholds in pulsed field ionization spectra by C. Y. Ng and coworkers.

DOE-SPONSORED PUBLICATIONS SINCE 2001

1. C. A. Raptis and S. T. Pratt
   TWO-PHOTON SPECTROSCOPY OF AUTOIONIZING STATES OF AMMONIA
   J. Chem. Phys. **115**, 2483-2491 (2001).

2. C. Ramos, P. R. Winter, T. S. Zwier, and S. T. Pratt
   PHOTOELECTRON SPECTROSCOPY VIA THE 1 $^1\Delta_u$ STATE OF DIACETYLENE
   J. Chem. Phys., **116**, 4011-4022 (2002).

3. S. T. Pratt
   PHOTOIONIZATION DYNAMICS OF THE B^1E'' STATE OF AMMONIA
   J. Chem. Phys. **117**, 1055-1067 (2002).

4. S. T. Pratt
   PHOTOIONIZATION OF DABCO VIA HIGH VIBRATIONAL LEVELS OF THE S_1 STATE
   Chem. Phys. Lett. **360**, 406-413 (2002).

5. F. Aguirre and S. T. Pratt
   VELOCITY MAP IMAGING OF THE PHOTODISSOCIATION OF CF_3I: VIBRATIONAL ENERGY DEPENDENCE OF THE RECOIL ANISOTROPY
   J. Chem. Phys., **118**, 1175-1183 (2003).

6. S. T. Pratt, J. A. Bacon, and C. A. Raptis
   VIBRATIONAL AUTOIONIZATION IN POLYATOMIC MOLECULES
   to appear in *Dissociative Recombination*, Edited by S. Guberman, Kluwer, New York, in press.

7. F. Aguirre and S. T. Pratt
   ION-IMAGING OF THE PHOTODISSOCIATION OF CF_3I^+
   J. Chem. Phys., **118**, 6318-6326 (2003).

Reactions of Atoms and Radicals in Pulsed Molecular Beams

Hanna Reisler

Department of Chemistry, University of Southern California

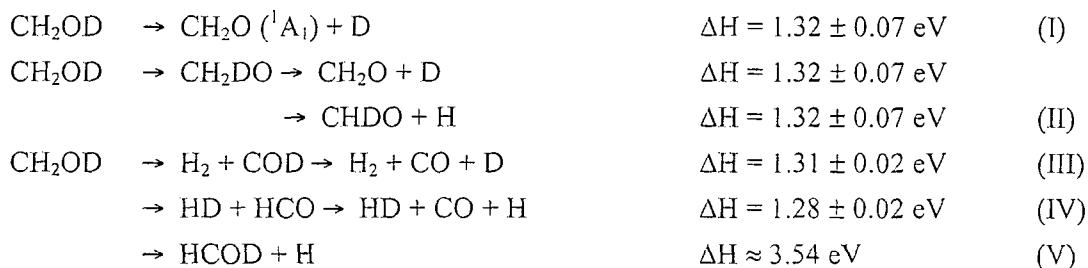Los Angeles, CA 90089-0482

reisler@usc.edu

Program Scope

We study photoinitiated reactions of molecules and free radicals that involve competitive pathways and/or isomerization by exploiting multiple-resonance excitation schemes, state-selected product detection, and photofragment translational spectroscopy and ion imaging for generation of correlated distributions. The current series of studies are concerned with mechanisms of photodissociation and isomerization of hydroxyalkyl radicals.

Photodissociation Dynamics of the Hydroxymethyl Radical in the $3s$, $3p_x$, and $3p_z$ states

The hydroxymethyl radical (CH_2OH) is a significant product in the reaction of $O(^1D)$ with methane. Similarly, reactions of Cl atoms and OH radicals with methanol yield predominantly CH_2OH. Because both CH_2OH and CH_3O have low barriers to dissociation, the photoisomerization $CH_2OH \leftrightarrow CH_3O$ has attracted considerable theoretical interest. It has been predicted theoretically that CH_2OH requires ~16,000 cm^{-1} to surmount the barrier to $H + CH_2O$ ($^1A_1$) on the ground state, while experiment has established that the corresponding barrier for CH_3O decomposition is ~ 11,000 cm^{-1} relative to the energy of CH_2OH. Since less energy is required to dissociate CH_2OH via the CH_3O route, the height of the isome-rization barrier (calculated at ~14,000 cm^{-1}) is of importance.

According to *ab initio* calculations, the lowest excited electronic states of the CH_2OH radical have a predominant Rydberg character, and are characterized, in turn, as the $3s$, $3p_x$, $3p_y$ and $3p_z$ states.[1,2] The UV absorption spectrum starts as a broad and structureless band with a threshold at ~ 385 nm, extending to below 351 nm. It has recently been assigned to $1^2A'(3s) \leftarrow 1^2A''$ excitation.[3] Vibrational structure is observed, however, in the transitions from the ground state to the higher $3p_x$ and $3p_z$ states, but no rotational features can be resolved due to lifetime broadening.[4,5]

In the past few years, we have been engaged in elucidating the photodissociative spectroscopy and dynamics of the $CH_2OH(D)$ via the origin band of the $3p_z$ state [~ 5.09 eV (244 nm)].[4,5] In more recent studies, we followed the dissociation on the $3s$, $3p_x$, and higher vibrational levels of the $3p_z$ states, and observed H and D atom formation. Below we report on the O-D and O-H photodissociation channels of CH_2OD via the channels listed below:

CH_2OD	$\rightarrow CH_2O$ ($^1A_1$) + D	$\Delta H = 1.32 \pm 0.07$ eV	(I)
CH_2OD	$\rightarrow CH_2DO \rightarrow CH_2O + D$	$\Delta H = 1.32 \pm 0.07$ eV	
	$\rightarrow CHDO + H$	$\Delta H = 1.32 \pm 0.07$ eV	(II)
CH_2OD	$\rightarrow H_2 + COD \rightarrow H_2 + CO + D$	$\Delta H = 1.31 \pm 0.02$ eV	(III)
	$\rightarrow HD + HCO \rightarrow HD + CO + H$	$\Delta H = 1.28 \pm 0.02$ eV	(IV)
	$\rightarrow HCOD + H$	$\Delta H \approx 3.54$ eV	(V)

O-D bond fission from the 3s State of CH₂OD

Since the $3s$ state is the lowest excited state of CH₂OH, studying its photodissociation dynamics simplifies interpretation. Absorption to this state commences at 26,000 cm⁻¹ (3.21 eV), and constitutes an underlying continuum in the regions where absorptions to the $3p_x$ and $3p_z$ states dominate.

We have examined the photodissociation from the $3s$ state at 365-318 nm, a wavelength region where O-D fission is the only observed channel, but since the results are similar, we only report detailed studies at 352.5 nm (3.51 eV). At this wavelength, the radicals can predissociate only via the ground electronic state. Comparison between our experimental results and the theoretical calculations of Hoffman and Yarkony[6] suggests that the intersection seam of the $3s$ and ground states is located in the repulsive region of the O-D coordinate, and the ensuing fast dissociation does not favor isomerization.

The c.m. translational energy distribution CH₂OD dissociating to D + CH₂O is shown in Fig 1. The negative β_{eff} value of -0.7 ± 0.1 is consistent with the 3s ^{2}A' ← 1^{2}A" transition. A large fraction of the available energy is partitioned into relative translation with $\langle f_T \rangle$ = 0.69. The nearly Gaussian shape of the distribution and the large value of $\langle f_T \rangle$ are consistent with fast dissociation. The arrow in Fig. 1 indicates the maximum allowed total c.m. translational energy of the products, 2.19 eV, calculated for photolysis via Channel I, and this value is in good agreement with the experimentally observed maximum translational energy.
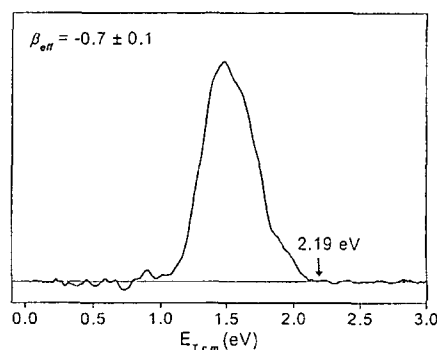
Fig. 1: D+CH₂O from CH₂OD(3s) at 352.5 nm

In an attempt to assess the importance of Channel (III), a search for CO (v=0) signal was carried out by using (2+1) REMPI via the B state at 230.1 nm. However, this experiment was hampered by a strong CO (v=0) background signal from the probe laser alone. Coincidentally, the detection wavelength of CO (~ 230 nm) overlaps an absorption band of CH₂OD to the $3p_z$ Rydberg state, and at this wavelength, the CH₂O (^{1}A₁) product from CH₂OD photodissociation has sufficient internal energy to predissociate to CO (v=0,1) (see below). The signal from this product overwhelms any other source of CO. We argue, however, that it unlikely that channel (III) is competitive, because of the tight transition state involved in H₂ elimination.

It has been shown before that the electronic wave function of the ground state of CH₂OH(D) complies with Cs A" symmetry (as a result of the shallowness of the CH₂ wag and O-H torsional potentials), while the *nuclear* equilibrium geometry of the radical calculated *ab initio* is nonplanar and belongs to the C₁ point group (A symmetry). In A symmetry, the ground state correlates with CH₂O (^{1}A₁) + D products, and *ab initio* calculations find that this channel proceeds over a barrier of ~ 1.98 eV (~ 16,000 cm⁻¹). Since electronic Rydberg states correlate diabatically with products in excited Rydberg states, the dissociation from the $3s$ state to channel (I) should involve crossing to the ground state PES. The calculations by Hoffman and Yarkony indicate that the excited state dissociation of CH₂OD is strongly affected by nonadiabatic transitions through conical intersections.[6] They find an efficient seam of conical intersections between the $3s$ and the ground states, with a low-energy (2.9 eV) crossing seam at an O-D distance of ~ 1.48 Å, i.e., extended by ~ 0.5 Å from the equilibrium distance in the ground state. This conical intersection is thought to greatly promote radiationless transitions from $3s$ to the ground state. The 3s/ground state coupling transports the radical to a repulsive part of the ground state PES, where it dissociates to H₂CO (1^{1}A₁) + D, apparently without isomerization.

The C-H fission channel in the photodissociation of CH_2OD

At wavelengths shorter than 318 nm, both D and H products are detected. The signal from the C-H fission channel increased rapidly and monotonically when the photolysis wavelength decreases from 318 to 247 nm (Fig. 2). No change in intensity is detected when the band origins of the transitions to the $3p_x$, and $3p_z$ states are accessed. The translational energy distributions of the D and H photofragments from CH_2OD are very different, and they are assigned to channels (I) and (V), respectively. Again, there is no evidence of isomerization. The H translational energy distributions are much colder than those of D at comparable photolysis wavelengths, and $\beta_{eff} = 0$ is obtained. From the highest translational energies of the H atom E_t distributions obtained following excitations to the $3s$, $3p_x$ and $3p_z$ states (see Fig. 3 for an example), the C-H bond dissociation energy $D_0(H\text{-}CHOD) \leq 81 \pm 2$ kcal/mol is derived. This is the first experimental determination of this bond dissociation energy, and it leads to an estimation of the heat of formation of CHOD, a value that can now be compared to calculations.
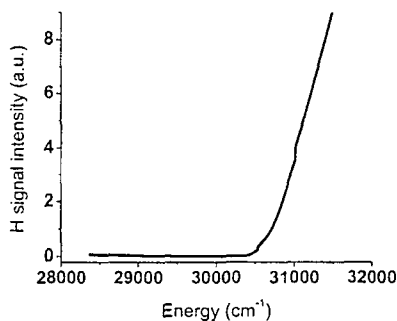
Fig. 2. H signal starts above 30,500cm^{-1} (328nm).
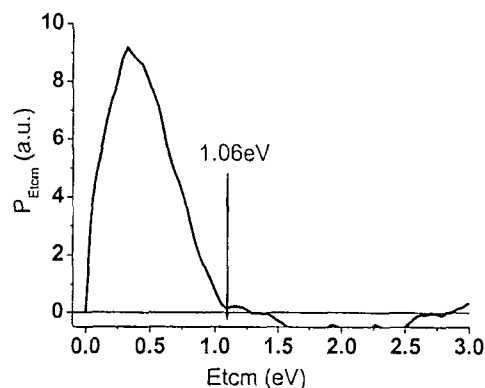
Fig.3. E_t distribution of the H fission channel
from $3p_x$ at 285.5 nm (35,026 cm^{-1})

"Hot" formaldehyde: A source of secondary H/D fragments

As the photolysis energy increases in the region of excitation to the $3p_z$ state (< 244 nm), the translational energy distributions of the D and H products from CH_2OD broaden, indicating the production of highly excited formaldehyde (and/or CHOD) fragments. When the internal energy of formaldehyde reaches the threshold of the H(D) + H(D)CO channel, a second peak of slow H(D) starts to appear. The width of this peak increases with increasing photolysis energy. It appears that the molecular fragments possess sufficient internal energy to undergo further unimolecular reactions. This secondary dissociation is also the source of the CO(v=0,1) products in photodissociation at 230 nm. It is intriguing that both H and D atoms are produced in the photodissociation of CH_2OD (Fig. 3 gives an example of secondary D production), indicating contributions from dissociation of "hot" CH_2O and/or CHOD, and the possible isomerization CHOD $\leftrightarrow$ CHDO. We hope that calculations of this relatively simple system will help in interpreting the results.

Fig. 4. D atoms from "hot" products generated in dissociation via the $3p_z$ state. The peak at slow E_{tcm} observed following excitation in the 6_0^2 band originates in secondary dissociation
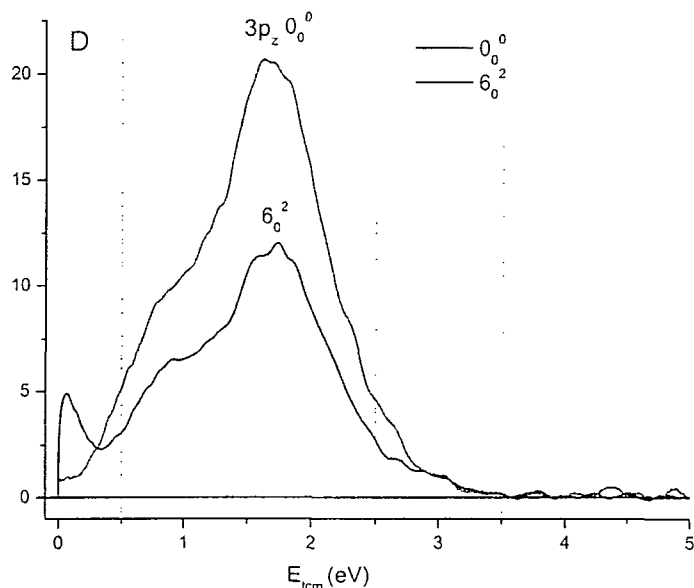
Future Plans

We have recently installed an OPO laser system that enables us to excite OH and CH stretch fundamentals. The spectroscopy and photoionization of CH_2OH via this channel will be studied. We are also installing an imaging system that will allow us to detect efficiently slow H/D atoms deriving from high overtone dissociation. The spectroscopy and photodissociation dynamics of higher hydroxyalkyl radicals will be examined as well.

[1] S. Rettrup, P. Pagsberg, and C. Anastasi, *Chem. Phys* **122**, 45 (1988).

[2] P. J. Bruna and F. Grein, *J. Phys. Chem.* A **102**, 3141(1998); **105**, 8599 (2001)

[3] L. Feng, X. Huang, and H. Reisler, *J. Chem. Phys.* **117**, 4820 (2002).

[4] V. Aristov, D. Conroy, and H. Reisler, *Chem. Phys. Lett.* **318**, 393 (2000).

[5] D. Conroy, V. Aristov, L. Feng, and H. Reisler, *J. Phys. Chem. A* **104**, 10288 (2000)

[6] B. C. Hoffman and D. R. Yarkony, *J. Chem. Phys.* **116**, 8300 (2002).

Publications in 2001-2003:

1. *Competitive pathways and nonadiabatic transitions in photodissociation*, D. Conroy, V. Aristov, L. Feng, A. Sanov, and H. Reisler, Acc. Chem. Res., **34**, 625-632 (2001).

2. Photodissociative spectroscopy of the hydroxymethyl radical (CH_2OH) in the $3s$ and $3p_x$ states, L. Feng, X. Huang, and H. Reisler, J. Chem. Phys. **117**, 4820 (2002).

3. O-D bond dissociation from the $3s$ state of deuterated hydroxymethyl radical (CH_2OD), L. Feng, A.V. Demyanenko, and H. Reisler, J Chem. Phys., in press. (2003)

Electronic Structure, Molecular Bonding and Potential Energy Surfaces

Klaus Ruedenberg

Ames Laboratory USDOE, Iowa State University, Ames, Iowa, 50011

ruedenberg@iastate.edu

Scope

Our work is predicated on approaching the construction of wavefunctions describing molecular electronic structures in two stages:

(i) Zeroth-order terms of the SCF or MCSCF type that determine the principal molecular orbitals and typically account for the fundamental understanding of bond forming, bond breaking and reaction paths.

(ii) Refinement terms that account for the dynamic inter-electronic correlations and establish chemical accuracy.

We consider the optimized full valence-space of deformed minimal-basis atomic orbitals a classical zeroth-order choice, which has proven effective and useful for elucidating many reaction paths and transition states. For the most effective correlation refinements, a variety of approaches are competing. Our work addresses the problem of extending ab-initio methods in both spaces to larger molecules as well as the question of chemical interpretations of complex wavefunctions.

Recent Results

A-priori Elimination of Configurational Deadwood from Zeroth-Order Space

Even though the zeroth-order wavefunctions are based on comparatively small orbital sets, their configuration spaces still grow too large for practical use even in moderately sized molecules. This growth is however largely due to vastly increasing amounts of ineffective configurations. We have developed a systematic method for eliminating *a-priori* all of this configurational deadwood. It involves the *a-priori* choice of appropriately localized molecular orbitals, which we call split-localized orbitals; an appropriate and effective open-ended *a-priori* ordering procedure; and a reliable *a-piori* truncation criterion. Thereby full valence space-type multi-configurational expansions are reduced by orders of magnitude and the reduction fraction moreover increases with the size of the molecule, so that larger systems become accessible.

This work has been contingent on a new direct determinantal CI procedure for arbitrary configuration selections recently developed by us.

Natural Orbitals Do Not Generate The Most Rapidly Convergent CI Expansions

In this context we have shown that, contrary to a very widely held belief, the natural orbitals of a molecular wavefunction do not generally generate its most rapidly converging configuration interaction expansion. In full valence spaces, split-localized orbitals lead to configurational expansions that typically converge faster, even when the natural orbitals are adapted to a higher symmetry.

Jacobi-Rotation-Based MCSCF Method for the Zeroth-Order Space

A new MCSCF method based on successive optimizations of Jacobi rotation angles is presented. For given one- and two-particle density matrices and an initial set of corresponding integrals, a technique is developed for the determination of a Jacobi angle for the mixing of two orbitals, such that the exact energy, written as a function of the angle, is *fully* minimized. Determination of the energy-minimizing orbitals for given density matrices is accomplished by successive optimization and updating of Jacobi angles and integrals. Alternating between CI and orbital optimization steps minimizes the total MCSCF energy. Efficiency is realized by optimizing CI and orbital vectors quasi-simultaneously by not fully optimizing each in each improvement step

Jacobi-Rotation-Based Excited State MCSCF Method.

On the basis of the Jacobi-rotation based approach, a novel MCSCF procedure is formulated for excited states. It is based on minimizing a functional that maintains the higher-root character during the minimization, thereby eliminating the root-flipping problem.

Exact Generation Of The Zeroth-Order Space From Quasi-Atomic Minimal Basis Sets

A method has been developed for determining, in the context of molecular SCF, DFT or MCSCF calculations, *quasi-atomic* orbitals with the following attributes:
– The orbitals are *molecule-intrinsic* and *basis-set independent.*
– The number of these orbitals is equal to the total number of minimal basis orbitals of the atoms in the molecule.
– The exact SCF, DFT or MCSCF MOs can nevertheless be exactly expanded in terms of these orbitals.
– Within the constraints of the preceding two requirements, these orbitals deviate as little as possible from the optimal minimal-basis-set orbitals of the corresponding *free* atoms.
– Concrete applications show that that these deviations are in fact extremely small (corresponding to overlap integrals >0.99).

On this basis, it has been possible to account for and analyze bond formation qualitatively as well as quantitatively in terms of interactions between molecule-intrinsic *minimal-basis set orbitals* on the various atoms that differ from the free-atom minimal-basis set orbitals only by very slight deformations. Notwithstanding their smallness, the deformations entail significant energy changes on the chemical scale.

In the *virtual* SCF orbital space, the method furnishes a basis-set-independent ab-initio quantification of the qualitative notion of the *virtual valence* space orbitals and, in particular, an unambiguous ab-initio identification of the unoccupied frontier orbitals. They are found to differ markedly from the equal-dimensional subspace spanned by the virtual orbitals with the lowest Fock operator energies. They also approximate the optimal correlating orbitals of a full-valence-space MCSCF calculation.

Accurate Recovery Of Dynamic Correlation By A Bilinear Formula In Terms Of Pair-Densities Between Localized Orbitals

Presuming zeroth-order electronic wavefunctions generated from localized SCF or FORS molecular orbitals, the correlation energy is expressed as a bilinear form in terms of the pair-populations of these orbitals and the projections of a correlation operator onto these orbitals. The values of the latter are determined by fitting the correlation energies of large sets of organic molecules, which are reproduced with a mean absolute deviation of 1-3 kcal/mol. The resulting formula provides a "back-of-the-envelope" method for estimating correlation energies and furnishes an analysis of these energies in terms of physical concepts and chemical structure. It predicts the correlation energy of diamond (per carbon atom) to within 6 kcal/mol.

Future Work

The methods described above will be extended and generalized for applications to reaction paths and transition states.

Publications 2001, 2002, 2003

A New Parallel Optimal-Parameter Fast Multipole Method
    Cheol Ho Choi, Klaus Ruedenberg, Mark S. Gordon,
    J. Computational Chem. **22**, 1484-1501 (2001)

Oriented Non-spherical Atoms in Crystals Deduced from X-Ray Scattering Data
    L. L. Miller, R. A. Jacobson, K. Ruedenberg, J. Niu, W. H. E. Schwarz
    Helvetica Chimica Acta **84**, 1907-1942 (2001)

Identification of Deadwood in Configuration Spaces through General Direct Configuration Interaction
    Joseph Ivanic and Klaus Ruedenberg
    Theor. Chem. Accounts **106**, 339-351 (2001)

Deadwood in Configuration Spaces. II. SD and SDTQ Spaces
    Joseph Ivanic and Klaus Ruedenberg,
    Theor. Chem. Accounts **107**, 220-228 (2002)

Electron Pairs, Localized Orbitals and Electron Correlation
    Laimutis Bytautas and Klaus Ruedenberg
    Molecular Physics, **100**, 757-781 (2002)

A MCSCF Method for Ground and Excited States Based on Full Optimizations of Successive Jacobi Rotations
    J. Ivanic and Klaus Ruedenberg
    J. Computational Chemistry, accepted

Economical Description of Electron Correlation
Laimutis Bytautas and Klaus Ruedenberg
2002 Symposium Volume on Recent Advances in Electron Correlation Methodology
(A. K. Wilson and K. A. Peterson Edtrs. ACS Books, 2003), accepted

Photoionization and Thermochemical Studies of Transient and Metastable Species

Branko Ruscic

Chemistry Division, Argonne National Laboratory, 9700 South Cass Avenue, Argonne, IL 60439

ruscic@anl.gov

Program Scope

In most general terms, the fundamental goal of this program is to explore, understand, and utilize the basic processes of interaction of VUV light with atoms and molecules. More specifically, the program uses photoionization mass spectrometry and other related methods to study transient and metastable species that are intimately connected to energy-producing processes, such as combustion, or play prominent roles in the associated environmental issues. The ephemeral species of interest are produced *in situ* using various techniques, such as sublimation, pyrolysis, microwave discharge, chemical abstraction reactions with H or F atoms, laser photodissociation, on-line synthesis, and others. The desired information is obtained by applying photoionization techniques in conjunction with conventional, coherent, and synchrotron light sources. The *spiritus movens* of these studies is the need to provide the chemical community with essential information on the species of interest, such as accurate and reliable thermochemical, spectroscopic and structural data, and thus contribute to the global comprehension of the underlying chemical reactions. The motivation is additionally fueled by the intent to extract, when possible, useful generalities, such as chemical bonding patterns, or unveil systematic behavior in the ubiquitous autoionization processes and other phenomena occurring during photoionization. In addition, results obtained in this program serve as testing ground for state-of-the-art electronic structure calculations, and have historically generated a significant impetus for theoretical developments. The experimental work of this program is coordinated with related experimental and theoretical efforts within the Argonne Chemical Dynamics Group to provide a broad perspective on this area of science.

Recent Progress

Development of Active Thermochemical Tables and of the underlying Thermochemical Network

Active Thermochemical Tables (ATcT), as the first actual example of the broader idea of Active Tables (*vide infra*), are aiming to bring the science of thermochemistry into the 21st century. At the core of ATcT is the explicit utilization and statistical treatment of underlying interdependences between thermochemical quantities, most conveniently expressed through a network of relationships. The current development of ATcT has several related components: The conceptual and practical advances in the underlying methodologies, as well as the construction and evaluation of actual Thermochemical Network and the resulting practical advances in thermochemistry of stable and ephemeral species, are a direct and continuing product of this project (funded by DOE BES), while the accompanying software development involved in bringing to life a practical instance of ATcT as a web-service is highly leveraged by an additional funding source (DOE MICS).

Briefly, traditional thermochemistry uses a sequential approach to develop thermochemical values (such as enthalpies of formation) from measurable quantities (such as bond dissociation energies, equilibrium constants, reaction enthalpies, etc.) and then presents the results in tabulations. Consequently, tabulated values have intricate, but hidden, progenitor-progeny dependences, frustrating proper updates with new knowledge: Update of one species based on latest measurements may improve things locally, but, unfortunately, inherently increases the overall inconsistency of the tables. (Note that overall consistency is crucial, since the primary use of tabulations is to obtain thermochemical properties of reactions, i.e. *sums and differences* between individual values.) Path selection and lack of corrective feedback inherent in the "adopt and freeze" approach results in cumulative errors and values (and associated uncertainties) that are path-dependent and do not properly reflect the globality of relationships used elsewhere in the table.

In reality, the measurable thermochemical quantities form a Thermochemical Network.[1,2] In graph-theoretical

---

[1] B. Ruscic, J. V. Michael, P. C. Redfern, L. A. Curtiss, and K. Raghavachari, *J. Phys. Chem. A.* **102**, 10889-10899 (1998)

[2] B. Ruscic, M. Litorja, and R. L. Asher, *J. Phys. Chem. A.* **103**, 8625-8633 (1999)

lingo, the vertices (nodes) of the graph depicting the Thermochemical Network represent the desired thermochemical quantities (enthalpies of formation), while the edges (links) are the measurable quantities. The Network has typically multiple paths connecting any two arbitrary vertices. Moreover, the same path often contains multiple edges (i.e. competing measurements). The traditional sequential approach is tantamount to selecting one particular path from one vertex to the next, and ignoring alternative paths. Contrary to the sequential approach, the *statistically optimal* set of enthalpies of formation is obtained by simultaneous solution of the whole Network through two major steps. The first step involves a statistical analysis of the Network, during which the internal consistency of all edges is critically examined and tested to identify and correct in a statistically meaningful way "optimistic" uncertainties. Once the Network is internally consistent, the solution can be obtained by executing the second step, namely a minimization of χ^2 in error-weighted space. This approach is the basis for ATcT, giving it multiple and significant advantages. The solutions obtained from ATcT are guaranteed to be globally consistent with all available data present in the Network. A huge additional advantage is the ability to painlessly propagate new data and its full consequences, opening a new venue of rapid availability of latest information. ATcT also allows "what if" tests that, for example, are able to probe a hypothesis or scrutinize the consistency (or lack thereof) of new data against the existing body of knowledge. Finally, statistical analysis of the Network allows the uncovering of "weakest links", and hence suggests which future experiments/calculations may have the highest impact. (The latter aspect is, by itself, a new paradigm of how to efficiently drive science.) It should also be mentioned that, since this approach is software/database oriented, it is very easy to incorporate links to supporting documents, such as complete scientific papers supporting the pedigree of the underlying information and/or original raw data as obtained in the laboratory.

The current version of ATcT (1.0 β) is running as a web service and is accessible to registered users via the Collaboratory for Multi-Scale Chemical Science.[3] The ATcT back-end kernel is quite complex (currently at ~40,000 lines of code). The underlying thermochemical data is organized in a number of Libraries and Notes. Libraries are intended to be large collections of data generated by thermochemical committees (e.g. NIST, IUPAC) who oversee and anoint their scientific soundness and completeness. Notes are lighter versions of Libraries, associated with individual users or collaborative workgroups. The current "MainLibrary" contains Network data that is being developed at Argonne (see below). Several other Libraries ("CODATALibrary", "JANAFLibrary", "GurvichLibrary") contain data that reproduce information in historical tables. Each Library or Notes collection contains a number of Dictionaries, Lexicons, Compendia, etc. that contain information needed to construct and manipulate the Thermochemical Network. While the kernel is only in the initial stages of development, many useful features are already built in. For example, the user can set/change options such as temperature schedule, reference temperature, output units, etc., and define how information is searched for (this allows user-provided information to supercede existing information in other Libraries as well as workgroup-sharing of information). The current function that analyses and solves the Network is based on the "worst offender" strategy. Other strategies will be incorporated as they will be developed.

Short-term and medium-term plans call for a number of additional developments and improvements to ATcT and an expansion of the underlying Thermochemical Network. Long-term, we would like to return to our original vision of Interacting Active Tables. Namely, one can envision adding similar "intelligence" to other databases. For example, Active Kinetic Rate Tables placed above the ATcT would make use of the relationships implied in a tabulation of elementary kinetic rate measurements and would be able to interact with ATcT, both as a user of information and as a contributor of new information.

Although composed with considerable scientific rigor, the primary aim of the initial Thermochemical Network was to provide testing grounds for ATcT software development. Now that we have a working initial version of the software, we have embarked upon constructing a Core Thermochemical Network with full scientific rigor and completeness. The Core Network is currently encompassing H/O/C/N. During the evaluation process that precedes the incorporation of information into the Network, we are finding a number of errors and inconsistencies in data that lies at the heart of thermochemistry. (To our total surprise, we have found – and

---

[3] http://swift.mcs.anl.gov:8080/jetspeed/index.jsp or http://cmcs.ca.sandia.gov/index.php

corrected − small inconsistencies/errors even in the early calorimetric determinations of the enthalpies of formation of H$_2$O, CO$_2$, etc., that stayed undiscovered for almost seven decades.)

The development strategy of the Core Network is partly driven by several immediate goals. The first goal is to provide definitive ATcT values for the O/H system. The relevant part of the Network is complete (except that HO$_2$ thermochemistry is still under construction, since it also involves halogen thermochemistry.) Using ATcT we have now derived definitive values (based on current knowledge) for all possible H/O species (except HO$_2$). (Last year we have reported here on a related simpler attempt using a semi-manual approach, rather than ATcT.) A full report will be published shortly. While the largest difference is for H$_2$O$_2$, our new values for other species slightly revise and supercede the prior best values that were recommended by CODATA and subsequently adopted in JANAF, Gurvich et al., etc. (with a dramatic drop in uncertainty in several cases).

The second goal is to improve on the enthalpy of formation (and particularly, on its uncertainty, if possible) of C atom in gas phase (equivalent to the vaporization enthalpy of graphite). This quantity is quite important, since all theoretical calculations that proceed via computation of the atomization enthalpy of the target species (such as G3 or W1), need it to derive the final enthalpy of formation. The existing value has an unpleasantly large uncertainty given its very fundamental nature (± 0.45 kJ/mol, currently the most uncertain atomic species relevant in combustion, albeit a few others are not much behind), which quickly becomes substantial as the number of C atoms in the target species increases. Similarly, the current uncertainty of this quantity diminishes the value of accurate experimental benchmarks, if they are used to derive atomization enthalpies for the purpose of comparison to theory. In order to examine this problem, we have thoroughly evaluated and implemented the relevant section of the Thermochemical Network. Based on currently available experimental results, we now have a slightly improved value. However, the Network suggests that, in this case, target state-of-the art computations could help. The calculations, which are in progress, are performed in collaboration with Attila Csaszar (Eotvos U. Budapest) and John Stanton (U. Texas Austin). The network also suggests a photoionization experiment that will be pursued at ALS Berkeley in collaboration with C.-Y. Ng (U. C. Davis).

The third goal was to provide definitive answers for the sequential bond dissociation energies in methane (and therefore for the resulting thermochemistry of CH$_n$-type species). Hence, the Network was expanded with relevant C$_1$ chemistry. Here, the Network suggests that the current experimental data are able to provide the thermochemistry of CH$_3$ and CH$_2$ in a very satisfactory manner. However, the final answer for the thermochemistry of CH (helped considerably by state-of-the-art electronic structure calculations) is awaiting progress with respect to the thermochemistry of C in gas phase, as discussed above.

We are currently expanding the C$_1$ thermochemistry present in the Core Network and starting to implement some C$_2$ thermochemistry, as well as some halogen thermochemistry (since many combustion-related kinetic measurements involve the latter). As the Core Network grows to encompass more combustion-related species, we will gradually make ATcT available for open public use, in response to considerable interest among a growing number of potential users (including heavy-weight entities such as NIST and IUPAC).

Other progress

We have completed a month-long campaign of measurements at the Chemical Dynamics Beamline at ALS Berkeley. During this campaign, we have implemented and thoroughly tested on two different end-stations the new quasi-CW laser dissociation radical source. While the performance of lasers that are part of the beamline left a bit to be desired, the source worked very well and performed exactly as designed. During the testing process we have acquired new spectra on several combustion-related species, such as HOCO and propargyl.

In collaboration with Robert Botto and Theobald Kupka (ANL) we have performed a theoretical study of NMR shifts. The effort aims to thoroughly evaluate various computational approaches that may be suitable for routine predictions of NMR shifts that will be used in the interpretation of spectra.

As part of the IUPAC Task Force on Thermochemistry of Radicals (where the Argonne effort is central to the project success), we have performed critical and meticulous evaluations of the thermochemistry of a number of small radicals important in combustion and atmospheric chemistry. The resulting "IUPAC recommended values"

will be soon published.

We have an ongoing collaboration with the group of Tamas Turany (Eotvosh U. Budapest) on extending the Active Table approach to Monte Carlo analysis of reaction mechanisms. We also have an ongoing collaboration with Attila Csaszar (Eotvos U. Budapest) and John Stanton (U. Texas Austin) on computing via state-of-the art theoretical approaches critical thermochemistry of several small radicals (where the choice of targets is driven via Active Tables). Finally, with J. A. Pople (NWU) and L. Curtiss (ANL) we are trying to develop an approach that will produce individual uncertainties for G3-type calculations.

Future Plans

Future plans of this program pivot around further developments of Active Tables, coupled to experimental investigation of radicals and transient species that are intimately related to combustion processes, particularly those that potentially define the initial attack of O_2 on hydrocarbon moieties during combustion, as well as other ephemeral species that are implicated in subsequent atmospheric chemistry (particularly hydrocarbon moieties· that contain oxygen and/or nitrogen). The experimental effort in our labs will be complemented with measurements at the Advanced Light Source at Lawrence Berkeley Laboratory. In collaboration with the theorists in the Argonne Chemical Dynamics Group, we also plan on determining in quantitative ways the effect of hindered rotations on thermochemical quantities of both transient and stable species. We also intend to further test and enhance our fitting methods for accurate determination of fragment appearance potentials.

Publications resulting from DOE sponsored research (2001-)

- *Evidence for a Lower Enthalpy of Formation of Hydroxyl Radical and a Lower Gas-Phase Bond Dissociation Energy of Water*, B. Ruscic, D. Feller, D. A. Dixon, K. A. Peterson, L. B. Harding, R. L. Asher, and A. F. Wagner, *J. Phys. Chem. A.* 105, 1-4 (2001)

- *Theoretical Investigation of the Transition States Leading to HCl Elimination in 2-Chloropropene*, B. Parsons, L. Butler, and B. Ruscic, *Mol. Phys.* 100, 865-874 (2002)

- *On the Enthalpy of Formation of Hydroxyl Radical and Gas-Phase Bond-Dissociation Energies of Water and Hydroxyl*, B. Ruscic, A. F. Wagner, L. B. Harding, R. L. Asher, D. Feller, D. A. Dixon, K. A. Peterson, Y. Song, X. Qian, C. Y. Ng, J. Liu, W. Chen, and D. W. Schwenke, *J. Phys. Chem. A* 106, 2727-2747 (2002).

- *Toward Hartree-Fock and Density Functional Complete Basis-Set-Predicted NMR Parameters*, T. Kupka, B. Ruscic, and R. E. Botto, *J. Phys. Chem. A.* 106, 10396-10407 (2002)

- *Hertree-Fock and Density Functional Complete Basis Set (CBS) Predicted Nuclear Shielding Anisotropy and Shielding Tensor Components*, T. Kupka, B. Ruscic, and R. E. Botto, *Solid State Nucl. Mag. Res.* 23, 000-000 (2003) (in press, available online since 26 March 2003)

- *A Grid Service-Based Active Thermochemical Table Framework*, G. von Laszewski, B. Ruscic, P. Wagstrom, S. Krishnan, K. Amin, S. Nijsure, S. Bittner, R. Pinzon, J. C. Hewson, M. L. Morton, M. Minkoff, and A. F. Wagner, in: *Grid Computing — GRID 2002 Proceedings*, M. Parashar Ed., (*Proc. 3rd Int. Workshop on Grid Computing, Baltimore, MD Nov. 18, 2002*) *Lecture Notes in Computer Science 2536*, Springer, Berlin-Heidelberg, 2002, pp 25-38

- *A Divertimento in Thermochemistry: From Photoionization Spectroscopy of Radicals to Active Tables*, B. Ruscic, *Abstr. Pap. 225th ACS National Meeting*, March 23-27, 2003, New Orleans, LA, PHYS-058 (2003)

- *Radical Photoionization Studies with VUV Synchrotron Radiation*, C. Nicolas, M. L. Morton, D. S. Peterka, M. Ahmed, L. Poisson, B. Ruscic, C.-Y. Ng, X. Tang, and T. Zhang, *Abstr. Pap. 225th ACS National Meeting*, March 23-27, 2003, New Orleans, LA, PHYS-269 (2003)

- *Further Refinements of the Bond Dissociation Energy in Water and Hydroxyl Radical Using the Active Thermochemical Table Approach*, B. Ruscic, R. E. Pinzon, M. L. Morton, B. Wang, A. F. Wagner, G. von Laszewski, S. G. Nijsure, K. A. Amin, S. J. Bittner, and M. Minkoff, *Proc. 58th Int. Symp. Mol. Spectrosc.*, June 16-20, 2003, Columbus, OH, WG09 (2003)

Next-Generation Electronic Structure Methods of Subchemical Absolute Accuracy: New Ansätze for Explicitly-Correlated Theories

Henry F. Schaefer III
Center for Computational Quantum Chemistry, University of Georgia
Athens, Georgia 30602-2525
Email: hfsiii@uga.edu
(706)542-2067

All *ab initio* electronic structure methods in common use today in some way involve the orbital approximation, wherein antisymmetrized products of one-electron functions are used to represent many-electron wavefunctions of chemical systems. To an increasing extent over the past few decades, these theories have delivered reliable predictions of molecular energies, geometric structures, and myriad properties for diverse fields of chemistry, certainly including the combustion community. In addition to their computational tractability, methods based on orbital expansions have indispensable interpretive merits, because they embody traditional bonding concepts. If pushed to technical limits, these conventional wavefunction methods can, on a broad scale, more or less approach chemical accuracy (1 kcal mol^{-1}) in relative energetics for small molecules, especially if some semi-empiricism is introduced. However, this level of accuracy is entirely unacceptable for many problems, particularly in establishing the building blocks of the world's thermochemical database. The saga of the heat of formation of the OH radical is a striking example of the general need for improved thermochemistry: within the last two years it was discovered that the accepted bond dissociation energy of water, and hence $\Delta H^{\circ}_{f,0}(OH)$, was too high by 0.5 kcal mol^{-1}. It is remarkable that such a sizable error in one the most fundamental thermochemical parameters of all of chemistry persisted into the 21st century, and it is sobering that comparable errors for similar species undoubtedly remain.

For very small systems, conventional coupled-cluster theory [CCSD(T)] aided by various complete basis set (CBS) extrapolations, with amendments for effects such as core correlation and special relativity, is now having an impact in resolving thermochemical discrepancies past the 1 kcal mol^{-1} benchmark. However, dreams of consistent and general subchemical accuracy (0.1-0.2 kcal mol^{-1}) cannot be realized with such methods due to a fundamental flaw in the orbital approximation itself, namely, the failure to properly describe electron cusp behavior. Accordingly, our proposal for theoretical development involves a continued pursuit of explicitly correlated wavefunctions that solve the cusp problem and promise to mature into a new generation of electronic structure methods of subchemical accuracy for combustion and other applications.

A depiction of the electron-electron cusp is a truly challenging task for many-electron molecular systems. In the region of the coalescence point, the exact wavefunction is linear in the interelectronic distance (r_{12}). In contrast, conventional quantum chemical wavefunctions effectively incorporate only even powers of r_{12}, do not have sufficient flexibility to fully relax into the conical region of the cusp, and thus are deficient in describing short-range electron correlation. The principal consequence of these deficiencies is a very protracted dependence of the computed correlation energy on higher angular momentum functions in the one-particle basis, making convergence of absolute energies to the mE_h level virtually impossible, and engendering particular problems in achieving accurate energetic predictions for processes that break electron pairs. The early work of Hylleraas on the helium atom showed that explicitly correlated methods, which directly incorporate the r_{12} variable into the wavefunction, have dramatically improved convergence characteristics. Indeed, Hylleraas CI computations on the ground state of He have now achieved better than 20 digits of accuracy in the absolute energy, at least 15 orders of magnitude better than the best conventional CI treatments!

In 2000 we started a long-term research program to further develop highly accurate *explicitly correlated* methods, to create attendant state-of-the-art computer codes, to undertake practical chemical applications of unprecedented size, and to disseminate such expertise to the community. Thus far our efforts have built upon the linear R12 methods of Kutzlenigg, Klopper, and co-workers, and have focused on the evaluation of nonstandard two-electron integrals required for R12/A and R12/B implementations in the *standard approximations*. The groundwork of our implementations of linear R12 methods and the successes of the resulting chemical applications now allow promising new theories to be pursued.

A unified formalism for explicitly correlated methods can be derived which centers on pair correlation functions of the type

$$u_{ij}(\mathbf{x}_1,\mathbf{x}_2) = \sqrt{\frac{N(N-1)}{2}}\langle\tilde{\psi}|\hat{a}_i\hat{a}_j|\Phi\rangle \tag{1}$$

$$= \sqrt{\frac{N!}{2}}\int d\mathbf{x}_3 d\mathbf{x}_4 \ldots d\mathbf{x}_N \tilde{\psi}(\mathbf{x}_1,\mathbf{x}_2,\ldots,\mathbf{x}_N)\left[\chi_1(\mathbf{x}_3)\cdots\chi_{i-1}(\mathbf{x}_{i+1})\chi_{i+1}(\mathbf{x}_{i+2})\cdots\chi_{j-1}(\mathbf{x}_j)\chi_{j+1}(\mathbf{x}_{j+1})\cdots\chi_N(\mathbf{x}_N)\right]$$

where Φ is the Hartree-Fock wavefunction comprised of N spin-orbitals χ_k, $\hat{a}_i$ and $\hat{a}_j$ are annihilation operators for a selected pair of occupied orbitals, and $\tilde{\psi}$ is an associated correlated wavefunction to be determined. To be specific and as simple as possible, let us consider the MP2 method, where $\tilde{\psi}$ is the first-order perturbation wavefunction, while the second-order energy is given by

$$E_2 = \sum_{i<j}^{occ} f_{ij}, \tag{2}$$

and the pair energies are evaluated as a single electron repulsion integral involving u_{ij} and the normalized, antisymmetrized orbital product $[ij]$, viz.,

$$f_{ij} = \left\langle[ij]\Big|\frac{1}{r_{12}}\Big|u_{ij}(1,2)\right\rangle. \tag{3}$$

Exact MP2 theory can be achieved by solving the set of two-electron integro-differential equations

$$\left[\hat{F}(1)+\hat{F}(2)-\varepsilon_i-\varepsilon_j\right]u_{ij}(1,2) = -\hat{Q}(1)\hat{Q}(2)\frac{[ij]}{r_{12}} \tag{4}$$

for the antisymmetric u_{ij} functions of all occupied ij pairs. In this equation, $\hat{F}$ is the Fock operator, and $\hat{Q}=1-\hat{P}$, where $\hat{P}$ is the projector onto the occupied orbital space. In intermediate normalization, we have the auxiliary constraint $\langle u_{ij}(1,2)|[ij]\rangle = \langle\tilde{\psi}|\Phi\rangle = 0$.

It is convenient and instructive to write the pair function in the MP2 case as

$$u_{ij}(1,2) = \sum_{a<b}^{uoc}\frac{\langle[ij]|r_{12}^{-1}|[ab]\rangle}{\varepsilon_i+\varepsilon_j-\varepsilon_a-\varepsilon_b}[ab] + \hat{Q}_{ext}(1,2)w_{ij}(1,2), \tag{5}$$

where the first term on the right is the conventional MP2 expansion involving products of unoccupied orbitals from a finite one-particle basis set. The exact integro-differential equation for the correction function $w_{ij}(1,2)$ is

$$\hat{Q}_{ext}(1,2)\left\{\left[\hat{F}(1)+\hat{F}(2)-\varepsilon_i-\varepsilon_j\right]w_{ij}(1,2) + \frac{[ij]}{r_{12}}\right\} = 0, \tag{6}$$

where

$$\hat{Q}_{ext}(1,2) = 1 - \hat{P}(1) - \hat{P}(2) + \hat{P}(1)\hat{P}(2) - \hat{Q}_{uoc}(1)\hat{Q}_{uoc}(2) \tag{7}$$

is the projector onto the external virtual space not spanned by the chosen basis set. In this form the exact MP2 pair energies (f_{ij}) are related to their conventional counterparts (e_{ij}) via

$$f_{ij} = e_{ij} + \left\langle[ij]\Big|\frac{1}{r_{12}}\Big|\hat{Q}_{ext}(1,2)w_{ij}(1,2)\right\rangle. \tag{8}$$

The most remarkable feature of this formalism is that it reduces the N-electron correlation problem down to the computation of two-electron functions [Eq. (6)] and two-electron integrals for the pair energies [Eq. (8)]! In other words, if robust analytical or numerical techniques were available to solve the two-electron problem in the field of (a) distributed nuclei, (b) instantaneous repulsions of a single electron pair, and (c) average interactions with the remaining electrons, then we could determine exact many-electron correlation energies at various levels of N-body theory. It should be emphasized that this possibility does not merely

apply to MP2 theory. For example, in coupled-cluster theory the $\hat{T}_2$ operator can be written using first quantization as

$$\hat{T}_2 = \sum_{m<n} \hat{t}(m,n) \tag{9}$$

where m and n are electron indices and

$$\hat{t}(1,2) = \sum_{i<j}^{occ} |u_{ij}\rangle\langle ij| \; . \tag{10}$$

Coupled integro-differential equations, analogous to Eq. (4), for the exact coupled-cluster u_{ij} functions have recently been developed.

Existing electron correlation methods can be categorized according to the ansatz adopted to approximate the pair correlation correction functions $w_{ij}(1,2)$. Conventional methods simply set $w_{ij}(1,2) = 0$. In contrast, current explicitly correlated methods choose some two-particle basis set to expand this function. The linear R12 methods, in their orbital-invariant form, invoke the simplest cusp-satisfying ansatz

$$w_{ij}(1,2) = \frac{1}{2} r_{12}\left(\sum_{k<l}^{occ} c_{kl}^{ij}[kl] \right), \tag{11}$$

where the summation is over occupied orbital product states. In the MP2 case the coefficients c_{kl}^{ij} are determined from Eq. (6). In the current grant period, we successfully implemented the MP2-R12 method embodied in Eq. (11) and completed several high-accuracy chemical applications by utilizing this theory in the context of coupled-cluster focal-point extrapolations. Our specific proposals for the upcoming grant period involve the development and programming of several more advanced, explicitly-correlated alternatives to Eq. (11) in the pursuit of even better accuracy and efficiency.

Publications Supported by DOE: 2001, 2002, 2003

1. T. D. Crawford, S. S. Wesolowski, E. F. Valeev, R. A. King, M. L. Leininger, and H. F. Schaefer, "The Past, Present, and Future of Quantum Chemistry," pages 219 - 246 in *Chemistry for the 21st Century*, editors E. Keinan and I. Schechter (Wiley-VCH, Weinheim, Germany, 2001).

2. M. Hofmann and H. F. Schaefer, "Structure and Reactivity of the Vinylcyclopropane Radical Cation," *Alfred Bauder Issue, J. Mol. Structure* **599**, 95 (2001).

3. R. I. Kaiser, C. C. Chiong, O. Asvany, Y. T. Lee, F. Stahl, P. R. Schleyer, and H. F. Schaefer, "Chemical Dynamics of d_1-Methyldiacetylene (CH_3CCCCD; $\tilde{X}\,^1A_1$) and d_1-Ethynylallene ($H_2CCCH(C_2D)$; $\tilde{X}\,^1A'$) Formation from Reaction of $C_2D(\tilde{X}\,^2\Sigma^+)$ with Methylacetylene, CH_3CCH ($\tilde{X}\,^1A_1$)," *J. Chem. Phys.* **114**, 3488 (2001).

4. F. Stahl, P. R. Schleyer, H. F. Bettinger, R. I. Kaiser, Y. T. Lee, and H. F. Schaefer, "Reaction of the Ethynyl Radical, C_2H, with Methylacetylene, CH_3CCH, Under Single Collision Conditions: Implications for Astrochemistry," *J. Chem. Phys.* **114**, 3476 (2001).

5. E. F. Valeev, A. G. Császár, W. D. Allen, and H. F. Schaefer, "MP2 Limit for the Barrier to Linearity of Water," *J. Chem. Phys.* **114**, 2875 (2001).

6. E. F. Valeev, W. D. Allen, H. F. Schaefer, A. G. Császár, and A. L. L. East, "Interlocking Triplet Electronic States of Isocyanic Acid: Sources of Nonadiabatic Photofragmentation Dynamics," *William H. Miller Issue, J. Phys. Chem. A* **105**, 2716 (2001).

7. R. I. Kaiser, T. N. Le, T. L. Nguyen, A. M. Mebel, N. Balucani, Y. T. Lee, F. Stahl, P. R. Schleyer, and H. F. Schaefer, "A Combined Crossed Molecular Beam and *Ab Initio* Investigation of C_2 and C_3 Elementary Reactions with Unsaturated Hydrocarbons – Pathways to Hydrogen Deficient Radicals in Combustion Flames," *Faraday Discuss. Chem. Soc.* **19**, 51 (2001).

8. F. Stahl, P. R. Schleyer, H. F. Schaefer, and R. I. Kaiser, "The Reactions of Ethynyl Radicals as a Source of C_4 and C_5 Hydrocarbons in Titan's Atmosphere," *Planetary and Space Sciences* **50**, 685 (2002).

9. B. G. Rocque, J. M. Gonzales, and H. F. Schaefer, "An Analysis of the Conformers of 1,5-Hexadiene," *Ernest R. Davidson Issue, Mol. Phys.* **100**, 441 (2002).

10. I. Hahndorf, Y. T. Lee, R. I. Kaiser, L. Vereecken, J. Peeters, H. F. Bettinger, P. R. Schreiner, P. R. Schleyer, W. D. Allen, and H. F. Schaefer, "A Combined Crossed-Beam, *Ab Initio*, and Rice-Ramsperger-Kassel-Marcus Investigation of the Reaction of Carbon Atoms $C(^3P_j)$ with Benzene, $C_6H_6(\tilde{X} \, ^1A_{1g})$ and d_6-Benzene, $C_6D_6(\tilde{X} \, ^1A_{1g})$," *J. Chem. Phys.* **116**, 3248 (2002).

11. H. F. Schaefer, "Computers and Molecular Quantum Mechanics: 1965-2001, A Personal Perspective," *J. Mol. Struct.* **573**, 129 (2001).

12. J. P. Kenny, K. M. Krueger, J. C. Rienstra-Kiracofe, and H. F. Schaefer, "C_5H_4: Pyramidane and Its Low Lying Isomers," *J. Phys. Chem. A* **105**, 7745 (2001).

13. L. Vereecken, J. Peeters, H. F. Bettinger, R. I. Kaiser, P. R. Schleyer, and H. F. Schaefer, "Reaction of Phenyl Radicals with Propyne," *J. Amer. Chem. Soc.* **124**, 2781 (2002).

14. J. C. Reinstra-Kiracofe, G. S. Tschumper, H. F. Schaefer, S. Nandi, and G. B. Ellison, "Atomic and Molecular Electron Affinities: Photoelectron Experiments and Theoretical Computations," *Chem. Revs.* **102**, 231 (2002).

15. N. R. Brinkmann, N. A. Richardson, S. S. Wesolowski, Y. Yamaguchi, and H. F. Schaefer, "Characterization of the $\tilde{X} \, ^2A_1$ and $\tilde{a} \, ^4A_2$ Electronic States of CH_2^+," *Chem. Phys. Lett.* **352**, 505 (2002).

16. R. I. Kaiser, I. Hahndorf, O. Asvany, Y. T. Lee, L. Vereecken, J. Peeters, H. F. Bettinger, P. R. Schleyer, and H. F. Schaefer, "Neutral-Neutral Reactions in the Interstellar Medium: Elementary Reactions of C_6H_5 and C_6H_6," *Astronomy and Astrophysics*, submitted (2003).

17. R. I. Kaiser, F. Stahl, P. R. Schleyer, O. Asvany, Y. T. Lee, and H. F. Schaefer, "Atomic and Molecular Hydrogen Elimination in the Crossed Beam Reaction of d_1-Ethynyl Radicals $C_2D(\tilde{X} \, ^2\Sigma^+)$ with Acetylene, $C_2H_2(\tilde{X} \, ^1\Sigma_g^+)$: Dynamics of d_1-Diacetylene (HCCCCD) and d_1-Butadiynyl (DCCCC) Formation," *Phys. Chem. Chem. Phys.* **4**, 2950 (2002).

18. N. D. K. Petraco, W. D. Allen, and H. F. Schaefer, "The Fragmentation Path for Hydrogen Atom Dissociation from Methoxy Radical," *J. Chem. Phys.* **116**, 10229 (2002).

19. L. Horny, N. D. K. Petraco, C. Pak, and H. F. Schaefer, "What Is the Nature of Polyacetylene Neutral and Anionic Chains $HC_{2n}H$ and $HC_{2n}H^+$ (n = 6-12) that Have Been Recently Observed in Neon Matrices?" *J. Amer. Chem. Soc.* **124**, 5861 (2002).

20. P. Jensen, S. S. Wesolowski, N. R. Brinkmann, N. A. Richardson, Y. Yamaguchi, H. F. Schaefer, and P. R. Bunker, "A Theoretical Study of $\tilde{a} \, ^4A_2 \, CH_2^+$," *J. Mol. Spectrosc.* **116**, 10229 (2002).

21. D. Moran, F. Stahl, E. D. Jemmis, H. F. Schaefer, and P. R. Schleyer, "Structures, Stabilities and Ionization Potentials of Dodecahedane Endohedral Complexes," *J. Phys. Chem. A* **106**, 5144 (2002).

22. Q. Li, J. F. Zhao, Y. Xie, and H. F. Schaefer, "Electron Affinities, Molecular Structures, and Thermochemistry of the Fluorine, Chlorine, and Bromine Substituted Methyl Radicals," Invited Article, *Mol. Phys.* **100**, 3615 (2002).

23. F. Stahl, P. R. Schleyer, H. Jiao, H. F. Schaefer, K.-H. Cheu, and N. L. Allinger, "The Resurrection of Neutral Tris-Homoaromaticity," *J. Org. Chem.* **67**, 6599 (2002).

24. K. W. Sattelmeyer and H. F. Schaefer, "The v_5 Vibrational Frequency of the Vinyl Radical: Conflict Between Theory and Experiment," *J. Chem. Phys.* **117**, 7914 (2002).

25. Y. Xie, W. Wang, K. Fan, and H. F. Schaefer, "The Ring Structure of the NO Dimer Radical Cation: A Possible New Assignment of the Mysterious IR Absorption at 1424 cm^{-1}," *J. Chem. Phys.* **117**, 9727 (2002).

26. L. Horny, N. D. K. Petraco, and H. F. Schaefer, "Odd Carbon Long Linear Chains $HC_{2n+1}H$ (n = 4-11): Properties of the Neutrals and Radical Anions," *J. Amer. Chem. Soc.* **124**, 14716 (2002).

27. P. R. Schreiner, A. A. Fokin, P. R. Schleyer, and H. F. Schaefer, "Model Studies on the Electrophilic Substitution of Methane with Various Electrophiles E (E = NO_2^+, F^+, Cl^+, Cl_3^+, HBr_2^+, HCO^+, OH^+, H_2O-OH^+, and Li^+)," *Fundamental World of Quantum Chemistry; A Tribute Volume to the Memory of Per-Olov Löwdin*, Editors E. J. Brändas and E. S. Kryachko (Kluwar, Dordrecht, Holland, 2003).

28. J. P. Kenny, W. D. Allen, and H. F. Schaefer, "Complete Basis Set Limit Studies of Conventional and R12 Correlation Methods: The Silicon Dicarbide (SiC_2) Barrier to Linearity", *J. Chem. Phys.*

29. A. A. Fokin, P. R. Schreiner, S. I. Kozhushkov, K. Sattelmeyer, H. F. Schaefer, and A. de Meijere, "Delocalization in Sigma Radical Cations: The Intriguing Structures of Ionized [n] Rotanes", *Organic Letters*

30. E. F. Valeev, W. D. Allen, R. Hernandez, C. D. Sherrill, and H. F. Schaefer, "On the Accuracy of Atomic Orbital Expansion Methods: Explicit Effects of k Functions on Atomic and Molecular Energies", *J. Chem. Phys.*

Picosecond Nonlinear Optical Diagnostics

T. B. Settersten and Xiangling Chen
Combustion Research Facility, Sandia National Laboratories
P.O. Box 969, MS 9056
Livermore, CA 94509-0969
Telephone: (925) 294-4701, email: tbsette@sandia.gov

Program Scope

This program focuses on two aspects of diagnostic research. First is the design of innovative sensing strategies for important combustion species. Second is the fundamental investigation of the physics and chemistry of laser-atom/molecule interactions in systems that are perturbed by inter-molecular collisions. This includes the study of fundamental spectroscopy, energy transfer, and photochemical processes. This aspect of the research is essential to the correct interpretation of diagnostic signals. We are particularly interested in resonant nonlinear optical techniques because they can provide high sensitivity, spatial resolution, and species selectivity. We use custom-built tunable picosecond lasers, which enable efficient nonlinear excitation, provide high temporal resolution for pump/probe studies of collisional processes, and are amenable to detailed physical models of laser-molecule interactions.

Recent Progress

Fluorescence quenching of NO A $^2\Sigma^+$ (v=0). Laser-induced fluorescence is an extremely sensitive technique that is often used for detection of NO concentration in flames. Its use for quantitative determination of NO concentrations requires knowledge of the rate of collisional quenching of the excited state, which can be calculated only if the cross sections for quenching by all collision partners are known. Recent measurements of temperature- and species-specific cross sections for the quenching of NO A $^2\Sigma^+$ (v=0) have enabled the development of models[1,2] that can be used to correct LIF measurements in flames for quenching. In [2], the model predicted total quenching rates in excellent agreement with measurements in premixed, low-pressure, slightly rich $CH_4/N_2/O_2$ flames. On the other hand, recently reported measurements of NO A fluorescence lifetimes in an atmospheric-pressure CH_4/air counterflow diffusion flame could not be reconciled with predictions based on either of the quenching cross-section models[1,2] and flame species calculations[3] (see Fig. 1). In particular, the computed fluorescence lifetimes were substantially lower in the fuel-rich region of the flame for temperatures below 1300 K where the dominant quenchers are H_2O and CO_2. This disagreement motivated our use of time-resolved ps-LIF to measure species- and temperature-specific cross sections for the quenching of fluorescence from NO A $^2\Sigma^+$ (v=0) by NO (X $^2\Pi$), CO_2, H_2O, CO, O_2, N_2, and C_2H_2 in the temperature range from 293 K to 1300 K.[4] A temperature- and pressure-controlled vacuum cell was used to prepare static gas samples of well-known composition. The use of picosecond excitation and fluorescence detection with sub-nanosecond resolution enables accurate measurement of NO fluorescence decays with lifetimes ranging from less than 10 ns to 200 ns. The large dynamic range provided by this instrument enables very accurate

measurement of quenching rate coefficients that are determined from the dependence of decay rates on quencher gas pressure.

Our new measurements of the quenching cross section for H_2O significantly disagree with the two commonly accepted quenching models, and generally agree with prior measurements[5] that were disregarded in formulating these models because these data were not fit by the assumed forms of the models. Using our new measurements of quenching cross sections to predict fluorescence lifetimes in the atmospheric-pressure diffusion flame of CH_4 and air described in [3] we now demonstrated excellent model-experiment agreement (see Fig. 1).
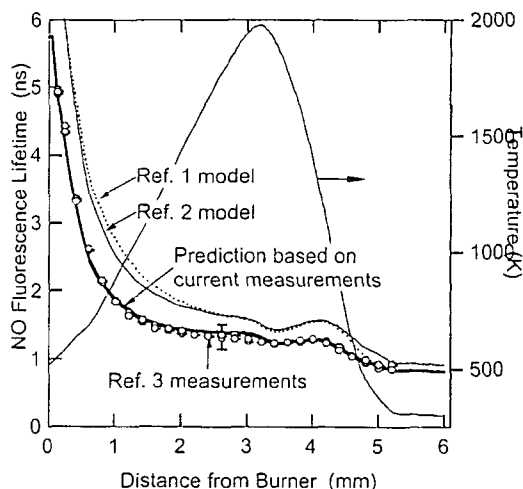

Figure 1. Measurements and model predictions of NO fluorescence lifetime in a CH_4/air diffusion flame.

Imaging of atomic oxygen in flames. Two-photon LIF detection of atomic oxygen requires UV pulses of sufficiently high energies that ambient, high-temperature CO_2 may be photolyzed to produce $O(2p\ ^3P)$ and $CO(X\ ^1\Sigma^+)$.[6] With a 5- to 10-ns UV laser pulse, ground-state O is photolytically produced and detected by the same pulse, limiting the detection sensitivity for the native population. Because the photolysis process is due to single-photon absorption while the signal generation process proceeds via two-photon absorption, picosecond excitation enables the generation of significantly larger signals while minimizing photolytic interference. We directly compared nanosecond and picosecond excitation for two-photon LIF detection of O-atom and investigated imaging applications[7] (for details, see abstract by J.H. Frank in this volume).

Nitric oxide ground-state population dynamics. Laser-induced fluorescence is commonly used for measurement of nitric oxide in combustion system. For saturated LIF the measured signal depends strongly on ground-state refilling during the laser pulse. In collaboration with Christof Schulz and Wolfgang Bessler (U. Heidelberg), Volker Sick (U. Michigan), and John Daily (U. Colorado), we have started pump-probe experiments designed to measure ground-state refilling rates. A weak ps pulse is tuned to a line in NO A-X (1,0) band and is scanned in time to probe via LIF the ground state population during intense nanosecond excitation of a line in NO A-X (0,0) band. Results of preliminary experiments suggest that efficient ground-state RET occurs during the ns laser pulse and that recycling of laser-excited population may not be a significantly important channel.

Picosecond IR-UV double-resonance spectroscopy. We previously reported[8] measurements using ns IR-UV double-resonance spectroscopy to detect OH and CH_3. These techniques are spatially resolved, absorption-based techniques in which an IR laser pumps a ro-

vibrational transition and an UV laser probes an electronic transition from the labeled level. These techniques are particularly advantageous for detection of species that are hindered by either spectral interferences in the IR or predissociation in the UV. The IR-UV techniques simplify complex electronic spectra, and can provide important characterization of electronic states that predissociate or internally convert, which is essential for the development of future diagnostics that involve these states. We are in the process of building a ps IR-UV spectrometer based on distributed-feedback dye lasers (DFDL). The single-mode picosecond laser pulses (~50 ps) are short enough to avoid collisional effects but long enough to allow for sufficient spectral resolution. High peak power will enable very efficient wavelength conversions and allow even weak transitions to be saturated. Studies at higher pressures will also be possible. The UV laser is operational, and the implementation of a next-generation DFDL for IR generation via difference-frequency mixing is almost complete.

Future Plans

Coherent picosecond double-resonance spectroscopy. The ps IR-UV spectrometer will be completed, and initial experiments will probe OH in atmospheric-pressure flames. Using the time-resolution afforded by this spectrometer, we will measure rotational energy transfer in OH X. Subsequent experiments will investigate the UV spectroscopy of methyl and propargyl.

We will investigate detection of atomic hydrogen using a single-laser, two-color polarization-spectroscopy technique that was introduced recently by Kulatilaka, *et al.*[8] We are currently building a DFDL to produce picosecond pulses at 486 nm. The DFDL output will be frequency-doubled to produce a 243-nm pump beam and the residual fundamental will be used as the probe beam. These experiments using single-mode laser pulses are particularly amenable to numerical simulations being developed by the Lucht group and will allow studies of population dynamics on sub-nanosecond timescales.

Quenching of laser-induced fluorescence at elevated temperatures. Our previous measurements of the species- and temperature-dependent quenching of the CO B $^1\Sigma^+$ (v=0) and NO A $^2\Sigma^+$ (v=0) have been limited to temperatures below 1300 K. We will build a ceramic fluorescence cell with flow control to extend these measurements to 1700K. Measurements in premixed, low-pressure flames will be used to investigate quenching at temperatures approaching 2000 K. Under low-pressure flame conditions (~ 30 Torr), we expect that the fluorescence decay rates for CO and NO will be on the order of 10^8 s^{-1} and 2.5×10^7 s^{-1}, respectively. Using ps excitation and sub-ns LIF detection, we will temporally resolve the fluorescence decays, and infer cross sections from computed species concentrations and temperature in a series of engineered flames. A variety of premixed low-pressure flames, using various fuels, oxidizers, diluents, and flow rates will be utilized to achieve desired conditions.

Photolytic interferences in two-photon LIF of O-atom and CO. We will continue our experiments to elucidate the photolysis mechanisms at play in two-photon LIF measurements of O-atom and CO concentrations. The experiment will employ a tunable ns

laser to photodissociate O_2 or CO_2 in a high-temperature fluorescence cell, and a delayed ps laser to probe the products (CO and O) with TP-LIF. Relative yields will be measured using two-photon ps LIF detection of O ($2p$ ^3P) following ns laser photolysis at 217, 226, and 230 nm. Absolute cross sections will be determined by calibrating two-photon ps LIF of CO to a known concentration.

Nitric oxide ground-state population dynamics. The experimental apparatus is being modified to improve signal levels and reproducibility. We will use the improved flow cell to measure room-temperature refilling rates during electronic excitation with a ns laser. The experimental data will be analyzed using simulations to be developed by John Daily.

References

1. P.H. Paul, J. A. Gray, J.L. Durant, and J.W. Thoman, AIAA J. **32**, 1670 (1994).
2. M. Tamura, P.A. Berg, J.E. Harrington, J. Luque, J.B. Jeffries, G.P. Smith, and D.R. Crosley, Combust. Flame **114**, 502 (1998).
3. J.J. Driscoll, V. Sick, P.E. Schrader, and R.L. Farrow, Proc. Combust. Inst. **29**, 2719 (2002).
4. T.B. Settersten, B.D. Patterson, and J.A. Gray, "Temperature-dependent cross sections for quenching of NO LIF by NO, H_2O, and CO_2," Proceedings of the 3rd Joint Meeting of the U.S. Sections of the Combustion Institute, March 2003.
5. M.C. Drake, and J.W. Ratcliffe, J. Chem. Phys. **98**, 3850 (1993).
6. see 1 below
7. J.H. Frank, T.B. Settersten, B.D. Patterson, and X. Chen, "Comparison of nanosecond and picosecond excitation for two-photon LIF detection of atomic oxygen in flames," Proceedings of the 3rd Joint Meeting of the U.S. Sections of the Combustion Institute, March 2003.
8. see 2 and 3 below
9. W.D. Kulatilaka, S.F. Hanna, and R.P. Lucht, "Two-color, two-photon laser-induced polarization spectroscopic (LIPS) measurement of atomic hydrogen," Proceedings of the 3rd Joint Meeting of the U.S. Sections of the Combustion Institute, March 2003.

BES-Supported Publications

1. T. B. Settersten, A. Dreizler, B. D. Patterson, P. E. Schrader, and R. L. Farrow, "Photolytic interference to two-photon laser-induced fluorescence detection of atomic oxygen in hydrocarbon flames," Appl. Phys. B. *in press* (2003).
2. T. B. Settersten, R. L. Farrow, and J. A. Gray, "Coherent infrared-ultraviolet double-resonance spectroscopy of CH_3," Chem. Phys. Lett. **370**, 204 (2003).
3. T. B. Settersten, R. L. Farrow, and J. A. Gray, "Infrared-ultraviolet double-resonance spectroscopy of OH in a flame," Chem. Phys. Lett. **369**, 584 (2003).
4. T. B. Settersten, A. Dreizler, and R. L. Farrow, "Temperature- and species-dependent quenching of CO *B* probed by two-photon laser-induced fluorescence using a picosecond laser," J. Chem. Phys. **117**, 3173 (2002).
5. T. B. Settersten and M. A. Linne, "Modeling Short-Pulse Excitation for Gas-Phase Laser Diagnostics," J. Opt. Soc. Am. B **19**, 954 (2002).

Theoretical Studies of Potential Energy Surfaces and Computational Methods

Ron Shepard
Chemistry Division
Argonne National Laboratory
Argonne, IL 60439
[email: shepard@tcg.anl.gov]

Program Scope: This project involves the development, implementation, and application of theoretical methods for the calculation and characterization of potential energy surfaces (PES) involving molecular species that occur in hydrocarbon combustion. These potential energy surfaces require an accurate and balanced treatment of reactants, intermediates, and products. This difficult challenge is met with general multiconfiguration self-consistent-field (MCSCF) and multireference single- and double-excitation configuration interaction (MRSDCI) methods. In contrast to the more common single-reference electronic structure methods, this approach is capable of describing accurately molecular systems that are highly distorted away from their equilibrium geometries, including reactant, fragment, and transition-state geometries, and of describing regions of the potential surface that are associated with electronic wave functions of widely varying nature. The MCSCF reference wave functions are designed to be sufficiently flexible to describe qualitatively the changes in the electronic structure over the broad range of molecular geometries of interest. The necessary mixing of ionic, covalent, and Rydberg contributions, along with the appropriate treatment of the different electron-spin components (e.g. closed shell, high-spin open-shell, low-spin open shell, radical, diradical, etc.) of the wave functions are treated correctly at this level. Further treatment of electron correlation effects is included using large scale multireference CI wave functions, particularly including the single and double excitations relative to the MCSCF reference space. This leads to the most flexible and accurate large-scale MRSDCI wave functions that have been used to date in global PES studies.

Electronic Structure Code Maintenance, Development, and Applications: A major component of this project is the development and maintenance of the COLUMBUS Program System. The COLUMBUS Program System computes MCSCF and MRSDCI wave functions, MR-ACPF (averaged coupled-pair functional) energies, MR-AQCC (averaged quadratic coupled cluster) energies, spin-orbit CI energies, and analytic energy gradients. Geometry optimizations to equilibrium and saddle-point structures can be done automatically for both ground and excited electronic states. The COLUMBUS Program System is maintained and developed collaboratively with several researchers including Isaiah Shavitt (University of Illinois), Russell M. Pitzer (Ohio State University), and Hans Lischka (University of Vienna, Austria). The COLUMBUS Program System of electronic structure codes has been maintained on the various machines used for production calculations by the Argonne Theoretical Chemistry Group, including IBM RS6000 workstations, DEC/COMPAC ALPHA workstations, the parallel IBM SP QUAD machine at ANL, the parallel IBM SP at NERSC, the Theoretical Chemistry Group's IBM SP parallel supercomputer, and the Group's 64-CPU Linux cluster. Most recently, the codes have been ported to the 512-CPU Linux cluster, Chiba City, and to the new 320-CPU JAZZ Teraflop facility at Argonne. The COLUMBUS codes also have been ported recently to the Macintosh personal computer, allowing sophisticated production-level electronic structure calculations on desktop and laptop computers. These computer codes are used in the production-level molecular applications by members and visitors of the Argonne Theoretical Chemistry Group. The next major release of the COLUMBUS codes will begin to incorporate the newer language features of F90/F95. This will facilitate future development and maintenance effort.

In collaboration with Hans Lischka (University of Vienna, Austria), Robert Harrison (Oak Ridge National Laboratory), and Thomas Mueller (Central Institute for Applied Mathematics, Juelich, Germany), the parallel version of the CI diagonalization program CIUDG and the parallel CI density code CIDEN have been developed and ported to several large parallel machines. Using the widely available TCGMSG and MPI libraries, these programs also run on networks of workstations, small-scale shared-memory parallel machines (e.g. Cray and IBM SMP nodes), and small-scale distributed memory machines (e.g. Linux clusters). The latest version of this parallel code uses the Global Array library, which allows for the elimination of unnecessary synchronization steps from earlier versions of this code and reduces the overall communications requirements for larger numbers of nodes. The current versions of the parallel CI and CI density codes allow for molecular geometry optimizations through a sequence of single-point calculations. The controlling scripts are being modified and tested to allow for automatic geometry optimization in the same way as that done for the sequential versions of these codes. The current version of the CIUDG program represents a merging of several previous programs, including the graphical unitary group approach (GUGA) spin-orbit CI code, the sequential GUGA (nonspin-orbit) CI code, the sequential AO-driven code, and the parallel GUGA CI code. At present, not all of the functionality of these ancestor codes, which have been developed separately over the past ten to fifteen years, is included in the current CI code; consequently, future effort will be directed towards enabling all of the important functionality.

In collaboration with David Yarkony (Johns Hopkins University) and Hans Lischka (University of Vienna), the ability to compute nonadiabatic coupling between different electronic states of molecules in being incorporated into the COLUMBUS Program System. This will result in the ability to compute branching ratios of chemical reactions that involve PES cusps and crossings. It will also allow for the ability to locate automatically the cusp and crossing geometries and the noncrossing regions of the PES that maximize the nonadiabatic coupling.

Iterative Matrix Diagonalization: A new iterative subspace diagonalization approach, called the Subspace Projected Approximate Matrix (SPAM) method, has been developed. In a subspace method, a new trial vector is added to an existing vector subspace each iteration. The choice of expansion vectors determines the convergence rate. The traditional Davidson and Lanczos methods are examples of iterative subspace methods. In the SPAM approach, an approximate matrix is constructed each iteration using a projection operator approach, and the eigenvector of this approximate matrix is used to define the new expansion vector. The convergence rate is improved in the SPAM method over the Davidson and Lanczos approaches because of these improved expansion vectors. The efficiency of the procedure depends on the relative expense of forming approximate and exact matrix-vector products. The SPAM method allows for the simultaneous optimization of several roots and it allows for an arbitrary number of levels of matrix approximations. This results in a multiroot-multilevel SPAM algorithm that has a wide range of possible applications. This matrix diagonalization method has been applied to a wide range of eigenvalue problems, including optimization of the lowest eigenpairs, the highest eigenpairs, and interior eigenpairs using both root-homing and vector-following. Approximations have been generated by neglecting small matrix elements, by tensor-product approximation, by expansion truncation, by neglect of off-diagonal matrix blocks, and by operator approximation. These applications demonstrate the wide range of applicability of the SPAM diagonalization method. Work in progress is directed toward approximation of MRSDCI Hamiltonian matrices based on repulsion integral approximation.

The SPAM method is also being applied to the molecular vibration eigenvalue problem. This is based on the TetraVib program of Yu and Muckerman (*J. Molec. Spec.* **214**, 11-20 (2002)) that was described at the 2002 Combustion Contractor Meeting. This code is based on a combination of spherical harmonic basis functions for the angular

degrees of freedom and discrete variable representation (DVR) of the radial degrees of freedom. In the course of debugging the SPAM method for this problem, a relatively simple approximation was used with moderate success. The normal calculation is done with 64-bit floating point arithmetic. An approximate hamiltonian operator was defined using 32-bit floating point arithmetic. The accompanying table shows the timing comparisons for a sequence of hamiltonian operators for the H_2CO molecule. On the particular hardware used for this calculation (2.4GHz Xeon), a 32-bit floating point matrix-vector product is about 20% faster than the 64-bit floating point product. The hamiltonian dimensions range from $1.1 \cdot 10^4$ to $2.2 \cdot 10^6$ and the corresponding matrix-vector product times range over three orders of magnitude. The Davidson and SPAM times shown are those for the entire calculation to converge the lowest eigenvalue (the zero point energy), including the hamiltonian setup, the iteration time, and a subsequent wave function analysis. The SPAM timings are faster than the reference Davidson timings for two reasons, the faster matrix-vector product times and also the smaller, more compact, subspace dimensions. In all cases, only two exact matrix-vector products were required with the SPAM method. The last column shows the total timing ratios for the sequence of hamiltonian operators. Although the SPAM timings are relatively modest (10% to 30% reductions of effort), this is the result of a very simple-minded approach to generating hamiltonian approximations and demonstrates the great flexibility of the method. We are optimistic that a deeper use of the underlying physics to generate approximate hamiltonian operators will result in much more significant performance advantages for the SPAM method for this problem.

SPAM Timings Using 32-Bit Floating Point Approximation

N	m	Timings/Seconds Hv	H^1v	Davidson [n]	Time	SPAM $[n,n_1]$	Time	$\dfrac{T_{SPAM}}{T_{Davidson}}$
11375	5	0.01	0.01	[12]	0.33	[2,12]	0.33	1.000
69972	7	0.08	0.06	[15]	3.31	[2,15]	2.56	0.773
280665	9	0.29	0.25	[17]	15.90	[2,16]	11.94	0.751
865150	11	1.02	0.89	[24]	82.83	[2,24]	59.45	0.718
2229955	13	2.73	2.39	[13]	99.91	[2,13]	86.90	0.870

Other planned extensions of the SPAM method include application to the generalized symmetric eigenvalue problem, the complex hermitian eigenvalue problem, the complex hermitian generalized eigenvalue problem, and the general (nonhermitian) eigenvalue problem. The application to other linear and nonlinear problems (including the coupled-cluster equation solution) will also be considered.

The TCG Beowulf Linux Cluster: The Argonne Theoretical Chemistry Group historically has maintained an advanced computer system. Over the years, these have included the FPS attached processor (1982), the Stardent Titan workstations (1988), the Alliant FX-8 (1989), and the FX-2800 (1991) shared-memory parallel computers, and more recently the IBM SP distributed memory parallel computer system (1994) which now consists of 44 nodes. It is now possible to configure commodity hardware and software with free (or relatively inexpensive) operating system software to create a machine capable of supplying much of the computational requirements of the Group. We have started to grow such a system with the purchase of a 16 node (32 CPUs) system in 2001, and this was expanded in January 2003 by an additional 16 nodes (32 additional CPUs). This cluster approach allows the group to exploit the rapidly dropping costs of CPUs, memory, switching technology, and disk storage, and the rapidly increasing processing power of commodity CPUs.

Public Distribution of Software: The COLUMBUS Program System is available using the *anonymous ftp* facility of the internet. The codes and online documentation are available from the web address http://www.itc.univie.ac.at/~hans/Columbus/columbus.html. The latest code version, 5.9.3, was released in December, 2002. In addition to the source code, the complete online documentation, installation scripts, sample calculations, and numerous other utilities are included in the distribution. A partial implementation of an IEEE POSIX 1009.3 library has been developed and is also available from ftp://ftp.tcg.anl.gov/pub/libpxf. This library simplifies the porting effort required for the COLUMBUS codes, and also may be used independently for other Fortran programming applications. The SPAM code described above is available from ftp://ftp.tcg.anl.gov/pub/spam.

Publications:

"Ab Initio Determination of Americium Ionization Potentials," J. L. Tilson, R. Shepard, C. Naleway, A. F. Wagner, and W. C. Ermler, *J. Chem. Phys.* **112**, 2292-2300 (2000).

"The Subspace Projected Approximate Matrix (SPAM) Modification of the Davidson Method," R. Shepard, A. F. Wagner, J. L. Tilson, and M. Minkoff, *J. Comp. Phys.* **172**, 472-514 (2001).

"High-Level Multireference Methods in the Quantum-Chemistry Program System COLUMBUS: Analytic MR-CISD and MR-AQCC Gradients and MR-AQCC-LRT for Excited States, GUGA Spin-Orbit CI, and Parallel CI," H. Lischka, R. Shepard, R. M. Pitzer, I. Shavitt, M. Dallos, T. Muller, P. G. Szalay, M. Seth, G. S. Kedziora, S. Yabushita, and Z. Zhang, *Phys. Chem. Chem. Phys.* **3**, 664-673 (2001).

"Geometry Optimization of Excited Valence States of Formaldehyde Using Analytical Multireference Configuration Interaction Singles and Doubles and Multireference Averaged Quadratic Coupled-Cluster Gradients, and the Conical Intersection Formed by the $1^1B_1(\sigma-\pi^*)$ and the $2^1A_1(\pi-\pi^*)$ States," M. Dallos, T. Muller, H. Lischka, and R. Shepard, *J. Chem. Phys.* **114**, 746-757 (2001).

"The Calculation of f-f Spectra of Lanthanide and Actinide Ions by the MCDF-CI Method," M. Seth, K. G. Dyall, R. Shepard, and A. Wagner, *J. Phys. B: At. Mol. Opt. Phys.* **34**, 2383-2406 (2001).

"An Ab Initio Study of the Ionization Potentials and the f-f Spectroscopy of Europium Atoms and Ions," C. Naleway, M. Seth, R. Shepard, A. F. Wagner, J. L. Tilson, W. C. Ermler, and S. R. Brozell, *J. Chem. Phys.* **116**, 5481-5493 (2002).

"An Ab Initio Study of the f-f Spectroscopy of Americium^{+3}," J. L. Tilson, C. Naleway, M. Seth, R. Shepard, A. F. Wagner, and W. C. Ermler, *J. Chem. Phys.* **116**, 5494-5502 (2002).

"Reducing I/O Costs For The Eigenvalue Procedure In Large-Scale CI Calculations," R. Shepard, I. Shavitt, and H. Lischka, *J. Computational Chem.* **23**, 1121-1125 (2002).

"Analytic MRCI Gradient for Excited States: Formalism and Application to the n-π^* valence- and n-(3s,3p) Rydberg States of Formaldehyde," H. Lischka, M. Dallos, and R. Shepard, *Mol. Phys.* **100**, 1647-1658 (2002).

STUDIES OF COMBUSTION KINETICS AND MECHANISMS

Irene R. Slagle
Research Center for Chemical Kinetics
Department of Chemistry
The Catholic University of America
Washington, DC 20064
slagle@cua.edu

PROGRAM SCOPE

The objective of the current research program is to gain new quantitative knowledge of the kinetics and mechanisms of polyatomic free radicals that are important in hydrocarbon combustion processes. Experimental studies are carried out in a heatable fast-flow reactor coupled to a photoionization mass-spectrometer. .Polyatomic free radicals (R) are generated in situ by excimer laser photolysis (193 or 248 nm) of suitable radical precursors and the radical decay is monitored in real-time experiments. Where possible, these experimental studies are coupled with theoretical ones to obtain an improved understanding of the factors governing reactivity.

RECENT PROGRESS

During the current reporting period our work has focused on radical-radical reactions which may lead to chain termination and molecular mass growth.

I. Ethyl Radical Self Reaction

The kinetics of the ethyl radical self reaction has been studied over the temperature range from 300 to 800K and bath gas (He) density $(3 - 12) \times 10^{16}$ molecule cm^{-3}. In most experiments, ethyl radicals were produced by 193-nm laser photolysis of oxalyl chloride $((CClO)_2 \rightarrow 2Cl + 2CO)$ followed by the instantaneous conversion of the chlorine atoms into ethyl radicals by the reaction with ethane $(Cl + C_2H_6 \rightarrow C_2H_5 + HCl)$. Initial concentrations of the C_2H_5 radical were determined using the measured depletion of oxalyl chloride. The kinetics of C_2H_5 decay was monitored in real time and the values of the rate constant were determined from the $[C_2H_5]$ temporal profiles. The temperature dependence of the high-pressure-limit rate constant can be represented as $k = 2.29 \times 10^{-6} \times T^{-1.66} \exp(-552K/T)$ $cm^3 molec^{-1}s^{-1}$. The disproportionation to recombination ratio at 297 and 400K was in agreement with the value of 0.14 found in previous studies (See, for example, the review in *CRC Handbook of Bimolecular and Termolecular Gas Reactions*, J.A. Kerr, Ed. 1981, Volume 2.). However, a strong ion fragmentation signal at mass 28 from both ethane and butane prevented the determination of the branching ratio at higher temperatures.

II. Propargyl Radical Self Reaction

The kinetics of the propargyl radical self reaction has been studied over the temperature interval $500 - 1000$ K and bath gas (He) density $(3 - 6) \times 10^{16}$ molecule cm^{-3}. Propargyl radicals were produced by 248-nm laser photolysis of oxalyl chloride $((CClO)_2 \rightarrow 2Cl + 2CO)$ followed by the instantaneous conversion of the chlorine atoms into propargyl radicals by the reaction with propyne $(Cl + C_3H_4 \rightarrow C_3H_3 + HCl)$. Thus, no active species other than C_3H_3 were present

in the system during the kinetics of C_3H_3 decay. Initial concentrations of the C_3H_3 radical were determined using the measured production of HCl. The kinetics of C_3H_3 decay was monitored in real time and the values of the rate constant were determined from the $[C_3H_3]$ temporal profiles. The rate constant was found to decrease with temperature from 3.3×10^{-11} cm^3 molecule^{-1} s^{-1} at 500 K to 2.8×10^{-11} cm^3 molecule^{-1} s^{-1} at 700K and 1.3×10^{-11} cm^3 molecule^{-1} s^{-1} at 1000K. The low value at 1000 K is due either to falloff or to the effects of secondary reactions regenerating the propargyl radical. Because of the lack of kinetic information available on possible secondary reactions at high temperatures (e.g., phenyl radical reacting with the excess propyne), modeling does not resolve this problem.

Products of the reaction were studied in real-time experiments as well as by GC/MS analysis. In the real-time experiments, only formation of products at mass of C_6H_6 was observed. No C_6H_5 could be detected since, under the experimental conditions employed in this study, phenyl radical would react with the excess of propyne present in the reactor. GC/MS analysis demonstrated the dependence of the distribution of products of on temperature with benzene becoming the major (>80%) product of the self reaction at temperatures above 900K. Benzene, fulvene, and 1,5-hexadiyne were identified as products by their retention times and fragmentation patterns along with two C_6H_6 unknowns that could not be identified due to the lack of standard compounds. 2,4-hexadiyne and 1,2-dimethylenecyclobutane were not detected among the products. In addition, C_8H_6 and C_9H_8 were detected in both real-time and GC/MS experiments at 1000K. GC/MS analysis suggests that these products are phenylacetylene and phenyl-1-propyne, species which can be attributed to a fast reaction of phenyl (formed directly by the C_3H_3 + C_3H_3 reaction) with propyne.

PUBLICATIONS ACKNOWLEDGING SUPPORT OF THIS GRANT

M. N. Kislitsyn, I. R. Slagle, V. D. Knyazev. Kinetics of the Reaction Between Methyl Radical and Acetylene. Symp. Int. Comb. Proc. In press. 2003.

V. D. Knyazev, I. R. Slagle. Kinetics of the Reaction Between Propargyl Radical and Acetylene. J. Phys. Chem. A, 106, 5613 (2002).

S. I. Stoliarov, V. D. Knyazev, I. R. Slagle. Computational Study of the Mechanism and Product Yields in the Reaction Systems C_2H_3 + $CH_3 \leftrightarrows C_3H_6 \leftrightarrows H$ + C_3H_5 and C_2H_3 + $CH_3 \rightarrow CH_4$ + C_2H_2. J. Phys. Chem. A, 106, 6952 (2002).

V. D. Knyazev. Theoretical Study of the Channel of Formation of CO in the Reaction of O Atoms with CH_3: Reaction Over a barrier but not Through a Saddle Point. J. Phys. Chem. A, 106, 8741 (2002).

V. D. Knyazev, I. R. Slagle. Kinetics of the Reactions of n-Alkyl (C_2H_5, n-C_3H_7, and n-C_4H_9) Radicals with CH_3. J. Phys. Chem. A, 105, 6490 (2001).

V. D. Knyazev, I. R. Slagle. Kinetics of the Reactions of Allyl and Propargyl Radicals with CH_3. J. Phys. Chem. A, 105, 3196 (2001).

S. I. Stoliarov, A. Bencsura, E. Shafir, V. D. Knyazev, I. R. Slagle. Kinetics of the Reaction of

the CHCl$_2$ Radical With Oxygen Atoms. J. Phys. Chem. A, 105, 76 (2001).

V. D. Knyazev, W. Tsang. Chemically and Thermally Activated Decomposition of Secondary Butyl Radical. J. Phys. Chem. A, 104, 10747 (2000).

S. I. Stoliarov, V. D. Knyazev, I. R. Slagle. Experimental Study of the Reaction between Vinyl and Methyl Radicals in the Gas Phase. Temperature and Pressure Dependence of Overall Rate Constants and Product Yields. J. Phys. Chem. A, 104, 9687 (2000).

COMPUTATIONAL AND EXPERIMENTAL STUDY OF LAMINAR FLAMES

M. D. Smooke and M. B. Long
Department of Mechanical Engineering
Yale University
New Haven, CT 06520
mitchell.smooke@yale.edu

Program Scope

Our research has centered on an investigation of the effects of complex chemistry and detailed transport on the structure and extinction of hydrocarbon flames in coflowing axisymmetric configurations. We have pursued both computational and experimental aspects of the research in parallel. The computational work has focused on the application of accurate and efficient numerical methods for the solution of the boundary value problems describing the various reacting systems. Detailed experimental measurements were performed on axisymmetric coflow flames using two-dimensional imaging techniques. Spontaneous Raman scattering and laser-induced fluorescence were used to measure the temperature, major and minor species profiles. Laser-induced incandescence has been used to measure soot volume fractions. Our goal has been to obtain a more fundamental understanding of the important fluid dynamic and chemical interactions in these flames so that this information can be used effectively in combustion modeling.

Recent Progress

The major portion of our work during the past year has focused on a combined computational and experimental study of time varying, axisymmetric, laminar unconfined methane-air diffusion flames and on a combined computational and experimental study of the formation of soot in axisymmetric, laminar ethylene-air diffusion flames. Additional research was begun on the implementation of high-order implicit compact methods for time-varying computations. The time varying systems can enable the investigator to bridge the gap between laminar and fully turbulent systems. In addition, time varying flames offer a much wider range of interactions between chemistry and fluid dynamics than do steady-state configurations. The sooting flames can enable the investigator to understand the detailed inception, oxidation and surface growth processes by which soot is formed in hydrocarbon flames. The compact methods have the potential of being able to solve accurately time-varying systems in a fraction of the time compared to more traditional low-order methods

Time-Varying Flames: Atmospheric pressure, overventilated, axisymmetric, coflowing, nonpremixed laminar flames were generated with a burner in which the fuel flows from an uncooled 4.0 mm inner diameter vertical brass tube (wall thickness 0.038 mm) and the oxidizer flows from the annular region between this tube and a 50 mm diameter concentric tube. The oxidizer is air while the fuel is a mixture containing methane and nitrogen 65%/35% by volume, to eliminate soot. The burner includes a small loudspeaker in the plenum of the fuel jet, which allows a periodic perturbation to be imposed on the exit parabolic velocity profile. Perturbations of 30% and 50% of the average velocity have been investigated. Because the flame is slightly lifted, there is no appreciable heat loss to the burner.

Two-dimensional profiles of temperature, mixture fraction, and mole fractions of N2, CO2, CH4, H2, CO, and H2O as well as CH* emission have been measured in the time-varying flame. We obtain CH* relative concentration from flame chemiluminescence, and species concentrations

and temperature with vibrational Stokes-shifted Raman scattering and Rayleigh scattering using the second harmonic of a Nd:YAG laser. Each measurement is averaged over 1200 laser pulses, with separate data acquisitions for each orthogonal polarization of the scattered light. Measurements are performed at heights above the burner ranging from 2.5 mm to 50 mm, in 0.5 mm increments. These line measurements are then tiled together to form images. Data are acquired for the steady state flame, and for five equally spaced phases of the forced flame over one period.

Computationally we have generalized the velocity-vorticity model to solve time-dependent problems such as the forced time varying flame. For a time-dependent system, the computer effort required to calculate the solution at each time step scales approximately linearly with the number of grid points used to discretize the domain. To employ a reduced number of grid points efficiently, we have applied the local rectangular refinement (LRR) solution-adaptive gridding method [1] --- an orthogonal, unstructured gridding technique for solving systems of coupled nonlinear elliptic PDEs --- to the two periodically time-varying axisymmetric laminar diffusion flames. The time-dependent LRR method is similar to the steady-state LRR method [1], with the following exceptions. First, in the time-dependent method, the grid undergoes remeshing every several time steps, as needed. Remeshing is an automatic process in which any unnecessary refinement is removed and any required additional refinement is added. Second, in the current work, temporal partial derivatives are discretized using second order backward differences. During the past year advances have been made in the procedure used to choose the time step and the model employed for the fuel jet exit velocity.

A new model for the fuel jet exit velocity at the burner surface has been implemented and shows promise. The old model applied a parabolic (fully developed) profile for the axial velocity; the amplitude of the parabola (value of axial velocity) varied sinusoidally in time according to the magnitude of the perturbation under investigation. This model, while a good approximation, may not be the best representation of the experimental conditions, since the experiment generates the perturbation via a loudspeaker placed in the plenum of the fuel jet (not at the burner surface). Therefore, the new computational model involves running a separate simulation of flow in the fuel tube itself prior to running the flame simulation. In the fuel tube flow simulation, which is run until it reaches true periodicity, a sinusoidal temporal oscillation is applied to a plug flow profile at the bottom of the fuel tube. The resulting velocity profile at the top of the fuel tube is stored in a file at each time step, producing a library of velocity profiles: data that are both spatially and temporally dependent. The desired flame simulation is then run, applying at the fuel jet exit the velocity profiles that are appropriately interpolated from the library. Thus far, this new model has produced preliminary results that closely resemble results obtained with the old model, except that the wake of the flame looks more realistic.

Soot Modeling: Soot kinetics are modeled as coalescing, solid carbon spheroids undergoing surface growth in the free molecule limit. The particle mass range of interest is divided into sections and an equation is written for each section including coalescence, surface growth, and oxidation. For the smallest section, an inception source term is included. The transport conservation equation for each section includes thermophoresis, an effective bin diffusion rate, and source terms for gas-phase scrubbing. The gas and soot equations are additionally coupled through non-adiabatic radiative loss in the optically-thin approximation. The inception model employed here is based on an estimate of the formation rate of two- and three-ringed aromatic species (naphthalene and phenanthrene), and is a function of local acetylene, benzene, phenyl and molecular hydrogen concentrations. Oxidation of soot is by O_2 and OH. The surface growth rate is based upon that of Harris and Weiner [2] with an activation energy as suggested by Hura and Glassman [3].

Using planar laser imaging, we obtain two-dimensional fields of temperature, fuel concentration, and soot volume fraction in the C2H4/N2 flame. The temperature field is determined using the two scalar approach of Starner et al. [4]. The soot volume fraction field is determined by laser-induced incandescence (LII). At sufficient laser intensities, the LII signal has been shown to be directly proportional to the soot volume fraction. Probe measurements of the soot volume fraction are used for calibration.

Three chemical kinetic mechanisms were utilized in the modeling work. They included a 49 species reaction set derived from GRIMech 1.2 [5] to which additional reactions describing the formation and oxidation of benzene, and related species were included [6], a 65 species mechanism based upon the work of Sun et al. [7] and a 101 reaction set from Appel, Bockhorn and Frenklach [8]. Fuel and nitrogen are introduced through the center tube (4mm id) and air through the outer coflow with plug flow velocity profiles. Both velocity profiles were those employed in the experiments. Flames containing 40% (60%), 60% (40%) and 80% (20%) mole fractions of ethylene (nitrogen) with a bulk averaged velocity of 35 cm/sec were studied. The coflow air velocity was 35 cm/sec. Reactant temperatures were assumed to be 298 K. All radial velocities were assigned to zero at the flame base. Calculations were performed on an SGI Origin 2000 computer. The computations included 20 soot sections.

We have found that by placing an upper bound on the size of the soot particles for which surface growth is allowed, we have dramatically improved the comparisons between the predicted soot volume fractions of the model and the experiments for all three mechanisms, though the magnitude and orientation of some key species still contain significant differences. These results clearly indicate that the ability to make quantitative soot predictions remains limited by some fundamental uncertainties in the soot model (including the lack of aging and aggregate formation effects), by the ability of the chemical kinetic mechanism to predict accurately the concentrations of important species (benzene, propargyl, acetylene and diacetylene) and possibly by the lack of quantitative information concerning the production of translucent particles.

Future Plans

During the next year we hope to expand our research in two main areas. First, we will continue our study of sooting hydrocarbon flames with the goal of understanding the differences in soot distribution between the computational and experimental results. A significant portion of this work will address radiation reabsorption in the computations. Second, we will continue our study of time-varying diffusion flames with the goal of incorporating high-order compact methods into the model. We will include a detailed soot model into the gas phase system with the goal of predicting soot volume fractions as a function of time. Laser induced incandescence (LII) will be used to measure soot volume fractions.

References

1. Bennett, B.A.V. and Smooke, M.D., *Combust. Theory Model.*, **2**, p. 221, (1998).

2. Harris, S.J., and Weiner, A.M., *Combust. Sci. Tech.*, **31**, p. 155, (1983).

3. Hura, H.S. and Glassman, I., *Proceedings of the Combustion Institute*, **22**, p. 371, (1988).

4. Starner, S., Bilger, R. W., Dibble, R. W., Barlow, R. S., *Combust. Sci. Tech.*, **86**, p. 223, (1992).

5. Bowman, C.T., Hanson, R.K., Davidson, D.F., Gardiner, Jr., W.C. Lissianski, `
Smith, G.P., Golden, D.M., Frenklach, M., Wang, H., and Goldenberg, M., GRI-Mech version
2.11, http://www.gri.org (1995).

6. McEnally, C. S., Schaffer, A. M., Long, M. B., Pfefferle, L. D., Smooke, M. D., Colket, M. B.,
and Hall, R. J., *Proceedings of the Combustion Institute*, **27**, p.1497, (1998).

7. Sun, C. J., Sung, C. J., Wang, H., and Law, C. K., *Comb and Flame*, **107**, p. 321, (1996).

8. Appel, J., Bockhorn, H. and Frenklach, M., *Comb. and Flame*, **121**, p. 122, (2000).

DOE Sponsored Publications since 2001

1. K.T. Walsh, J. Fielding, M.D. Smooke, and M.B. Long, "Experimental and Computational
Study of Temperature, Species, and Soot in Buoyant and Nonbuoyant Coflow Laminar Diffusion
Flames," *Proceedings of the Combustion Institute*, **28**, (2001).

2. C.S. McEnally, L.D. Pfefferle, A.M. Schaffer, M.B. Long, R.K. Mohammed, M.D. Smooke,
and M.B. Colket, "Characterization of a Coflowing Methane Air Nonpremixed Flame with
Computer Modelling, Rayleigh-Raman Imaging, and On-Line Mass Spectrometry," *Proceedings
of the Combustion Institute*, **28**, (2001).

3. B.A.V. Bennett, C.S. McEnally, L.D. Pfefferle, M.D. Smooke, and M.B. Colket,
"Computational and Experimental Study of Axisymmetric Coflow Partially Premixed
Ethylene/Air Flames," *Comb. and Flame*, **127**, (2001).

4. B.A.V. Bennett and M.D. Smooke, "The Effect of Overall Discretization Scheme on Jacobian
Structure, Convergence Rate, and Solution Accuracy within the Local Rectangular Refinement
Method," *Numerical Linear Algebra with Applications*, **8**, (2001).

5. J. Fielding. J. H. Frank, S. A. Kaiser, M. D. Smooke, and M. B. Long, "Polarized/Depolarized
Rayleigh Scattering for Determining Fuel Concentration in Flames," *Proceedings of the
Combustion Institute*, **29**, (2002).

6. S. V. Naik, N. M. Laurendeau, J. A. Cooke and M. D. Smooke, "A Soot Map for Methane-
Oxygen Counterflow Diffusion Flames," to be published *Combust. Sci. and Tech.*, (2003).

7. S. V. Naik, N. M. Laurendeau, J. A. Cooke, and M. D. Smooke, "Effect of Radiation on Nitric
Oxide Concentrations Under Sooting Oxy-Fuel Conditions," to be published, *Comb. and Flame*,
(2003).

8. M. D. Smooke, R. J. Hall and M. B. Colket, "Modeling the Transition from Non-Sooting to
Sooting Coflow Ethylene Diffusion Flames," to appear, *Comb. Theory and Modeling*, (2003).

Universal/Imaging Studies of Chemical Dynamics

Arthur G. Suits
Chemistry Department
Brookhaven National Laboratory
Upton, NY 11973
and
Department of Chemistry
Stony Brook University
Stony Brook, NY 11794
arthur.suits@sunysb.edu

Program Scope

Detailed investigations are conducted into: the dynamics of elementary reactions important in combustion and atmospheric chemistry; the decay mechanisms and dynamics of excited molecular states and transient radicals; nonadiabatic reaction dynamics; the photochemistry and reactivity of complex molecules; and the spectroscopy of important transient species. The focus of this program is on combining universal probes, providing global insight, with state-resolved probes providing quantum mechanical detail, to develop a molecular-level understanding of chemical phenomena. This research is conducted using state-of-the-art molecular beam machines, reactive scattering, and vacuum ultraviolet lasers in conjunction with ion imaging technqiues. An ongoing parallel effort is made to develop new tools and experimental methods with which to achieve these goals. The program benefits greatly from interactions with the other members of the Gas Phase Molecular Dynamics group at BNL, with strongly coupled dynamics, spectroscopy, kinetics and theoretical studies often brought to focus on a single issue.

Recent Progress

<u>Rotationally-resolved Ion Pair Imaging Spectroscopy of CH_3^+</u>. Using the "second-generation" velocity mapping system mentioned below, we have achieved rotationally resolved Ion Pair Imaging Spectra (IPIS) for numerous vibrational levels of the methyl cation. The results yield new vibrational frequencies and rotational constants for this fundamental system and show the capability of the IPIS technique to provide high resolution results despite the larger angular momenta in the fragments compared to photoelectron spectroscopy.

<u>Development of high-resolution multi-lens velocity mapping and "DC Slice Imaging"</u>. For conventional velocity map imaging, high fields in the ionization region lead to a strong dependence of the magnification on the birthplace of the ion on the time-of-flight axis and compression of the temporal spread in the ion arrival time at the detector. Use of a two-stage or three-stage lens system allows for acceleration fields an order of magnitude smaller, leading to greatly reduced dependence on ionization position, and allowing for larger ionization volumes that are critical for the VUV probes we employ. Furthermore, we find that this lens geometry automatically makes it possible to obtain the equatorial "slice" of the image under pure velocity mapping conditions simply by applying a brief gate pulse to the detector. This obviates the need for reconstruction techniques that can introduce noise and artifacts into the results, leading to greatly enhanced S/N and improved resolution. We have applied this technique to achieve improved velocity resolution and S/N for photochemistry and, recently, reactive scattering studies.

Direct imaging of O(^{3}P) + alkane reactions: energy dependence of the dynamics. We have obtained the first direct differential cross sections for reaction of ground state oxygen with alkanes, via single-photon VUV probe of the hydrocarbon radical product in these reactions. Crossed-beam reaction of O(^{3}P) with the a variety of hydrocarbon target molecules show direct back scattering and a large fraction of energy in internal modes of the hydrocarbon radical – on the order of 60% of the available energy – clearly showing the inadequacy of the quasi-triatomic model often invoked to understand these reactions. We have augmented these studies with ab initio calculations and Monte Carlo simulations of Doppler spectra performed by Jim Muckerman and Greg Hall. Virtually all that is known about these systems comes from laser-induced fluorescence spectra of the OH product. Only one previous study described differential cross sections for these systems, and that was obtained only for the OH (v=1) product. Our results provide the first detailed global insight into translational energy and angular distributions for these reactions. The results suggest that in these reactions the H abstraction is a "vertical" process such that the radical relaxation energy is not available for translational energy release.

Photodissociation of chlorobutane and the energy dependence of the photoionization efficiency of alkyl radicals. An important issue that arises with our use of 157 nm single photon ionization of hydrocarbon radicals as a probe technique is the possibility of the detection efficiency varying strongly with internal energy in the product. Indeed, this problem is faced by most molecular probe techniques, from electron impact ionization to REMPI to LIF. Rarely is much of an effort to investigate this issue but it can have a profound impact on the distributions one obtains. We have measured the relative efficiency of our 157 nm probe using 193 nm photodissociation of chlorobutane, with probe of the Cl product using established REMPI methods, and compared that result with 157 nm probe of the alkyl fragment. We find no significant dependence of the VUV probe on the internal energy in the radical produced at 193nm, affording some confidence in our use of this probe technique.

Imaging O(^{3}P) vs. O(^{1}D) + alkane reactions: the role of electronic excitation. We have extended our studies of oxygen atom reactions with alkanes to include a direct comparison of ground state and electronically excited oxygen atom reaction with hydrocarbons. The purpose of these studies is severalfold. First we are interested in the nature of the H abstraction pathway in the O(^{1}D) reactions, which are believed to proceed largely through insertion and formation of a long-lived intermediate, but may also include a direct component. Second, we wish to take advantage of the opportunity afforded by our sensitive single-photon probe to perform a direct comparison of the dynamics of reaction on the triplet and singlet potential energy surfaces at the same energy. Finally, C-C bond fission leading to formation of the hydroxyalkyl radical has been proposed as an important channel in these reactions, and our probe is extremely sensitive to this product. The results we have obtained for O(^{1}D) and O(^{3}P) reaction with n-pentane yield some anticipated results as well as some surprises. The results for the ground state reaction are consistent with our previous studies and our proposed picture of "vertical" H abstraction. For the singlet reaction, we clearly see two components in the translational energy release and considerable coupling of the energy release and differential cross sections. We can associate the faster forward scattered component with formation of a transient insertion intermediate (which paradoxically is associated with vibrationally excited OH) while the slower isotropic component is associated with the statistical decay of an activated alcohol. We see no evidence of the C-C bond fission process, and we ascribe this to the likely secondary decomposition of these hot hyroxyalkyl radical products to the corresponding aldehydes.

Future Plans

Cl + alkane reactions. Our sensitive VUV probe of alkyl radicals, combined with our recently developed DC slice imaging technique, will allow detailed measurement of the product velocity-flux contour map directly in these crossed-beam scattering studies. Work on the Chemical Dynamics Beamline has shown strongly coupled angular and translational energy release distributions for this system, but the detailed nature of the dynamics, in particular the link between the differential cross sections and the primary vs. secondary H abstraction question, remain clouded.

State-resolved imaging study of the O(^{1}D) + methane reaction. We will compare our VUV studies of H abstraction dynamics in C-4 to C-6 alkanes to the reaction with methane, using a 2+1 state-resolved probe of the methyl radical product. In this case we expect to see correlated product state information for the undetected OH cofragment in the translational energy release distributions. These studies will complement the theoretical direct dynamics calculations being performed in the group.

Application of four-wave mixing in Hg vapor to produce intense VUV for scattering studies. Our sensitive crossed-beam imaging studies now rely on single photon ionization by the 7.9 eV F_2 laser. This unfortunately limits the range of systems we may study to those having an ionization energy below 7.9 eV. Many interesting systems, including, for example, those involving abstraction of a primary hydrogen atom, have an ionization energy in the vicinity of 8 to 9 eV. We have tested four-wave mixing in Hg vapor as a convenient, intense source of 10 eV photons, and it looks very promising. The Hg four-wave mixing system benefits from a double resonance, yielding the most efficient laser-based VUV source. We can then apply this source to reaction dynamics studies in simpler systems such as O(^{3}P) or Cl + CH$_4$.

Ion Pair Imaging studies with an XUV-FEL. Brookhaven National Laboratory is unique in the U.S. in that a successful extreme ultraviolet (XUV) free electron laser has been developed and is now in operation. Furthermore, this source is unique in the world in that it operates on a principle of high-gain harmonic generation from a laser seed, thereby providing intense, fully coherent, transform-limited, sub-picosecond radiation in the extreme ultraviolet. We are currently using this source to extend our ion pair imaging studies into the XUV, with an eye to ion pair dissociation dynamics and superexcited state decay processes. Theoretical studies of these superexcited states are being conducted by Hua-Gen Yu in parallel with the experimental work.

DOE Publications 2001-present

F. Qi, O. Sorkhabi, A. G. Suits, S.-H. Chien and W.-K. Li, "Photodissociation of ethylene sulfide at 193nm : A photofragment translational spectroscopy study with VUV synchrotron radiation and ab initio calculations," *J. Am. Chem. Soc.*, **123**, 148 (2001).

Julie A. Mueller, Johanna L. Miller, Laurie J. Butler, Fei Qi, Osman Sorkhabi and Arthur G. Suits, "Internal Energy Dependence of the H + Allene / H + Propyne Product Branching from the Unimolecular Dissociation of 2-Propenyl Radicals," *J. Phys. Chem. A* **104**, 48 (2001).

O. Sorkhabi, F. Qi, A.H. Rizvi and A.G. Suits, "The ultraviolet photochemistry of phenylacetylene and the enthalpy of formation of 1,3,5-Hexatriyne," *J. Am. Chem. Soc.*, **123**, 671 (2001).

C. L. Berrie, C. A. Longfellow, A. G. Suits and Y. T. Lee, "Infrared multiphoton dissociation of acetone in a molecular beam," *J. Phys. Chem. A.*, **105**, 2557 (2001).

M. Ahmed, D. S. Peterka, P. Regan, X. Liu and A. G. Suits, "Ion pair imaging spectroscopy: $CH_3Cl \rightarrow CH_3^+ + Cl$," *Chem. Phys. Lett.* **339**, 203 (2001).

A. G. Suits and F. Qi, "The photodissociation of cyclic sulfides probed with tunable undulator radiation," *J. Elect. Spec. Rel. Phenom.*, **119**, 127 (2001).

X. Liu, R. L. Gross and A. G. Suits, "'Heavy electron' photoelectron spectroscopy: rotationally resolved ion pair imaging of CH_3^+," *Science* **294**, 2527 (2001).

A.G. Suits, "Photodissociation and Reaction Dynamics Studies Using Third-Generation Synchrotron Radiation." In **Chemical Applications of Synchrotron Radiation, Part I**, T.K. Sham, ed., (World Scientific, Singapore, 2002.)

X. Liu, R. L. Gross and A. G. Suits, "Differential cross sections for $O(^3P)$ + alkane reactions by direct imaging," *J. Chem. Phys.* **116**, 5341 (2002).

R. L. Gross, X. Liu and A. G. Suits, "The ultraviolet photodissociation of 2-chlorobutane: an imaging study comparing universal and state-resolved probe techniques," *Chem. Phys. Lett.* **362**, 229 (2002).

X. Liu, R. L. Gross, G. E. Hall, J. T. Muckerman and A. G. Suits, "Imaging $O(^3P)$ + alkane reaction dynamics in crossed molecular beams: Vertical versus adiabatic H abstraction dynamics," *J. Chem. Phys.* **117**, 7947 (2002).

F. Qi and A. G. Suits, "Photodissociation of propylene sulfide at 193 nm: A photofragment translational spectroscopy study with VUV synchrotron radiation," *J. Phys. Chem. A.* **106** 11017 (2002).

J. K. C. Lau, W. K. Li, F. Qi and A. G. Suits, "A Gaussian-3 study of the photodissociation channels of propylene sulfide," *J. Phys. Chem. A.* **106** 11025 (2002).

X. Liu and A. G. Suits, "The dynamics of hydrogen abstraction in polyatomic molecules," in **Modern Trends in Chemical Reaction Dynamics**, X. M. Yang and K. Liu, eds. (World Scientific, Singapore: in press.)

Elementary Reaction Kinetics of Combustion Species

Craig A. Taatjes

Combustion Research Facility, Mail Stop 9055, Sandia National Laboratories,
Livermore, CA 94551-0969
cataatj@sandia.gov   www.ca.sandia.gov/CRF/staff/taatjes.html

SCOPE OF THE PROGRAM

This program aims to develop new laser-based methods for studying chemical kinetics and to apply these methods to the investigation of fundamental chemistry relevant to combustion science. The central goal is to perform accurate measurements of the rates at which important free radicals react with stable molecules. Understanding the reactions in as much detail as possible under accessible experimental conditions increases the confidence with which modelers can treat the inevitable extrapolation to the conditions of real-world devices. Another area of research is the investigation and application of new detection methods for precise and accurate kinetics measurements. Absorption-based techniques are emphasized, since many radicals critical to combustion are not amenable to fluorescence detection.

An important part of our strategy is using experimental data to test and refine detailed calculations (working in close cooperation with Stephen Klippenstein and Jim Miller), drawing on the calculational results to gain insight into the interpretation of our results and to guide experiments that will probe key aspects of potential energy surfaces. This strategy has been very successful in our investigations of the reactions of alkyl radicals with O_2, where the combination of rigorous theory and validation by detailed experiments has made great strides toward a general quantitative model for alkyl oxidation. Reactions of unsaturated hydrocarbon radicals that may play a role in soot formation chemistry are also targets of investigation.

PROGRESS REPORT

The current efforts of the laboratory center on developing high-sensitivity absorption-based techniques for kinetics measurements, and on applying these techniques to investigate important combustion reactions. In the last year we have continued to concentrate on the application of cw infrared frequency-modulation spectroscopy to measuring product formation in the reaction of alkyl radicals with O_2.

Measurements of Product Formation in Alkyl + O_2 Reactions

Master equation simulations and ab initio calculations on the ethyl and propyl reactions with O_2 have been compared with LIF and FM measurements of product formation in these reactions to produce and validate a phenomenological model capable of explaining the body of kinetic data on these reactions. One key result is the need to include formally direct pathways for chemically activated reactions. For example, the experiments are very sensitive to the direct formation of OH from R + O_2, which occurs

by isomerization and elimination of OH from the incipient RO_2 complex before collisional stabilization can occur.

Neopentyl + O_2 The OH formation from Cl-initiated neopentane oxidation has been measured to complement previous measurements of HO_2 production in the same system. Ab initio calculations of stationary states in the neopentyl + O_2 system carried out by Stephen Klippenstein have been used to construct a provisional model for neopentyl oxidation, by extending the parameterized results of detailed master equation calculations on the analogous n-propyl + O_2 reaction. Once again, including formally direct pathways for bimolecular product formation and isomerization is critical for a correct description of the reaction. In addition, HO_2 is postulated to be formed from the reaction of OH with the neopentylperoxy radical; although this reaction has not been experimentally investigated it is calculated to be barrierless. The model predicts the observed HO_2 and OH formation remarkably well, and also nearly quantitatively models published OH LIF experiments of Pilling and coworkers. These earlier experiments had been interpreted as a direct measurement of the key $RO_2 \leftrightarrow QOOH$ isomerization rate; however, the present master-equation-based model implies an isomerization rate sixty times greater than that derived under the earlier interpretation.

C_2D_5, $C_3D_7 + O_2$ The kinetic isotope effect for DO_2 production is a convolution of kinetic isotope effects for the stabilization, redissociation, and elimination channels, and successful modeling of the deuterated system will place additional demands on the theoretical description of the alkyl + O_2 potential energy surface. In both ethyl and propyl + O_2 reactions, the increased density of states in the RO_2 radical leads to a more pronounced role for the stabilization channel, as reflected in smaller prompt and total DO_2 yields than HO_2 yields, and slower secondary formation of DO_2. The overall yield of DO_2 nears 100% only at low radical densities. Because the overall yield is governed by the competition between reactive removal of RO_2 by self reaction and elimination of HO_2, this observation may be affected by a kinetic isotope effect in the alkylperoxy self reaction. Measurements of DO_2 formation in the C_2D_5 and $C_3H_7 + O_2$ reactions have been completed as a function of temperature and pressure. Full analysis of the data and preparation for publication is ongoing.

Infrared Spectroscopy of HO_2 Radical

The high-resolution spectrum of the overtone of the $H-O_2$ stretch ($2v_1$) has been measured with transient laser FM spectroscopy. This transition has been extensively used to monitor HO_2 yet an adequate high-resolution spectrum had not previously been reported. The overtone appears to be heavily perturbed, possibly by the nearby (v_2+5v_3) state. The successful assignment of the lines of this transition may enable temperature-dependent absorption cross sections to be calculated from room temperature measurements.

Laser Photolysis/cwLPA Measurements of C_2H_3 Reactions

Long-path absorption spectroscopy of the vinyl radical has been applied to kinetic investigations of its reactions with stable species. The vinyl radical is detected using a

vibrational band of the $A \leftarrow X$ transition near 403 nm after 266 nm photolysis of C_2H_3I. The pulsed laser photolysis / cw laser absorption technique has been employed to investigate the vinyl + NO reaction as a function of pressure in the temperature range from 300 to 700 K. This reaction has been calculated to proceed via a stable C_2H_3NO species, and to form HCN + CH_2O at elevated temperature. At room temperature, the rate constant is $1.6 \pm 0.4 \times 10^{-11}$ cm^3 molecule^{-1} s^{-1} and no pressure dependence is observable at pressures above 10 Torr of helium. At higher temperatures, falloff of the rate constant at lower pressures is observed, which has been fit using the Troe formalism. A publication on these results is currently in preparation.

Infrared Absorption Measurements of C_3H_3 Reactions

Infrared laser absorption spectroscopy has been used to investigate recent discrepancies in measurements of the propargyl radical self-reaction rate coefficient and product formation in 193 nm photolysis of propyne. The cross section of propargyl radical has been measured relative to that of HCl using the Cl + propyne reaction, yielding a peak absorption cross section, assuming Doppler-limited lines, of $(1.9 \pm 0.4) \times 10^{-18}$ cm^2 for the P(12) line of the ν_1 fundamental at 296 K and 6 Torr He. The rate coefficient for the propargyl radical (CH_2CCH) self-reaction was then determined by modeling the infrared absorption of the propargyl radical formed in the 193 nm photolysis of propargyl chloride ($HCCCH_2Cl$) and propargyl bromide ($HCCCH_2Br$). The propargyl self-reaction rate coefficient so obtained, $(3.9 \pm 0.6) \times 10^{-11}$ cm^3 molecule^{-1} s^{-1}, is consistent with measurements from Hudgens's group and Fahr's group, as well as with recent work by Slagle and Knyazev and by Hippler and coworkers. However, it disagrees significantly with the one previous infrared absorption determination.

The 193 nm photolysis of propyne has been thought to produce the 1-propynyl radical; however, recent H-atom time-of-flight measurements by Ashfold's group of propyne photolysis at slightly longer wavelengths have suggested that ground state dissociation, forming the propargyl radical, is dominant. In our experiments both the propargyl radical and acetylene (HCCH) are observed in room temperature 193 nm photolysis of propyne (CH_3CCH). The propargyl is formed promptly following the UV photolysis pulse, and the magnitude of the signal is unaffected by the addition of O_2. The observed propargyl signal is consistent with direct CH_2CCH formation in the 193 nm photolysis of propyne and appears inconsistent with formation by secondary reactions of the 1-propynyl radical (CH_3CC). The observed CH_2CCH yield per 193 nm photon absorbed is 0.49 ± 0.10.

FUTURE DIRECTIONS

Characterization of R + O_2 reactions will continue. The ability to simultaneously probe various reactants and products will play a key role in extending these measurements. In future experiments, photolysis of selected alkyl halides or reactions of Br with alkanes may be used to generate individual alkyl isomers. Selective deuteration also may make it possible to distinguish among different internal abstraction pathways in R + O_2 reactions. Interpretation of isotopic labeling experiments will require detection of

both HO_2 and DO_2 and an understanding of the kinetic isotope effects on the overall reaction. Probing the electronic transition of the DO_2 using difference frequency generation of a cw Nd:YAG and a dye laser in $LiNbO_3$ will enable simultaneous detection of HO_2 (in the H-O overtone) and DO_2 (in the $A \leftarrow X$ band). In the long term, detection of the hydroperoxy radical intermediate in the $R + O_2 \rightarrow RO_2 \rightarrow QOOH \rightarrow QO + OH$ mechanism might be possible in the infrared. In addition to characterizing saturated alkyl radical reactions with O_2 at a higher level of detail, the present methodology will be extended to reactions of unsaturated radicals with O_2. Investigation of the kinetics of vinyl radical reactions using visible absorption detection will continue with measurements of reactions of C_2H_3 with unsaturated hydrocarbons as a function of temperature and pressure.

Publications acknowledging BES support 2001-present

1. John D. DeSain, Eileen P. Clifford, and Craig A. Taatjes, "Infrared Frequency-Modulation Probing of Product Formation in Alkyl + O_2 Reactions: II. The Reaction of C_3H_7 with O_2 between 296 and 683 K," *J. Phys. Chem. A*, **105**, 3205 –3213 (2001).
2. Craig A. Taatjes and John F. Hershberger, "Recent Progress in Infrared Absorption Probing of Elementary Reaction Kinetics," *Annu. Rev. Phys. Chem.* **52**, 41-70 (2001).
3. Holger Thiesemann, Eileen P. Clifford, Craig A. Taatjes, and Stephen J. Klippenstein, "Temperature Dependence and Deuterium Kinetic Isotope Effects in the CH (CD) + C_2H_4 (C_2D_4) Reaction between 295 and 726 K," *J. Phys. Chem. A*, **105**, 5393-5401 (2001).
4. Leonard E. Jusinski and Craig A. Taatjes, "Efficient and Stable Operation of an Ar^+-Pumped Continuous-Wave Ring Laser from 505-560 nm Using a Coumarin Laser Dye," *Rev. Sci. Instrum.* **72**, 2837-2838 (2001).
5. John D. DeSain and Craig A. Taatjes, "Infrared Frequency-Modulation Probing of Product Formation in Alkyl + O_2 Reactions: III. The Reaction of Cyclopentyl Radical (c-C_5H_9) with O_2," *J. Phys. Chem. A* **105**, 6646-6654 (2001).
6. John D. DeSain, Craig A. Taatjes, James A. Miller, Stephen J. Klippenstein, and David K. Hahn, "Infrared Frequency-Modulation Probing of Product Formation in Alkyl + O_2 Reactions: IV. Reactions of Propyl and Butyl Radicals with O_2," *Faraday Discuss.* **119**, 101-120 (2001).
7. Craig A. Taatjes and Stephen J. Klippenstein, "Kinetic Isotope Effects and Variable Reaction Coordinates in Barrierless Recombination Reactions," *J. Phys. Chem. A* **105**, 8567-8578 (2001).
8. John D. DeSain, Leonard E. Jusinski, Andrew D. Ho, and Craig A. Taatjes, "Temperature Dependence and Deuterium Kinetic Isotope Effects in the Reaction of HCO (DCO) with O_2 between 298 and 673 K," *Chem. Phys. Lett.* **347**, 79-86 (2001).
9. Milena Shahu, Chun-Hui Yang, Charles D. Pibel, Andrew McIlroy, Craig A. Taatjes, and Joshua B. Halpern, "Vinyl Radical Visible Spectroscopy and Excited State Dynamics," *J. Chem. Phys.* **116**, 8343-8352 (2002).
10. Jared D. Smith, John D. DeSain, and Craig A. Taatjes, "Infrared Laser Absorption Measurements of HCl(v=1) Production in Reactions of Cl Atoms with Isobutane, Methanol, Acetaldehyde, and Toluene," *Chem. Phys Lett* **366**, 417-425 (2002).
11. John D. DeSain, Stephen J. Klippenstein, Craig A. Taatjes, Michael D. Hurley, and Timothy J. Wallington, "Product Formation in the Cl-Initiated Oxidation of Cyclopropane" *J. Phys. Chem. A* **107**, 1992-2002 (2003).
12. Michael D. Hurley, William F. Schneider, Timothy J. Wallington, David Mann, John D. DeSain, and Craig A. Taatjes, "Kinetics of Elementary Reactions in the Chain Chlorination of Cyclopropane," *J. Phys. Chem. A* **107**, 2003-2010 (2003).
13. John D. DeSain, Stephen J. Klippenstein, and Craig A. Taatjes, "Time-resolved Measurements of OH and HO_2 Formation in Pulsed-Photolytic Chlorine Atom Initiated Oxidation of Neopentane," *Phys. Chem. Chem. Phys.* **5**, 1584 - 1592 (2003).
14. John D. DeSain, Andrew D. Ho, and Craig A. Taatjes, "High Resolution Diode Laser Absorption Spectroscopy of the O-H stretch overtone band (2,0,0) $\leftarrow$ (0,0,0) of the HO_2 Radical," *J. Mol. Spectrosc.*, in press.
15. John D. DeSain, Stephen J. Klippenstein, James A. Miller and Craig A. Taatjes, "Measurement, Theory, and Modeling of OH Formation From the Reactions of Ethyl and Propyl Radicals with O_2," *J. Phys. Chem. A*, in press.
16. John D. DeSain and Craig A. Taatjes, "Infrared Laser Absorption Measurements of the Kinetics of Propargyl Radical Self-Reaction and the 193 nm Photolysis of Propyne," *J. Phys .Chem. A*, in press.

The Extraction of Underlying Molecular Vibrational Dynamics from Complex Spectral Regions

H. S. Taylor, Principal Investigator

Department of Chemistry, SSC 704

University of Southern California

Los Angeles, CA 90089-0482

E-mail: taylor@chem1.usc.edu

PHONE: (213) 740-4112; FAX: (213) 740-3972

Perhaps the best way to simultaneously remind the reader of the aims of our project, to present the new work done in the last year and to establish an appreciation of what we are now working on and where we see new challenges is to first reprint an abstract written a year and a half ago for another meeting and entitled "Nonlinear Dynamics and Molecular Spectroscopy: A Successful Marriage".

The abstract reads:

The object of our research program, done in collaboration with Dr. C. Jung is to take the results of a measured complex spectra of the high vibrational levels of polyatomic molecules and to extract from them the various internal motions that when quantized give rise to these spectra. In short we are learning how the atoms in the molecules move and how energy is transferred when specific amounts of energy are put locally into the molecule. All this can be done if the experimental results can be represented by a spectroscopic Hamiltonian. No potential surfaces or large-scale calculations are needed. Given this Hamiltonian, if the number of degrees of freedom minus the number of constants of motion are two, we can use the semiclassical limit of the spectroscopic Hamiltonian and canonical transforms to reduce the problem to one of a configuration space of two canonical angles. Then by comparing the two-

dimensional density and phase accumulation plots of eigenfunctions, which are trivially obtained from the Hamiltonian, to the tori and organizing periodic orbits projected from the phase space onto the configuration space, we can: (1) classify the eigenstates into several series that are each quantization ladders of similar dynamics, (2) assign meaningful quasiconserved quantum numbers for each state by counting nodes in the density plots if the density is localized in angle space and by counting phase advances in directions where the density is delocalized; (3) relate these series to special organizing structures in phase space which are then transformed back to the full dimension action-angle space and then (4) with appropriate assumptions further transform back into motions in physical space. The result is that we obtain for highly excited spectra various ladders of levels each based on a definitive type of motion and assignment. These ladders overlap in energy and when merged yield the spectra which was observed and previously thought to be too complex to be interpretable by previously known methods. Application has been made to C_2H_2[1,2] CHBrClF[3], DCO[5] and N_2O[4].

Relative to this abstract probably the biggest progress has been the completion to the stage of writing up of an anlysis of two more molecules both studied experimentally by Quack and coworkers, CF_3CHFI[6] and CDBrCl[7]. The key difference for these molecules from past ones studied is that the effective Hamiltonian given in Quacks' papers had four degrees of freedom and one constant of the motion, the Polyad number. This means that the reduced angle space in which we must represent pictorially the magnitude of each eigenfunction and graphically it's phase, is now three-dimensional. The good news is that our methods were able to identify for the large majority of the 161 states in the 5th Polyad (the most spectroscopically complex Polyad measured) the underlying dynamics and assignment. Unexpected motions that result from frequency locking of three normal modes via multiple Fermi interactions are uncovered. These papers are in the write up stage. The "bad news" albeit not unexpected is that we are now confronting two natural limitations of the "detailed extraction of internal motions" type of spectral inturpretation that we carry out. The first barrier is simply viewing the wave functions in three-dimensions. We remind the readers that our methods depend on visually sorting our reduced dimensions (here 3) angle space representation of the eigenstates into energetically overlapping ladders of different dynamics, ordering the states on a ladder by node and phase advance counts (which with the Polyad number gives the assignment) and then

identifying from the appearance and location (in angle space) of the wave function an idealized classical trajectory which when transformed back to displacement coordinate space yields pictures of the internal motions upon which the state is quantized. Even though our highly excited wave functions in reduced 3D angle space are very much simpler than the usual ones in 4D displacement space, the graphics and slice by slice inspections needed to carry out our analysis are highly labor intensive (this is how we spent much of the year) and present big challenges for moving on to more degrees of freedom. The second limitation is the fact that in higher dimension, the density of states in a Polyad has increased so much that the basis state mixing is so extensive and complex for about 50 state functions that it is impossible to make an assignment or find an organizing structure. Such states are in a loose sense "unassignable" because they are based on motions that are "classically chaotic". As dimension increases we anticipate larger and larger regions of the spectra will be of this nature. Statistical concepts can be used to classify such spectra but such classifications are too generic and molecule unspecific to be of interest to chemists. For example given only the values of all statistical measures for a spectra would not even hint at which molecule was studied.

Another challenge we are addressing is that many molecules have low potential barriers and double wells (e.g., the inversion of H_2O) which ruin the unique definition of action-angle variables upon which the whole concept of a simplifying (dominant dynamics only) spectroscopic Hamiltonian is based. We hope to extend the concept of H(spect.) to such cases but we face formidable theoretical challenges.

We are also writing a major review of our past analysis, which can now be presented much more simply. Experience has made us better pedagogies.

We also plan to analyze more molecular systems by our simplified method. Examples are HOCl, HOBr, HCP, and NH_2.

REFERENCES

1. State-by State Assignment of the Bending Spectrum of Acetylene at 15000 cm-1: A Case Study of Quantum-Classical Correspondence, with M. P. Jacobson, C. Jung, and R.W. Field, J. Chem. Phys., 111, 600-618 (1999)

2. The Acetylene Bending spectrum at ~10,000 cm^{-1}: Quantum Assignment in the Midst of Classical Chaos, C. Jung, M. Jacobson and H.S. Taylor, J. Phys. Chem. A, 105, 681-693 (2001).

3. Extracting the CH Chromophore Vibrational Dynamics of CHBrClF Directly from Spectra: Unexpected Constants of the Motion and Symmetries, C. Jung, E. Ziemniak and H.S. Taylor, J. Chem. Phys., 115, 2449 (2001).

4. Semiclassical Assignment of the Vibrational Spectrum of N_2O, H. Waalkens, C.Jung and H.S. Taylor, 106, 911-924 (2002).

5. Extraction of the Vibrational Dynamics from Spectra of Highly Excited Polyatomics: DCO, C. Jung, H.S. Taylor and E. Atilgan, J. Phys. Chem. A., 106, 3092-3101 (2002).

6. Vibrational Spectra and Intramolecular Vibrational Redistribution in Highly Excited Deuterobromochlorofluoromethane CDBr-ClF: Experiment and Theory, A. Beil, H. Hollenstein, O.L.A. Monti, M. Quack and J. Stohner, J. Chem. Phys., 113, 2701-2718 (2000).

7. Ab Initio Calculation and Spectroscopic Analysis of the Intramolecular Vibrational Redistribution in 1, 1, 1,2-Tetrafluoroiodoethane CF_3CHFl, J. Pochert, M. Quack, J. Stohner and M. Willeke, J. Chem. Phys, 113, 2719-2735 (2000).

REFERENCES FOR DOE SPONSERED RESEARCH

1. Extracting the CH Chromophore Vibrational Dynamics of CHBrClF Directly from Spectra: Unexpected Constants of the Motion and Symmetries, C. Jung, E. Ziemniak and H.S. Taylor, J. Chem. Phys., 115, 2449 (2001).

2. Semiclassical Assignment of the Vibrational Spectrum of N_2O, H. Waalkens, C.Jung and H.S. Taylor, 106, 911-924 (2002).

3. Extraction of the Vibrational Dynamics from Spectra of Highly Excited Polyatomics: DCO, C. Jung, H.S. Taylor and E. Atilgan, J. Phys. Chem. A., 106, 3092-3101 (2002).

THEORETICAL CHEMICAL DYNAMICS STUDIES OF ELEMENTARY COMBUSTION REACTIONS

Donald L. Thompson
Department of Chemistry, Oklahoma State University, Stillwater, Oklahoma 74078

I. Program Scope

The aim of this theoretical research program is to contribute to improvements in theoretical and computational methods for studying the chemical dynamics of large, complex systems and to a better understanding of the elementary reactions that occur in hydrocarbon combustion. We are developing methods, performing simulations, and computing rates for elementary gas-phase reactions. The studies are, for the most part, based on classical trajectory simulations, semiclassical approaches, diffusion theory, and variational transition-state theory. A particularly strong emphasis of our work is the development of better ways for formulating accurate potential energy surfaces based on *ab initio* results for use in simulations of many-atom system.

II. Recent Progress

A. Interpolating moving least squares (IMLS) methods for fitting *ab initio* energies for many-atom systems

The speed with which quantum chemistry calculations can now be done allows for the direct use of *ab initio* forces in MD simulations. However, high-level quantum calculations are often too costly in computer time for practical applications and the levels of theory that must be used are often inadequate for reactions. Thus, among the immediate problems that need to be dealt with are the efficiency in using expensive high-level quantum chemistry methods (which often do not provide the necessary gradients directly) and ways to correct the errors of *ab initio* energies when necessary. The error in *ab initio* results can be dealt with in analytic PESs by simply scaling to empirical data. There is a need to develop better methods for fitting analytic potential energy surfaces (PESs) and techniques for making direct dynamics more efficient (e.g., reducing the number of points that must be computed). Within the context of modern quantum chemistry capabilities it is sensible to focus on local fitting schemes (which could be used with scaling if necessary). In the 1970's we proposed using a scheme based on local fitting with cubic splines.[1] Splines provide a very flexible and numerically efficient approach to fitting a surface with smooth first and continuous second derivatives; however, they require a fairly high density of points for a good fit. A more useful approach is the interpolating moving least squares (IMLS) introduced by Ischtwan and Collins.[2] It is based on a modified Shepard interpolation, the simplest case of IMLS. The Shepard method is a zero-degree IMLS method. It has a serious problem because the derivative of the interpolant is zero at every data point; however, this problem can be "fixed" by using Taylor expansions instead of just data points; and the method has been widely applied. Nevertheless, there is a need to explore more efficient and accurate interpolation schemes. We are exploring higher-order IMLS solutions to this problem in collaboration with Drs. Al Wagner and Michael Minkoff at Argonne National Laboratory.

The IMLS methods use weighted polynomial least squares fits to the *ab initio* points that are usually weighted by functions that depend on where the PES fit is desired. While position-dependent weights mean that the least-squares fit must be done from scratch at each location a PES fit is needed, such weights greatly improve fit accuracy by adding non-linear flexibility to the polynomial fit. The IMLS approach can be compactly programmed for any number of degrees of freedom and for any polynomial degree. The weights have a structure that allows only "nearest neighbor" *ab initio* points to significantly influence the fit. Consequently software strategies can be used to make the fit evaluation a local, rather than global, process. Initial results on few dimensional applications indicate that the number of *ab initio* points required is better than inversely proportional to the degree of the IMLS polynomial. Scaling studies are in progress.

B. Constructing PESs for large systems from component PESs

Empirical and semiempirical formulations are often the most practical approaches for constructing PESs. In fact, there exist a large number of tested analytical surfaces, many of which were accurately fit for the critical regions of interactions, i.e., near equilibrium and saddle points. As we move to larger systems, it would be beneficial if we could incorporate these potentials into the larger ones such that we take advantage of the proven accuracy of these often laboriously validated potentials. Also, given the costs of obtaining high-level *ab initio* energies, it is often necessary to focus those calculations only on the regions around the critical points on the PES. These regions of the PES can usually be fit by relatively simple analytic functions. However, describing the global PES requires that we "ties" these together, and this has often been done by using switching functions, which can involve guesses about the functional behavior and huge numbers of parameters that must be adjusted. Thus, methods are needed for combining PESs to build a PES for larger systems.

The empirical valence bond (EVB) approach used by Warshel[3] and modified by Chang and Miller[4] is physically intuitive and straightforward to implement, and thus it has been widely used for large systems. The basic idea is that given analytical forms (e.g., zeroth-order potentials) for two wells, the global PES is constructed by an exchange potential term that connects the two wells via a barrier. This is done so that PES exactly reproduces a harmonic force field about the saddle point geometry (which can be obtained from *ab initio* calculations). This is straightforward to do if only up to quadratic terms are included in the exchange potential. However, this exchange term is often not convergent or does not decay rapidly enough away from the transition-state region. To avoid this problem, we have added a damping function to the exchange term along the reaction coordinate. We have illustrated this for the *cis-trans* isomerization of HONO, including tunneling effects for which an accurate description of the reaction barrier is crucial. Based on our studies,[5] we have concluded that EVB is a practical method of constructing PES from "components" for certain types of reactions; however, care must be taken to ensure proper behavior of the potential.

C. Semiclassical Methods for Polyatomic Molecules

An important problem in realistic molecular dynamics simulations is the neglect of quantum effects. The obvious "fix" is to use semiclassical corrections, and practical methods for semiclassical treatments of chemical processes remain a very active area of

research. Our interests have focused on treating tunneling effects in polyatomic molecules by using a semiclassical method,[6] developed in our group. This method, based on the Makri-Miller[7] tunneling model, provides a practical way to include proton tunneling in MD simulations. The gist of the method is to propagate classical trajectories to determine turning points at the potential barrier and then compute WKB tunneling probabilities; that is, the method is basically a surface-hopping model. Our most recent application[8] of this was a study of the mode selectivity of hydrogen peroxide level splitting, motivated by the recent publication of an accurate PES[9] and quantum mechanical[10] and experimental results.[11] The study not only shows the validity of this tunneling model but also provides a sensitive probe of the intramolecular dynamics. Thus, the study provides a test of the validity of classical dynamics for excited vibrational states of this polyatomic molecule. The calculated level splittings for the ground and selected vibrationally excited states of HOOH are in good agreement with the trends of the experimental and quantum results. This is a method that can be applied to systems of any size.

D. The Quasiclassical Approximation: Bond Dissociations in HONO and HOOH

Nitrous acid and hydrogen peroxide are among the more thoroughly studied four-atom molecules and there is a lot of experimental and theoretical information available for them. There are some similarities between the two molecules that invite comparisons – excitation of the OH overtones can lead to dissociations of the O-N bond in HONO and the OO bond in HOOH, and the dissociation energies are close in value. The OH local-mode spectroscopy and overtone-induced dissociation of HOOH into OH fragments have been extensively studied both experimentally and theoretically.[12] There are experimental values of lower limits of the lifetimes for some rovibrational states of HOOH available for comparison. In a recent work by Reiche et al.[13] on the O-N bond dissociation of trans-HONO upon excitation of the O-H bond, the unimolecular dissociation rates for several rovibrational states of the $v_{OH}=5$ level were measured, and rough estimates of the lower limits of the lifetimes for the $v_{OH}=6$ and 7 states were given. They find that the IVR is not fast compared to reaction and thus the system is nonstatistical for the energies studied.

We have investigated the accuracy of the quasiclassical trajectory approach for describing the intramolecular dynamics and predicting the dissociation rates for the two systems. We used the Kuhn et al.[9] 6-D analytical potential based on high-level ab initio calculations in the study of HOOH and have used our recently developed EVB for HONO. The purpose was to test the validity of the quasiclassical trajectory approach for these systems. Despite the similarities, the quasiclassical approximation does not seem to be equally accurate for the two systems. The quasiclassical method seems to work well for HONO. The calculated dissociation rates for the $v_{OH}=6$ and 7 states are within the experimental ranges, and the finding that the system is nonstatistical is in accord with the results of Reiche et al.[13] On the other hand, the quasiclassical trajectory approach breaks down for HOOH near the reaction threshold region due to aphysical zero-point energy flow, although the results are better for the higher states.

III. Future Work

We will continue studies of (a) the basic formal and numerical aspects of higher degree interpolated moving least squares (IMLS) methods (in collaboration with Drs. A. Wagner and M. Minkoff at ANL); (b) studies of practical methods for simulating reactions in many-atom systems, with an emphasis on hydrocarbon radical reactions; and (c) further development of methods for treating nonstatistical (e.g., intrinsic non-RRKM) unimolecular reactions (examples: formic acid and acetyl radical); in particular, further development of the intramolecular dynamics diffusion theory approach (IDDT). We also plan to initiate studies of methods to extend our work to catalytic processes (this will be done in collaboration with Dr. D. C. Sorescu, NETL, Pittsburgh)

IV. References

1. D. R. McLauglin and D. L. Thompson, J. Chem. Phys. **59**, 4393 (1973).
2. J. Ischtwan and M. A. Collins, J. Chem. Phys. **100**, 8080 (1994).
3. A. Warshel, Accts. Chem. Res. **14**, 284 (1981).
4. Y. T. Chang and W. H. Miller, J. Phys. Chem. **94**, 5884 (1990).
5. Y. Guo and D. L. Thompson, J. Chem. Phys. **118**, 1673 (2003).
6. See: Y. Guo and D. L. Thompson, in *Modern Methods for Multidimensional Dynamics Computations in Chemistry*, D. L. Thompson, Ed., World Scientific, Singapore, 1998; p. 713.
7. N. Makri and W. H. Miller, J. Chem. Phys. **91**, 4026 (1989).
8. Y. Guo and D. L. Thompson, J. Phys. Chem. A **106**, 8374 (2002).
9. B. Kuhn, T. R. Rizzo, D. Luckhaus, M. Quack, and M. A. Suhn, J. Chem. Phys. **111**, 2565 (1999).
10. R. Chen, G. Ma, and H. Guo, J. Chem. Phys. **114**, 4763 (2001).
11. D. Luckhaus, J. Chem. Phys. **113**, 1329 (2000).
12. B. Kuhn, T. R. Rizzo, J. Chem. Phys. **112**, 7461 (2000); and references therein.
13. F. Reiche, B. Abel, R. D. Beck, and T. R. Rizzo, J. Chem. Phys. **112**, 8885 (2000); *ibid.* **116**, 10267 (2002).

Publications

1. Yin Guo and Donald L. Thompson, "Semiclassical Calculations of Tunneling Splitting in Hydrogen Peroxide and Its Deuterated Isotopomers," J. Phys. Chem. A **118**, 1673-1678 (2003). (Special Don Setser issue).
2. Yin Guo and Donald L. Thompson, "A Theoretical Study of Cis-Trans Isomerization in HONO Using an Empirical Valence Bond Potential," J. Chem. Phys. **118**, 1673-1678 (2003).
3. Gia G. Maisuradze and Donald L. Thompson, "Interpolating Moving Least-Squares Method for Fitting Potential Energy Surfaces: Illustrative Approaches and Applications," J. Phys. Chem. A, Donald J. Kouri Special Issue, submitted.
4. Yin Guo and Donald L. Thompson, "A Classical Trajectory Study of Bond Dissociation in HONO and HOOH," J. Phys. Chem. A, submitted.

Terascale High-Fidelity Simulations of Turbulent Combustion with Detailed Chemistry
http://scidac.psc.edu/

SciDAC: Computational Chemistry
(DOE Office of Science, Basic Energy Sciences: Chemical Sciences, Program Manager:
William H. Kirchhoff)

Work-in-progress Report – *Period from 03/31/02 to 03/31/03*

List of Principal Investigators

- Arnaud Trouvé (University of Maryland, UMD, *atrouve@eng.umd.edu*)
- Jacqueline Chen (Sandia National Laboratories, SNL, *jhchen@ca.sandia.gov*)
- Hong G. Im (University of Michigan, UMI, *hgim@umich.edu*)
- Christopher J. Rutland (University of Wisconsin, UWI, *rutland@engr.wisc.edu*)
- Raghurama Reddy, Sergiu Sanielevici (Pittsburgh Supercomputing Center, PSC, Carnegie Mellon Univ., *rreddy@psc.edu, sergiu@psc.edu*)

Project Summary

The present project is a multi-institution collaborative effort aimed at adapting an existing high-fidelity turbulent reacting flow solver called S3D for efficient implementation on terascale massively parallel processors (MPP) computers. S3D adopts the direct numerical simulation (DNS) approach: DNS is a unique tool in combustion science proposed to produce both high-fidelity observations of the micro-physics found in turbulent reacting flows as well as the reduced model descriptions needed in macro-scale simulations of engineering-level systems. The new MPP S3D software is enhanced by adding new numerical and physical modeling capabilities, such as: an implicit/explicit additive Runge-Kutta method for efficient time integration; an immersed boundary method to allow for geometrical complexity; an adaptive mesh refinement (AMR) capability to provide flexible spatial resolution; a thermal radiation capability to allow for more realistic heat transfer descriptions; a soot formation capability to enhance pollutant emission predictions; and a liquid spray capability to capture fuel vaporization effects. In addition, the new MPP S3D software is modified to become object-oriented and fit into an advanced software environment based on an adaptive mesh refinement (AMR) framework called GrACE and the Common Component Architecture (CCA).

Program Scope

Direct numerical simulation (DNS) is a mature and productive research tool in combustion science that is based on first principles of continuum mechanics. Because of its high demand for computational power, current state-of-the-art DNS remains limited to small computational domains (*i.e.* weakly turbulent flows) and to simplified problems corresponding to adiabatic, non-sooting, gaseous flames in simple geometries. The objective of this research project is to use terascale technology to overcome many of the current DNS

limitations and allow for first-principles simulations of pollutant emissions (NO_x, soot) from turbulent combustion systems.

The effort leverages an existing DNS capability, named S3D, developed at Sandia National Laboratories and a collaborative effort between Sandia and the Pittsburgh Supercomputing Center for efficient implementation of S3D on massively parallel computers. S3D is a compressible Navier-Stokes solver coupled with an integrator for detailed chemistry (CHEMKIN-compatible), and is based on high-order finite differencing, high-order explicit time integration, conventional structured meshing, and MPI-based parallel computing implementation. The objective here is to both re-design S3D for effective use on terascale high-performance computing platforms, and to enhance the code with new numerical and physical modeling capabilities. The list of numerical developments includes: an implicit/explicit additive Runge-Kutta method for efficient time integration; an immersed boundary method to allow for geometrical complexity; and an adaptive mesh refinement (AMR) capability to provide flexible spatial resolution. The list of physical modeling developments includes: a thermal radiation capability; and a multi-phase capability including soot particles and liquid fuel droplets.

The new MPP S3D software is being modified to be object-oriented and fit into an advanced software framework, known as the Grid Adaptive Computational Engine (GrACE). GrACE is a MPP framework targeted for AMR applications and includes load-balancing capabilities. In addition, S3D will be made compliant to a software interoperability standard, the Common Component Architecture (CCA) developed by the SciDAC ISIC in Ref. [1]. The CCA environment will allow exchanging software components developed by different teams working on complementary tasks. It will allow in particular the re-use of components developed by a separate Sandia-led research project called CFRFS [2]. The CFRFS project is closely related to, and coordinated with, the present effort, and focuses for instance on developing an AMR component. This exchange of software components between different projects is a unique feature allowed by the SciDAC structure that promotes interactions between different teams of application scientists (our project and CFRFS [2]) and between application scientists and computer scientists (our project, CFRFS and the CCA ISIC [1]).

Recent Progress

As explained above, the present developments for S3D include a complete software re-design, new numerical methods and new physical modeling capabilities. We present here a summary of progress made during the first 19 months work period of this project extending from 09/01/01 to 03/31/03.

Software design developments:

• A new Fortran90 version of S3D has been developed and released by SNL (Scott Mason, Jacqueline Chen)

• GrACE has been ported on the PSC TCS computing system (TCS is a Compaq Alphaserver Cluster) and S3D is currently being adapted to the GrACE/CCA framework (PSC/Yang Wang, Roberto Gomez, Raghurama Reddy, Junwoo Lim)

Numerical developments:

- An implicit/explicit (IMEX) additive Runge-Kutta (ARK) time integration scheme has been developed and implemented into S3D (SNL/Christopher Kennedy; PSC/Roberto Gomez, Raghurama Reddy). A separate implicit solver (VODE) has also been implemented into S3D for auto-ignition problems (UWI/Christopher Rutland, [3]).

- A new pseudo-compressibility method has been developed and implemented into S3D (UMD/Arnaud Trouvé, [4]). This method allows for more efficient computations of slow flow problems while still using a fully compressible formulation.

- The S3D inflow boundary scheme (using a characteristic-based analysis) has been modified to allow for injection of laminar/turbulent flow perturbations while minimizing spurious acoustic wave reflections (UMI/Hong Im, [5]).

Physical model developments:

- A new thermal radiation solver (discrete ordinate method, DOM, grey and non-scattering medium) has been implemented into S3D (UMI/Hong Im). A second separate solver based on the discrete transfer method (DTM) is currently under development (UMD/Arnaud Trouvé).

- A phenomenological soot model based on transport equations for the soot volume fraction and particle number density has been implemented into S3D (UMD/Arnaud Trouvé).

- A Lagrangian particle model to describe dilute liquid sprays has been developed and coupled to the gas-phase Eulerian solver in S3D (UWI/Christopher Rutland, [3]).

Note that our strategy is to both work on new developments for S3D and exploit the most recently up-dated version of the solver to produce results and learn about combustion physics. Recent contributions to combustion science based on S3D may be found in Refs. [6-9] (SNL/Jacqueline Chen).

Future Plans

The main focus of the coming work period will be two-fold: (1) to release a CCA/GrACE-based version of S3D; (2) to initiate two pilot demonstration studies. The two pilot studies correspond to: the simulation of compression-ignition of a gaseous or liquid, hydrocarbon fuel in a turbulent inhomogeneous mixture; and the simulation of NO_x and soot emissions from hydrocarbon-air turbulent jet diffusion flames. The generation of these new DNS databases will also be associated with the development of adequate post-processing tools including tools for data visualization, flamelet-based analysis and statistical analysis.

References

[1] Armstrong, R. C., *et al.* "Center for Component Technology for Terascale Simulation Software", SciDAC Integrated Software Infrastructure Center (ISIC), http://www.cca-forum.org/ccttss/

[2] Najm, H., *et al.* "A Computational Facility for Reacting Flow Science", SciDAC project, http://cfrfs.ca.sandia.gov/

[3] Wang, Y. & Rutland, C. J. (2003) "On the Combustion of Normal Heptane Fuel Droplets in Isotropic Turbulence with DNS", *3rd Joint Meeting US Sections of Combustion Institute*, Chicago, IL.

[4] Wang, Y. & Trouvé, A. (2003) "Artificial Acoustic Stiffness Reduction in Fully Compressible, Direct Numerical Simulation of Combustion", *3rd Joint Meeting US Sections of Combustion Institute*, Chicago, IL.

[5] Yoo, C. & Im, H. G. (2003) "A Computational Study on the Dynamics of Counterflow Hydrogen-Air Edge Flames", *3rd Joint Meeting US Sections of Combustion Institute*, Chicago, IL.

[6] Chen, J. H., Mason, S. D. & Hewson, J. C. (2003) "The Effect of Temperature Inhomogeneity on Low-Temperature Autoignition of Fuel-Lean Premixed Hydrogen/Air Mixtures", *3rd Joint Meeting US Sections of Combustion Institute*, Chicago, IL.

[7] Hawkes, E. R. & Chen, J. H. (2003) "Turbulent Stretch Effects on Hydrogen Enriched Lean Premixed Methane-Air Flames", *3rd Joint Meeting US Sections of Combustion Institute*, Chicago, IL.

[8] Liu, S. & & Chen, J. H. (2003) "The Effect of Product Gas Enrichment on the Chemical Response of Premixed Diluted Methane/Air Flames", *3rd Joint Meeting US Sections of Combustion Institute*, Chicago, IL.

[9] Sutherland, J. C., Smith, P. J. & Chen, J. H. (2003) "DNS of a Nonpremixed CO-H2 Jet using Detailed Chemistry – Toward Improved LES Models", *3rd Joint Meeting US Sections of Combustion Institute*, Chicago, IL.

VARIATIONAL TRANSITION STATE THEORY

Principal investigator, mailing address, and electronic mail

Donald G. Truhlar
Department of Chemistry, University of Minnesota, 207 Pleasant Street SE,
 Minneapolis, Minnesota 55455
truhlar@umn.edu

Program scope

This project involves the development of variational transition state theory (VTST) with multidimensional tunneling (MT) contributions, the development of new electronic structure methods to provide input for such rate constant calculations, research on the interface of electronic structure theory and dynamics, and application of these techniques to gas-phase reactions. The work involves development of new theory, development and implementation of practical techniques for applying the theory to various classes of reactions and transition states, and applications to specific reactions, with special emphasis on combustion reactions and reactions that provide good test cases for methods needed to study combustion reactions. A theme that runs through our current work is the development of consistently and generally defined electronic structure methods with empirical elements, including molecular mechanics, density functionals, and scaled-electron-correlation components and the use of these methods in direct dynamics calculations of chemical reaction rates.

Recent progress

We have developed powerful new multi-coefficient correlation methods (MCCMs) that allow accurate evaluation of bond energies, reaction energies, and potential energy surfaces at relatively low cost compared to previously available methods. These methods are multi-level electronic structure methods in that they involve extrapolating two or more electronic structure levels to the limit of infinite-order electron correlation (i.e., full configuration interaction) and a complete one-electron basis set—the combination of extrapolating both elements yields complete configuration interaction. Five particularly promising methods of this type have been developed into the MCCM/3 suite, and they span a range of convenience and accuracy, from very inexpensive methods with no iterative post-Hartree-Fock steps to more expensive and demanding but very accurate methods; individual steps are based on Moller-Plesset perturbation theory and quadratic configuration interaction. The resulting methods are well suited for geometry optimization and direct dynamics calculations as well as energy and gradient calculations, and they have performance-to-cost ratios that are very much better than using single-level methods. We have also shown how even greater accuracy can be obtained by using parameters specifically optimized for combustion problems.

We developed a multi-configuration version of molecular mechanics (MCMM) that allows a convenient interface of high-level ab initio calculations with molecular mechanics force fields. MCMM accomplishes much the same purpose as direct dynamics because it does not require artfulness in surface fitting, and yet it yields a semiglobal potential energy surface that is valid in the whole reaction swath, not just along a one-dimensional path. It has the great advantage that it allows the use of high-level electronic methods at minimal cost. We have now developed a general strategy that demonstrates that one can obtain

useful semiglobal fits to potential energy surfaces with on the order of only a dozen Hessians or less.

We have developed a new hybrid density functional method parameterized for kinetics, and we have tested this and other density functional methods with several extended and polarized double zeta basis sets. The results have been tested against conformational energies and against a 22-reaction database of barrier heights that we developed specifically for this purpose; the importance of diffuse functions for density functional theory has been demonstrated. The mean unsigned error in barrier heights is only 1.5 kcal/mol, and the new methods have also been shown to provide excellent quality for saddle point geometries.

We recently improved the large-curvature tunneling (LCT) method so that it is more robust for anharmonic potential energy surfaces. The new method is called large-curvature tunneling, version 4.

VTST with multidimensional tunneling contributions has now been tested against newly available accurate benchmark rate constants for CH_4 + H and O on given realistic potential energy surfaces. The VTST/MT calculations agree quite well with the benchmark results over a wide temperature range.

We have made several applications of our methods to calculate rate constants for specific chemical reactions. Recent applications of this type include a series of very accurate dynamics calculations on H + CH_4, H_2 + CH_3, and several isotopologs. We obtained good agreement with experimental results over the temperature range 348 K to 2400 K.

Software distribution

We have developed several software packages for applying variational transition state theory with optimized multidimensional tunneling coefficients to chemical reactions and for carrying out MCCM calculations, hybrid Hartree-Fock density functional theory calculations, and direct dynamics applications. The URL for our software distribution site is http://comp.chem.umn.edu/Truhlar. The number of license requests that we fulfilled during the period Jan. 1, 2001–April 11, 2003 for selected software packages developed under DOE support is as follows:

	Total	academic	government/DoD	industry
POLYRATE	161	143	11	7
GAUSSRATE	58	52	5	1
MORATE	28	23	2	3
ABCRATE	8	5	2	1
MC-TINKERATE	3	3	0	0
HONDOPLUS	66	56	5	5
MULTILEVEL	16	16	0	0
MC-TINKER	6	6	0	0

Future plans

Our objective is to increase the applicability and reliability of variational transition state theory with optimized multidimensional tunneling calculations for combustion reactions. An important part of how we plan to do this is further improvement of the interface with high-level electronic structure calculations. We will continue to develop single-level and dual-level direct dynamics methods as well as multi-configuration molecular mechanics methods for carrying out rate calculations with potential energy surfaces based on high-level electronic structure theory, and we will continue to develop new multi-level

electronic structure methods and hybrid density functional methods for kinetics. In addition to developing the methods, we are putting them into user-friendly packages that will allow more researchers to carry out calculations conveniently by the new methods.

VTST is being applied and will be applied to selected reactions of three types: (i) important test cases for the new methods, (ii) reactions of fundamental importance for further development of dynamical theory, and (iii) important combustion reactions, for example, reactions of atoms and other radicals with unsaturated and aromatic systems, reactions of hydrogen atoms with alcohols and ethers, and reactions of sulfur-containing compounds. We are also developing new methods that should be useful for the calculation of substituent effects.

Publications, 2001-present
Journal articles

1. "Improved Algorithm for Corner Cutting Calculations," A. Fernandez-Ramos and D. G. Truhlar, Journal of Chemical Physics 114, 1491-1496 (2001).

2. "Thermal and State-Selected Rate Coefficients for the $O(^3P)$ + HCl Reaction and New Calculations of the Barrier Height and Width," S. Skokov, S. Zhou, J. M. Bowman, T. C. Allison, D. G. Truhlar, Y. Lin, B. Ramachandran, B. C. Garrett, and B. J. Lynch, Journal of Physical Chemistry A 105, 2298-2307 (2001).

3. "How Well Can Hybrid Density Functional Methods Predict Transition State Geometries and Barrier Heights?" B. J. Lynch and D. G. Truhlar, Journal of Physical Chemistry A 105, 2936-2941 (2001).

4. "Multi-Coefficient Correlation Method: Comparison of Specific-Range Reaction Parameters to General Reaction Parameters for $C_nH_xO_y$ Compounds," P. L. Fast, N. Schultz, and D. G. Truhlar, Journal of Physical Chemistry A 105, 4143-4149 (2001).

5. "POTLIB 2001: A Potential Energy Surface Library for Chemical Systems," R. J. Duchovic, Y. L. Volobuev, G. C. Lynch, T. C. Allison, J. C. Corchado, D. G. Truhlar, A. F. Wagner, and B. C. Garrett, Computer Physics Communications 144, 169-187 (2002).

6. "Molecular Mechanics for Chemical Reactions. A Standard Strategy for Using Multi-Configuration Molecular Mechanics for Variational Transition State Theory with Optimized Multidimensional Tunneling," T. Albu, J. C. Corchado, and D. G. Truhlar, Journal of Physical Chemistry A 105, 8465-8487 (2001).

7. "Test of Variational Transition State Theory with Multidimensional Tunneling Contributions Against an Accurate Full-dimensional Rate Constant Calculation for a Six-Atom system," J. Pu, J. C. Corchado, and D. G. Truhlar, Journal of Chemical Physics 115, 6266-6267 (2001).

8. "Parameterized Direct Dynamics Study of Rate Constants of H with CH_4 from 250 to 2400 K," J. Pu and D. G. Truhlar, Journal of Chemical Physics 116, 1468-1478 (2002).

9. "What are the Best Affordable Multi-Coefficient Strategies for Calculating Transition State Geometries and Barrier Heights?" B. J. Lynch and D. G. Truhlar, Journal of Physical Chemistry A 106, 842-846 (2002).

10. "Interpolated Algorithms for Large-Curvature Tunneling Calculations," A. Fernandez-Ramos, D. G. Truhlar, J. C. Corchado, and J. Espinosa-Garcia, Journal of Physical Chemistry A 106, 4957-4960 (2002).

11. "Tests of Potential Energy Surfaces for H + CH_4 ↔ CH_3 + H_2: Deuterium and Muonium Kinetic Isotope effects for the Forward and Reverse Reaction," J. Pu and D. G. Truhlar, Journal of Chemical Physics 117, 10675-10687 (2002).

12. "Obtaining the Right Orbitals is the Key to Calculating Accurate Binding Energies for Cu+ Ion," B. J. Lynch and D. G. Truhlar, Chemical Physics Letters **361**, 251-258 (2002).

13. "Validation of Variational Transition State Theory with Multidimensional Tunneling Contributions Against Accurate Quantum Mechanical Dynamics for H + CH$_4$ -> H$_2$+ CH3 in an Extended Temperature Interval," J. Pu and D. G. Truhlar, Journal of Chemical Physics **117**, 1479-1481 (2002).

14. "Reply to Comment on Molecular Mechanics for Chemical Reactions," D. G. Truhlar, Journal of Physical Chemistry A **106**, 5048-5051 (2002).

15. "The Effectiveness of Diffuse Basis Functions for Calculating Relative Energies by Density Functional Theory," B. J. Lynch, Y. Zhao, and D. G. Truhlar, Journal of Physical Chemistry A **107**, 1384-1388 (2003).

16. "Robust and Affordable Multi-Coefficient Methods for Thermochemistry and Thermochemical Kinetics: The MCCM/3 Suite and SAC/3," B. J. Lynch and D. G. Truhlar, Journal of Physical Chemistry A, in press.

17. "Force Field Variations along the Torsional Coordinates of CH$_3$OH and CH$_3$CHO," T. V. Albu and D. G. Truhlar, Journal of Molecular Spectroscopy, in press.

18. "Small Basis Sets for Calculations of Barrier Heights, Energies of Reaction, Electron Affinities, Geometries, and Dipole Moments," B. J. Lynch and D. G. Truhlar, Theoretical Chemistry Accounts, in press.

Book chapters

1. "Molecular Scale Modeling of Reactions and Solvation," D. G. Truhlar, in *Proceedings of FOMMS 2000: Foundations of Molecular Modeling and Simulation*, Keystone, Colorado, July 23-28, 2000, edited by P. T. Cummings. P. R. Westmoreland, and B. Carnahan (American Institute of Chemical Engineers Symposium Series Vol. 97, New York, 2001), pp. 71-83.

2. "Multilevel Methods for Thermochemistry and Thermochemical Kinetics," B. J. Lynch and D. G. Truhlar, American Chemical Society Symposium Series, edited by A. K. Wilson, American Chemical Society, Washington, in press.

Computer programs

"POLYRATE–version 9.1," J. C. Corchado, Y.-Y. Chuang, P. L. Fast, J. Villà, W.-P. Hu, Y.-P. Liu, G. C. Lynch, K. A. Nguyen, C. F. Jackels, V. S. Melissas, B. Lynch, I. Rossi, E. L. Coitiño, A. Fernandez-Ramos, J. Pu, R. Steckler, B. C. Garrett, A. D. Isaacson, and D. G. Truhlar, University of Minnesota, Minneapolis, July 2002.

"MORATE–version 8.5," Y.-Y. Chuang, P. L. Fast, W.-P. Hu, G. C. Lynch, Y.-P. Liu, and D. G. Truhlar, University of Minnesota, Minneapolis, May 2001.

"GAUSSRATE–version 9.0," J. C. Corchado, Y.-Y. Chuang, E. L. Coitiño, and D. G. Truhlar, University of Minnesota, Minneapolis, May 2002.

"HONDOPLUS–version 4.3," H. Nakamura, J. Xidos, J. Thompson, J. Li, G. D. Hawkins, T. Zhu, B. J. Lynch, Y. Volobuev, D. Rinaldi, D. A. Liotard, C. J. Cramer, and D. G. Truhlar, University of Minnesota, Minneapolis, January 2003.

"MULTILEVEL–version 3.0.1," J. M. Rodgers, B. J. Lynch, P. L. Fast, Y.-Y. Chuang, Y. Zhao, J. Pu, and D. G. Truhlar, University of Minnesota, Minneapolis, Aug. 2002.

"MC-TINKER–version 1.0," T. V. Albu, J. C. Corchado, Y. Kim, J. Villa, J. Xing, and D. G. Truhlar, University of Minnesota, Minneapolis, March 2002.

"MC-TINKERATE–version 8.8," T. V. Albu, J. C. Corchado, Y. Kim, J. Villa, J. Xing, and D. G. Truhlar, University of Minnesota, Minneapolis, March 2002.

KINETIC DATA BASE FOR COMBUSTION MODELING

Wing Tsang
National Institute of Standards and Technology
Gaithersburg, MD 20899
wing.tsang@nist.gov

Program Scope or Definition: The aim of this work is to develop data sets of thermal rate constants that are the essential ingredients for the understanding of the chemistry of combustion. It is of particular pertinence due to advances in Computational Fluid Dynamics. Programs are becoming available that can deal with large chemical kinetics data sets. Complete description of combustion requires understanding of both fluid dynamics and chemistry. It should be increasingly possible to describe the behavior of real systems. This can lead to the development of powerful design tools. It will bring combustion technology to the same level as other areas of technology where simulations have made possible revolutionary advances. An important aspect of the work is a close examination of existing data sets with the view of filling in the most blatant gaps. Real fuels are complex mixtures of large hydrocarbons(1). A characteristic of large organics is the multiplicity of reaction paths. Unimolecular reactions are of particular importance since they reduce the size of the fuel to compounds that are the inputs of soot and oxidation models. Soot formation involves condensation reactions that are the reverse of unimolecular decompositions and thus can be treated in a similar manner. The present discussion concentrates on the treatment of the multiple channel nature of such reactions.

Recent Progress: The high temperatures characteristic of combustion processes make energy transfer of great importance in unimolecular reactions. Rates of reactions are pressure as well as temperature dependent. The general principles are well understood(2). The quantitative treatment of multichannel reactions leads to complications. In recent reports we have described a program CHEMRATE(3,4) designed to deal rigorously with these situations. We have been distributing this program to other experimentalists and the present work represents an application of the program.

When a molecule decomposes or isomerizes via a multiplicity of pathways the individual processes are independent of each other only at the high pressure limit. Under such conditions all reactants have a Boltzmann distribution. Energy transfer effects lead to new distribution functions and consequently new rate constants. It is known that such processes are much effected by the nature and magnitude of the energy transfer. However there has been virtually no consideration of the quantitative consequences. Aside from developing a better understanding of the phenomenon, it is also useful to examine how such rate information can be made compatible with the requirements of CHEMKIN(5) At present the most widely used formalism is that developed by Troe (6). It is applicable only for single step unimolecular decomposition or non reversible isomerization processes. There are two general types of multichannel unimolecular reactions. The first involves one reactant decomposing through a variety of channels. The other includes reversible isomerization together with decomposition channels. Our procedure is to use CHEMRATE to convert experimental measurements to high pressure rate expressions and then to use it again to project results to all temperatures and pressures.

Table 1. High Pressure Unimolecular Rate Expressions for Ethanol Decomposition

Reactions	Rate Expressions (s^{-1}) $AT^n\exp(-E/RT)$		
	Log A	N	E/R
$C_2H_5OH = C_2H_4 + H_2O$	9.69	1.36	33094
$C_2H_5OH = CH_3 + CH_2OH$	23.82	-2.16	44304
$C_2H_5OH = C_2H_5 + OH$	22.47	-2.16	48600

A: Ethanol Decomposition: We illustrate the first situation with the decomposition of ethanol. The experimental situation has been dealt with in an earlier report. The present work uses this reaction as a model system and is focussed on determining the effects arising from the multichannel nature of the problem. High pressure rate expressions for the three important channels are summarized in Table 1(7). The elimination reaction is the main process. The C-C bond cleavage reaction releases radicals and will be of more significance in the initial stages of combustion. The C-O bond cleavage reaction is of less significance than the C-C bond breaking reaction and from a practical point of view it will not make significant contributions.

Figure 1 gives results for the elimination reaction as a function of pressure for several temperatures. At every temperature there are two lines. The upper line is for the exponential down collisional model while the lower one is for a step ladder model. Both calculations are carried out with a 500 cm^{-1} step size down. Differences are very small. The use of a 700 cm^{-1} step size down for the step ladder model will lead to an exact match of the results. The exact same results were obtained with or without the secondary channels. Figure 2 contains results for the C-C bond cleavage channel. Also included are results for calculations assuming that this is the only channel. The presence of the elimination channel becomes increasingly important with decreasing pressure. The rate of decrease with pressure is much larger with the step ladder model. The difference in the rate constants for reactions with and without the additional channels are also plotted in Figure 2. This is a sigmoidal shaped curve for the exponential down model but an exponential increase to a constant value for the step ladder model.

Clearly it will be impossible to make a Troe type fit for the C-C bond cleavage reaction over the entire pressure range. We have found it possible to use the Troe parameters as empirical constants by limiting the fitting to the region where the dependence of the rate constants on pressure are no more than linearly dependent on pressure. This severely limits the pressure range where the Troe parameters can be used. In the present case this lower limit is about 10^{-2}
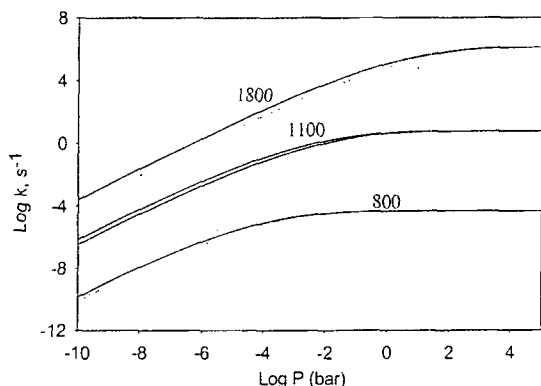

Figure 2: Rate constants as a function pressure for H$_2$O elimination from ethanol at various temperatures. Solid line is for exponential down model and dotted line is for step ladder model. Step size down is 500 cm^{-1}.
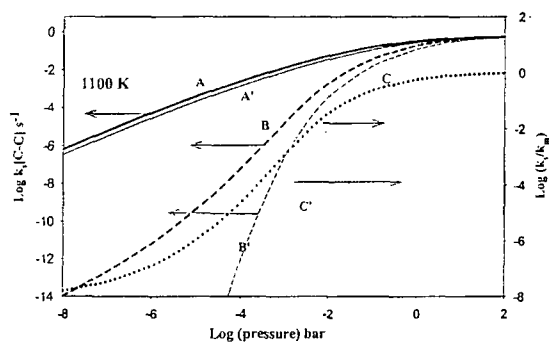
Figure 2: (left axis) Rate constants for C-C bond cleavage. Based on assumption that it is only channel with exponential down model (A) and stepladder model(A') C-C bond cleavage on the basis of multichannel decomposition (B) exponential down and (B') step ladder down models. (right axis). Ratio of rate constants for single channel and multichannel as a function of pressure. C exponential down and C' step ladder models.

Table 2. High pressure rate expressions and constant ratios for the decomposition of heptyl radicals.
$k=AT^n exp(-E/T)$

Reactions:	A	N	E/T	Log (k/k∝) for reactions at 1 bar and various temperatures with 1-heptyl as reactant				
				700	800	900	1000	1150
k1: C7H15-1 ----> C2H4 + nC5H11	11.07	0.614	13358	-.17	-.34	-.60	-.85	-.89
k2: C7H15-2 ----> C3H6 + nC4H9	11.94	0.431	13702	.21	.15	.06	-.12	-.10
k3: C7H15-3 ----> 1-C4H8 + nC3H7	11.91	0.434	13674	.16	.06	-.06	-.26	-.24
k4: C7H15-3 ----> CH3 + 1-C6H12	11.94	0.44	14748	.17	.04	-.11	-.33	-.32
k5: C7H15-4 ----> 1-C5H10 + C2H5	11.35	0.68	13397	.35	.22	.08	-.13	-.13
k6: C7H15-2 <---> C7H15-1	2.721	2.429	8599.3	.12	.13	.10	-.01	0
k7: C7H15-3 <---> C7H15-1	3.647	2.362	8862.6	.10	.07	.01	-.12	-.12
k8: C7H15-4 <---> C7H15-1	5.805	1.961	12509.7	.36	.22	.07	-.15	-16
k9: C7H15-2 <---> C7H15-3	5.291	2.117	10854.8	.17	.15	-.35	-.07	-.07
k10: C7H15-1 <---> C7H15-2	3.473	2.205	7185.3	-.05	-.20	-.35	-.50	-.47
k11: C7H15-1 <---> C7H15-3	4.26	2.211	7504.9	-.07	-.25	-.40	-.56	-.54
k12: C7H15-1 <---> C7H15-4	6.592	1.734	11136.3	-.13	-.37	-.59	-.82	-.79
k13: C7H15-3 <---> C7H15-2	5.438	2.042	10841.2	.15	.11	.01	-.16	-.15

bar at 800 K and 1 bar at 1800 K. For the C-O bond cleavage reaction the applicable range are much higher. Thus this approach is not useful for this channel. Additional parameters must be introduced into Chemkin for such cases. Noted that either the step-ladder or exponential down model will lead to similar results at the beginning of the fall-off region in the present case where k/k_α is larger than 0.03. Of course it is always possible to express results at constant pressure. Probably the best way of expressing results is by presenting data in a tabular form. The magnitude of the differences in rate constants depend on the differences in the activation energy. The general shape of the curve characterizing the differences (see Figure 2) stays the same.

B: Heptyl Radical Decomposition: The more complicated situation is encountered for the cases when reversible isomerization and decomposition must both be considered. We have discussed some of the problems in last years report for hexyl radicals. We now consider the situation for heptyl radicals. As before, the experimental results are from single pulse shock tube decomposition of 1-heptyl iodide radical. Under the conditions of the experiments one obtains the cracking pattern for 1-heptyl radical decomposition. This includes all the 1-olefin radicals from ethylene to 1-hexene. From these results we were able to derive a set of high pressure rate expressions for the decomposition and isomerization processes. We then use these high pressure rate expressions to project rate constants over all pertinent temperature and pressure ranges. The consequence of such calculations is the following. At the lower temperatures high pressure rate constants for the decomposition and isomerization rate constants can be used. At temperatures above 700 K energy transfer effects begin to be important with rate constants becoming pressure dependent. As the temperature is increased, rate constants arising from steady state distributions become effected by the changes in the distribution function with time. At first it is still possible to talk about an average rate constant. However at temperature above 1200 K the temporal behavior of the 4 heptyl isomers can no longer be reproduced in this fashion. Fortunately at such temperatures rate constants are so large that the only expression that is needed is for the cracking pattern and in fact one can remove the heptyl radicals from consideration. That is the reactions RH+Rad=R*+ RadH and R*=alkyl+olefin can now be written as RH+Rad=alkyl+olefin.

The competing reaction under all conditions is the reaction of the heptyl radical with O_2, since this is the beginning of the oxidation sequence of reactions. The derived high pressure rate expressions can be found in Table 2. Also included in the table are $k/k\alpha$ values at temperatures where it is applicable. Note that results are for 1 bar and applicable only with 1-heptyl radical as the starting reactant. Thus the stability of each radical will depend on how it originated. This is a very serious complicating factor, since it implies a further increase in the number of species. Clearly there is need for mechanism reduction. Nevertheless it is very important to have as complete a set of reactions as possible before trying simplification procedures.

Future Plans: We will extend our treatment of multichannel processes to consider the consequences with respect to chemical activation processes. The reactions of interest involve the combination of unsaturated radicals. These are the precursors of soot and examination of existing data sets indicate that for only a few reactions have the rigorous treatment been employed.

Publications 2001-2003
Tsang, W. and Lifshitz, A., "Single Pulse Shock Tube" in Part III "Chemical Reactions in Shock Waves, in Handbook of ShockWaves", Academic Press, New York, 108, 2001
Tsang, W., A Pre-processor for the Generation of Chemical Kinetic Data for Simulations AIAA Paper #2001-0359, Proc. 39th Aerospace Sciences Meeting, Reno, Nevada, 2001
Herzler, J., Manion, J. A., and Tsang, W. "1,2-Pentadiene Decomposition", Int. J. Chem. Kin., 33, 755, 2001
Tsang, W., "Important Factors in the Development of Combustion Mechanisms for Realistic Fuels", AIAA Paper #2002-1098, Proc. 40th Aerospace Sciences Meeting, Reno, Nevada, 2002
Karin Roy, Iftikhar A. Awan, Jeffrey A. Manion, and Wing Tsang, Thermal Decomposition of 2-Bromo-propene and 2-chloro-propene, Phys. Chem. Chem. Phys.(in press) 2003
Tsang, W., "Progress in the Development of a Kinetic Database for Heptane Combustion" AIAA Paper #2003-0663. Proc. 40th Aerospace Sciences Meeting, Reno, Nevada, (2003)
Babushok, V. I., Tsang, W. and McNesby, K. L., "Additive Influence on PAH formation"30th Symp (int'l) on Combustion. (in press, 2003)

References

1. Edwards, T., Harrison, W. E. III, and Maurice, L. Q., "Properties and Usage of Air Force Fuel: JP-8", AIAA 2001-0498, 39th AIAA Aerospace Sciences Meeting and Exhibit, Jamuary 8-11, 2001 Reno. NV
2. Holbrooke, K. A., Pilling. M. J., and Robertson, S. H., "Unimolecular Reactions" John Wiley and Sons., New York , 1996
3. Tsang, W., Bedanov, V., and Zachariah, M.R., J. Phys. Chem. 100, 4011 (1996).
4. Tsang, W., "A Pre-processor for the Generation of Chemical Kinetics Data for Simulations" AAIA-2001-0359, 39th AIAA Aerospace Sciences Meeting and Exhibit, Jamuary 8-11, 2001 Reno. NV
5. Kee, R.J., Grcar, J.F., Smooke, M.D., Miller, J.A. A Fortran Computer Program for Modeling Steady Laminar One-Dimensional Premixed Flames, Sandia National Lab., Rep. SAND85-8240, 1990.
6. Troe, J. J. chem. Phys., 66, 4758, 1977
7. Tsang, W.,"Multichannel Decomposition of Ethanol" in preparation

SINGLE-COLLISION STUDIES OF
ENERGY TRANSFER AND CHEMICAL REACTION

James J. Valentini
Department of Chemistry
Columbia University
3000 Broadway, MC 3120
New York, NY 10027
jjv1@chem.columbia.edu

PROGRAM SCOPE

This research program aims to elucidate the dynamics of bimolecular reactions—reactions that are actually important in combustion media, those that are prototypes of such reactions, and those that illustrate fundamental dynamical principles that govern combustion reactions. The study of reaction dynamics involves asking many different questions. The principal one that we pose in our current work is how "many-body" effects influence bimolecular reactions. By many-body effects we mean anything that results from a reaction with a potential energy surface of more than three mathematical dimensions. This means polyatomic reactions, reactions in which one or both of the reactants and one or both of the products are triatomic or larger. A major interest at present is in reactions for which the reactants offer multiple, identical reaction sites. Our aim is not to provide a complete description of any one molecular system, but rather to develop a general understanding of how the factors of energetics, kinematics, and reactant/product structure control the dynamics in a series of analogous systems.

Our experiments are measurements of quantum-state-resolved partial cross sections under single-collision conditions. We use pulsed uv lasers to produce reactive radical species and thereby initiate chemical reactions. The reaction products are detected and characterized by resonant multi-photon ionization (REMPI) and time-of-flight mass spectrometry.

RECENT PROGRESS

We have explored an extensive series of reactions of the general form H + RH $\rightarrow$ H$_2$ + R, where RH is an alkane. We have studied the reaction of many different alkanes—methane, ethane, propane, butane, n-pentane, n-hexane, neopentane, isobutane, cyclopropane, cyclobutane, cyclopentane, and cyclohexane. The reactant H atoms are prepared by uv-pulsed-laser photolysis. H2 is detected with rotational- and vibrational-state-selectivity under single-collision conditions by uv-pulsed-laser REMPI.

Our results have led to a local reaction model of the H + RH reaction dynamics, a model which is applicable beyond the class of reactions on which it has been developed. This local reaction model describes the structural and stereochemical features of reactions in which there are multiple, nearly identical reaction sites in a polyatomic molecule. The model is based on the idea of a local impact parameter, defined as the distance between the relative velocity vector and a line parallel to it that passes through a particular reactive

atom in a polyatomic molecule. The local impact parameter replaces the ordinary impact parameter as the organizing principle of the collision dynamics. Associated with this local impact parameter is a local opacity function and a local orbital angular momentum. In any collision involving a molecule with multiple reaction sites there are several different local impact parameters and local opacities and local orbital angular momenta. The outcome of the collision—whether reaction will occur, where it will occur if it does, and what the energies of the products will be—is determined by the dependence of reactivity on these local descriptors of the collision. This model can explain the differentiation of the reactions in terms of their energy disposal, accounting for the changes in energy disposal both between and within classes of RH.

This year we studied a series of fluorine-substituted alkanes as a way of expanding our selection and control of structural and stereochemical factors. Many such fluoroalkanes are readily available commercially, providing from one F-for-H substitution to complete fluorination, with almost all possible choices of the sites that are F substituted. These fluoroalkanes allow us to select the number of competing C-H reaction sites and their orientation. This permits us to do careful tests of the postulates of the local reaction model, because we can select the stereochemical features of the reactant very specifically. F-for-H substitution at a particular C-H site removes that site from the "competition" for reaction, since the reaction to produce HF is very endoergic and not appreciable even at the high collision energies of our experiments. These substituted alkanes also allow us to change the moments of inertia, and thus the rotational constants, of the R radical product, exploring further the H_2-R angular momentum coupling effects that we suggest are important in the reactions.

The analysis of the energy disposal in these reactions is done incorporating the kinematic constraint on product rovibrational energy that came from our kinematic model of reactions at suprathreshold collision energies. Our results for the H + RH reactions show that the kinematic constraint expresses fully the consequences of conservation of total energy. By using the kinematically constrained energy in the linear surprisal analysis of the H_2 product rovibrational state distributions, we separately extract the expression of angular momentum conservation. We find that in some of the H + RH reactions the H_2 rotational distribution shows a zero surprisal parameter, indicating that all rotational states that are energetically accessible are populated statistically. This outcome is expected from our local reaction model, but would be difficult to account for otherwise.

This year we have worked on enhancement of the capabilities of our experimental apparatus to extend the range and detail of our measurements. We are adding an ion imaging capability to our experiments to allow us to do determine the quantum-state-resolved differential cross sections of the H_2 product of the H + RH reactions. Determination of the product differential cross sections will characterize the "many-body" effects on the dynamics in more detail and more meaningfully. To make these measurements possible we need to improve the overall sensitivity of our apparatus, and so we have

spent much of the past few months redesigning and reconstructing our set-up. We have succeeded in enhancing our experimental sensitivity—measured as the size of the smallest partial cross section we can reasonably sample—by almost a factor of 100, through improvements in the pulsed molecular beam, the photolysis laser system, and the REMPI detection system.

This year we also began a collaboration with David Chandler to produce ultra-cold molecules by velocity cancellation in molecular collisions. The experiment takes advantage of the fact that in some molecular collisions the velocity vector of a scattered product in the center-of-mass frame is exactly the negative of the velocity vector of the center-of-mass, yielding a lab-frame product velocity that is identically zero. We have succeeded in making NO (from NO + Ar collisions) with a mean velocity of zero and a spread corresponding to a temperature of less than 1K. The cold NO is produced in sufficient densities for trapping and subsequent spectroscopic and collision dynamics studies. A publication describing our first results is being prepared now. An increase in product density and a reduction in product velocity spread, i. e. temperature, seem accessible with modest improvements in the experiment.

FUTURE PLANS

In the next few months we expect to complete our state-to-state studies of $H + C_lH_mF_n \rightarrow H_2(v',j') + C_lH_{m-1}F_n$ reactions. We will then begin to use the new ion imaging capability to obtain state-to-state differential cross sections, starting with the prototype $H + CH_4 \rightarrow H_2 + CH_3$ reaction. We believe that we will have enough velocity resolution to observe the population of individual vibrational states of the CH_3 product in the translational energy distribution of the $H_2(v',j')$.

We will continue our cold molecule studies with David Chandler, exploring different collisional systems. Simple analysis of the kinematics and energetics of the scattering in a crossed beam arrangement indicates that there are particular combinations of scattering partners and collision energies that are very favorable for production of zero-lab-velocity products.

PUBLICATIONS

1. C.A. Picconatto, A. Srivastava, and J.J. Valentini, "Reactions at Suprathreshold Energy: Evidence of a Kinematic Limit to the Internal Energy of the Products," J. Chem. Phys. <u>114</u>, 1663-1671 (2001).

2. C.A. Picconatto, A. Srivastava, and J.J. Valentini, "The H + n-C_5H_{12}/n-$C_6H_{14} \rightarrow H_2(v', j') + C_5H_{11}/C_6H_{13}$ Reactions: State-to-State Dynamics and Models of Energy Disposal," J. Chem. Phys. <u>114</u>, 4837-4845 (2001).

3. C.A. Picconatto, H. Ni, A. Srivastava, and J.J. Valentini, "Quantum State Distribution of HCl from the uv Photodissociation of HCl Dimer," J.

Chem. Phys. <u>114</u>, 7073-7080 (2001).

4. C.A. Picconatto, A. Srivastava, and J.J. Valentini, "State-to-State Dynamics of the H + $CD_3(CH_2)_4CD_3 \rightarrow H_2 + CD_3((CH_2)_3CH)CD_3$ Reaction: Dynamics of Abstraction of Secondary H in Linear Alkanes," Chem. Phys. Lett. <u>340</u> 317-321 (2001).

5. J.J. Valentini, "State-to-State Chemical Reaction Dynamics in Polyatomic Systems: Case Studies," Ann. Rev. Phys. Chem. <u>52</u>, 15-39 (2001).

7. A. Srivastava, C.A. Picconatto, and J.J. Valentini, "State-to-State Dynamics of the H + $c\text{-}C_6H_{12} \rightarrow H_2(v',j') + c\text{-}C_6H_{11}$ Reaction," J. Chem. Phys. <u>115</u>, 2560-2565 (2001).

8. A. Srivastava, C.A. Picconatto, and J.J. Valentini, "State-to-State Dynamics of H + c-RH ® $H_2(v',j')$ + c-R Reactions: The Influence of Reactant Stereochemistry, Chem. Phys. Lett. <u>354</u>, 25-30 (2002).

9. J.J. Valentini, " Mapping Reaction Dynamics via State-to-State Measurements: Rotations Tell the Tale," J. Phys. Chem. <u>106</u>, 5745-5759 (2002)

Theoretical Studies of the Dynamics of Chemical Reactions

Albert F. Wagner

Gas Phase Chemical Dynamics Group, Chemistry Division
Argonne National Laboratory, Argonne, IL 60439
wagner@tcg.anl.gov

Program Scope

The goal of this program is to apply and extend dynamics and kinetics theories to elementary reactions of interest in combustion. Typically, the potential energy surfaces used in these applications are determined from *ab initio* electronic structure calculations, usually by other members of the group. Generally the calculated kinetics or dynamics is compared to experimental results, often generated by other members of the group.

Recent Progress

Addition of D to Acetylene and Ethylene: In collaboration with J. Michael and L. Harding in our group, we are investigating the addition of D atoms to small unsaturated hydrocarbons, as in:

$$D + HCCH \leftrightarrow \quad DHCCH^* \to H + DCCH \qquad (1)$$
$$\downarrow M$$
$$DHCCH$$
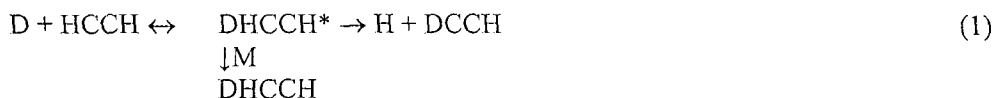
At low pressures (<20 torr for M = Kr) and high temperatures (~1100 K – 1650 K), Michael finds identical rates for D atom loss and H atom gain, implying that the exoergic isotopic exchange is the dominant process in Rxn (1). The addition of H or D to acetylene has a long history. Measurements on the H+HCCH reaction at low temperatures (< 500 K) twenty years ago by Payne et al., Keil et al., and Ellul et al., consistently showed an apparent high pressure limit at low pressures (<1 atm) and a shallow temperature dependence for that limit implying a relatively low reaction barrier. Theoretical attempts by several groups to reproduce these measurements largely failed to reproduce the pressure dependence in detail and argued for a much higher high-pressure limit. Much more recently, Knyazev et al. measured vinyl radical dissociation at low pressures and higher temperatures and produced a theoretical model that systematically approaches a higher high pressure limit than measurements at low temperatures, but was consistent with the dissociation measurements. Like Knyazev, the measurements Michael reports this year are at much higher temperatures and lower pressures than the early addition experiments, but unlike Knyazev, are much closer to the addition high pressure limit because of the isotopic exchange. Using high level electronic structure calculations, Harding has calculated the reaction paths for Rxn. (1) and for H+HCCH addition. When corrected for the zero point corrections at a harmonic level, the computed potential along the reaction path is remarkably similar to an Eckart potential derived from just the computed barrier height, reaction exoergicity, and imaginary frequency at the barrier. They are also quite similar to the semi-empirical fitted reaction path potential derived by Knyazev. High pressure addition rate constants calculated with POLYRATE show inconsequential variational effects and tunneling that is very similar to Eckart tunneling over the broad temperatures range (200K – 2000K) characterizing all the measurements. Without any adjustment of the computed potential energy properties, RRKM calculations with Eckart tunneling reproduce the high temperature measurements of Michael, and the earlier low temperature measurements of Hoyermann et al. are reproduced. Like Knyazev, comparable calculations for H+HCCH show a steeper temperature dependence and higher high-pressure limiting rate constant than

the early addition rate constant measurements suggest. Similar calculations are in progress for D(H) + H_2CCH_2 to compare to Michael's measurements and those of others.

Thermalization Measurements in Alkane Dissociation: In collaboration with Kiefer (UIC), master equation (ME) calculations are being used to model dissociation measurements of simple hydrocarbons such as neopentance, isobutene, and propane. These experiments are carried out under weak shock conditions in which both the rate of thermalization of the reaction mixture [e.g., neopentane (C_5H_{12}) in Kr] to the shock temperature and the subsequent rate of dissociation of the hydrocarbon (e.g, $C_5H_{12} \rightarrow C_4H_9 + CH_3$) can be measured. Thermalization is dominated by energy transfer where the hydrocarbon is initially vibrationally cold. Dissociation is dominated by energy transfer where the hydrocarbon is vibrationally hot. In most dissociation experiments, energy transfer characteristics, such as ΔE_{down}, are fit to the dissociation kinetics with little independent confirmation of the size and physical meaning of such quantities. But in these weak shock experiments, if one underlying exponential gap model would apply to both thermalization and dissociation, then parameters such as ΔE_{down} would be more highly constrained and more directly connected to energy transfer. Calculations of the thermalization rates on the neopentane/Kr system using exact state counts for the vibrational density of states show that convergence of the lower eigenvalues of the ME require a large number of discretized energy grains. To handle such large numbers of grains, a banded inverse iteration eigenvalue approach is being used to get the lower eigenvalues of the ME one at a time. This approach gives only the slowest thermalization rates and ignores fast transients. By varying ΔE_{down} reasonable agreement with experimental measurements of Pτ, where P is the pressure and τ is the relaxation lifetime, can be reached at the temperatures of the shock tube experiments (~600K – 1850K). These calculations are also in qualitative agreement with room temperature relaxation measurements by Holmes et al. more than thirty years ago. Extensive, analytic, but approximate theories have been developed by Herzfeld and Litovitz, among others, to explain early relaxation experiments. The ME results are being analyzed in the context of these approximate theories to more fully understand the mechanisms of thermalization.

Transferable Pairwise Additive Potentials for Hindered Rotations: Barrierless reactions can be significantly influenced by complicated, large-amplitude hindered rotations. The *ab initio* description of such hindered rotations can be computationally intensive. However, the increasing number of comprehensive *ab initio* studies of the potential energy surfaces controlling barrierless reactions now invites systematic tests of much simpler and perhaps transferable pairwise additive models for hindered rotations. This is now being carried out for four hydrocarbon reactions recently studied by Harding and Klippenstein: CH_3+CH_3, $H+CH_3$, $H+C_2H_5$, and $H+C_3H_3$. In a pairwise additive approach, the potential energy $V(\mathbf{q})$, where $\mathbf{q}$ is the hindered rotor deviation from the minimum energy path (MEP), is given by:

$$V(\mathbf{q}) = V_{NB}(\mathbf{q}) + [V_{MEP} - V_{NB}(\mathbf{q}_{MEP})]S(\mathbf{q}) \qquad (2)$$

where $S(\mathbf{q})$ is a normalized switch from 1 on the reaction path to 0 far away from the path and where the non-bonded interaction $V_{NB} = \Sigma_i \Sigma_j V_{pw,ij}$ where $V_{pw,ij}$ is a pairwise interaction between the ith atom and jth atom. Each $V_{pw,ij}$ can be approximated by a power series expansion in a basis. For example, a 3 term expansion in $e^{-bR_{ij}}$ gives a Morse Oscillator (MO) representation of $V_{pw,ij}$. Similar expansion are possible for S (or R_{ij}^{-b}). Determining the best representation within the context of Eq. (2) ultimately involves finding the most compact and accurate basis set for S and V_{NB} to fit the kinetically important region for the four reactions selected. Preliminary results indicate that between 5% - 15% rms relative error can be obtained with an MO expansion. Transferability tests indicate that families of reactions, for example $H+CH_3$ and $H+C_2H_5$, can be fit with common parameters with modest degradation in accuracy.

Future Plans

Besides continuing work in the above projects, we are interested in the following projects:

Reaction Kinetics of CN + OH: The experimental studies by G. Macdonald for both the overall rate and the branching ratio of the CN+OH will be compared to theoretical kinetics calculations. Mebel et al. has performed density functional electronic structure calculations on the ground triplet state potential energy surface. All the major stationary points and transition states were characterized. With supplemental information on the barrierless reaction path for the initial CN+OH approach, a FTST/RRKM calculation will be performed with the VariFlex software to estimate the rate constant and branching ratios. The comparison between theory and experiment should help define the accuracy of the computed stationary points on the surface. The first excited triplet surface has recently been studied by Schaefer's group. They found that this surface interacts with the lowest triplet surface to produce conical intersections. The kinetic import of these conical intersections will be an issue in this study.

Soot Morphology Modeling: Small angle X-ray scattering (SAXS) by Hessler and Winans characterize *in situ* the size and shape of soot and its polycyclic aromatic hydrocarbons (PAHs) down to <1nm in scale. Unlike diffraction experiments, SAXS gives several moments of the soot distribution, instead of the exact location of every atom. How many moments and to what accuracy is not well known. What is needed is the approximate, but rapid conversion of the SAXS signals into families of plausible soot shapes and sizes. Using PAHs as the known building blocks of soot and generalizing hard-sphere models, we plan to apply Reverse Monte Carlo (RMC) techniques to optimize building block arrangements to best match the synthetic signal to the real signal. We believe RMC methods can be made reasonably fast, leading to a rapid first cut rendering of X-ray scattering information into molecular assemblies. We expect families of RMC solutions will be found that depend on the initial starting configurations. Common moments of all the families have will measure the number of moments that can be reliably extracted from SAXS data. The RMC solutions could become starting points for much more realistic MD simulations.

Publications from DOE Sponsored Work from 2001 - Present

Evidence for a Lower Enthalpy of Formation of Hydroxyl Radical and a Lower Gas Phase Bond Dissociation Energy of Water
B. Ruscic, D. Feller, D. A. Dixon, K. A. Peterson, L. B. Harding, R. A. Asher, and A. F. Wagner
J. Phys. Chem. A 105, 1-4 (2001)

The Subspace Projected Approximate Matrix (SPAM) Modification of the Davidson Method
R. Shepard, A. F. Wagner, M. Minkoff, and J. L. Tilson
J. Comp. Phys. 172, 472-514 (2001)

Mapping the OH + CO → HOCO Reaction Pathway Through Infrared Spectroscopy of the OH-CO Reactant Complex
M. I. Lester, B. V. Pond, M. D. Marshall, D. T. Anderson, L. B. Harding, and A. F. Wagner
Faraday Discussions, 118, 373-385(2001)

Thermodynamic Functions for the Cyclopentadienyl Radical: The Effect of Jahn-Teller Distortion
J. H. Kiefer, R. S. Tranter, H. Wang, A. F. Wagner
Int. J. Chem. Kin. 33, 834-845 (2001)

The Calculation of f-f Spectra of Lanthanide and Actinide Ions by the MCDF-CI Method
M. Seth, R. Shepard, A. F. Wagner, K. G. Dyall
J. Phys. B. 34, 2383-2406 (2001)

POTLIB 2000: A Potential Energy Surface Library for Chemical Systems
R. J. Duchovic, Y. L. Volobuev, G. C. Lynch, T. C. Allison, D. G. Truhlar, A. F. Wagner, B. C. Garrett
Comp. Phys. Comm. 144, 169-187 (2002)

An Ab Initio Study of the f-f Spectroscopy of Americium^{+3}
J. Tilson, M. Seth, C. Naleway, M. Seth, R. Shepard, A. F. Wagner, W. Ermler
J. Chem. Phys. 116, 5494 (2002)

An Ab Initio Study of the Ionization Potential and f-f Spectroscopy of Europium Atoms and Ions
C. Naleway, M. Seth, R. Shepard, A. F. Wagner, J. Tilson, W. C. Ermler, and S. R. Brozell
J. Chem. Phys. 116, 5481 (2002)

Flexible Transition State Theory for a Variable Reaction Coordinate:Analytic Expressions and an Application
S. Robertson, A. F. Wagner, and D. M. Wardlaw
J. Phys. Chem. A 106, 2598 (2002).

On the Enthalpy of Formation of Hydroxy Radical and Gas-Phase Bond Dissociation Energy of Water and Hydroxyl
B. Ruscic, A. F. Wagner, L. B. Harding, R. L. Asher, D. Feller, D. A. Dixon, K. A. Peterson, Y. Song, X. Qian, C.-Y. Ng, J. Liu and W. Chen
J. Phys. Chem. 106, 2727 (2002)

Rate Constants, $1100 \leq T \leq 2000$ K, for the Reaction, $H + NO_2 \rightarrow OH + NO$, Using Two Shock Tube Techniques: Comparison of Theory to Experiment
M.-C. Su, S. S. Kumaran, K. P. Lim, A. F. Wagner, L. B. Harding, and J. V. Michael
J. Phys. Chem. A 106, 8261 (2002)

Rate Constants for $H + O_2 + M \rightarrow HO_2 + M$ in Seven Bath Gases
J. V. Michael, M.-C. Su, J. W. Sutherland, J. J. Carroll, and A. F. Wagner
J. Phys. Chem. A, 106, 5297 (2002)

Flexible Transition State Theory for a Variable Reaction Coordinate: Derivation of Canonical and Microcanonical Forms with Angular Momentum Conservation
S. H. Robertson, D. M. Wardlaw, A. F. Wagner
J. Chem. Phys. 117, 593 (2002)

The Challenges of Combustion for Chemical Theory
A. F. Wagner
29th Symposium (International) on Combustion (in press)

Kinetic Modeling of Combustion Chemistry

Charles K. Westbrook and William J. Pitz
Lawrence Livermore National Laboratory
Livermore, CA 94550

This program consists of several interconnected activities, beginning with development of detailed chemical kinetic reaction mechanisms for selected fuels, followed by application of those mechanisms to laboratory experiments to refine and validate the mechanisms, and finally to application of the mechanisms to applied problems of industrial and other interest. During these activities, individual and groups of reactions and thermochemical data which are most in need of further study are identified and communicated to other contractors who could address those needs.

During the past year, three major types of fuels were studied and had detailed reaction mechanisms developed, tested and applied. The first consisted of conventional hydrocarbon species, including toluene and the nine isomers of heptane. Both are important species for study because they illustrate the role that fuel molecular size and structure play in determining many combustion properties. The second class of fuels studied in the past year consisted of a group of large oxygenated hydrocarbons which are of interest because such oxygenates have recently been shown to be effective in reducing soot emissions when used as diesel engine fuels. Finally, the third class of fuels consist of a variety of organophosphate species which are interesting as flame suppressants but are currently much more important because they include chemical warfare (CW) nerve agents such as Sarin, VX and others. For all of these fuels, reaction mechanisms have been developed and the work has been published in refereed papers.

Ignition of isomers of heptane

There are 9 structurally distinct isomers of heptane (C_7H_{16}), and some of their combustion properties, such as flame speed and heat of reaction, are very similar. However, their relative rates of high temperature ignition are not the same, affecting their ignition in shock tubes and leading to different detonation properties. Even more variation is seen in their relative rates of low temperature ignition, which produces a significant variability in their octane and cetane ratings, reflecting their differing ignition in spark-ignition and diesel engines. We have used systematic mechanism generation techniques to develop reaction mechanisms for each isomer. Each mechanism is based on a common C_1 - C_6 submechanism, with the reactions and species specific to the particular heptane isomer then built on top of that base. Each heptane mechanism then includes approximately 1000 different chemical species and 4000 elementary, reversible reactions. Reaction pathways and rates depend on relevant C-H and C-O bond energies, geometries of each elementary reaction, and ring strain energies for intramolecular transfers.

Systematics of the influence of molecular structure on shock tube ignition [1] were then explained in terms of the relative production of H atoms during fuel consumption, since H atoms generate the majority of reactive chain branching from its reaction with molecular oxygen. Another very interesting result of this study was that, while ignition of each isomer varies predictably from the other isomers, overall the isomers ignite at very similar rates, rates that are very similar in turn to all other alkane fuels from propane (C_3H_8) to decane ($C_{10}H_{22}$). All of these alkanes ignite much more rapidly than methane (CH_4) and significantly slower than ethane (C_2H_6). Methane is slowest to ignite because all possible alkyl radicals (methyl in the case of methane) produce no H atoms directly, and ethane is fastest because all of its alkyl radicals (ethyl) produce H atoms. All of the larger alkanes ignite at intermediate rates because its multitude of alkyl radicals produces mixtures of H atoms and methyl radicals, and thus the influence of H atom chain branching is intermediate between methane and ethane. These results have then been related to detonation parameters [2].

Ignition of the same isomers of heptane were then studied [3] at low and intermediate temperatures where structural factors influence reactivity in rapid compression machines, spark-ignition engines, diesel engines, and homogeneous charge, compression ignition (HCCI) engines. Following our extensive studies in previous years, the low temperature reaction paths and rates, especially the rates of alkylperoxy radical isomerizations and other intramolecular reactions that all depend strongly on molecular structure factors, were found to be most important. Current kinetic models can be used to predict reliably the tendency of these fuels to produce knocking behavior in SI engines and their tendency to produce soot in diesel combustion.

A very detailed chemical kinetic reaction mechanism was published during the past year [4] to describe combustion of iso-octane. This mechanism, together with a preceding study developing a mechanism for n-heptane, provides a thorough modeling tool for the two components which are the primary reference fuels (PRF) for measuring knocking behavior and octane ratings in spark-ignition engines. These mechanisms have attracted widespread use in the combustion modeling community.

Combustion of oxygenated hydrocarbons and soot production
Recent engine experiments have shown that addition of oxygenates species to diesel fuel can reduce soot emissions, but there was no fundamental explanation of the reasons for these effects, and no way to extrapolate the phenomenon to other oxygenated additive species. We found that it was possible to simulate ignition under fuel-rich conditions at elevated pressures and relate the compositions of the rich ignition to species which lead to soot production. When oxygenated species such as methanol, ethanol, dimethyl ether, and dimethoxy methane were added to a typical diesel fuel, the levels of soot precursors were reduced [5-7]. During the past year, we developed reaction mechanisms for two new oxygenated species that are much closer to realistic diesel fuel in their physical properties than the above oxygenates. These species were tri-propylene glycol monomethyl ether (TPGME) and dibutyl maleate (DBM). We found that

TPGME is much more effective than DBM in reducing soot precursor levels and therefore sooting because the oxygen atoms in TPGME remove more C atoms in the diesel fuel from the pool of species which produce soot. The differences in soot reducing potential are linked to structural factors of the oxygenated additives.

Combustion of organophosphorus compounds

An important class of organophosphorus compounds (OPC's) is closely related to many hydrocarbons for which we already have detailed kinetic reaction mechanisms. Building on past experience with phosphate species thermochemistry and kinetics, and on fluorine chemistry models, we have developed models for a wide range of non-toxic OPC's, including dimethyl methyl phosphonate (DMMP), di-isopropy methyl phosphonate (DIMP), trimethyl phosphate (TMP), triethyl phosphate (TEP) and others. These models have been tested extensively through comparison between computed model results and experimental data from seeded hydrocarbon flames. These models were then adapted to describe CW agent kinetics by including the features that are unique to such toxic species as Sarin, VX, and others.

We have used these kinetic models to study incineration of toxic OPC species [8,9]. Because of the extreme toxicity of CW agents, it is very desirable to be able to use surrogate fuels to estimate the rates of incineration of the CW chemicals. We found that the destruction of the toxic Sarin is best simulated by DIMP, although many current studies use DMMP instead. The computed model results show that for incineration conditions, Sarin is consumed at a rate very similar to DIMP, and DMMP is much less reactive.

Other projects

Additional applied modeling projects [10,11] have addressed hydrocarbon ignition in homogeneous charge, compression ignition (HCCI) engines, an attractive hybrid concept that combines the premixed, homogeneous gas phase conditions familiar in spark-ignition engines with the compression ignition of diesel engines. Due to the extreme lean or dilute operation of HCCI engines, NOx emissions can be completely avoided, but considerable unburned hyrocarbon and CO emissions are a problem that still needs a solution. Finally, we have been studying hybrid molecular dynamics/kinetic Monte Carlo techniques to address multi-time-scale problems involved in soot polymerization and soot production in diesel engines [12].

Charles K. Westbrook (email: westbrook1@llnl.gov)
William J. Pitz (email: pitz1@llnl.gov)

References

1. Westbrook, C.K., Pitz, W.J., Curran, H.C., Boercker, J., and Kunrath, E., "A Detailed Chemical Kinetic Modeling Study of the Shock Tube Ignition of Isomers of Heptane", **Int. J. Chem. Kinetics** 33, 868-877 (2001).

2. Romano, M.P., Radulescu, M.I., Higgins, A.J., Lee, J.H.S., Pitz, W.J., and Westbrook, C. K., "Sensitization of Hydrocarbon-Oxygen Mixtures to Detonation Via Cool Flame Oxidation", **Proc. Comb. Inst.** 29, in press (2003).

3. Westbrook, C., Pitz, W., Boercker, J., Curran, H.J., Griffiths, J.F., Mohamed, C., and Ribaucour, M., "Detailed Chemical Kinetic Reaction Mechanisms for Autoignition of Isomers of Heptane Under Rapid Compression", **Proc. Comb. Inst.** 29, in press (2003).

4. Curran, H.J., Gaffuri, P., Pitz, W.J. and Westbrook, C.K., "A Comprehensive Modeling Study of iso-Octane Oxidation", **Combust. Flame** 129, 253-280 (2002).

5. Fisher, E. M., Pitz, W. J., Curran, H. J., and Westbrook, C. K., "Detailed Chemical Kinetic Mechanisms for Combustion of Oxygenated Fuels", **Proc. Comb. Inst.** 28: 1579-1586 (2000).

6. Kaiser, E. W., Wallington, T. J., Hurley, M. D., Platz, J., Curran, H. J., Pitz, W. J., and Westbrook, C. K., "Experimental and Modeling Study of Premixed Atmospheric-Pressure Dimethyl Ether-Air Flames", **J. Phys. Chem. A** 104, No. 35, 8194-8206 (2000).

7. Curran, H. J., Fisher, E. M., Glaude, P.-A., Marinov, N. M., Pitz, W. J., Westbrook, C. K., Layton, D. W., Flynn, P. F., Durrett, R. P., zur Loye, A. O., Akinyemi, O. C., and Dryer, F. L., "Detailed Chemical Kinetic Modeling of Diesel Combustion with Oxygenated Fuels," **SAE Trans.** 110, pp. 1019-1029 (2001).

8. Glaude, P.-A., Curran, H.J., Pitz, W.J., and Westbrook, C.K., "Kinetic Study of Combustion of Organophosphorus Compounds", **Proc. Comb. Inst.** 28: 1749 (2000).

9. Glaude, P.-A., Melius, C., Pitz, W. J., and Westbrook, C. K., "Detailed Chemical Kinetic Reaction Mechanisms for Incineration of Organophosphorus and Fluoro-Organophosphorus Compounds", **Proc. Comb. Inst.** 29, in press (2003).

10. Aceves, S.M., Flowers, D.L., Martinez-Frias, J., Smith, J.R., Westbrook, C.K., Pitz, W.J., Dibble, R., Wright, J.F., Akinyemi, W.C., and Hessel, R.P., "A Sequential Fluid Mechanic Chemical-Kinetic Model of Propane HCCI Combustion," SAE Transactions, Section 4, Volume 110, pp. 514-521 (2001).

11. Flowers, D., Aceves, S., Westbrook, C.K., Smith, J.R., and Dibble, R. "Detailed Chemical Kinetic Simulation of Natural Gas HCCI Combustion: Gas Composition Effects and Investigation of Control Strategies", **J. Eng. Gas Turb. Power** 123, 433 (2001).

12. Violi, A., Kubota, A., Pitz, W.J., Westbrook, C.K. and Sarofim, A. "A Fully-Integrated Molecular Dynamics - Kinetic Monte Carlo Approach for the Simulation of the Growth of Soot Precursors, **Proc. Comb. Inst.** 29, (2003).

PROBING FLAME CHEMISTRY WITH MBMS, THEORY, AND MODELING

Phillip R. Westmoreland

Department of Chemical Engineering
University of Massachusetts Amherst
159 Goessmann Laboratory, 686 N. Pleasant
Amherst, MA 01003-9303

Phone 413-545-1750
FAX 413-545-1647
westm@ecs.umass.edu
http://www.ecs.umass.edu/che/westmoreland.html

Program Scope

This program's objective is to establish kinetics of combustion and molecular-weight growth in hydrocarbon flames as part of an ongoing study of flame chemistry. Our approach combines molecular-beam mass spectrometry (MBMS) experiments on low-pressure flat flames; *ab initio* thermochemistry and transition-state structures; rate constants predicted by transition-state and chemical activation theories; and whole-flame modeling using mechanisms of elementary reactions. The MBMS technique is powerful because it can be used to measure a wide range of species, including radicals, quantitatively with high sensitivity and low probe perturbation. The present focus is on ethylene, vinyl, propargyl, and allene chemistry in flames, in addition to fundamental improvements in measurements and reactive-flow models of flames.

Recent Progress

In the past year, we have focused on three new insights. First, our MBMS experiments at UMass have been used to resolve puzzles about oxidation kinetics of lean ethylene combustion by modeling these and a range of other data. Second, measurements establish that $C_3H_3+C_3H_3$ kinetics can account for C_6H_6 formation in a lean allene-doped ethylene flame but not in a doped fuel-rich flame. Third, our experiments in a new MBMS at the LBNL Advanced Light Source, conducted in collaboration with Terry Cool and Andy McIlroy, reveal the isomeric split between allene and propyne, between acetaldehyde and the previously speculated intermediate ethenol (vinyl alcohol), and between benzene and other C_6H_6 isomers.

Flame mapping and modeling. Two similar fuel-lean ethylene flames were mapped, distinguished from each other by the addition of 0.20% allene in the second flame. The intent was to boost C_3H_3 concentrations and C_3H_3 chemistry while leaving most concentrations of stable and radical species little changed. These flames are maintained at $\phi = 0.70$ (70% of the fuel required stoichiometrically), 56.5% Ar diluent, $P = 30$ Torr, and $v_o = 30.6$ cm/s. These are similar conditions to the undoped fuel-lean ethylene flame of Bhargava and Westmoreland,[1] although on a smaller, standard McKenna burner used so that the burners and results in the UMass, ALS, and Sandia MBMS apparata can be matched with no uncertainty. Mole-fraction profiles were measured for 35 stable and radical species in both fuel-lean flames, where our recently installed quadrupole MS proved its value by separating several hitherto unresolved isomers through small mass defects.

We then used these data to test rate constants in full flame-chemistry mechanisms, identifying key reactions and kinetics that had caused mispredictions in simple fuel-lean ethylene flames in all other proposed reaction sets. Key improvements in the kinetics came by modeling not just the flames but also the DOE-sponsored flow-reactor measurements of Fred Dryer and co-workers [DOE Publ. 3]. The latter data included only stable species but were at lower temperature (850-950 K) and higher pressure (5-10 atm) than in the flames.

The wider parameter space revealed three reactions in particular that led to improved flame kinetics and predictions. First, HO_2 kinetics were more detectable in the high-pressure flow reactor, which trapped H atoms more effectively as HO_2 and clarified the kinetics and the roles of the two reactions $C_2H_4 + HO_2 = c-CH_2CH_2O$ (oxirane) $+ OH$ and $CH_2O + HO_2 = HCO + H_2O_2$. The former reaction controlled the delicate balance of OH production through an effectively one-step chemically activated addition and decomposition, while the second reaction is an abstraction step four times slower than that in GRI-Mech 3.0, crucial to capturing the fuel consumption rate.

---

[1] A. Bhargava and P. R. Westmoreland, *Combustion and Flame* 115, 456-467 (1998).

Second and more important for the flame, crucial corrections were established to $C_2H_3+O_2$ kinetics. New kinetic parameters for the $C_2H_3+O_2$ system were proposed based on combined experimental, reactor-modeling, and theoretical results. Again, chemically activation is of central importance, as association makes chemically activated $CH_2CHOO^{\cdot}$ (vinylperoxy radical), which isomerizes and decomposes to give a pseudo-single-step production of $HCO+CH_2O$, dominant at 800 to 2300 K. A product channel of CH_2CHO+O, proposed to be dominant by other workers, proved instead to be secondary, and the corrected rate constant and products kept fuel consumption from being excessive in the flow reactor and the flame [DOE Publ. 3].

These corrections and the new data also resolve a puzzle with post-flame CO profiles, seen in modeling the data of Ref. 1 by us and other investigators. One hypothesis that we had previously examined and discarded had been uncertainty in the temperature and/or pressure dependence of $CO+OH$. Instead, the new measurements show that CO surprisingly persists into the post-flame zone even at the lean, high-temperature conditions. Furthermore, the new reaction set gives the correct maximum and the correct low levels of CO in the post-flame zone.

Theoretical analyses of $C_2H_3+O_2$ PES and kinetics. The results described above for $C_2H_3+O_2$ have prompted a collaboration among our group, Barry Carpenter, and Steve Klippenstein to resolve theoretical uncertainties and to establish $C_2H_3+O_2$ kinetics that would be valid over the entire range of interest for temperature and pressure (or density). Recent CASPT2 ab initio calculations by the Carpenter group had given different, lower energy barriers to the cyclization of $CH_2CHOO^{\cdot}$ and subsequent isomerizations on the path to $HCO+CH_2O$, seeming to make it more favorable than the homolytic bond scission that gives CH_2CHO+O.

We computed a detailed potential energy surface for CH_2CHOO in the coordinates of CCOO dihedral angle and OO bond length at B3LYP / 6-31G(d) with full optimization of other coordinates at each point. The result was that the minimum energy path has an energy barrier of 38.7 kcal/mol at a dihedral angle of 116 degrees and OO=2.026 angstroms. This energy is lower than the 41.6 kcal/mol of the fully separated CH_2CHO+O, which also shows modest energy minima of 37.4 and 37.9 at OO=2.4 angstroms and dihedrals of zero and 180 degrees. These are apparently weak dipole-quadrupole interactions. Selected calculations at B3LYP/6-311G(d,p) with diffuse functions on oxygen supported this picture.

Further analysis among the collaborators has incorporated high-level quantum chemical simulations (up to MRCI, RS2C, and CASPT2/cc-pvtz with extrapolation to the infinite basis-set limit), direct transition state theory calculations (B3LYP/6-311G**), multiwell master equation modeling, and direct trajectory simulations (with B3LYP/6-31G* energies).[2] Preliminary results show uncertainty as to whether a classical (zero-K) barrier is present in the OO coordinate, but they confirm the tight CH_2CHO-O transition state and consequent low value of the step's Arrhenius pre-exponential (high-pressure limit).

Propargyl chemistry in C_6H_6 formation. Propargyl (CH_2CCH, C_3H_3) has become widely accepted as the likely sole precursor of single-ring aromatics in flames. Analysis of our data from a fuel-rich ethylene flame[3] and its allene-doped analogue reveals a less restricted picture. Within experimental uncertainty, allene doping left C_3H_3 levels unchanged or slightly lower, yet C_6H_6 increased 20-fold. We have made an initial examination[4] of other possible channels using the screening technique of high-pressure-limit association rate constants and measured reactant concentrations, which implied that $C_4H_3+C_2H_2$ and $C_3H_3+C_3H_3$ both were contributing. Work is continuing with pressure-dependent rate constants and with the key reactants re-measured in ways that will allow comparison with no relative calibration uncertainties.

[2] S.J. Klippenstein, Y. Georgievskii, J.A. Miller, J.A. Nummela, B.K. Carpenter, and P.R. Westmoreland, "Vinyl+O_2: A Complete Theoretical Treatment," Joint Meeting of the US Sections of the Combustion Institute, Chicago IL, Mar. 16-19, 2003; paper A39.

[3] A. Bhargava and P. R. Westmoreland, *Combustion and Flame* 113, 333-347 (1998).

[4] M.E. Law, G.E. Oulundsen, T. Carriere, and P.R. Westmoreland, "Aromatic Ring Formation within Premixed Allene-Doped Ethylene Flat Flames," Joint Meeting of the US Sections of the Combustion Institute, Chicago IL, Mar. 16-19, 2003; paper F25.

The story in the allene-doped lean flame is simpler. The change in propargyl (increase of x3.7) seems sufficient to account for the increase in C_6H_6 formation, although only a threshold level of C_6H_6 can be used for the estimated increase (greater than x10). The same screening tests as used above show $C_3H_3+ C_3H_3$ as the dominant feasible channel, although $C_3H_5+ C_3H_5$ could contribute at its high-pressure limit after sufficient H removal. However, this route may be eliminated as a potential contributor: falloff would be significant because the nascent allyl-allyl bond is so easily broken.

Improved flame models of the energy equation. We have developed a solution method for solving the nonadiabatic energy equation in a flat flame [DOE Publ. 2] that modifies the Chemkin II / Premix code to explicitly incorporate radiative losses (with NIST's RADCAL subroutine) and burner losses into the energy equation and boundary conditions. Significant improvements are observed relative to adiabatic flame-profile calculations. Further comparisons with the data are in progress.

Photoionization MBMS using the LBNL ALS. In collaboration with Terry Cool and Andy McIlroy, a flame-sampling MBMS apparatus using vacuum-ultraviolet photoionization has been constructed on the Chemical Dynamics Beamline at Lawrence Berkeley National Laboratory's Advanced Light Source (http://www.chemicaldynamics.lbl.gov/es3/flamediagnostic.htm). With the intense, finely tuned VUV photons, we can discriminate many isomeric species by their photoionization thresholds. A McKenna burner has been chosen as in the Sandia and UMass MBMS configurations, giving complementary measurement capabilities for identical flames.
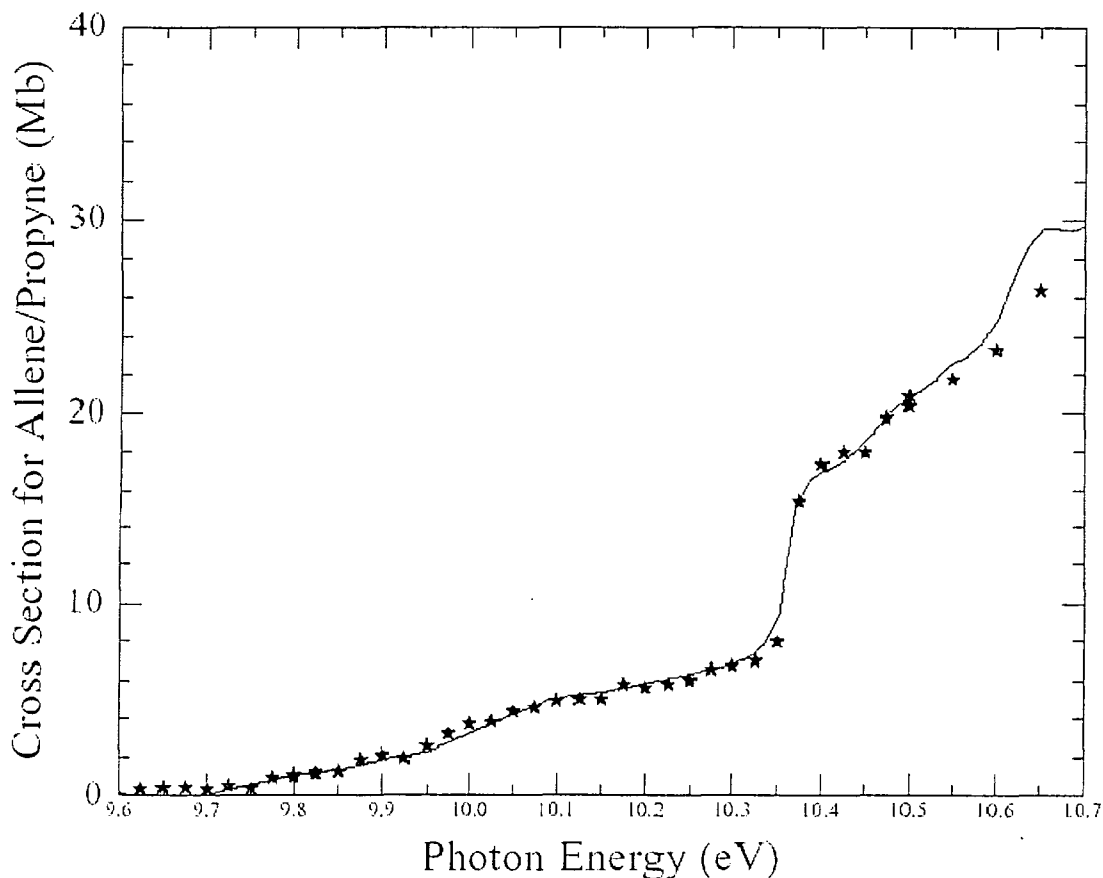
Fig. 1. Photon ionization efficiency for mass 40 in the fuel-rich ethylene flame (phi=1.9, 30 Torr) at 6 mm distance from burner (uncorrected). Solid lines show cross-section based on calbrated cross-sections combined for 43% allene and 57% propyne.

Following an opening campaign of equipment shakedown and testing in March 2002, we participated in initial flame studies in July and then in more extensive measurements in December. Figure 1 shows example data that resolve allene and propyne in the fuel-rich ethylene flame. In this set, the time-of-flight mass spectrometer was used with a sweep of energy-selected VUV photons in steps of 0.25 eV. At 10.375 eV, propyne adds to the allene signal observed below that energy. Using pure-species cross-sections, the split of allene and propyne at this position was found to be 0.43/0.57.

Mass 78 was analyzed similarly, revealing signals that were dominated by benzene and 1,5-hexadiyne. Based on computed electron density of radical molecular orbitals, we have previously proposed that the latter species would dominate over 1,2,4,5-hexatetraene and 4,5-hexadiene-1-yne, the other simple combination products of $C_3H_3+C_3H_3$. Other interesting results include separation of ethenol (vinyl alcohol) and acetaldehyde at mass 44.

Future Plans

We have begun moving the UMass MBMS experiments toward mapping cyclohexane flames. Cyclohexane has the advantage of having only secondary hydrogens to abstract, which will give us a clean measurement of these rate constants at high temperatures. The abstraction product cyclohexyl (C_6H_{11}) should mainly decompose, forming $2C_2H_4+C_2H_3$ rather cleanly. Kinetics of the smaller amounts of 1-hexene and other heavy products should thus be easier to isolate.

Meanwhile, we will extract rate constants and improve overall kinetic mechanisms using the ethylene flame data. In that direction, we are continuing our collaboration to improve theoretical rate constants for $C_2H_3+O_2$, Also, the full nonadiabatic energy equation solutions will be used to probe causes of low heat release in the fuel-lean flame. Finally, we will discriminate more isomers using the ALS MBMS, expanding the value of earlier MBMS data for development and testing of combustion kinetics.

Publications of DOE-sponsored Research, 2000-2003

1. M. E. Law, T. Carrière, and P.R. Westmoreland, "New Insights into Fuel-Lean Ethylene Flames," *Chem. Phys. Prop. Combustion*, 194-197 (2001).
2. T. Carrière and P.R. Westmoreland, "Complete Solution of the Flat-Flame Equations in the Non-Adiabatic Case," *Chem. Phys. Prop. Combustion*, 241-244 (2001).
3. T. Carrière, P.R. Westmoreland, A. Kazakov, Y.S. Stein, and F.L. Dryer, "Modeling Ethylene Combustion from Low to High Pressure," *Proc. Combust. Inst.*, **29** (in press).

Photoinduced Molecular Dynamics in the Gas and Condensed Phases

M. G. White and R. J. Beuhler

*Chemistry Department, Brookhaven National Laboratory, Upton, NY 11973*

(mgwhite@bnl.gov, beuhler@bnl.gov)

1. Project Scope

The goal of this program is to elucidate the dynamics of photoinduced fragmentation processes of molecules in the gas-phase and on surfaces through measurements of the state- and energy-distributions of the products. Particular emphasis is placed on processes that provide information on chemical intermediates or reactions that are important in combustion or energy-related catalysis. State- and energy-resolved measurements on the gas-phase products resulting from photodesorption, and photo-initiated and thermal reactions are used to infer the dynamics of product formation and desorption, *i.e.* the surface-bound transition state. Thermal oxidation and atom-atom recombination reactions important in energy-related catalysis are also being studied with the goal of obtaining microscopic description of the surface reaction dynamics.

2. Recent Progress

Reaction dynamics on well-characterized O/Ag(111) surfaces. We have successfully employed a gas-phase O-atom source for producing well-defined O-atom coverages on a Ag(111) surface. The dissociative sticking probability or molecular oxygen onto Ag(111) is extremely small ($<10^{-7}$), so that the formation of saturated coverages of O-atoms needed for reactivity studies requires high pressure exposures (~10 Torr) and elevated temperatures (400K-500K). Exposures of this type, however, result in uncontrolled deposition of O-atoms which occupy surface sites, as well as penetrate the Ag surface to sub-surface and bulk sites. By supplying oxygen *atoms* to the surface (unit sticking probability), we have been able to prepare O-covered Ag(111) surfaces under UHV conditions with well-defined overlayer structures and coverages. With increasing coverage, thermal desorption measurements show that it is possible to produce surface O-atoms only (0.25 monolayers), surface and sub-surface species (0.25-0.4M), and at higher coverages, all three O-atom species are present (surface, sub-surface and bulk). The O-atom source is based on electron beam heating of molecular O_2 at low pressures (typically, $<10^{-6}$ Torr) resulting in more than 60% dissociation to O-atoms.
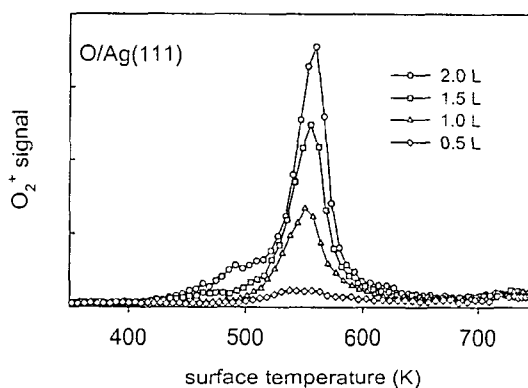

Thermal desorption curves for O_2 resulting from chemisorbed O-atom recombination on Ag(111) as a function of coverage. The peak at 550K at highest coverage is due to the formation of sub-surface O-atoms.

These well-characterized O/Ag surfaces are being used for state-resolved measurements of the $O_{(a)} + O_{(a)} \rightarrow O_{2(g)}$ recombination reaction which we have recently studied on an oxygenated polycrystalline Ag-foil whose surface structure is highly faceted and difficult to characterize. Preliminary measurements for thermally-activated O-atom recombination indicate that the desorbed O_2 molecules exhibit a Boltzmann velocity distribution near the desorption temperature (~500K) and a relatively broad angular distribution relative to the surface normal (~$\cos^3\theta$). The latter is consistent with a small, but non-zero barrier for desorption (≤ 0.1 eV). These results are consistent with our earlier measurements on the polycrystalline Ag surface where the desorbed O_2 velocity distributions are well described by near-Boltzmann distributions at 510-525K, independent of rotational state. Current efforts involve the use of pump-probe methods where the O-atom recombination reaction is activated by transient heating of the Ag

surface induced by pulsed IR or visible laser radiation, and extension to the more reactive Ag(110) surface.

Gas-phase clusters and size-selected deposition: Gas-phase sources for generating clusters of a few atoms to a few hundred atoms are being developed for size-dependent reactivity studies in the gas-phase and deposited on surfaces. The focus is on generating clusters of the early transition metal compounds (carbides, nitrides, sulfides, phosphides), which are known in their bulk form to be active catalysts for a wide range of heterogeneous reactions, such as hydrodesulfurization, and hydrocarbon isomerization and dehydrogenation. In collaboration with Philip Johnson at Stony Brook University, we have successfully employed a laser-ablation plasma source to generate neutral clusters of molybdenum carbide, nitride and sulfide that exhibit a wide range of stoichiometry and size distributions. The neutral mass distributions were characterized by time-of-flight mass spectrometry following photoionization with 193 nm radiation.

The most prominent cluster in the carbide mass distribution corresponds to Mo_8C_{12}, which is assigned to a Met-Car-like structure analogous to that observed for other early transition metal carbides (Ti, V, Zr, Nb). All-electron quantum calculations by James Muckerman (BNL/Chemistry) confirm that the Mo_8C_{12} cluster can form a highly stable caged-like structure, with two inequivalent sets of four Mo atoms at the corners of the cage interconnected by C_2 units. At higher mass, the yield of carbide clusters decreases, but varies smoothly out to clusters containing >25 Mo atoms. The stoichiometry of the heavier carbide clusters is Mo_xC_{x+2} and Mo_xC_{x+3} which we ascribe to near cubic nanocrystallites. The nitride clusters are found to be very different, with at most three nitrogen atoms contained in clusters with up to 40 Mo atoms. This observation is somewhat surprising since Mo metal is known to form stable interstitial alloys with both carbon *and* nitrogen. The mass distributions for the sulfide clusters indicate a "magic number" structure at Mo_6S_4, which is attributed to a stable cage structure previously ascribed to the $[Cu_6S_4]^-$ anion. Such caged structures could be anticipated from other synthetic studies that show that molybdenum sulfide can form large fullerene and tubular nanostructures.
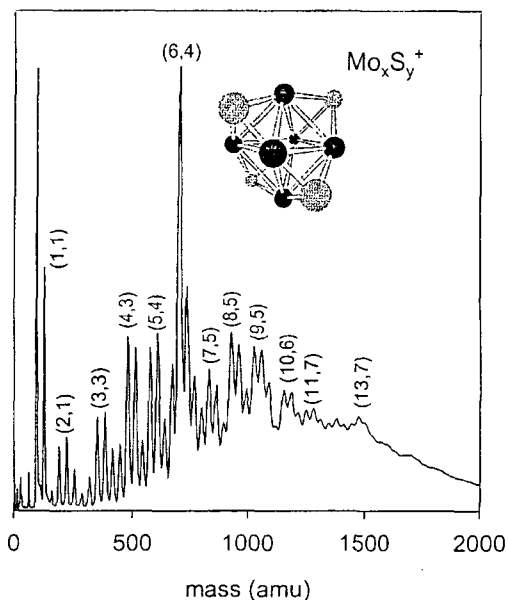
Cluster ion mass distribution for molybdenum clusters formed by laser ablation and detected by 193nm ionization. The inset shows a possible structure for the

Current work involves the construction of a new gas-phase cluster ion source and beam line for the production, mass selection and deposition of Mo compound clusters onto surfaces for subsequent reactivity studies. The first part of this project involves testing and development of a magnetron sputtering source which will be tried in place of the laser ablation source used in our initial cluster studies. The apparatus consists of a cluster ion source, mass-selector, kinetic energy-analyzer and ion guide transport optics which will provide mass-selected clusters up to 25,000 amu. The latter has been designed to fit on the X-24 beam line at the National Synchrotron Light Source, where we plan to perform Mo L-edge XAS and/or EXAFS experiments via soft x-ray fluorescence or total electron yield measurements. The latter will allow us to probe the local electronic (oxidation state, coordination number) and atomic structure of Mo atoms within the supported nanoclusters.

3. Future

Reaction dynamics on well-characterized O/Ag surfaces. In the near future, we will investigate the dynamics of the ethylene epoxidation reaction by using Ag single-crystal surfaces [(111) and (110)] and the gas-phase O-atom source for the formation of well-characterized O-atom coverages and chemical

speciation (surface, sub-surface and bulk). Current models suggest that chemisorbed O-atoms on the surface insert into the C=C double bond of adsorbed ethylene, whereas, sub-surface O-atoms enhance ethylene binding by decreasing the electron density on nearby Ag atoms. In conjunction with molecular beam preparation of the ethylene reactant, it should be possible to elucidate unambiguously the role of sub-surface and surface O-atom species, as well as explore the velocity and surface temperature effects independently for this important reaction system. The experimental studies will be complimented by theoretical calculations for the ethylene oxidation reaction by James Muckerman and coworkers at BNL.

Reactivity of Supported Metal Nanoclusters: New efforts will be directed towards exploring the reactivity of Ag, Mo and MoX (MoC, MoS_2) nanoclusters supported on metal or metal-oxide surfaces by molecular beam methods and IR spectroscopy. Supported metal clusters represent models for "real world" catalysts that typically consist of small metal particles dispersed on a porous metal-oxide support, e.g., Ag on α-alumina (Al_2O_3). Furthermore, the catalytic activity of such supported particles is strongly dependent on particle size, morphology and chemical environment. Nanoparticles will be prepared by self-limiting growth on metal-oxide thin films and single crystals ($Ag/TiO_2(110)$) or thin films prepared by PVD, and by templating on reconstructed metal surfaces ($Mo/MoS_2/Au(111)$-($\sqrt{3}$ x 22)). We propose to investigate the size-dependent activity of supported metal nanoclusters towards reactive adsorbates using molecular beam scattering (sticking, reaction) and IR surface spectroscopy at the U4IR beam line at the NSLS. The low frequency output ($100 - 1000$ cm^{-1}) of IR radiation from the U4IR beam line at the NSLS is ideally suited for investigating vibrational modes that are strongly coupled to the surface, as well as the Mo-C and MoS phonon modes in the nanoparticles themselves. These experiments will address activation for adsorption, dissociation and reaction on bare, oxidized (Ag) and carbided/sulfided (Mo) metal particles.

Publications

1. Gas-Phase Production of Molybdenum Carbide, Nitride and Sulfide Clusters and Nanocrystallites, J. M. Lightstone, H. Mann, M. Wu, P. M. Johnson, and M. G. White, *J Phys. Chem*, accepted.

Reactions of Small Molecular Systems

Curt Wittig
Department of Chemistry
University of Southern California
Los Angeles, CA 90089-0482
wittig@usc.edu

Program Scope

The goals of our program are: (i) a detailed understanding of elementary molecular processes relevant to combustion; and (ii) the development of associated diagnostic tools. This includes experimental and theoretical studies of bimolecular and unimolecular reactions and energy transfer, including the concurrent development of new experimental methods and atom/radical sources.

Recent Results

Last year, experiments were carried out with H_2Te that demonstrated a source of reasonably monoenergetic H atoms at low energies. Photodissociation at 355 nm yielded E_{trans} centered at 1650 cm^{-1}, with a spread due to TeH rotational excitation: $\langle E_{rot} \rangle = 60$ cm^{-1}. The ability to carry out long wavelength photolysis that is selective toward the TeH $^2\Pi_{1/2}$ excited spin-orbit component is due to stong spin-orbit coupling in TeH. This is the only case in the literature in which a one-photon process yields such low energy, tunable H atoms. This energy range is germane to combustion environments, and the work is ongoing. We also wrote a paper on superelastic scattering of fast H atoms from $I(^2P_{1/2})$, which increases the speed of the incident H atom by nearly the 7603 cm^{-1} iodine spin-orbit splitting. Again, relativity (strong spin-orbit coupling) plays a large role.

The most recent experiments have examined two-photon excitation of gaseous H_2O by using 266.2 nm radiation. There have been three reports of OH $A^2\Sigma^+ \rightarrow X^2\Pi$ emission following two-photon excitation,[1-3] and Crim and coworkers have reported OH $A^2\Sigma^+ \leftarrow X^2\Pi$ signals that they have attributed to two-photon excitation.[4] These previous observations were, however, limited to minor product channels. Specifically, as shown below, the $A^2\Sigma^+$ state accounts for less than 1% of the total OH product channel, and the $X^2\Pi$ state is formed with considerable internal excitation (mainly rotational), which is not amenable to detection via LIF because of $A^2\Sigma^+$ predissociation.

The method-of-choice for determining product branching ratios in this system is the high-n Rydberg time-of-flight (HRTOF) method. It misses nothing: all OH internal excitations are encoded in the $c.m.$ translational energy distributions. As we have used this for a broad range of studies in the past, the method will not be elaborated here. Figure 1 shows the essential features.

Figure 2 shows a low-resolution absorption spectrum of gaseous H_2O at 300 K. Two-photon excitation accesses the B^1A_1 state at an *equivalent* one-photon wavelength of 133.1 nm.
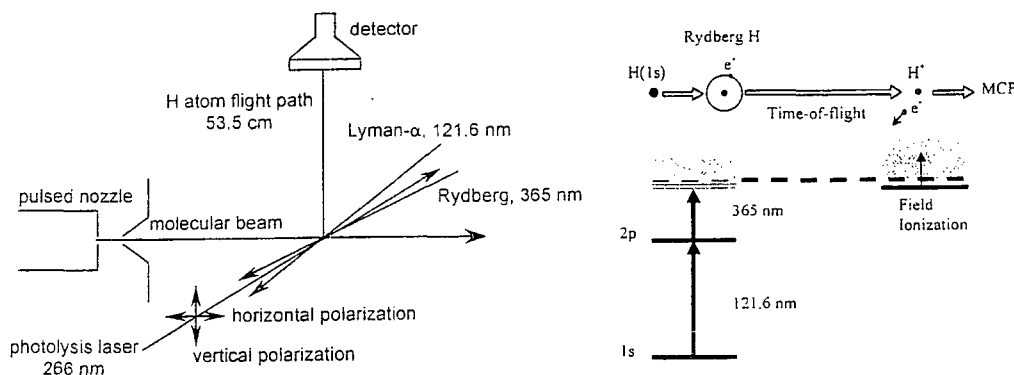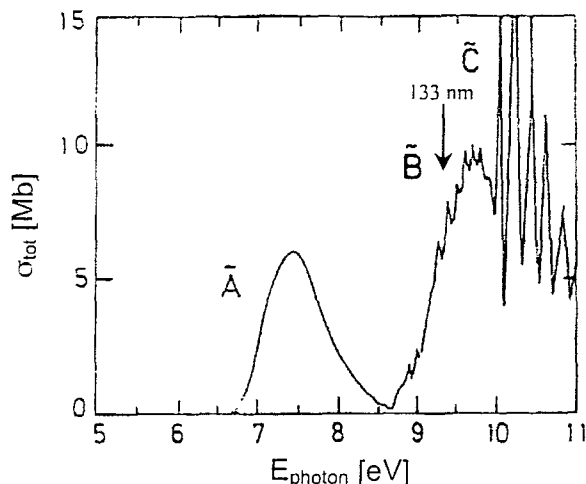

Fig. 1. Schematic of HRTOF arrangement.

Fig. 2. The *B* state is accessed via two-photon excitation at 266 nm.

It is noteworthy that two-photon excitation of the A^1B_1 state is much less efficient than two-photon excitation of B^1A_1.[5] There is a conical intersection of the B^1A_1 and X^1A_1 PES's that is believed to play an important role in the photodissociation dynamics of B^1A_1,[6] in contrast to A^1B_1, which undergoes direct photodissociation.

The first experiments were carried out with a relatively long focal length lens (43 cm). Since then, shorter focal length lenses have arrived, and a 6 cm lens is now in place and will be used soon. Because of the 43 cm focal length, it was expected that the two-photon excitation efficiency would be modest. Consequently, the length of the TOF region was shortened from 53 cm to 14 cm. [The maximum length we have ever used is 110 cm.] This increases the collection efficiency at the expense of resolution. It is expected that the 6 cm focal length lens will improve S/N by an order of magnitude, thereby enabling higher resolution to be obtained.

Figure 3 shows time-of-flight distributions. Had OH $A^2\Sigma^+$ been produced, it would have yielded a signal (for $v = 0$, $J = 0$) at the position indicated by the arrow. The fact that there is no discernible signal at long times shows that $A^2\Sigma^+$ is indeed a minor product.

Figure 4 shows translational energy distributions that correspond to the TOF spectra shown in Fig. 3. They do not show sharp structure, but instead several lumpy features that are reproducible.
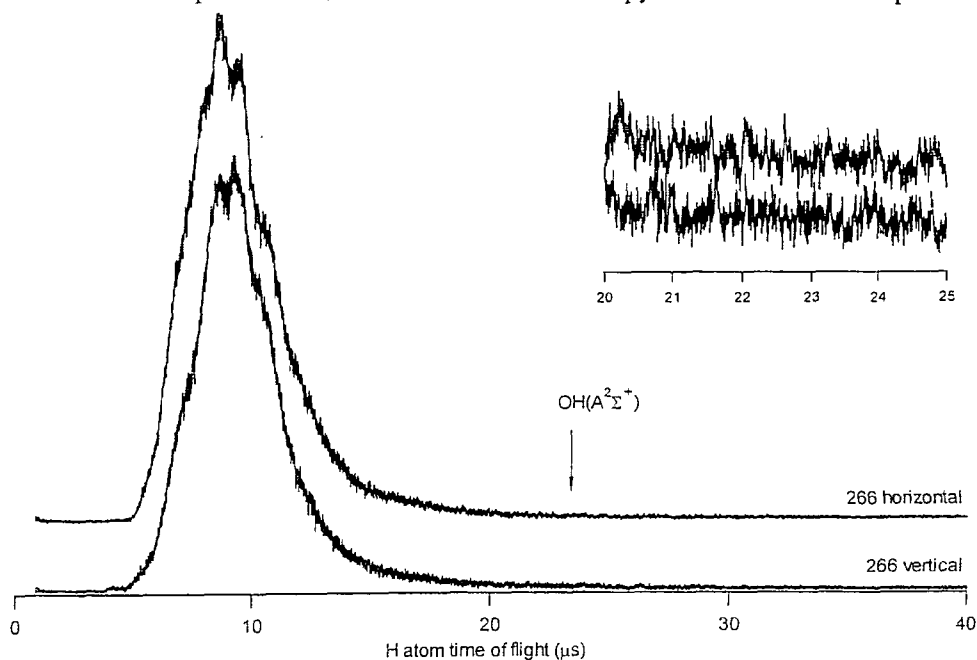
Fig. 3. The TOF spectrum shows that OH(*A*) is a minor product channel.
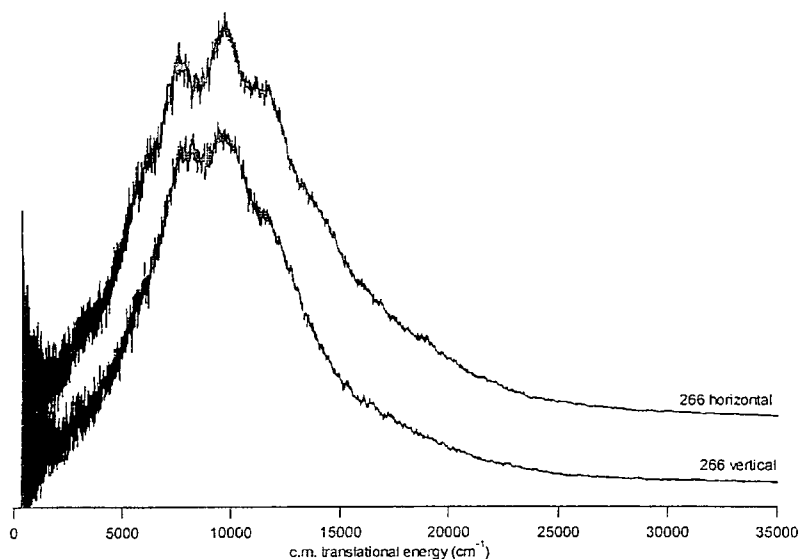
Fig. 4. The lumpy features are believed to be maxima in rotational distributions.

On the basis of the extremely high rotational excitation observed with 121.6 nm photolysis,[7] we tentatively assign the spectra to high rotational levels of low-lying vibrational levels. The modest difference for vertical and horizontal polarizations is consistent with coupling between B^1A_1 and X^1A_1.

The dissociation mechanism is not clear at this time. Though B^1A_1 and X^1A_1 are coupled via the conical intersection, X^1A_1 does not dominate the dynamics, *i.e.*, from Fig. 4, it is obvious that OH contains very little low-J population of low vibrational levels. There is a significant degree of direct character. Finally, we note that these results have implications for liquid·water, where two-photon excitation can be used to create radicals within a bulk sample.

References

1. N. Shafizadeh, J. Rostas, J. L. Lemaire, and F. Rostas, Chem. Phys. Lett. 152, 75 (1988).
2. C. G. Atkins, R. G. Briggs, J. P. Halpern, and G. Hancock, Chem. Phys. Lett. 152, 81 (1988).
3. R. G. Briggs, J. P. Halpern, G. Hancock, N. Shafizadeh, J. Rostas, J. L. Lemaire, and F. Rostas, Chem. Phys. Lett. 156, 363 (1989).
4. R. L. Vander Waal, J. L. Scott, and F. F. Crim, J. Chem. Phys. 94, 1859 (1991).
5. C. L. Thomsen, D. Madsen, S. R. Keiding, J. Thogersen, and O. Christiansen, J. Chem. Phys. 110, 3453 (1999).
6. R. v. Harrevelt and M. C. v. Hemert, J. Chem. Phys. 112, 5777 (2000).
7. S. Harich, D. W. H. Hwang, X. Yang, J. J. Lin, X. Yand, and R. N. Dixon, J. Chem. Phys. 113, 10073 (2000).

DOE Publications: 2000 – Present

1. Photoinitiated H_2CO unimolecular decomposition: accessing H + HCO products via S_0 and T_1 pathways, L.R. Valachovic, M.F. Tuchler, M. Dulligan, Th. Droz-Georget, M. Zyrianov, A. Kolessov, H. Reisler and C. Wittig, J. Chem. Phys. 112, 2752 (2000).
2. Fundamental Aspects of Molecular Photochemistry, C. Wittig, Encyclopedia of Physical Science and Technology, Third Edition, (Academic Press, 2001), supported by many agencies.
3. Intriguing near-ultraviolet photochemistry of H_2Te, J. Underwood, D. Chastaing, S. Lee, P. Boothe, T. C. Flood, and C. Wittig, Chem. Phys. Lett. 362, 483-490 (2002).
4. Intracluster superelastic scattering via sequential photodissociation in small HI clusters, D. Chastaing, J. Underwood, S. Lee, and C. Wittig, J. Chem. Phys., in press (2003).

Theoretical Studies of the Reactions and Spectroscopy of Radical Species Relevant to Combustion Reactions and Diagnostics

David R. Yarkony
Department of Chemistry, The Johns Hopkins University, Baltimore, MD 21218
yarkony@jhu.edu

Our research employs computational techniques to study spin-nonconserving and spin-conserving electronically nonadiabatic processes involving radical species that are relevant to combustion reactions and combustion diagnostics.

Conical Intersections of Three Electronic States

The realization that conical intersections of two states of the same symmetry are not rare occurrences has revolutionized the way we think about nonadiabatic processes. On the other hand conical intersections of three states have been ignored except when required by symmetry. Three state conical intersections, intersections of state (I,J,K) are of interest in their own right as they provide new branching patterns for radiationless decay (a wave packet exiting a three state 'cone' has electronic state, as well as geometric, options). However three state intersections also represent sources of linked pairs (I,J) and (J,K) of two state intersections. These linked pairs of conical intersections are considerable more difficult to treat since they result in derivative couplings that may be double valued.[1] Recently we have developed an efficient algorithm for locating points on a seam of conical intersection of three states which is not required by symmetry.[2] The algorithm represents an extension of the algorithm we currently use to locate conical intersections of two electronic states[3] and derives considerable efficiency from the use of an analytic gradient, and Lagrange multiplier, techniques. We showed, using wave functions comprised of over 1.2 million configuration state functions, that changes in the molecular framework can cause the 3p Rydberg states of ethyl radical to become degenerate. For the allyl radical (see below) a three state intersection, involving Rydberg states with both s and p character. In addition, for the first time, sections of the seams corresponding to the linked pairs of conical intersections have been mapped.

COLUMBUS

One of the goals of our research program is to make the tools we have developed for locating, describing and analyzing conical intersections freely available to the general scientific community. In addition we would like to extend the range of accessible problems by taking advantage of the enormous power of parallel computing. To accomplish these goals a collaboration has been established with Hans Lischka's group (Vienna) and Ron Shepard's group (Argonne), principal developers of the COLUMBUS codes. COLUMBUS is a state of the art, highly efficient, suite of electronic structure codes that can determine state-averaged multiconfigurational self consistent field/ multireference configuration interaction wave functions, as well as the corresponding energy gradients and most recently first derivative couplings. COLUMBUS runs on both sequential

(single processor) and parallel (multiprocessor) platforms. It is freely available from the website, http://www.itc.univie.ac.at/~hans/Columbus/columbus.html. We are in the process of including in COLUMBUS our algorithms for locating and analyzing two state and three state conical intersections. The new version of COLUMBUS will provide the general scientific community with the tools to treat an increased range of problems in nonadiabatic chemistry. The calculations reported below on the allyl radical used COLUMBUS.

Photodissociation: $CH_2COH \rightarrow CH_2CO + H$

Predissociation of the vinoxy radical after the excitation $X^2A'' \rightarrow B^2A''$, the subject of work by Neumark and coworkers[4] and by Rohlfing and coworkers,[5] exhibits a sudden onset approximately 2000cm^{-1} above threshold. This precipitous onset of rapid photodissociation suggested that conical intersections were involved in the internal conversion. We undertook a study to confirm this hypothesis. The results however were quite surprising. Critical points on the A^2A' and B^2A'' potential energy surfaces were determined at the multireference configuration interaction level using expansions of five million configuration state functions. A mechanism consisting of a sequence of internal conversions, $B^2A'' \rightarrow A^2A' \rightarrow X^2A''$ to the ground state was proposed. B^2A'' - A^2A' conical intersections, are shown to be too high in energy to participate in this process. Instead the B^2A'' - A^2A' radiationless transition is enabled by an avoided crossing which is accessible after a barrier (TSB- in Fig. 1) of ca. 2000cm^{-1}, in agreement with experimental observations.
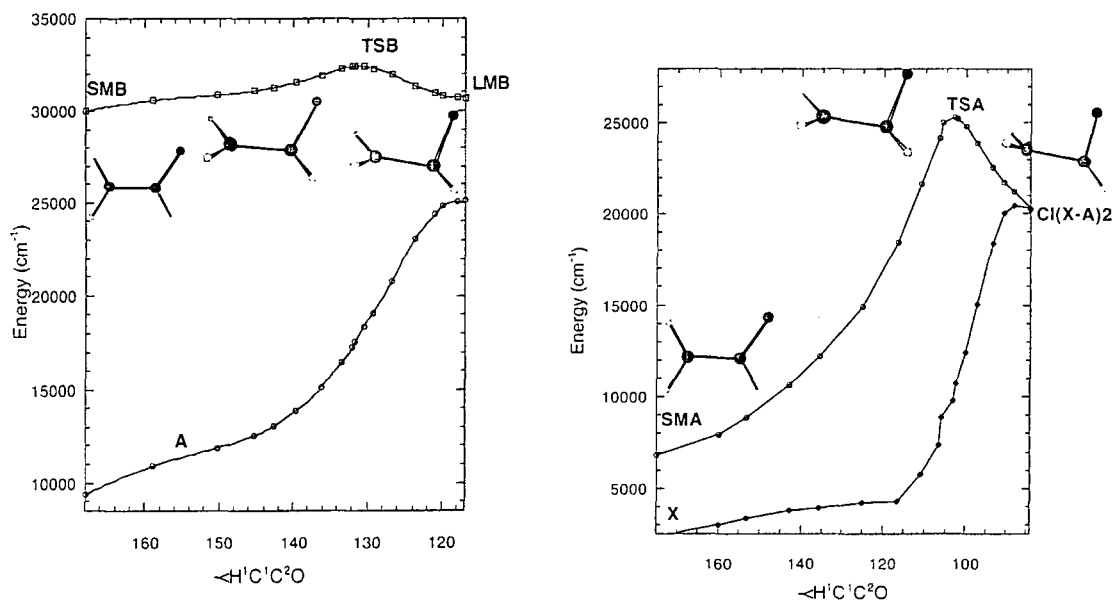

Figure 1 (Left panel) Path from spectroscopic minimum of the B state (SMB) to a region of large derivative coupling (LMB). (Right panel) Paths on A state following B $\rightarrow$ A nonadiabatic transition, ending near TSA. Shorter path leads to X state via A -X conical intersection.

Subsequently a $A^2A' \rightarrow X^2A'$ radiationless transition can occur very efficiently through easily accessible conical intersections (CI(X-A)2 in Fig.1).. A one-dimensional coupled adiabatic state

model of the process was developed. The radiationless decay rates of the vibrational levels obtained from this model serve to validate the proposed mechanism.

Photodissociation of Allyl

The photodissociation of the allyl radical (pictured below), which is relevant to hydrocarbon combustion, has recently been the object of detailed experimental work.[6,7] Although the allyl radical is discussed in many organic chemistry textbooks as the simplest unsaturated radical, the detailed structure of its electronically excited states remains unclarified. Our current work focuses on the three closely spaced excited states at approximately 5 eV,[8] the $B(1^2A_1)(4.97$ eV) , $C(2^2B_1)(5.00eV)$ and $D(1^2B_2)(5.15$ eV), states. We are currently using multireference configuration interaction methods to determine whether three state conical intersections exist for this system and how they might impact the B, C, and D electronic states, their spectra and photodissociation dynamics.
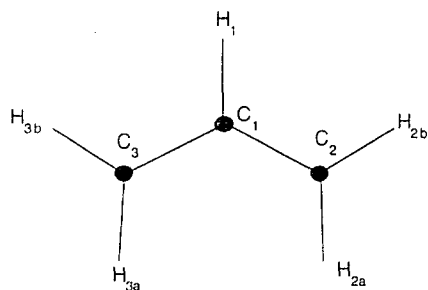
A key result of this, in progress, study is shown in the Figure on the right The point labelled BCD-CI is a three state conical intersection of states equivalent to the experimentally designated B, C and D states. Emerging from that point are energy optimized sections
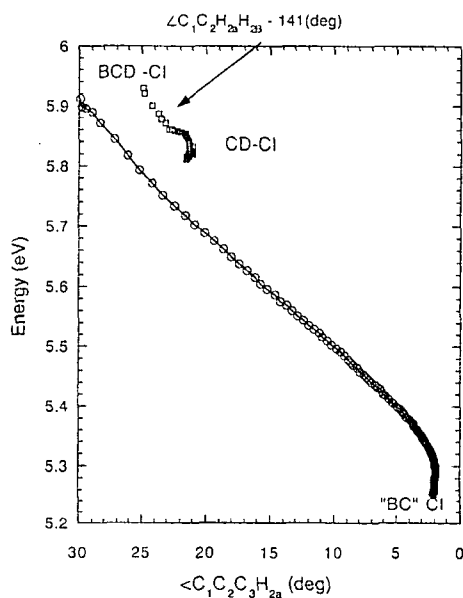
(in progress at time of writing) of the upper (C,D) (squares), and of the lower (B,C) (circles) linked pairs of conical intersection. This represents, to our knowledge. the first time seams of linked conical intersections merging into a single three state conical lintersection have been located.

The Future

We will continue our study of the allyl radical and the significance of its three state and linked conical intersections. We will also continue to work on the assignment of the symmetry of the closely spaced C and D states which is at present is opposite to the experimental result. We will also extend our studies to consider the photodissociation of the propargyl radical in particular and

the energetics of three state conical intersection in general. Our goal here is to determine how the energy of these intersections, changes, relative to the vertical excitation energy, with substituent substitution. It will be particularly interesting to consider the 3p Rydberg manifold in molecules including hydroxymethyl for which the splitting of the 3p manifold at the ground state equilibrium geometry is much larger than that of ethyl.[9]

References

1   S. Han and D. R. Yarkony, J. Chem. Phys., to be submitted (2003).
2   S. Matsika and D. R. Yarkony, work in progress (2003).
3   D. R. Yarkony, Rev. Mod. Phys. **68**, 985 (1996).
4   D. L. Osborn, H. Choi, D. H. Mordaunt, R. T. Bise, D. M. Neumark, and C. M. Rohlfing, J. Chem. Phys. **106**, 3049 (1997).
5   L. R. Brock and E. A. Rohlfing, J. Chem. Phys. **106**, 10048 (1997).
6   H.-J. Deyerl, I. Fischer, and P. Chen, J. Chem. Phys. **110**, 1450 (1999).
7   T. Gilbert, I. Fischer, and P. Chen, J. Chem. Phys. **113**, 561 (2000).
8   J. Blush, D. W. Minsek, and P. Chen, J. Phys. Chem. **96**, 10150 (1992).
9   P. J. Bruna and F. Grein, J. Phys. Chem. A. **102**, 3141 (1998).

PUBLICATIONS SUPPORTED BY DE-FG02-91ER14189: 2001 - present

[1]   *Conical intersections: The New Conventional Wisdom* – Feature Article, D. R. Yarkony, *J. Phys. Chem. A* **105**, 6277-6293 (2001).

[2]   *Conical Intersections and the Spin-Orbit Interaction,* Spiridoula Matsika and David R. Yarkony, in **The Role of Degenerate States in Chemistry**, Advances in Chemical Physics, Michael Baer and Gert. D. Billing, eds, J. Wiley, New York, 2002, pp. 557-583

[3]   *Conical Intersections: Their description and consequences,* David. R. Yarkony, in **Conical Intersections: Electronic Structure,Dynamics and Spectroscopy**, *Wolfgang Domcke, David R. Yarkony and Horst Köppel, eds. World Scientific Publishing, Singapore, (2003).*

[4]   *Determination of potential energy surface intersections and derivative couplings in the adiabatic representation* David. R. Yarkony, in **Conical Intersections: Electronic Structure,Dynamics and Spectroscopy**, *Wolfgang Domcke, David R. Yarkony and Horst Köppel, eds. World Scientific Publishing, Singapore, (2003)*

[5].   *Characterizing the Local Topology of Conical Intersections Using Orthogonality Constrained Parameters: Application to the internal conversion $S_1 \rightarrow S_0$* David R. Yarkony, J. Chem. Phys. 114, 2614 (2001)

[6].   *Intersecting Conical Intersection Seams in Tetra atomic Molecules : The S_1 - S_0 Internal Conversion in HNCO,* David R. Yarkony, *Molec. Phys.* 99, 1463-1467 (2001).

[7]   *Photodissociation of the Hydroxymethyl Radical I. The Role of Conical Intersections in LineBroadening and Decomposition Pathways* Brian C. Hoffman and David R. Yarkony, J. Chem. Phys. **116** 8300-8306, (2002).

[8].   *Spin-orbit Coupling and Conical Intersections. IV: A perturbative determination of the electronic energies,derivative couplings and a rigorous diabatic representation near a conical intersection. The general case* S. Matsika and D. R. Yarkony, *J. Phys. Chem* B. **106** 8108-8116 (2002)

[9].   *Photdissociation of the vinoxy radical through conical and avoided intersections* S. Matsika and D. R. Yarkony, J. Chem. Phys. **117**, 7198 (2002).

[10].   *Accidental Conical Intersections of three states of the same symmmetry: Location and Relevance,* S. Matsika and D. R. Yarkony, J. Chem. Phys. **117**, 6907 (2002).

The Chemistry and Spectroscopy of Combustion Species: Isomer-Specific Excitation and Detection

Timothy S. Zwier

Department of Chemistry, Purdue University, West Lafayette, IN   47907-2084

zwier@purdue.edu

Program Definition and Scope

Combustion models necessarily face a daunting task as they seek to describe the complex array of reactions that produce and destroy aromatics and polyaromatic hydrocarbons in flames. Many of these reactions involve species with several isomers, only some of which are efficiently transformed into aromatics. The objectives of this research program are to develop and utilize laser-based methods for photoexciting, detecting, and spectroscopically characterizing structural or conformational isomers relevant to soot formation. We are applying these methods to key reactions that lead toward the prototypical aromatics benzene and naphthalene, and their simple derivatives, in flames.

Recent Progress

A. Spectroscopy and dynamics of the diethynyl benzenes

A major thrust of our work over the past year has been to characterize the vibronic spectroscopy of *ortho-*, *meta-*, and *para*-diethynylbenzene (*o*-DEB, *m*-DEB, and *p*-DEB). These molecules are important intermediates along the way from benzene to larger polyaromatic hydrocarbons in flames. The symmetry allowed S_0-S_1 origins were located at 33515 cm^{-1}, 33806 cm^{-1}, and 34255 cm^{-1}, with vibronic structure extending about 2000 cm^{-1} above the origin in *o*-DEB and *m*-DEB, but more than 3000 cm^{-1} in *p*-DEB. Major peaks in each spectrum were attributed to vibronically induced bands indicating strong coupling of the S_1 state to the S_2 state. Ground state infrared spectra in the C-H stretch region (3000-3300 cm^{-1}) were obtained using resonant ion-dip infrared spectroscopy (RIDIRS). In all three isomers, the C-H stretch fundamental was split by Fermi resonance with a combination band composed of the C≡C stretch and two quanta of C≡C-H bend. This Fermi resonance is detuned in the overtone region of *p*-DEB, which shows a single peak at 6556 cm^{-1}. Infrared spectra were also recorded in the excited electronic state using a UV-IR-UV version of RIDIR spectroscopy. In all three isomers the C-H stretch fundamental was unshifted from the ground state, but no Fermi resonance was seen.

One of our most exciting results from the first year of the grant was the observation of a broad absorption in the S_1-state infrared spectrum of *ortho*-diethynyl benzene, stretching from 3050-3250 cm^{-1}. Selective deuteration of *o*-DEB at the acetylenic hydrogens led to infrared spectra that retained the broad absorption despite the absence of the acetylenic C-H stretch absorption, proving that the IR absorption is electronic in nature. The nature of this state is still unclear, but its presence only in *ortho*-diethynylbenzene and the breadth of the absorption both suggest a state that could be a gateway for Bergman cyclization to form the 1,4-didehydronaphthalene diradical:
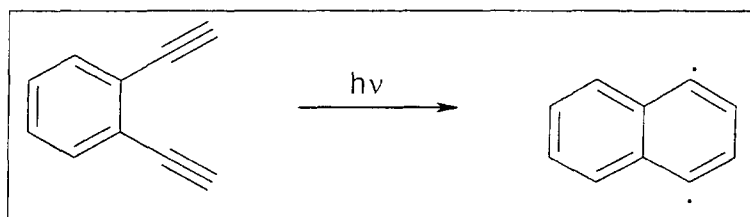
B. Spectroscopic characterization of C_6H_6 isomers

A second major focus of the present work is a detailed, isomer-specific study of the C_6H_6 potential energy surface that connects two propargyl radicals to benzene. After aborted attempts to synthesize specific C_6H_6 isomers, we are learning to make and handle the non-benzene C_6H_6 isomers by pyrolysis of 1,5-hexadiyne, one of the primary adducts formed when two propargyl radicals recombine. We have built a high temperature furnace / flow cell for this purpose, and are using photoacoustic spectroscopy to characterize the products so formed.

C. Methods Development

We have also made several improvements to our experimental capabilities over the last year. First, we have successfully generated mid-infrared light (~0.5 mJ/pulse at 6-7 μm) by difference frequency mixing the output of our KTA-based parametric converter in $AgGaSe_2$. This will enable us to look at C-H bend and C=O stretch fundamentals. Second, we have built and tested a fast ion gate capable of selectively removing adjacent ion masses in a time-of-flight mass spectrum. Such selective removal can be crucial in photochemical studies, where interferences can swamp out the desired ion signal if not removed. Third, we have designed and built a modified ion source region that will skim the molecular beam before interrogation. The open source design that has been so useful in past photochemical studies has also put significant limitations on our allowable gas flow conditions. The skimmer will reduce these restrictions significantly. Finally, we are modifying an existing chamber for fluorescence detection in the source chamber so that we can detect some of the aromatic products with even greater sensitivity in fluorescence.

Future Plans

Over the coming year, we will pursue the isomer-specific spectroscopy and photoisomerization dynamics of (1) the C_6H_6 isomers 1,5-hexadiyne, fulvene, and 3,4-dimethylene cyclobutene, (2) the *ortho*-diethynylbenzene ($C_{10}H_6$) isomer, and (3) the *ortho-, meta-,* and *para*-ethynylstyrene ($C_{10}H_8$) isomers.

We will further characterize the high-temperature flow cell that will be used to pyrolyze 1,5-hexadiyne to form either 3,4-dimethylene cyclobutene in nearly pure form at 450 °C, or fulvene/benzene mixtures at higher temperatures (610 °C). We plan to record R2PI, non-resonant ion-gain and resonant ion-dip infrared spectra, seeking clean UV wavelengths for detection of these species. We will work to obtain pure samples of fulvene for study of its photoisomerization to benzene. We will also study the photoisomerization of 1,5-hexadiyne, which is commercially available.

In *ortho*-diethynylbenzene, we will pursue direct evidence for the photochemical reaction to form 1,4-didehydronaphthalene diradical. This photochemistry will be probed by exciting *ortho*-diethynyl benzene with an ultraviolet laser pulse while it is in our reaction tube, and using cyclohexadiene as a trap to form naphthalene, which we can detect sensitively in R2PI.

Finally, we will also explore the spectroscopy and dynamics of the $C_{10}H_8$ ethynylstyrene isomers **1-3** shown below, which could isomerize to naphthalene following photoexcitation. Samples of these molecules are currently being synthesized.

ortho-ethynyl	*meta*	*para*
styrene		
1	**2**	**3**
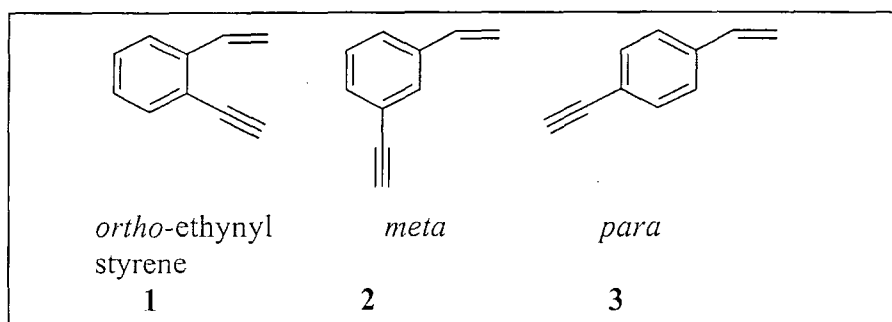
Publications acknowledging DOE support, 2000-present:

Allison G. Robinson, Paul R. Winter, Christopher Ramos, and Timothy S. Zwier, "Ultraviolet Photochemistry of Diacetylene: Reactions with Benzene and Toluene", *J. Phys. Chem. A* **104**, 10312-10320 (2000).

Charles S. McEnally, Allison G. Robinson, Lisa D. Pfefferle, and Timothy S. Zwier, "Aromatic Hydrocarbon Formation in Nonpremixed Flames Doped with Diacetylene, Vinylacetylene, and Other Hydrocarbons: Evidence for Pathways Involving C4 Species", Combustion and Flame **123**, 344-357 (2000).

Christopher Ramos, Paul R. Winter, Timothy S. Zwier, and Stephen T. Pratt, "Photoelectron Spectroscopy via the $1^1\Delta_u$ state of Diacetylene", J. Chem. Phys. **116**, 4011 (2002).

Allison G. Robinson, Paul R. Winter, and Timothy S. Zwier, "The singlet-triplet spectroscopy of 1,3-butadiene using cavity ring-down spectroscopy", J Chem. Phys. 116 (18): 7918-7925 (2002).

Allison G. Robinson, Paul R. Winter, and Timothy S. Zwier, "The Ultraviolet Photochemistry of Diacetylene with Styrene", J. Phys. Chem. A **106** (24): 4789-4796 (2002).

Jaime Stearns and Timothy S. Zwier, "The Infrared and Ultraviolet Spectroscoy of jet-cooled *ortho-*, *meta-*, and *para*-diethynylbenzene: In search of a spectroscopic link to photochemical Bergman cyclization", (in preparation).

Participants

Dr. Musahid Ahmed
Lawrence Berkeley Laboratory
One Cyclotron Road
Berkeley, CA 94720
Phone: (510)486-6355
mahmed@lbl.gov

Prof. Wesley D. Allen
The Center for Computational
Quantum Chemistry
The University of Georgia
Athens, GA 30602-2525
Phone: (706)542-7729
wdallen@ccqc.uga.edu

Dr. Sarah W. Allendorf
Combustion Research Facility
Mail Stop 9055
Sandia National Laboratories
PO Box 969
Livermore, California 94551-0969
Phone: (925)294-3379
swallen@sandia.gov

Prof. Tomas Baer
Department of Chemistry
University of North Carolina
Chapel Hill, North Carolina 27599-3290
Phone: (919)962-1580
baer@unc.edu

Dr. Robert S. Barlow
Combustion Research Facility
MS9051
Sandia National Laboratories
Livermore, California 94551-0969
Phone: (925)294-2688
barlow@ca.sandia.gov

Prof. Joel M. Bowman
Department of Chemistry
Emory University
1515 Pierce Drive
Atlanta, Georgia 30322
Phone: (404)727-6590
bowman@euch4e.chem.emory.edu

Professor Kenneth Brezinsky
Chemical Engineering Dept.
810 S. Clinton
The University of Illinois at Chicago
Chicago, Illinois 60607-7022
Phone: (312)996-9430
kenbrez@uic.edu

Dr. Nancy Brown
Environmental Technologies
Division
Advanced Energy Technology
Lawrence Berkeley National
Laboratory MS 51-208
One Cyclotron Road
Berkeley, California 94720
Phone: (510)486-4241
njbrown@lbl.gov

Prof. Laurie J. Butler
The James Franck Institute
The University of Chicago
5640 S. Ellis Avenue
Chicago, Illinois 60637
Phone: (773)702-7206
ljb4@midway.uchicago.edu

Dr. Robert W. Carling
MS 9054
Combustion Research Facility
Sandia National Laboratories
Livermore, California 94551-0969
Phone: (925)294-2206
rwcarli@sandia.gov

Prof. Barry K. Carpenter
Department of Chemistry &
Chemical Biology
Cornell University
Ithaca, NY 14853-1301
Phone: (607)255-3826
bkc1@cornell.edu

Dr. David W. Chandler
Combustion Research Facility
MS 9054
Sandia National Laboratories
Livermore, California 94551-0969
Phone: (925)294-3132
chandler@ca.sandia.gov

Dr. Robert K. Cheng
Energy and Environment Division
University of California
Lawrence Berkeley National
Laboratory
One Cyclotron Road
Berkeley, California 94720
Phone: (510)486-5438
rkcheng@lbl.gov

Prof. Robert E. Continetti
Department of Chemistry and
Biochemistry, 0340
University of California, San Diego
9500 Gilman Drive
La Jolla, CA 92093-0340
Phone: (858)534-5559
rcontinetti@ucsd.edu

Prof. Terrill A. Cool
College of Engineering
School of Applied & Engineering
Physics
Cornell University
Ithaca, New York 14853-1301
Phone: (607)255-4191
tac13@cornell.edu

Prof. F. Fleming Crim
Department of Chemistry
University of Wisconsin
1101 University Avenue
Madison, Wisconsin 53706
Phone: (608)263-7364
fcrim@chem.wisc.edu

Prof. Robert F. Curl, Jr.
Department of Chemistry
Rice University
P.O. Box 1892
Houston, Texas 77005
Phone: (713)348-4816
rfcurl@rice.edu

Prof. Hai-Lung Dai
Department of Chemistry
University of Pennsylvania
Philadelphia, Pennsylvania 19104-6323
Phone: (215)898-5077
dai@sas.upenn.edu

Prof. H. Floyd Davis
Department of Chemistry &
Chemical Biology
Baker Laboratory
Cornell University
Ithaca, New York 14853-1301
Phone: (607)255-0014
hfd1@cornell.edu

Dr. Michael J. Davis
Chemistry Division
Argonne National Laboratory
9700 South Cass Avenue
Argonne, Illinois 60439
Phone: (630)252-4802
davis@tcg.anl.gov

Prof. Frederick L. Dryer
Department of Mechanical &
Aerospace Engineering
Princeton University
Princeton, New Jersey 08544
Phone: (609)258-5206
fldryer@princeton.edu

Prof. G. Barney Ellison
Department of Chemistry
University of Colorado
Boulder, Colorado 80309-0215
Phone: (303)492-8603
barney@jila.colorado.edu

Prof. Kent M. Ervin
Department of Chemistry/216
College of Arts and Sciences
University of Nevada, Reno
Reno, Nevada 89557-0020
Phone: (775)784-6676
ervin@chem.unr.edu

Dr. Askar Fahr
Chemical Kinetics and Thermo-
Dynamics Division
National Institutes of Standards and
Technology
Gaithersburg, MS 20899
Phone: (301)975-2511
askar.fahr@nist.gov

Prof. Robert W. Field
Department of Chemistry
Room 6-219
Massachusetts Institute of
Technology
77 Massachusetts Ave.
Cambridge, Massachusetts 02139
Phone: (617)253-1489
rwfield@mit.edu

Dr. Christopher Fockenberg
Chemistry Department
Building 555A
Brookhaven National Laboratory
Upton, NY 11973-5000
Phone: (631)344-4372
fknberg@bnl.gov

Dr. Jonathan H. Frank
Combustion Research Facility
MS 9051
Sandia National Laboratories
Livermore, CA 94511
Phone: (925)294-4645
jhfrank@ca.sandia.gov

Prof. Michael Frenklach
Department of Mechanical
Engineering
Lawrence Berkeley National
Laboratory
University of California at Berkeley
Berkeley, California 94720-1740
Phone: (510)643-1676
myf@me.berkeley.edu

Dr. David Golden
Department of Mechanical
Engineering; Bldg. 520
Stanford University
Stanford, CA 94305
Phone: (650)723-5009
david.golden@stanford.edu

Dr. Stephen K. Gray
Chemistry Division
Argonne National Laboratory
9700 South Cass Ave.
Argonne, Illinois 60439
Phone: (630)252-3594
gray@tcg.anl.gov

Prof. William H. Green, Jr.
Department of Chemical
Engineering, 66-448
Massachusetts Institute of
Technology
77 Massachusetts Ave.
Cambridge, Massachusetts 02139
Phone: (617)253-4580
whgreen@mit.edu

Dr. Gregory E. Hall
Chemistry Department
Brookhaven National Laboratory
Upton, New York 11973
Phone: (631)344-4376
gehall@bnl.gov

Prof. Ronald K. Hanson
Department of Mechanical
Engineering
Stanford University
Stanford, California 94305
Phone: (650)723-4023
hanson@me.stanford.edu

Dr. Lawrence Harding
Chemistry Division
Argonne National Laboratory
9700 South Cass Avenue
Argonne, Illinois 60439
Phone: (630)252-3591
harding@anl.gov

Dr. Alex Harris
Chemistry Department, Bldg. 555
Brookhaven National Laboratory
Upton, NY 11973
Phone: (631)344-4301
alexh@bnl.gov

Dr. Carl C. Hayden
Combustion Research Facility
MS 9055
Sandia National Laboratories
Livermore, California 94551-0969
Phone: (925)294-2298
cchayde@sandia.gov

Prof. Martin Head-Gordon
Department of Chemistry
University of California at Berkeley
Berkeley, California 94720
Phone: (510)642-5957
mhg@cchem.berkeley.edu

Prof. John Hershberger
Department of Chemistry
North Dakota State University
Fargo, ND 58105-5516
Phone: (701)231-8225
john.hershberger@ndsu.nodak.edu

Dr. Jan P. Hessler
Chemistry Division
Argonne National Laboratory
9700 South Cass Avenue
Argonne, Illinois 60439
Phone: (630)252-3717
hessler@anl.gov

Prof. Paul L. Houston
Department of Chemistry
122 Baker Laboratory
Cornell University
Ithaca, New York 14853-1301
Phone: (607)255-4303
plh2@cornell.edu

Dr. Wen Hsu
Combustion Research Facility
MS9056
Sandia National Laboratories
Livermore, CA 94551
Phone: (925)294-2379

Prof. Philip M. Johnson
Department of Chemistry
State University of New York
at Stony Brook
Stony Brook, New York 11794
Phone: (631)632-7912
philip.Johnson@sunysb.edu

Prof. Michael E. Kellman
Department of Chemistry
University of Oregon
Eugene, Oregon 97403
Phone: (541)346-4196
kellman@oregon.uoregon.edu

Prof. John Kiefer
Department of Chemical
Engineering
810 S. Clinton
University of Illinois at Chicago
Chicago, Illinois 60607
Phone: (312)996-5711
john.h.kiefer@uic.edu

Dr. Stephen J. Klippenstein
Combustion Research Facility
MS 9055
Sandia National Laboratories
Livermore, California 94551-0969
Phone: (925)294-2289
SJKLIPP@sandia.gov

Prof. Stephen R. Leone
Department of Chemistry
University of California
Berkeley, CA 94720-1460
Phone: (510)643-5467
srl@cchem.berkeley.edu

Prof. Marsha I. Lester
Department of Chemistry
University of Pennsylvania
231 South 34th Street
Philadelphia, Pennsylvania 19104-
6323
Phone: (215)898-4640
milester@sas.upenn.edu

Prof. William A. Lester, Jr.
Department of Chemistry
University of California at Berkeley
Berkeley, California 94720-1460
Phone: (510)643-9590
walester@cchem.berkeley.edu

Prof. John C. Light
The James Franck Institute
The University of Chicago
5640 S. Ellis Avenue
Chicago, Illinois 60637
Phone: (773)702-7197
j-light@uchicago.edu

Prof. Ming-Chang Lin
Department of Chemistry
Emory University
1515 Pierce Drive
Atlanta, Georgia 30322
Phone: (404)727-2825
chemmcl@emory.edu

Prof. Robert P. Lucht
School of Mechanical Engineering
Purdue University
West Lafayette, IN 47907-2088
Phone: (765)494-0539
lucht@purdue.edu

Dr. R. Glen Macdonald
Chemistry Division
Argonne National Laboratory
9700 South Cass Avenue
Argonne, Illinois 60439
Phone: (630)252-7742
rgmacdonald@anl.gov

Dr. Andrew McIlroy
Combustion Research Facility
MS 9055
Sandia National Laboratories
Livermore, California 94551-0969
Phone: (925)294-3054
amcilr@sandia.gov

Dr. William J. McLean
Combustion Research Facility
MS9054
Sandia National Laboratories
Livermore, California 94551-0969
Phone: (925)294-2687
wjmclea@sandia.gov

Professor Gregory J. McRae
Department of Chemical
Engineering; Room 66-372
Massachusetts Institute of
Technology
Cambridge,MA 02139
Phone: (617)253-6564
mcrae@mit.edu

Dr. Joe V. Michael
Chemistry Division
Argonne National Laboratory
9700 South Cass Avenue
Argonne, Illinois 60439
Phone: (630)252-3171
michael@anlchm.chm.anl.gov

Dr. Hope A. Michelsen
Combustion Research Facility
M/S 9054
Sandia National Laboratories
Livermore, CA 94551
Phone: (925)294-2335
hamiche@sandia.gov

Dr. James A. Miller
Combustion Research Facility
MS-9055
Sandia National Laboratories
Livermore, California 94551-0969
Phone: (925)294-2759
jamille@ca.sandia.gov

Prof. Terry A. Miller
Department of Chemistry
Ohio State University
140 West 18th Avenue
Columbus, Ohio 43210
Phone: (614)292-2569
tamiller+@osu.edu

Prof. William H. Miller
Department of Chemistry
University of California at Berkeley
Berkeley, California 94720
Phone: (510)642-0653
miller@cchem.berkeley.edu

Prof. C. Bradley Moore
Office of Research
208 Bricker Hall
Ohio State University
190 N. Oval Mall
Columbus, Ohio 43210
Phone: (614)292-1582
moore.1@osu.edu

Dr. James Muckerman
Chemistry Department
Brookhaven National Laboratory
Upton, NY 11973
Phone: (631)344-4368
muckerma@bnl.gov

Dr. Habib N. Najm
Combustion Research Facility
MS9051
Sandia National Laboratories
Livermore, California 94551-0969
Phone: (925)294-2054
hnnajm@ca.sandia.gov

Prof. Daniel M. Neumark
Department of Chemistry
University of California at Berkeley
Berkeley, California 94720
Phone: (510)642-3502
neumark@cchem.berkeley.edu

Prof. Cheuk-Yiu Ng
Department of Chemistry
One Shields Avenue
University of California at Davis
Davis, CA 95616
Phone: (530)754-9645
cyng@chem.ucdavis.edu

Dr. David L. Osborn
Combustion Research Facility
MS 9055
Sandia National Laboratories
Livermore, California 94551-0969
Phone: (925)294-4622
dlosbor@sandia.gov

Prof. David S. Perry
Department of Chemistry
University of Akron
Akron, Ohio 44325
Phone: (330)972-6825
dperry@uakron.edu

Dr. Stephen Pratt
Chemistry Division
Argonne National Laboratory
9700 South Cass Avenue
Argonne, Illinois 60439
Phone: (630)252-4199
stpratt@anl.gov

Dr. Jack M. Preses
Chemistry Department
Brookhaven National Laboratory
Upton, New York 11973
Phone: (631)344-4371
preses@bnl.gov

Dr. Larry A. Rahn
Combustion Research Facility
MS 9056
Sandia National Laboratories
Livermore, California 94551-0969
Phone: (925)294-2091
rahn@sandia.gov

Prof. Hanna Reisler
Department of Chemistry
University of Southern California
Los Angeles, California 90089-0482
Phone: (213)740-7071
reisler@usc.edu

Dr. Branko Ruscic
Chemistry Division
Argonne National Laboratory
9700 South Cass Avenue
Argonne, Illinois 60439
Phone: (630)252-4079
ruscic@anl.gov

Dr. Trevor Sears
Chemistry Department
Brookhaven National Laboratory
Upton, New York 11973
Phone: (631)344-4374
sears@bnl.gov

Dr. Thomas B. Settersten
Combustion Research Facility
MS 9056
Sandia National Laboratories
Livermore, California 94551-0969
Phone: (925)294-4701
tbsette@sandia.gov

Dr. Ron Shepard
Chemistry Division
Argonne National Laboratory
9700 South Cass Avenue
Argonne, Illinois 60439
Phone: (630)252-3584
shepard@tcg.anl.gov

Prof. Irene Slagle
Department of Chemistry
The Catholic University of America
Michigan Avenue at 7th Street, N.E.
Washington, D.C. 20064
Phone: (202)319-5384
slagle@cua.edu

Prof. Mitchell Smooke
Department of Mechanical
Engineering
Yale University
P.O. Box 208284
New Haven, Connecticut 06520-
8284
Phone: (203)432-4344
mitchell.smooke@yale.edu

Prof. Arthur G. Suits
Department of Chemistry
State University of New York
 at Stony Brook
Stony Brook, NY 11794
Phone: (631)632-1702
arthur.suits@sunysb.edu

Dr. Craig Taatjes
Combustion Research Facility
MS 9055
Sandia National Laboratories
Livermore, California 94551-0969
Phone: (925)294-2764
cataatj@sandia.gov

Prof. Howard S. Taylor
Department of Chemistry
University of Southern California
Los Angeles, California
Phone: (213)740-4112
taylor@usc.edu

Professor Donald L. Thompson
Department of Chemistry
Oklahoma State University
Stillwater, OK 74078
Phone: (405)744-5174
dlt@okstate.edu

Dr. Alison Tomlin
Argonne National Laboratory
9700 South Cass Avenue
Argonne, IL 60439
Phone: (630)252-5034
fueast@leeds.ac.uk

Dr. Robert Tranter
Dept. of Chemical Engineering
The University of Illinois at Chicago
810 S. Clinton Street
Chicago, IL 60607
Phone: (312)996-0808
rtranter@uic.edu

Prof. Donald G. Truhlar
Department of Chemistry
139 Smith Hall
University of Minnesota
207 Pleasant St. SE
Minneapolis, Minnesota 55455
Phone: (612)624-7555
truhlar@umn.edu

Dr. Wing Tsang
Chemical Kinetics Division
Center for Chemical Technology
A147 Chemistry Building
Natl. Inst. of Standards and
Technology
Gaithersburg, Maryland 20899
Phone: (301)975-2507
wing.tsang@nist.gov

Dr. Frank P. Tully
Division of Chemical Sciences,
 Geosciences and Biosciences SC-14
Office of Basic Energy Sciences
U.S. Department of Energy
19901 Germantown Road
Germantown MD 20874-1290
Phone: (301)903-5998
frank.tully@science.doe.gov

Prof. James J. Valentini
Department of Chemistry
Columbia University
3000 Broadway, MC 3120
New York, New York 10027
Phone: (212)854-7590
jjv1@chem.columbia.edu

Dr. Albert F. Wagner
Chemistry Division
Argonne National Laboratory
9700 South Cass Avenue
Argonne, Illinois 60439
Phone: (630)252-3597
wagner@tcg.anl.gov

Dr. Charles K. Westbrook
Division of Computational Physics
Lawrence Livermore National
Laboratory
P. O. Box 808, L-091
Livermore, California 94550
Phone: (925)422-4108
westbrook1@llnl.gov

Prof. Phillip R. Westmoreland
Department of Chemical
Engineering
University of Massachusetts
Amherst, Massachusetts 01003
Phone: (413)545-1750
westm@ecs.umass.edu

Dr. Michael G. White
Department of Chemistry
Brookhaven National Laboratory
Upton, New York 11973
Phone: (631)344-4345
mgwhite@bnl.gov

Prof. Curt Wittig
Department of Chemistry
University of Southern California
Los Angeles, California 90089-0484
Phone: (213)740-7368
wittig@usc.edu

Prof. David R. Yarkony
Department of Chemistry
Johns Hopkins University
3400 N. Charles Street
Baltimore, Maryland 21218
Phone: (410)516-4663
yarkony@jhu.edu

Prof. Timothy S. Zwier
Department of Chemistry
Purdue University
West Lafayette, Indiana 47907
Phone: (765)494-5278
zwier@purdue.edu

Author Index